

# IL NUOVO CIMENTO

ORGANO DELLA SOCIETÀ ITALIANA DI FISICA

SOTTO GLI AUSPICI DEL CONSIGLIO NAZIONALE DELLE RICERCHE

Vol. III, N. 5

Serie decima

1° Maggio 1956

## Charge Renormalization Group in Quantum Field Theory.

N. N. BOGOLJUBOV and D. V. ŠIRKOV

*Steklov Mathematical Institute of the Academy of Sciences of the USSR - Moscow*

(ricevuto il 24 Novembre 1955)

**Summary.** — Lie differential equations are obtained for the multiplicative charge renormalization group in quantum electrodynamics and in pseudo-scalar meson theory with two coupling constants. By the employment of these equations there have been found the asymptotic expressions for the electro-dynamical propagation functions in the «ultraviolet» and in the «infrared» regions. The asymptotic high momenta behaviour of meson theory propagation functions is also discussed, for the weak coupling case.

### 1. — Introduction.

An increasingly keen interest is being given of late to the idea of surpassing the framework of usual perturbation theory. This is due both to the direct evidences that the meson coupling constants are not at all small and to the fact that even in quantum electrodynamics, where the coupling constant is really a small quantity, there are domains in the momentum space, where the effective parameter of the perturbation power series can grow to infinity.

Our implication refers here to the so called «ultraviolet» region

$$|\kappa^2| \gg m^2,$$

and «infrared» region

$$\kappa^2 \sim m^2.$$

For instance, in the first case the  $n$ -th term of the usual power series contains expressions of the type:

$$\left( e^2 \ln \frac{\kappa^2}{m^2} \right)^n.$$

Owing to this fact, the effective parameter of the development is no longer  $e^2$ , but  $e^2 \ln (\kappa^2/m^2)$ .

The attempts to arrive at the non perturbational approach were based primarily on extensive and intricate investigations of Schwinger-Dyson equations for appropriate Green's functions, at various approximations.

By this method EDWARDS <sup>(1)</sup> arrived at an interesting approximate integral equation and in some cases succeeded in obtaining appropriate solutions.

Later on LANDAU, ABRIKOSOV and HALATNIKOV <sup>(2)</sup> investigated this problem in a more consistent way and succeeded in finding the asymptotic forms of quantum electrodynamical Green's functions for a significant high momenta region.

Analogous methods were successfully employed by ABRIKOSOV in the treatment of the infrared region <sup>(3)</sup>.

The problem of finding the asymptotic expressions of Green's functions in this regions has been treated independently by one of the authors (N.N. BOGOLJUBOV) with his assistants <sup>(4)</sup> by means of the Fock proper time method.

A new type of non-perturbational approach, essentially based on group theoretical properties of propagation functions was suggested by GELL-MANN and Low <sup>(5)</sup>. Their work, however, was not completed owing to some errors which shall be pointed out below.

A more consistent development of the ideas put forward by GELL-MANN and Low can be achieved by the investigation of the multiplicative charge renormalization group.

STÜCKELBERG and PETERMANN <sup>(6)</sup> appear to be the first to have drawn attention to this group and to its role in the general quantum field theory.

These authors have also pointed out the possibility of defining the corresponding infinitesimal operators and hence the possibility of constructing the Lie differential equations.

<sup>(1)</sup> S. F. EDWARDS: *Phys. Rev.*, **90**, 284 (1953).

<sup>(2)</sup> L. D. LANDAU, A. A. ABRIKOSOV and I. M. HALATNIKOV: *Dokl. Akad. Nauk SSSR*, **95**, 497, 773, 1177 (1954); **96**, 261 (1954).

<sup>(3)</sup> A. A. ABRIKOSOV: *Doctoral Thesis* (Institute for Physical Problems of the Academy of Sciences of the USSR, 1955).

<sup>(4)</sup> Communicated by N. N. BOGOLJUBOV at the All-Union Conference on Problems of Quantum Electrodynamics and of Elementary Particles (Moscow, March 1955).

<sup>(5)</sup> M. GELL-MANN and F. E. LOW: *Phys. Rev.*, **95**, 1300 (1954).

<sup>(6)</sup> E. C. G. STÜCKELBERG and A. PETERMANN: *Helv. Phys. Acta*, **26**, 499 (1953).



The development of these group ideas is the chief purpose of the present paper.

We shall obtain here the Lie differential equations for the charge renormalization group in question and consider their applications to the construction of the asymptotic forms of Green's functions. It will be shown that by this method considerable improvement in the results of the usual perturbation theory can be achieved directly, with no recourse to the complicated integral equations of the Schwinger-Dyson type.

## 2. - The Multiplicative Renormalization Group in Quantum Electrodynamics.

It is well known that the usual subtraction procedure is equivalent to the introduction of certain divergent counter-terms into the expression of the interaction lagrangian. In order to get rid of actual infinities in intermediate calculations it is advisable to proceed with some kind of cut-off, for instance with a regularization of the Pauli-Villars type. The cut-off is removed from the final formulae by a limiting process. Making the necessary suppositions of summability of the resulting power series we arrive thus at the finite expressions for the considered propagation functions.

These expressions contain arbitrary constants due to the ambiguity of the subtraction procedure or, what is the same, to the possibility of adding finite terms of the same operational structure as that of the divergent counter-terms to the interaction lagrangian.

This ambiguity may be removed from the theory by putting the condition that it should describe particles with the given experimental values of mass and charge.

However, Green's functions and coupling parameter still contain arbitrary constants, so that the same physical situation may correspond to two different sets of their values. This is the cause of the existence of the renormalization group.

As was pointed out by DYSON<sup>(7)</sup> the introduction of counter-terms (with the exception of the self mass counter-term) is equivalent to a multiplicative renormalization of Green's functions and charge. We intend here to investigate this point more closely. Since the mentioned counter-terms have the form<sup>(8)</sup>

$$(1) \quad (Z-1)\sqrt{4\pi e}\bar{\psi}\hat{A}\psi + (Z-1)\bar{\psi}(\hat{\kappa}-m)\psi - \frac{Z_3-1}{2} \sum_{m,n} A_m (g^{mn}\kappa^2 - \kappa^m\kappa^n) A_n,$$

<sup>(7)</sup> F. J. DYSON: *Phys. Rev.*, **75**, 1736 (1949).

<sup>(8)</sup> We use Feynman's system of Dirac matrices and

$$g^{ik} = 0 \quad (i \neq k), \quad g^{00} = -g^{11} = -g^{22} = -g^{33} = 1.$$

the inclusion of the finite terms of the same structure:

$$(2) \quad (z-1)\sqrt{4\pi e}\bar{\psi}\hat{A}\psi + (z-1)\bar{\psi}(\hat{\kappa} - m)\psi - \frac{z_3-1}{2} \sum_{m,n} A_m (g^{mn}\kappa^2 - \kappa^m\kappa^n) A_n,$$

in the interaction lagrangian leads to an allowed modification of the subtraction procedure.

Such an inclusion must be accompanied by a corresponding transformation of Green's functions and of  $e$ .

Now, it should be noted that the contribution of the first term of (2) in the equations for Green's functions combines simply with that of the interaction lagrangian.

The contribution of the second term combines with that of the fermion part of the free lagrangian. Thus the multiplicative effect of these two terms is clear.

The difficulty arises with the third term of (2).

The fact is that its contribution in the corresponding equation

$$g^{mn}\kappa^2 - \kappa^m\kappa^n$$

is not proportional to the inverse electromagnetic pairing

$$g^{mn}\kappa^2$$

and it can be shown that, aside from the multiplicative effect, the considered term modifies the photon propagation function by adding an expression of the longitudinal form

$$\frac{1-z_3}{z_3} \frac{\kappa^m\kappa^n}{(\kappa^2)^2}.$$

Such a supplementary term is not relevant when (as in DYSON's paper) only  $S$ -matrix elements between real states are considered, because of the Lorentz condition. But the situation is different with Green's functions, which are represented by sums of Feynman graphs containing only internal lines.

Nevertheless, a purely multiplicative effect of the third term may still be obtained if we choose a free photon propagation function in the transverse form

$$(3) \quad D_{mn}^{tr} = \frac{1}{i\kappa^2} \left( g^{mn} - \frac{\kappa_m\kappa_n}{\kappa^2} \right), \quad \kappa_m = g^{mn}\kappa^n$$

instead of its usual Feynman's form

$$(4) \quad D_{mn}^c = \frac{1}{i\kappa^2} g^{mn}.$$

To arrive at such transverse form the following gradient transformation



of the functional argument of Green's functions is to be carried out:

$$(5) \quad A_n(\kappa) \rightarrow A'_n(\kappa) = A_n(\kappa) - \frac{\kappa_n}{\kappa^2} (\kappa \cdot A(\kappa)).$$

In fact, we have:

$$(6) \quad i \langle T(A_n(\kappa) A_m(\kappa')) \rangle_0 = \frac{g^{mn}}{\kappa^2} \delta(\kappa + \kappa')$$

and thus

$$(7) \quad i \langle T(A'_n(\kappa) A_m(\kappa')) \rangle_0 = \frac{g^{mn} - (\kappa_m \kappa_n / \kappa^2)}{\kappa^2} \delta(\kappa + \kappa').$$

By means of the transverse form (3) it can be shown<sup>(9)</sup> that the finite introduction of finite counter-terms (2) into the interaction lagrangian is equivalent to the multiplicative transformations of the full propagation functions (Green's functions with the functional argument  $A$  put to zero) and of the vertex part. Taking into account the necessary renormalization of the coupling constant we come to the following system of equations:

$$(8) \quad \begin{cases} a) & G_1 \rightarrow G_2 = z G_1 & b) & \Gamma_1 \rightarrow \Gamma_2 = z^{-1} \Gamma_1 \\ c) & D_1 \rightarrow D_2 = z_3 D_1 & d) & e_1 \rightarrow e_2 = z_3^{-\frac{1}{2}} e_1. \end{cases}$$

Their meaning resides in the physical equivalence of two different sets  $G_1, D_1, \Gamma_1, e_1$ , and  $G_2, D_2, \Gamma_2, e_2$ , both describing the same particles with experimental values of mass and charge.

As has been pointed out the transformations (8) are valid only for the case (3). This important fact was not duly taken into account by GELL-MANN and Low in their paper, where they proceeded from the usual form of the free photon propagation function.

For the sake of correct employment of the transformation properties (8) only the transverse form (3) will be considered in the present paper.

It should be noted that the transition from the usual form to this form of the free photon propagation function does not modify the transverse part of the photon Green's function  $D(x, x' | A)$ , while the electron function  $G(x, x' | A)$  undergoes multiplication by a « longitudinal » exponential factor<sup>(10)</sup>.

To close this section let us recall that the equations (8) are often written with the divergent constants  $Z, Z_3$  being interpreted as the relations between renormalized and unrenormalized quantities.

In such a presentation, due to DYSON, they are only of symbolic character

<sup>(9)</sup> N. N. BOGOLJUBOV and D. V. ŠIRKOV: *Usp. Fiz. Nauk*, **57**, 3 (1955).

<sup>(10)</sup> L. D. LANDAU and I. M. HALATNIKOV: *Žu. Èksper. Teor. Fiz.*, **29**, 89 (1955).

and the attempts to render them meaningful by a cut-off procedure must be carried out with great care.

It may be mentioned for instance that following POMERANČUK<sup>(11)</sup> one can render  $Z_3$  negative by a special limiting process.

This seemingly paradoxical property can also be established directly in the following way (\*).

Let us introduce two cut-offs  $\Lambda_p, \Lambda_e$  for the photon and electron momenta respectively.  $\Lambda_p$  being fixed we let  $\Lambda_e \rightarrow \infty$ , thus coming to the situation where all the relevant divergencies will arise only from the second order term of the photon self energy part.

Therefore the corresponding subtraction procedure leads to the formula

$$(9) \quad Z_3 = 1 - \frac{e^2}{3\pi} \ln \frac{\Lambda_e^2}{m^2} - e^2 C(\Lambda_p, \Lambda_e, e^2),$$

where  $C$  does not depend on  $\Lambda_e$  in the limit  $\Lambda_e \rightarrow \infty$ . Hence by giving  $\Lambda_p$  an arbitrary large value we can choose  $\Lambda_e$  so that the second term in (9) prevails.

We thus have the limiting process in which

$$Z_3 \rightarrow -\infty.$$

### 3. - Renormalization Group Equations in Quantum Electrodynamics and their Partial Solutions.

Having in mind the obtainment of functional equations of the renormalization group, let us write the propagation functions  $G$  and  $D$  in the form:

$$(10) \quad G(\kappa) = i \frac{s_1(\kappa^2)\hat{\kappa} + s_2(\kappa^2)m}{\kappa^2 - m^2},$$

$$(11) \quad D_{mn}(\kappa) = \frac{1}{i\kappa^2} \left( g^{mn} - \frac{\kappa_m \kappa_n}{\kappa^2} \right) d(\kappa^2)$$

(the vertex part  $\Gamma$  shall be considered later).

Now, the arbitrary finite constants  $z$  and  $z_3$  in the definitions of  $G$  and  $D$  can be fixed by the following conditions

$$(12) \quad d = 1, \quad s_1 = 1, \quad \text{at } \kappa^2 = \lambda^2,$$

<sup>(11)</sup> I. POMERANČUK: *Dokl. Akad. Nauk SSSR*, **103**, 1005 (1955).

(\*) See also: N. N. BOGOLJUBOV and D. V. ŠIRKOV: *Dokl. Akad. Nauk SSSR*, **105**, 685 (1955).



where  $\lambda^2 < 0$ . The considerations below may be trivially generalized also to the case  $\lambda^2 > 0$ , by dealing separately with the real parts of the Green functions in the domain  $\kappa^2 > 0$ , where these functions take on complex values. Owing to the uniformity in the momentum space the functions  $s_1$ ,  $s_2$  and  $d$  can be represented in the form

$$f\left(\frac{\kappa^2}{\lambda^2}, \frac{m^2}{\lambda^2}, e^2\right)$$

and, by the definition of  $\lambda$

$$(13) \quad s_1\left(1, \frac{m^2}{\lambda^2}, e^2\right) = d\left(1, \frac{m^2}{\lambda^2}, e^2\right) = 1.$$

It should be noted that the second of the conditions (13) is not necessary. Since, for instance,  $s_1 = s_1^0$  with  $\kappa^2 = \lambda^2$ , in further considerations the constant  $s_1^0$  becomes but an irrelevant factor.

The «normalization» momentum  $\lambda^2$  can be expressed directly in terms of the charge  $e$ . Inserting (11) into the third of eq. (8), and with due account of the fourth eq. (8), we obtain

$$(14) \quad d\left(\frac{\kappa^2}{\lambda_2^2}, \frac{m^2}{\lambda_2^2}, e_2^2\right) = z_3 d\left(\frac{\kappa^2}{\lambda_1^2}, \frac{m^2}{\lambda_1^2}, e_1^2\right),$$

while

$$(15) \quad e_2^2 = z_3^{-1} e_1^2.$$

Assuming that  $\kappa^2 = \lambda_1^2$  and with account of (13), then (14) becomes

$$z_3 = d\left(\frac{\lambda_1^2}{\lambda_2^2}, \frac{m^2}{\lambda_2^2}, e_2^2\right),$$

which gives the functional equation for  $d$

$$(16) \quad d\left(\frac{\kappa^2}{\lambda_1^2}, \frac{m^2}{\lambda_1^2}, e_1^2\right) = \frac{d(\kappa^2/\lambda_2^2, m^2/\lambda_2^2, e_2^2)}{d(\lambda_1^2/\lambda_2^2, m^2/\lambda_2^2, e_2^2)},$$

with

$$(17) \quad e_1^2 = e_2^2 d\left(\frac{\lambda_1^2}{\lambda_2^2}, \frac{m^2}{\lambda_2^2}, e_2^2\right).$$

Now, let us relate  $e^2$  in (16) and (17) to the observed value of the electronic charge  $e_0^2$ . In that case the true photon propagation function is normalized at

$\kappa^2 = 0$  and therefore has the form

$$d = d^0 \left( \frac{\kappa^2}{m^2}, e_0^2 \right).$$

Thus

$$(18) \quad e^2 = e_0^2 d \left( \frac{\lambda^2}{m^2}, e_0^2 \right).$$

Let us now consider the fermion propagation function. The calculations will be performed simultaneously both for  $s_1$  and  $s_2$  suppressing the indices 1 and 2.

After having written an equation for  $s$  similar to (14), we define  $z$ , and eliminating  $z$  we obtain a functional equation for  $s$ :

$$(19) \quad s \left( \frac{\kappa^2}{\lambda_1^2}, \frac{m^2}{\lambda_1^2}, e_1^2 \right) = s \left( 1, \frac{m^2}{\lambda_1^2}, e_1^2 \right) \frac{s(\kappa^2/\lambda_2^2, m^2/\lambda_2^2, e_2^2)}{s(\lambda_1^2/\lambda_2^2, m^2/\lambda_2^2, e_2^2)}.$$

Now we shall derive the differential equations for  $d$  and  $s$ . By introducing

$$\frac{\kappa^2}{\lambda_2^2} = x, \quad \frac{m^2}{\lambda_2^2} = y, \quad \frac{\lambda_1^2}{\lambda_2^2} = t,$$

we can express (16) and (19) as:

$$(20) \quad e^2 d(x, y, e^2) = e^2 d(t, y, e^2) d \left( \frac{x}{t}, \frac{y}{t}, e^2 d(t, y, e^2) \right)$$

$$(21) \quad \ln s(x, y, e^2) = \ln s \left( \frac{x}{t}, \frac{y}{t}, e^2 d(t, y, e^2) \right) + \\ + \ln s(t, y, e^2) - \ln s \left( 1, \frac{y}{t}, e^2 d(t, y, e^2) \right).$$

Differentiating (20) and (21) with respect to  $x$  and assuming  $t = x$  we obtain the Lie group equations

$$(22) \quad \frac{\partial e^2 d(x, y, e^2)}{\partial x} = \frac{e^2 d(x, y, e^2)}{x} \left[ \frac{\partial}{\partial \xi} d \left( \xi, \frac{y}{x}, e^2 d(x, y, e^2) \right) \right]_{\xi=1},$$

$$(23) \quad \frac{\partial \ln s(x, y, e^2)}{\partial x} = \frac{1}{x} \left[ \frac{\partial}{\partial \xi} \ln s \left( \xi, \frac{y}{x}, e^2 d(x, y, e^2) \right) \right]_{\xi=1}.$$

Formulae (22) and (23) show that to obtain expressions for  $d$  and  $s$  valid for all the values of their arguments one has only to define  $d(\kappa^2/\lambda^2, y, e^2)$  and



$s(\kappa^2/\lambda^2, y, e^2)$  in the vicinity of  $\kappa^2 = \lambda^2$ . This can be done by means of the usual perturbation theory.

The equations obtained express the fact that, owing to the existence of the renormalization group, the momentum scale can be altered with a simultaneous alteration of the charge value.

We point out that the only equation which is to be solved is equation (22) inasmuch as the function  $d$  being known,  $s$  is obtained from (23) by a simple integration

$$(24) \quad \ln \frac{s(x, y, e^2)}{s(x_0, y, e^2)} = \int_{x_0}^x \frac{dz}{z} \left[ \frac{\partial}{\partial \xi} \ln s \left( \xi, \frac{y}{z}, e^2 d(z, y, e^2) \right) \right]_{\xi=1}.$$

Note that  $e^2$  is related to the experimental charge  $e_0^2$  by means of

$$e^2 d \left( \frac{\kappa^2}{\lambda^2}, \frac{m^2}{\lambda^2}, e^2 \right) = e_0^2 d^0 \left( \frac{\kappa^2}{m^2}, e_0^2 \right),$$

which allows us to view  $e^2$  as a function of  $\lambda^2$ .

The general group equations so obtained are now employed to investigate the asymptotic region of high momenta

$$|\kappa^2| \gg m^2, \quad \kappa^2 < 0.$$

Putting  $\lambda^2 \sim \kappa^2$ , we see that in this asymptotic region the expression

$$(25) \quad e_\lambda^2 d \left( \frac{\kappa^2}{\lambda^2}, e_\lambda^2 \right) \equiv e_\lambda^2 d \left( \frac{\kappa^2}{\lambda^2}, 0, e_\lambda^2 \right),$$

approximates asymptotically the function

$$e_0^2 d^0 \left( \frac{\kappa^2}{m^2}, e_0^2 \right).$$

On the other hand, (25) is identical to

$$e_m^2 d \left( \frac{\kappa^2}{m^2}, e_m^2 \right).$$

Therefore, we have

$$e_0^2 d_{as}^0 \left( \frac{\kappa^2}{m^2}, e_0^2 \right) = e^2 d \left( \frac{\kappa^2}{m^2}, e^2 \right),$$

where

$$e^2 = e_m^2 = e_0^2 d_{as}^0(1, e_0^2)$$

and  $d_{as}^0$  stands for the asymptotical part of  $d^0$ . Quite similarly we come to see that

$$s\left(\frac{\kappa^2}{m^2}, e^2\right)$$

approximates (up to an insignificant constant factor) the asymptotic part of  $s$ .

Hence to obtain the asymptotic parts of the functions in question we may put:  $x = |\kappa^2|/m^2$  and omit  $y$ . Then we have:

$$(26) \quad a) \quad \frac{\partial e^2 d(x, e^2)}{\partial x} = \frac{e^2 d(x, e^2)}{x} \varphi\{e^2 d(x, e^2)\},$$

where

$$(27) \quad \varphi(e^2) = \left[ \frac{\partial}{\partial \xi} d(\xi, e^2) \right]_{\xi=1}$$

and

$$(28) \quad b) \quad \ln \frac{s(x, e^2)}{s(x_0, e^2)} = \int_{x_0}^x \frac{dz}{z} \left[ \frac{\partial}{\partial \xi} \ln s(\xi, e^2 d) \right]_{\xi=1}.$$

Equation (26) can be solved by the usual method of separation of variables, and we come to the equation obtained by GELL-MANN and LOW in their paper, cited above

$$(29) \quad \int_{e^2}^{e^2 d} \frac{dz}{z \cdot \varphi(z)} = \ln x.$$

Further on, introducing in the integral (28) a new variable  $z' = e^2 d$ , with due use of (26) we obtain an equation for  $s$  in the form

$$(30) \quad \ln \frac{s(x, e^2)}{s(x_0, e^2)} = \int_{e^2 d(x_0)}^{e^2 d(x)} \frac{dz'}{z' \cdot \varphi(z')} \left[ \frac{\partial}{\partial \xi} \ln s(\xi, z') \right]_{\xi=1}.$$

Now we shall make some remarks on the GELL-MANN and LOW equation in the form (29).

It is clear that, to use this equation for the actual evaluation of  $d$ , we



first have to obtain an expression for  $\varphi(z)$ . This is easily done by the help of perturbation theory. Indeed

$$d^{-1}(\xi, e^2) = 1 - \frac{e^2}{3\pi} \ln \xi - \frac{e^4}{4\pi^2} \ln \xi + \dots$$

and therefore in virtue of (27)

$$(31) \quad \frac{1}{\varphi(z)} = \frac{3\pi}{z} \left( 1 - \frac{3z}{4\pi} + a_1 z^2 + \dots \right).$$

Now it is easily seen from (29) that  $e^2 d(x)$  cannot remain small at all values of  $x$ . Indeed, for small values of  $z$  we have

$$\frac{1}{\varphi(z)} \leq \frac{3\pi}{z} (1 + c),$$

$c$  being a constant. Therefore, as long as  $e^2 d$  is small, we have the inequality

$$\ln x < 3\pi(1 + c) \int_{e^2}^{e^2 d} \frac{dz}{z^2} < 3\pi(1 + c) \int_{e^2}^{\infty} \frac{dz}{z^2} = \frac{3\pi(1 + c)}{e^2}$$

and thus the corresponding possible values of  $|\kappa^2|$  are restricted.

However, since we have at present no other information as to the behaviour of  $\varphi(z)$  but the expansion (31), we are limited to work in the region of the momentum space for which:

$$(32) \quad \frac{e^2}{3\pi} \ln \left| \frac{\kappa^2}{m^2} \right| < 1.$$

Here we can approach the problem of transforming the asymptotic form of the normal perturbation expansion to

$$(33) \quad f_0 \left( e^2 \ln \left| \frac{\kappa^2}{m^2} \right| \right) + e^2 f_1 \left( e^2 \ln \left| \frac{\kappa^2}{m^2} \right| \right) + \dots$$

Trying to solve this problem directly, we would have to sum up an infinite number of Feynman's graphs to obtain each function  $f_0, f_1, \dots$  for instance, by solving the corresponding Schwinger-Dyson integral equation. Precisely this method was used in (2) to calculate  $f_0$  for the main propagation functions. On the other hand, the group equations obtained above enable us to solve this problem directly (for the domain (32)).

Inserting (31) into (29) we have

$$1 - d^{-1} + \frac{3}{4\pi} e^2 \ln d^{-1} + a_1 e^4 (d-1) + \dots = \frac{e^2}{3\pi} \ln x$$

and the required expansion follows immediately

$$(34) \quad d^{-1}(x, e^2) = 1 - \frac{e^2}{3\pi} \ln x + \frac{3}{4\pi} e^2 \ln \left( 1 - \frac{e^2}{3\pi} \ln x \right) + e^4 \dots$$

Expansions of the type (33) for the asymptotic parts of  $s_1$  and  $s_2$  defining the electron Green's functions, can be obtained in quite similar way. Making use of the eq. (30) and of the usual perturbation series

$$(35) \quad \begin{cases} s_1(x, e^2) = 1 + ce^4 \ln x + \dots \\ s_2(x, e^2) = s_2^0 \left[ 1 - \frac{3e^2}{4\pi} \ln x + \frac{e^4}{\pi^2} (\alpha_1 \ln^2 x + \alpha_2 \ln x) + \dots \right] \end{cases}$$

( $c, s_2^0, \alpha_1, \alpha_2$  being numbers)

we obtain easily

$$(36) \quad \begin{cases} \ln s_1(x, e^2) = 3\pi ce^2(d-1) \\ \ln \frac{s_2(x, e^2)}{s_2(1, e^2)} = \frac{9}{4} \ln d^{-1} + \frac{3}{\pi} e^2 \left( \frac{9}{16} + \alpha_2 \right) (d-1). \end{cases}$$

To get the required representations of the type (33) for  $s_1$  and  $s_2$  we have only to insert (34) into (36).

Restricting ourselves to the leading terms we arrive to the relations obtained in (2).

It is to be emphasized that formulae (35) were obtained by perturbation theory using the purely transversal photon causal function (3). It is easily seen, that had we made use of the usual photon pairing (4) instead of (3), we would have come to results not coinciding with the correct asymptotic expressions<sup>(2)</sup>. In fact, as we have mentioned before, this contradiction had been met by GELL-MANN and Low who had employed the usual photon pairing (4).

As it is seen, the method presented does not call for summing the infinite systems of Feynman's graphs. To obtain the terms of the series (33) up to the term of the  $2n^{\text{th}}$  order in  $e$ , it is sufficient to get the usual renormalized perturbation formulae of the order  $(2n+2)e^{2n+2}$ . Their reduction to the form (33) is performed by purely algebraical manipulation.

Heretofore we have employed the general Lie equations only to obtain the



asymptotic behaviour of propagation functions in the high momenta region. It should be emphasized that the significance of these equations is not at all exhausted by such employment.

Let us consider for instance the case  $\kappa^0 \sim m^2$ , when the electron Green's function has a singularity. The function  $d$  being regular in this region, we shall place our interest only in  $s_1$  and  $s_2$ . For the sake of convenience we present them in the following form:

$$(37) \quad s\left(\frac{\kappa^2}{\lambda^2}, \frac{m^2}{\lambda^2}, e^2\right) = S\left(\frac{\kappa^2 - m^2}{\lambda^2 - m^2}, \frac{\lambda^2 - m^2}{m^2}, e^2\right).$$

Now we turn back to (24) and assume that  $y = 1$ . Using (37) we find:

$$(38) \quad \ln \frac{s(\kappa^2/m^2, e^2)}{s(\kappa_0^2/m^2, e^2)} = \int_{\frac{\kappa_0^2}{m^2}}^{\frac{\kappa^2}{m^2}} \frac{dx}{x-1} \left[ \frac{\partial}{\partial \xi} \ln S\left(\xi, x-1, e^2 d(x, 1, e^2)\right) \right]_{\xi=1}.$$

This calls for such choice of the integration limits as to keep outside of the pole  $x = 1$ .

With this in view, assume:

$$\frac{\kappa^2}{m^2} > 1, \quad \frac{\kappa_0^2}{m^2} > 1$$

or

$$\frac{\kappa^2}{m^2} < 1, \quad \frac{\kappa_0^2}{m^2} < 1.$$

Apparently, to use (38) for the actual evaluation of  $s$ , we have to know the behaviour of the function

$$S(\xi, x-1, e^2)$$

only in the infinitesimal vicinity of its « point of normalization »

$$\xi = \frac{\kappa^2}{\lambda^2} - \frac{m^2}{m^2} = 1.$$

Therefore to obtain the expression in brackets of formula (38) we can make use again of the perturbation theory.

Taking the second approximation for  $s_1$  and  $s_2$ , after a simple calculation <sup>(12)</sup>

<sup>(12)</sup> See N. N. BOGOLJUBOV and D. V. ŠIRKOV: *Dokl. Akad. Nauk SSSR*, **103**, 391 (1955).

we arrive to

$$(39) \quad \frac{s_1(x, 1, e^2)}{s_1(x_0, 1, e^2)} = (|x-1|)^{-3e^2/2\pi x} (|x_0-1|)^{3e^2/2\pi x_0},$$

$$(40) \quad \frac{s_2(x, 1, e^2)}{s_2(x_0, 1, e^2)} = (|x-1|)^{-(3e^2/4\pi)(1+x/x)} (|x_0-1|)^{(3e^2/4\pi)(1+x_0/x_0)}.$$

Hence, with  $\kappa^2 \rightarrow m^2$  the functions  $s_1$  and  $s_2$  have the known infrared singularity

$$(41) \quad s_1, s_2 \sim \left( \left| \frac{\kappa^2 - m^2}{m^2} \right| \right)^{-3e^2/2\pi}.$$

Now we turn to the vertex part. Consider, for instance, the vertex part  $\Gamma$  with two electron and one photon lines. According to (8) we have the transformation law of  $\Gamma$  under the multiplicative renormalization group

$$(42) \quad \Gamma \rightarrow \Gamma' = z^{-1} \Gamma$$

and

$$(43) \quad s'_1 = z s_1.$$

On the other hand, « $\lambda$ -normalization» being assumed, for the sake of uniformity it must have, in the momentum space, the form

$$\Gamma_\lambda = \Gamma\left(\frac{\kappa}{\lambda}, \frac{\kappa-q}{\lambda}, \frac{m}{\lambda}, e_\lambda^2\right).$$

Hence from (42) and (43) we get

$$(44) \quad \Gamma\left(\frac{\kappa}{\lambda_2}, \frac{\kappa-q}{\lambda_2}, \frac{m}{\lambda_2}, e_2^2\right) s_1\left(\frac{\lambda_1^2}{\lambda_2^2}, \frac{m^2}{\lambda_2^2}, e_2^2\right) = \Gamma\left(\frac{\kappa}{\lambda_1}, \frac{\kappa-q}{\lambda_1}, \frac{m}{\lambda_1}, e_1^2\right) s_1\left(1, \frac{m^2}{\lambda_1^2}, e_1^2\right)$$

where

$$e_1^2 = e_2^2 d\left(\frac{\lambda_1^2}{\lambda_2^2}, \frac{m^2}{\lambda_2^2}, e_2^2\right).$$

This relation enables us to reduce the study of  $\Gamma$  at arbitrary values of  $|\kappa/\lambda|$ ,  $|(\kappa-q)/\lambda|$ ,  $|q/\lambda|$  to the case when the greatest of their values is of the order of unity, with the assumption that  $\lambda^2$  is of the order of the largest of  $|\kappa^2|$ ,  $|(\kappa-q)^2|$ ,  $|q^2|$ .



#### 4. — Renormalization Group Equations in Pseudoscalar Meson Theory.

The renormalization group method can be employed in any renormalizable meson theory. Consider, for example, the pseudoscalar meson theory with pseudoscalar coupling. The essential difference between this case and spinor electrodynamics lies in the fact, that here we have two kinds of charges. The point is, that to remove all the infinities we have to introduce, besides all the counter-terms corresponding to those in electrodynamics, an extra-term, the so-called « fourmesonic » counter-term  $H\varphi^4$ . The divergent part of the coefficient  $H$  is defined by the subtraction procedure, but with a certain ambiguity in the finite part. Hence the theory contains in fact not only one mesonic charge  $g$  but another finite constant, say  $h$  <sup>(13)</sup>. Consequently the initial interaction lagrangian should be presented in the form (\*)

$$(45) \quad L = \sqrt{4\pi} \cdot g \bar{\psi} \gamma^5 \psi \varphi + h \varphi^4.$$

Writing down the multiplicative counter-terms in the following form:

$$(46) \quad (Z_1 - 1) \sqrt{4\pi} \cdot g \bar{\psi} \gamma^5 \psi \varphi + (Z_2 - 1) \bar{\psi} (\hat{\kappa} - M) \psi + \\ + (Z_3 - 1) \varphi (\kappa^2 - m^2) \varphi + (Z_4 - 1) h \varphi^4$$

and introducing the nucleon propagator  $G(\kappa)$ , the meson propagator  $D(\kappa)$ , the 3-vertex part  $\Gamma^5(\kappa, q)$  and the 4-vertex part  $\square(\kappa, q, p)$

$$(47) \quad \begin{cases} G(\kappa) = i \frac{\hat{\kappa} s(\kappa^2) + M s'(\kappa^2)}{\kappa^2 - M^2}, & D(\kappa) = \frac{i d(\kappa^2)}{\kappa^2 - m^2}, \\ \Gamma^5(\kappa, 0) = \gamma^5 \Gamma(\kappa^2), & \square(\kappa, 0, 0) = \square(\kappa^2), \end{cases}$$

we obtain the renormalization group equations

$$(48) \quad \begin{cases} s_1 \rightarrow s_2 = z_2 s_1, & \Gamma_1 \rightarrow \Gamma_2 = z_1^{-1} \Gamma_1, & g_1 \rightarrow g_2 = z_1 z_2^{-1} z_3^{-1} g_1, \\ d_1 \rightarrow d_2 = z_3 d_1, & \square_1 \rightarrow \square_2 = z_4^{-1} \square_1, & h_1 \rightarrow h_2 = z_4 z_3^{-2} h_1, \end{cases}$$

with  $z_1, \dots, z_4$  being arbitrary finite constants.

<sup>(13)</sup> This circumstance has been emphasized also by G. BONNEVAY: *Compt. Rend.* **238**, 1641 (1954).

(\*) To simplify the notation we omit the isotopic spin matrices  $\tau$ , and view  $q$  as real. However, this does not produce any effect upon the group equations obtained below.

Equations (48) serve to show that with the introduction of the functions

$$(49) \quad \delta(\kappa^2) = s^2 \Gamma^2 d, \quad \varphi(\kappa^2) = d^2 \square,$$

their transformation laws will be

$$(50) \quad g_1^2 \delta_1 = g_2^2 \delta_2, \quad h_1 \varphi_1 = h_2 \varphi_2.$$

The inspection of the corresponding graphs brings to light that the function  $\delta$  has the role of an effective interaction between two nucleons, while  $\varphi$  corresponds to interactions between two mesons.

Through proper employment of the uniformity in the momentum space and through «  $\lambda$ -normalization »

$$(51) \quad \delta\left(\frac{\kappa^2}{\lambda^2}, \frac{m^2}{\lambda^2}, \frac{M^2}{\lambda^2}, g^2, h\right) \Big|_{\kappa^2=\lambda^2} = \varphi\left(\frac{\kappa^2}{\lambda^2}, \frac{m^2}{\lambda^2}, \frac{M^2}{\lambda^2}, g^2, h\right) \Big|_{\kappa^2=\lambda^2} = 1,$$

we arrive to the following system of functional equations

$$(52) \quad \delta(x, y, Y, g^2, h) = \delta(t, y, Y, g^2, h) \delta\left(\frac{x}{t}, \frac{y}{t}, \frac{Y}{t}, g_1^2, h_1\right),$$

$$(53) \quad \varphi(x, y, Y, g^2, h) = \varphi(t, y, Y, g^2, h) \varphi\left(\frac{x}{t}, \frac{y}{t}, \frac{Y}{t}, g_1^2, h_1\right),$$

$$(54) \quad \Delta(x, y, Y, g^2, h) \Delta\left(1, \frac{y}{t}, \frac{Y}{t}, g_1^2, h_1\right) = \Delta(t, y, Y, g^2, h) \Delta\left(\frac{x}{t}, \frac{y}{t}, \frac{Y}{t}, g_1^2, h_1\right),$$

where  $\Delta$  stands for any of  $s, \Gamma, d, \square$  and

$$(55) \quad \begin{cases} x = \frac{\kappa^2}{\lambda^2}, & y = \frac{m^2}{\lambda^2}, & Y = \frac{M^2}{\lambda^2}, & t = \frac{\lambda_1^2}{\lambda^2}, \\ g_1^2 = g^2 \delta(t, y, Y, g^2, h), & h_1 = h \varphi(t, y, Y, g^2, h). \end{cases}$$

Equations (52)-(55) express the fact that owing to the existence of the re-normalization group, the alteration of the scale of masses and momenta is possible with simultaneous alteration of the values of the mesonic charges  $g$  and  $h$ .

As to the relation between the constants  $g$  and  $h$  in these equations and their experimental values, note that in the meson theory, as distinct from electrodynamics with a single charge  $g$ , so far there has not been found a method for unique determination of their value by various experiments<sup>(15)</sup>. Evidently this may be due to the fact that really there are two charges  $g$  and  $h$  in the meson theory and their values should be obtained by experimental data.

<sup>(15)</sup> This fact was pointed out by G. KÄLLÉN: *Nuovo Cimento*, **12**, 217 (1954).



Differentiating (52), (53) and the logarithm of (54) with respect to  $x$  and assuming  $t = x$  we obtain the Lie differential equations of the meson two-charge theory

$$(56) \quad \frac{\partial \delta(x, y, Y, g^2, h)}{\partial x} = \frac{\delta(x, y, Y, g^2, h)}{x} \Psi\left(\frac{y}{x}, \frac{Y}{x}, g^2 \delta, h \varphi\right),$$

$$(57) \quad \frac{\partial \varphi(x, y, Y, g^2, h)}{\partial x} = \frac{\varphi(x, y, Y, g^2, h)}{x} \Phi\left(\frac{y}{x}, \frac{Y}{x}, g^2 \delta, h \varphi\right),$$

$$(58) \quad \frac{\partial \ln \Delta(x, y, Y, g^2, h)}{\partial x} = \frac{1}{x} \left[ \frac{\partial}{\partial \xi} \ln \Delta\left(\xi, \frac{y}{x}, \frac{Y}{x}, g^2 \delta, h \varphi\right) \right]_{\xi=1}.$$

Here  $\Psi$  and  $\Phi$  being obtained by

$$(59) \quad \Psi(y, Y, g^2, h) = \left[ \frac{\partial}{\partial \xi} \delta(\xi, y, Y, g^2, h) \right]_{\xi=1},$$

$$(60) \quad \Phi(y, Y, g^2, h) = \left[ \frac{\partial}{\partial \xi} \varphi(\xi, y, Y, g^2, h) \right]_{\xi=1}.$$

Thus the problem is reduced to consider the system of two equations (56) and (57): when the functions  $\delta$  and  $\varphi$  are known, all the other functions  $\Delta$  can be determined from (58) by quadrature

$$(61) \quad \ln \frac{\Delta(x, y, Y, g^2, h)}{\Delta(x_0, y, Y, g^2, h)} = \int_{x_0}^x \frac{dz}{z} \left[ \frac{\partial}{\partial \xi} \ln \Delta\left(\xi, \frac{y}{z}, \frac{Y}{z}, g^2 \delta(z, y, Y, g^2, h), h \varphi(z, y, Y, g^2, h)\right) \right]_{\xi=1}.$$

These group equations are applied now to the high momenta region, with

$$(62) \quad |\kappa^2| \gg M^2 > m^2.$$

Assuming the normalization momentum  $\lambda^2$  much greater than  $M^2$ , we see that the limiting case corresponding to (62) is achieved in (56)–(61) assuming  $y = 0$ ,  $Y = 0$ . With the abbreviations

$$(63) \quad g^2 \delta(x, g^2, h) = \sigma(z, g^2, h),$$

$$(64) \quad h \varphi(x, g^2, h) = \varrho(z, g^2, h),$$

$$(65) \quad z = \ln x,$$

we find instead of (56), (57)

$$(66) \quad \frac{d\sigma}{dz} = \sigma \Psi(\sigma, \varrho),$$

$$(67) \quad \frac{d\rho}{dz} = \rho \Phi(\sigma, \rho),$$

where

$$(68) \quad \Psi(\sigma, \rho) = \left[ \frac{\partial}{\partial \xi} \delta(\xi, \sigma, \rho) \right]_{\xi=1},$$

$$(69) \quad \Phi(\sigma, \rho) = \left[ \frac{\partial}{\partial \xi} \varphi(\xi, \sigma, \rho) \right]_{\xi=1}$$

and

$$(70) \quad \ln \frac{A(x, g^2, h)}{A(x_0, g^2, h)} = \int_{\ln x_0}^{\ln x} dz \left\{ \frac{\partial}{\partial \xi} \ln A(\xi, \sigma(z, g^2, h), \rho(z, g^2, h)) \right\}_{\xi=1}.$$

Dividing (66) by (67) we eliminate the variable  $z$

$$(71) \quad \frac{d\rho}{d\sigma} = \frac{\rho \Phi(\sigma, \rho)}{\sigma \Psi(\sigma, \rho)}.$$

The last equation can be easily analyzed in the weak coupling case, when the constants  $g^2$  and  $h$  are small compared to unity.

In that case one can obtain the power series for  $\Phi$  and  $\Psi$  by the usual perturbation theory. With the aid of the lowest order graphs we find that the first terms of these series have the form

$$(72) \quad \Psi(\sigma, \rho) = \psi_1 \sigma + \psi_2 \sigma^2 + \psi_3 \sigma \rho + \psi_4 \rho^2 + \dots,$$

$$(73) \quad \rho \Phi(\sigma, \rho) = \varphi_1 \sigma^2 + \varphi_2 \sigma \rho + \varphi_3 \rho^2 + \varphi_4 \sigma \rho^2 + \dots,$$

$\psi_1, \psi_2, \dots, \varphi_1, \varphi_2, \dots$ , being numerical coefficients.

From the form of expansions (72) and (73) it immediately appears that in the vicinity of the point  $\sigma = 0$  equation (71) has two special solutions of the form

$$(74) \quad \rho(\sigma) = a_1 \sigma + a_2 \sigma^2 + \dots,$$

the coefficients  $a_1, a_2$  being the roots of the quadratic equation

$$(75) \quad \varphi_3 a_1^2 + (\varphi_2 - \psi_1) a_1 + \varphi_1 = 0.$$

Substituting (74) into (72) and into (66) we see that in the case of the special solutions (74), the leading term of (66) has the same form as at  $h = 0$

$$(76) \quad \frac{d\sigma}{dz} = \psi_1 \sigma^2 + \dots$$



For the purpose of illustration we solve (76), and obtain the asymptotic expressions of  $s$ ,  $d$ ,  $\Gamma$  and  $\square$  for the neutral pseudoscalar theory. In this case  $\psi_1 = -5/4\pi$ ; integrating (76) we find

$$(77) \quad \sigma(z, g^2, h) = g^2 \delta(x, g^2, h) = \frac{g^2}{1 - (5/4\pi)g^2 \ln x}.$$

Employing this relations for the determination of  $s$ ,  $d$ ,  $\Gamma$  and  $\square$  with the aid of lowest order perturbation calculations we find <sup>(16)</sup>

$$(78) \quad s(x, g^2) = \left(1 - \frac{5}{4\pi} g^2 \ln x\right)^{-\frac{1}{10}},$$

$$(79) \quad d(x, g^2) = \left(1 - \frac{5}{4\pi} g^2 \ln x\right)^{-\frac{2}{5}},$$

$$(80) \quad \Gamma(x, g^2) = \left(1 - \frac{5}{4\pi} g^2 \ln x\right)^{-\frac{1}{5}},$$

$$(81) \quad \square(x, g^2) \sim \left(1 - \frac{5}{4\pi} g^2 \ln x\right)^{-\frac{1}{5}}.$$

From (77) follows that, as in electrodynamics, the function  $\sigma = g^2 \delta$  becomes of the order of unity even for small  $g^2$ , if the momentum is large enough. We are thus led beyond the limits of the weak coupling case.

Now we turn to general solutions of (71). In the phase plane  $(\sigma, \varrho)$  it is easily seen that solutions which do not pass through the singular point  $\sigma = 0$ ,  $\varrho = 0$  bring us to finite values of  $\varrho$  in the vicinity of the point  $\sigma = 0$  and hence the perturbation approach breaks down in these cases, even when the momenta are yet relatively small.

<sup>(16)</sup> Formulae (78), (79), (80) coincide with the results of A. D. GALANIN, B. L. IOFFE and I. JA. POMERANČUK: *Žu. Eksper. Teor. Fiz.*, **29**, 51 (1955).

#### RIASSUNTO (\*)

Si ottengono delle equazioni differenziali di Lie per il gruppo moltiplicativo di rinormalizzazione della carica nell'elettrodinamica quantistica e nella teoria mesonica pseudo-scalare con due costanti d'accoppiamento. Coll'impiego di queste equazioni si sono trovate le espressioni asintotiche per le funzioni elettrodinamiche di propagazione nell'« ultravioletto » e nell'« infrarosso ». Si discute inoltre per il caso di accoppiamento debole il comportamento asintotico dei momenti elevati delle funzioni di propagazione della teoria mesonica.

(\*) Traduzione a cura della Redazione.

## Polarization of Nucleons from Photonuclear Reactions.

W. CZYZ

*Physical Institute, Jagiellonian University - Kraków (Poland)*

J. SAWICKI

*Institute of Theoretical Physics, University of Warsaw - Warsaw (Poland)*

(ricevuto il 21 Dicembre 1955)

**Summary.** — A method is given to calculate the polarization of nucleons produced in photonuclear reactions if the photonucleon is assumed to interact with the residual nucleus through a potential containing in general a spin-orbit coupling. The method is applied to the  ${}^9\text{Be}(\gamma, n){}^8\text{Be}$  reaction where for the  ${}^9\text{Be}$  nucleus the one particle model is assumed with the central interactions of GUTH and MULLIN. The maximum polarization  $P_{\max} \sim 45\%$  results for  $\hbar\omega = 2\text{ MeV}$  at the scattering angle  $\theta \sim 45^\circ$ . The dependance of  $P$  on  $\theta$  is shown graphically for some energies  $\hbar\omega$  near the threshold of the reaction. The polarization of photonucleons from a nucleus being in a  $S_{\frac{1}{2}}$  ground state is discussed. Further applications of the method and the results are indicated.

In the recent years many authors have investigated the polarization of nucleons elastically scattered from nuclei or produced in some nuclear reactions of the stripping type. The aim of the present paper is to give a method of calculation of the degree of polarization of nucleons produced in photonuclear reactions with some applications.

On applying the time dependent theory of perturbations to the calculation of the cross-section for photodisintegration <sup>(1,2)</sup> we represent the wave function of the system: photonucleon-final nucleus  $\Psi(\mathbf{r}, t)$  as a superposition of the stationary energy eigenfunctions.

---

<sup>(1)</sup> H. A. BETHE: *Handbuch der Physik*.

<sup>(2)</sup> H. A. BETHE: *Ann. der Phys.*, **4**, 443 (1930).



Let the photonucleon interact with the final nucleus through a potential containing in general a spin-orbit term. Then the operators  $\hat{Y}^2$ ,  $\hat{L}^2$ ,  $\hat{M}_J$ ,  $\hat{\sigma}^2$  (where  $\hat{Y}^2$  is the square of the total angular momentum,  $\hat{L}^2$  the square of the orbital angular momentum,  $\hat{M}_J$  the projection of the total angular momentum and  $\hat{\sigma}^2$  the square of the spin) are constants of the motion. The energy eigenfunctions  $\Psi_E(L, J, M_J)$  are then simultaneous eigenfunctions of these operators. Thus we may write

$$(1) \quad \Psi(\mathbf{r}, t) = \left( \sum_{E'} + \int dE' \right) \left\{ \sum_{L, J, M_J} a_{E'}(L, J, M_J; t) \cdot R_{LJ}(E') Y(L, J, M_J) \exp \left[ -i \frac{E' t}{\hbar} \right] \right\},$$

where  $R_{LJ}(E')$  is a function of  $r$  and the total angular momentum eigenfunction  $Y(L, J, M_J)$  depends on  $\vartheta$ ,  $\varphi$  and  $\sigma_n$ . In view of the asymptotical form of  $R_{LJ}(E') \sim r^{-1} \sin(kr - \frac{1}{2}L\pi + \eta_{LJ})$  (\*) in analogy to ref. (2) only the outgoing wave is obtained; the integration over  $E'$  destroys the ingoing wave in the asymptotical form of  $\Psi(\mathbf{r}, t)$ :

$$(2) \quad \Psi(\mathbf{r}, t) \sim r^{-1} \exp \left[ ikr - i \frac{Et}{\hbar} \right] N(E) \sum_{L, J, M_J} \exp[i(\eta_{LJ} - \frac{1}{2}L\pi)] Y(L, J, M_J) H'^{L, J, M_J}_{l, j, m_j},$$

where  $N(E)$  is a factor dependent only on energy and  $H'^{L, J, M_J}_{l, j, m_j} = \int R_{LJ}^*(E) \cdot Y^*(L, J, M_J) H'(R_{l_j}(E) Y(l, j, m_j))$ ,  $H'$  being the interaction of the nucleon with the electromagnetic field,  $R_{l_j}(E) Y(l, j, m_j)$  and  $R_{LJ}(E) Y(L, J, M_J)$  are single particle model wave functions of the initial and final states.

The polarization vector is  $\mathbf{P} = \{ \langle f\chi | \boldsymbol{\sigma}_n | f\chi \rangle \}_{\text{av}} / \{ \langle f\chi | f\chi \rangle \}_{\text{av}}$ , where  $f\chi$  is the scattering amplitude obtained from (2) and equal to  $f_{\frac{1}{2}\frac{1}{2}}\chi_{\frac{1}{2}}(\sigma_n) + f_{\frac{1}{2}\frac{-1}{2}}\chi_{-\frac{1}{2}}(\sigma_n)$ :

$$\begin{aligned} \Psi(\mathbf{r}, t) &\sim r^{-1} \exp \left[ ikr - i \frac{Et}{\hbar} \right] N(E) \cdot f\chi = \\ &= r^{-1} \exp \left[ ikr - i \frac{Et}{\hbar} \right] N(E) [f_{\frac{1}{2}\frac{1}{2}}\chi_{\frac{1}{2}}(\sigma_n) + f_{\frac{1}{2}\frac{-1}{2}}\chi_{-\frac{1}{2}}(\sigma_n)], \end{aligned}$$

$\chi_{\mu_n}(\sigma_n)$  is the spin function of the ejected nucleon of the spin number  $\mu_n$  and

$$(3) \quad f_{\mu_n} = \sum_{L, J, M_J} i^{-L} \exp[i\eta_{LJ}] C_{L\frac{1}{2}}(J, M_J; M_J - \mu_n, \mu_n) Y_{L, M_J - \mu_n}(\bar{\vartheta}, \bar{\varphi}) H'^{L, J, M_J}_{l, j, m_j} \dots,$$

where  $C_{L\frac{1}{2}}(J, M_J; M_J - \mu_n, \mu_n)$  is a Clebsch-Gordan coefficient;  $Y_{L, M_J - \mu_n}(\alpha, \beta)$  is a spherical harmonic and  $\bar{\vartheta}, \bar{\varphi}$  are the polar angles of the vector  $\mathbf{k}$  of the out-

(\*) It is valid for neutrons, the generalization for protons is straightforward.

going neutron; the symbol  $\{\}_{\text{av}}$  denotes averaging over the directions of the  $\gamma$  quantum polarization and magnetic quantum numbers of the initial nucleus.

We shall confine ourselves to the electric dipole approximation. Then  $H'$  is proportional to  $\mathbf{e} \cdot \mathbf{r} = r \cos \alpha$  where  $\mathbf{e}$  is the polarization vector of the incident photon. The system of reference is chosen so that the  $xy$  plane is identical with the reaction plane and the  $z$  axis with the direction of the vector  $\mathbf{k} \times \mathbf{k}_0$ , where  $\mathbf{k}_0$  is the wave vector of the photon.

Then

$$(4) \quad \mathbf{e} \cdot \mathbf{r} = r \cos \alpha = r(\cos \vartheta \cos \Phi + \sin \vartheta \sin \Phi \cos \varphi) = z \cos \Phi + x \sin \Phi.$$

The meaning of all the angles involved is indicated in Fig. 1. With the quantization axis chosen ( $\bar{\vartheta} = \pi/2$ ,  $\bar{\varphi} = (\pi/2) - \theta$ , where  $\theta$  is the scattering angle, see Fig. 1) it may be easily verified that  $P_x$  and  $P_y$  vanish. The degree of polarization is

$$(5) \quad P = P_z = \frac{\{|f_{+\frac{1}{2}}|^2 - |f_{-\frac{1}{2}}|^2\}_{\text{av}}}{\{|f_{+\frac{1}{2}}|^2 + |f_{-\frac{1}{2}}|^2\}_{\text{av}}}.$$

In our case we may write

$$(6) \quad f_{\mu_n} = f_{\mu_n}^z \cos \Phi + f_{\mu_n}^x \sin \Phi.$$

On averaging over the directions of the photon polarization we have

$$(7) \quad \{|f_{\mu_n}|^2\}_{\text{av}} = \frac{1}{2(2j+1)} \sum_{m_j=-j}^j (|f_{\mu_n}^z|^2 + |f_{\mu_n}^x|^2).$$

Since the  $|f_{\mu_n}^x|^2$  give zero contribution to the numerator of the expression for  $P$ , the polarization becomes

$$(8) \quad P = \frac{\sum_{m_j=-j}^j (|f_{+\frac{1}{2}}^z|^2 - |f_{-\frac{1}{2}}^z|^2)}{\sum_{\mu_n} \sum_{m_j} (|f_{\mu_n}^z|^2 + |f_{\mu_n}^x|^2)}.$$

At first this method may be applied to the calculation of the polarization of low and medium energy  $(^+)$  photoneutrons from the  $^9\text{Be}(\gamma, n)^8\text{Be}$  reaction. The one particle model of Guth and Mullin  $(^3)$  may be assumed for the  $^9\text{Be}$  nucleus its ground state being  $P_{\frac{3}{2}}$ . The final neutron is now assumed to interact with the residual core through the potential containing a spin-orbit coupling.

$(^+)$  I. e. the quantum energy in the range of validity of the model used.

$(^3)$  E. GUTH and C. MULLIN: *Phys. Rev.*, **76**, 234 (1949).

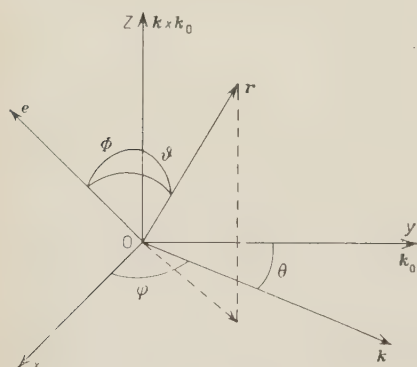


Fig. 1.

After calculating all the coefficients, angular integrals and performing the summations in eq. (8) we may express  $P$  in terms of the radial integrals  $R_J$  appearing in  $H'_{l,j,m_j}^{L,J,M_J}$  in the form

$$(9) \quad P = \frac{i[AB^* - A^*B + \frac{1}{2}(C^*D - CD^*)] \sin 2\theta}{I + (AA^* + B\bar{B}^*) + \frac{1}{3}(CC^* + D\bar{D}^*) + [AB^* + A^*B + \frac{1}{3}(CD^* - C^*D)] \cos 2\theta}$$

where:

$$\begin{aligned} A &= R_{\frac{1}{2}} - \frac{1}{5} R_{\frac{3}{2}} - \frac{3}{10} R_{\frac{5}{2}}, & B &= \frac{3}{2} R_{\frac{3}{2}}, \\ C &= R_{\frac{1}{2}} + \frac{5}{2} R_{\frac{3}{2}} - \frac{9}{10} R_{\frac{5}{2}}, & D &= \frac{3}{5} R_{\frac{3}{2}} + \frac{9}{10} R_{\frac{5}{2}}, \\ R_J &= \exp[i\eta_{LJ}] \int_0^\infty R_{LJ}^* R_{1\frac{1}{2}} r^3 dr. \end{aligned}$$

If the spin-orbit coupling is equal zero then  $R_{\frac{3}{2}} = R_{\frac{5}{2}}$  and  $A = C$ ,  $B = D$ . This is in the case of the interactions of Guth and Mullin (square well depths are  $V_{1\frac{1}{2}} = 12.16$  MeV,  $V_{0\frac{1}{2}} = V_{2\frac{1}{2}} = V_{2\frac{3}{2}} = 3$  MeV). In this case

$$(10) \quad P = \frac{2R_{PS}R_{PD} \sin(\eta_2 - \eta_0) \sin 2\theta}{[\frac{4}{3}R_{PS}^2 + \frac{7}{3}R_{PD}^2 + \frac{2}{3}R_{PS}R_{PD} \cos(\eta_2 - \eta_0)] + [-R_{PD}^2 + 2R_{PS}R_{PD} \cos(\eta_2 - \eta_0)] \cos 2\theta},$$

where  $\eta_0$ ,  $\eta_2$  are the  $S$  and  $D$  state phaseshifts defined in ref. (3) and

$$R_{PS} = \int_0^\infty R_{0\frac{1}{2}}^* R_{1\frac{1}{2}} r^3 dr, \quad R_{PD} = \int_0^\infty R_{2\frac{3}{2}}^* R_{1\frac{1}{2}} r^3 dr = \int_0^\infty R_{2\frac{5}{2}}^* R_{1\frac{1}{2}} r^3 dr.$$

$P$  was calculated for some energies of the incident  $\gamma$  quantum  $\hbar\omega$  close above the threshold of the reaction = 1.6 MeV. For these energies the dependance of  $P$  (in %) on  $\theta$  is shown graphically in Fig. 2. The maximum  $P$  is considerable only in the energy range for which both  $R_{PS}$  and  $R_{PD}$  are simultaneously considerable that is in a width of about 1 MeV near the threshold of the reaction.

For larger energies  $\hbar\omega$   $P$  is negligible. From Fig. 2 it is seen that  $P_{\max} (\sim 45\%$  for  $\hbar\omega = 2$  MeV) comes in near  $\theta = 45^\circ$ .

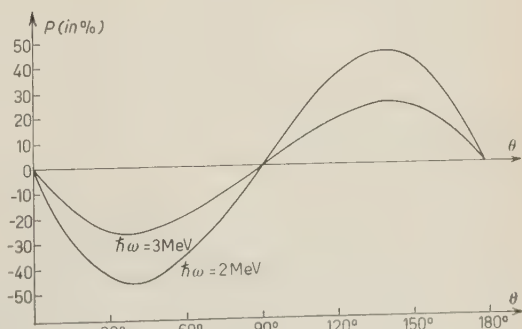


Fig. 2.



It is interesting here that  $P \neq 0$  comes in for the central interactions  $V_{LJ}$ . But if the initial state of some nucleus is  $S_{\frac{1}{2}}$ , we obtain for an interaction with the spin-orbit coupling the polarization:

$$(11) \quad P = \frac{i[FG^* - F^*G] \sin 2\theta}{Z + (FF^* + GG^*) + (FG^* + F^*G) \cos 2\theta},$$

where

$$F = -\bar{R}_{\frac{3}{2}} - 2\bar{R}_{\frac{1}{2}}, \quad G = 3\bar{R}_{\frac{3}{2}}, \quad Z = 4|\bar{R}_{\frac{3}{2}} - \bar{R}_{\frac{1}{2}}|,$$

$$\bar{R}_J = \exp[i\eta_{LJ}] \int_0^\infty R_{LJ}^* R_{0\frac{1}{2}} r^3 dr.$$

This result may be applied to the calculation of polarization of photo-neutrons from deuterium and in particular to the examination of the  $L \cdot \vec{\sigma}$  coupling as proposed by CASE and PAIS <sup>(4)</sup> and used by AUSTERN <sup>(5)</sup>.

From eq. (12) it follows that if the spin-orbit coupling vanishes ( $\bar{R}_{\frac{3}{2}} = \bar{R}_{\frac{1}{2}}$ ) then  $P = 0$ .

The experimental investigation of  $P$  seems to be important because it might give valuable informations concerning the types of interactions for some simple nuclei as  $^2\text{H}$ ,  $^6\text{Li}$ ,  $^7\text{Li}$ ,  $^9\text{Be}$ , for which two body models may be applied. We hope to develop the method for the assumption that the outgoing nucleon interacts with the residual core through the «clouded crystal ball» potential of FESHBACH *et al.* <sup>(6)</sup> modified by ADAIR *et al.* <sup>(7)</sup> by an additional spin-orbit term.

\* \* \*

We wish to thank Professors L. INFELD and H. NIEWODNICZAŃSKI for their kind interest.

<sup>(4)</sup> K. M. CASE and A. PAIS: *Phys. Rev.*, **80**, 203 (1950).

<sup>(5)</sup> N. AUSTERN: *Phys. Rev.*, **85**, 283 (1952).

<sup>(6)</sup> H. FESHBACH, C. E. PORTER and V. F. WEISSKOPF: *Phys. Rev.*, **96**, 448 (1954).

<sup>(7)</sup> P. ADAIR, P. FIELDS and C. DARDEN: *Phys. Rev.*, **96**, 503 (1954).

## RIASSUNTO (\*)

Si dà un metodo per calcolare la polarizzazione dei nucleoni prodotti nelle reazioni fotonucleari se si assume che il fotonucleone interagisca col nucleo residuo per mezzo di un potenziale contenente generalmente un accoppiamento spin-orbita. Si applica il metodo alla reazione  ${}^9\text{Be}(\gamma, n){}^8\text{Be}$ , dove per il nucleo  ${}^9\text{Be}$  si assume il modello a particella singola con le interazioni centrali di Guth e Mullin. La massima polarizzazione  $P_{\text{max}} \sim 45\%$  risulta per  $\hbar\omega = 2\text{ MeV}$  con l'angolo di scattering  $\theta \sim 45^\circ$ . Si mostra graficamente la dipendenza di  $P$  da  $\theta$  per alcune energie  $\hbar\omega$  prossime alla soglia della reazione. Si discute la polarizzazione dei fotonucleoni dovuta ad un nucleo in uno stato fondamentale  $S_{\frac{1}{2}}$ . Si indicano ulteriori applicazioni del metodo.

---

(\*) Traduzione a cura della Redazione.

# Die Eigenschaften der quantentheoretischen Phasenraumdichte.

H. KÜMMEL

*Institut für theoretische Physik der Freien Universität Berlin  
West-Berlin (Deutschland)*

(ricevuto il 25 Dicembre 1955)

**Zusammenfassung.** — In einer früheren Arbeit des Verfassers <sup>(1)</sup> war die Phasenraumdichte quantentheoretisch begründet worden. Es wird jetzt gezeigt, daß die Entartung der Energieeigenwerte keine Schwierigkeiten macht. Dazu werden die Eigenschaften der Wellenfunktionen aus den Gleichgewichtseigenschaften des Systems erschlossen. Ferner ist eine Beschränkung auf wirkliche makroskopische Messungen notwendig. Dann gilt im Grenzfall hoher Temperatur die klassische Physik. Ferner ist die Dichte fast überall positiv (im Gegensatz zur üblichen Wignerschen quantentheoretischen Dichtefunktion). Während man diese Eigenschaft in der klassischen Physik also — nnschaulich selbstverständliche — Zusatzhypothese einführt, folgt sie hier aus den Gesetzen der quantentheoretischen Aussagenlogik.

## 1. — Einleitung.

Vom Verfasser ist eine Phasenraumdichte aus der Quantentheorie hergeleitet worden <sup>(1)</sup>, die näherungsweise klassischen Bewegungsgleichungen genügt. Damit konnte man die klassische Thermodynamik und Hydromechanik auf die Quantentheorie zurückführen. Inzwischen ist es auch gelungen, diese Dichte für die Fragen der irreversiblen Thermodynamik heranzuziehen, insbesondere die Onsagersche Form der irreversiblen Thermodynamik herzu-

<sup>(1)</sup> H. KÜMMEL: *Nuovo Cimento*, **2**, 877 (1955), als II zitiert.



leiten<sup>(2)</sup>. Auch die Boltzmann-Gleichung in ihrer der Quantentheorie angepaßten Form konnte mit dieser Phasenraumdicke begründet werden<sup>(3)</sup>. Diese hat sich so als sehr brauchbar erwiesen.

Bei der Ableitung der Bewegungsgleichungen sind in II einschneidende Voraussetzungen gemacht worden. Es ist die Frage, ob diese wirklich erfüllt sind. Wegen der ungenügenden Kenntnis der Wellenfunktionen ist dies natürlich schwer zu entscheiden. Man kann jedenfalls die Voraussetzungen sinnvoll abschwächen, sodaß der tatsächlich vorhandenen Entartung (oder Fast-Entartung) der Energie Rechnung getragen wird (vgl. Anm. 13 in II). Dies werden wir unten durchführen, indem wir die Gleichgewichtseigenschaften des Systems verwerten.

Außerdem wollen wir noch zeigen, daß die Phasenraumdicke fast überall positiv ist. Zu den in II behandelten oben erwähnten physikalischen Anwendungen war diese Aussage nicht erforderlich, weil es nur notwendig war, die Gleichung.

$$(1) \quad \bar{A} = \int A(p, q) f_N(p, q, t) dp dq$$

für den Erwartungswert einer Größe  $A$  zu verstehen. Dann aber, wenn man den Übergang ins Gleichgewicht *quantitativ* untersuchen will (wie in III), muß man von dieser Eigenschaft Gebrauch machen. Hier erweist sich wieder die besondere Stärke der in II vorgeschlagenen Definition: Während die Wignersche Verteilung diese Eigenschaft nicht hat, kann durch die in II eingeführte Integration über kleine Gebiete im Phasenraum die gewünschte Vorzeichenrelation mit beliebiger Genauigkeit erreicht werden.

## 2. – Voraussetzungen über die Wellenfunktionen.

Wir machen für  $\psi_n$  den Ansatz (mit  $A_n$ ,  $W_n$  reell;  $P$  — Permutation):

$$(2) \quad \psi_n = \sum_p (\pm 1)^p A_n^p(\mathbf{r}_i) \exp \left[ \frac{i}{\hbar} W_n^p(\mathbf{r}_i) - \frac{i}{\hbar} \varepsilon_n t \right].$$

Das gibt die Schrödingergleichungen:

$$(3) \quad 2m(\varepsilon_n - \sum_{i < k} V_{ik}) = \sum_i (W_{n|v}^2)_i - \frac{\hbar^2}{A_n} \sum_i A_{n|i|v} A_{n|i|v}$$

$$(4) \quad \sum_i W_{n|i|v} + 2A_{n|i|v} W_{n|i|v} = 0.$$

<sup>(2)</sup> H. KÜMMEL: *Zeits. f. Naturf.*, **11a**, 15 (1956) als III zitiert.

<sup>(3)</sup> H. KÜMMEL: *Zeits. f. Phys.*, **143**, 219 (1955), als IV zitiert.

Wir machen folgende Näherungsannahmen:

$$(5) \quad \lambda_{n,\nu}^{(i)} = \frac{\hbar}{|W_{n|v}|} \ll \Delta X_\nu,$$

$$(6) \quad \lambda_{n,\nu} \ll \frac{|A_n|}{|A_{n|v}|}, \quad \frac{|A_{n|v}|}{|A_{n|v|\mu}|}, \quad \dots$$

$$(7) \quad \lambda_{n,\nu} \ll \frac{\lambda_{n,\nu}}{|\lambda_{n,\nu|\mu}|} = \frac{|W_{n|v|\mu}|}{|W_{n|v}|}, \quad \dots$$

Ein Kommentar erübrigt sich, zumal in I <sup>(4)</sup> ganz ähnlich vorgegangen wird. Wir bemerken nur, daß (5) bis (7) besagt, daß die  $\psi_n$  innerhalb des durch  $\Delta X_\nu$  gekennzeichneten Intervalls den Charakter ebener Wellen haben sollen. Damit werden z.B. die Operatoren der lokalen Dichte und Stromdichte (vgl. I):

$$(8) \quad R_{nm}(\mathfrak{R}, t) = \frac{N}{\Delta V} \int_{\Delta V(\mathfrak{R})} d\mathbf{r}_1 \int_V d\mathbf{r}_2 \dots d\mathbf{r} \psi_n^* \psi_m,$$

$$(9) \quad J_{mn}^\nu(\mathfrak{R}, t) = \frac{N}{\Delta V} \int_{\Delta V(\mathfrak{R})} d\mathbf{r}_1 \int_V d\mathbf{r}_2 \dots d\mathbf{r}_N \frac{i\hbar}{2m} \{ \psi_{m|v}^* \psi_n - \psi_m^* \psi_{n|v} \}$$

mit

$$\Delta V(\mathfrak{R}) = (\Delta X)^3$$

als « kleinstem makroskopischen Volumen » und  $V$  = Gesamtvolumen. Wenn man nun (5) bis (7) voraussetzt, so wird

$$R_{nm} = 0 \quad \text{für} \quad \frac{1}{\hbar} |\varepsilon_n - \varepsilon_m| \rightarrow \infty \quad \text{und} \quad J_{nm}^\nu = 0 \quad \text{für} \quad \frac{1}{\hbar} |\varepsilon_n - \varepsilon_m| \rightarrow \infty.$$

Diese Operatoren sind also « fast-diagonal », d.h. makroskopische Operatoren im Sinne von I. Wegen dieser Eigenschaft bezeichnen wir die obigen Näherungsannahmen (5) (6) und (7) auch als « *Diagonalitätsforderungen* ».

Es gibt aber noch eine zweite Gruppe von Annahmen über die Wellenfunktionen. Denn man muß ja in die Theorie irgendwie einbauen, daß im Gleichgewicht (bei Abseparation der Schwerpunktsbewegung) kein lokaler Strom fließt und daß die Dichte überall konstant ist.

Dazu benutzen wir die an der statischen Form des Ergodenzatzes gemachten Erfahrungen (LUDWIG <sup>(5)</sup>): Danach geben im Gleichgewicht (im Zeitmittel

<sup>(4)</sup> H. KÜMMEL: *Nuovo Cimento*, **1**, 1057 (1955), als I zitiert.

<sup>(5)</sup> G. LUDWIG: *Zeits. f. Phys.*, **135**, 483 (1953).

über genügend lange Zeit) nur die Diagonalelemente des statistischen Operators und der makroskopischen Operatoren Beiträge. D.h. man kann *praktisch* den Erwartungswert jedes solchen Operators durch

$$(10) \quad \text{Erw}_0(A) = \sum_{nn'} w_{nn'} A_{nn'}$$

mit  $\varepsilon_n = \varepsilon_n$  ersetzen. Berechnet man speziell den Erwartungswert bei Kenntnis der Energie (mit makroskopischer Genauigkeit  $\Delta E$ ), so wird stattdessen

$$(11) \quad \text{Erw}_0(A) = \sum_{\substack{n \\ \varepsilon_n \in (E, E + \Delta E)}} w_{nn} A_{nn},$$

wenn man gleich innerhalb  $(E, E + \Delta E)$  diagonalisiert. Wenn man also erreichen will, daß im Gleichgewicht die Dichte räumlich konstant wird, hat man

$$(12) \quad \sum_{\substack{n \\ \varepsilon_n \in (E, E + \Delta E)}} w_{nn} R_{nn} = \text{Const}$$

zu fordern. Nun ist der Gleichgewichtszustand dadurch charakterisiert, daß nichts weiter als die Energie bekannt ist, d.h. es müssen alle  $w_{nn}$  gleich sein. Daher haben wir statt (12):

$$\sum_{\substack{n \\ \varepsilon_n \in (E, E + \Delta E)}} R_{nn} = \text{Const}$$

oder:

$$(13) \quad \int_V d\mathbf{r}_2 \dots d\mathbf{r}_N \frac{\partial}{\partial \mathbf{r}_v} \sum_{\substack{n \\ \varepsilon_n \in (E, E + \Delta E)}} \psi_n^* \psi_n = 0.$$

Da im Gleichgewicht der Strom verschwinden muß, folgt weiterhin:

$$(14) \quad \int_V d\mathbf{r}_2 \dots d\mathbf{r}_N \sum_{\substack{n \\ \varepsilon_n \in (E, E + \Delta E)}} [\psi_n^* \psi_{n|v} - \psi_{n|v}^* \psi_n] = 0.$$

Aus (13) und (14) erhalten wir mit dem Ansatz (2) für  $\psi_n$ :

$$(13a) \quad \int d\mathbf{r}_2 \dots d\mathbf{r}_N \sum_{n \neq p'} (\pm 1)^{p+p'} \frac{1}{h} A_n^p A_n^{p'} (W_n^p - W_n^{p'})_1 \exp \left[ \frac{i}{h} (W_n^p - W_n^{p'}) \right] + \text{Glieder mit } A_{n|v, \dots} = 0,$$

$$(14a) \quad \int d\mathbf{r}_2 \dots d\mathbf{r}_N \sum_{n \neq p'} (\pm 1)^{p+p'} \frac{1}{h} A_n^p A_n^{p'} (W_n^p - W_n^{p'})_1 \exp \left[ \frac{i}{h} (W_n^p - W_n^{p'}) \right] + \text{Glieder mit } A_{n|v, \dots} = 0.$$



Nennen wir  $A_{n|v}/A_n$  und  $W_{n|v,\mu}/W_{n|\mu}$  «klein von erster Ordnung» (ohne das vorerst näher zu präzisieren), so folgt aus diesen Gleichungen, daß auch

$$(15) \quad \int dr_2 \dots dr_N \sum_{\substack{n \\ \varepsilon_n \in (E, E + \Delta E)}} (\pm 1)^{p+p'} \frac{1}{\hbar} A_n^p A_n^{p'} W_{n|v}^p \exp \left[ \frac{i}{\hbar} (W_n^p - W_n^{p'}) \right],$$

klein von erster Ordnung ist. Diese Größe stellt im wesentlichen den Impuls einer Überlagerung ebener Wellen im Gase dar. Daher ist dies Ergebnis (für  $A_{n|v} = 0$ ) selbstverständlich.

Bevor wir dies weiter verwerten, wollen wir auf die Bedeutung dieser Überlegungen hinweisen. Solche makroskopische Operatoren wie  $R$  und  $J_v$  nach (8) und (9) sind nicht sehr sinnvoll. Denn  $\psi_n^* \psi_n$  ist eine im allgemeinen *schnell* veränderliche Funktion der Koordinaten (wenn man die Symmetrieforderung an die Wellenfunktionen sowie die Form (2) benutzt, sieht man das sehr leicht). Daher hängen die Integrale sehr von Lage und Breite des Integrationsintervalles  $\Delta V$  ab, was sicherlich unvernünftig ist. Das war der Grund, weshalb wir, statt die einzelnen Matricelemente zu betrachten, alle zu derselben Energie gehörigen zusammenfassen mußten.

Wir wollen nun für den interessanteren Nicht-Gleichgewichtsfall die Folgerungen ziehen. Dazu verwenden wir erstens die Tatsache, daß wir die Integrationen über alle anderen Koordinaten weglassen können, weil dadurch an der *Größenordnungs* beziehung sicher nichts geändert wird. Zweitens nehmen wir an, daß die statistische Matrix nicht allzusehr vom Gleichgewicht abweiche. d.h. daß sie auch noch einigermaßen diagonal sei. Die hieraus zu folgernden physikalischen Gesetze sind also nur unter dieser Voraussetzung richtig. Wenn wir das also erst einmal hinnehmen, folgt sofort, daß (13a) zu

$$(16) \quad \sum_{\substack{p, p', n, m \\ \varepsilon_n, \varepsilon_m \in (E, E + \Delta E)}} (\pm 1)^{p+p'} w_{nm} \frac{1}{\hbar} A_n^p A_m^{p'} (W_n^p - W_m^{p'})|_v \exp \left[ \frac{i}{\hbar} (W_n^p - W_m^{p'}) \right] \\ = \text{klein von erster Ordnung}$$

verallgemeinert werden kann. Dagegen gilt das Entsprechende für (14a) nicht mehr, weil durchaus ein endlicher Strom auftreten kann. Die Gleichung (16) stellt die zweite Annahme über die Wellenfunktionen dar. Wir wollen sie mit dem Schlagwort «*Gleichgewichtsforderung*» kennzeichnen.

Wenden wir uns nun der Diskussion der hierin steckenden Voraussetzungen zu: Erstens hatten wir die physikalischen Eigenschaften des Gleichgewichtszustandes hineingesteckt, also gewissermaßen einen Ersatz für die nicht mögliche Berechnung der Wellenfunktionen des vorliegenden Problems gefunden und benutzt. Zweitens sollten die Abweichungen vom Gleichgewicht nicht sehr groß sein. Dies aber bedeutet keine wesentliche Einschränkung, weil die zulässigen Abweichungen *makroskopisch gesehen* durchaus *groß* sein können.

Nehmen wir nämlich an, daß  $A_n$  innerhalb  $\Delta V$  nicht allzusehr veränderlich ist, (wir werden gleich darauf noch zurückkommen), so bedeutet (16), daß der dort stehende Ausdruck klein ist, oder die Dichte

$$\sum_{p p'} \sum_{n m} (\pm 1)^{p+p'} w_{nm} A_n^p A_m^{p'} \exp \left[ \frac{i}{\hbar} (W_n^p - W_m^{p'}) \right]$$

innerhalb  $\Delta V$  langsam veränderlich. Wir haben also nichts anderes vorausgesetzt, als die Berechtigung, über solche Intervalle  $\Delta V$  hinwegzuintegrieren. Wir lassen demnach nur solche physikalischen Situationen zu, die innerhalb mikroskopischer Gebiete keine Dichteschwankung aufweisen. Alle anderen statistischen Matrizen würden einer *mikroskopischen* Messung am *makroskopischen* Objekt entsprechen, die wir bei einer Theorie makroskopischer Körper tunlichst auszuschalten haben.

Schließlich gehen wir noch auf eine dritte Vernachlässigung ein, die wir durch das Wort « *Klassizitätsforderung* » charakterisieren wollen. Sie ist erfüllt, wenn wir noch

$$(17) \quad \frac{A_n|_v}{A_n} \ll \frac{1}{\Delta X_v}, \text{ d.h. } \frac{A_n|_v}{A_n} \text{ « klein von erster Ordnung »}$$

annehmen. Das ist nämlich die Forderung, die die Gültigkeit der klassischen Physik garantieren wird. Wir wollen dies unten weiter untersuchen. Vorerst bemerken wir, daß dann, wenn wir (17) annehmen, auch

$$(18) \quad \sum_{\substack{p p' n m \\ \epsilon_n, \epsilon_m \in (E, E + \Delta E)}} (\pm 1)^{p+p'} w_{nm} \frac{1}{\hbar} A_n^p A_m^{p'} (W_n^p - W_m^{p'}) \exp \left[ \frac{i}{\hbar} (W_n^p - W_m^{p'}) \right] \ll \\ \ll \frac{1}{\Delta X_v} \sum_{p p' n m} (\pm 1)^{p+p'} w_{nm} A_n^p A_m^{p'} \exp \left[ \frac{i}{\hbar} (W_n^p - W_m^{p'}) \right] \\ \text{ (« klein von erster Ordnung »)}$$

gilt. Ferner ist dann  $A_n|_v / A_n$  klein « von zweiter Ordnung », sodaß wir (wie in I und II) das letzte Glied in (3) weglassen können. Was bedeutet (17) physikalisch? Offenbar sollen die  $\psi_n$  innerhalb  $\Delta X_v$  mit großer Genauigkeit immer den Charakter ebener Wellen haben. Das ist natürlich in Strenge nicht richtig. Wir haben in II 2.5 gezeigt, daß bei genügend hoher kinetischer Energie, d.h. bei hinreichend hoher Temperatur, (17) angenommen werden darf, wenn das Wechselwirkungspotential die bei den Molekülen übliche Form hat.

Wenn man (17) nicht annimmt, bekommt man quantenmechanische Korrekturen gegenüber dem klassischen Verhalten. Sie sind in Einzelfällen, z.B. bei der Boltzmann-Gleichung<sup>(3)</sup>, durchführbar.

Wir wollen jetzt (17) voraussetzen und benutzen, weil uns das klassische Verhalten interessiert. Wesentlich für die Gültigkeit der klassischen Bewegungsgleichung ist die Richtigkeit von

$$(19) \quad \int_{\Delta V(\mathfrak{R})} \int_V \mathrm{d}r_1 \int \mathrm{d}r_2 \dots \mathrm{d}r_N \frac{\partial}{\partial r^{(1)}} \sum_{nm} w_{nm} \psi_n^* \psi_m = \frac{\Delta}{\Delta \mathfrak{R}} \int_{\Delta V(\mathfrak{R})} \int_V \mathrm{d}r_1 \int \mathrm{d}r_2 \dots \mathrm{d}r_N \sum_{nm} w_{nm} \psi_n^* \psi_m.$$

Wir stellen erstens fest, daß (19) erfüllt ist: Denn der Integrand ist nach (17) und (18) langsam veränderlich ( $\Delta/\Delta \mathfrak{R}$  bedeutet den mit  $\Delta X_v$  gebildeten Differenzenquotienten, vgl. z.B. I). Zweitens folgt daraus die klassische Bewegungsgleichung für die Verteilungsfunktion nach II, Anhang 1, Gl. (10) ff. Wir haben damit die Anwendung der dortigen Gleichung A.(12) vermieden, die wegen der tatsächlich vorhandenen Entartung (ebene Wellen gleicher Energie, aber verschiedener Richtung) physikalisch schwer zu rechtfertigen ist.

### 3. – Vorzeichen der Phasenraumdichte.

Wir wollen uns nun der Frage nach dem Vorzeichen der in II eingeführten Phasenraumdichte zuwenden. Letztere war ja durch

$$(20) \quad f_N(\mathfrak{B}_l, \mathfrak{R}_l, t) = \frac{1}{\Delta \tau^N} \int_{\Delta \tau_i} \mathrm{d}v_i \mathrm{d}r_i f(v_i, r_i, t)$$

mit

$$(21) \quad f(v_i, r_i, t) = \left( \frac{m}{2\pi\hbar} \right)^{3N} \int \mathrm{d}\bar{r}_i \exp \left[ \frac{i}{\hbar} m \Sigma v_i \bar{r}_i \right] \sum_{nm} w_{nm} \psi_n^* \left( \mathfrak{s} + \frac{\bar{r}}{2} \right) \psi_m \left( \mathfrak{s} - \frac{\bar{r}}{2} \right)$$

und

$$\Delta \tau = \Delta V(\mathfrak{B}) \cdot \Delta V(\mathfrak{R})$$

als kleinstem makroskopischen Phasenraumintervall definiert. Dabei ist  $w_{nm}$  ein positiv definiter hermitescher Operator, d.h. es ist

$$(22) \quad w_{nm} = w_{mn}^*$$

und

$$(23) \quad \sum_{nm} w_{nm} x_n x_m \geq 0$$

für beliebige  $x_n$ . Aus (22) folgt leicht, daß  $f$ , also ebenfalls  $f_N$ , reell ist. Es



gilt aber auch

$$(24) \quad f_N(\mathfrak{R}_i, \mathfrak{R}_i, t) \gtrsim 0,$$

wenn die Nichtdiagonalglieder von  $w_{nm}$  klein sind im Verhältnis zu den Diagonalgliedern; und zwar um so besser, je größer das Volumen  $\Delta\tau$  gewählt wird. Zum Beweise benutzen wir erstens, daß nach (22) (23)

$$(25) \quad w_{nn} \geq 0$$

ist. Zweitens zeigen wir, daß die Diagonalglieder positiv sind, was nach unserer Voraussetzung genügt. Dazu greifen wir ein solches Glied heraus (die Symmetrieeigenschaften der Wellenfunktionen sind belanglos, wir lassen sie hier daher weg):

$$(26) \quad \frac{1}{\Delta\tau} \int d\mathbf{v} d\mathfrak{s} \int d\bar{\mathbf{r}} w_{nn} \left\{ A_n \left( \mathfrak{s} + \frac{\bar{\mathbf{r}}}{2} \right) A_n \left( \mathfrak{s} - \frac{\bar{\mathbf{r}}}{2} \right) \cdot \right. \\ \left. \cdot \exp \left[ -\frac{i}{\hbar} m \mathbf{v} \bar{\mathbf{r}} \right] \exp \left[ \frac{i}{\hbar} \left[ W_n \left( \mathfrak{s} + \frac{\bar{\mathbf{r}}}{2} \right) - W_n \left( \mathfrak{s} - \frac{\bar{\mathbf{r}}}{2} \right) \right] \right] \right\} + \text{konjug. kompl.} \}.$$

Wegen der Integration über  $\mathbf{v}$  bleibt  $\mathbf{r}$  klein. Da  $A_n$  reell ist, ist also  $A_n(\mathfrak{s} + (\bar{\mathbf{r}}/2)) A_n(\mathfrak{s} - (\bar{\mathbf{r}}/2))$  fast immer positiv, und zwar um so besser, je langsamer  $A_n(\mathbf{r})$  mit  $\mathbf{r}$  veränderlich und je kleiner  $\mathbf{r}$  ist, was wiederum um so besser erfüllt ist, je größere  $\Delta V(\mathfrak{R})$  gewählt wird. Aus den gleichen Gründen kann man

$$W_n \left( \mathfrak{s} + \frac{\bar{\mathbf{r}}}{2} \right) = W_n(\mathfrak{s}) + \frac{1}{2} W_{n|\mathbf{v}} \bar{\mathbf{r}}_{\mathbf{v}}$$

entwickeln. Dann ergibt die Integration über  $\mathbf{r}$  eine (unscharfe)  $\delta$ -Funktion, die ebenfalls positiv ist. Daher ist der ganze Ausdruck positiv. Wir bemerken noch, daß man an die langsame Veränderlichkeit der  $A_n$  und  $W_{n|\mathbf{v}}$  nicht allzu große Ansprüche zu stellen braucht. Insbesondere braucht nicht etwa die Klassizitätsforderung (17) erfüllt zu sein. Je besser sie aber erfüllt ist, desto exakter ist andererseits (26) positiv.

Wählen wir weiterhin  $\Delta V(\mathbf{v})$  sehr groß, dann wird  $\mathbf{r}$  sehr klein und es ist

$$f_N(\mathfrak{R}_i, \mathfrak{R}_i, t) \approx \left( \frac{m}{2\pi\hbar} \right)^{3N} \frac{1}{\Delta\tau^N} \int d\bar{\mathbf{r}}_i \int d\mathbf{v}_i d\mathfrak{s}_i \exp \left[ -\frac{i}{\hbar} m \sum \mathbf{v}_i \bar{\mathbf{r}}_i \right] \sum_{nm} w_{nm} \psi_n^*(\mathfrak{s}) \psi_m(\mathfrak{s}),$$

was mit (23) positiv ist.  $\Delta V(\mathbf{v})$  darf man nur dann sehr groß wählen, wenn  $f(\mathbf{v}_i, \mathbf{r}_i, t)$  mit  $\mathbf{v}_i$  langsam veränderlich ist: Das wiederum ist eine Forderung an die  $w_{nm}$ . Denn wir setzen voraus, daß es zu jeder Energie aus  $(E, E + \Delta E)$

alle möglichen mit  $E$  verträglichen Werte  $W_{n|v}$  gibt. Das bedeutet ja nichts anderes als die Zulassung aller möglichen fast-ebenen Wellen gleicher Energie. Dann gibt es zu jedem vorgegebenen  $v$  auch ein  $W_{n|v}$  und  $W_{m|v}$  mit  $v^{(i)} = (1/2m)(W_{n|v} + W_{m|v})$ , und zu jedem benachbarten  $v'$  auch ein benachbartes  $W_{n'|v}$  und  $W_{m'|v}$  mit  $v^{(i')} = (1/2m)(W_{n'|v} + W_{m'|v})$ . Wenn nun in

$$f(v_i, r_i, t) = \int d\bar{r}_i \exp \left[ -\frac{i}{\hbar} m \sum v_i \bar{r}_i \right] \sum_{nm} w_{nm} A_n \left( \bar{s} + \frac{\bar{r}}{2} \right) A_m \left( \bar{s} - \frac{\bar{r}}{2} \right) \cdot \exp \left[ \frac{i}{\hbar} \left[ W_n \left( \bar{s} + \frac{\bar{r}}{2} \right) - W_n \left( \bar{s} - \frac{\bar{r}}{2} \right) \right] \right]$$

zu  $w_{nm}$  ein benachbartes  $w_{n'm'}$  gehört, dann ändert sich  $f$  langsam mit  $v$ . Wir haben also die « Stetigkeit » des von  $n$  und  $m$  fast kontinuierlich abhängenden  $w_{nm}$  zu verlangen. Andernfalls hätten wir wieder eine mikroskopische Messung an dem makroskopischen System gemacht, was wir bereits einmal als nicht zur makroskopischen Beschreibung gehörig erwähnten.

#### 4. – Schluß.

Wir haben gesehen, daß der Charakter von  $f_N$  als *positive* Dichtenfunktion mit dem klassischen Verhalten parallel geht und darüber hinaus die Beschränkung auf makroskopische Messungen voraussetzt. Dies haben wir mit den Mitteln der Quantentheorie nachgewiesen. *Die Eigenschaft der Dichtefunktion, positiv zu sein, ist also quantentheoretisch zu begründen. In der klassischen Theorie ist sie eine anschaulich als selbstverständlich angesehene Zusatzannahme* (vgl. hierzu eine demnächst an anderer Stelle erscheinende Arbeit des Verf.). Wenn wir die obigen Überlegungen noch einmal durchdenken, sehen wir, daß entscheidend zwei Dinge eingehen: Erstens die quantenmechanische Aussagenlogik, die die Existenz positiver definiter Dichteoperatoren voraussetzt. Zweitens die Einführung von Zellen im Phasenraum. Das letzte hat in der hier und in den früheren Arbeiten vorgetragenen Form nur dann Sinn, wenn die Annahme fast-ebener Wellen gerechtfertigt ist. Wir sind natürlich hier sehr viel weiter gekommen, als eine Störungstheorie uns zu bringen vermag. (Eine Anwendung der Störungstheorie bei einem Problem vieler Teilchen ist in jedem Falle unerlaubt, vgl. hierzu VAN KAMPEN <sup>(6)</sup>). Die uns gezogenen

<sup>(6)</sup> N. G. VAN KAMPEN: *Physica*, **20**, 603 (1954). Auch die sonst sehr überzeugende Darstellung von M. BORN, in *Natural Philosophy of Cause and Chance* (Oxford, 1949) ist nicht frei von der Verwendung der Störungstheorie.

Grenzen sind: Beschränkung auf Gase <sup>(7)</sup> (und allenfalls Flüssigkeiten), sowie für die praktische Auswertbarkeit die Beschränkung auf nicht zu niedrige Temperaturen (wobei freilich in wohlbekannten Ausnahmefällen auch hier ziemlich weit herunter gegangen werden kann).

Der Vorzug der quantentheoretischen Behandlung liegt darin, daß sie gewisse Feinheiten enthält, so z.B. die Symmetrierelationen, die die irreversible Thermodynamik (vgl. III) begründen. Letztere kann man eben nicht mehr anschaulich als Zusatzannahme in die klassische Theorie einbauen. Es gibt allerdings eine interessante Ausnahme: Wenn man sich auf die Phasenraum-dichte für ein Teilchen beschränkt und die « Boltzmannsche Unordnungs-annahme » als plausibel annimmt, erhält man zusätzlich die erwähnten Symmetrierelationen (vgl. IV und die erwähnte demnächst erscheinende Arbeit).

\* \* \*

Herrn Prof. LUDWIG habe ich für fördernde und klärende Diskussionen sehr zu danken.

---

<sup>(7)</sup> Der Begriff « Gas » ist dabei ziemlich weit zu fassen: Auch alle gasähnlichen Modelle (Schallquanten im Festkörper) gehören hierzu. Für solche Probleme, die nicht einmal behelfsmäßig wie Gase behandelt werden dürfen, fehlt jede Berechtigung für eine Beschreibung mit den üblichen statistischen Methoden.

---

#### RIASSUNTO (\*)

In un precedente lavoro dell'Autore è stata motivata dal punto di vista della teoria quantistica la densità dello spazio delle fasi. Si mostra ora che la degenerazione degli autovalori dell'energia non offre difficoltà. A tal uopo si deducono le proprietà delle funzioni d'onda dalle proprietà d'equilibrio del sistema. È necessario inoltre limitarsi a vere misurazioni macroscopiche. Nel caso limite di temperature elevate vale allora la fisica classica. Inoltre la densità è quasi dappertutto positiva (in contrapposto alla consueta funzione quantistica della densità di Wigner). Mentre nella Fisica classica questa proprietà si introduce come ipotesi aggiuntiva intuitiva, questa consegue nel presente lavoro dalle leggi della logica dei postulati della teoria quantistica.

---

(\*) Traduzione a cura della Redazione.



## Zerfall eines gebundenen $\Lambda^0$ -Teilchens.

G. EDER

*Max-Planck-Institut für Physik - Göttingen (\*)*

(ricevuto il 20 Gennaio 1956)

**Zusammenfassung.** — Aus einem einfachen Modell soll das Energiespektrum der Protonen abgeschätzt werden, die beim  $p\pi^-$ -Zerfall eines gebundenen  $\Lambda^0$ -Teilchens entstehen.

Beim Zerfall eines freien, ruhenden  $\Lambda^0$ -Teilchens (Masse  $M$ ) in ein Proton (Masse  $m$ ) und ein negatives Pion (Masse  $\mu$ ) ist die Protonenergie eindeutig zu  $T = 0.5 Q(2\mu + Q)(m + \mu + Q)^{-1}$  mit  $Q = 37$  MeV bestimmt ( $\hbar = c = 1$ ). Ist nun entsprechend einer Bindungsenergie von 1 MeV für ein gebundenes  $\Lambda^0$ -Teilchen  $Q = 36$  MeV, so wäre für einen reinen Zweiteilchenzerfall  $T = 5.1$  MeV. Durch die Konzentration der  $\Lambda^0$ -Wellenfunktion auf ein endliches Volumen mit dem Radius  $a$  ergibt sich aber eine Impulsunschärfe des  $\Lambda^0$ -Teilchens  $\Delta k \approx a^{-1}$ . Es kann also eine kinetische Energie bis zu  $k^2/(2M) \approx (2Ma^2)^{-1} \approx 1.8$  MeV annehmen, wenn wir  $a \approx 3 \cdot 10^{-13}$  cm setzen. Die größte und kleinste Protonenergie ergeben sich daraus zu  $T \approx 12$  MeV und 1 MeV. Man wird daher ein Protonenspektrum mit einer Breite von ca. 10 MeV und einem Maximum bei  $T \approx 5$  MeV erwarten.

Es soll nun angenommen werden, daß im Kern auf das  $\Lambda^0$ -Teilchen ein Potential  $V_0$  mit der Reichweite  $a$  wirkt. Für das emittierte Pion werden die freien Wellenfunktionen eingesetzt. Die Einwirkung des Coulombfeldes auf das Pion soll dadurch berücksichtigt werden, daß die Zerfallswahrscheinlichkeit mit  $\varrho(1 - e^{-\varrho})^{-1}$  multipliziert wird.  $\varrho = 2\pi Z\alpha/v_\pi$ . Dabei ist  $Z$  die Kernladungszahl,  $\alpha$  die Feinstrukturkonstante und  $v_\pi$  die Piongeschwindigkeit.

(\*) Jetzt in der theoretischen Studienabteilung von CERN am Institut for theoretical Physics, Kopenhagen.

Das emittierte Proton steht unter dem Einfluß des Coulomb- und Kernfeldes. Da der Coulombwall für die leichtesten Kerne im Vergleich zu den Kernkräften sehr niedrig ist, soll sein Einfluß vernachlässigt werden. Um den Einfluß der Proton-Kern-Wechselwirkung bloß qualitativ abzuschätzen, nehmen wir an, daß auf das entstehende Proton ein Potential

$$(25) \quad U(\mathbf{x}) = -U_0 b^3 \delta(\mathbf{x})$$

wirkt. Ist  $B$  die Bindungsenergie des  $\Lambda^0$ -Teilchens, so wird seine Wellenfunktion

$$(2) \quad \varphi_\Lambda(\mathbf{x}) = (C/r) \sin(\beta r/a) \text{ bzw. } e^\gamma \sin \beta(C/r) \exp[-\gamma r/a]$$

für  $r < a$  bzw.  $r > a$ .  $r = |\mathbf{x}|$ . Dabei ist wegen der Stetigkeit von  $(d/dr)\varphi_\Lambda$  in  $r = a$ :  $\gamma \operatorname{tg} \beta = -\beta$ . Es bedeutet

$$\beta = a\sqrt{2M(V_0 - B)}, \quad \gamma = a\sqrt{2MB}$$

und

$$C^2 = (\beta\gamma/2\pi a) \{ \gamma(\beta - \sin \beta \cos \beta) + \beta \sin^2 \beta \}^{-1}.$$

Aus (1) folgt für die  $l$ -te Protoneigenfunktion zur kinetischen Energie  $T = p^2/(2m)$ :

$$(3) \quad \begin{cases} \varphi_{ep} = p\sqrt{(2l+1)/(2\pi R)} j_l(pr) P_l(\cos \vartheta) & \text{für } l > 0, \\ \varphi_{op} = (p^2/2\pi R)^{\frac{1}{2}} \{ j_0(pr) + (mb^3 U_0/2\pi r) \exp[ipr] \}. \end{cases}$$

$R$  ist der Radius der Normierungskugel,  $\vartheta$  der Winkel zwischen  $\mathbf{x}$  und dem Protonimpuls  $\mathbf{p}$ ,  $p = |\mathbf{p}|$ . Mit einem Wechselwirkungsglied

$$(4) \quad H' = -(g/\sqrt{2m})(\varphi_x^* \sigma_i \varphi_\Lambda)(\partial \Phi / \partial x_i),$$

wo  $\Phi$  die Mesonwelle bedeutet, wird das Matrixelement für die Emission eines Protons in den  $l$ -ten Eigenszustand:

$$\begin{aligned} M'_l &= (g/\sqrt{2m}) \int d\mathbf{x} (\varphi_{xi}^* \sigma_i \varphi_\Lambda) i q_i \exp[i\mathbf{q}\mathbf{x}] (2\omega)^{-\frac{1}{2}} = \\ &= i^{l+1} (gp/2m) \sqrt{(2l+1)/(2\pi R\omega V)} (\boldsymbol{\sigma}\mathbf{q}) 4\pi \int_0^\infty dr r^2 \varphi_\Lambda(r) j_l(pr) j_l(qr) P_l(\cos \theta) \quad \text{für } l > 0. \end{aligned}$$

Hier ist  $\mathbf{q}$  der Mesonimpuls,  $q = |\mathbf{q}|$ ,  $\omega = (\mu^2 + q^2)^{\frac{1}{2}}$ ,  $\theta$  ist der Winkel

zwischen  $\mathbf{p}$  und  $\mathbf{q}$  und  $V$  ist das Normierungsvolumen der Pionwelle,

$$M'_0 = i(gp/2m\sqrt{2\pi R\omega V})4\pi \int_0^\infty dr r^2 \varphi_\Lambda(r) \{j_0(pr) + (mb^3 U_0/2\pi r) \exp[ipr]\} j_0(qr).$$

Mit

$$\sum_{\mathbf{q}} = V(2\pi)^{-3} \int d\mathbf{q}$$

wird

$$\begin{aligned} (5) \quad & \sum_{\mathbf{q}} \sum_{l=0}^{\infty} (2l+1) |\overline{M'_l}|^2 \delta(E_e - E_a) = \\ & = (g^2 p^2 / 8\pi^2 m^2 R) \int d\mathbf{q} (q^2/\omega) \int_0^\pi d\theta \sin \theta \left\{ \int_0^\infty dr r^2 \varphi_\Lambda(r) j_0(kr) \right\}^2 \delta(E_e - E_a) + \\ & + (g^2 p b^3 U_0 / 2\pi^2 R m) \int d\mathbf{q} (q^4/\omega) \int_0^\infty dr r \varphi_\Lambda(r) j_0(qr) \int_0^\infty dr' r' \varphi_\Lambda(r') j_0(qr') \cdot \\ & \cdot (\sin pr \exp[-ipr'] + \sin pr' \exp[ipr]) \delta(E_e - E_a). \end{aligned}$$

Der in  $U_0$  quadratische Term wurde vernachlässigt,

$$(6) \quad E_e - E_a = T + \omega - \mu - Q.$$

$k = |\mathbf{p} + \mathbf{q}|$ . Das erste Integral in (5) läßt sich ausführen, wenn man  $\mathbf{q} = \mathbf{k} - \mathbf{p}$ , substituiert. Für festes  $p$  bzw.  $T$  läuft dabei  $k$  von  $k_1$  bis  $k_2$ , wobei aus (5) und (6) folgt:

$$k_1 = \sqrt{Q(2\mu + Q) - T[2(\mu + Q) - T]} - \sqrt{2mT} \quad \text{bzw.} \quad \sqrt{2T(m + \mu + Q) - Q(2\mu + Q)}$$

$$\text{für } T < \text{bzw. } > 0.5 Q(2\mu + Q)(m + \mu + Q)^{-1},$$

$$k_2 = \sqrt{Q(2\mu + Q) - T[2(\mu + Q) - T]} + \sqrt{2mT}.$$

Für das zweite Integral nähern wir (2) durch

$$(7) \quad \varphi_\Lambda = (2\lambda/\pi a^2)^{\frac{3}{2}} \exp[-\lambda r^2/a^2]$$

an, wobei  $\lambda$  so zu bestimmen ist, daß der Verlauf von (2) möglichst gut wiedergegeben wird. Aus

$$j_l(pR) \approx (pR)^{-1} \cos \{pR + \frac{1}{2}(l+1)\pi\} = 0$$

folgt für die Dichte der Protonenzustände  $dn = (R/\pi) dp = (mR/\pi p) dT$ . Damit wird die Zerfallswahrscheinlichkeit

$$w = 2\pi \sum_{p,q} \sum_{l=0}^{\infty} (2l+1) |\overline{M_l}|^2 \delta(\mu + Q - T - \omega) = \int_0^Q dT w(T),$$

wo

$$(8) \quad w(T) = 4(g^2/4\pi)(C^2/m)(qa)^2 \{F(ak_2) - F(ak_1)\} \varrho(1 - e^{-\varrho})^{-1} + \\ + \delta(2/\pi^2)(g^2/4\pi)\sqrt{2\lambda}qa^2(e^{-\xi^2} - e^{-\eta^2})\{g(\xi) + g(\eta)\}\varrho(1 - e^{-\varrho})^{-1}$$

Dabei ist

$$F(x) = \int_0^x dt f^2(t)/t \quad \text{mit} \quad f(t) = (\sin \beta \cdot t \cos t - \beta \cos \beta \cdot \sin t)/(\beta^2 - t^2) - \\ - \sin \beta (t \cos t - \gamma \sin t)/(\gamma^2 + t^2).$$

$$\delta = (U_0/Q)(b/a)^3, \quad \xi = (p - q)(a/2\sqrt{\lambda}), \quad \eta = (p + q)(2a/\sqrt{\lambda}),$$

$$p^2 = 2mT, \quad q^2 = (Q - T)(2\mu + Q - T), \quad g(x) = \sum_{n=0}^{\infty} \frac{(-2)^n x^{2n+1}}{(2n+1)!!}.$$

Um ein numerisches Beispiel zu geben, nehmen wir  $a = 3 \cdot 10^{-13}$  cm und  $B = 1$  MeV an. Mit  $M = 1114$  MeV folgt daraus  $Q = 36$  MeV;  $\gamma = 0.747$  und  $\beta = 1.939$ , d.h.  $V_0 = 7.7$  MeV,  $C^2/m = 0.00459$ ;  $\lambda \approx 0.67$ .

Abb. 1 zeigt den Verlauf von  $w(T)$  für  $Z = 3$ .

(4) ergibt für die Zerfallswahrscheinlichkeit eines freien  $\Lambda^0$ -Teilchens

$$(9) \quad w_{tr} = (g^2/4\pi)(p_0/m)^3 \cdot (m/2M)(M^2 + m^2 - \mu^2)m,$$

wobei  $p_0^2 = (M^2 + m^2 - \mu^2)^2/(2M)^2 - m^2$ . Vergleicht man (8) mit (9), so findet man für die obigen Annahmen

$$w/w_{tr} = 0.59 \quad \text{bzw.} \quad 0.99 \quad \text{für} \quad \delta = 0 \quad \text{bzw.} \quad \frac{1}{4}.$$

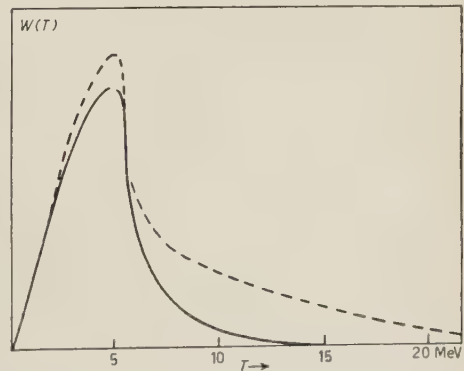


Abb. 1. - Energiespektrum der Protonen für  $\delta = 0$  (—) und  $\delta = \frac{1}{4}$  (-----).



Experimentell kann noch wenig über das Energiespectrum der Protonen ausgesagt werden <sup>(1)</sup>.

---

(1) J. CRUSSARD *et al.*; K. GOTTSTEIN *et al.*: *Pisa Conference*, 1955.

---

#### RIASSUNTO (\*)

In base a un modello semplice si vuol stimare lo spettro d'energia dei protoni che si originano nel decadimento  $p-\pi^-$  di una particella  $\Lambda^0$  legata.

---

(\*) *Traduzione a cura della Redazione.*

## Zur Photonvielfacherzeugung.

G. EDER

*Max-Planck-Institut für Physik - Göttingen (\*)*

(ricevuto il 20 Gennaio 1956)

**Zusammenfassung.** — Für energiereiche Elektronen und Vektormesonen wird die mittlere Anzahl von Bremsquanten in niedrigster störungstheoretischer Näherung diskutiert. Für kleinere Photonenergien ist die mittlere Photonenzahl  $n$  spinunabhängig und wächst logarithmisch mit der Primärenergie und der maximalen Photonenergie. Bei größeren Photonenergien nimmt  $n$  für Vektormesonen quadratisch mit der maximalen Photonenergie zu.

Zunächst soll eine Verallgemeinerung der Resultate von GUPTA <sup>(1,2)</sup> auf beliebige Streuwinkel gegeben werden. Der differentielle Wirkungsquerschnitt für die Erzeugung von  $n$  Photonen bei der Streuung eines hochenergetischen Elektrons am Coulombfeld einer Punktladung ergibt sich zu

$$(1) \quad \frac{d\sigma}{d\Omega} = \left(\frac{\alpha Z}{2m}\right)^2 \frac{1 - \beta^2}{\beta^4 \sin^4(\vartheta/2)} \left\{ 1 + \frac{\beta^4 \sin^2 \vartheta}{6(1 - \beta^2)} \right\} \frac{\bar{n}(\vartheta)^n}{n!},$$

wo

$$(2) \quad \bar{n}(\vartheta) = \frac{\alpha}{\pi} \left( \ln \frac{\varepsilon_2}{\varepsilon_1} \right) \ln \left\{ \left( \frac{2\omega}{m} \right)^2 \sin^2 \frac{\vartheta}{2} + \cos^2 \frac{\vartheta}{2} \right\}.$$

Dabei ist  $\alpha$  die Feinstrukturkonstante,  $Z$  die Ladungszahl des Streuzentrums,  $m$  die Elektronenmasse,  $\beta$  die Geschwindigkeit und  $\omega$  die Primärenergie des Elektrons.  $\varepsilon_1$  und  $\varepsilon_2$  bedeuten die minimale und maximale Photonenergie;  $\vartheta$  ist der Streuwinkel. Weithers wurde  $\hbar = c = 1$  gesetzt. Das Ergebnis (2)

(\*) Jetzt in der theoretischen Studienabteilung von CERN am Institut for teoretisk Fysik, Kopenhagen.

(1) S. N. GUPTA: *Phys. Rev.*, **98**, 502 (1955).

(2) S. N. GUPTA: *Phys. Rev.*, **99**, 1015 (1955).

erhält man quantentheoretisch dadurch, daß man

$$\begin{aligned} i\{i\gamma(k - q^{(1)} - \dots - q^{(i)} - m)\}^{(e^{(i)})\gamma} u_k & \quad \text{durch} \quad -u_k \cdot 2(e^{(i)}k), \\ \bar{u}_{k'}(e^{(i)}\gamma)i\{i\gamma(k' + q^{(i)} + \dots + q^{(n)} - m)\} & \quad \text{durch} \quad -2(e^{(i)}k')\bar{u}_{k'}, \end{aligned}$$

und in den Nennern der  $S_x$ -Funktionen

$$\begin{aligned} (k - q^{(1)} - \dots - q^{(i)})^2 + m^2 & \quad \text{durch} \quad -2k(q^{(1)} + \dots + q^{(i)}) \\ (k' + q^{(i)} + \dots + q^{(n)})^2 + m^2 & \quad \text{durch} \quad 2k'(q^{(i)} + \dots + q^{(n)}) \end{aligned}$$

ersetzt. Dabei sind  $k$  und  $k'$  die Viererimpulse des Elektrons vor und nach der Streuung.

$$(i\gamma k + m)u_k = \bar{u}_{k'}(i\gamma k' + m) = 0.$$

$e^{(i)}$  ist der Polarisationsvektor des  $i$ -ten Protons. Die Näherungen bedeuten, daß die Photonenergien gegenüber der Primärenergie des Elektrons vernachlässigt werden. In halbklassischer Behandlung <sup>(3)</sup> erhält man (2) dadurch, daß man den Elektronenstrom klassisch behandelt. Seine Impulsraumdarstellung lautet dann

$$j(p) = ie\{k/(kp) = k'/(k'p)\}$$

und

$$\bar{n}(\vartheta) = (2\pi)^{-3} \int_{\epsilon_1 \leq p_0 \leq \epsilon_2} d^4p |j(p)|^2 \delta(p^2) \theta(p),$$

woraus mit  $kk' = \beta^2 \omega^2 \cos \vartheta$  und  $\beta \approx 1$  das Ergebnis (2) folgt. Aus (2) erhalten wir

$$(2a) \quad \bar{n}(\pi) = (2\alpha/\pi) \ln(\epsilon_2/\epsilon_1) \ln(2\omega/m).$$

Die Elektron-Positron-Paarvernichtung liefert unter der Annahme, daß zwei Photonen den Hauptbeitrag der Paarenergie übernehmen, für  $n$  das gleiche Resultat. Beschränkt man den Winkel  $\theta_i$  zwischen dem Ausbreitungsvektor des  $i$ -ten Photons und  $k$  auf  $0 \leq \theta_i \leq \delta \ll 1$ , so wird

$$\bar{n}(\pi) = (4\alpha/\pi) \ln(\epsilon_2/\epsilon_1) \ln(\omega\delta/m),$$

in Übereinstimmung mit den Berechnungen von GUPTA <sup>(1)</sup>. Für  $m/\omega < \vartheta \ll 1$  wird

$$\bar{n}(\vartheta) = (2\alpha/\pi) \ln(\epsilon_2/\epsilon_1) \ln(\omega\vartheta/m).$$

<sup>(3)</sup> Vgl. W. THIRRING: *Elektrodynamik* (Wien).

Die Näherungsannahmen für die  $\Theta_i$  bei GUPTA <sup>(2)</sup> ergeben für  $\bar{n}(\vartheta \ll 1)$  einen Wert, der um den Faktor 2 zu groß ist. Der Unterschied zwischen (2a) und (2b) ist nur durch verschiedene  $\vartheta$ -Werte bedingt, bedeutet aber keinen Unterschied für die mittlere Photonenzahl bei Bremsstrahlungs- und Paarvernichtungsprozessen (vgl. GUPTA <sup>(2)</sup>).

Der schwache Anstieg von  $n$  mit der Energie macht die Erzeugung vieler Photonen unwahrscheinlich. Es soll nun untersucht werden, ob man von Vektormesonen größere mittlere Photonenzahlen erwarten kann, ohne daß auf die Schwierigkeiten eingegangen werden soll, die sich durch die Nichtrenormierbarkeit der vektoriellen Mesontheorie ergeben. Wir gehen aus von einer Wechselwirkungsenergiedichte

$$H' = ieA_\mu \{ \psi_\nu^* (\partial_\mu \psi_\nu - \partial_\nu \psi_\mu) - (\partial_\mu \psi_\nu^* - \partial_\nu \psi_\mu^*) \psi_\nu \} + e^2 A_\mu \psi_\nu^* (A_\mu \psi_\nu - A_\nu \psi_\mu).$$

Dabei genügen die Mesonfeldgrößen den Gleichungen

$$\partial_\nu \psi_\nu = 0, \quad (\partial_\nu^2 - \mu^2) \psi_\mu = 0. \quad \mu \text{ ist die Mesonmasse}$$

Betrachten wir den Prozess in niedrigster störungstheoretischer Näherung, so können im zugehörigen Feynmandiagramm für einen Punkt drei verschiedene Ausdrücke eingesetzt werden:

$$(3a) \quad \begin{cases} 1. & -e \sum_{q^{(i)} e^{(i)}} a^*(e^{(i)} q^{(i)}) (2q_0^{(i)})^{-\frac{1}{2}} B(i, i-1), \\ \text{wo} & B(i, i-1) = \delta_{\beta_i \alpha_{i-1}} (e^{(i)}, p^{(i-1)} + p^{(i)}) - p_{\beta_i}^{(i-1)} e_{\alpha_{i-1}}^{(i)} - p_{\alpha_{i-1}}^{(i)} e_{\beta_i}^{(i)}. \end{cases}$$

$p^{(i)} = p^{(i-1)} - q^{(i)}$  ist der Viererimpuls des  $i$ -ten Photons.  $a^*$  sind die Photonerzeugungsoperatoren.

$$(3b) \quad \begin{cases} 2. & e^2 \sum_{q^{(i)} q^{(i+1)} e^{(i)} e^{(i+1)}} a^*(e^{(i)} q^{(i)}) a^*(e^{(i+1)} q^{(i+1)}) (4q_0^{(i)} q_0^{(i+1)})^{-\frac{1}{2}} C(i+1, i-1), \\ \text{wo} & C(i+1, i-1) = (e^{(i)} e^{(i+1)}) \delta_{\beta_{i+1} \alpha_{i-1}} - e_{\beta_{i+1}}^{(i+1)} e_{\alpha_{i-1}}^{(i)}. \end{cases}$$

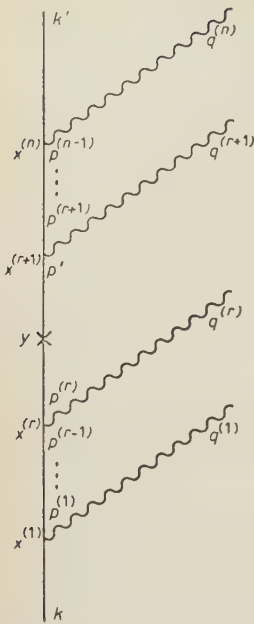
Oder im Falle eines Coulombfeldes:

$$(3c) \quad \begin{cases} 3. & D(s, r) = \delta_{\beta_s \alpha_r} (\bar{A}_\mu, p_\mu^{(n)} + p'_\mu) - \bar{A}_{\alpha_r} p_{\beta_s}^{(n)} - \bar{A}_{\beta_s} p'_{\alpha_r}, \\ \text{wo} & \bar{A} = (0, -ie^2 Z(\mathbf{p}^{(\mu)} - \mathbf{p}')^{-2}). \end{cases}$$

Für eine innere Mesonlinie ist

$$(4) \quad F(i) = -i(\delta_{\alpha_i \beta_i} + \mu^{-2} p_{\alpha_i}^{(i)} p_{\beta_i}^{(i)})(p^{(i)2} + \mu^2)^{-1}$$





einzusetzen. Die Indizes  $\alpha_i$ ,  $\beta_i$  durchlaufen die Zahlen 1 bis 4.

$$p^{(1)} = k - q^{(1)}, \dots, p^{(r)} = k - q^{(1)} - \dots - q^{(r)},$$

$$p' = k' + q^{(r+1)} + \dots + q^{(n)},$$

$$p^{(r+1)} = k' + q^{(r+2)} + \dots + q^{(n)}, \dots, p^{(n-1)} = k' + q^{(n)}.$$

Betrachten wir zunächst den Fall  $\varepsilon_2 \omega \ll \mu^2$ . In den Nennern der  $F(i)$  ersetzen wir wieder  $p^{(i)2} + \mu^2$  durch

$$-2k(q^{(1)} + \dots + q^{(i)}) \quad \text{für } 1 \leq i \leq r$$

bzw. durch

$$2k'(q^{(r+1)} + \dots + q^{(n)}) \quad \text{für } r+1 \leq i \leq n-1$$

$$p'^2 = 2k'(q^{(r+1)} + \dots + q^{(n)}). \quad (\text{Vgl. Abb. 1}).$$

Abb. 1. – Feynmandiagramm zur Photonvielfacherzeugung.

Die Photonerzeugung kann auf  $B(i, i-1)$  beschränkt werden. Nun ist

$$\begin{aligned} -i_{\alpha_i \beta_i} (\delta_{\alpha_i \beta_i} + \mu^{-2} p_{\alpha_i}^{(i)} p_{\beta_i}^{(i)}) \{ \delta_{\beta_i \gamma_{i-1}} (e^{(i)} p^{(i-1)} + p^{(i)}) - p_{\beta_i}^{(i-1)} e_{\gamma_{i-1}}^{(i)} - e_{\beta_i}^{(i)} p_{\gamma_{i-1}}^{(i)} \} \psi_{\alpha_{i-1}}(k) &\approx \\ \approx -i (\delta_{\alpha_i \beta_i} + \mu^{-2} k_{\alpha_i} k_{\beta_i}) \{ 2 \delta_{\beta_i \alpha_{i-1}} (e^{(i)} k_{\beta_i} e_{\alpha_{i-1}}^{(i)} - e_{\beta_i}^{(i)} k_{\alpha_{i-1}}) \} \psi_{\alpha_{i-1}}(k) &= \psi_{\alpha_i}(k) \cdot 2i(e^{(i)} k), \\ \text{für } 1 \leq i \leq r, \text{ da } k_\nu \psi_\nu(k) = 0 \text{ und } k_\nu^2 &= -\mu^2. \end{aligned}$$

Analog erhält man  $2i(e^{(i)} k') \psi_{\beta_{i-1}}^*(k')$  für  $r+1 \leq i \leq n$ , wenn man  $\psi_{\beta_i}^*(k')$  von rechts mit dem obigen Ausdruck multipliziert. Dadurch haben wir dasselbe Problem wie im Falle der Elektronen. Es wird das Übergangselement für die Erzeugung von  $n$  Photonen mit den Impulsen  $k^{(1)}, \dots, k^{(n)}$ :

$$\begin{aligned} \langle k^{(1)}, \dots, k^{(n)}; k' | S | 0; k \rangle &= \\ = \frac{n}{\sqrt{n!}} \left( \frac{e^2}{2} \right)^{n/2} \int dy_0 \exp[-i(k_0 - k'_0) y_0] \psi_s^*(k') (2\omega \bar{A}_0 \delta_{sr} + \bar{A}_r k_s + \bar{A}_s k'_r) \psi_r(k) \cdot L(k, k'), \end{aligned}$$

wo

$$L(k, k') = \sum_{r=0}^n \sum_{p'} \frac{(e^{(1)} k) \cdot \dots \cdot (e^{(r)} k) (e^{(r+1)} k') \cdot \dots \cdot (e^{(n)} k')}{(-k k^{(1)}) \cdot \dots \cdot (-k, k^{(r)}) (k' k^{(r+1)}) \cdot \dots \cdot (k' k^{(n)})} = \prod_{i=1}^n \left( e^{(i)}, \frac{k'}{k' k^{(i)}} - \frac{k}{k k^{(i)}} \right).$$

$\sum_{p'}$  ist die Summe aller Ausdrücke, welche aus dem ursprünglichen durch Vertauschung von Vektoren aus  $(k^{(1)}, \dots, k^{(r)})$  mit solchen aus  $(k^{(r+1)}, \dots, k^{(n)})$

entstehen. Es wird schliesslich:

$$(5) \quad \frac{d\sigma}{d\Omega} = \left(\frac{\alpha Z}{2\mu}\right)^2 \frac{1 - \beta^2}{\beta^4 \sin^4(\vartheta/2)} \left\{ 1 + \frac{\beta^4 \sin^2 \vartheta}{6(1 - \beta^2)} \right\} \frac{\bar{n}(\vartheta)^n}{n!},$$

wo  $\bar{n}(\vartheta)$  durch (2) gegeben ist. Für kleine Photonenergien ist also die mittlere Photonenzahl vom Spin unabhängig.

Schwächen wir die Annahme über die Photonenergien ab zu  $\varepsilon_2 \ll \mu$ , so sind die größten Beiträge von den Termen  $\sim p_{\alpha_i}^{(i)} p_{\beta_i}^{(i)}$  in  $F(i)$  zu erwarten. Wir betrachten daher Ausdrücke der Form

$$K_{ij} = -ip_{\beta_i}^{(i)} \{ B(i, i-1)(-i)\delta_{\alpha_{i-1}\beta_{i-1}} B(i-1, i-2) \dots (-i)\delta_{\alpha_{j+1}\beta_{j+1}} B(j+1, j) + \\ + i[(p^{(i-1)^2} + \mu^2) C(i, i-2)(-i)\delta_{\alpha_{i-2}\beta_{i-2}} B(i-2, i-3) \dots (-i)\delta_{\alpha_{j+1}\beta_{j+1}} B(j+1, j) + \\ + \dots + (p^{(j+1)^2} + \mu^2) B(i, i-1)(-i)\delta_{\alpha_{i-1}\beta_{i-1}} \dots B(j+3, j+2)(-i)\delta_{\alpha_{j+2}\beta_{j+2}} C(j+2, j)] \} p_{\alpha_j}^{(j)}.$$

Der Faktor  $i$  vor der eckigen Klammer kommt daher, daß die entsprechenden Ausdrücke nicht vom  $n$ -ten, sondern vom  $(n-1)$ -ten Entwicklungsglied der  $S$ -Matrix stammen. Höhere Potenzen in  $C$  würden niedrigere Potenzen von  $\omega$  liefern.

Durch vollständige Induktion zeigt man:

$$(6) \quad K_{ij} \sim \mu^2 (-i)^{i-j} (i-j-1)(e^{(j)} p^{(j)}) \dots (e^{(i)} p^{(i)}).$$

Als gemeinsamer Faktor bleibt nur  $\mu^2$ ; die Terme  $\sim k q^{(1)}$  heben sich gegenseitig weg.

Somit bleibt noch die Annahme  $\omega \gg \varepsilon_2 \gg \mu$ . Beschränken wir uns auf longitudinal polarisierte Mesonen im Anfangs- und Endzustand, so kommt für  $n = 2m + 1$  der Hauptbeitrag zur Photonvielfacherzeugung von folgendem Ausdruck:

$$S' = (-i)^{n+1} (-e/\sqrt{2})^n \int dy_0 \exp[-i(k_0 - k'_0)y_0] \sum_{q(i)e(i)} (q_0^{(1)} \dots q_0^{(n)})^{-\frac{1}{2}} \cdot \\ \cdot a^*(q^{(1)}e^{(1)}) \dots a^*(q^{(n)}e^{(n)}) \cdot (-i)^{m+1} (-i/\mu^2)^m \cdot 2^{-m} \cdot \\ \cdot \left\{ \sum_{r \text{ ger.}}^{n-1} \psi_{\beta_n}^*(k') Q(n, n-2) p_{\alpha_{n-2}}^{(n-2)} p_{\beta_{n-2}}^{(n-2)} Q(n-2, n-4) \dots p_{\beta_{r+1}}^{(r+1)} Q(r+1, r) \dots \right. \\ \cdot p_{\beta_r}^{(2)} Q(2, 0) \psi_{\alpha_0}(k) + \sum_{r \text{ ung.}}^n \psi(k') Q(n, n-2) p_{\alpha_{n-2}}^{(n-2)} p_{\beta_{n-2}}^{(n-2)} Q(n-2, n-4) \dots \\ \cdot p'_{\beta_s}(Q(s, r) \dots p_{\beta_s}^{(2)} Q(2, 0) \psi_{\alpha_0}(k)) \cdot \{(k', q^{(n)}) \dots (k', q^{(r+1)} + \dots + q^{(n)}) \cdot \\ \cdot (-k, q^{(1)} + \dots + q^{(r)}) \dots (-k, q^{(1)})\}^{-1}.$$

Dabei bedeutet:

$$Q(i+1, i-1) = B(i+1, i) \delta_{\alpha_i \beta_i} B(i, i-1) - (p^{(i)^2} + \mu^2) C(i+1, i-1),$$

$$\begin{aligned}
Q(r+1, r) &= B(r+1, s) \delta_{\alpha_s \beta_s} D(s, r) - (p'^2 + \mu^2) C(r+1, r), \\
Q(s, r-1) &= D(s, r) \delta_{\beta_r \alpha_r} B(r, r-1) - (p'^2 + \mu^2) C(s, r-1), \\
C(r+1, r) &= e_{\beta_{r+1}}^{(r+1)} \bar{A}_{\alpha_r}, \quad C(s, r-1) = -\bar{A}_{\beta_s} e_{\alpha_{r-1}}^{(r)}, \\
\text{da } \bar{A} e^{(r)} &= \bar{A} e^{(r+1)} = 0.
\end{aligned}$$

Nun ist

$$\begin{aligned}
(7) \quad \bar{Q}(i+1, i-1) &= p_{\beta_{i+1}}^{(i+1)} Q(i+1, i-1) p_{\alpha_{i-1}}^{(i-1)} \sim \\
&\sim - (q^{(i)} q^{(i+1)}) (p^{(i)} e^{(i+1)}) (p^{(i)} e^{(i)}) - (p^{(i)} q^{(i+1)}) (p^{(i)} q^{(i)}) (e^{(i)} e^{(i+1)}).
\end{aligned}$$

Der Erzeugungsquerschnitt läßt sich nun nicht mehr in geschlossener Form auswerten. Wir spezialisieren uns daher auf solche Photonen, für die  $\mathbf{q} \parallel \mathbf{k}^{(1)}$  und  $\mathbf{e}^{(i)} | \mathbf{e} \perp \mathbf{k}, \mathbf{k}^{(1)}$  ist. Damit wird

$$\begin{aligned}
(8a) \quad \bar{Q}(i+1, i-1) &= - (p^{(i)} q^{(i+1)}) (p^{(i)} q^{(i)}), \\
(8b) \quad \bar{Q}(r+1, r) &= p_{\beta_{r+1}}^{(r+1)} Q(r+1, r) p_{\alpha_r}^{(r)} = -\omega A_0(\mathbf{e}\mathbf{k}') (p'^2 - p^{(r)} q^{(r+1)}), \\
(8c) \quad \bar{Q}(s, r-1) &= p_{\beta_s}' Q(s, r-1) p_{\alpha_{r-1}}^{(r-1)} = \omega A_0(\mathbf{e}\mathbf{k}') (p^{(r)2} + k q^{(r)}).
\end{aligned}$$

Für longitudinale Mesonen gilt

$$\psi(k) = (2\omega\mu^2)^{-\frac{1}{2}} (\mathbf{k}|\beta, i\beta\omega) \sim (2\omega\mu^2)^{-\frac{1}{2}} \cdot k, \quad \text{wenn } \beta \sim 1.$$

Daher wird

$$p_{\beta_2}^{(2)} Q(2, 0) \psi_{\alpha_0} \sim \bar{Q}(2, 0) (2\omega\mu^2)^{-\frac{1}{2}}, \quad \psi_{\beta_n}^* Q(n, n-2) p_{\alpha_{n-2}}^{(n-2)} = \bar{Q}(n, n-2) (2\omega\mu^2)^{-\frac{1}{2}}.$$

Dasselbe gilt für  $Q(r+1, r)$  und  $Q(s, r-1)$ .

Mit den Bezeichnungen  $\vartheta = \angle(\mathbf{k}, \mathbf{k}')$ ,  $\theta = \angle(\mathbf{k}, \mathbf{k}^{(1)})$ ,  $\theta' = \angle(\mathbf{k}', \mathbf{k}^{(1)})$  und  $\varphi = \angle\{E(\mathbf{k}, \mathbf{k}), E(\mathbf{k}, \mathbf{k}^{(1)})\}$  wird

$$\cos \theta' = \cos \theta \cos \vartheta + \sin \theta \sin \vartheta \cos \varphi, \quad (\mathbf{e}\mathbf{k}') = \beta\omega \sin \vartheta \sin \varphi$$

und

$$\begin{aligned}
Q(r+1, r) &= -\beta\omega^2 A_0 \sin \vartheta \sin \varphi \{2(k', q^{(r+1)} + \dots + q^{(n)}) - q^{(r+1)} k\}, \\
Q(s, r-1) &= \beta\omega^2 A_0 \sin \vartheta \sin \varphi \{-2k(q^{(1)} + \dots + q^{(r)}) + kq\}.
\end{aligned}$$

Damit wird

$$S' = -i(e/\sqrt{2})^n \int dy_0 \exp[-i(k_0 - k'_0)y_0] \sum_{\sigma^{(i)} e^{(i)}} (q_0^{(1)} \dots q_0^{(n)})^{-\frac{1}{2}} a^*(q^{(1)} e^{(1)}) \dots a^*(q^{(n)} e^{(n)}) \cdot \\ \cdot \mu^{-n+1} (-)^{(n-1)/2} (2\omega\mu^2)^{-1} 2^{-n} \\ \cdot \left\{ \sum_{r \text{ ger.}}^{n-1} \frac{(q^{(1)} k) \dots (q^{(r)} k) (q^{(r+2)} k') \dots (q^{(n)} k') [-2k' (q^{(r+1)} + \dots + q^{(n)}) + q^{(r+1)} k]}{(-k q^{(1)}) \dots (-k, q^{(1)} + \dots + q^{(r)}) (k', q^{(r+1)} + \dots + q^{(n)}) \dots (k', q^{(n)})} + \right. \\ \left. + \sum_{r \text{ unger.}}^n \frac{(q^{(1)} k) \dots (q^{(r-1)} k) (q^{(r+1)} k') \dots (q^{(n)} k') [-2k (q^{(1)} + \dots + q^{(r)}) + q^{(r)} k]}{(-k, q^{(1)}) \dots (-k, q^{(1)} + \dots + q^{(r)}) (k', q^{(r+1)} + \dots + q^{(n)}) \dots (k', q^{(n)})} \right\} \cdot \beta \omega^2 \bar{A}_0 \sin \vartheta \sin \varphi.$$

$$\langle k'; k^{(1)}, \dots, k^{(n)} | S' | k; 0 \rangle = \frac{-i}{\sqrt{n!}} (-)^{(n-1)/2} e^n \beta \omega^2 2^{-\frac{n}{2}} \mu^{-n-1} \bar{A}_0 (k_0^{(1)} \dots k_0^{(n)})^{-\frac{1}{2}} \sin \vartheta \sin \varphi \cdot$$

$$\cdot \int dy_0 \exp[-i(k_0 - k'_0)y_0] \left\{ \sum_{r \text{ ger.}}^{n-1} (-)^r \binom{n}{r} \left[ 2(n-r) - \frac{1-\beta \cos \theta}{1-\beta \cos \theta'} \right] + \right. \\ \left. + \sum_{r \text{ unger.}}^n (-)^r \binom{n}{r} (2r-1) \right\} = \bar{A}_0 (\beta^2 \omega^2 / 4\mu) (\cos \theta - \cos \theta') (1 - \beta \cos \theta')^{-1} \cdot \\ \cdot \sin \vartheta \sin \varphi (k_0^{(1)} \dots k_0^{(n)})^{-\frac{1}{2}} (n!)^{-\frac{1}{2}} (-ie/\sqrt{2}\mu)^n.$$

Daraus folgt

$$(9) \quad \frac{d\sigma}{d\Omega_0} = \left( \frac{\alpha Z}{4\beta\mu} \cdot \frac{\sin \vartheta \sin \varphi}{\sin^2(\vartheta/2)} \cdot \frac{\cos \theta (1 - \cos \vartheta) - \sin \vartheta \sin \theta \cos \varphi}{1 - \beta(\cos \theta \cos \vartheta + \sin \theta \sin \vartheta \cos \varphi)} \right)^2 \frac{\bar{n}^n}{n!}.$$

Dabei ist

$$(10) \quad \bar{n} = (e^2/2\mu^2) (\Delta\Omega/8\pi^3) \int_0^{\varepsilon_1} dq_0 q_0 = (\alpha\Delta\Omega/2) (\varepsilon_2/2\pi\mu)^2.$$

$\Omega_0 = \Omega_0(\vartheta, \varphi)$ .  $\Delta\Omega$  ist jenes Raumwinkelelement, innerhalb dessen (8a) noch eine gute Näherung für (7) darstellt. Mit  $(\alpha/8\pi^2) = 0.924 \cdot 10^{-1}$  und  $\Delta\Omega = 10^{-1}$  wird

$$(11) \quad \bar{n} = 0.9 \cdot 10^{-5} (\varepsilon_2/\mu)^2.$$

Nach (11) nimmt  $\bar{n}$  sehr rasch mit der maximalen Photonenergie zu. Für  $n \sim 10$  müßte  $\varepsilon_2 \sim 10^3 \mu$  betragen. Dies würde für  $\omega \sim 10^3$  bis  $10^4$  MeV bedeuten, daß die Masse des Vektorteilchens in der Größenordnung der Elektronenmasse läge. Die Schwierigkeit der Interpretation liegt darin, dass  $\bar{n}$  wegen seines raschen Anstieges mit  $\varepsilon_2$  auch wesentlich größere Werte annehmen kann.



## RIASSUNTO (\*)

Per elettroni e mesoni vettoriali di elevata energia si discute il numero medio di quanti di frenamento nella più bassa approssimazione della teoria delle perturbazioni. Per energie fotoniche minori il numero medio di fotoni  $m$  è indipendente dallo spin e cresce logaritmicamente con l'energia primaria e l'energia fotonica massima. A energie fotoniche maggiori, pei mesoni vettoriali  $n$  aumenta quadraticamente con l'energia fotonica massima.

---

(\*) *Traduzione a cura della Redazione.*

**Electronic States of Diatomic Molecules: the  $O_2^+$  Molecular Ion (\*).**

F. BASSANI (+), E. MONTALDI and F. G. FUMI

*Istituto di Scienze Fisiche dell'Università - Milano  
Gruppo di Fisica dei Solidi*

(ricevuto il 25 Gennaio 1956)

**Summary.** — The scheme proposed by FUMI and PARR for the calculation of electronic energy levels of diatomic molecules is applied to the oxygen molecular ion in the  $\pi$ -electron approximation, using one empirical parameter. The vertical excitation energies from the ground state  $^2H_g$  to the  $^4H_u$  and  $^2H_u$  states are computed as functions of distance between 1.01 Å and 1.46 Å, and they agree with the observed values within 0.1 eV. The relative position of the  $^4H_u$  and  $^2H_u$  states is predicted correctly. The excitation energies to the unobserved states  $^2\Phi_u$ ,  $^4H_g$  and  $^2\Phi_g$  were also computed, but should be considered of purely indicative value.

1. — Two years ago FUMI and PARR <sup>(1)</sup> proposed a scheme to calculate the electronic energy levels of diatomic molecules «with fair accuracy and minimum labour» and they applied it to the oxygen molecule with excellent results. The scheme is based on the method of antisymmetrized molecular orbitals, with configuration interaction, and uses the atoms-in-molecules correction <sup>(2,3)</sup> and the approximation of zero overlap in the core terms and zero differential overlap in the electronic repulsion terms <sup>(4)</sup>.

(\*) This work was supported by grants from the National Research Council. A preliminary report on it was presented by R. FIESCHI at the Symposium on the Quantum Theory of Molecules held in Stockholm and Uppsala on March 21-25, 1955 (*Svensk Kemisk Tidskrift*, **67**, 394 (1955)).

(+) Currently at the Department of Physics, University of Illinois USA, for the academic years 1954-55 and 1955-56.

(1) F. G. FUMI and R. G. PARR: *Journ. Chem. Phys.*, **21**, 1864 (1953). In Table I of this paper, for  $g$  read  $\bar{g}$ .

(2) W. MOFFITT: *Proc. Roy. Soc. (London)*, **A 210**, 246 (1951).

(3) R. PARISER: *Journ. Chem. Phys.*, **21**, 568 (1953).

(4) R. G. PARR: *Journ. Chem. Phys.*, **20**, 1499 (1952).

For a second application of this scheme we have chosen the oxygen molecular ion which has in common with the oxygen molecule the simplifying feature that its low excited states can be accounted for qualitatively on the  $\pi$ -electron approximation. We refer to the states  ${}^2\Pi_g$ ,  ${}^4\Pi_u$  and  ${}^2\Pi_u$  in order of increasing energy; the next higher observed state,  ${}^4\Sigma_g^-$ , requires the excitation of  $\sigma$  electrons and has not been considered in our treatment.

2. - The qualitative interpretation of the low excited states of  $O_2^+$  requires only two configurations (5):

$$(1) \quad (A) \quad [KK(\sigma_g 2s)^2(\sigma_u 2s)^2(\sigma_g 2p)^2](\pi_u 2p)^4(\pi_g 2p)$$

$$(2) \quad (B) \quad [KK(\sigma_g 2s)^2(\sigma_u 2s)^2(\sigma_g 2p)^2](\pi_u 2p)^3(\pi_g 2p)^2.$$

The (A) configuration gives a  ${}^2\Pi_g$  state, while the (B) configuration gives three  ${}^2\Pi_u$  states, a  ${}^4\Pi_u$  state and a  ${}^2\Phi_u$  state. These include the three lower observed states of  $O_2^+$ .

To develop a quantitative treatment of these states on the  $\pi$ -electron approximation we must consider two other configurations:

$$(3) \quad (C) \quad [KK(\sigma_g 2s)^2(\sigma_u 2s)^2(\sigma_g 2p)^2](\pi_u 2p)^2(\pi_g 2p)^3$$

$$(4) \quad (D) \quad [KK(\sigma_g 2s)^2(\sigma_u 2s)^2(\sigma_g 2p)^2](\pi_u 2p)(\pi_g 2p)^4.$$

TABLE I. - Wave functions for some electronic states of  $O_2^+$ .

State	Configuration	Wave function (*)
${}^2\Pi_g$	A	$(u^+\bar{u}^+u^-\bar{u}^-g^+) = \Psi_A$
	C	$(g^+g^-\bar{g}^-u^+\bar{u}^+) = \Psi_{C_1}$
	C	$6^{-\frac{1}{2}}[(g^+\bar{g}^+g^-u^+\bar{u}^-) + (g^+\bar{g}^+g^-\bar{u}^+u^-) - 2(g^+\bar{g}^+\bar{g}^-u^+u^-)] = \Psi_{C_2}$
	C	$2^{-\frac{1}{2}}[(g^+\bar{g}^+g^-u^+\bar{u}^-) - (g^+\bar{g}^+g^-\bar{u}^+u^-)] = \Psi_{C_3}$
${}^2\Pi_u$	D	$(g^+\bar{g}^+g^-\bar{g}^-u^+) = \Psi_D$
	B	$(u^+u^-\bar{u}^-g^+\bar{g}^+) = \Psi_{B_1}$
	B	$6^{-\frac{1}{2}}[(u^+\bar{u}^+u^-g^+\bar{g}^-) + (u^+\bar{u}^+u^-\bar{g}^+g^-) - 2(u^+\bar{u}^+\bar{u}^-g^+g^-)] = \Psi_{B_2}$
	B	$2^{-\frac{1}{2}}[(u^+\bar{u}^+u^-g^+\bar{g}^-) - (u^+\bar{u}^+u^-\bar{g}^+g^-)] = \Psi_{B_3}$
	B	$(u^+\bar{u}^+u^-g^+g^-) = \Psi_B$

(\*) Here  $(u^+\bar{u}^+u^-\bar{u}^-g^+)$ , for example, represents the normalized Slater determinant, a typical term in the expansion of which is  $(5!)^{-\frac{1}{2}}[(\pi_u^+\alpha)^2(\pi_u^+\beta)^2(\pi_u^-\alpha)^2(\pi_u^-\beta)^2(\pi_g^+\alpha)^2]$  where  $\alpha$  and  $\beta$  are one-electron spin functions and superscripts denote electrons.

(5) G. HERZBERG: *Spectra of Diatomic Molecules* (New York, 1950), pp. 343, 346 and 560.

The first of these gives rise to three  ${}^2\Pi_g$  states, a  ${}^4\Pi_g$  state and a  ${}^2\Phi_g$  state, while the second gives a  ${}^2\Pi_u$  state.

The wave functions for these states are constructed by the standard procedure. A peculiarity arises in the resolution of the degeneracy of the Slater determinants for the (B) and (C) configurations, which is formally analogous to one discussed in Slater's lectures <sup>(6)</sup> and is resolved in an analogous fashion.

Table I gives the wave functions for the states  ${}^2\Pi_g$ ,  ${}^4\Pi_u$  and  ${}^2\Pi_u$ : since we neglect spin-orbit coupling, it is sufficient to give only the simplest multiplet component for each state. We will not quote the detailed results for the states  ${}^2\Phi_u$ ,  ${}^4\Pi_g$  and  ${}^2\Phi_g$  (see section 5).

3. — The energy formulas for the states  ${}^2\Pi_g$ ,  ${}^4\Pi_u$  and  ${}^2\Pi_u$  in terms of integrals over *MO*'s are given in Table II.

Table III gives the energy formulas in terms of integrals over *AO*'s. To obtain these formulas from Table II one uses the appropriate LCAO forms for the molecular orbitals  $\pi_u^\pm$  and  $\pi_g^\pm$ , the assumption of zero overlap in the core terms and the assumption of zero differential overlap in the electronic repulsion terms <sup>(1)</sup>. A justification for the approximations of zero overlap and zero differential overlap in diatomic molecules has been given by FUMI and PARR (ref. <sup>(1)</sup>, appendix).

4. — Table IV gives the values we have used for the integrals over atomic orbitals which appear in Table III. For the two-centre integrals ( $aa|bb$ ) and ( $aa|b_s b_s$ ) we take the *theoretical* values given by KOPINECK <sup>(7)</sup> for Slater  $2p\pi$  *AO*'s of effective charge 4.725, equal to the average of the effective charges of O and  $O^+$ .

To determine the values of the one-centre integrals we follow a procedure of the type proposed by PARISER <sup>(8)</sup> which had been applied successfully in the case of the oxygen molecule <sup>(1)</sup>. This procedure is based on an analysis of the valence states of interest. The valence states to be considered for O,  $O^+$  and  $O^-$  are listed in the paper by FUMI and PARR (ref. <sup>(1)</sup>, Table VI) and their energies were determined by a Mulliken-type treatment (ref. <sup>(1)</sup>, Table VII). Here we need to consider anew only the valence state  $O^{++}(V_2)$ ,  $\sigma\pi$ : the energy of this state referred to O,  ${}^3P$  is  $49.4 \text{ eV} = (13.6 + 35.2 + 0.6) \text{ eV}$ , where 35.2 eV is the value of the ionization potential for  $O^+$  and

$$0.6 \text{ eV} = \frac{1}{4} \left[ \frac{O^{++}(1D) - O^{++}(3P)}{2} + \frac{O^{++}(1S) - O^{++}(3P)}{5} \right] \quad (8).$$

<sup>(6)</sup> J. C. SLATER: *Electronic Structure of Atoms and Molecules*, in *Technical Report No. 3, M.I.T. Solid State and Molecular Theory Group* (1953), pp. 24-25.

<sup>(7)</sup> H. J. KOPINECK: *Zeits. f. Naturforsch.*, **5a**, 420 (1950).

<sup>(8)</sup> Spectral data and ionization potentials are taken from Landolt-Börnstein Tables, Vol. I, 1950, as in reference <sup>(1)</sup>.



TABLE II. — Energy formulas in terms of integrals over molecular orbitals (\*,†).

$I(\pi_u)$	$I(\pi_g)$	$J(\pi_u^+, \pi_u^+)$	$J(\pi_g^+, \pi_g^+)$	$J(\pi_u^+, \pi_g^+)$	$K(\pi_u^+, \pi_u^+)$	$K(\pi_g^+, \pi_g^+)$	$K(\pi_u^+, \pi_g^+)$	$K(\pi_u^+, \pi_g^-)$
${}^2\Pi_g(A)$	4	1	6	0	4	-2	-1	-1
${}^2\Pi_g(C_1)$	2	3	1	3	6	0	-2	-1
${}^2\Pi_g(C_2)$	2	3	1	3	6	-1	-1	-1
${}^2\Pi_g(C_3)$	2	3	1	3	6	1	-1	-1
${}^2\Pi_g(AC_1)$	...	...	...	...	...	...	...	...
${}^2\Pi_g(AC_2)$	...	...	...	...	...	...	...	...
${}^2\Pi_g(AC_3)$	...	...	...	...	...	...	...	...
${}^2\Pi_g(C_1C_2)$	...	...	...	...	...	...	...	...
${}^2\Pi_g(C_1C_3)$	...	...	...	...	...	...	...	...
${}^2\Pi_g(C_2C_3)$	...	...	...	...	...	...	...	...
${}^2\Pi_u(D)$	1	4	0	6	4	0	-1	-1
${}^2\Pi_u(B_1)$	3	2	3	1	6	-1	-2	-1
${}^2\Pi_u(B_2)$	3	2	3	1	6	-1	-1	-1
${}^2\Pi_u(B_3)$	3	2	3	1	6	-1	-1	-1
${}^2\Pi_u(DB_1)$	...	...	...	...	...	...	...	...
${}^2\Pi_u(DB_2)$	...	...	...	...	...	...	...	...
${}^2\Pi_u(DB_3)$	...	...	...	...	...	...	...	...
${}^2\Pi_u(B_1B_2)$	...	...	...	...	...	...	...	...
${}^2\Pi_u(B_1B_3)$	...	...	...	...	...	...	...	...
${}^2\Pi_u(B_2B_3)$	...	...	...	...	...	...	...	...
${}^4\Pi_u(B)$	3	2	3	1	6	-1	-2	-1

(\*) Here  ${}^2\Pi_g(A)$ , for example, denotes the energy of the  ${}^2\Pi_g$  state of the (A) configuration, while  ${}^2\Pi_g(AC_1)$  denotes the interaction matrix element between the  ${}^2\Pi_g$  state of the (A) configuration and the first  ${}^2\Pi_g$  state of the (C) configuration.

(†) The integrals are defined as follows:  $I(\phi) = \int \phi^* H_{\text{core}} \phi dv$ ,  $J(\phi_k, \phi_l) = \int \phi_k^*(1) \phi_l^*(2) (e^2/r_{12}) \phi_k(1) \phi_l(2) dr_1 dr_2$ ,  $K(\phi_k, \phi_l) = \int \phi_k^*(1) \phi_l^*(2) (e^2/r_{12}) \phi_k(1) \phi_l(2) dr_1 dr_2$ , and  $(\phi_k \phi_l | \phi_k \phi_l) = \int \phi_k^*(1) \phi_l^*(2) \phi_k(1) \phi_l(2) dr_1 dr_2$ .

TABLE III. — Energy formulas in terms of integrals over atomic orbitals (\*), (+), (×).

	$\frac{1}{8}(aa aa)$	$\frac{1}{8}(aa a_s a_s)$	$\frac{1}{8}(aa bb)$	$\frac{1}{8}(aa b_s b_s)$	Core contribution
${}^2\Pi_g(A)$ , ${}^2\Pi_u(D)$	6	30	18	26	$5\alpha+3\beta$ , $5\alpha-3\beta$
${}^2\Pi_g(C_1)$ , ${}^2\Pi_u(B_1)$	6	30	26	18	$5\alpha-\beta$ , $5\alpha+\beta$
${}^2\Pi_g(C_2)$ , ${}^2\Pi_u(B_2)$	9	29	15	27	$5\alpha-\beta$ , $5\alpha+\beta$
${}^2\Pi_g(C_3)$ , ${}^2\Pi_u(B_3)$	11	23	29	17	$5\alpha-\beta$ , $5\alpha+\beta$
${}^2\Pi_g(AC_1)$ , ${}^2\Pi_u(DB_1)$	2	2	-2	-2	0 , 0
${}^2\Pi_g(AC_2)$ , ${}^2\Pi_u(DB_2)$	$-\sqrt{6}$	$3\sqrt{6}$	$\sqrt{6}$	$-3\sqrt{6}$	0 , 0
${}^2\Pi_g(AC_3)$ , ${}^2\Pi_u(DB_3)$	$3\sqrt{2}$	$-\sqrt{2}$	$-3\sqrt{2}$	$\sqrt{2}$	0 , 0
${}^2\Pi_g(C_1C_2)$ , ${}^2\Pi_u(B_1B_2)$	$\sqrt{6}$	$\sqrt{6}$	$-\sqrt{6}$	$-\sqrt{6}$	0 , 0
${}^2\Pi_g(C_1C_3)$ , ${}^2\Pi_u(B_1B_3)$	$-3\sqrt{2}$	$5\sqrt{2}$	$-5\sqrt{2}$	$3\sqrt{2}$	0 , 0
${}^2\Pi_g(C_2C_3)$ , ${}^2\Pi_u(B_2B_3)$	$-\sqrt{3}$	$3\sqrt{3}$	$\sqrt{3}$	$-3\sqrt{3}$	0 , 0
${}^4\Pi_u(B)$	0	32	24	24	$5\alpha+\beta$

(\*) See Table II footnote (\*).

(+) The matrix elements  ${}^2\Pi_g(A)$  and  ${}^2\Pi_u(D)$  differ only in their core contributions, which are respectively  $5\alpha+3\beta$  and  $5\alpha-3\beta$ . Similar statements hold for the matrix elements listed in the following lines.

(×) The integrals are defined as follows:  $(pq|rs) = \int \chi_p(1)\chi_q(1)(e^2/r_{12})\chi_r(2)\chi_s(2)d\mathbf{v}$ ,  $\alpha = \int \chi_a H_{\text{core}} \chi_a d\mathbf{v}$  and  $\beta = \int \chi_b H_{\text{core}} \chi_a d\mathbf{v}$ , where  $\chi_p$ ,  $\chi_q$ ,  $\chi_r$  and  $\chi_s$  are Slater AO's from the set  $a$ ,  $a_s$ ,  $b$ ,  $b_s$ .

TABLE IV. — Values of integrals (eV) (\*).

	Internuclear distance (Å)					
	0	1.008	1.120	1.232	1.344	1.456
$(aa bb)$	16.90	12.680	11.646	10.750	9.972	9.292
$(aa b_s b_s)$	14.98	12.389	11.444	10.610	9.874	9.223
$-\beta$	—	5.546	4.257	3.291	2.500	1.918

(\*) See Table III, footnote (×), for definitions of integrals.

To determine  $(aa|aa)$  and  $(aa|a_s a_s)$  we use processes of the type  $O^+ + O \rightarrow O^{++} + O^-$ , for which the differences between the various  $\alpha$ 's should average out in the net value for the energy change involved. There are three such processes:

$$(5) \quad O^+({}^1V_1) + O(V_2) \rightarrow O^{++}(V_2) + O^-(V_1), \quad \Delta E = -(aa|aa) + 3(aa|a_s a_s) = 28.1 \text{ eV}$$

$$(6) \quad O^+(V_1) + O(V_2) \rightarrow O^{++}(V_2) + O^-(V_1), \quad \Delta E = 2(aa|a_s a_s) = 29.8 \text{ eV}$$

$$(7) \quad O^+({}^3V_1) + O(V_2) \rightarrow O^{++}(V_2) + O^-(V_1), \quad \Delta E = (aa|aa) + (aa|a_s a_s) = 32.0 \text{ eV}$$

and by a least-squares method we find

$$(8) \quad (aa|aa) = 16.90 \text{ eV}, \quad (aa|a_s a_s) = 14.98 \text{ eV}.$$

The core parameter  $\alpha$  does not enter in the excitation energies. The core parameter  $\beta$  is taken as an empirical parameter and is fitted to the observed excitation energy  ${}^4\Pi_u - {}^2\Pi_g$ , obtained from Morse curves for these states. The appendix describes the procedure adopted to perform the fitting. The values obtained for  $\beta$  are included in Table IV. An alternative fitting of  $\beta$  to the observed excitation energy  ${}^2\Pi_u - {}^2\Pi_g$  has also been done, and gave almost identical results.

It should be noted here that the justification given by FUMI and PARR (ref. (1), appendix) for the approximations of zero overlap and zero differential overlap in diatomic molecules is strictly valid only if one uses for the one-centre and two-centre integrals values which correspond to the same effective charge, in particular if one uses *theoretical* values also for the one-centre integrals. In this respect two attitudes are possible (9): 1) one may simply *assume* with PARISER and PARR (9) that the atoms-in-molecules correction (2,3) and the approximations of zero overlap and zero differential overlap (4) are compatible, or 2) one may introduce appropriate corrections for the slight incompatibility, following the attitude that PARISER and PARR (9) attribute to MOSER (10). In either case the formulas for the excitation energies in terms of integrals over AO's for the states of  $O_2$  considered by FUMI and PARR (1), and the analogous formulas for the states of  $O_2^+$  considered here, remain unchanged. This is at once obvious if one adopts the first attitude: it is true also if one adopts the second attitude because the corrections practically cancel out (\*). The quantity which is affected if one adopts the attitude of MOSER is the empirical  $\beta$ : obviously, if one adopts the attitude of PARISER and PARR  $\beta$  is also unchanged. For the moment we do not wish to attach any particular significance to the empirical  $\beta$ , and thus we can safely take the attitude of PARISER and PARR (9).

5. - Table V gives the electronic excitation energies from the ground state  ${}^2\Pi_g$  to the  ${}^4\Pi_u$  and  ${}^2\Pi_u$  states of  $O_2^+$ , computed with the energy formulas of

(9) R. G. PARR and R. PARISER: *Journ. Chem. Phys.*, **23**, 711 (1955): section IV C.

(10) C. M. MOSER: *Journ. Chem. Phys.*, **21**, 2098 (1953).

(\*) Formally this is so because the molecular integrals  $J(\pi_u^+, \pi_u^+)$  and  $J(\pi_g^+, \pi_g^+)$  which have equal and opposite corrections of the first order in  $S$  ( $S$ , overlap integrals for  $2p\pi$  AO's) appear always in the same fashion in these excitation energies, while the other molecular integrals of interest have only small corrections of the first order in  $S$ , or corrections of the second order in  $S$ . The corrections are as follows:  $J(\pi_u^+, \pi_u^+)$ ,  $+\frac{1}{2}SA_1$ ;  $J(\pi_g^+, \pi_g^+)$ ,  $-\frac{1}{2}SA_1$ ;  $J(\pi_u^+, \pi_g^+)$ ,  $-\frac{1}{4}S^2A_1$ ;  $K(\pi_u^+, \pi_u^-)$ ,  $+SA_2$ ;  $K(\pi_g^+, \pi_g^-)$ ,  $-SA_2$ ;  $K(\pi_u^+, \pi_g^-)$ ,  $-\frac{1}{2}S^2A_2$ ;  $K(\pi_u^+, \pi_g^+)$ ,  $-\frac{1}{4}S^2A_1$ ;  $(\pi_u^+ \pi_u^+ | \pi_g^- \pi_g^-)$ ,  $-\frac{1}{2}S^2A_2$ , where  $A_1 = [(aa|aa)_t - (aa|aa)_c] + [(aa|a_s a_s)_t - (aa|a_s a_s)_c]$  and  $A_2 = [(aa|aa)_t - (aa|aa)_c] - [(aa|a_s a_s)_t - (aa|a_s a_s)_c]$  ( $t$ , theoretical integral;  $c$ , integral with the atoms-in-molecules correction).

Table III and the values for the integrals given in Table IV. The experimental values for the excitation energies quoted in Table V are obtained by computing Morse curves for the states involved from the experimental data (<sup>5</sup>): they are accurate to about 0.1 eV. The values of the Morse parameters for the states  ${}^2\Pi_g$ ,  ${}^4\Pi_u$  and  ${}^2\Pi_u$  are given in Table VI.

TABLE V. — *Electronic excitation energies in  $O_2^+$  (eV) (\*)*.

		Internuclear distance (Å) (+)				
		1.008	1.120	1.232	1.344	1.456
${}^4\Pi_u$	calculated	8.874	6.062	4.015	2.573	1.607
	observed	8.874	6.062	4.015	2.573	1.607
${}^2\Pi_u$	calculated	9.743	6.961	4.930	3.457	2.452
	observed	9.745	7.002	4.947	3.459	2.401

(\*) Excitation energies are relative to the  ${}^4\Pi_g$  ground state.

(+) The equilibrium internuclear distance for the ground state is 1.1227 Å.

TABLES VI. — *Morse parameters for some states of  $O_2^+$  (\*)*.

State	$D_e$ (eV)	$\beta$ (Å <sup>-1</sup> )	$r_e$ (Å)
${}^2\Pi_g$	6.5958	2.8013	1.1227
${}^4\Pi_u$	2.6421	2.4430	1.3813
${}^2\Pi_u$	1.7875	2.5811	1.4089

(\*) For definitions of the Morse parameters see HERZBERG: *Spectra of Diatomic Molecules* (New York, 1950), p. 101, eqs. (III-98) and (III-100). In particular  $D_e({}^2\Pi_g) = D_0 + \frac{1}{2}\omega_e({}^2\Pi_g)$ ;  $D_e({}^4\Pi_u) = D_e({}^2\Pi_g) - T_e({}^4\Pi_u)$  and  $D_e({}^2\Pi_u) = D_e({}^2\Pi_g) - T_e({}^2\Pi_u)$ .

Our theoretical results agree with the experimental values within 0.1 eV. This indicates that the  $\pi$ -electron approximation is valid for the  ${}^2\Pi_g$ ,  ${}^4\Pi_u$  and  ${}^2\Pi_u$  states of  $O_2^+$  to a surprising accuracy.

We do not quote the detailed results that we have obtained for the unobserved states  ${}^2\Phi_u$ ,  ${}^4\Pi_g$ , and  ${}^2\Phi_g$  since we feel that they can have only an indicative value. Indeed the  ${}^2\Phi_u$  state turns out to fall in the energy region of the  ${}^4\Sigma_g$  state, which involves the excitation of the  $\sigma$ -electrons, and the states  ${}^4\Pi_g$  and  ${}^2\Phi_g$  come out well above it. We find that the  ${}^2\Phi_u$  state is roughly 1 eV above the  ${}^2\Pi_u$  state, while the  ${}^4\Pi_g$  and  ${}^2\Phi_g$  states are several volts above the  ${}^2\Pi_u$  state, the  ${}^2\Phi_g$  state being above the  ${}^4\Pi_g$  state by a couple of volts. The  ${}^2\Phi_u$  state appears to be stable, with a  $D_e$  of the order of 2.5 eV. The  ${}^4\Pi_g$  and  ${}^2\Phi_g$  states seem also to be stable.



\* \* \*

One of us (F.G.F.) is happy to thank Professor ROBERT G. PARR for the helpful discussions he had with him in Milan in November 1953 when this work was first undertaken. The absence of two of us (F.G.F. and F.B.) from Italy for the academic year 1954-55 unfortunately delayed the completion of the work (\*).

## APPENDIX

### Determination of the empirical $\beta$ .

The most obvious method to fit  $\beta$  to the observed excitation energy  ${}^4\Pi_u - {}^2\Pi_g$  is numerically rather laborious since it involves for each internuclear distance the solution of the fourth-order secular equation for the  ${}^2\Pi_g$  state for different values of  $\beta$ , to find the value of  $\beta$  for which the calculated excitation energy  ${}^4\Pi_u - {}^2\Pi_g$  equals the observed one. We have avoided this procedure by the formal artifice of transforming the secular equation for the  ${}^2\Pi_g$  state into a linear equation in  $\beta$ . The secular equation for the  ${}^2\Pi_g$  state reads

$$(9) \quad \|H_{ik} - \delta_{ik}W'\| = 0, \quad (i, k = 1, 2, 3, 4)$$

where for convenience of notation we have used the indices 1, 2, 3 and 4 to denote respectively the  ${}^2\Pi_g$  state of the  $A$  configuration and the first, second and third  ${}^2\Pi_g$  state of the  $C$  configuration. If we put now  $W' = x + H_{44}$ , equation (9) becomes

$$(10) \quad \|H'_{ik} - \delta_{ik}x\| = 0,$$

where  $H'_{ik} = H_{ik}$  for  $i \neq k$ , and  $H'_{kk} = H_{kk} - H_{44}$ . Equation (10) is linear in  $\beta$  since only  $H'_{11}$  depends on  $\beta$  and this dependence is linear. We can then easily solve equation (10) for  $\beta$  as a function of  $x$ , and plot the results in a graph. Now, if we denote by  $W$  the experimental value of the excitation energy  ${}^4\Pi_u - {}^2\Pi_g$ , we have:

$$(11) \quad W = H_{BB} - H_{44} - x = 2\beta - x + A$$

where  $A = \frac{1}{8}[-11(aa|aa) + 9(aa|a_s a_s) - 5(aa|bb) + 7(aa|b_s b_s)]$ . In the  $x, \beta$  plane, equation (11) represents a straight line and the intersections of this straight line with the  $\beta, x$  curve obtained from equation (10) give the solutions

(\*) Professor PARR now informs the authors that the formulas of Tables I-III had recently been derived independently by his coworker Dr. PETER G. LYKOS, who had also obtained numerical results in substantial agreement with Table V.

of the system formed by equations (10) and (11). Obviously we must take the solution which corresponds to the lowest value of  $x$ . The procedure is repeated for each internuclear distance, taking in each case the appropriate values for the observed excitation energy  $W$  and for the two-centre integrals.

The alternative fitting of  $\beta$  to the observed excitation energy  ${}^2\Pi_u$ - ${}^2\Pi_g$  can be done quite easily by transforming both the secular equations for the  ${}^2\Pi_g$  and  ${}^2\Pi_u$  states into linear equations in  $\beta$ .

---

### RIASSUNTO

Lo schema proposto da FUMI e PARR per il calcolo dei livelli elettronici di molecole biatomiche viene applicato allo ione molecolare di ossigeno nella approssimazione degli elettroni  $\pi$  usando un parametro empirico. Le energie di eccitazione verticali dallo stato fondamentale  ${}^2\Pi_g$  agli stati  ${}^4\Pi_u$  e  ${}^2\Pi_u$  sono calcolate in funzione della distanza fra 1.01 Å ed 1.46 Å, e concordano con i valori osservati entro 0.1 eV. La posizione relativa degli stati  ${}^4\Pi_u$  e  ${}^2\Pi_u$  è prevista correttamente. Le energie di eccitazione agli stati non osservati  ${}^2\Phi_u$ ,  ${}^4\Pi_g$  e  ${}^2\Phi_g$  sono anche state calcolate, ma devono essere considerate puramente indicative.

## Les équations approchées de la théorie du champ unifié d'Einstein-Schrödinger.

M. A. TONNELAT

*Faculté des Sciences - Institut Henri Poincaré - Paris*

(ricevuto il 3 Febbraio 1956)

**Summary.** — Approximated equations are obtained from rigorous and general solutions  $\Gamma_{\mu\nu}^0(g_{\lambda\epsilon})$  and without any hypotheses about the order of the  $\gamma_{\mu\nu}=g_{\mu\nu}$ . Some physical interpretations of these results are given. The stress-moment tensor is pointed out of the equations of gravitation and some possibilities appear of obtaining the equations of motion of a charged particle.

Les principes de la théorie d'Einstein-Schrödinger <sup>(1)</sup> conduisent à étendre les équations de la Relativité générale valables dans le cas extérieur. Les lois du champ unifié se traduisent encore par les équations sans second membre:

$$(I) \quad R_{\mu\nu}(I) - \lambda g_{\mu\nu} = 0 ;$$

$R_{\mu\nu}$  étant le tenseur de Ricci formé à partir d'une connexion quelconque  $\Gamma_{\sigma\epsilon}^0$ :

$$(1) \quad R_{\mu\nu} = \partial_\epsilon \Gamma_{\mu\nu}^0 - \partial_\nu \Gamma_{\mu\epsilon}^0 + \Gamma_{\mu\nu}^\lambda \Gamma_{\lambda\epsilon}^0 - \Gamma_{\mu\epsilon}^\lambda \Gamma_{\lambda\nu}^0 .$$

Il faut alors que le tenseur d'énergie-impulsion — tenseur « matériel » et tenseur électromagnétique — soit extrait de  $R_{\mu\nu}$  lui-même.

Pour obtenir les équations du champ, il est nécessaire de remplacer dans (I)

<sup>(1)</sup> A. EINSTEIN: *The Meaning of Relativity* (1953): Appendice à la 4<sup>ème</sup> édition.

les coefficients de connexion affine  $\Gamma_{\mu\nu}^o$  par leur valeur en fonction du tenseur fondamental  $g_{\mu\nu}$ . L'expression des  $\Gamma_{\mu\nu}^o$  est déduite d'une 2<sup>e</sup> groupe d'équations:

$$(II) \quad \begin{cases} (a) \quad g_{\mu\nu;\varrho} = \frac{2}{3}(g_{\mu\varrho}\Gamma_\nu + g_{\nu\varrho}\Gamma_\mu) \\ (b) \quad \partial_\varrho(\sqrt{-g} f^{\mu\varrho}) = 0 \end{cases}$$

en posant

$$(2) \quad \Gamma_\mu = \Gamma_{\mu\varrho}^o = \frac{1}{2}(\Gamma_{\mu\varrho}^o - \Gamma_{\varrho\mu}^o)$$

$$(3) \quad f^{\mu\nu} = g_{\mu\nu}^{\mu\nu} = \frac{1}{2}(g^{\mu\nu} - g^{\nu\mu}).$$

Aux termes en  $\lambda$  près, (I) et (II) découlent nécessairement d'un principe variationnel appliqué à la densité scalaire  $A = \int G^{\mu\nu} R_{\mu\nu} d\tau$ .

Enfin, en effectuant le changement de connexion

$$(4) \quad L_{\mu\nu}^o = \Gamma_{\mu\nu}^o + \frac{2}{3}\delta_\mu^\varrho \Gamma_\nu \quad L_\mu = L_{\mu\varrho}^o = 0$$

les équations (I) et (II) ont l'expression suivante en fonction de la nouvelle connexion  $L_{\sigma\varrho}^o$  à vecteur de torsion nul:

$$(I)' \quad W_{\mu\nu}(L) - \lambda g_{\mu\nu} = \frac{2}{3}(\partial_\mu \Gamma_\nu - \partial_\nu \Gamma_\mu);$$

$$(II)' \quad \begin{cases} (a) \quad D_\varrho g_{\mu\nu} = \partial_\varrho g_{\mu\nu} - L_{\mu\varrho}^\sigma g_{\sigma\nu} - L_{\nu\varrho}^\sigma g_{\mu\sigma} = 0, \\ (b) \quad \partial_\varrho(\sqrt{-g} f^{\mu\varrho}) = 0, \end{cases}$$

$W_{\mu\nu}(L)$  étant le tenseur de Ricci formé à partir de la connexion  $L_{\sigma\varrho}^o$ :

$$(1)' \quad W_{\mu\nu} = \partial_\varrho L_{\mu\nu}^o - \partial_\nu L_{\mu\varrho}^o + L_{\mu\nu}^\lambda L_{\lambda\varrho}^o - L_{\mu\varrho}^\lambda L_{\lambda\nu}^o.$$

## 1. — Les équations rigoureuses des champs.

Scindons le tenseur fondamental  $g_{\mu\nu}$  et la connexion affine  $L_{\mu\nu}^o$  en parties symétrique et antisymétrique. Posons

$$(5) \quad g_{\mu\nu} = \gamma_{\mu\nu} + \varphi_{\mu\nu},$$

$$(6) \quad L_{\mu\nu}^o = L_{\mu\nu}^o + L_{\mu\nu}^o = \left\{ \begin{matrix} \varrho \\ \mu\nu \end{matrix} \right\} + u_{\mu\nu}^c + L_{\mu\nu}^o,$$



$\left\{ \begin{smallmatrix} \varrho \\ \mu\nu \end{smallmatrix} \right\}$  représentant les symboles de Christoffel formés à l'aide des  $\gamma_{\sigma\tau}$  et  $u_{\mu\nu}^{\varrho}$  désignant le reste de la partie symétrique de la connexion.

Les équations (I)' se partagent en 2 groupes, antisymétrique et symétrique qui s'écrivent ainsi:

$$(7) \quad W_{\underset{\vee}{\mu}\nu} = \nabla_{\varrho} L_{\underset{\vee}{\mu}\nu}^{\varrho} + L_{\underset{\vee}{\mu}\nu}^{\varrho} u_{\varrho} - (u_{\mu\varrho}^{\lambda} L_{\underset{\vee}{\lambda}\nu}^{\varrho} + u_{\lambda\nu}^{\varrho} L_{\underset{\vee}{\mu}\varrho}^{\lambda}) = -\frac{\chi}{2} F_{\mu\nu} + \lambda \varphi_{\mu\nu},$$

$$(8) \quad W_{\underset{\vee}{\mu}\nu} = G_{\mu\nu} + \nabla_{\varrho} u_{\mu\nu}^{\varrho} - \frac{1}{2} \nabla_{\mu} \nabla_{\nu} \log g + \\ + u_{\mu\nu}^{\varrho} u_{\varrho} - (u_{\mu\varrho}^{\lambda} u_{\lambda\nu}^{\varrho} + L_{\underset{\vee}{\mu}\varrho}^{\lambda} L_{\underset{\vee}{\lambda}\nu}^{\varrho}) = \lambda \gamma_{\mu\nu}$$

en posant

$$(9) \quad \partial_{\mu}^{\lambda} \Gamma_{\nu} - \partial_{\nu} \Gamma_{\mu}^{\lambda} = -\frac{3\chi}{4} F_{\mu\nu}.$$

$\chi$  est un invariant.  $G_{\mu\nu}$  et  $\nabla_{\varrho}$  représentent le tenseur de Ricci riemannien et la dérivation covariante formés avec les  $\left\{ \begin{smallmatrix} \varrho \\ \mu\nu \end{smallmatrix} \right\}$  écrits eux-mêmes avec les  $\gamma$ .

Remplaçons maintenant dans (7) et dans (8) les  $u_{\mu\nu}^{\varrho}$  et les  $L_{\mu\nu}^{\varrho}$  par leurs valeurs tirées de (II)'. La résolution de (II)' sur laquelle nous ne reviendrons pas ici <sup>(1)</sup> nous montre:

1) Que la partie symétrique  $u_{\mu\nu,\varrho} = \gamma_{\varrho\sigma} u_{\mu\nu}^{\sigma}$  de la connexion s'exprime de la façon suivante en fonction de la partie antisymétrique

$$(10) \quad u_{\mu\nu,\varrho} = -(\varphi_{\mu\lambda} L_{\nu\varrho}^{\lambda} + \varphi_{\nu\lambda} L_{\mu\varrho}^{\lambda}).$$

On a d'autre part

$$(11) \quad u_{\varrho} = u_{\varrho\lambda}^{\lambda} = \frac{1}{2} \partial_{\varrho} \text{Log} \frac{g}{\gamma} - \frac{1}{2} \nabla_{\varrho} \text{Log} g \quad (1)$$

2) Que la partie antisymétrique  $L_{\underset{\vee}{\mu}\nu,\varrho} = \gamma_{\varrho\sigma} L_{\underset{\vee}{\mu}\nu}^{\sigma}$  de la connexion s'exprime

(1) Cf. M. A. TONNELAT: *Journ Phys.*, **12**, 81 (1951); **16**, 21 (1955); cf. aussi: *La théorie du champ unifié d'Einstein* (Paris, 1955).

Suivant les notations habituelles  $g$ ,  $\gamma$ ,  $\varphi$  = déterm.  $g_{\mu\nu}$ ,  $\gamma_{\mu\nu}$  et  $\varphi_{\mu\nu}$ ,  $gg^{\mu\nu}$ ,  $\gamma\gamma^{\mu\nu}$ ,  $\varphi\varphi^{\mu\nu}$ , ... = mineurs  $g_{\mu\nu}$ ,  $\gamma_{\mu\nu}$ ,  $\varphi_{\mu\nu}$ .

comme suit en fonction du tenseur fondamental  $g_{\mu\nu}$  <sup>(2)</sup>

$$(12) \quad (a^2 + b^2) L_{\mu\nu, \varrho} = a S_{\mu\nu, \varrho}^* + b S_{\mu\nu, \varrho}^*$$

avec

$$(13) \quad a = 2 - \frac{g}{\gamma} + \frac{6\varphi}{\gamma}, \quad b = \frac{2\sqrt{\varphi}}{\sqrt{-\gamma}} \left( 3 - \frac{g}{\gamma} + \frac{\varphi}{\gamma} \right),$$

$$(14) \quad S_{\mu\nu, \varrho}^* = \left( 2 - \frac{g}{\gamma} + \frac{\varphi}{\gamma} \right) R_{\mu\nu, \varrho} - \frac{2\sqrt{\varphi}}{\sqrt{-\gamma}} R_{\mu\nu, \varrho}^* - R_{\mu\nu, \varrho}^*,$$

$$(15) \quad R_{\mu\nu, \varrho}^* = -\frac{1}{2} \varphi_{\mu\nu\varrho} + \nabla_{\varrho} \varphi_{\mu\nu} + \frac{\sqrt{\varphi}}{2\sqrt{-\gamma}} \varphi_{[\mu\nu]\varrho}^* + \frac{\sqrt{\varphi}}{4\sqrt{-\gamma}} \varphi_{\mu\nu}^* \varphi^{\sigma\varrho} \varphi_{\sigma\varrho} - \varphi_{\mu\nu} \varphi_{\varrho} \text{Log} \frac{g}{\gamma} + \\ + \frac{\sqrt{\varphi}}{2} \varepsilon_{\mu\nu\varrho\sigma} \varphi^{\lambda\sigma} \varphi_{\lambda} \text{Log} \frac{g}{\gamma} - \frac{\varphi}{2\sqrt{-\gamma}} \varepsilon_{[\mu\nu]\varrho\lambda}^* \varphi^{\sigma\lambda} \varphi_{\sigma} \text{Log} \frac{g}{\varphi} + \frac{\sqrt{\varphi}}{2\sqrt{-\gamma}} \varphi_{\mu\nu}^* \varphi_{\varrho} \text{Log} \frac{g}{\varphi}.$$

En substituant (10) dans (7) et dans (8) et en tenant compte de (II)<sub>h</sub> qui s'écrit encore

$$(16) \quad \partial_{\varrho} \left[ \sqrt{-g} \left( \frac{\varphi}{g} \varphi^{\mu\varrho} + \frac{\gamma}{g} \varphi^{\mu\varrho} \right) \right] = \nabla_{\varrho} \left[ \frac{\gamma}{g} \left( \frac{\varphi}{g} \varphi^{\mu\varrho} + \varphi^{\mu\varrho} \right) \right]^{(3)} = 0.$$

Les équations rigoureuses du champ unifié sont alors :

a) Pour l'électromagnétisme.

$$(E) \quad \nabla_{\varrho} \left[ \frac{\gamma}{g} \left( \frac{\varphi}{g} \varphi^{\mu\varrho} + \varphi^{\mu\varrho} \right) \right] = 0,$$

$$(E)' \quad \frac{1}{\sqrt{-g}} \nabla_{\varrho} \sqrt{-g} L_{\mu\nu}^{\varrho} + 2 \gamma^{\tau\lambda} \gamma^{\sigma\varrho} L_{\mu\tau, \sigma} L_{\nu\lambda, \varrho} - \\ - \gamma^{\lambda\tau} \gamma^{\sigma\delta} \gamma^{\varrho\varrho} L_{\varrho\tau, \delta} (\varphi_{\mu\sigma} L_{\nu\lambda, \varrho} - \varphi_{\nu\sigma} L_{\mu\lambda, \varrho}) = -\frac{\chi}{2} F_{\mu\nu} \cdot \lambda_{\mu\nu}.$$

(2) Rappelons que

$$(17) \quad \varphi_{\mu\nu\varrho} = \partial_{\mu} \varphi_{\nu\varrho} + \partial_{\varrho} \varphi_{\mu\nu} + \partial_{\nu} \varphi_{\varrho\mu}.$$

D'autre part, pour toute grandeur  $A_{\mu\nu\dots}$  antisymétrique en  $\mu, \nu$ :

$$(18) \quad A_{\mu\nu\dots}^* = (\sqrt{-\gamma}/2) \varepsilon_{\mu\nu\lambda\tau} \gamma^{\lambda\varrho} \gamma^{\tau\sigma} A_{\varrho\sigma\dots}$$

Enfin pour toute grandeur  $B_{\varrho}$

$$(19) \quad B_{\varrho}^* = \varphi_{\varrho\sigma} \gamma^{\sigma\lambda} \varphi_{\lambda\tau} \gamma^{\tau\mu} B_{\mu}.$$

(3) En ce qui concerne les  $\varphi_{\mu\nu}$ , les notations soulignées  $\varphi_{\mu\nu}^{\underline{\mu\nu}}$  indiquent que les indices ont été élevés à l'aide des  $\gamma^{\mu\nu}$  ( $\varphi_{\mu\nu}^{\underline{\mu\nu}} = \gamma^{\mu\varrho} \gamma^{\nu\sigma} \varphi_{\varrho\sigma}$ ). Cela afin d'éviter des confusions avec  $\varphi\varphi^{\mu\nu} = \text{mineur } \varphi_{\mu\nu}$ .

b) *Pour la gravitation.*

$$(G) \quad G_{\mu\nu} - \frac{1}{\sqrt{-g}} \nabla^\rho \sqrt{-g} (\varphi_{\mu\lambda} L_{\nu\rho}^\lambda + \varphi_{\nu\lambda} L_{\mu\rho}^\lambda) - \frac{1}{2} \nabla_\mu \nabla_\nu \text{Log } g - L_{\mu\rho}^\lambda L_{\lambda\nu}^\rho - \\ - \gamma^{\lambda\sigma} \gamma^{\rho\tau} (\varphi_{\mu\epsilon} L_{\rho\sigma}^\epsilon + \varphi_{\rho\epsilon} L_{\mu\sigma}^\epsilon) (\varphi_{\lambda\delta} L_{\nu\tau}^\delta + \varphi_{\nu\delta} L_{\lambda\tau}^\delta) = \lambda \gamma_{\mu\nu}.$$

Dans toutes ces équations,  $L_{\mu\nu}^\rho = \gamma^{\rho\sigma} L_{\mu\nu,\sigma}^\rho$  admet, en fonction du tenseur fondamental  $g_{\mu\nu}$ , l'expression complètement déterminée par (12), (13), (14) et (15).

## 2. — Les équations approchées.

Nous allons supposer que le champ  $\varphi_{\mu\nu}$  ( $= g_{\mu\nu}$ ) est petit devant l'unité ainsi que ses dérivées des différents ordres. Développons  $\varphi_{\mu\nu}$  suivant les puissances croissantes d'un paramètre infiniment petit  $\varepsilon$ :

$$\varphi_{\mu\nu} = \varepsilon \varphi_{\mu\nu}^1 + \varepsilon^2 \varphi_{\mu\nu}^2 + \varepsilon^3 \varphi_{\mu\nu}^3 + \dots$$

Pour obtenir les équations approchées du champ unifié, il n'est pas nécessaire d'introduire a priori une hypothèse sur l'ordre de grandeur des  $\gamma_{\mu\nu}$  ( $= g_{\mu\nu}$ ) <sup>(4)</sup>.

D'autre part, à l'aide de (12), (14) et (15) on écrit facilement l'expression de la connexion affine à un ordre quelconque sans qu'il soit nécessaire d'utiliser des approximations successives.

### APPROXIMATION DU 3<sup>e</sup> ORDRE.

Cherchons, par exemple, à expliciter les équations rigoureuses (E) et (G) en négligeant les termes du 4<sup>e</sup> ordre introduits par les  $\varphi_{\mu\nu}$  et par leurs dérivées. On a <sup>(5)</sup>:

$$(20) \quad \frac{g}{\gamma} = 1 + \frac{\varphi}{\gamma} + \frac{1}{2} \gamma^{\mu\epsilon} \gamma^{\nu\sigma} \varphi_{\mu\nu} \varphi_{\rho\sigma} = 1 + F,$$

(4) Cf. M. A. TONNELAT: *Journ. Phys.*, **13**, 177 (1952), et aussi LENOIR: *Compt. Rend. Ac. Sci.*, **240**, 1400 (1955).

(5) Cf. M. A. TONNELAT: *La théorie du champ unifié d'Einstein et quelques-uns de ses développements* (Paris, 1955).

Signalons des erreurs d'impression dans les formules (4.27) à (4.35) de cet ouvrage, rectifiées ici par (21) à (27).

avec

$$F = \frac{1}{2} \gamma^{\mu\sigma} \gamma^{\nu\sigma} \varphi_{\mu\nu} \varphi_{\sigma\sigma} = \frac{1}{2} \varphi_{\mu\nu} \varphi^{\mu\nu}.$$

$F$  et  $\frac{\varphi}{\gamma}$  sont des termes en  $\varepsilon^2$  et en  $\varepsilon^4$ . A l'approximation considérée, c'est-à-dire aux termes du 4<sup>e</sup> ordre près, il résulte ainsi de (12), (13) et (14)

$$(21) \quad a = 1 - F, \quad b = \frac{4\sqrt{\varphi}}{\sqrt{-\gamma}},$$

$$(22) \quad (1 - 2F + \dots) L_{\sqrt{\varphi}, e} = (1 - F + \dots) S_{\sqrt{\varphi}, e} + \frac{4\sqrt{\varphi}}{\sqrt{-\gamma}} S_{\sqrt{\varphi}, e}^*,$$

d'où:

$$(23) \quad L_{\sqrt{\varphi}, e} = (1 + F + \dots) S_{\sqrt{\varphi}, e} + \frac{4\sqrt{\varphi}}{\sqrt{-\gamma}} S_{\sqrt{\varphi}, e}^*.$$

Mais, d'après (14):

$$(24) \quad S_{\sqrt{\varphi}, e} = (1 - F + \dots) R_{\sqrt{\varphi}, e} - \frac{2\sqrt{\varphi}}{\sqrt{-\gamma}} R_{\sqrt{\varphi}, e}^* - R_{\sqrt{\varphi}, e}^{\bar{}}.$$

En substituant dans (23):

$$(25) \quad L_{\sqrt{\varphi}, e} = R_{\sqrt{\varphi}, e} + \frac{2\sqrt{\varphi}}{\sqrt{-\gamma}} R_{\sqrt{\varphi}, e}^* - R_{\sqrt{\varphi}, e}^{\bar{}},$$

et, en se limitant aux termes en  $\varepsilon^3$ , on obtient à partir de l'expression rigoureuse (15) de  $R_{\sqrt{\varphi}, e}$ :

$$(26) \quad L_{\sqrt{\varphi}, e} = -\frac{1}{2} \varphi_{\mu\nu} + \nabla_e \varphi_{\mu\nu} + \frac{1}{3} \sqrt{\varphi}, e$$

en posant

$$(27) \quad \begin{aligned} \frac{1}{3} \sqrt{\varphi}, e &= -\frac{\sqrt{\varphi}}{\sqrt{-\gamma}} \varphi_{[\mu\nu], e}^* + \frac{\sqrt{\varphi}}{4\sqrt{-\gamma}} \varphi_{\mu\nu} \varphi^{\sigma\sigma} \varphi_{\sigma e} - \varphi_{\mu\nu} \partial_e \text{Log} \frac{g}{\gamma} + \\ &+ \frac{\sqrt{\varphi}}{2} \varepsilon_{\mu\nu\sigma} \varphi^{\lambda\sigma} \partial_\lambda \text{Log} \frac{g}{\gamma} + \sqrt{\varphi} \varepsilon_{[\mu\nu], e}^* \varphi^{\sigma\lambda} \partial_\sigma \frac{\sqrt{\varphi}}{\sqrt{-\gamma}} - \varphi_{\mu\nu} \partial_e \frac{\sqrt{\varphi}}{\sqrt{-\gamma}} + \\ &+ \frac{2\sqrt{\varphi}}{\sqrt{-\gamma}} \nabla_e^1 \varphi_{\mu\nu}^* + \frac{1}{2} \varphi_{\mu\nu}^{\bar{}} - \nabla_e^{\bar{}} \varphi_{\mu\nu}. \end{aligned}$$



Bien entendu, toutes les contributions du 1<sup>er</sup> et du 2<sup>e</sup> ordre ne peuvent provenir que des 2 premiers termes  $(-\frac{1}{2}\varphi_{\mu\nu e} + \nabla_e \varphi_{\mu\nu})$  de  $L_{\mu\nu, e}^{\nu}$ .

En substituant (26) dans (E) et dans (G), on constate qu'au 4<sup>e</sup> ordre près les équations du champ unifié sont les suivantes:

a) *Pour l'électromagnétisme.*

$$(28) \quad \nabla_e \varphi_{\mu e}^{\mu e} + \nabla_e \left( \frac{\varphi}{\gamma} \varphi^{\mu e} + F \varphi^{\mu e} \right) = 0,$$

$$(29) \quad \nabla_e \left( -\frac{1}{2} \varphi_{\mu\nu e} + \nabla_e \varphi_{\mu\nu} \right) + \frac{\chi}{2} F_{\mu\nu} - \lambda \varphi_{\mu\nu} + \nabla_e A_{\mu\nu, e}^{\nu} + \\ + \frac{1}{2} \left( -\frac{1}{2} \varphi_{\mu\nu e} + \nabla_e \varphi_{\mu\nu} \right) \partial^e \text{Log} \frac{g}{\gamma} + \frac{1}{2} \varphi^{\sigma e} (\varphi_{\mu\sigma}^{\lambda} - 2 \nabla_{\sigma} \varphi_{\mu}^{\lambda}) (\varphi_{\nu\lambda e} - 2 \nabla_e \varphi_{\nu\lambda}) + \\ + \frac{1}{4} (\varphi^{\epsilon\lambda\sigma} - 2 \nabla^{\sigma} \varphi^{\epsilon\lambda}) [(\varphi_{\mu\sigma} \varphi_{\nu\epsilon\lambda} - \varphi_{\nu\sigma} \varphi_{\mu\epsilon\lambda}) + \varphi_{\mu\sigma} \nabla_e \varphi_{\nu\lambda} - \varphi_{\nu\sigma} \nabla_e \varphi_{\mu\lambda}] = 0.$$

b) *Pour la gravitation.*

$$(30) \quad G_{\mu\nu} + \frac{1}{2} \nabla^e [\varphi_{\mu}^{\lambda} (\varphi_{\nu e\lambda} - 2 \nabla_{\lambda} \varphi_{\nu e}) + \varphi_{\nu}^{\lambda} (\varphi_{\mu e\lambda} - 2 \nabla_{\lambda} \varphi_{\mu e})] - \\ - \frac{1}{2} \nabla_{\mu} \nabla_{\nu} \text{Log} g + \frac{1}{4} (\varphi_{\mu e\sigma} - 2 \nabla_{\sigma} \varphi_{\mu e}) (\varphi_{\nu}^{\sigma e} - 2 \nabla^e \varphi_{\nu}^{\sigma}) - \lambda \gamma_{\mu\nu} = 0.$$

#### APPROXIMATION DU 2<sup>e</sup> ORDRE.

En négligeant les termes qui ne peuvent donner qu'une contribution du 3<sup>e</sup> ordre, on déduit immédiatement de (28), (29) et (30):

a) *Pour l'électromagnétisme.*

$$(31) \quad \nabla_e \varphi_{\mu e}^{\mu e} = \partial_e \sqrt{-\gamma} \varphi_{\mu e}^{\mu e} = 0,$$

$$(32) \quad \nabla_e \nabla^e \varphi_{\mu\nu} - \frac{1}{2} \nabla_e \varphi_{\mu\nu e} = -\frac{\chi}{2} F_{\mu\nu} + \lambda \varphi_{\mu\nu}.$$

b) *Pour la gravitation.*

$$(33) \quad G_{\mu\nu} - \nabla^{\lambda} (\varphi_{\mu\lambda} \nabla^{\lambda} \varphi_{\nu e} + \varphi_{\nu\lambda} \nabla^{\lambda} \varphi_{\mu e}) + \frac{1}{2} \nabla^e (\varphi_{\mu\lambda} \varphi_{\nu e}^{\lambda} + \varphi_{\nu\lambda} \varphi_{\mu e}^{\lambda}) - \\ - \frac{1}{2} \nabla_{\mu} \nabla_{\nu} \text{Log} g + (\nabla_{\sigma} \varphi_{\mu e} - \frac{1}{2} \varphi_{\mu e\sigma}) (\nabla^e \varphi_{\nu}^{\sigma} - \varphi_{\nu}^{\sigma e}) = \lambda \gamma_{\mu\nu}.$$

### 3. — Les équations électromagnétiques.

Considérons maintenant les équations (31) et (32) au 2<sup>e</sup> ordre d'approximation. Pour transformer (32), formons l'expression  $\nabla^e \varphi_{\mu\nu\rho}$  à partir de la définition des  $\varphi_{\mu\nu\rho} = \partial_\mu \varphi_{\nu\rho} + \partial_\rho \varphi_{\mu\nu} + \partial_\nu \varphi_{\rho\mu}$ :

$$(34) \quad \nabla^e \varphi_{\mu\nu\rho} = \square \varphi_{\mu\nu} + \\ + \gamma^{\rho\lambda} [(\nabla_\lambda \nabla_\mu - \nabla_\mu \nabla_\lambda) \varphi_{\nu\rho} + (\nabla_\lambda \nabla_\nu - \nabla_\nu \nabla_\lambda) \varphi_{\rho\mu} + (\nabla_\lambda \nabla_\rho - \nabla_\rho \nabla_\lambda) \varphi_{\mu\lambda}]$$

avec

$$(35) \quad \square = \nabla_\rho \nabla^\rho.$$

D'autre part, nous devons tenir compte des identités suivantes valables dans un espace de Riemann dont la métrique est  $\gamma_{\mu\nu}$

$$(36) \quad (\nabla_\rho \nabla_\sigma - \nabla_\sigma \nabla_\rho) \varphi_{\mu\nu} = G_{\mu\rho\sigma}^\tau \varphi_{\tau\nu} + G_{\nu\rho\sigma}^\tau \varphi_{\mu\tau},$$

$$(37) \quad G_{\mu\nu\sigma}^\tau + G_{\sigma\mu\nu}^\tau + G_{\nu\sigma\mu}^\tau = 0,$$

$$(38) \quad G_{\mu\nu\rho\sigma} = -G_{\nu\mu\rho\sigma} = -G_{\mu\nu\sigma\rho} = G_{\rho\sigma\mu\nu} \quad (6).$$

En tenant compte de ces identités et aussi de (31), on obtient à partir de (34):

$$(39) \quad \nabla^e \varphi_{\mu\nu\rho} = \square \varphi_{\mu\nu} - G_{\mu\nu}^{\rho\sigma} \varphi_{\rho\sigma} - (G_{\mu}^{\tau\rho} \varphi_{\nu\tau} + G_{\nu}^{\tau\rho} \varphi_{\tau\mu}),$$

c'est-à-dire, d'après (33), et en négligeant les termes du 3<sup>e</sup> ordre:

$$(40) \quad \nabla^e \varphi_{\mu\nu\rho} = \square \varphi_{\mu\nu} - G_{\mu\nu}^{\rho\sigma} \varphi_{\rho\sigma} - 2\lambda \varphi_{\mu\nu}.$$

En comparant (32) et (40) on a donc:

$$(41) \quad \square \varphi_{\mu\nu} + G_{\mu\nu}^{\tau\sigma} \varphi_{\tau\sigma} = -\chi F_{\mu\nu}$$

et

$$(42) \quad \nabla^e \varphi_{\mu\nu\rho} = -\chi F_{\mu\nu} - 2\lambda \varphi_{\mu\nu} - G_{\mu\nu}^{\rho\sigma} \varphi_{\rho\sigma}.$$

(6) La définition du tenseur de Riemann-Christoffel est celle qu'adopte habituellement EINSTEIN

$$G_{\mu\nu\sigma}^\tau = \partial_\sigma \left\{ \begin{matrix} \tau \\ \mu\nu \end{matrix} \right\} - \partial_\nu \left\{ \begin{matrix} \tau \\ \mu\sigma \end{matrix} \right\} + \left\{ \begin{matrix} \lambda \\ \mu\nu \end{matrix} \right\} \left\{ \begin{matrix} \tau \\ \lambda\sigma \end{matrix} \right\} - \left\{ \begin{matrix} \lambda \\ \mu\sigma \end{matrix} \right\} \left\{ \begin{matrix} \tau \\ \lambda\nu \end{matrix} \right\}.$$

Les équations fondamentales de l'électromagnétisme — c'est-à-dire (31) et (32) — s'écrivent donc encore au 3<sup>e</sup> ordre près:

(31)

$$\nabla_{\varrho} \varphi^{\mu\varrho} = 0 \quad (\text{ou } \nabla^{\varrho} \varphi_{\mu\varrho} = 0)$$

(41)

$$\square \varphi_{\mu\nu} = -\chi F_{\mu\nu} - G^{\tau\sigma}_{\mu\nu} \varphi_{\tau\sigma}$$

De ces équations, on peut déduire les 2 conséquences suivantes:

1) Appliquons  $\nabla^{\nu} = \gamma^{\nu\lambda} \nabla_{\lambda}$  à (41). On obtient:

(43)

$$\nabla^{\nu} (\nabla^{\varrho} \nabla_{\varrho} \varphi_{\mu\nu}) = -\nabla^{\nu} (\chi F_{\mu\nu}) - (\nabla^{\nu} G^{\tau\sigma}_{\mu\nu}) \varphi_{\tau\sigma} - G^{\tau\sigma}_{\mu\nu} \nabla^{\nu} \varphi_{\tau\sigma},$$

c'est-à-dire, en tenant compte des identités (36), (37), (38) et de la condition (31):

(44)

$$2G^{\lambda\nu}_{\mu\varrho} \nabla^{\varrho} \varphi_{\lambda\nu} + \frac{3}{2} (\nabla_{\varrho} G^{\varrho\lambda\nu}_{\mu}) \varphi_{\lambda\nu} = -\nabla^{\nu} (\chi F_{\mu\nu}).$$

Mais, d'après les identités

(45)

$$\nabla_{\varrho} G^{\tau}_{\mu\sigma\nu} + \nabla_{\nu} G^{\tau}_{\mu\varrho\sigma} + \nabla_{\sigma} G^{\tau}_{\mu\nu\varrho} = 0$$

valables aussi dans un espace de Riemann, on obtient par contraction:

(46)

$$\nabla_{\varrho} G^{\varrho}_{\mu\nu\sigma} = \nabla_{\sigma} G_{\mu\nu} - \nabla_{\nu} G_{\mu\sigma}$$

et, en vertu de (33), cette expression est au plus du 2<sup>e</sup> ordre. Il en résulte qu'à l'approximation admise, le 2<sup>e</sup> terme de (44) est négligeable. On a donc simplement (7):

(47)

$$\nabla^{\nu} (\chi F_{\mu\nu}) = -2G^{\lambda\nu}_{\mu\varrho} \nabla^{\varrho} \varphi_{\lambda\nu}.$$

2) Appliquons maintenant  $\nabla_{\lambda}$  à (41) et effectuons une permutation circulaire sur  $\lambda, \mu, \nu$ . En tenant compte de (36), (37) et (38) et aussi de la condition (31), on obtient

(48)

$$\square \varphi_{\mu\nu\lambda} = \lambda \varphi_{\mu\nu\lambda} + 2(G^{\tau\varrho}_{\mu\lambda} \nabla_{\nu} \varphi_{\tau\varrho} + G^{\tau\varrho}_{\lambda\nu} \nabla_{\mu} \varphi_{\tau\varrho} + G^{\tau\varrho}_{\nu\mu} \nabla_{\lambda} \varphi_{\tau\varrho}) - \\ - (G^{\tau\varrho}_{\mu\lambda} \varphi_{\tau\varrho\nu} + G^{\tau\varrho}_{\lambda\nu} \varphi_{\tau\varrho\mu} + G^{\tau\varrho}_{\nu\mu} \varphi_{\tau\varrho\lambda}).$$

(7) La même condition peut être obtenue en appliquant  $\nabla^{\nu}$  à la relation (42).

En tenant compte de (38) et à l'approximation admise, le 3<sup>e</sup> terme du second membre de (48) se réduit à :

$$(49) \quad G^{\rho\sigma}{}_{\rho\sigma} \varphi_{\mu\nu\lambda} + 2\lambda \varphi_{\mu\nu\lambda} = -2\lambda \varphi_{\mu\nu\lambda},$$

(48) s'écrit donc encore :

$$(50) \quad \square \varphi_{\mu\nu\lambda} = -\lambda \varphi_{\mu\nu\lambda} + 2(G^{\tau\rho}{}_{\mu\lambda} \nabla_\nu \varphi_{\tau\rho} + G^{\tau\rho}{}_{\lambda\nu} \nabla_\mu \varphi_{\tau\rho} + G^{\tau\rho}{}_{\nu\mu} \nabla_\lambda \varphi_{\tau\rho})$$

ou, en multipliant par  $\frac{1}{6} \varepsilon^{\mu\nu\lambda\sigma}$  et en sommant

$$(51) \quad \frac{1}{6} \varepsilon^{\mu\nu\lambda\sigma} \square \varphi_{\mu\nu\lambda} = -\frac{\lambda}{6} \varepsilon^{\mu\nu\lambda\sigma} \varphi_{\mu\nu\lambda} - \varepsilon^{\mu\nu\lambda\sigma} G^{\tau\rho}{}_{\mu\nu} (\nabla_\lambda \varphi_{\tau\rho}).$$

Sous cette forme, et en négligeant le terme en  $\lambda$ , on reconnaît l'expression indiquée par Schrödinger pour mettre en évidence l'existence d'un courant lié directement à la présence d'une courbure riemannienne <sup>(8)</sup>.

#### 4. — Les équations de la gravitation.

Les équations (33) s'écrivent encore :

$$(52) \quad G_{\mu\nu} - \varphi_{\mu\lambda} (\nabla^\rho \nabla^\lambda - \nabla^\lambda \nabla^\rho) \varphi_{\nu\rho} - \varphi_{\nu\lambda} (\nabla^\rho \nabla^\lambda - \nabla^\lambda \nabla^\rho) \varphi_{\mu\rho} - (\nabla^\rho \varphi_{\nu\lambda}) (\nabla^\lambda \varphi_{\mu\rho}) - \\ - \frac{1}{4} \nabla_\mu \nabla_\nu (\varphi_{\rho\sigma} \varphi^{\rho\sigma}) - \frac{1}{2} (\varphi_\mu{}^\tau \nabla^\rho \varphi_{\nu\tau\rho} + \varphi_\nu{}^\tau \nabla^\rho \varphi_{\mu\tau\rho}) - \frac{1}{4} \varphi_{\mu\tau\rho} \varphi_\nu{}^{\tau\rho} = \lambda \gamma_{\mu\nu},$$

c'est-à-dire, en tenant compte des identités (36), (40) et (41) :

$$(53) \quad G_{\mu\nu} + \frac{1}{2} \varphi^{\rho\sigma} (\varphi_{\mu\tau} G^{\tau}{}_{\nu\rho\sigma} + \varphi_{\nu\tau} G^{\tau}{}_{\mu\rho\sigma}) - (\nabla^\rho \varphi_{\nu\lambda}) (\nabla^\lambda \varphi_{\mu\rho}) - \frac{1}{4} \nabla_\mu \nabla_\nu (\varphi_{\rho\sigma} \varphi^{\rho\sigma}) - \\ - \frac{1}{4} \varphi_{\mu\tau\rho} \varphi_\nu{}^{\tau\rho} + \frac{1}{2} (\varphi_\mu{}^\tau F_{\nu\tau} + \varphi_\nu{}^\tau F_{\mu\tau}) + (\varphi_\mu{}^\tau G^{\rho\sigma}{}_{\nu\tau} + \varphi_\nu{}^\tau G^{\rho\sigma}{}_{\mu\tau}) \varphi_{\rho\sigma} = \lambda \gamma_{\mu\nu}.$$

Or, cette équation peut s'écrire ainsi :

$$(54) \quad \boxed{G_{\mu\nu} - \frac{1}{2} \gamma_{\mu\nu} G + \lambda \gamma_{\mu\nu} = \chi(\tau_{\mu\nu} + M_{\mu\nu} + X_{\mu\nu} + Y_{\mu\nu})}$$

à condition de poser :

$$(55) \quad \tau_{\mu\nu} = -\frac{1}{2} (\varphi_{\mu\tau} F_\nu{}^\tau + \varphi_{\nu\tau} F_\mu{}^\tau) + \frac{1}{4} \gamma_{\mu\nu} \varphi_{\lambda\tau} F^{\lambda\tau},$$

<sup>(8)</sup> E. SCHRÖDINGER: *Proc. Roy. Ir. Acad.*, A 56, 13 (1954).



$$(56) \quad M_{\mu\nu} = \frac{1}{4\chi} \left( \varphi_{\mu\tau\varrho} \varphi_{\nu}^{\tau\varrho} - \frac{1}{6} \gamma_{\mu\nu} \varphi_{\varrho\sigma\lambda} \varphi^{\varrho\sigma\lambda} \right),$$

$$(57) \quad X_{\mu\nu} = \frac{1}{\chi} \left[ (\nabla^{\varrho} \varphi_{\nu\lambda})(\nabla^{\lambda} \varphi_{\mu\varrho}) + \frac{1}{4} \nabla_{\mu} \nabla_{\nu} (\varphi_{\varrho\sigma} \varphi^{\varrho\sigma}) - \right. \\ \left. - \frac{1}{2} \gamma_{\mu\nu} (\nabla_{\lambda} \varphi_{\tau\varrho})(\nabla^{\lambda} \varphi^{\tau\varrho}) + \frac{\chi}{2} \gamma_{\mu\nu} \varphi_{\varrho\sigma}^{\varrho\sigma} F_{\varrho\sigma} \right],$$

$$(58) \quad Y_{\mu\nu} = -\frac{1}{2\chi} \left[ (G^{\varrho\sigma}{}_{\nu\tau} \varphi_{\mu}^{\tau} + G^{\varrho\sigma}{}_{\mu\tau} \varphi_{\nu}^{\tau}) \varphi_{\varrho\sigma} - \frac{3}{2} \gamma_{\mu\nu} G^{\varrho\sigma}{}_{\lambda\tau} \varphi_{\varrho\sigma} \varphi^{\lambda\tau} \right].$$

$\tau_{\mu\nu}$  est le tenseur électromagnétique d'impulsion-énergie, symétrisé, dans le cas où existent à la fois champ et induction;  $M_{\mu\nu}$  dépend uniquement du courant  $\varphi_{\mu\nu\varrho}$ ;  $X_{\mu\nu}$  introduit des termes supplémentaires qui font intervenir les dérivées du champ électromagnétique; enfin  $Y_{\mu\nu}$  introduit explicitement la courbure riemannienne rapportée aux  $\gamma_{\tau\sigma}$  <sup>(9)</sup>.

Formons la divergence des différents tenseurs qui figurent au second membre de (54). On a:

$$(59) \quad \nabla^{\nu} \tau_{\mu\nu} = \frac{1}{4} \varphi_{\mu\tau\lambda} F^{\tau\lambda} - \frac{1}{\chi} G_{\tau\varrho}^{\lambda\sigma} \varphi_{\mu}^{\tau} \nabla^{\varrho} \varphi_{\lambda\sigma} - \tau_{\mu\nu} \nabla^{\nu} \text{Log } \chi,$$

$$(60) \quad \nabla^{\nu} M_{\mu\nu} = -\frac{1}{4} \varphi_{\mu\tau\lambda} F^{\tau\lambda} - \frac{\lambda}{4\chi} \varphi_{\mu\tau\varrho} \varphi^{\tau\varrho} + \frac{1}{2\chi} G_{\lambda\pi}^{\tau\varrho} \varphi_{\tau\mu\varrho} \varphi^{\lambda\pi} - M_{\mu\nu} \nabla^{\nu} \text{Log } \chi,$$

$$(61) \quad \nabla^{\nu} X_{\mu\nu} = \frac{\lambda}{2\chi} \varphi_{\mu\tau\varrho} \varphi^{\tau\varrho} - \frac{1}{2\chi} G_{\lambda\pi}^{\tau\varrho} \varphi_{\tau\mu\varrho} \varphi^{\lambda\pi} + \frac{1}{\chi} G_{\tau\varrho}^{\lambda\sigma} \varphi_{\mu}^{\tau} \nabla^{\varrho} \varphi_{\lambda\sigma} - \\ - X_{\mu\nu} \nabla^{\nu} \text{Log } \chi + \frac{1}{4\chi} G_{\tau}^{\varrho\lambda\sigma} \varphi_{\lambda\sigma} \varphi_{\mu\varrho}^{\tau} - \frac{1}{2\chi} G_{\mu}^{\tau\nu\lambda} \varphi_{\tau\varrho} \nabla^{\varrho} \varphi_{\nu\lambda} - \\ - \frac{1}{2\chi} \varphi^{\varrho\sigma} \varphi_{\lambda\pi} \nabla_{\mu} G^{\lambda\pi}{}_{\varrho\sigma} - \frac{5}{4\chi} G_{\varrho\sigma}^{\lambda\pi} \varphi^{\varrho\sigma} \nabla_{\mu} \varphi_{\lambda\pi} + \frac{1}{2\chi} G_{\varrho}^{\tau\nu\lambda} \varphi_{\mu\tau} \nabla^{\varrho} \varphi_{\nu\lambda},$$

$$(62) \quad \nabla^{\nu} Y_{\mu\nu} = \frac{1}{2\chi} (\nabla_{\mu} G^{\varrho\sigma}{}_{\nu\tau}) \varphi_{\varrho\sigma} \varphi^{\nu\tau} - \frac{1}{4\chi} G_{\nu}^{\varrho\tau\sigma} \varphi_{\tau\sigma} \varphi_{\mu\varrho}^{\nu} - Y_{\mu\nu} \nabla^{\nu} \text{Log } \chi + \\ + \frac{1}{2\chi} G_{\mu}^{\tau\nu\sigma} \varphi_{\tau\varrho} \nabla^{\varrho} \varphi_{\nu\sigma} - \frac{1}{2\chi} G^{\varrho\sigma}{}_{\nu\tau} \varphi_{\mu}^{\tau} \nabla^{\varrho} \varphi_{\varrho\sigma} + \frac{5}{4\chi} G^{\varrho\sigma}{}_{\lambda\tau} \varphi^{\lambda\tau} \nabla_{\mu} \varphi_{\varrho\sigma},$$

c'est-à-dire:

$$(63) \quad \nabla^{\nu} (\tau_{\mu\nu} + M_{\mu\nu} + X_{\mu\nu} + Y_{\mu\nu}) = -(\tau_{\mu\nu} + M_{\mu\nu} + X_{\mu\nu} + Y_{\mu\nu}) \nabla^{\nu} \text{Log } \chi,$$

(9) M. A. TONNELAT: *Compt. Rend. Ac. Sci.*, **241** (1955).

ou

$$(64) \quad \nabla^\nu \chi(\tau_{\mu\nu} + M_{\mu\nu} + X_{\mu\nu} + Y_{\mu\nu}) = 0.$$

Ainsi, l'ensemble du tenseur impulsion-énergie vérifie, au 3<sup>e</sup> ordre près, une identité en divergence nulle. Or on sait que le 1<sup>er</sup> membre de (54) satisfait rigoureusement l'identité:

$$(65) \quad \nabla^\nu (G_{\mu\nu} - \frac{1}{2}\gamma_{\mu\nu}G + \lambda\gamma_{\mu\nu}) \equiv 0,$$

toujours valable dans un espace de Riemann. Au 2<sup>e</sup> ordre d'approximation, le second membre de (54) a les propriétés qui caractérisent le tenseur d'impulsion-énergie.

### 5. — Introduction d'approximations sur les $\gamma_{\mu\nu}$ .

Supposons maintenant que les  $\gamma_{\mu\nu}$  admettent le développement suivant en fonction du paramètre  $\varepsilon$ :

$$\gamma_{\mu\nu} = \eta_{\mu\nu} + \varepsilon\gamma_{\mu\nu}^1 + \varepsilon^2\gamma_{\mu\nu}^2 + \dots$$

L'écart entre les  $\gamma_{\mu\nu}$  et leurs valeurs galiléennes est d'un ordre de grandeur égal au plus à  $\varepsilon$ . Il en est de même de l'ordre de grandeur des dérivées de  $\gamma_{\mu\nu}$ .

On obtient ainsi

#### 1. AU 1<sup>er</sup> ORDRE.

##### a) Pour l'électromagnétisme.

$$(66) \quad \eta^{\rho\sigma}\partial_\rho\varphi_{\mu\sigma}^1 = 0$$

$$(67) \quad \overset{\circ}{\square}\varphi_{\mu\nu}^1 = -\chi_1 F_{\mu\nu} \quad (\overset{\circ}{\square} = \partial^\rho\partial_\rho)$$

avec les conditions

$$(68) \quad \eta^{\rho\sigma}\partial_\sigma\varphi_{\mu\nu\rho}^1 = -\chi_1 F_{\mu\nu}$$

$$(69) \quad \eta^{\rho\sigma}\partial_\rho(\chi_1 F_{\mu\sigma}) = 0$$

$$(70) \quad \overset{\circ}{\square}\varphi_{\mu\nu\rho}^1 = 0.$$

(Ces relations étant obtenues en négligeant les termes en  $\lambda$ ).

b) *Pour la gravitation.*

$$(71) \quad \mathcal{L}_{\mu\nu} = 0$$

en posant

$$(72) \quad \mathcal{L}_{\mu\nu} = \frac{1}{2} \eta^{\rho\sigma} \mathcal{L}_{\sigma\mu\nu\rho}$$

$$(73) \quad \mathcal{L}_{\sigma\mu\nu\rho} = \partial_\rho \partial_\mu \gamma_{\nu\sigma} + \partial_\sigma \partial_\nu \gamma_{\mu\rho} - \partial_\rho \partial_\sigma \gamma_{\mu\nu} - \partial_\mu \partial_\nu \gamma_{\rho\sigma}.$$

## 2. AU 2<sup>e</sup> ORDRE.

a) *Pour l'électromagnétisme.*

$$(74) \quad \eta^{\rho\sigma} \partial_\rho \varphi_{\mu\sigma} + \gamma^{\rho\sigma} \partial_\rho \varphi_{\mu\sigma} + \eta^{\rho\sigma} (\nabla_\rho - \partial_\rho) \varphi_{\mu\sigma} = 0$$

$$(75) \quad \square_2 \varphi_{\mu\nu} + \gamma^{\rho\sigma} \partial_\rho \partial_\sigma \varphi_{\mu\nu} + \eta^{\rho\sigma} (\nabla_\rho \nabla_\sigma - \partial_\rho \partial_\sigma) \varphi_{\mu\nu} = -\chi_2 F_{\mu\nu} - 2G_{\mu\nu}^{\rho\sigma} \varphi_{\rho\sigma}$$

avec les conditions:

$$(76) \quad \eta^{\rho\sigma} \partial_\sigma \varphi_{\mu\nu\rho} + \gamma^{\rho\sigma} \partial_\sigma \varphi_{\mu\nu\rho} + \eta^{\rho\sigma} (\nabla_\rho - \partial_\rho) \varphi_{\mu\nu\sigma} = -\chi_2 F_{\mu\nu} - 2G_{\mu\nu}^{\rho\sigma} \varphi_{\rho\sigma}$$

$$(77) \quad \eta^{\rho\sigma} \partial_\rho (\chi_2 F_{\mu\sigma}) + \eta^{\rho\sigma} (\nabla_\rho - \partial_\rho) (\chi_2 F_{\mu\sigma}) + \gamma^{\rho\sigma} \partial_\rho (\chi_2 F_{\mu\sigma}) = -2G_{\mu\rho}^{\lambda\nu} \eta^{\rho\sigma} \partial_\sigma \varphi_{\lambda\nu}$$

$$(78) \quad \frac{1}{6} \varepsilon^{\mu\nu\lambda\sigma} [\square_2 \varphi_{\mu\nu\lambda} + \gamma^{\rho\tau} \partial_\rho \partial_\tau \varphi_{\mu\nu\lambda} + \eta^{\rho\tau} (\nabla_\rho \nabla_\tau - \partial_\rho \partial_\tau) \varphi_{\mu\nu\lambda}] = -\varepsilon^{\mu\nu\lambda\sigma} G_{\mu\nu}^{\tau\rho} (\partial_\lambda \varphi_{\tau\rho}).$$

b) *Pour la gravitation.*

$$(79) \quad G_{\mu\nu} - \frac{1}{2} \eta_{\mu\nu} G = \chi(\tau_{\mu\nu} + \frac{M}{2}_{\mu\nu} + \frac{X}{2}_{\mu\nu})$$

avec

$$(80) \quad G_{\mu\nu} = \mathcal{L}_{\mu\nu} + \frac{1}{2} \gamma^{\rho\sigma} \mathcal{L}_{\mu\nu\rho\sigma} + \eta^{\rho\lambda} \eta^{\sigma\tau} ([\mu\rho, \sigma][\lambda\nu, \tau] - [\mu\nu, \sigma][\lambda\rho, \tau]).$$

## 6. - Interprétation des résultats obtenus. Le champ électromagnétique $F_{\mu\nu}$ . Cas d'un champ de Schwarzschild.

L'apparition du champ  $F_{\mu\nu}$  n'est pas une simple possibilité que présente la théorie du champ unifié. Elle découle nécessairement des équations fonda-

mentales de la théorie telles qu'on les obtient par application du principe variationnel à une densité invariante formée à l'aide du tenseur de Ricci (système faible).

La condition

$$(81) \quad F_{\mu\nu} = 0$$

est, en particulier, réalisée à tous les ordres dans le cas du « système fort » où l'on postule la condition supplémentaire  $\Gamma_\mu = I_{\mu\rho}^{\rho} = 0$ . Cette disparition du vecteur de torsion, suffisante pour entraîner celle de  $F_{\mu\nu}$ , n'est d'ailleurs pas nécessaire. Il suffit de supposer, très arbitrairement

$$(82) \quad \Gamma_\mu = I_{\mu\rho}^{\rho} = \partial_\mu \psi,$$

$\psi$  étant un scalaire quelconque, pour supprimer  $F_{\mu\nu}$  et aboutir à la conséquence suivante tirée de (77):

$$(83) \quad G_{\mu\rho}^{\lambda\nu} \eta^{\rho\sigma} \partial_\sigma \varphi_{\lambda\nu} = 0$$

ou

$$(84) \quad (\partial_\nu \partial_\mu \gamma_{\lambda\tau} + \partial_\lambda \partial_\tau \gamma_{\mu\nu}) \partial^\tau \varphi^{\lambda\nu} = 0.$$

Sous cette forme, on reconnaît l'une des relations obtenues par A. EINSTEIN et B. KAUFMAN dans le cas du système fort <sup>(10)</sup>. Or, en choisissant un champ de Schwarzschild, A. EINSTEIN et B. KAUFMAN ont précisément montré que le lien établi par (84) entre les grandeurs du 1<sup>er</sup> ordre  $\varphi_{\mu\nu}$  et  $\gamma_{\mu\nu}$  est beaucoup trop étroit. L'équation (84) demeurant physiquement inadmissible il faut donc revenir à (77) en supposant toujours

$$F_{\mu\nu} \neq 0$$

au moins au deuxième ordre.

Développons dans ce cas l'expression (77). On trouve:

$$(85) \quad \eta^{\rho\sigma} [\partial_\rho (\chi_2 F_{\mu\sigma}) + \chi([\mu\rho, \lambda]_1 F_{\sigma}^{\lambda} - [\sigma\rho, \lambda]_1 F_{\mu}^{\lambda}) - \gamma_{\sigma\tau} \partial_\rho (\chi_1 F_{\mu}^{\tau}) + \\ + (\partial_\tau \partial_\rho \gamma_{\varepsilon\mu} - \partial_\tau \partial_\mu \gamma_{\rho\varepsilon} - \partial_\varepsilon \partial_\rho \gamma_{\mu\tau} + \partial_\varepsilon \partial_\mu \gamma_{\rho\tau}) (\partial_\sigma \eta^{\lambda\varepsilon} \eta^{\nu\tau} \varphi_{\lambda\nu})] = 0$$

ou

$$(86) \quad \eta^{\rho\sigma} \partial_\rho (\chi_2 F_{\mu\sigma} - \chi \gamma_{\sigma\tau} F_{\mu}^{\tau} + \chi \gamma_{\mu\tau} F_{\sigma}^{\tau}) + \\ + 2\eta^{\rho\sigma} \partial_\tau \left[ (\partial_\rho \gamma_{\varepsilon\mu} - \partial_\mu \gamma_{\rho\varepsilon}) \partial_\sigma \varphi^{\varepsilon\tau} + \frac{\chi}{1} \gamma_{\rho\sigma} F_{\mu}^{\tau} \right] = 0.$$

<sup>(10)</sup> A. EINSTEIN et B. KAUFMAN: *Sur l'état actuel de la théorie de la gravitation généralisée* (Louis de Broglie. Physicien et Penseur, Paris, 1952).

Supposons, comme le font A. EINSTEIN et B. KAUFMAN, que le champ de gravitation soit un champ de Schwarzschild. On a :

$$(87) \quad \gamma_{\mu\nu} = -\delta_{\mu\nu} \frac{2m}{\varrho}$$

avec

$$(88) \quad \varrho^2 = \sum_{p=1}^{p=3} (x^p - a^p)^2 \quad (a^4 = 0)$$

en reprenant les notations d'Einstein-Kaufman, c'est-à-dire en désignant par  $a^p$  les coordonnées de la particule de masse  $m$  qui crée, au point  $x^p$ , le champ à symétrie sphérique.

En calculant, au voisinage de l'origine, les termes  $\partial_\varrho \gamma_{\mu\nu}$ ,  $\partial_\varrho \partial_\sigma \gamma_{\mu\nu}$  on obtient d'après (87) et (88)

$$(89) \quad \gamma_{\mu\nu} = -\delta_{\mu\nu} \frac{2m}{a}, \quad \partial_\varrho \gamma_{\mu\nu} = -\frac{2m}{a^3} \delta_{\mu\nu} a_\varrho,$$

$$(90) \quad \partial_\varrho \partial_\sigma \gamma_{\mu\nu} = -\frac{2m}{a^5} \delta_{\mu\nu} (3a_\varrho a_\sigma - \varepsilon_{\varrho\sigma} a^2)$$

en utilisant toujours les notations Einstein-Kaufman

$$(91) \quad \varepsilon_{\varrho\sigma} = \begin{vmatrix} 1 & & & \\ & 1 & & \\ & & 1 & \\ & & & 0 \end{vmatrix}.$$

En choisissant en outre un système de coordonnées particulier tel que la masse créant le champ soit sur l'axe  $0x$  ( $a_1 = -a$ ,  $a_2 = a_3 = 0$ ), on obtient le résultat trouvé par EINSTEIN et par B. KAUFMAN <sup>(10)</sup> en ce qui concerne les termes de (86) en  $\varphi^{\sigma\tau}$ . Mais ici, il faut tenir compte en outre des termes supplémentaires dus à la présence de  $F_{\mu\nu}$ . On trouve alors :

Pour  $\mu = 1$

$$(92) \quad \eta^{\sigma\sigma} \partial_\varrho (\chi F_{1\sigma}) + \frac{4m}{a} \partial_4 (\chi F_{14}) + \frac{12m}{a^3} \partial_4 \varphi_{14} = 0$$

Pour  $\mu = p$ ,  $p = 2$  ou  $3$

$$(93) \quad \eta^{\sigma\sigma} \partial_\varrho (\chi F_{p\sigma}) + \frac{4m}{a} \partial_4 (\chi F_{p4}) - \frac{12m}{a^3} (\partial_{11} \varphi_{1p} + \partial_{11} \varphi_{p1}) = 0$$



Pour  $\mu = 4$

$$(94) \quad \eta^{\sigma\sigma} \partial_{\sigma} (\chi F_{4\sigma}) - \frac{2m}{a^2} \chi F_{14} + \frac{12m}{a^3} \partial_1 \varphi_{14} = 0.$$

Si l'on suppose la disparition de  $F_{\mu\nu}$  au 1<sup>er</sup> ordre ( $F_{\mu\nu} = 0$ ), il faut nécessairement supposer l'existence de termes en  $F_{\mu\nu}$  ( $F_{\mu\nu} \neq 0$ ) sous peine d'aboutir à des conditions physiquement inadmissibles portant sur les  $q_{\mu\nu}$ , conditions signalées par A. EINSTEIN et B. KAUFMAN <sup>(10)</sup>.

## 7. - Le courant $\varphi_{\mu\nu\rho}$ .

Des conclusions analogues interviennent au sujet du courant  $q_{\mu\nu\rho}$ . La condition (78) qui ne fait pas intervenir de termes en  $F_{\mu\nu}$  et qui est valable, par conséquent, quel que soit  $\Gamma_{\sigma} = \Gamma_{\sigma}^{\sigma}$ , a été mise en évidence par E. SCHRÖDINGER: Si  $\varphi_{\mu\nu\rho} = 0$ , la présence d'une courbure riemannienne  $R_{\mu\nu\rho\sigma}^{\sigma} \neq 0$  entraîne nécessairement l'existence d'un courant du second ordre  $q_{\mu\nu\rho}$ .

Dans le cas particulier d'un champ de Schwarzschild (87), on obtiendrait à partir de (78):

$$(95) \quad \square \varphi_{234} + \frac{2m}{a} \partial_4^2 \varphi_{234} - \frac{4m}{a^3} \varphi_{234} = -\frac{12m}{a^3} \partial_1 \varphi_{23},$$

$$(96) \quad \square \varphi_{341} + \frac{4m}{a} \partial_4^2 \varphi_{341} + \frac{2m}{a^2} \partial_{\sigma} \varphi_{\sigma 34} - \frac{4m}{a^3} \varphi_{341} = -\frac{12m}{a^3} \partial_3 \varphi_{14},$$

$$(97) \quad \square \varphi_{214} + \frac{4m}{a} \partial_4^2 \varphi_{214} + \frac{2m}{a^2} \partial_{\sigma} \varphi_{\sigma 24} - \frac{4m}{a^3} \varphi_{214} = -\frac{12m}{a^3} \partial_2 \varphi_{14},$$

$$(98) \quad \square \varphi_{123} + \frac{4m}{a} \partial_4^2 \varphi_{123} - \frac{2m}{a^2} \partial_{\sigma} \varphi_{\sigma 23} - \frac{4m}{a^2} \partial_1 \varphi_{123} - \frac{4m}{a^3} \varphi_{123} = -\frac{12m}{a^3} \partial_1 \varphi_{23}.$$

## 8. - Le tenseur d'énergie et les équations du mouvement.

Il résulte de la discussion précédente qu'on ne peut faire disparaître arbitrairement au 1<sup>er</sup> et au 2<sup>e</sup> ordre d'approximation les termes en  $F_{\mu\nu}$  qui interviennent dans l'expression du tenseur d'impulsion-énergie. Celui-ci comprend donc un terme électromagnétique:

$$(55) \quad \tau_{\mu\nu} = -\frac{1}{2} (\varphi_{\mu\rho} F_{\nu}^{\rho} + \varphi_{\nu\rho} F_{\mu}^{\rho}) + \frac{1}{4} \gamma_{\mu\nu} \varphi_{\lambda\rho} F^{\lambda\rho},$$

et un terme « matériel »

$$(56) \quad M_{\mu\nu} = \frac{1}{4\chi} \left( \varphi_{\mu\tau\varrho} \varphi_{\nu}^{\tau\varrho} - \frac{1}{6} \gamma_{\mu\nu} \varphi_{\varrho\sigma\lambda} \varphi^{\varrho\sigma\lambda} \right),$$

$\tau_{\mu\nu}$  est un terme en  $\varepsilon^2$  si  $F_{\mu\nu} \neq 0$ .

L'intervention explicite de termes en  $F_{\mu\nu}$  dans les équations électromagnétiques en  $\square\varphi_{\mu\nu}$  provient du fait que ces équations se déduisent de (I)'. Ces termes disparaissent, bien entendu, si l'on substitue à (I)', les conséquences

$$(99) \quad \partial_{\varrho} W_{\underset{\vee}{\mu\nu}} + \partial_{\nu} W_{\underset{\vee}{\varrho\mu}} + \partial_{\mu} W_{\underset{\vee}{\nu\varrho}} = 0.$$

D'autre part, dans les équations (33) du champ de gravitation, les termes en  $F_{\mu\nu}$  sont introduits par les expressions équivalentes en  $\square\varphi_{\mu\nu}$  et en  $\nabla^{\varrho}\varphi_{\mu\nu\varrho}$ , comme il ressort de (67) et de (68). Ces termes n'interviennent donc pas d'après (9), dans les équations d'Infeld déduites du « système fort » ( $\Gamma_{\mu} = 0$ ). Dans les équations de Callaway (où ils seraient liés au vecteur appelé  $B_{\mu}$ ), le choix de champs quasi-statiques ayant la forme particulière (100), supprime automatiquement l'apparition de termes de ce genre.

En effet, avec les notations habituelles, on choisit une solution quasi-statique:

$$(100) \quad \varphi_{\underset{2}{x}\underset{2}{a}} = \sum_{k=1}^N \varepsilon_{\underset{2}{x}\underset{2}{a}r} \partial_{\underset{2}{r}} \varphi_{\underset{2}{}}^{\underset{2}{k}}, \quad \varphi_{\underset{3}{r}\underset{3}{0}} = \sum_{k=1}^N \varepsilon_{\underset{3}{r}\underset{3}{0}0} \partial_{\underset{3}{r}} \varphi_{\underset{3}{}}^{\underset{3}{k}}.$$

Pour la  $k^{\text{e}}$  particule dont le mouvement est déterminé par 3 fonctions du temps  $\hat{a}^{\underset{2}{k}}(t)$ , on a posé en effet:

$$(101) \quad \varphi_{\underset{2}{}}^{\underset{2}{k}} = \frac{\underset{2}{e}^{\underset{2}{k}}}{\underset{2}{r}}, \quad \varphi_{\underset{3}{}}^{\underset{3}{a}} = \frac{\underset{3}{e}^{\underset{3}{a}}}{\underset{3}{r}}.$$

Les champs (100) définis en fonction d'un infiniment petit  $\lambda = \sqrt{\varepsilon}$ , correspondent aux champs dits du 1<sup>er</sup> ordre dans le reste de ce travail. Une solution de la forme (100) entraîne donc

$$(102) \quad \varphi_{\underset{1}{\mu\nu}\varrho} = 0$$

et, d'après (68):

$$(103) \quad F_{\underset{1}{\mu\nu}} = 0.$$

Par conséquent:

$$(104) \quad \tau_{\underset{2}{\mu\nu}} = 0, \quad M_{\underset{2}{\mu\nu}} = 0.$$

Le seul tenseur non nul qui demeure au second membre de (79) est donc le tenseur  $X_{\mu\nu}$ . Sa contribution — qui se réduit à une divergence — ne peut conduire aux équations du mouvement.

Pour éviter cette conclusion négative, il faudrait

a) Ou bien déterminer un champ  $\varphi_{\mu\nu}$  tel que :

$$(105) \quad \varphi_{\mu\nu} \neq 0, \quad F_{\mu\nu} \neq 0.$$

b) Ou bien introduire dans l'hamiltonien initial des termes supplémentaires qui permettent l'adjonction d'un tenseur de Maxwell :

$$(106) \quad \theta_{\mu\nu} = -\varphi_{\mu\sigma}\varphi_{\nu}^{\sigma} + \frac{1}{4}\eta_{\mu\nu}\varphi_{\sigma\sigma}\varphi^{\sigma\sigma},$$

dans les équations du champ : Telle est l'intéressante mais assez artificielle suggestion de BONNOR <sup>(11)</sup>.

En résumé, il nous paraît souhaitable de chercher à obtenir les équations du mouvement en nous laissant guider par l'expression (54) du tenseur  $S_{\mu\nu} = G_{\mu\nu} - \frac{1}{2}\gamma_{\mu\nu}G$ . On peut alors reprendre en les modifiant quelque peu les approximations quasi statiques usuelles de façon à ménager une intervention possible des termes  $\varphi_{\mu\nu}$ ,  $F_{\mu\nu}$  et par conséquent des tenseurs  $M_{\mu\nu}$  et  $\tau_{\mu\nu}$ . Il peut être opportun, dans ce cas, de supprimer certaines restrictions de la théorie <sup>(12)</sup>. Quoi qu'il en soit, ce programme dépasse le cadre de cette étude.

Il est possible de supposer que l'obtention des équations du mouvement exige des modifications plus profondes de la théorie. Telle est l'interprétation

<sup>(11)</sup> W. B. BONNOR : *Proc. Roy. Soc.*, A **226**, 366 (1954).

<sup>(12)</sup> On sait qu'il est possible d'obtenir assez naturellement une forme de la théorie qui ne contienne pas la condition

$$(II) \quad \partial_\sigma \mathcal{G}_{\nu}^{\mu\sigma} = \partial_\sigma (\sqrt{-g} f^{\mu\sigma}) \doteq 0.$$

Celle-ci résulte en effet obligatoirement de l'application d'un principe variationnel à la densité scalaire.  $\mathcal{G}^{\mu\nu}R_{\mu\nu}(I)$ ,  $R_{\mu\nu}(I)$  étant le tenseur de Ricci formé avec une connexion quelconque  $\Gamma_{\lambda\tau}^0$ .

Par contre la condition (II b) n'intervient pas quand la variation porte au départ sur une densité  $\mathcal{G}^{\mu\nu}W_{\mu\nu}(L)$ ,  $W_{\mu\nu}(L)$  étant le tenseur de Ricci formé avec la connexion  $L_{\sigma\tau}^0$  à vecteur de torsion nul. Le courant

$$\sqrt{-g} f^\mu = \partial_\sigma (\sqrt{-g} f^{\mu\sigma}) \neq 0$$

se manifeste alors dans les équations du champ.

proposée en 1936 par la théorie non linéaire de Born-Infeld, interprétation étendue depuis par plusieurs auteurs <sup>(13)</sup> à la récente théorie unitaire.

Quoi qu'il subsiste de cette discussion, nous pouvons tirer de l'ensemble de cette étude les conclusions suivantes:

Il est avantageux de déduire les équations de la théorie du champ unifié de la solution rigoureuse des équations  $g_{\mu\nu,0} = 0$  substituée dans (7) et dans (8). On obtient ainsi à partir des équations rigoureuses (E) et (G) leur expression à un ordre donné sans utiliser des approximations successives et sans faire aucune hypothèse sur l'ordre de grandeur des  $\gamma_{\mu\nu} = g_{\mu\nu}$ . Enfin il est souhaitable de développer les calculs ultérieurs (approximations quasi-statiques aux divers ordres, portant aussi sur les  $\gamma_{\mu\nu}$ ) à partir des équations (54) de la gravitation, complétée au besoin par des termes en  $f_{\mu}$  <sup>(12)</sup>. Une éventuelle déduction des équations du mouvement d'une particule chargée basée sur l'intervention simultanée des tenseurs  $\tau_{\mu\nu}$  et  $M_{\mu\nu}$  ne semble pas totalement hors d'atteinte de la théorie du champ unifié.

---

<sup>(13)</sup> Cf. KURSUNOGLU: *Phys. Rev.*, **88**, 1369 (1952); S. MAVRIDÈS: *Journ. Phys.*, **16**, 482 (1955).

---

#### RIASSUNTO (\*)

Da soluzioni rigorose e generali  $\Gamma_{\mu\nu}^e(g_{\lambda e})$  e senza alcuna ipotesi sull'ordine dei  $\gamma_{\mu\nu} = g_{\mu\nu}$ , si ottengono delle equazioni approssimate. Si danno alcune interpretazioni fisiche di questi risultati. Il tensore del momento dello sforzo delle equazioni è messo in evidenza nelle equazioni della gravitazione ed appaiono alcune possibilità di ottenere le equazioni di moto di una particella carica.

---

(\*) Traduzione a cura della Redazione.

## Star Produced by the Capture of a Hyperon $\Sigma^-$ .

TSAI-CHÜ

*Faculté des Sciences, Sorbonne, France*

(ricevuto il 4 Febbraio 1956)

**Summary.** — A flat track of 876  $\mu\text{m}$  emitted from a primary star of 19 prongs came to rest in the emulsion and produced a small star of three prongs. Direct mass determinations of the above track give  $2830 \pm 560 m_e$  by ionization and  $2560 \pm 790 m_e$  by scattering. Two prongs of the secondary star can be identified as  $\alpha$ -particles; the star has a visible energy of 18 MeV. The small star has been explained by the reaction  $\Sigma^- + p \rightarrow \Lambda^0 + n$ ; the capture of a negative hyperon by a proton inside a nucleus with a few low energy nucleons knocked out of the target nucleus. The present event may be the break-up of a light nucleus by the neutron and  $\Lambda^0$ .

We have studied <sup>(1,2)</sup> the strange particles giving rise to nuclear interactions or slow secondaries from a stack S 36 of 600 microns G5 stripped emulsion sheets developed to a low minimum ionization. Among the nuclear interactions examined, there was one having the characteristics of a hyperon capture star. A slow particle, with a range of 876 microns and a mass of the order of a proton, emitted from a primary star came to rest in the emulsion and produced a small star. Of the twelve examples of hyperon capture events <sup>(3,4)</sup> published up to date, nearly half are stars with only small prongs and having an energy below 35 MeV. Incidentally, the stars are small because a part of the hyperon energy is carried away by the  $\Lambda^0$  formed during the

<sup>(1)</sup> M. MORAND and TSAI-CHÜ: *Suppl. Nuovo Cimento*, **12**, 280 (1954).

<sup>(2)</sup> TSAI-CHÜ: *Compt. Rend.*, **241**, 294 (1955); *Nuovo Cimento*, in the press.

<sup>(3)</sup> R. H. W. JOHNSTON and C. O'CEALLAIGH: *Phil. Mag.*, **45**, 424 (1954); *Nuovo Cimento*, **10**, 468 (1955).

<sup>(4)</sup> M. CECCARELLI, N. DALLAPORTA, M. GRILLI, M. MERLIN, G. SALANDIN, B. SECHI and M. LADU: *Nuovo Cimento*, **2**, 542 (1955).



capture process. The low granulation of this stack is more favorable for the visual study of short tracks. The mass determination by ionization using the method of gaps and blobs can be extended to the whole trajectory of the particles with satisfactory results as a large number of gaps is still present near the end of the tracks. The short prongs of the secondary star can be identified as  $\alpha$  particles by comparing with the radioactive  $\alpha$  particles found in the emulsion. The density of radioactive  $\alpha$  stars leads to the conclusion that the probability of an accidental coincidence between the end of a proton and a radioactive  $\alpha$  star is negligible for this event.

### 1. — The Direct Mass Determinations.

The mass of the particle producing the secondary star was determined both by ionization and by scattering. The grain density of a particle in emulsion is roughly proportional to its ionization. It depends only on the velocity and specific charge of a particle and is independent of its mass. The grains in emulsion take different shapes and dimensions and for higher ionization they begin to overlap, making visual counting difficult. Much information can be obtained about the ionization of a particle by measuring the lengths of the grains or gaps, but the process is too time-consuming. However it is more expedient to proceed by counting gaps and blobs <sup>(5)</sup> than by measuring gap lengths. « Gap and blob » counting is also more accurate than blob counting in the determination of the mass of an unknown particle. Supposing  $N(L)$  is the number of gaps with a projected length longer than  $L$ ,  $N(0)$  will be the total number of gaps in a section or simply the number of blobs, we have

$$(1) \quad N(L) = N(0) \exp [-gL],$$

or

$$(2) \quad g = \frac{1}{L} \log_e \frac{N(0)}{N(L)};$$

and

$$(3) \quad g = \frac{2.303}{L \sec \beta} \log_{10} \frac{N(0)}{N(L)},$$

for a section with an angle of dip  $\beta$  in emulsion. The coefficient  $g$  depends on the velocity and specific charge of the particle. The number of blobs  $N(0)$  decreases with the increase of velocity of the particle; the number of long

---

<sup>(5)</sup> P. H. FOWLER and D. H. PERKINS: in the press.

gaps  $N(L)$  increases slightly with the increase of velocity, so their ratio  $N(0)/N(L)$  is more sensitive to the variation of velocity than the blobs  $N(0)$ .

We counted the number of gaps with  $L$  longer than 0.63 microns, or equivalent to 0.2 divisions of the scale in the eyepiece of the microscope. The measurements were made from the end of the trajectory in sections of 25 microns. Near the end of the track, there may be some sections containing only gaps under the specified limit, so we had to count smaller gaps and to calculate the coefficient  $g$  by means of the equation

(3). We selected nine protons close to the particle to be measured for its mass determination. The curve in Fig. 1 shows the average results of every 100 microns for the protons; the ordinate represents the average of  $\cos \beta \log_{10} \cdot (N(0)/N(L))$  and the abscissa the logarithm of range in units of 25 microns;

the points marked with  $\times$  are the corresponding values for the unknown particle. The coefficient  $g$  can be obtained by multiplying the ordinate with  $3.70 \text{ microns}^{-1}$ . The mass of the

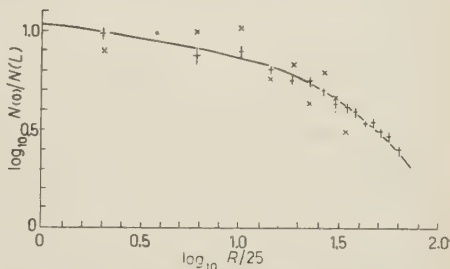


Fig. 1. - Logarithm of ratio between blob number and gap number against logarithm of range for protons and hyperons ( $\times$ ).

particle, relative to that of a proton, which is equal to the mean ratio of ranges with the same ordinate is  $1.73 \pm 0.62$ . A similar result is obtained by counting gaps longer than 0.3 divisions. The weighted mean is  $1.54 \pm 0.31$  and is obtained by assigning to each ratio a weight inversely proportional to the square of its deviation from the mean one. The mass of the particle is  $2830 \pm 560 m_e$ .

The scattering of the particle was measured with the constant sagitta method by means of the microscope Koritska. The Koritska MS2 has no one-micron graduation for the movement along the trajectory, but it provides 4 cogged disks permitting an automatic displacement in  $\pi$ -cells. The first disk begins at 124 microns from the end of the trajectory; the four disks cover a total distance of about 2000 microns. Starting from the end of the trajectory, we measured the scattering in cells of 5 microns until 125 microns, then continued with the four disks. Measurements were repeated several times in order to reduce the observational errors. For the second difference in ordinate of the fundamental cells, we obtained, by eliminating the noise between

(6) C. DILWORTH, S. J. GOLDSACK and L. HIRSCHBERG: *Nuovo Cimento*, **11**, 113 (1954).

the fundamental and the double cells, the following values:

	within 125 $\mu$ m	above 124 $\mu$ m
unknown particle	1.51	3.53
proton	$1.96 \pm 0.03$	$3.57 \pm 0.03$

The above values are in divisions of a scale on the eyepiece of the microscope, each division is calibrated to 0.0564 microns. The values for the protons are deduced from a trajectory of about 1000 microns and they stand for the weighted means of 14 protons found in the neighborhood of the unknown particle. Scattering angles four times larger than the mean values were eliminated and replaced by one equal to four times the mean one. Corrections for inclinations of the tracks in emulsion were applied to the protons as well as to the unknown particle; for the unknown particle, they were 1.5% for the trajectory within 125 microns from the end and only 0.2% for the other part. Other corrections<sup>(6)</sup> on the second differences due to the variation of the scattering constant, range and energy relation and relativistic effect were estimated for the proton and a particle with a mass 1.25 times that of a proton. The total correction on the ratio of the second differences between the proton and the unknown particle was 0.9995 for that portion of the trajectory farther from the end and it was 1.021 for the portion nearer the end, the latter including another correction due to the deviation from a constant sagitta scheme. The mass of the particle which is deduced from the average of the two ratios of the second differences is  $2560 \pm 790 m_e$ . The average is obtained by taking account of the number of measurements and the error is the standard deviation estimation from the number of independent double cells.

The mass of the particle giving rise to the secondary star is higher than that of a proton and is compatible with that of the hyperon  $\Sigma$ .

## 2. — The $\alpha$ -Particles in Emulsion.

In order to identify the nature of the short prongs of the secondary star and to estimate the probability of accidental coincidence of this event, we studied a small sample of radioactive  $\alpha$  particles present in the emulsion around the event found. We measured the projected length and the angle of dip of 264  $\alpha$  particles and counted their number of gaps. The number of gaps of the  $\alpha$  particles was normalized to a standard length of 25 microns; the histogram of Fig. 2 shows their distributions. Apparently there is a large number of  $\alpha$  particles from zero to two gaps. The inclination of a particle may have some influence on the detection of gaps. After having grouped the  $\alpha$  particles without gap in different angular intervals, we found that they began to

increase for an angle of dip greater than  $40^\circ$ . The histogram in broken lines indicates the corrected distributions. Many  $\alpha$  particles have actually 2 to 6 gaps per 25 microns, and only one has 12.9 gaps; while protons have, on the average,  $13.2 \pm 0.8$  gaps on the last 25 microns from the end of the track. Therefore it is generally possible to distinguish an  $\alpha$  particle from a short proton by gap counting.

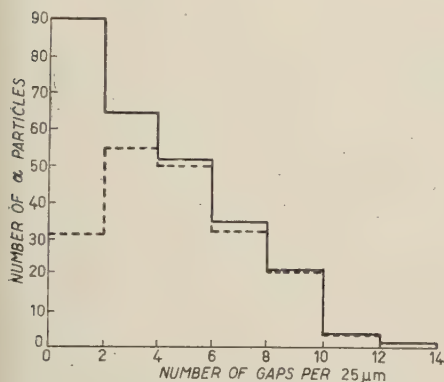


Fig. 2. — Gap distributions of  $\alpha$ -particles. Solid line for all particles and dotted line for those with an angle of dip greater than  $40^\circ$ .

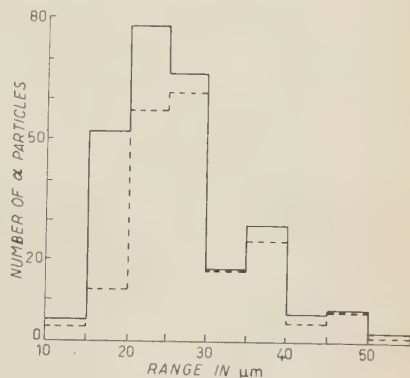


Fig. 3. — Length distributions of  $\alpha$ -particles. Solid line for all particles and broken line for those forming stars.

The  $\alpha$  particles observed in emulsion appear either as single tracks or as stars. Those forming stars are often not emitted from the same point, because some diffusion of the radioactive nuclei may take place during the intervals between two emissions. The total density of  $\alpha$  particles in this emulsion is  $5.1 \cdot 10^2$  particles per  $\text{cm}^2$ ; nearly two thirds of them are formed in stars and the average number of  $\alpha$  particles per star is  $4.1 \pm 0.3$ . The density of 3-prong  $\alpha$  stars is  $4 \cdot 10^{-10}$  per cubic micron.

The histogram of Fig. 3 shows the distribution of the lengths of the  $\alpha$  particles; the one in broken line shows the same for associated particles. In agreement with the Geiger and Nuttall law,  $\alpha$  particles with higher energy are produced by radioactive nuclei with shorter half-period of life, so the majority of  $\alpha$  particles with longer tracks form stars. A group of short single tracks with a range from 15 to 20 microns and an energy of about 4.5 MeV may have been produced by the traces of thorium contained in the emulsion. Two groups of associated  $\alpha$  particles, one with a range from 20 to 30 microns and an energy of about 5.8 MeV and the other from 35 to 40 microns and an energy of 7.6 MeV may have been produced by radon and its product  $\text{RaC}'$  respectively. A very small group with a range from 45 to 50 microns, and energy of 8.9 MeV may have been produced by  $\text{ThC}'$ . Consequently, the single  $\alpha$  par-



ticles in stripped emulsion may issue from the long lived thorium present in the emulsion, while the associated ones, constituting a higher percentage, may indicate that they are mainly produced by another short lived radioactive element, probably the radon in the atmosphere or in the surroundings.

### 3. - The Primary and the Secondary Stars.

We observed nineteen particles coming out from the primary star. There were thirteen prongs with a grain density four times higher than the minimum of ionization (six of these prongs including the hyperon came to rest in the same plate); one prong with a grain density about 3 times and 5 prongs with a grain density less than twice the minimum. As the plates were developed to a minimum of only about 11 grains per 100 microns, some relativistic prongs may have escaped observation.

Besides the hyperon  $\Sigma$ , there were some other prongs showing interesting features.

A particle, next to the hyperon, was emitted with a grain density equal to about six times the minimum and made a large single angle scattering after describing a trajectory of 8.5 mm. The particle increased its grain density after the single scattering. It came to rest in the next plate with a total residual range of 4500 microns and could be a proton. Before the single scattering, the particle could have a smaller multiple scattering and a smaller variation of granulation than those of a proton.

Another particle with a grain density 3 times the minimum had a trajectory of 300 microns only and produced two particles: one with higher grain density and another with a black trajectory. The latter particle had a large angle of dip and came to rest after traversing six plates with a total range of about 4000 microns; the former traversed 24 plates and left the stack after travelling a distance of about 4.5 cm in the emulsion, it could have a residual range of 4000 microns if it were a proton.

Detailed study of these and other tracks is still in progress.

A negative hyperon, like negative  $K^-$  and  $\pi^-$  mesons is usually captured by a nucleus and produces a star when it comes to rest. Fig. 4 shows the hyperon  $\Sigma^-$  and the secondary star. The hyperon whose mass was determined in the previous section must be a negative one. The secondary star had three small prongs, all terminated in the emulsion. At the centre of the star there could be an electron of very low energy (of the order of keV) which was not indicated in the figure. Table I shows their range, orientations, energy and momentum.  $\alpha$  is the angle made by the projection of a track on the plane of the plate and another arbitrary direction chosen in the plate;  $\beta$  is the angle between the track and this projection. Prongs *A* and *C* have 5.0 and 2.2 gaps



per 25 microns, they have nearly the same number of gaps (2 to 6) as do most  $\alpha$  particles. So prongs *A* and *C* are more probably  $\alpha$  particles than protons, prong *B* could also be an  $\alpha$  particle but it is too short to be identified defini-



Fig. 4. — The hyperon  $\Sigma^-$  and the secondary star.

TABLE I.

Prong	Range ( $\mu\text{m}$ )	$\alpha$	$\beta$	Energy (MeV)	Momentum (MeV/c)
<i>A</i>	56.0	203° 40'	—22° (glass)	9.9	271
<i>B</i>	4.9	190°	+33° (air)	1.5 (0.49)	104 (29.7)
<i>C</i>	34.3	121° 50'	+49°	7.2	230
total	—	178° (176°)	+18° (+15°)	18.6 (17.6)	416 (347)
Pri.	876	153° 20'	+ 2°	—	—

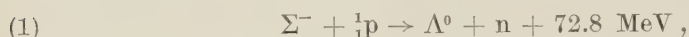
tely. Among the radioactive  $\alpha$  particles studied, none had a range as long as prong *A*; and none as short as prong *B*. Therefore the possibility of an accidental coincidence between a radioactive  $\alpha$  star and the end of a proton seems quite small for this event. An upper limit for such accidental coincidence can be estimated from the number of ordinary 3-prong radioactive stars within a sphere of, say 3 microns radius, i.e.  $27.4 \cdot 10^{-10}$  or  $10^{-8}$ . It should be remarked that long-range radioactive  $\alpha$  particles<sup>(7)</sup> do exist, for example 20 in  $10^6$  of  $\text{RaC}'$   $\alpha$  particles have 10.422 MeV and 2 in  $10^6$  of  $\text{ThC}'$   $\alpha$  particles have 10.0735 MeV; the probability of an accidental coincidence should be reduced by a factor of  $10^{-4}$ .

The momentum and energy of prong *B* in Table I were calculated as an  $\alpha$  particle, those in parentheses for *B* as a proton. The hyperon star has a

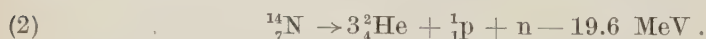
(7) G. H. BRIGGS: *Rev. Mod. Phys.*, **26**, 4 (1954).

total visible energy of 18.6 MeV if we assume prong  $B$  as an  $\alpha$  particle, or 17.6 MeV if prong  $B$  were a proton. The three prongs of the hyperon star have a resultant momentum of 416 MeV/c orientated with an angle  $\alpha$  equal to  $178^\circ$  and an angle  $\beta$  equal to  $18^\circ$ ; the numbers in parentheses indicate the corresponding values for prong  $B$  as a proton.

According to theory and experiments, the small star can be explained <sup>(4,5)</sup> as the capture of a hyperon by a proton inside a nucleus, namely



the  $\Lambda^0$  and the neutron formed inside may leave the nucleus in opposite directions and knock out a few low energy nucleons. For  $\Sigma^- = 2326 m_e$ ,  $p = 1836 m_e$ ,  $\Lambda^0 = 2181 m_e$ ,  $n = 1838.5 m_e$  and for the capture of  $\Sigma^-$  by a free proton, the energy released will be equal to  $142.5 m_e c^2$  or 72.8 MeV; the  $\Lambda^0$  and the neutron have each a momentum of 275 MeV/c and an energy of 33.3 MeV for  $\Lambda^0$  and 39.5 MeV for neutron respectively. In the present example, the  $\alpha$  particles actually have small energies but their resultant momentum is too high in comparison with 275 MeV/c, this high momentum 416 or 347 MeV/c can only be balanced by a  $\Lambda^0$  accompanied by some neutrons moving in an opposite direction to that of the  $\alpha$  particles. So the break-up of a  ${}^{12}_6\text{C}$  into three  $\alpha$  particles is energetically possible but ruled out by momentum considerations. Supposing the break-up of a nitrogen nucleus  ${}^{14}_7\text{N}$ ,



Reactions (1) and (2) worked together will produce three  $\alpha$  particles, one  $\Lambda^0$  and two neutrons with an energy of 34.6 for the three neutral particles. The momentum of the  $\alpha$  particles can easily be balanced by giving each neutron an energy less than 10 MeV. If prong  $B$  were a proton, one may consider the carbon nucleus



Because a larger amount of energy is required to release the protons and neutrons than  $\alpha$  particles, we have only 19.8 MeV available for the distribution among the three neutrons and one  $\Lambda^0$ ; each of them may have only 5 MeV.

<sup>(8)</sup> M. W. FRIEDLANDER, Y. FUJIMOTO, D. KEEFE and M. G. K. MENON: *Nuovo Cimento*, **2**, 90 (1955).

#### 4. - Conclusion.

The primary particle of the small star has a mass value compatible with that of a hyperon. The probability of an accidental coincidence between a radioactive  $\alpha$  star and a proton is negligible for this event. The small secondary star indicates that the primary particle is a hyperon  $\Sigma^-$  and the capture of this hyperon could probably lead to the break-up of a nitrogen nucleus. The  $\Lambda^0$  emitted has a smaller kinetic energy than what the capture by a hydrogen nucleus would produce.

\* \* \*

I wish to express my sincere thanks to Professor MAX MORAND, Science Faculty, University of Paris, for his guidance and encouragement in this work and to each one of my colleagues in the laboratory for his or her collaboration.

#### RIASSUNTO (\*)

Una traccia piana di  $876 \mu\text{m}$  emessa da una stella primaria di 19 rami si è arrestata nell'emulsione producendo una piccola stella di 3 rami. Determinazioni di massa dirette eseguite sulla traccia di cui sopra danno per ionizzazione  $2830 \pm 560 m_e$  e per scattering  $2560 \pm 790 m_e$ . Due rami della stella secondaria si possono identificare con particelle  $\alpha$ ; la stella ha un'energia visibile di 18 MeV. La stella piccola è stata spiegata con la reazione  $\Sigma^- + p \rightarrow \Lambda^0 + n$ ; cattura di un iperone negativo all'interno di un nucleo con qualche nucleone di bassa energia espulsi dal nucleo bersaglio. Il presente evento potrebbe essere la frammentazione di un nucleo leggero da parte del neutrone e del  $\Lambda^0$ .

---

(\*) Traduzione a cura della Redazione.

## Observations on the Multiply Charged Particles of the Cosmic Radiation.

C. J. WADDINGTON

*H. H. Wills Physical Laboratory, University of Bristol, England*

(ricevuto l'8 Febbraio 1956)

**Summary.** — A nuclear emulsion technique has been used to measure the fluxes of the  $\alpha$ -particles of the primary cosmic radiation at three different geographical positions. Two of these determinations were made on the same geomagnetic latitude, one over America, which has been previously reported <sup>(1)</sup>, and the other over England. The two flux values found were unexpectedly significantly different, and this difference could be entirely attributed to the absence over England of those  $\alpha$ -particles with energies of less than about 0.65 GeV per nucleon. Measurements on the protons and heavy primary particles detected in those two stacks of emulsions also indicated that the cut-off energy over England at the time of the exposure was between 0.60 and 0.70 GeV per nucleon, instead of the 0.33 GeV per nucleon calculated from the known geomagnetic latitude. Similarly, the data from the American stack suggest that when this was exposed the cut-off energy was less than 0.15 GeV per nucleon. An analysis has been made of the various experimental flux values obtained at different points on the earth's surface, and it is concluded that the cut-off energies should be calculated, not from the geomagnetic latitudes, but from latitudes which are from four to six degrees lower over Europe, and three or more degrees higher over America.

### Introduction.

In a previous experiment on the properties of the  $\alpha$ -particles in the primary cosmic radiation <sup>(1)</sup> a determination was made of the incident flux and energy distribution. A stack of glass backed nuclear emulsions exposed by high altitude balloon was employed to detect these particles. This exposure

---

<sup>(1)</sup> C. J. WADDINGTON: *Phil. Mag.*, **1**, 105 (1956).

was made at Minnesota, at a geomagnetic latitude of  $55^{\circ}$  N. In the present paper it is proposed to compare the results of this investigation, henceforth referred to as Part I, or «the American investigation», with the results obtained from a similar experiment made in a stack of stripped emulsions exposed on the same geomagnetic latitude but at a different geographic position. This later investigation will be referred to as Part II, or «the English investigation». In addition, the results of another flux determination, Part III, «the Italian investigation», made in a stack of stripped emulsions exposed in Northern Italy in 1954, will be considered because of its significance in the interpretation of the conflicting results obtained from the two earlier experiments.

Part II was undertaken in a stack exposed over Southern England in 1954. It was originally intended to use the greatly increased path lengths available in stripped emulsions to resolve the existing controversy concerning the energy distribution <sup>(1)</sup>, and to study the types of interactions induced by the  $\alpha$ -particles. The results relating to the interactions have been published <sup>(2)</sup>. With regard to the energy spectrum it was found that the greater statistical weight available on the determinations of the energies of the particles was more than offset by the higher level of distortion in these emulsions. For this reason, and for others which will become apparent later, it was not possible, from the direct energy measurements, to resolve the previously mentioned controversy. Instead it is suggested that neither of the previous methods of obtaining the spectra at these energies <sup>(3)</sup> were entirely correct.

However, it was found that there were considerable discrepancies between the results obtained in the two experiments. Pronounced differences were observed between the absolute flux values, and between the form of the low energy ends of the energy spectra. It is with these differences, their experimental confirmation, and the interpretation of their existence that this paper is primarily concerned. The main features of this work were reported at the Mexico Conference (1955).

## 1. — Experimental Method.

1.1. *Stack Details.* — The relevant details of the three stacks of nuclear emulsions used in these investigations are given in Table I.

In this table the value quoted for the residual matter consists of the total quantity of matter, in  $\text{g/cm}^2$ , due to the vertical residual atmosphere, together with that due to packing material above the emulsions.

<sup>(2)</sup> C. J. WADDINGTON: *Phil. Mag.*, **1**, 105 (1956).

<sup>(3)</sup> M. F. KAPLON, B. PETERS, H. L. REYNOLDS and D. M. RITSON: *Phys. Rev.*, **85**, 295 (1952).



TABLE I.

	No. of plates	Size of plates cm	Geo- mag. latitude	Time of exposure hrs	Mean altitude ft	Residual matter g/cm <sup>2</sup>	Date
Stack I (American)	24*	15 × 15 × 0.04	55° N	4	97 000	14.5	4-10-50
Stack II (English)	40	30 × 25 × 0.06	55° N	4	101 000	12.5	9-7-54
Stack III (Italian)	80	15 × 20 × 0.06	46° N	6	106 000	9.5	14-9-54

(\*) Glass backed.

1'2. *Particle Selection.* — The methods of track selection employed were very similar to those described previously <sup>(1)</sup>.

The emulsions were scanned along horizontal lines parallel to the top edges for tracks satisfying the following criteria:

i) The track must have had a projected length in the emulsions of greater than eight millimetres in Stack I, greater than ten in Stack II, and greater than six in Stack III.

ii) The track must have had a grain density greater than about three times the plateau value in that particular emulsion.

These scanning lines were separated from each other by a distance of ten millimetres, and from the edges of the emulsions by a distance of at least ten millimetres. When allowance was made for tracks which crossed two or more scans, each scan could be considered independently.

1'3. *Track Measurement.* — Somewhat different procedures of measurement were used in the later investigations than in the American one. In particular, due to the use of stripped emulsions, which permitted the singly charged particles to be followed either to rest, or until they revealed their nature, scattering measurements in the English stack were made only on those tracks already identified as being due to  $\alpha$ -particles. Also, because of the low level of ionization in the emulsions of this stack, accurate ionization measurements were made on all the  $\alpha$ -particle tracks. These measurements were made with the primary objective of determining the form of the low energy end of the energy-spectrum.

1'3.1. Ionization measurements. - In order to determine the grain density, more than 600 grains were counted on each track found in the English stack, compared with the 200 to 400 in the other stacks. As a result the grain density measurements in the English stack were considered to be the most reliable. Those in the American stack must be regarded as being somewhat unreliable, since at the time when they were made the author had not established a reliable and invariable grain counting convention. These various grain density measurements are shown in Fig. 9, Appendix I.

Blob-gap measurements, of the type introduced by FOWLER and PERKINS <sup>(4)</sup>, were made on all the  $\alpha$ -particle tracks observed in the English stack. On each track determinations of  $G$ , the coefficient of the exponent of the gap-length distribution, were made on a number of individual segments. These segments were selected so that they each contained 50 gaps. The length of the gaps,  $l$ , was such that  $G \cdot l$  was approximately 2.5. Measurements were made on six such segments in each track, and as far as possible their positions were selected so that they lay near the middle of the emulsions. No more than three were counted in any one emulsion, thus reducing the possibility that a local variation in the ionization of one emulsion should severely affect the mean value of  $G$  obtained for the track.

These measurements were corrected for the variation of development from emulsion to emulsion, and for that due to the variation with depth in a single emulsion. The magnitude of these corrections was obtained by making blob-gap measurements over the entire lengths of relativistic  $\alpha$ -particle tracks passing through the emulsions. These particles were selected by their low scattering parameters, and by the high energy disintegration they produced.

The normalized mean values of  $G$ ,  $\bar{G}$ , obtained on all the particle tracks observed in the English stack are shown in Fig. 1. In this figure the  $\bar{G}$  values obtained on tracks with a scattering parameter of less than  $0.01^\circ/100 \mu\text{m}$  are shown in black. Also shown is the value obtained from the tracks used to normalize the emulsions, and those values corresponding to energies of about 0.65 and 0.35 GeV per nucleon at the top of the atmosphere. These values were obtained from the known variation of  $G$  with velocity on singly charged particles <sup>(4)</sup>. It can be seen that the number of  $\alpha$ -particles which entered the atmosphere

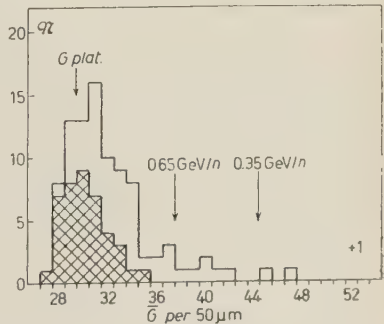


Fig. 1. - The distribution of the blob-gap density on the particles observed in the English stack. The value obtained on relativistic  $\alpha$ -particles is shown by  $G_{\text{plat}}$ .

<sup>(4)</sup> P. H. FOWLER and D. H. PERKINS: *Phil. Mag.*, **46**, 587 (1955).

with energies of less than 0.65 GeV per nucleon was small. The measurements made on the fast  $\alpha$ -particles to normalize the emulsions indicate that there is no appreciable «trough» in the ionization of doubly charged particles analogous to that observed for the singly charged particles. This observation supports that of FOWLER and PERKINS (4) who state that if there is a «trough» it must be less than 5%.

13.2. Multiple scattering measurements – In making the multiple scattering measurements in the English investigation a  $4\bar{D}$  replacement cut-off was employed instead of the  $4\bar{D}$  block cut-off used in the American one. Noise elimination was used, both between  $\bar{D}_2$  and  $\bar{D}_c$ , and between  $\bar{D}_{3c}$  and  $\bar{D}_c$ , and a weighted mean taken of the resulting scattering parameters (5). A correction for C-shaped distortion (6) was applied to all tracks. All the scattering parameters were measured on a basic cell size of 400  $\mu\text{m}$ , and as far as possible about 100 cells were measured.

The noise elimination was calculated assuming a dependence on  $c^{\frac{1}{2}}$ , where  $c$  was the cell size in hundreds of microns, since this dependence was found to be a better representation of the experimentally observed variation than the  $c^{\frac{1}{4}}$  assumed previously. The data obtained in the American stack have been recalculated for this dependence, since measurements made at that time show a similar variation, and the energy spectra shown later are derived from these new energy values. In practice it is found that the effect of this change is to raise the individual energy values only slightly.

No scattering measurements were made in the Italian stack.

## 2. – The Flux of Primary $\alpha$ -Particles.

In the conditions of an experiment of this type the flux of particles at the point of detection in the emulsion,  $J_n(x)$ , is given by

$$(1) \quad J_n(x) = \frac{N}{t \cdot a \cdot \varphi} \frac{\int_0^{\theta_{\max}} d\theta}{\int_0^{\theta_{\max}} \cos \theta d\theta},$$

where  $N$  is the total effective number of particles crossing a detecting area  $a$ ,  $\theta$  is the zenith angle,  $t$  is the time of exposure of the emulsions in seconds, and  $\varphi$  is the solid angle over which particles may enter and be detected.

(5) R. R. DANIEL and D. H. PERKINS: *Proc. Roy. Soc., A* **221**, 351 (1954).

(6) P. H. FOWLER: *Phil. Mag.*, **41**, 169 (1950).

To extrapolate  $J_{\lambda}(x)$  to the top of the atmosphere it is necessary to correct for the absorption of primary  $\alpha$ -particles in the matter above the point of detection, and for the production of secondary  $\alpha$ -particles produced by the fragmentation of the heavy primary particles ( $Z \geq 3$ ). In order to make these corrections values must be assumed for the mean free paths of  $\alpha$ -particles and heavy primaries in the relevant materials, for the fluxes of the heavy primaries, and for the fragmentation probabilities of these heavy particles in the various media. None of the values quoted in the literature for the mean free paths or fragmentation probabilities in air, or light elements, appear to be very reliable, since they nearly all depend on an extrapolation from values observed in media predominantly composed of heavy elements, such as nuclear emulsion. Similarly the values quoted for the heavy primary fluxes differ widely, partly perhaps because they depend quite seriously on the values taken for the mean free paths and fragmentation probabilities. Fortunately these uncertainties do not seriously affect the  $\alpha$ -particles, since the correction for the effects of secondary particles at the depths in the atmosphere applicable to these experiments is less than 15%. The major uncertainty is introduced by the existing doubt as to the true value of the absorption mean free path of  $\alpha$ -particles in air. However, the extrapolations from the observed mean free paths of  $\alpha$ -particles in media such as brass, glass and emulsion made by BRADT and PETERS<sup>(7)</sup>, and that made by the author<sup>(2)</sup> both give the same value of about 45 g/cm<sup>2</sup>. This value has been used throughout.

The primary flux,  $J_{\lambda 0}$ , was calculated by using a method due to KAPLON *et al.*<sup>(8)</sup>, see also GOTTSTEIN<sup>(9)</sup>. These authors considered parallel beams of nuclei travelling through the atmosphere, and neglected ionization losses. They solved the diffusion equations of these nuclei for the various components of the heavy primaries. These equations have also been solved for the  $\alpha$ -particles, so that they may be used to find  $J_{\lambda 0}$ . Using these equations the primary flux found in Part I was recalculated, and those of Parts II and III determined.

The flux values in the emulsions of Stacks I, II and III were from equation (1).

$$J_{I\alpha}(x) = 207 \pm 23 \text{ } \alpha\text{-particles/m}^2\text{/steradian/s}$$

$$J_{II\alpha}(x) = 138 \pm 16 \text{ } \alpha\text{-particles/m}^2\text{/steradian/s}$$

$$J_{III\alpha}(x) = 72 \pm 8 \text{ } \alpha\text{-particles/m}^2\text{/steradian/s}$$

and these values, when extrapolated to the top of the atmosphere,

(7) H. L. BRADT and B. PETERS: *Phys. Rev.*, **77**, 54 (1950).

(8) M. F. KAPLON, J. H. NOON and G. W. RACETTE: *Phys. Rev.*, **95**, 1408 (1954).

(9) K. GOTTSTEIN: *Phil. Mag.*, **45**, 347 (1954).



became

$$J_{I\alpha^0} = 292 \pm 32 \text{ } \alpha\text{-particles/m}^2\text{/steradian/s}$$

$$J_{II\alpha^0} = 172 \pm 19 \text{ } \alpha\text{-particles/m}^2\text{/steradian/s}$$

$$J_{III\alpha^0} = 88 \pm 13 \text{ } \alpha\text{-particles/m}^2\text{/steradian/s}.$$

It can be seen that there is a very significant, and unexpected difference between  $J_{I\alpha^0}$  and  $J_{II\alpha^0}$ . Discussion of this point will be deferred until Section 5, where it will be shown that this difference can hardly be due to an experimental error, but must be physically significant. In addition it will become apparent that the true value of  $J_{III\alpha^0}$  is obtained if the flux values of the heavy primaries are reduced by about one third from those assumed when calculating  $J_{I\alpha^0}$  when making the extrapolation to the top of the atmosphere. Under these conditions  $J_{III\alpha^0}$  becomes

$$J_{III\alpha^0} = 182 \pm 21 \text{ } \alpha\text{-particles/m}^2\text{/steradian/s}.$$

This value will be used henceforth.

Two previous comparable flux determinations exist. Both of these were made at approximately the same *geographic* position as that of the American investigation. NEY and THON <sup>(10)</sup>, who used a scintillation counter flown in a conventional counter array, found  $J_{\alpha}(x)$ , under less than 10 g/cm<sup>2</sup>, to be  $280 \pm 8 \text{ } \alpha\text{-particles/m}^2\text{/steradian/s}$ . Extrapolating in the same manner as above, this results in a value of  $J_{\alpha^0}$  of  $318 \pm 9 \text{ } \alpha\text{-particles/m}^2\text{/steradian/s}$ . DAVIS *et al.* <sup>(11)</sup> obtained a value for  $J_{\alpha^0}$  of  $310 \pm 30$  (\*)  $\alpha\text{-particles/m}^2\text{/steradian/s}$  when using a proportional counter. It can be seen that both these values are in good agreement with that obtained for  $J_{I\alpha^0}$ .

The significance of the value obtained for  $J_{III\alpha^0}$  will become apparent later. At this stage in the discussion it will merely be remarked that this value, which is the only other one made over Europe, is considerably lower than that which would have been predicted from a consideration of previous results obtained over America.

### 3. - The Energy Spectrum.

From the values of the scattering parameters obtained on each of the  $\alpha$ -particle tracks observed in the American and English stacks it is possible

<sup>(10)</sup> E. P. NEY and D. M. THON: *Phys. Rev.*, **81**, 1068 (1951).

<sup>(11)</sup> L. R. DAVIS, H. M. CAULK and C. Y. JOHNSON: *Phys. Rev.*, **91**, 431 (1953).

(\*) Value quoted by HORWITZ <sup>(12)</sup>.



to determine either the energy, or a lower limit to the energy. In view of the doubt that has recently been cast by BISWAS *et al.* <sup>(12)</sup> on the significance of scattering measurements made on particles of high energy, the precise significance of the energy values obtained is uncertain. However, evidence is presented in Appendix II which suggests that the experimental energy values of less than about 1 GeV per nucleon can be considered generally reliable.

It was originally intended to use the blob-gap density measurements as a means of checking and improving the energy values obtained from scattering measurements on the relatively slow  $\alpha$ -particles, thus determining the shape of the low energy end of the spectrum with greater precision than hitherto. However, due to the absence of any appreciable number of low energy  $\alpha$ -particles (see Fig. 1) this became impossible, and the use of these measurements was restricted to confirming that the majority of the particles observed had energies greater than about 0.65 GeV per nucleon.

The integral and differential energy spectra of Parts I and II, when extrapolated to the top of the atmosphere, are shown in Fig. 2. Only tracks with zenith angles less than  $60^\circ$  or  $65^\circ$  in Parts I and II respectively are considered. The position of the cut-off energy calculated from the geomagnetic latitude is shown on each of these spectra. Also shown is the mean

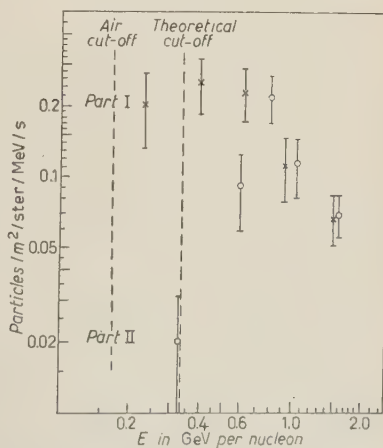
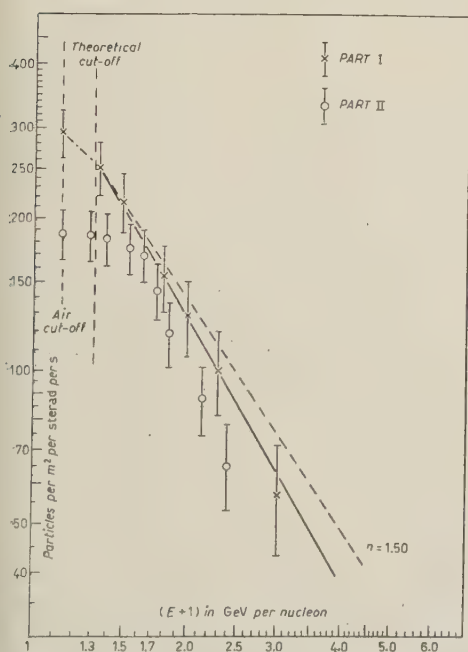


Fig. 2. — The integral and differential energy spectra extrapolated to the top of the atmosphere in the American and English stacks. Values are shown for the geomagnetic cut-off energy, and for the air cut-off energy.

<sup>(12)</sup> S. BISWAS, B. PETERS and RAMA: *Proc. Ind. Acad.*, **41**, 154 (1955).

energy of incidence for which an  $\alpha$ -particle would be absorbed by the overlying matter before being detected in the emulsions, the «air cut-off». It may be noted that the integral spectrum in the American investigation appears to rise fairly steadily to this value.

These spectra show that the flux discrepancy previously noted can be entirely attributed to a lack of low energy particles in the English stack. This conclusion is supported by the grain density measurements, see Fig. 9, which suggest that there are far fewer tracks with high ionizations in Stack II than in Stack I.

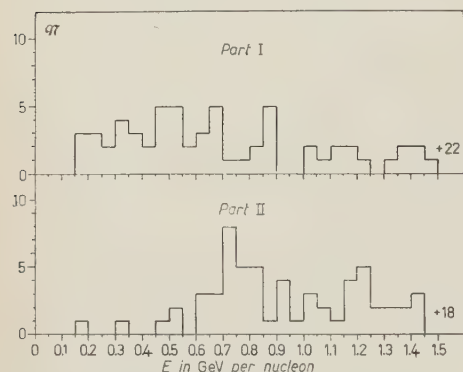


Fig. 3. The distribution of the energies of the  $\alpha$ -particles at the top of the atmosphere in the American and English stacks.

In order to assist in a clear appreciation of the precise nature of the data represented in Fig. 2, the top-of-the-atmosphere energy values obtained in the two experiments are also shown plotted as a histogram on a linear scale, Fig. 3. It should be appreciated that as approximately equal numbers of particles were studied in each experiment, the discrepancy is greater than is at first apparent, since those in the American stack arrived over a wider range of energies than those in the English one.

The data presented so far suggest that the English stack was exposed in such conditions that the true cut-off energy at the time of the exposure was between 0.60 and 0.70 GeV per nucleon, instead of the expected 0.33 GeV per nucleon. In order to verify this conclusion a number of subsidiary investigations were made of the characteristics of various types of particles entering these emulsions. These will now be considered.

#### 4. — Subsidiary Experiments.

4.1. *The Flux of Slow Alpha Particles.* — In order to determine whether the absence of slow particles in the English stack suggested by the results of the main experiment was real, a more extensive scan was made of the emulsions around those previously scanned. A single line, ten millimetres from the top edge, was scanned across a number of those emulsions whose grain densities had been normalized but which had not been previously scanned. The same criteria of acceptance were applied as before, except that only tracks with grain densities of greater than five times the minimum value were

accepted. The total length scanned in this manner was almost exactly twice that scanned previously.

Each track found in this scan, and identified as that of an  $\alpha$ -particle, was grain counted. These grain densities are shown in Fig. 4. They provided a method of checking the scanning efficiencies achieved. In this figure the results obtained in the present experiment, shown in black, are compared with those of the main experiment, when allowance is made for the different scanning areas in the two experiments. It has been assumed that at the point where the two distributions become indistinguishable the scanning losses have become negligible. This occurs at a grain density corresponding to an energy of approximately 0.45 GeV per nucleon.

It is then possible to compare the relative fluxes of  $\alpha$ -particles with energies of less than 0.45 GeV per nucleon observed in the two stacks. In the American stack this flux was:

$$J_{I\alpha} (< 0.45 \text{ GeV}/n) = 46.5 \pm 9.5 \text{ } \alpha\text{-particles}/\text{m}^2/\text{ster}/\text{s}$$

while in the English stack it was

$$J_{II\alpha} (< 0.45 \text{ GeV}/n) = 5.3 \pm 1.5 \text{ } \alpha\text{-particles}/\text{m}^2/\text{ster}/\text{s}.$$

It can be seen that there was a significant lack of low energy  $\alpha$ -particles in the English stack, thus confirming the previous results.

**4.2. The Proton Flux.** — It would be interesting to see whether there was a lack of protons incident on the English stack which corresponded to the lack of slow  $\alpha$ -particles. Such protons may be assumed to be those of equal magnetic rigidity to the missing  $\alpha$ -particles, which had energies of less than about 0.65 GeV per nucleon. These protons will be those with energies of less than 1.9 GeV.

The question as to whether or not these protons are present has been studied by comparing the densities of disintegrations produced by singly charged particles in the two stacks. Since these stacks were exposed for the same

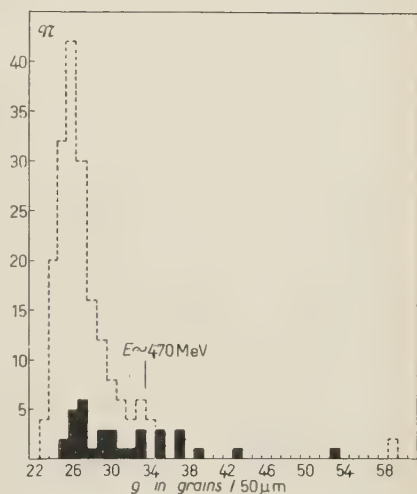


Fig. 4. — A comparison of the grain densities of the  $\alpha$ -particles observed in the English stack in the main experiment, and in the subsidiary experiment, shown in black.

duration of time, the results were made directly comparable by scanning the emulsions of the English stack for stars at a depth corresponding to the mean depth at which those of the American stack had been scanned, plus an amount which allowed for the slight difference in altitude.

The ratio,  $R$ , of the number of stars per unit volume in the English stack to that in the American was found to have the value:

$$R = 0.88 \pm 0.05,$$

which must either mean that the American stack was flown at a lower altitude than assumed, or that the fluxes at the top of the atmosphere were not equal. Arguments will be presented in Section 5 to show that it is unlikely that this stack should have been exposed under much more than the assumed amount of residual matter. Thus it appears that the total flux of singly charged particles into the emulsions was different in the two stacks.

It will be shown in the next sub-section that the flux of all the multiply charged particles may be assumed to be smaller in the English than in the American stack. Consequently the number of singly charged particles produced above the emulsions will also have been reduced. These singly charged particles will in general have the same energy as that per nucleon of the multiply charged particles which produce them, and as a result those that may be missing would have had less than 0.70 GeV energy. Such particles are, as a rule, incapable of producing stars with shower particles, unlike the protons of primary origin which may be missing, as these have between 1.0 and 1.9 GeV energy. It is therefore more significant to compare the numbers of stars observed with one or more shower particles. The ratio obtained in this case is:

$$R = 0.82 \pm 0.10.$$

The fact that this value is significantly less than unity suggests that the primary proton flux was less when the English stack was exposed than it was when the American stack was exposed. It is not, however, possible to demonstrate from these measurements that this decrease is due solely to a lack of low energy protons, although this seems a plausible assumption.

4.3. *The Heavy Primaries in the English Stack.* — Since very extensive measurements have been made of the fluxes of the heavy primaries in the American stack by DAINTON *et al.* <sup>(13)</sup> it was possible to compare them with those observed in the English one. In view of the controversy that exists

(<sup>13</sup>) A. D. DAINTON, P. H. FOWLER and D. W. KENT: *Phil. Mag.*, **43**, 729 (1952).



as to the significance of the observed flux of Lithium, Beryllium and Boron in the above experiment, only the fluxes of particles with charges greater than that of Boron have been compared.

In the English stack, in addition to the heavy primary tracks found in the scans made for the  $\alpha$ -particles and slow  $\alpha$ -particles, extra scans were made for additional heavy primary tracks in other emulsions of the stack. These extra scans were designed to detect tracks which had a length of more than six millimetres and which were heavier than those of relativistic Lithium nuclei. As a result it is unlikely that there could have been any failure to detect particles heavier than Boron.

Measurements were made of the  $\delta$ -ray density of each track found and identified from its appearance as being due to a heavy primary particle. On those tracks where the length per emulsion was greater than one centimetre, a measurement was also made of the scattering parameter, thus determining the energy. In addition each track was followed through the emulsions until it interacted, left the stack, or was brought to rest by ionization losses. As a result it was possible in many cases to obtain an independent estimate of a lower limit to the energy of the particle. From a combination of the energy measurements and the  $\delta$ -ray densities it was generally possible to determine the charge of the particle. In those few cases where this was not possible the assumption was made that the track was relativistic, so that the charge could be obtained from the  $\delta$ -ray density alone.

The comparison of the results obtained in this stack with those obtained by DAINTON *et al.* (13), may be conveniently divided into two separate sections:

*a)* The fluxes of the heavy primaries:

The total flux of particles with charges greater than that of Boron at the top of the atmosphere has been recalculated from the data of DAINTON *et al.*, (13) using the same values for the relevant constants, such as the fragmentation probabilities, as in the rest of this work. The value obtained was:

$$J_{I_{HM}^0} = 17.6 \pm 1.4 \text{ particles/m}^2/\text{steradian/s}.$$

In the English stack the analogous value was:

$$J_{II_{HM}^0} = 15.5 \pm 2.2 \text{ particles/m}^2/\text{steradian/s}.$$

These two values are not significantly different, but are quite consistent with the flux in the English stack being up to 30% less than that in the American one. Thus a consideration of the fluxes alone does not allow any conclusions to be drawn as to whether or not the conditions of exposure of these stacks were different.



### b) The energies of the heavy primaries:

In Fig. 5 a comparison is made between the distributions in energies at the top of the atmosphere of the heavy primaries observed in the two stacks.

The data for the American stack (I) are taken from a group of tracks which were under almost exactly the same mean residual matter as those observed in the English stack (II), so that the charge distributions should be closely similar. It should be noted that these energy values are not critically dependent on the precise identification of the charges of the individual tracks.

From this figure it can be seen that there is a significant difference in the energy distributions observed in the two stacks. In particular there was a definite lack of low energy heavy primary particles incident on the atmosphere when the English stack was exposed. Within the limitations imposed by the small number of particles considered it appears that this stack could have been exposed under such conditions that the true cut-off energy was between 0.60 and 0.70 GeV per nucleon. Similarly the particles observed in the American stack cover an energy range which extends right down to the air cut-off value, which, for example, is 0.34 GeV per nucleon for an oxygen nucleus incident at the average azimuthal angle.

Thus the characteristics of the heavy primaries in the English stack are quite consistent with the assumption that they show the same behaviour, relative to those observed in the American stack, as do the  $\alpha$ -particles.

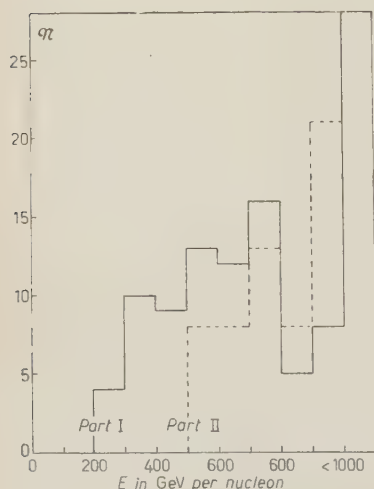


Fig. 5. The energies at the top of the atmosphere of the heavy primary particles observed by DANTON *et al.* (13) in the American stack, and of those observed in the English one. These two distributions have been normalized for particles with energies greater than 1 GeV per nucleon.

### 4.4. The Flux of Heavy Primaries in the Italian Stack.

A determination of the flux of particles with charge greater than that of Boron has been made in the Italian stack by the author working in collaboration with P. H. FOWLER and R. HILLIER. Full details of this experiment will be published later, but the provisional value found for the flux is:

$$J_{\text{III}_{HM^0}} = 6.8 \pm 0.5 \text{ particles/m}^2\text{/steradian/s.}$$

It will be seen later that this value is considerably lower than that which would have been expected from a consideration of the values found over the

American continent. This result is in agreement with the low value found for the  $\alpha$ -particle flux in this stack.

## 5. — Discussion.

There are two possible ways of attempting to explain the observations in the English stack as being due to an experimental error. Neither appears convincing.

Firstly it may be suggested that the results on the  $\alpha$ -particles, which are those of the greatest weight, could be misleading due to an unexpected detection inefficiency. The numerous checks on the scanning efficiency described in Appendix I make such an assumption difficult to support. The validity of this conclusion is strengthened by the subsidiary experiment described in Section 4.1, in which a particular search was made for the missing  $\alpha$ -particles without success. Further, the fact that these particles all lie in one energy range, and that they are those with the highest ionizations, and are therefore presumably the easiest to detect, must surely mean that the observed results cannot be explained in this manner.

Secondly an attempt may be made to attribute the discrepancy between these stacks to an incorrect flight curve of either or both the balloons.

A study of the characteristics of the heavy primaries observed by DAINTON *et al.* <sup>(13)</sup> in the American stack, in particular the apparently excessive flux of light nuclei, could be interpreted as suggesting that the amount of overlying matter had been underestimated. The implications of such an assumption would be that the real  $\alpha$ -particle flux would be higher than the value quoted here, and that the energies of the individual particles would also be higher. The total amount of residual matter cannot, however, have been seriously underestimated, since these authors observed an appreciable flux of high charge particles ( $Z \geq 10$ ), which are rapidly absorbed by matter. For example, if it were assumed that the true mean residual matter was 5 g/cm<sup>2</sup> greater than that assumed, which would imply an altitude difference of 7000 feet, then the true flux of the  $Z \geq 10$  component at the top of the atmosphere would be  $6.0 \pm 0.9$  particles/m<sup>2</sup>/steradian/s, which is a higher value than any previously reported. Such an addition amount of residual matter would only raise the primary  $\alpha$ -particle flux to  $316 \pm 35$   $\alpha$ -particles/m<sup>2</sup>/steradian/s, and increase the energy of a 300 MeV per nucleon  $\alpha$ -particle by 20 MeV per nucleon. It is apparent that no serious errors can have been introduced by an uncertainty in the true flight curve of the American stack.

If on the other hand, the English stack was flown at a lower altitude than assumed, then again the true flux at the top of the atmosphere and the individual energies of the particles would be increased. As a result the discrepancy

between the two observed energy spectra would be still further increased. As in the case of the other stack the effect of a few thousand feet error in the mean altitude would be less than the statistical uncertainties.

Thus the difference between the results obtained in these two stacks cannot be plausibly explained as being due to an experimental error. Instead it is necessary to assume that they have a genuine physical significance. From the nature of these differences they would seem to be due to the English stack having been exposed under conditions of a higher cut-off energy than the American. Such a difference in the cut-off energies could be due to a temporary increase, which would imply that the observed results in the English investigation were due to a time variation; or it could be permanent, implying that the use of the geomagnetic latitude to determine the true cut-off energy was unjustifiable.

All the time variations hitherto observed which resulted in a decrease in the intensity have been world wide, and were observed both at high and low altitudes. As a result they cannot have been due only to a change in the earth's field producing a change in the geomagnetic cut-off <sup>(14)</sup>. It is difficult therefore, to explain the results observed in these experiments as being due to a time variation of the types that are well known, since it would appear that the only variation has been in the cut-off energy.

However, although the observed flux differences in the two stacks are large, it is not certain that such differences would be detected at sea level, since they are due solely to an absence of low energy particles. Thus the possibility of a time variation which only alters the true cut-off energies cannot be excluded as an explanation of these results. For this reason it is necessary to consider the data obtained by other workers, in order to see whether there are other anomalous results, and if there are, to try and correlate them either with time or with geographic position.

*Comparison with other results.* — The majority of the values known for the  $\alpha$ -particle fluxes are listed in Table IIa, and presented in Fig. 6a, while those for the total fluxes of nuclei with charges greater than that of Boron appear in Table IIb and Fig. 7a.

In these tables,  $\lambda$  is the geomagnetic latitude,  $A$  is the geographic longitude,  $E_c$  is the cut-off energy per nucleon derived from  $\lambda$ ,  $E'_c$  is the assumed cut-off energy, calculated from considerations to be discussed, the date is that of the exposure, and « Class » is the classification of this date in terms of the magnetic variations observed on that date. These last data are obtained from the *Journal of Geophysical Research*, where for each month ten days are classified

<sup>(14)</sup> B. Rossi: *Suppl. Nuovo Cimento*, **2**, 275 (1955).

as quiet (Q), five as disturbed (D), and the other are not classified (NC). For those determinations where the date is not given it has either been impossible to find it from the literature, or the value quoted is the mean from several determinations. Of all the results only that of KAPLON *et al.* <sup>(3)</sup> at  $\lambda = 55^\circ$  N, was made on a magnetically disturbed day.

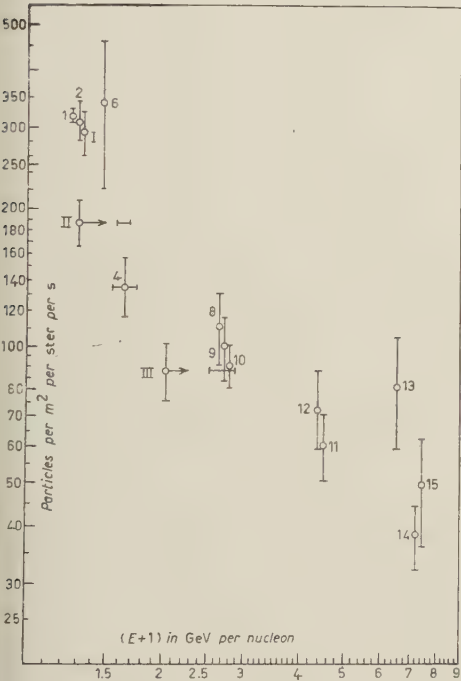


Fig. 6. - a) The experimental  $\alpha$ -particle flux values as a function of the cut-off energy calculated from the geomagnetic latitude. The effect of the change in the cut-off energy deduced from the results of the English investigation is shown for the determinations made over Europe.

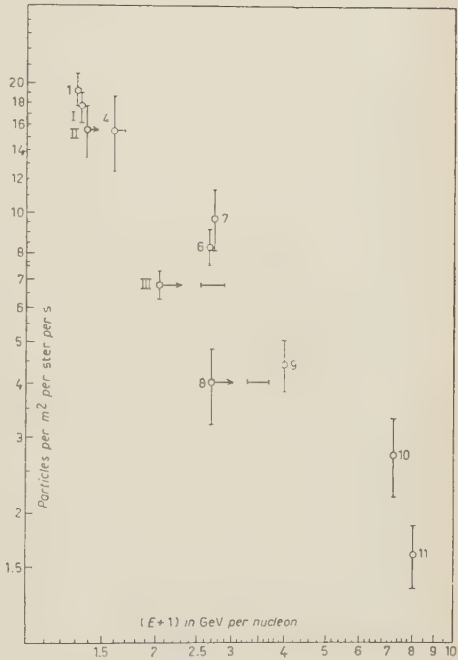


Fig. 7. - a) The experimental heavy primary flux values as a function of the cut-off energy calculated from the geomagnetic latitude. The effect of the change in the cut-off energy deduced from the results of the English investigation is shown for the determinations made over Europe.

It may be seen from Figs. 6a and 7a that if these experimental values are plotted at the cut-off energies calculated from the geomagnetic latitudes, apart from those where there are experimental reasons for not doing so, then there is an extremely wide dispersion of the experimental points, which appears to be considerably greater than that which could be expected from purely statistical considerations:

These determinations may be roughly classified into three separate groups,

TABLE IIa. — *Flux Determinations*

No.	$\lambda$	$E_c$	$E'_c$	$A$	D <sub>0</sub>
1	55° N	0.33	0.15	90° W	4-1
2	55° N	0.33	0.15	90° W	4-1
3	55° N	0.33	0.15	90° W	4-1
4	55° N	0.33	$0.67 \pm 0.10$ (×)	90° W	12-2
5	55° N	0.33	$0.65 \pm 0.05$	0°	9-4
6	51° N	0.60	0.40	80° W	29-4
7	46° N	1.05	1.55 — 1.90	10° E	14-4
8	41° N	1.70	1.30	90° W	2-4
9	41° N	1.70	1.30	105° W	2-4
10	41° N	1.70	1.30	105° W	2-4
11	30° N	3.50	2.95	80° W	2-4
12	30° N	3.50	2.95	80° W	2-4
13	18° N	5.50	?	80° E	19-4
14	10° N	6.20	6.00	90° W	6-4
15	3° N	6.40	?	80° E	19-4

(×) The threshold energy is defined by the Čerenkov detector rather than by the earth's magnetic field.

TABLE IIb. — *Flux Determinations*

No.	$\lambda$	$E_c$	$E'_c$	$A$
1	55° N	0.33	0.15	90°
2	55° N	0.33	0.15	90°
3	55° N	0.33	$0.65 \pm 0.05$	0°
4	51° N	0.60	0.40	80°
5	46° N	1.05	$1.55 \div 1.90$	10°
6	41° N	1.70	1.30	105°
7	41° N	1.30	1.30	105°
8	41° N	1.70	$2.3 \div 2.7$	10°
9	30° N	3.50	2.95	80°
10	10° N	6.20	6.00	90°
11	3° N	7.00	?	—
12	10° N	6.20	6.00	90°

(<sup>15</sup>) J. LINSLEY: *Phys. Rev.*, **93**, 899 (1954).

(<sup>16</sup>) L. GOLDFARB, H. L. BRADT and B. PETERS: *Phys. Rev.*, **77**, 751 (1950).

(<sup>17</sup>) G. J. PERLOW, L. R. DAVIS, C. W. KISSINGER and J. D. SHIPMAN JR.: *Phys. Rev.*, **88**, 321 (1952).

(<sup>18</sup>) N. HORWITZ: *Phys. Rev.*, **98**, 165 (1955).

(<sup>19</sup>) L. BOHE: *Ph.D. Thesis*, University of Minnesota (1954).

(<sup>20</sup>) B. PETERS: *Progress in Cosmic Ray Physics*, vol. I (1952).



## Primary Alpha Particles.

Flux parts/m <sup>2</sup> /ster/s	Method	Authors
318 ± 9 (*)	Scintillation counter	NEY and THON <sup>(9)</sup>
310 ± 30 (+)	Proportional counter	DAVIS <i>et al.</i> <sup>(11)</sup>
292 ± 32	Emulsions	WADDINGTON <sup>(1)</sup> , Stack I
135 ± 20	Cloud chamber plus Čerenkov Detector	LINSLEY <sup>(15)</sup>
186 ± 21	Emulsion	WADDINGTON, Stack II
340 ± 120	Emulsions	GOLDFARB <i>et al.</i> <sup>(16)</sup>
88 ± 13	Emulsions	WADDINGTON, Stack III
110 ± 20	Proportional counter	PERLOW <i>et al.</i> <sup>(17)</sup>
99 ± 16	Čerenkov Counter	HORWITZ <sup>(18)</sup>
88 ± 10 (†)	Double Scintillation counter	BOHL <sup>(19)</sup>
60 ± 10	Emulsions	GOLDFARB <i>et al.</i> <sup>(16)</sup>
72 ± 15	Emulsions	PETERS <sup>(20)</sup>
81 ± 22	Ionisation chamber Integral type	POMERANTZ <sup>(21)</sup>
38 ± 6	Ionization chamber Differential type	MCCLURE <sup>(22)</sup>
49 ± 13	Ionization chamber Integral type	POMERANTZ <sup>(21)</sup>

The value quoted by the authors when extrapolated to the top of the atmosphere.

A corrected value quoted by HORWITZ <sup>(18)</sup>.

The quoted value has been recalculated using a value of 45 gms/cm<sup>2</sup> for the mean free path of  $\alpha$ -particles and allowing for the effects of secondary production.

## Particles Heavier than Boron

Date	Class.	Flux (*) parts/m <sup>2</sup> /ster/s	Authors
-8-50	D	19.3 ± 1.7	KAPLON <i>et al.</i> <sup>(3)</sup>
-9-50	NC	17.6 ± 1.4 (**)	DAINTON <i>et al.</i> <sup>(13)</sup> , Stack I
-7-54	Q	15.2 ± 2.2	WADDINGTON, Stack II
-5-49	NC	15.5 ± 3.1	PETERS <sup>(20)</sup>
-9-54	NC	6.8 ± 0.5	FOWLER <i>et al.</i> , Stack III
2-51	NC	8.3 ± 0.8	KAPLON <i>et al.</i> <sup>(3)</sup>
—	—	9.7 ± 1.6	KAPLON <i>et al.</i> <sup>(8)</sup>
7-53	NC	4.0 ± 0.8	FAY <sup>(23)</sup>
4-49	Q	4.4 ± 0.6	PETERS <sup>(20)</sup>
—	—	2.7 ± 0.6	HOUD <i>et al.</i> <sup>(24)</sup>
—	—	1.6 ± 0.3	LAL <i>et al.</i> <sup>(25)</sup>
—	—	0.96 ± 0.10	DANIELSON <sup>(26)</sup>

All these determinations were made in nuclear emulsions.  
Recalculated value.

<sup>(21)</sup> M. A. POMERANTZ: *Journ. Frank. Inst.*, **258**, 443 (1954).

<sup>(22)</sup> G. W. MCCLURE: *Phys. Rev.*, **96**, 1391 (1954).

<sup>(23)</sup> H. FAY: *Zeits. f. Naturf.*, **10a**, 572 (1955).

<sup>(24)</sup> R. F. HOUD, J. R. FLEMING and J. J. LORD: *Phys. Rev.*, **95**, 647 (1954).

<sup>(25)</sup> D. LAL, YASH PAL, M. F. KAPLON and B. PETERS: *Phys. Rev.*, **86**, 569

(1952).

<sup>(26)</sup> R. E. DANIELSON: *Ph. D. Thesis*, University of Minnesota (1954).

depending on whether they were conducted over the American continent, over western Europe or over India. A study of the data shows that the flux determinations made over America are consistently higher than those made over Europe, but are apparently lower than those made over India. An explanation of these discrepancies may be attempted in the following manner.

As a provisional assumption, to be justified later, it has been assumed that the cut-off energy determined in the English stack is not due to a time variation, but instead represents the true value over southern England. Accepting this cut-off value implies that for this stack the cut-off energy should have been calculated from a latitude which is between four and six degrees lower than the geomagnetic latitude. As a first approximation it appears reasonable to assume that such an alteration in the latitudes will be applicable to all the results obtained over western Europe. The effect of applying such a correction to the cut-off energies is shown in Figs. 6*a* and 7*a*, where the positions taken up by these European results is shown. It can be seen that the effect is to bring the results into far better agreement with those obtained over America, thus apparently justifying the initial assumption that the results observed in the English stack were not due to a time variation.

Since the geomagnetic latitudes do not appear to determine accurately the cut-off energies over Europe, there seems to be no valid reason why they should necessarily be assumed to do so elsewhere. For this reason it is interesting to study the results obtained over America. It may be noticed that the integral energy spectrum obtained in the American stack continued to rise beyond the theoretical cut-off value, and ceased to do so only at the air cut-off value. In addition, a re-analysis has been made by FOWLER and WADDINGTON (to be published), of the large number of slow  $\alpha$ -particles observed by DAINTON *et al.* (13) in this stack. It has been shown that these slow  $\alpha$ -particles cannot be attributed to particles of secondary origin, as had been previously assumed, but must represent a significant number of primary  $\alpha$ -particles entering the atmosphere with energies less than the theoretical cut-off value.

For these reasons it has been assumed that over America the cut-off energies should be calculated from latitudes which are at least three degrees higher than the geomagnetic ones. It is not possible to calculate the correction more closely, since the only data available at present are that from this stack, and the air cut-off would prevent any difference greater than three degrees from being observed. One other result is available which supports this conclusion, and that is the  $\alpha$ -particle flux determination of LINSLEY (15). In this experiment the cut-off energy was defined by the threshold of the Čerenkov detector rather than by the geomagnetic cut-off. The flux value obtained may be seen to be much lower than the value that would have been expected from a consideration of other American results if the geomagnetic latitudes did give the correct cut-off values.

The total effect of these assumptions as to the corrections that need to be applied to the geomagnetic latitudes over America and Europe are shown in Fig. 6*b* and 7*b*. It can be seen that the agreement between the various results is quite within the statistical limits, thus suggesting that the various assumptions made during the argument were essentially correct. It should, however,

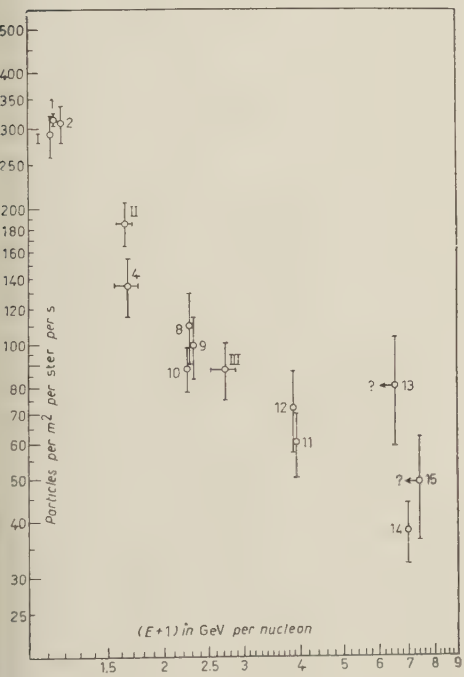


Fig. 6. - *b*) The experimental  $\alpha$ -particle flux values as a function of the suggested cut-off values.

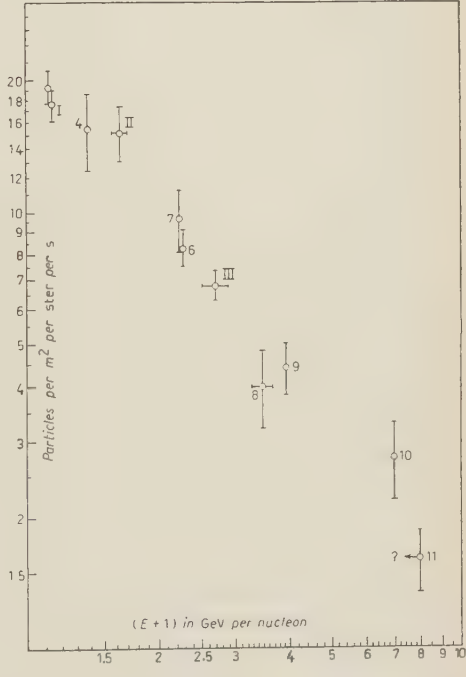


Fig. 7. - *b*) The experimental heavy primary flux values as a function of the suggested cut-off values.

be stressed that the evidence for a correction over America rests mainly on the results obtained from one stack, flown more than two years before any of the European stacks. The possibility that this stack was exposed during a period of time variation cannot be excluded. Nevertheless, it appears reasonably established that some correction, in the direction postulated here, must be made to the cut-off energies over America.

The measurements made over India are still not in agreement with those made elsewhere. Unfortunately nothing is known about the true cut-off energies over India, and so it is difficult to know how to treat these results. In order to explain the results of POMERANTZ<sup>(21)</sup> in terms of a correction to the cut-off energies it would be necessary to assume that they should be cal-

culated from latitudes which were at least ten degrees higher than the geomagnetic ones. The justification of such an assumption must await further experimental measurements.

That the assumptions made here as to the corrections that have to be made to the geomagnetic latitudes over America and Europe are valid has received support from recent measurements of the positions of the cosmic ray minimum intensities over the Pacific and Atlantic by SIMPSON *et al.* <sup>(27)</sup> (reported at the Mexico Conference) using neutron counters. These workers found that the positions of minimum intensity did not lie on the geomagnetic equator, but were shifted from it in directions which appear to agree with those suggested by the above considerations.

Therefore, contrary to previously accepted belief, it must be assumed that the geomagnetic field as determined on the earth's surface does not completely define the paths of the cosmic ray particles as they arrive from outer space. The question as to the nature of the additional fields that are apparently present to modify the effect of the earth's field cannot as yet be answered. The preliminary requirement for the elucidation of this problem must be a much better knowledge of the true cut-off energy as a function of geographic position, and the mapping of lines of equal cosmic ray intensity. These measurements will need to be made over several years, as the possibility that the additional fields may be time dependent cannot be neglected.

\* \* \*

The author wishes to acknowledge his indebtedness to Professor C. F. POWELL, F.R.S. for affording him the facilities of this laboratory, and to the Department of Scientific and Industrial Research for a maintenance grant. He is grateful to Messrs. P. H. FOWLER, and R. HILLIER for permission to quote from unpublished work. He thanks Dr. J. A. SIMPSON for an interesting correspondence, and Mr. P. H. FOWLER for many inspiring conversations. Finally, he is extremely grateful to Miss B. J. BOLT, without whose careful scanning this experiment would never have been completed.

## APPENDIX I

### Scanning Efficiencies in the Main Experiments.

Because of the importance of demonstrating that there were no serious systematic errors introduced by a failure to detect particles in any of the main

---

<sup>(27)</sup> J. A. SIMPSON, D. C. ROSE, K. B. FENTON and J. KATZMAN (to be published) (1955).



experiments, the scanning efficiencies achieved in each have been considered in detail in this Appendix.

In the American stack, all the scanning was done by the author, while in the others it was undertaken by a particularly reliable observer. As an additional check on the scanning efficiency in the English stack, which was of particular importance, the author re-scanned about one quarter of the total scanned length, without finding evidence for any scanning inefficiencies.

In spite of the supposedly high scanning efficiency, there are a number of possible ways in which tracks could have been missed. For this reason various tests were made on the experimental data in order to determine whether such missing of tracks had actually occurred.

i) Tracks with ranges only slightly in excess of the minimum accepted could have been missed due to the scanner underestimating their potential lengths when observing them crossing the scan. This possibility was investigated by considering the integral length distributions of all the tracks observed, Fig. 8. Within the limits of the statistical errors there appears to be no evidence for any missing of tracks of short range in Stack I or III, but a slight indication of missing in Stack II. As a result, in the English investigation only those tracks with a length greater than eleven millimetres have been considered in the systematic analysis.

The deviation from a power law observed at high ranges must be attributed to the limited ranges and non-linearity of the tracks of the singly charged particles.

ii) Tracks with grain densities only just greater than the minimum accepted could have been missed due to an underestimation of their grain densities, or because of a failure to detect them. The possibility that any  $\alpha$ -particles should be missed in this manner was reduced by ensuring that the minimum grain density accepted was considerably less than the minimum grain density of an  $\alpha$ -particle. The amount of «overlap» is illustrated in Fig. 9, which shows, for each experiment, the observed grain density distributions of the singly and doubly charged particles.

iii) It was possible that there could have been an indiscriminate missing of tracks, but of the fifty-four and thirty-four cases in Stack I and II respectively where a track was observed in one scan, and should have been observed in a second, only in Stack I one was missed in a manner which could not be explained. For this reason the influence of any such indiscriminate missing was considered to be negligible.

Overlapping scans were not used in the Italian stack, since it was desired

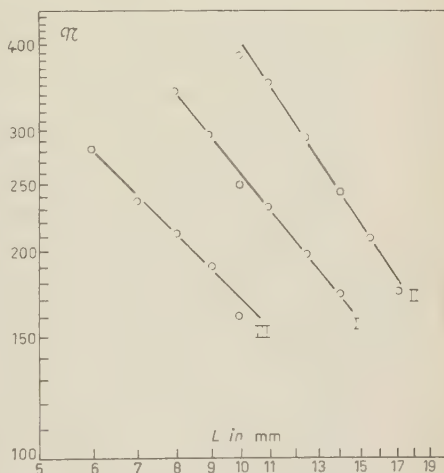


Fig. 8. — The integral length distribution of the tracks observed in stacks I, II and III. For convenience of representation the data of stack III have been multiplied by a factor of two.



to keep the amount of overlying matter as small as possible. However, in view of the higher ionization level in this stack, compared with that in the English one, and the experience and proven ability of the observer, the possibility of serious indiscriminate missing was neglected.

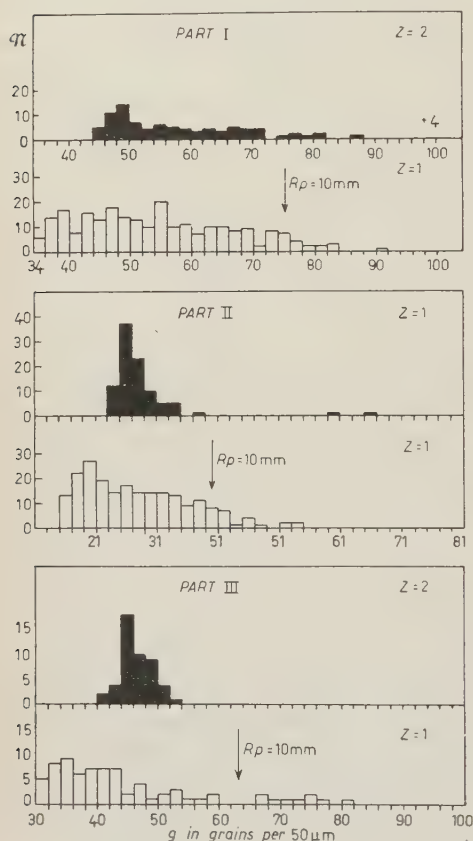


Fig. 9. — The grain density distributions observed for the singly and doubly charged particles in stack I, II and III.

iv) Tracks which appeared to the observer to be steeply dipping and which were therefore neglected, could have been scattered into the plane of the emulsion elsewhere along the path, and thus have had a total length greater than the minimum accepted. This effect could be of importance only for those particles with large scattering parameters. Thus it is unlikely that any of the  $\alpha$ -particles would have been missed, since these particles generally have small scattering parameters. Also, for just this reason, particular attention was devoted in the scanning to tracks of high grain density, which were possibly those of highly scattered particles.

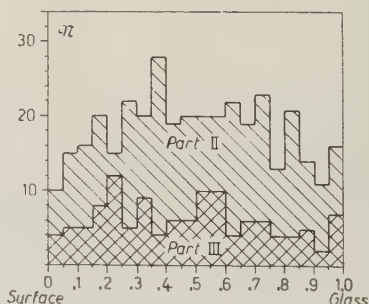


Fig. 10. — The distribution of the depth in the emulsions at which tracks were found in stack II and III.

v) In emulsions where there is a pronounced variation in the grain density throughout their thickness, the detection efficiency may well be a function of the depth at which the track crosses the scan.

In the American stack, there was no appreciable grain density gradient, and such an effect could hardly occur. In the English stack, and to a lesser degree in the Italian stack, there was a considerable variation, which was distinguished by a pronounced fall in the grain density at the surface of the emulsions, and although less severely, at the glass. For this reason, in these stacks, the depth at which each track crossed the scan was determined, and a histogram drawn of the depth distributions, Fig. 10. It appears that in the

English stack there was a lack of tracks found near the surface of the emulsions, and as a result those found within the top 5% of these emulsions have not been considered.

It appears therefore, that provided the corrections to the data of the English investigation given in i) and v) are applied, it is permissible to assume that the influence of an inefficient detection of particles was negligible.

## APPENDIX II

### The Effect of Spurious Scattering.

It has been suggested by BISWAS *et al.* <sup>(12)</sup> that, due to the influence of local forms of distortion in emulsions, measurements of the scattering parameter, and thus of the energies, of fast particles are liable to serious errors. These authors predict that energy values greater than about 0.30 GeV per nucleon determined from multiple scattering measurements may only represent lower limits to the true energies. If this is true in the present experiments, then the experimentally determined value of the cut-off energy in the English stack can only represent a lower limit to the true value. In view of the importance of finding the true cut-off energy, the problem as to whether there is serious spurious scattering in these stacks has been studied more closely.

Two methods of studying this problem present themselves. The first consists of comparing the energy distribution of the  $\alpha$ -particles found from multiple scattering measurements with that found from a study of the latitude effect. It is generally assumed that the integral energy spectrum of the multiply charged particles, except at energies of less than about 0.35 GeV per nucleon, may be represented by an expression of the form

$$N(> E) = \frac{C}{(1 + E)^n},$$

where  $C$  and  $n$  are constants, and  $E$  is the kinetic energy in GeV per nucleon. It can be seen from Figs. 6 and 7 that over the energy range which concerns us here, between 0.50 and 2.0 GeV per nucleon, the above relation is a reasonable representation of the energy spectrum. Values quoted for  $n$  vary between about 1.2 and 1.9 but from Figs. 6*b* and 7*b* it appears that  $n$ , over this restricted range of energies, may be taken as being about 1.2. This value is unlikely to be in error by much more than 0.2. On the other hand the experimentally observed integral energy spectra over this energy range are fitted by values for  $n$  of about 1.8 and 2.0 in Parts I and II respectively. It appears that the greater steepness of these spectra must be due to the influence of spurious scattering.

Now the data of BISWAS *et al.* <sup>(12)</sup>, as presented in their Fig. 7, represent their measurements made on particles all of which had assumed energies greater than 5.0 GeV per nucleon. These measurements are summarized in Table III.

TABLE III. - *The Effect of Spurious Scattering (Taken from BISWAS *et al.* (1955)). On Particles with a Nominal Energy of More than 5 GeV per Nucleon.*

$E$ in GeV/nucleon	$E > 5$	$5 > E \geq 2$	$2 > E \geq 1$	$1 > E \geq 0.6$	$0.6 > E \geq 0.4$	$E < 0.4$
(a) 1000 $\mu\text{m}$ cells						
Number of particles	2	15	20	13	14	7
% of total	3	22	29	19	17	10
(b) 500 $\mu\text{m}$ cells						
Number of particles	1	10	28	24	13	18
% of total	1	11	30	25	14	19

Since the effect of spurious scattering,  $\bar{\alpha}_s$ , and of true scattering,  $\bar{\alpha}_t$ , will add as the squares, it is possible to assume that a given value of the scattering parameter will be due entirely to either  $\bar{\alpha}_s$  or  $\bar{\alpha}_t$ . Hence it is possible to calculate the distortion of the true energy spectrum that would be produced by spurious scattering of the magnitude suggested by BISWAS *et al.* It is found that even if it is assumed, in order to allow for any possible correction to the cut-off, that actually all the particles had energies greater than only 4.0 GeV per nucleon, spurious scattering of this magnitude would give an apparent value for  $n$  of 3.3. This result must indicate that the level of spurious scattering in the emulsions used in this experiment was considerably less than that observed in those used by BISWAS *et al.* <sup>(12)</sup>.

The second method of considering the spurious scattering in these emulsions is to consider the results of measurements made on high energy particles.

(i) In the emulsions of the English stack, seven of the observed  $\alpha$ -particles produced high energy nuclear disintegrations and could be assigned energies of more than 3 GeV per nucleon. Six of these particles had apparent energies, from the multiple scattering, of more than 2 GeV per nucleon,  $\bar{\alpha}_{100\mu\text{m}}^0 \leq 0.006$ . The other particle appeared to have an energy of 0.70 GeV per nucleon. The results of BISWAS *et al.* <sup>(12)</sup> would suggest that even on 1000  $\mu\text{m}$  cells, not more than two of these particles should have had an apparent energy higher than 2 GeV per nucleon.

(ii) In the emulsions of the American stack three high energy particles identified as such by the disintegrations produced, and having true energies of at least 10 GeV per nucleon, all gave extremely small, less than 0.003, scattering parameters. The results of the above authors would suggest that there was only a 5% probability that even one of the particles should give such a value.

It appears, therefore, that the influence of spurious scattering in the emulsions used in these experiments is not nearly as severe as that suggested by BISWAS *et al.* <sup>(12)</sup>. That the level of spurious scattering can be considerably lower than that observed by these authors has been shown by recent measurements made by BRISBOUT *et al.* <sup>(28)</sup> in this laboratory. On the other hand,

<sup>(28)</sup> F. A. BRISBOUT, C. DAHANAYAKE, A. ENGLER, P. H. FOWLER and P. B. JONES (to be published).

it is also apparent that it cannot be entirely neglected, particularly for energies greater than about 1.0 GeV per nucleon,  $\bar{\alpha}_{100\mu m}^0 \leq 0.01$ . For this reason the values obtained for  $n$  from the energy spectrum can be regarded as being only upper limits to the true values. However, it appears justifiable to assume that for energies of the order of 0.70 GeV per nucleon the effects of spurious scattering can be safely neglected in these particular emulsions. Hence the cut-off energy determined in the English stack can hardly have been in serious error due to this effect, and the value found experimentally can be regarded as being physically significant, rather than only representing a lower limit to the true value.

---

### RIASSUNTO (\*)

Una tecnica basata sull'impiego di emulsioni nucleari è stata usata per misurare il flusso delle particelle  $\alpha$  della radiazione cosmica primaria in tre posizioni geografiche differenti. Due di tali determinazioni furono fatte alla stessa latitudine geomagnetica, una in America già precedentemente riferita (<sup>1</sup>), e l'altra in Inghilterra. I due valori del flusso trovati furono, contrariamente alle aspettative, significativamente differenti e tale differenza potè essere interamente attribuita alla assenza sull'Inghilterra di particelle  $\alpha$  con energie inferiori a circa 0.65 GeV per nucleone. Misure sui protoni e sulle particelle primarie pesanti scoperte in questi due pacchi di emulsioni indicarono anche che l'energia di taglio sull'Inghilterra era all'epoca dell'esposizione tra 0.60 e 0.70 GeV per nucleone invece dei 0.33 GeV per nucleone calcolati dalla latitudine geomagnetica nota. Similmente, i dati del pacco americano indicano che, all'epoca in cui fu esposto, l'energia di taglio era inferiore a 0.15 GeV per nucleone. Si è eseguita un'analisi dei vari valori sperimentali del flusso ottenuti in diversi luoghi della superficie terrestre e si conclude che le energie di taglio si debbono calcolare non in base alla latitudine geomagnetica, bensì a latitudini di quattro gradi inferiori sull'Europa e di tre o più gradi superiori in America.

---

(\*) Traduzione a cura della Redazione.

## Kinematics of the Reaction $K + p \rightarrow \pi + \Sigma$ and of the Elastic Scattering $K + p \rightarrow K + p$ .

E. PEDRETTI

*Istituto di Fisica dell'Università - Bologna*

(ricevuto il 9 Febbraio 1956)

**Summary.** — To facilitate the identification of K-mesons interactions, particularly in G5 emulsion, the kinematics of the reaction  $K + p \rightarrow \pi + \Sigma$  and of the scattering  $K + p \rightarrow K + p$  have been calculated and plotted for various kinetic energies of the incident K-meson.

In the present paper we give some families of curves relative to the kinematics of the following processes

$$(1) \quad K + p \rightarrow \pi + \Sigma$$

$$(2) \quad K + p \rightarrow K + p.$$

For the reaction (1) we have used the formulas <sup>(1)</sup>

$$(3) \quad \operatorname{tg} \theta = \sqrt{1 - \beta^2} \frac{\sin \chi}{\frac{\beta e_{m'}^*}{b} + \cos \chi},$$

$$(4) \quad \operatorname{tg} \Phi = \sqrt{1 - \beta^2} \frac{\sin \chi}{\frac{\beta e_{M'}^*}{b} - \cos \chi},$$

<sup>(1)</sup> J. BLATON: *Danske Vidensk. Selsk. Mat. Fys.*, **24**, no. 20 (1950).



$$(5) \quad T_{m'} = \frac{e_{m'}^*}{\sqrt{1-\beta^2}} - m' + \frac{\beta b}{\sqrt{1-\beta^2}} \cos \chi,$$

$$(6) \quad T_{M'} = T_m + m + M - m' - M' - T_{m'},$$

where

$m$  = rest mass of the incident particle (K-meson) in energy units;

$M$  = rest mass of the target particle (proton) in energy units;

$m'$  = rest mass of the first reaction product (pion) in energy units;

$M'$  = rest mass of the second reaction product (hyperon) in energy units;

$T_m$  = kinetic energy of the incident particle in the laboratory system;

$\theta$  = angle of the first reaction product in the laboratory system with respect to the incident particle (Fig. 1);

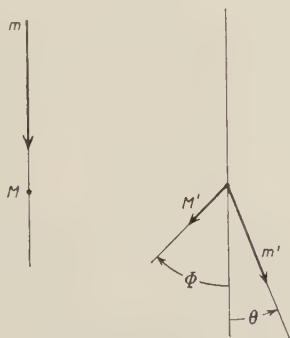


Fig. 1.

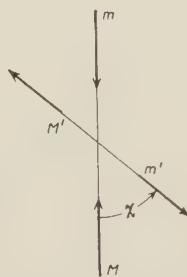


Fig. 2.

$\Phi$  = angle of the second reaction product in the laboratory system with respect to the incident particle (Fig. 1);

$\chi$  = angle corresponding to  $\theta$  in the center of mass system (Fig. 2);

$T_{m'}$  = kinetic energy of the first reaction product in the laboratory system;

$T_{M'}$  = kinetic energy of the second reaction product in the laboratory system;

and the quantities

$$(7) \quad \beta = \frac{\sqrt{T_m^2 + 2mT_m}}{T_m + m + M},$$

$$(8) \quad b = \sqrt{\frac{T_m^2 + 2mT_m}{(2T_m/M) + (1 + (m/M))^2}},$$

$$(9) \quad e_{m'}^* = \frac{2MT_m + (m + M)^2 + m'^2 - M'^2}{\sqrt{8MT_m + 4(m + M)^2}},$$

$$(10) \quad e_{M'}^* = \frac{2MT_m + (m + M)^2 - m'^2 + M'^2}{\sqrt{8MT_m + 4(m + M)^2}},$$

are respectively the velocity of the center of mass in the laboratory system in units of light velocity  $c$ , the momentum of both interacting particles in the center of mass system in energy units and the total energies of the reaction products in the center of mass system.

For the scattering (2) we have used the same formulas by putting  $m' = m$  and  $M' = M$ .

In the calculations we have adopted the values

$$m = 492 \text{ MeV for the K-meson}$$

$$M = 938 \quad \gg \quad \gg \quad \text{proton}$$

$$m' = 140 \quad \gg \quad \gg \quad \text{pion}$$

$$M' = 1189 \quad \gg \quad \gg \quad \text{hyperon } ^{(2)}.$$

We have carried out the calculations relative to the reaction (1) for the following kinetic energies of the incident K-meson

$$T_m = 60, 80, 100, 120, 140, 160 \text{ MeV}$$

and those relative to the scattering (2) for the energies

$$T_m = 10, 25, 50, 100, 125, 150, 200 \text{ MeV.}$$

To obtain the ranges in G5 emulsion of the hyperon produced in the process (1) and of the proton scattered in the process (2) we have used the Tables of H. FAY, K. GOTTSTEIN and K. HAIN plates table <sup>(3)</sup>.

The results are shown in the following tables where angles are expressed in degrees, energies in MeV and ranges in microns.

<sup>(2)</sup> B. ROSSI: *Suppl. Nuovo Cimento*, **2**, 163 (1955).

<sup>(3)</sup> H. FAY, K. GOTTSTEIN and K. HAIN: *Suppl. Nuovo Cimento*, **11**, 234 (1954).

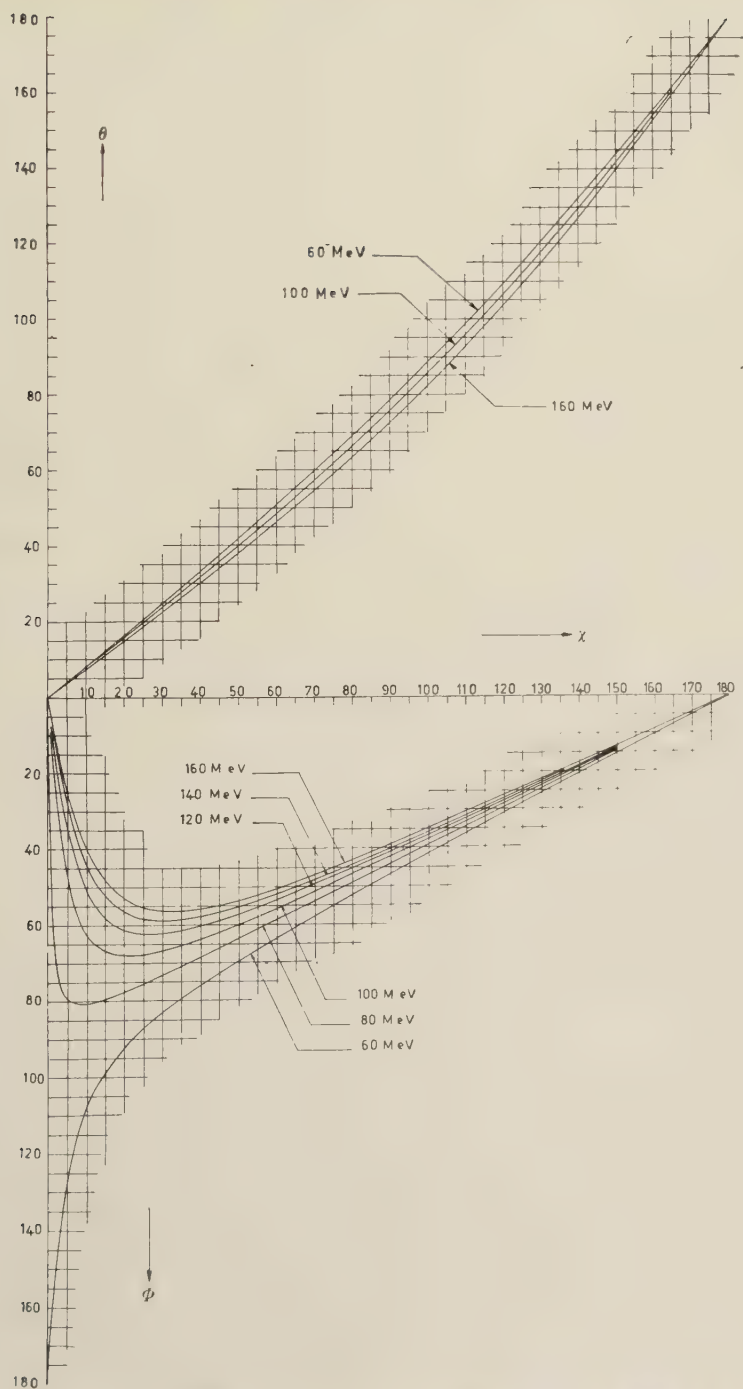


PLATE 1. -- Relations between the angle  $\chi$  (c.m. syst.) and the angles  $\theta$ ,  $\Phi$  (lab. syst.) for the reaction  $K+p \rightarrow \pi+\Sigma$ .

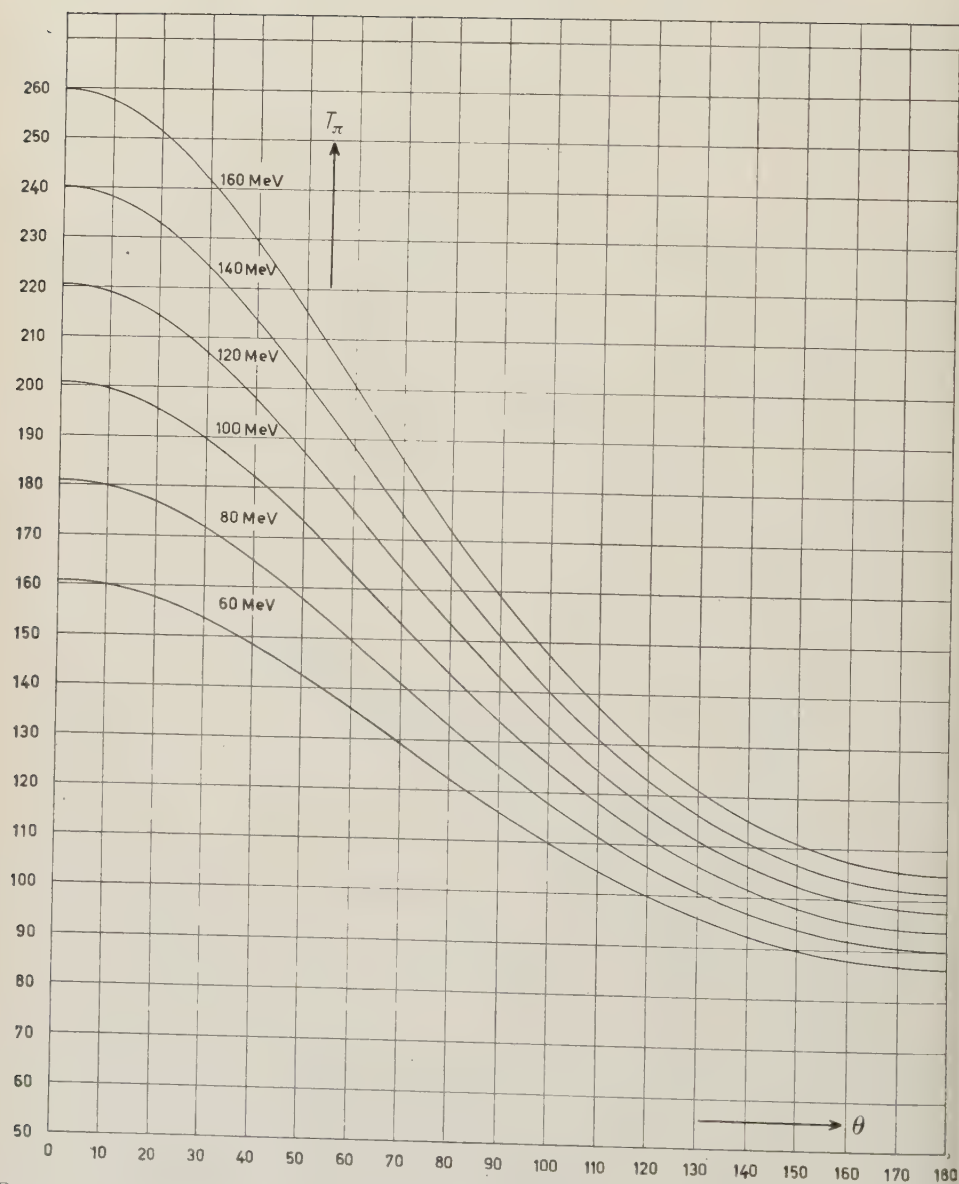


PLATE 2. - Kinetic energy  $T_\pi$  of the pion in the lab. syst. vs. the angle  $\theta$  in the reaction  $K + p \rightarrow \pi + \Sigma$ .

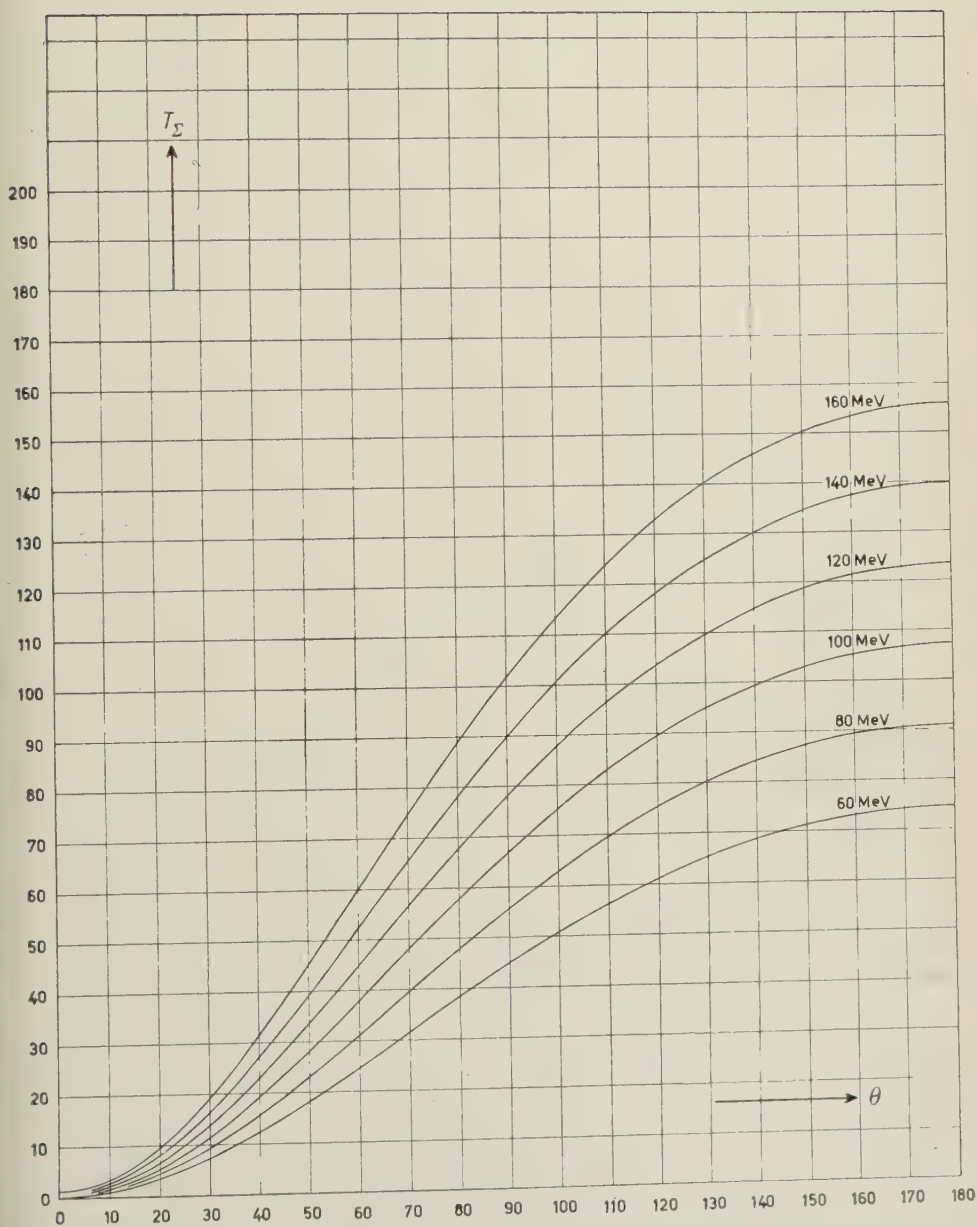


PLATE 3. — Kinetic energy  $T_\Sigma$  of the hyperon in the lab. syst. vs. the angle  $\theta$  in the reaction  $K + p \rightarrow \pi + \Sigma$ .



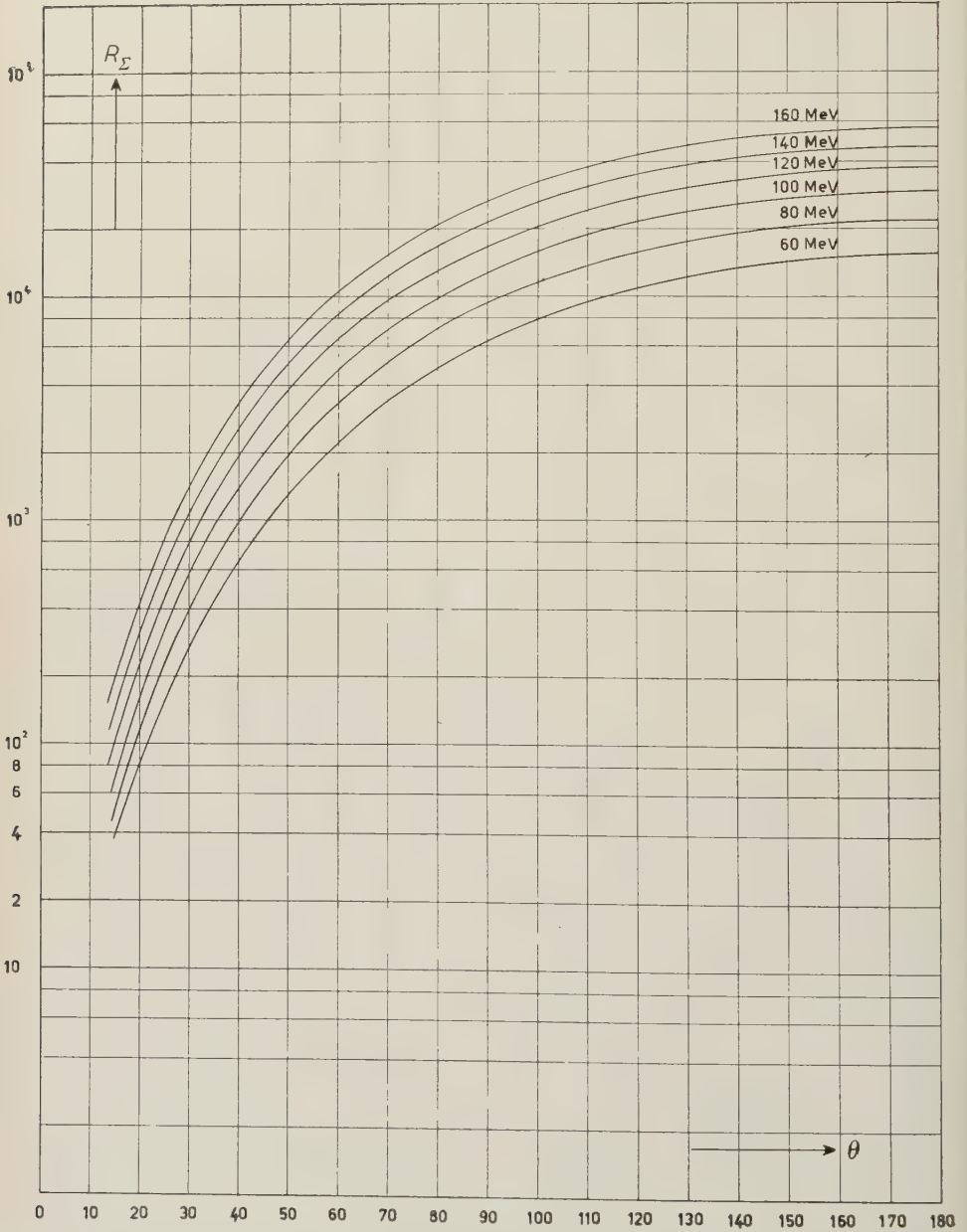


PLATE 4. - Range  $R_\Sigma$  of the hyperon in G5 emulsion vs. the angle  $\theta$  in the reaction  $K + p \rightarrow \pi + \Sigma$ .

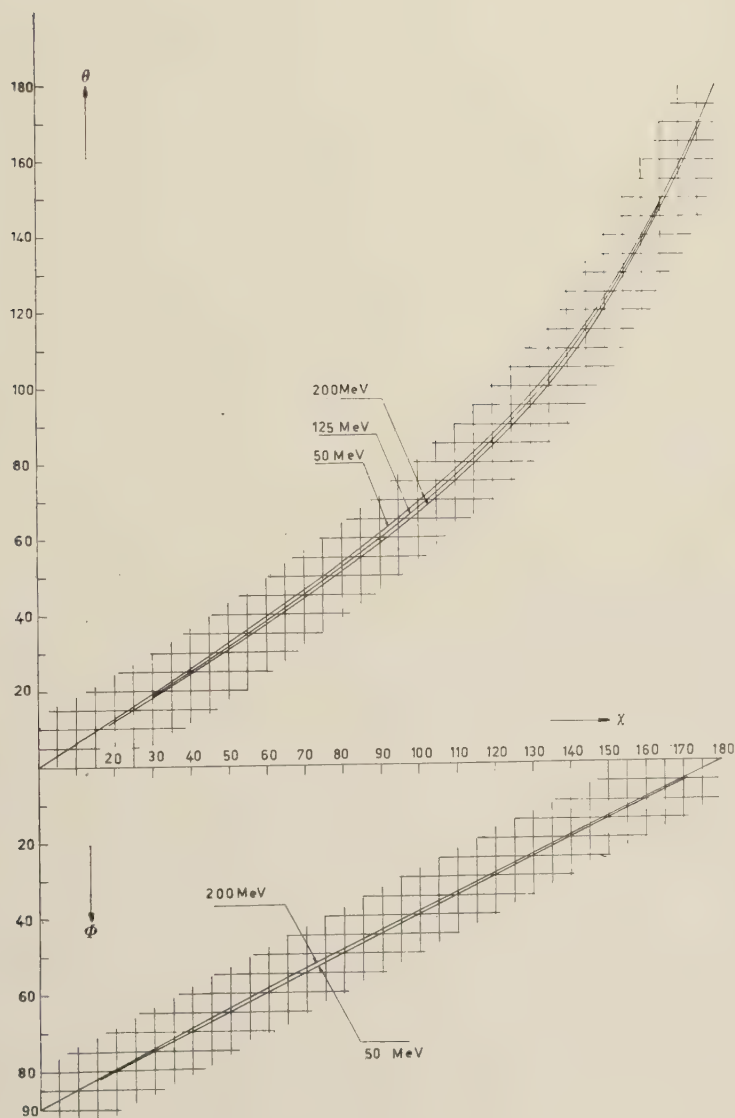


PLATE 5. — Relations between the angle  $\chi$  (c.m. syst.) and the angles  $\theta$ ,  $\Phi$  (lab. syst.) for the scattering  $K + p \rightarrow K + p$  (only for the energies  $T_m = 50, 125$  and  $200$  MeV).

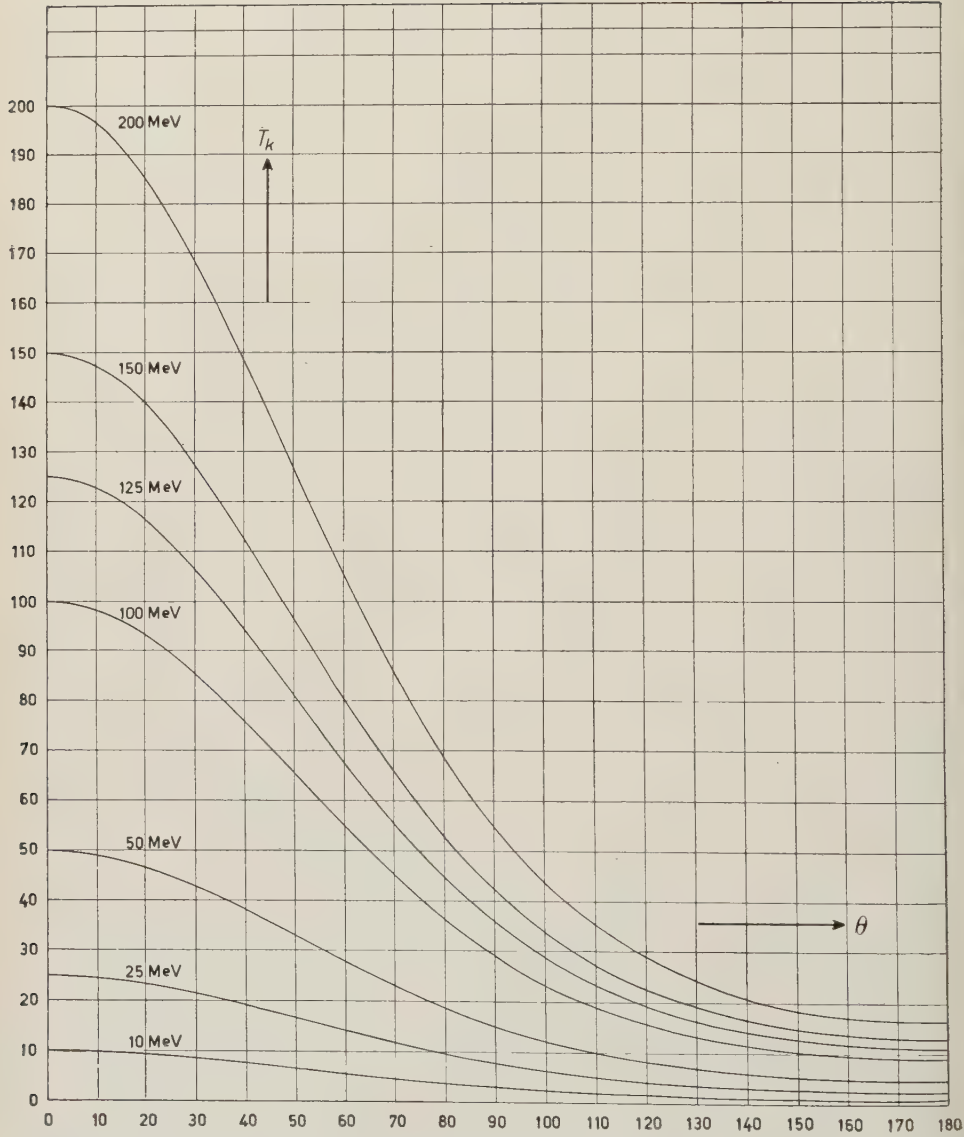


PLATE 6. - Kinetic energy  $T_K$  in the lab. syst. of the scattered K-meson vs. the angle  $\theta$  in the scattering  $K+p \rightarrow K+p$ .

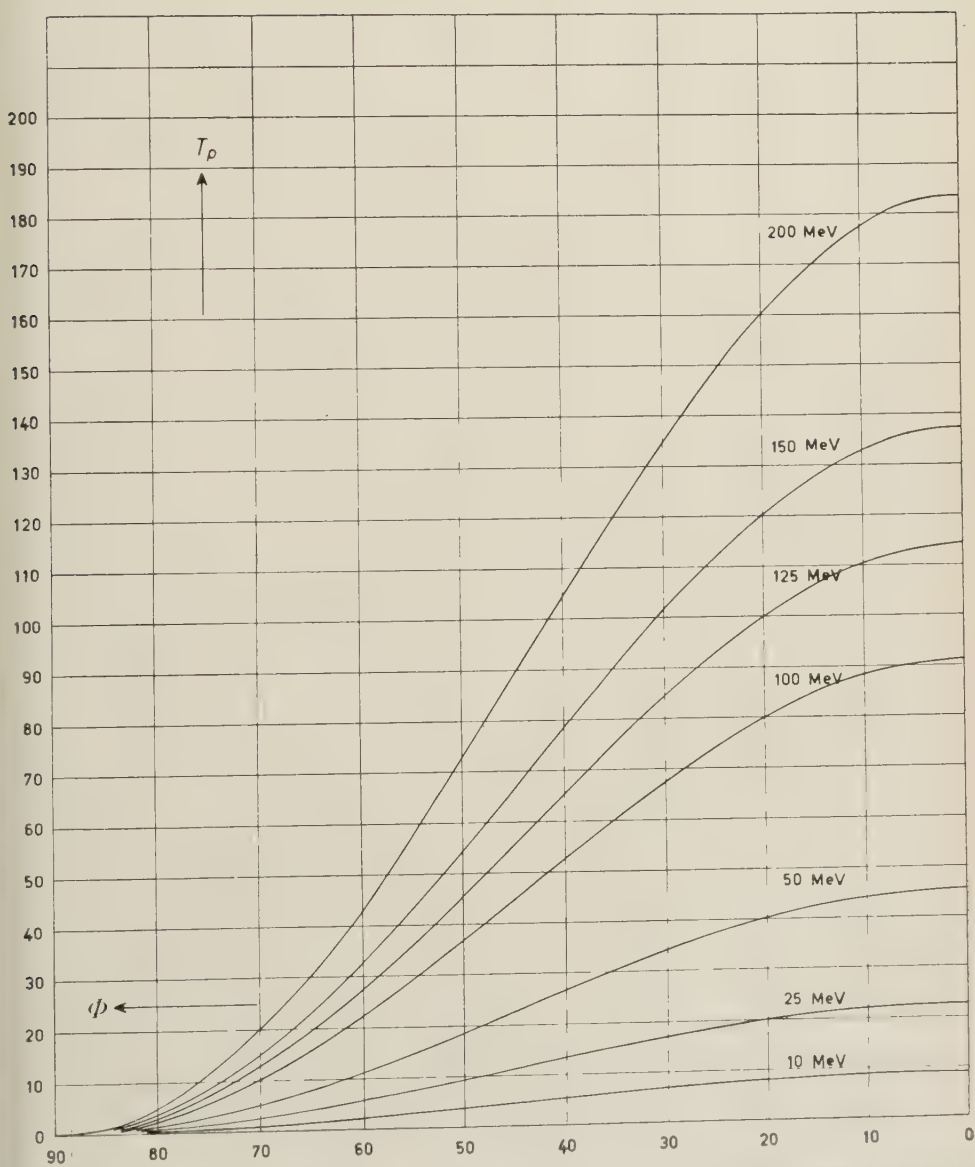


PLATE 7. - Kinetic energy  $T_p$  in the lab. syst. of the proton vs. the angle  $\phi$  in the scattering  $K + p \rightarrow K + p$ .

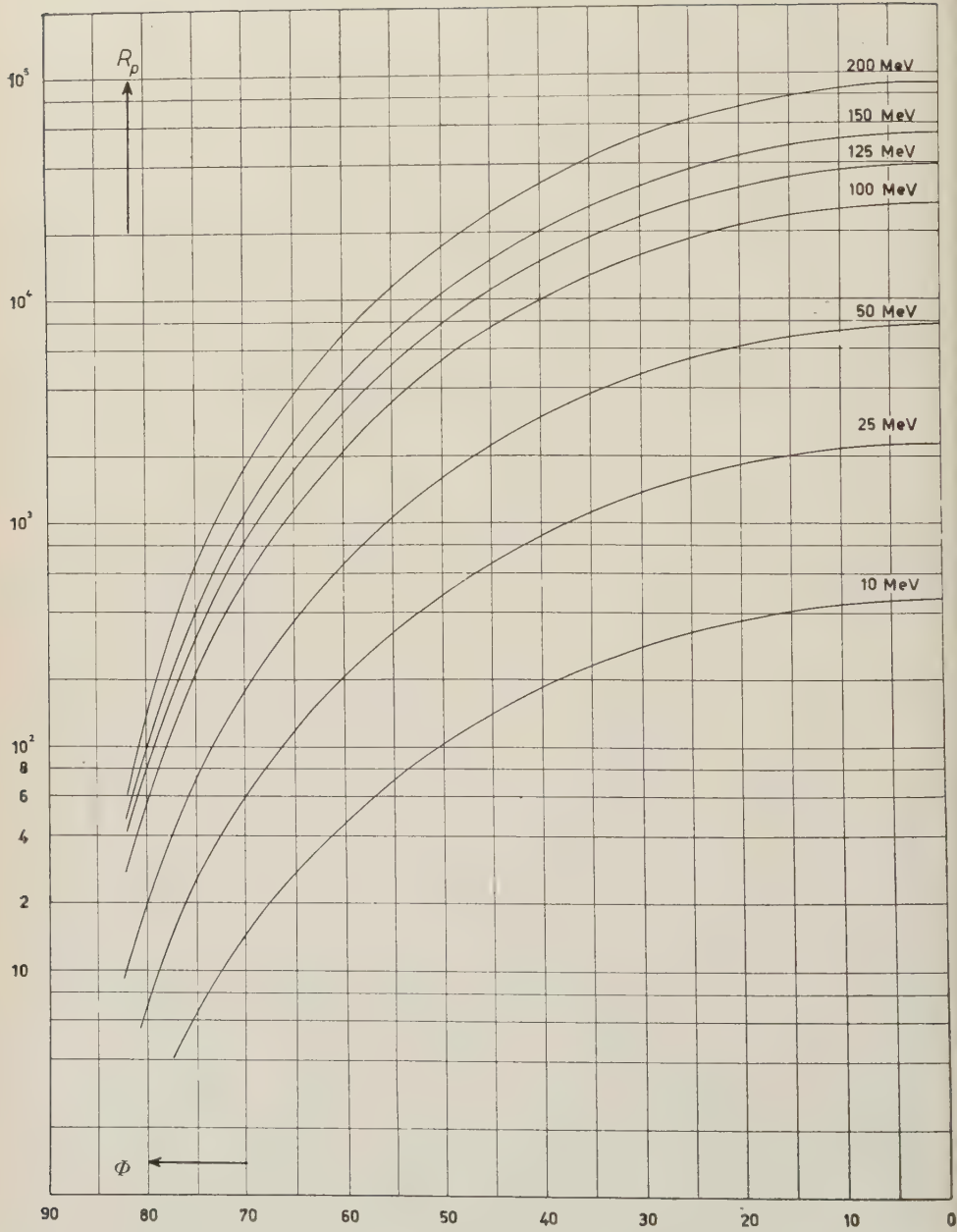


PLATE 8. - Range  $R_p$  of the proton in G5 emulsion vs. the angle  $\phi$  in the scattering  $K + p \rightarrow K + p$ .



\* \* \*

I wish to thank Misses V. BORELLI and A. VIGNUDELLI for making the numerical calculations and Mr. A. NANNINI for tracing the diagrams.

---

## RIASSUNTO

Per facilitare l'identificazione delle interazioni dei mesoni K, particolarmente in emulsione G5, sono state calcolate e graficate le cinematiche della reazione  $K + p \rightarrow \pi + \Sigma$  e dello scattering  $K + p \rightarrow K + p$  per varie energie cinetiche del mesone K incidente.

## Su una teoria bilocale dell'interazione tra una particella con spin $1/2$ e il campo elettromagnetico.

E. MINARDI

*Società Nazionale Cogne - Aosta*  
*Istituto Nazionale di Fisica Nucleare - Sezione di Torino*

(ricevuto il 10 Febbraio 1956)

**Riassunto.** — Si presenta una teoria bilocale per una particella libera con spin  $\frac{1}{2}$  fondata su una semplice generalizzazione lineare dell'equazione di Dirac. Si risolve tale equazione introducendo una condizione di quantizzazione della massa e una nuova condizione supplementare che sostituisce la condizione di Yukawa usata in un precedente lavoro. La generalizzazione della teoria è tale che nelle equazioni le coordinate del moto osservabile e le coordinate interne appaiono in maniera formalmente simmetrica. Si introduce poi l'interazione tra il campo bilocale non quantizzato e il campo elettromagnetico quantizzato in modo da soddisfare alla precedente simmetria. La teoria così ottenuta è differenziale e lineare; essa soddisfa alla invarianza di gauge ed alla conservazione della carica purchè si tenga conto della variazione della quadricorrente dovuta alla parte interna del campo bilocale. Si mostra infine che la teoria conduce alla comparsa, negli elementi di matrice dell'interazione, di fattori che tagliano in modo invariante gli impulsi elevati.

### Introduzione.

È stato originariamente suggerito da MARKOV e YUKAWA <sup>(1,3)</sup> di considerare campi non locali dipendenti da una nuova variabile cosiddetta « interna »  $\eta$ . Successivamente questo punto di vista « bilocale » nella trattazione della teoria dei campi è stato nuovamente studiato soprattutto da YUKAWA <sup>(1)</sup> e da RAYSKI <sup>(2)</sup> e posto in connessione con il problema della quantizzazione della massa. È stata così indicata, assumendo la separabilità tra le coordinate

---

<sup>(1)</sup> M. MARKOV: *Žu. Èksper. Teor. Fiz.*, **10**, 1311 (1940); H. YUKAWA: *Phys. Rev.*, **91**, 415 (1953).

<sup>(2)</sup> J. RAYSKI: *Nuovo Cimento*, **10**, 1792 (1953); **2**, 255 (1955).

<sup>(3)</sup> H. YUKAWA: *Phys. Rev.*, **77**, 219 (1950).

interne le coordinate spazio-temporali ordinarie, con la massa come costante di separazione, la possibilità che la funzione  $q(\eta)$  descrivente le proprietà interne sia determinata mediante un operatore di massa e che le masse note possano essere autovalori di tale operatore.

Nella presente nota si propone una teoria bilocale del genere sopra indicato nel caso delle particelle con spin  $\frac{1}{2}$  e si introduce in questa teoria l'interazione con il campo elettromagnetico.

Nella Sez. 1 si presenta l'equazione generalizzata del campo bilocale per una particella neutra libera e si imposta il problema degli autovalori dell'operatore di massa mediante una nuova condizione supplementare (che è introdotta al posto della condizione di Yukawa <sup>(1)</sup> usata in una nota precedente <sup>(2)</sup>) e mediante una speciale condizione di quantizzazione della massa, coinvolgente una lunghezza universale  $l$ .

La nuova condizione supplementare esprime l'indipendenza del problema della determinazione della struttura interna della particella dal problema del calcolo del suo moto osservabile.

Nella presente formulazione, al contrario della formulazione di Rayski, le variabili separabili  $x$  ed  $\eta$  non sono necessariamente variabili di Yukawa (cfr. <sup>(1)</sup> formula (6)), nè si raddoppiano le variabili di spin e le matrici di Dirac.

Nella Sez. 2 si introduce, partendo dall'equazione precedente, l'interazione tra una particella con spin  $\frac{1}{2}$  e il campo elettromagnetico quantizzato.

Si parte da un'equazione differenziale lineare per il campo bilocale in interazione con il campo elettromagnetico, la quale è simmetrica rispetto alle coordinate  $x$  ed  $\eta$  ed è invariante rispetto ad una trasformazione di gauge. Negli elementi di matrice dell'interazione compare un fattore che taglia i fotoni di impulso elevato.

Infine nell'Appendice si ottiene una soluzione relativistica e soddisfacente alle condizioni supplementari dell'equazione generalizzata del campo bilocale in assenza di interazione, nella forma di uno sviluppo in serie di onde piane.

## 1. - L'equazione bilocale per una particella neutra libera <sup>(\*)</sup>.

Sia  $\psi(x, \eta)$  il campo bilocale descrivente una particella elementare, con  $x$  che rappresenta lo spazio-tempo del moto osservabile e con  $\eta$  come coordinata interna.

<sup>(1)</sup> G. WATAGHIN: *Nuovo Cimento*, **7**, 166 (1950); **8**, 592 (1951); **10**, 500 (1953); *Symp. on New Res. Techn. in Phys.*, Rio de Janeiro, Luglio 1952; *Suppl. Nuovo Cimento*, **1**, 103 (1954); *Atti Acc. Lincei*, **17**, 116 (1954).

<sup>(\*)</sup> L'autore ringrazia il prof. G. WATAGHIN per un'illuminante discussione concernente questo paragrafo.

Poichè è compito della teoria bilocale dedurre in maniera automatica il valore delle differenti masse delle particelle, sembra opportuno che l'equazione per il campo  $\psi(x, \eta)$ , al contrario dell'equazione di Dirac, non contenga la costante  $m$  esplicitamente. La più semplice generalizzazione bilocale dell'equazione di Dirac che soddisfa a questa esigenza è la seguente:

$$(1) \quad \alpha_\nu \left( \frac{\partial}{\partial x_\nu} + \frac{\partial}{\partial \eta_\nu} \right) \psi(x, \eta) = 0 \quad (\nu = 1, 2, 3, 4).$$

Separiamo tale equazione nelle variabili  $x$  ed  $\eta$ , ponendoci nel sistema del baricentro della particella. In tale sistema si deve porre:

$$(2) \quad \nabla_x \cdot \psi(x, \eta) = 0,$$

cosicchè la (1) diviene:

$$(3) \quad \left( \frac{\partial}{\partial x_4} - i\alpha_\nu \frac{\partial}{\partial \eta_\nu} \right) \psi(x_4, \eta) = 0.$$

Ponendo  $\psi(x_4, \eta) = f(x_4) \cdot \varphi(\eta)$ , ove  $f(x_4)$  è una funzione di  $x_4$  e  $\varphi(\eta)$  una matrice a una colonna e a quattro righe i cui elementi sono funzioni di  $\eta$ , si ottengono le seguenti due equazioni per il campo  $f(x_4)$  di Dirac e per il campo interno rispettivamente <sup>(5)</sup>:

$$(4) \quad - \frac{\partial f(x_4)}{\partial x_4} = m f(x_4),$$

$$(5) \quad - i\alpha_\nu \frac{\partial \varphi(\eta)}{\partial \eta_\nu} = m \varphi(\eta).$$

Occorre ora porre un problema di autovalori onde derivare uno spettro di masse dalla (5). Per questo assumiamo anzitutto la seguente condizione supplementare, la quale sostituisce la condizione di Yukawa usata in una precedente nota <sup>(6)</sup>:

$$(6) \quad \frac{\partial^2}{\partial x_\nu \partial \eta_\nu} \psi(x, \eta) = 0.$$

<sup>(5)</sup> Nel procedimento di separazione si suppone  $m \neq 0$ . Se  $\psi$  non dipende da  $\eta$  si ottiene dalla (6) l'equazione di Dirac per una particella di massa nulla. La massa  $m = 0$  è così ottenuta senza porsi nel riferimento  $\mathbf{p}^{(x)} = 0$ , ciò che porterebbe ad un'inconsistenza.

<sup>(6)</sup> E. MINARDI: *Nuovo Cimento*, **11**, 694 (1954). Tale lavoro sarà nel seguito indicato con I. Notiamo che l'equazione generalizzata (11) di I non ha le corrette proprietà relativistiche di trasformazione e deve essere sostituita con la (1) di questo lavoro.

Nella Sezione seguente si soddisferà a questa condizione ponendo  $\eta_4 = 0$  nel sistema del baricentro. Avendosi allora, in tale sistema,  $\partial\psi(\eta_4=0)/\partial\eta_4=0$ , ed inoltre  $\nabla_x\psi(x, \eta) = 0$ , si vede che la (6) è soddisfatta. La (5) nel sistema del baricentro assume quindi la forma (cfr. I, formula (12)):

$$(7) \quad -i\alpha \cdot \nabla_\eta \varphi(\eta) = m\varphi(\eta).$$

Introducendo allora una speciale condizione ai limiti, o condizione di quantizzazione della massa per il campo interno  $\varphi$  soddisfacente alla (7), si può ottenere uno spettro di masse. Sembra naturale ritenere che la condizione di quantizzazione della massa, la quale si riferisce ad un campo interno  $\varphi$  le cui leggi non coincidono con quelle tradizionali, coinvolga altresì una nuova costante universale. In I si è assunta, come condizione di quantizzazione della massa, che la soluzione  $\varphi$  della (7), nel sistema del baricentro (ove  $\mathbf{p}^{(x)} = 0$ ,  $p_4^{(\eta)} = 0$ ) sia nulla sulla superficie di una sfera spaziale con centro nel punto  $\eta = 0$  e raggio uguale ad una lunghezza universale  $l$ . La parte radiale della soluzione  $\varphi$  della (7) può rappresentarsi (cfr. I, formula (15)) con una matrice a una colonna e con due elementi  $Y(r)$  e  $Z(r)$  ( $r = (\eta_1^2 + \eta_2^2 + \eta_3^2)^{\frac{1}{2}}$ ) (analogamente alla trattazione di Dirac di una particella spinoriale in campo centrale); si ottiene che l'elemento  $Y(r)$  deve soddisfare all'equazione sferica di Bessel:

$$(8) \quad \frac{d^2 Y}{dr^2} + \frac{2}{r} \frac{dY}{dr} + \left( m^2 - \frac{k(k+1)}{r^2} \right) Y = 0.$$

Per soddisfare alla condizione di quantizzazione della massa basta porre  $Y(ml) = 0$ .

D'altra parte anche la parte radiale del campo interno di una particella scalare o pseudoscalare soddisfa alla (8) (cfr. I, formula (4)) e vi sono soluzioni della (8) (cfr. con il seguito e con nota (7)) che possono attribuirsi ad ambedue i tipi di particelle. È necessaria pertanto una regola di selezione che attribuisca le masse ottenute all'uno o all'altro tipo di particella (cfr. con nota (7)).

Risolvendo la (8) la condizione di quantizzazione della massa si scrive:

$$(9) \quad Y_k(ml) = \frac{c_k}{\sqrt{ml}} J_{k+\frac{1}{2}}(ml) = 0,$$

ove  $k$ , nel caso di particelle pseudoscalari o scalari, assume tutti i valori interi positivi da 0 a  $+\infty$ , mentre, come si può vedere facilmente (cfr. I) il valore  $k = 0$  è escluso nel caso di particelle con spin  $\frac{1}{2}$  (7).

(7) Lo spettro di masse che si ottiene dalla (9) è presentato in I. Una discussione dei risultati numerici ottenuti per le masse è molto prematura. Tuttavia osserviamo



All'esterno della sfera baricentrica sopra considerata si assume la soluzione nulla delle (7) e (8) e quindi la  $Y_k(mr)$  è continua sulla superficie della sfera. Pertanto il campo interno  $\varphi$  delle particelle pseudoscalari soddisfacente alla (8) è continuo sulla sfera, mentre nel caso delle particelle con spin  $\frac{1}{2}$  tale continuità vale solo per una componente della matrice  $\varphi$  a una colonna e a due righe, l'altra potendo essere discontinua. È questa una caratteristica differenza tra particelle con spin  $\frac{1}{2}$  e particelle pseudoscalari.

Osserviamo infine che la soluzione precedentemente considerata è ottenuta nel sistema del baricentro e non possiede le corrette proprietà spinoriali di trasformazione. In appendice si presenterà una soluzione che possiede tali proprietà.

## 2. - L'interazione con il campo elettromagnetico.

Vogliamo ora introdurre nella teoria l'interazione con il campo elettromagnetico. Nell'equazione generalizzata (1) e nella condizione supplementare (6) le variabili  $x$  ed  $\eta$  compaiono in modo simmetrico. Sembra naturale assumere che tale simmetria sia conservata quando si introduce l'interazione. La più semplice equazione che soddisfa alla precedente esigenza è la seguente:

$$(10) \quad \alpha_v \left( \frac{\partial}{\partial x_v} - ieA_v(x + \eta) + \frac{\partial}{\partial \eta_v} \right) \psi(x, \eta, q) = 0.$$

Nella precedente il potenziale  $A_v(x')$  ( $x' = x + \eta$ ) è un operatore spazio-temporale definito dalle seguenti relazioni:

$$(11) \quad A_v(x') = \exp[iH_0 t'] A_v(\mathbf{x}') \exp[-iH_0 t'],$$

che l'operatore di massa proposto implica un momento angolare totale interno  $\mathbf{M}^{(\eta)} = \mathbf{L}^{(\eta)} + \frac{1}{2}\boldsymbol{\sigma}'$  (ove  $\mathbf{L}^{(\eta)} = \boldsymbol{\eta} \wedge \mathbf{p}^{(\eta)}$ ), la cui componente secondo l'asse  $z$  ha autovalori semi-interi. Invece dall'operatore di massa per particelle pseudoscalari (cfr. I, formula (3)) può ottenersi un momento angolare interno totale con autovalori interi rispetto a questo asse e con  $\mathbf{M}^{(\eta)^2} = k(k+1)$ . Sembra così possibile identificare il momento angolare totale interno  $\mathbf{M}^{(\eta)}$  con lo spin. Lo spettro di masse delle particelle con spin  $\frac{1}{2}$  è allora dato in I nel caso  $k=1$ , mentre i valori più alti di  $k$  corrispondono a spin semi-interi maggiori di  $\frac{1}{2}$ . Inoltre se si suppone che il campo interno delle particelle con spin intero non debba soltanto dipendere da  $\eta_v \eta_v$  ma che vi sia anche una dipendenza angolare, occorre ammettere l'esistenza di particelle di questo tipo con spin maggiore di zero ( $k > 0$ ) le cui masse sono pure ottenute con la condizione (9). È tuttavia presumibile che valga una regola di selezione tale che nel caso delle particelle con spin intero siano ammessi nella (9) solo i valori pari di  $k$ , mentre per le particelle con spin semi-intero siano ammessi solo i valori dispari.

Al mesone  $\tau$ , la cui massa compare per  $k=2$ , dovrebbe quindi ascriversi lo spin intero 2. Inoltre non potrebbero esistere particelle con spin intero dispari.

$$(12) \quad \square A_\nu(x') = 0,$$

$$(13) \quad [A_\nu(x'), A_{\nu'}(x'')] = -i\delta_{\nu\nu'} D(x' - x'').$$

$H_0$  è l'operatore hamiltoniano del campo elettromagnetico nel vuoto e  $D(x' - x'')$  la nota funzione invariante di Jordan-Pauli. Il campo bilocale  $\Psi(x, \eta, q)$ , oltre che una funzione delle coordinate  $x$  ed  $\eta$ , sarà un funzionale delle coordinate  $q$  del campo elettromagnetico. In generale esso potrà svilupparsi in serie delle autofunzioni dei campi liberi relativi alle differenti masse ed agli autostati di  $H_0$ :

$$(14) \quad \psi(x, \eta, q) = \sum_n \sum_k a_{m_n, k} \psi_{0, m_n}(x, \eta) \Psi_{0, k}(q).$$

La (10) è un'equazione differenziale lineare non separabile nelle coordinate  $x$  ed  $\eta$ . Essa è invariante rispetto ad una trasformazione di gauge,  $A_\nu(x') \rightarrow A_\nu(x') + \partial A(x')/\partial x' = A_\nu + \frac{1}{2}\partial A/\partial x + \frac{1}{2}\partial A/\partial \eta$ , purchè simultaneamente il campo  $\psi$  si trasformi in questo modo:

$$(15) \quad \psi \rightarrow \exp[iA(x + \eta)/2]\psi.$$

Al campo bilocale  $\psi$  è associata la quadricorrente  $s_\nu(x, \eta) = \psi^* \alpha_\nu \psi$ . Tale quadricorrente soddisfa alla seguente legge di conservazione:

$$(16) \quad \left( \frac{\partial}{\partial x_\nu} + \frac{\partial}{\partial \eta_\nu} \right) s_\nu(x, \eta) = 0.$$

Pertanto, affinchè si abbia conservazione differenziale della carica occorre tener conto della variazione di quadricorrente dovuta alla parte interna del campo bilocale.

È ora interessante mostrare che negli elementi di matrice dell'interazione tra gli stati imperturbati del campo bilocale  $\psi_0(x, \eta)$  e del campo elettromagnetico, compare un fattore che taglia gli impulsi elevati del fotone. Tali elementi di matrice sono:

$$(17) \quad \left\{ \begin{aligned} H'_{\text{II/Iem.}} &= -e \sqrt{\frac{2\pi}{k}} \int d^3x \int d^4\eta \exp[-ik_\nu(x_\nu + \eta_\nu)] \psi_{0, \text{II}}^\dagger \gamma_\alpha \psi_{0, \text{I}} = \\ &= -e \sqrt{\frac{2\pi}{k}} \exp[ik_0 t] \delta(\mathbf{p}_\text{I}^{(x)} - \mathbf{p}_\text{II}^{(x)} - \mathbf{k}) \int q_{\text{II}}^\dagger \gamma_\alpha q_\text{I} \exp[-ik_\nu \eta_\nu] d^4\eta, \\ H'_{\text{II/Ia.e.}} &= -e \sqrt{\frac{2\pi}{k}} \int d^3x \int d^4\eta \exp[ik_\nu(x_\nu + \eta_\nu)] \psi_{0, \text{II}}^\dagger \gamma_\alpha \psi_{0, \text{I}} = \\ &= -e \sqrt{\frac{2\pi}{k}} \exp[ik_0 t] \delta(\mathbf{p}_\text{I}^{(x)} - \mathbf{p}_\text{II}^{(x)} + \mathbf{k}) \int q_{\text{II}}^\dagger \gamma_\alpha q_\text{I} \exp[ik_\nu \eta_\nu] d^4\eta, \end{aligned} \right. \quad (\psi^\dagger = i\psi^* \beta).$$

Come sarà mostrato nell'Appendice (formula (27)) il campo bilocale  $\psi_0(x, \eta)$  potrà rappresentarsi per  $\eta_v^2 < l^2$  (esso è altrimenti nullo) con uno sviluppo in serie di onde piane.

Usando nella prima della (17) questa rappresentazione (ed analogamente per la seconda) si ottiene:

$$(18) \quad H'_{\text{II/Iem.}} = -e \sqrt{\frac{2\pi}{k}} \exp[ik_0 t] \delta(\mathbf{p}_I^{(\omega)} - \mathbf{p}_{\text{II}}^{(\omega)} - \mathbf{k}) \cdot \\ \cdot \sum_{\mathbf{p}_I^{(\eta)}, \mathbf{p}_{\text{II}}^{(\eta)}} e^{i\eta_{\text{II}}^*} (p_{\eta, \text{II}}^{(\eta)}) e^{i\eta_I} (p_{\nu, I}^{(\eta)}) u_{\text{II}}^\dagger \gamma_\lambda u_I V_{\eta}^{-1} \int_{V_I} \exp[i\eta_\nu (p_{\nu, \text{II}}^{(\eta)} - p_{\nu, I}^{(\eta)} - k_\nu)] d^4 \eta \cdot$$

ove  $V_\eta$  è il volume della sfera baricentrica di raggio  $l$  e  $u$  una matrice a una colonna e a quattro righe definita in Appendice formule (22) e (23).

Nell'eseguire l'integrazione nelle variabili  $\eta$  del fattore integrale della (18), occorre ricordare che devono essere soddisfatte le condizioni supplementari enunciate nella Sez. 1. Si soddisfa più comodamente a tali condizioni eseguendo l'integrazione nella (18) nel sistema del baricentro e ponendo poi il risultato in una forma relativisticamente invariante; invero il risultato che si ottiene integrando in tale sistema, in conseguenza del carattere invariante del fattore integrale, deve considerarsi legittimamente uguale a quello che si otterrebbe integrando in ogni altro riferimento.

Soddisfiamo alla condizione supplementare (6) ponendo  $\eta_4 = 0$  nel sistema del baricentro (cfr. Sez. 1). Pertanto, se si esegue l'integrazione nel sistema del baricentro, soltanto l'iperpiano  $\eta_4 = 0$  dovrà dare contributo alla integrazione rispetto a  $\eta_4$ , se non si vuole contraddire alla condizione precedente. Occorre quindi moltiplicare l'integrando per  $\delta(\eta_4)$ .

D'altra parte, in conseguenza della condizione di quantizzazione della massa, il campo bilocale è nullo all'esterno della sfera baricentrica. Ciò fissa il dominio dell'integrazione spaziale come quello dato da tale sfera. Ma il fattore integrale della (18) è allora la trasformata tridimensionale di Fourier di una funzione costante entro la sfera baricentrica e nulla all'esterno. Esso ha così la stessa forma del semplice fattore di taglio introdotto da WATAGHIN:

$$V_{\eta}^{-1} \int_{\text{sfera}} d^3 \eta \int d\eta_4 \exp[i\eta_\nu P_\nu] \delta(\eta_4) = 3 \frac{\sin Pl - Pl \cos Pl}{(Pl)^3} = 3 \sqrt{\frac{\pi}{2}} (Pl)^{-\frac{3}{2}} J_{\frac{3}{2}}(Pl) = G(P).$$

Nella precedente si è posto  $P_\nu = p_{\nu, \text{II}}^{(\eta)} - p_{\nu, I}^{(\eta)} - k_\nu$  e  $P = |\mathbf{P}| = (P_1^2 + P_2^2 + P_3^2)^{\frac{1}{2}}$ . Tale fattore di taglio è posto in forma invariante, in accordo con le considerazioni precedenti, sostituendo l'argomento  $P$  con l'invariante di Wataghin

$$\left[ - \left( \frac{+ p_\nu^{(\omega)} P_\nu}{im} \right)^2 + P_\nu^2 \right]^{\frac{1}{2}},$$

il quale è appunto uguale a  $P$  nel sistema del baricentro.

Nel caso del termine  $\alpha = 4$  (fotoni scalari) l'elemento di matrice dell'interazione assume una forma particolarmente semplice. Infatti, ricordando le condizioni supplementari, il fattore integrale dell'ultimo membro delle (17) è semplicemente la trasformata tridimensionale di Fourier di una funzione uguale a  $\varphi_{II}^* \varphi_I$  entro la sfera baricentrica e nulla all'esterno. In approssimazione non relativistica (e quindi non considerando transizioni coinvolgenti stati del vuoto o cambiamenti di massa) tale termine dà luogo all'energia mutua elettrostatica, secondo l'elettrodinamica classica, della densità di carica  $e\varphi_I^* \varphi_I$  entro la sfera baricentrica di raggio  $l$  <sup>(8)</sup>.

\* \* \*

L'autore ringrazia il Prof. G. WATAGHIN per le numerose discussioni. Ringrazia inoltre la Società Nazionale Cogne, segnatamente nelle persone del Direttore Generale ed Amministratore Delegato, Ing. G. ANSELMETTI, e del Capo del Laboratorio Chimico e Spettrochimico Dr. L. BENUZZI, per le facilitazioni concesse.

#### APPENDICE

##### Soluzione dell'equazione generalizzata in assenza di interazione.

In quest'Appendice vogliamo trovare una soluzione dell'equazione generalizzata (1) in assenza di interazione, la quale abbia le corrette proprietà spinoriali di trasformazione e sia tale da soddisfare alla condizione supplementare (6) e inoltre sia una autofunzione dell'operatore di massa corrispondente ad un certo autovalore  $m_n$  dello spettro di masse.

Per questo è conveniente esprimere il campo bilocale  $\psi(x, \eta)$  come sviluppo in serie delle autofunzioni del campo bilocale relativo a stati interni liberi. È questo il campo bilocale rappresentato da una matrice a una colonna e a quattro righe il quale soddisfa all'equazione generalizzata

$$(19) \quad \alpha_\nu \left( \frac{\partial}{\partial x_\nu} + \frac{\partial}{\partial \eta_\nu} \right) \psi(x, \eta) = 0,$$

ma non a una condizione di quantizzazione della massa, per cui non si ha uno spettro discreto di masse, bensì uno spettro continuo. Pertanto il campo bilocale relativo a stati interni liberi non ha significato fisico, ma è un artificio matematico. Esso è evidentemente determinato dall'equazione (19) con un'al-

<sup>(8)</sup> Cfr. E. MINARDI: *Nuovo Cimento*, **12**, 950 (1954).

gebra analoga a quella dell'equazione di Dirac per l'elettrone libero. La (19) può infatti soddisfarsi ponendo  $\psi(x, \eta) = N \exp[-ip_v^{(x)}x_v] \exp[-ip_v^{(\eta)}\eta_v]u_p$ , ove  $N$  è un fattore di normalizzazione e  $u_p$  è una matrice a una colonna e a quattro righe la quale soddisfa all'equazione:

$$(20) \quad \alpha_v(p_v^{(x)} + p_v^{(\eta)})u_p = 0.$$

Ponendo  $p_v = p_v^{(x)} + p_v^{(\eta)}$  si trova che, affinchè esistano soluzioni della (20), deve valere la relazione (della quale si vedrà più sotto il significato fisico)

$$(21) \quad p^4 = p_0^4 \quad (p_4 = ip_0, \quad p = (p_1^2 + p_2^2 + p_3^2)^{\frac{1}{2}}),$$

le cui uniche radici reali sono  $p = \pm p_0 = \pm (p_0^{(x)} + p_0^{(\eta)})$ .

In conseguenza della condizione supplementare (6) occorre porre nel sistema del baricentro  $p_4^{(\eta)} = -i \partial \psi / \partial \eta_4 = 0$ , cosicchè la (21) stabilisce che in tale sistema è  $(p_1^{(\eta)^2} + p_2^{(\eta)^2} + p_3^{(\eta)^2})^{\frac{1}{2}} = \pm m$ .

Poichè l'impulso interno  $p^{(\eta)}$ , come  $p^{(x)}$ , è arbitrario, la massa  $m$  può assumere un qualsiasi valore reale del continuo.

Esistono quattro soluzioni linearmente indipendenti dalla (20) le quali, analogamente al caso dell'equazione di Dirac per l'elettrone libero, possono scriversi convenientemente nel modo seguente:

$$(22) \quad u_{+,1} = \frac{1}{\sqrt{2}} \begin{pmatrix} 1 \\ 0 \\ \frac{p_3}{p_0} \\ \frac{p_1 + ip_2}{p_0} \end{pmatrix}, \quad u_{+,2} = \frac{1}{\sqrt{2}} \begin{pmatrix} 0 \\ 1 \\ \frac{p_0^2 - p_3^2}{p_0(p_1 + ip_2)} \\ -\frac{p_3}{p_0} \end{pmatrix}; \quad (p_0 > 0)$$

$$(23) \quad u_{-,1} = \frac{1}{\sqrt{2}} \begin{pmatrix} -\frac{p_3}{p_0} \\ -\frac{p_1 + ip_2}{p_0} \\ 1 \\ 0 \end{pmatrix}, \quad u_{-,2} = \frac{1}{\sqrt{2}} \begin{pmatrix} -\frac{p_0^2 - p_3^2}{p_0(p_1 + ip_2)} \\ \frac{p_3}{p_0} \\ 0 \\ 1 \end{pmatrix}; \quad (p_0 < 0).$$

Il fattore  $(2)^{-\frac{1}{2}}$  segue dalla condizione di normalizzazione  $u_{\pm,i}^* u_{\pm,i} = 1$ .

Per ogni dato valore di  $q$  le quattro soluzioni precedenti formano un sistema completo ortogonale:

$$(24) \quad \sum^p u_q^* u_{q'} = \delta_{qq'}.$$

L'indice  $p$  indica che la sommatoria è svolta tenendo  $p$  fisso.



Le seguenti relazioni possono essere utili:

$$(25) \quad \begin{cases} u_{\pm, i}^* \alpha_v u_{\pm, i} = \pm \frac{p_v}{p_0} = \pm \frac{1}{p_0} (p_v^{(x)} + p_v^{(\eta)}), & u_{\pm, i}^* \alpha_v u_{\pm, j} = 0, \\ u_{\pm, i}^* \beta u_{\pm, i} = 0, & u_{\pm, i}^* \beta u_{\pm, j} = 0, \quad (v = 1, 2, 3; i, j = 1, 2; i \neq j). \end{cases}$$

Poichè ogni combinazione lineare delle soluzioni precedenti soddisfa ancora alla (19), possiamo esprimere in questo modo il campo bilocale  $\psi_n(x, \eta)$  corrispondente ad un certo autovalore  $m_n$  dell'operatore di massa. Limitandosi al caso delle particelle con momento angolare totale interno uguale a  $\frac{1}{2}$  ( $k=1$ ), non si ha dipendenza angolare e nel sistema del baricentro il campo interno è dato dalla soluzione della (8) soddisfacente alla condizione di quantizzazione della massa (9). I coefficienti della combinazione lineare dei termini  $u_p \exp[-i\mathbf{p}^{(\eta)} \cdot \boldsymbol{\eta}]$  sono allora determinati in questo riferimento dalla condizione che l'elemento della matrice  $\psi_n(x, \eta)$  ottenuto combinando linearmente gli elementi  $\exp[-i\mathbf{p}^{(\eta)} \cdot \boldsymbol{\eta}]$  della matrice  $u_p \exp[-i\mathbf{p}^{(\eta)} \cdot \boldsymbol{\eta}]$  (cfr. formule (22) e (23)) sia uguale alla precedente soluzione della (8). Questi coefficienti sono quindi dati dai coefficienti dello sviluppo in onde piane, entro la sfera baricentrica, della soluzione della (8) per  $k=1$ , soddisfacente alla condizione (9). Si ha quindi nel sistema del baricentro:

$$(26) \quad \psi_n(x_1, \boldsymbol{\eta}) = V_x^{-\frac{1}{2}} \exp[itE] V_\eta^{-\frac{1}{2}} \sum_{\mathbf{p}^{(\eta)}} c^{(n)}(\mathbf{p}^{(\eta)^2}) \exp[-i\mathbf{p}^{(\eta)} \cdot \boldsymbol{\eta}] \quad (\mathbf{p}^{(x)}=0, p_4^{(\eta)}=0).$$

Per  $\boldsymbol{\eta}^2 > l^2$  si assume la soluzione nulla della (19). Pertanto, mentre l'elemento della matrice  $\psi_n$  corrispondente all'elemento 1 della matrice  $u_p$  è una funzione continua sulla superficie della sfera baricentrica, gli altri elementi della matrice  $\psi_n$  corrispondenti agli elementi non nulli della matrice  $u_p$ , (cfr. formule (22) e (23)) in generale non lo sono.

La (26) è subito generalizzata al caso di un riferimento qualsiasi in modo che abbia le corrette proprietà spinoriali di trasformazione. Poichè infatti nel sistema del baricentro è  $p_4^{(\eta)}=0$  possiamo sostituire  $p_v^{(\eta)} p_v^{(\eta)}$  a  $\mathbf{p}^{(\eta)^2}$  e  $p_v^{(\eta)} \eta_v$  a  $\mathbf{p}^{(\eta)} \cdot \boldsymbol{\eta}$ ; inoltre  $V^{-\frac{1}{2}}$ , essendo espresso solo con la costante universale  $l$  che è scalare, è esso stesso uno scalare. Si ha allora

$$(27) \quad \psi_n(x, \boldsymbol{\eta}) = V_x^{-\frac{1}{2}} \exp[-ix_p p_v^{(x)}] V_\eta^{-\frac{1}{2}} \sum_{\mathbf{p}^{(\eta)}} c^{(n)}(p_v^{(\eta)} p_v^{(\eta)}) u_p \exp[-i p_v^{(\eta)} \eta_v],$$

che si trasforma appunto come uno spinore.

Possiamo ora indicare il significato fisico della relazione (21). Con la (27) abbiamo infatti espresso lo stato interno relativo alla massa  $m_n$  come una sovrapposizione di stati di quadri-impulso interno  $p_v^{(\eta)}$ , ciascuno con peso statistico  $c^{(n)*}(p_v^{(\eta)^2}) c^{(n)}(p_v^{(\eta)^2})$ . Poichè ciascun impulso interno  $p_v^{(\eta)}$  soddisfa alla relazione  $p^2 = (p_0^{(x)} + p_0^{(\eta)})^2$  (la quale consegue appunto dalla (21) quando si ammettano solo radici reali) lo stato risultante dalla sovrapposizione degli stati di quadri-impulso  $p_v^{(\eta)}$ , che è proprio lo stato fisico della particella, dovrà soddisfare alla relazione:

$$(28) \quad \sum_{\mathbf{p}^{(\eta)}} c^{(n)*}(p_v^{(\eta)^2}) c^{(n)}(p_v^{(\eta)^2}) p^2 = \sum_{\mathbf{p}^{(\eta)}} c^{(n)*}(p_v^{(\eta)^2}) c^{(n)}(p_v^{(\eta)^2}) (p_0^{(x)} + p_0^{(\eta)})^2, \quad (v = 1, \dots, 4).$$

Dalla precedente, avendosi  $p_v^{(x)} p_r^{(\eta)} = 0$ ,  $\sum_{\mathbf{p}^{(\eta)}} c^{(n)*} (p_v^{(\eta)2}) c^{(n)} (p_v^{(\eta)2}) p_r^{(\eta)2} = m_n^2$ , ( $v=1, \dots, 4$ ) segue la formula

$$29) \quad p_0^{(x)2} = \mathbf{p}^{(x)2} + m_n^2,$$

che esprime la relazione usuale tra l'energia e l'impulso del moto osservabile.

### SUMMARY (\*)

A bilocal theory is presented for a free particle with spin  $\frac{1}{2}$  based on a simple general generalization of the Dirac equation. This equation is resolved introducing a condition for the mass quantization and a new supplementary condition substituting Yukawa's condition used in a preceding paper. The generalization of the theory is such that in the equations the co-ordinates of the observable motion and the internal co-ordinates appear formally symmetric. Then interaction is introduced between the non quantized bilocal field and the quantized electromagnetic field so as to satisfy aforesaid symmetry. The so obtained theory is differential and linear; it satisfies gauge invariance and charge conservation, provided one allows for the variation of the four-current due to the internal part of the bilocal field. It is finally shown that our theory leads to the appearance in the interaction matrix elements of factors which invariantly cut high pulses.

(\*) Traduzione a cura della Redazione.

## The Theorem on Incoming Waves.

D. PARK (\*)

*University of Ceylon - Colombo, Ceylon*

(ricevuto il 13 Febbraio 1956)

**Summary.** - The general form of the following theorem is stated and proved: if a particle is scattered by two potentials, then the resulting amplitude for a real transition may be written as the sum of two parts. The first is the amplitude for scattering by either of the potentials acting alone. The second is that for scattering by the other potential, where the incident wave is the wave function belonging to the first potential in which the asymptotic form of the « scattered » wave moves inward. Some remarks are added concerning the applications of this theorem in quantum mechanics and the theory of fields.

### 1. - Introduction.

The object of this note is to state and prove a simple theorem about scattering (or, more generally, about the  $S$ -matrix), and to make a few remarks about its implications. The general content of the theorem is well known <sup>(1)</sup>, but the discussions already available may well be supplemented by an explicit statement and a simple proof. These are given in Section 2; the following sections give a few remarks on applications of the theorem.

### 2. - The Theorem on Incoming Waves.

Suppose that a quantum mechanical system is described by the Schrödinger equation

$$(1) \quad i\hbar\partial_t\psi = H\psi, \quad H = H_0 + V$$

(\*) On leave from Williams College, Williamstown, Mass., U.S.A.

<sup>(1)</sup> G. BREIT and H. BETHE: *Phys. Rev.*, **93**, 888 (1954) and other references given there.

and that one knows how to solve

$$(2) \quad i\hbar\partial_t\varphi = H_0\varphi.$$

Then one can write  $\psi$  as  $\varphi + \chi$ , where  $\chi$  is attributable to the effect of the additional energy  $V$ . The general  $\chi$  can be formed out of two special cases:  $\chi^{(+)}$ , describing a system which was originally in the state  $\varphi$  and would have remained so except for the action of  $V$ , and  $\chi^{(-)}$ , whose temporal behavior is the inverse of this, i.e.  $\chi^{(+)}(-\infty) = \chi^{(-)}(\infty) = 0$ . These can be called the causal and anticausal solutions. They can be written formally from (1) or (2) as <sup>(2)</sup>

$$(3) \quad \chi^{(\pm)} = \lim_{\gamma \rightarrow +0} (E - H \pm i\gamma)^{-1} V\varphi \quad \text{or} \quad (E - H_0 \pm i\gamma)^{-1} V\psi,$$

where  $E$  is the energy eigenvalue assumed common to  $\psi$  and  $\varphi$ . The probability of transitions out of the state which originated as  $\varphi$  is given by the transition amplitude

$$T = (\varphi', V\psi^{(+)}) ,$$

where  $\varphi'$  describes the new state. Real transitions occur only between states of the same energy, and  $T$  will be written in bold face type when we wish to show that only real transitions are to be considered.

Suppose now that  $V$  is divided, naturally or artificially, into two parts,  $V_1$  and  $V_2$ , and that  $\psi_1^{(+)}$  describes the causal solution of the wave equation when only  $V_1$  is acting. Let the corresponding transition amplitude  $(\varphi', V_1\psi_1^{(+)})$  be called  $T_1$ . The theorem we wish to prove states that

$$(4) \quad \mathbf{T} = \mathbf{T}_1 + \mathbf{T}_{12}, \quad \mathbf{T}_{12} = (\psi_1^{(-)}, V_2\psi^{(+)}) ,$$

where  $\psi^{(-)}$  is the anticausal wave function whose final state is  $\varphi'$ .

*Proof:* Write  $\psi^{(+)}$  as  $\psi_1^{(+)} + \psi_2$  and

$$\begin{aligned} T &= (\varphi', V_1\psi_1^{(+)}) + (\varphi', V_1\psi_2 + V_2\psi^{(+)}) \\ &= \mathbf{T}_1 + \mathbf{T}_{12}. \end{aligned}$$

To evaluate  $T_{12}$ , we write  $H_0 + V_1$  as  $H_1$  and

$$\begin{aligned} \psi_2 &= \chi^{(+)} - \chi_1^{(+)} \\ &= (E - H + i\gamma)^{-1} V\varphi - (E - H_1 + i\gamma)^{-1} V_1\varphi \\ &= [(E - H + i\gamma)^{-1} - (E - H_1 + i\gamma)^{-1}] V\varphi + (E - H_1 + i\gamma) V_2\varphi. \end{aligned}$$

<sup>(2)</sup> The reason for the introduction of the terms  $\pm i\gamma$  is discussed in the Appendix.

To simplify this we use the second relation of the pair

$$(5) \quad a^{-1} - b^{-1} = a^{-1}(b - a)b^{-1} = b^{-1}(b - a)a^{-1}$$

to get

$$\begin{aligned} \psi_2 &= (E - H_1 + i\gamma)^{-1} V_2 [(E - H + i\gamma)^{-1} V\varphi + \varphi] \\ &= (E - H_1 + i\gamma)^{-1} V_2 \psi^{(+)} . \end{aligned}$$

Thus to evaluate  $T_{12}$  we need

$$V_1 \psi_2 + V_2 \psi^{(+)} = (E - H_0 + i\gamma)(E - H_1 + i\gamma)^{-1} V_2 \psi^{(+)}$$

so that

$$T_{12} = (E - E' + i\gamma)(\varphi', (E - H_1 + i\gamma)^{-1} V_2 \psi^{(+)}) ,$$

where  $E'$  is the energy of the state  $\varphi'$ . We have therefore, assuming that  $H_1$  is Hermitian,

$$T_{12} = (E - E' + i\gamma)((E - H_1 - i\gamma)^{-1} \varphi', V_2 \psi^{(+)}) .$$

If  $E' = E$ , then it follows easily that

$$T_{12} = (\psi_1'^{(-)}, V_2 \psi^{(+)})$$

and the theorem is proved. If further one can expand  $\varphi'$  in eigenfunctions of  $H_1$  then it is also valid off the energy shell. But even in quite simple cases such an expansion involves singular coefficients<sup>(3)</sup>, so that the extension of the theorem would rarely be possible.

### 3. - The Construction of Anticausal Wave Functions.

If one starts with an expression for the causal wave function (in any quantum mechanical representation), then the corresponding anticausal wave function may be constructed in a straightforward way. First form the time-reversed wave function, in which the « scattered » wave clearly moves inward. (The complete time reversal includes the reversal of external currents and hence of the magnetic fields which they produce). But one has now reversed also the direction of the incident beam. Therefore, next carry out a reflection of the wave function in the origin of coordinates. The passage from  $\psi^{(+)}$  to  $\psi'^{(-)}$

(3) S. BOROWITZ: *Phys. Rev.*, **89**, 441 (1953).



is thus effected by a total inversion in space-time. A simple example which is often useful is the Schrödinger wave function of a particle in a symmetrical field of force:

$$(6) \quad \psi^{(-)}(\theta) = \psi^{(+)*}(\pi - \theta),$$

where the star denotes the complex conjugate.

A further relation between the causal and anticausal wave functions results from taking  $V_1$  and  $V_2$  in (4) equal and opposite:

$$(7) \quad (\varphi', V\psi^{(+)} ) = (\psi'^{(-)}, V\varphi).$$

This rule helps one to compute transition probabilities from (4).

The result (6) is useful in deriving the expression of the theorem in terms of phase angles. Let  $U(r)$  denote  $(2m/\hbar^2)V(r)$ , and let the momentum of the incident particles be  $\hbar k$ . Then if  $V$  is spherically symmetrical, the transition amplitudes for the different angular momentum states are conveniently expressed in terms of phase angles. Let  $\varphi$  denote a plane wave,

$$\exp[ikz] = \sum (2l+1)i^l f_l(r) P_l(\cos \theta), \quad f_l(r) = (\pi/2kr)^{\frac{1}{2}} J_{l+\frac{1}{2}}(kr)$$

and correspondingly let the total causal wave function be

$$\psi = \sum (2l+1)i^l R_l(r) P_l(\cos \theta).$$

Then it is easy to show that

$$\exp[2i\delta_l] - 1 = -2ik \int_0^\infty f_l(r) U(r) R_l(r) r^2 dr.$$

The integral is, except for a constant factor, a single component of  $T$ , so that if  $U = U_1 + U_2$  and  $\delta_{1l}$  and  $R_{1l}$  are produced by  $U_1$  alone, we have by (4) and (6)

$$\exp[2i\delta_l] = \exp[2i\delta_{1l}] - 2ik \int_0^\infty R_{1l}^*(r) U_2(r) R_l(r) r^2 dr.$$

#### 4. - The Cross-Section Theorem.

The decomposition which we have made splits the scattering amplitude into two parts. We shall show that an analogous decomposition exists for

the total cross-section. Take the time derivative of

$$(\chi^{(+)}, \chi^{(+)}) = (\psi^{(+)}, \psi^{(+)}) + (\varphi, \varphi) - 2 \operatorname{Re} (\varphi, \psi^{(+)}).$$

The left side is clearly related to the total transition probability per unit time. Since  $H$  and  $H_0$  are Hermitian, the first two terms on the right are constant provided that they exist or can be made to exist in some limiting sense. The use of (1) and (2) gives

$$\begin{aligned} \partial_t (\chi^{(+)}, \chi^{(+)}) &= - (2/\hbar) \operatorname{Im} (\varphi, V \psi^{(+)}) \\ &\equiv - (2/\hbar) \operatorname{Im} T_0. \end{aligned}$$

This is the so-called cross-section theorem in its most general form<sup>(4)</sup>. The decomposition of  $T$  leads therefore to a corresponding decomposition of the total cross-section.

## 5. — Relation to Perturbation Theory.

The representation (4) amounts to a rather violent rearrangement of the expression which would result by considering  $V_1$  and  $V_2$  on an equal footing. It has however a close relationship to the expression of transition amplitudes by means of chronologically ordered operators in the interaction representation (see Section 7) or the corresponding formulas in the usual stationary state theory of perturbations. As an example of the latter, we can calculate  $T$  to the lowest order of approximation in which  $V_1$  and  $V_2$  each occur once. Only  $T_{12}$  matters here; if we write

$$\begin{aligned} \psi_1^{(-)} &= \varphi' + (E - H_0 - i\gamma)^{-1} V_1 \varphi' + \dots \\ \psi^{(+)} &= \varphi + (E - H_0 + i\gamma)^{-1} V_1 \varphi + \dots \end{aligned}$$

then the relevant part of  $T_{12}$  is

$$M_{12} = (\varphi', V_2 (E - H_0 + i\gamma)^{-1} V_1 \varphi) + (\varphi', V_1 (E - H_0 + i\gamma)^{-1} V_2 \varphi)$$

in which one can see quite clearly the origin of the usual prescription for forming the matrix elements.

<sup>(4)</sup> E. FEENBERG: *Phys. Rev.*, **40**, 40 (1932); N. BOHR, R. PEIERLS and G. PLACZEK: *Nature*, **144**, 200 (1939); D. PARK: *Ind. Journ. Theor. Phys.*, in the press.

## 6. — Application to Bremsstrahlung.

The earliest application of these considerations was to the theory of bremsstrahlung, when it was desired to use exact Coulomb wave functions instead of those given by the first Born approximation <sup>(5)</sup>. We let  $V_1$  be the external potential and  $V_2$  be the interaction with the radiation field. Let  $\varphi'$  be a state consisting of one bare electron moving freely and one bare photon. We shall write this as  $\varphi'_{1e}\varphi'_{1p}$ . The corresponding  $\psi^{(\pm)}$  when the electron's Coulomb interaction  $V_1$  has been taken into account is  $\psi'^{(\pm)}_{1e}\varphi'_{1p}$ . The initial one-electron wave function is  $\varphi_{1e}\varphi_{0p}$ , and its value after the Coulomb interaction only is  $\psi^{(+)}_{1e}\varphi_{0p}$ . The transition amplitude is

$$T = (\varphi'_{1e}\varphi'_{1p}, V_1\psi^{(+)}_{1e}\varphi_{0p}) + (\psi'^{(-)}_{1e}\varphi'_{1p}, V_2\psi^{(+)}),$$

where  $\psi^{(+)}$ , the exact final wave function, is in general a mixture of states containing different numbers of dressed electrons and quanta. Since  $\varphi'_{1p}$  is orthogonal to  $\varphi_{0p}$ , the first term vanishes. To the lowest order in  $V_2$ ,  $\psi^{(+)}$  is  $\psi^{(+)}_{1e}\varphi_{0p}$ , where only  $n = 0$  and  $2$  appear. Of these,  $n = 0$  is of lower order, so that, writing  $V_2$  symbolically as  $-\int jA$ , we have

$$(8) \quad T \approx - \int (\psi'^{(-)}_{1e}, i\psi^{(+)}_{1e})(\varphi'_{1p}, A\varphi_{0p}).$$

This well known result is of course obvious from (4), and it is derived here by way of illustration. It is also clearly apparent from this formula or the exact form preceding it that the total cross-section for the emission of a particular photon (or photons), independent of the scattered electrons, may be calculated using either  $\psi'^{(-)}_{1e}$  or  $\psi'^{(+)}_{1e}$ , indifferently <sup>(6)</sup>.

## 7. — Relation to Field Theory.

For simplicity we shall first consider the radiative corrections to scattering, or some analogous problem in which the interactions between the quantized fields do not give rise to observable transitions. In this case it is convenient to reverse the roles of  $V_1$  and  $V_2$  in the previous section, and let  $V_1$  be the interaction between fields and  $V_2$  be the interaction with a piece of apparatus classically described.  $T_1$  now describes the change in the system due to the field's self-interaction only, and  $\psi^{(\pm)}_1$  is the state in which this self inter-

<sup>(5)</sup> H. BETHE and L. MAXIMON: *Phys. Rev.*, **93**, 768 (1954) and earlier work cited there.

<sup>(6)</sup> H. OLSEN: *Phys. Rev.*, **99**, 1335 (1955).

action has been taken into account. The observable change in the system is now entirely due to  $T_{12}$ . Suppose that the interaction with  $V_2$  is one which in the absence of  $V_1$  would be amenable to expansion in powers of  $V_2$ . In the presence of  $V_1$ , the expansion can be carried out by writing  $\psi^{(+)}$  in (4) as  $\psi_1^{(+)} + \psi_2$  and using the first relation of (5) to get

$$\psi_2 = (E - H + i\gamma)^{-1} V_2 \psi_1^{(+)}.$$

With this, (4) is

$$(9) \quad T = (\varphi', V_1 \psi_1^{(+)}) + (\psi_1^{(-)}, V_2 \psi_1^{(+)}) + (\psi_1^{(-)}, V_2 (E - H + i\gamma)^{-1} V_2 \psi_1^{(+)}) ,$$

of which the last term can be further expanded in powers of  $V_2$ .

This equation has two points of interest. The first is that renormalization can very simply be characterized as the addition of counter terms to  $V_1$  (and their subtraction from  $H_0$ ) so as to make the first term vanish once for all. The second is that after this has been done, the remaining terms of (9) represent transitions between fields which have essentially identical characterizations in terms of the theory of interacting fields. The difficulties which arise from the attempt to express a field with one set of interactions in terms of the stationary states of a field with a different set (7) do not arise here, and there should be no difficulty about the convergence of the expansion of (9) in powers of  $V_2$  (after  $V_2$  has itself been renormalized by a multiplicative constant) provided that  $V_2$  is small enough to begin with. This conclusion is quite independent of the fact that the above-mentioned difficulties arise notoriously in the first term of (9), which cannot therefore be evaluated without renormalization and almost certainly has no expression as an expansion in positive powers of the coupling constant. The utility of the theorem (4) in field theory is therefore that it divides the transition amplitude into a generally analytic part and a probably non-analytic part, of which only the former gives the observable effects.

Suppose that one wishes to evaluate  $T_{12}$ , renormalizing step by step, as a power series in  $V_1$ . To do so, one goes into the interaction representation by carrying out successively the contact transformations generated by  $K$ ,  $U$  and  $W$ , with

$$\begin{aligned} i\hbar \partial_t K &= H_0 K, & K(-\infty) &= 1, \\ i\hbar \partial_t U_1 &= V_{1i} U_1, & U_1(-\infty) &= 1, & V_{1i} &= K^{-1} V_1 K \\ i\hbar \partial_t W &= V_{2r} W, & W(-\infty) &= 1, & V_{2r} &= U^{-1} K^{-1} V_2 K U. \end{aligned}$$

(7) L. VAN HOVE: *Physica*, **18**, 145 (1952).

In terms of these, we have

$$\begin{aligned}\psi_1^{(+)} &= K U_1 \varphi(-\infty) \\ \psi_1^{(-)} &= K U_1 U_1^{-1}(\infty) \varphi(-\infty) \\ \psi^{(+)} &= K U_1 W \varphi(-\infty)\end{aligned}$$

and

$$T_{12} = (\psi_1^{(-)}, V_2 \psi^{(+)}) = (\varphi'(-\infty), U_1(\infty) V_{2r} W \varphi(-\infty)).$$

If only the first order in  $V_2$  is needed,  $W$  may be replaced by unity. What remains is to expand the product  $U_1(\infty)V_2$ , and it is exactly this quantity which is given by the usual expansion in chronological products<sup>(8)</sup>. In the steady-state situation considered above, the renormalized  $U_1(\infty)$  is of course equal to unity, but the transition amplitudes for non-steady-state process may also be written down, formally at least, in the terms of a completely renormalized theory<sup>(9)</sup>.

## APPENDIX

The device of defining  $\psi^{(-)}$  by the addition of what amounts to a negative imaginary part to the Hamiltonian  $H_0$  has often been justified by an argument in which the interaction is thought of as having been turned on adiabatically over an infinite period of time. Not only is it difficult to imagine ways in which the interaction may be established adiabatically; it is also well known that such an argument fails for a stationary state. The «  $\gamma$  trick » is of course quite independent of such an assumption, and is introduced merely to pick out of the manifold of solutions of (1) those satisfying the principle of causality: as if one changes the interaction term  $V$  at a certain time  $t$ , then all the associated changes in  $\psi$  will occur subsequently to  $t$ . This specification is quite independent of whether the states involved are bound, free, or both.

The equation (3) for example, are valid when  $\varphi$  and  $\psi^{(+)}$  are eigenstates of the  $H_0$  and  $H$  respectively belonging to the energy  $E$ <sup>(10)</sup>. For generality, consider the second form, and let  $H_0$ , if one wishes, include a potential energy strong enough to produce binding;  $V$  is to be thought of in that case as an

<sup>(8)</sup> F. J. DYSON: *Phys. Rev.*, **75**, 486 (1949).

<sup>(9)</sup> G. KÄLLÉN: *Helv. Phys. Acta*, **25**, 417 (1952).

<sup>(10)</sup> In situations involving interacting fields, renormalization must be carried out in order for this to be possible.



additional interaction energy. Let  $\psi^{(+)}$  be written as

$$(A.1) \quad \psi^{(+)}(t) = \frac{1}{2\pi\hbar} \int_{-\infty}^{\infty} dE dt' \exp[-iE(t-t')/\hbar] \psi(t'),$$

so that

$$\chi^{(+)}(t) = \lim_{\gamma \rightarrow 0} \frac{1}{2\pi\hbar} \int_{-\infty}^{\infty} dE dt' \frac{\exp[-iE(t-t')/\hbar]}{E - H_0 + i\gamma} V \psi^{+}(t').$$

Since the eigenvalues of  $H_0$  are real, one can at once evaluate the  $E$ -integral.

If  $t$  is greater than  $t'$  the contour can be closed below to include the singularity; otherwise one gets zero, and in the limit

$$(A.2) \quad \chi^{(+)}(t) = - (i/\hbar) \int_{-\infty}^t dt' \exp[-iH_0(t-t')/\hbar] V \psi^{+}(t'),$$

in which the causality condition is evidently satisfied, since any possible external interference with the system subsequent to  $t$  does not affect its value at  $t$ . This expression is more familiar in the interaction representation or its generalization when bound states are present. Writing

$$\chi^{(+)}(t) = \exp[-iH_0 t/\hbar] \chi_i^{(+)}(t), \quad \psi^{(+)}(t) = \exp[-iH_0 t/\hbar] \psi_i^{(+)}(t)$$

$$\exp[iH_0 t/\hbar] V \exp[-iH_0 t/\hbar] = V_i(t)$$

we have

$$\chi_i^{(+)}(t) = - (i/\hbar) \int_{-\infty}^t dt' V_i(t') \psi_i^{+}(t').$$

This illustrates the way in which one can translate the expressions of the algebraic theory into those of the more usual computational methods when such a transcription is possible.

#### RIASSUNTO (\*)

Si enuncia e si dimostra il seguente teorema nella sua forma generale: se una particella subisce scattering da parte di due potenziali, l'ampiezza risultante per una transizione reale si può scrivere come somma di due parti. La prima è l'ampiezza dello scattering dovuto ad uno dei due potenziali agente singolarmente. La seconda è lo scattering dovuto al secondo potenziale, dove l'onda incidente è la funzione d'onda del primo potenziale in cui la forma asintotica dell'onda « diffusa » si muove verso l'interno. Si aggiungono alcune osservazioni sulle applicazioni di questo teorema nella meccanica quantistica e nella teoria dei campi.

(\*) Traduzione a cura della Redazione.

## On a Conform-Invariant Spinor Wave Equation.

FEZA GÜRSEY

*Mathematics Department, University of Istanbul*

(ricevuto il 14 Febbraio 1956)

**Summary.** — As a possible basis for a unitary description of particles a new spinor wave equation is proposed which is similar to Heisenberg's non-linear generalization of Dirac's equation but exhibits in addition an invariance with respect to conformal transformations. A  $2 \times 2$  matrix formalism is developed in view of obtaining a synthetic expression for conformal transformations as well as for spinor equations of Dirac's type. A direct proof of the conform-invariance of the new equation is then given with the aid of this formalism and an explicit transformation law for the wave function is derived. It is further shown that the unquantized equation allows for the propagation of plane waves corresponding to particles of different rest masses.

### 1. — Introduction.

One of the greatest obstacles encountered by modern field theories is the need to account for all the elementary particles the number of which seems to be growing as one moves into regions of higher energies. Under the present formalism one has to set up a separate field equation for each particle characterized by its rest mass and spin and any additional specific quantum number like isotopic spin, attribute, etc. One then introduces semiempirical interaction terms for each pair of particles, these terms involving coupling constants to be determined by experiment and being formally restricted by general principles of invariance like relativistic invariance. Apparently all these particles are not on the same footing, some like nucleons and electrons being much more stable than some transient « new particles » with very short life-times. The physicist feels therefore unjustified in labelling each particle by a different equation giving them an equivalent status thereby. This unsatisfactory procedure has worried many theoreticians who have felt the need

for a unitary field theory from which all the separate « elementary » particles and their interactions could be derived simultaneously.

If the unitary hypothesis is true there are strong arguments in favour of a non-linear theory. Indeed, in a linear theory, plane wave solutions are all independent, and, to introduce any interaction between them, one needs an auxiliary field which destroys the unitary hypothesis. Conversely, virtual transitions in quantized field theories introduce such interactions between plane waves which result in non-linear effects (like scattering of light by light). This seems to establish that even in the absence of actual electrons the quantized Maxwell equations are effectively non-linear.

Another advantage of non-linear classical field theories is the possibility to derive in some cases the equation of motion of a particle regarded as a singularity from the field equation itself. General relativity provides the most satisfactory model in this respect.

Other points have been stressed by EINSTEIN, BORN <sup>(1)</sup> and more recently by HEISENBERG <sup>(2)</sup>. HEISENBERG's idea is to base the unitary field theory on a spinor wave equation, since a tensor equation like those arising in general relativity will not serve to describe fermions. On the other hand, he has chosen an equation formally as similar as possible to the Dirac equation which certainly describes the electron correctly and is believed to be of value for the description of the nucleon. HEISENBERG's tentative equation reads:

$$(1.1) \quad \gamma^\mu \partial_\mu \psi + l^2 (\bar{\psi} \psi) \psi = 0,$$

where the  $\gamma^\mu$ 's are the conventional Dirac-Pauli matrices,  $\bar{\psi}$  is the adjoint wave function and  $l$  is a relativistically invariant fundamental length. HEISENBERG and others <sup>(3)</sup> were able to show that the existence of bosons and fermions of different rest masses follow from the quantized field equation.

The disadvantage of dealing with non-linear theories may be traced to the mathematical difficulties encountered in the solution and quantization of the equations, as the principle of the superposition (mathematically expressed in the form of Fourier expansions) can no longer be used. However, if the equation possesses remarkable properties of invariance, as in the case of the equations of general relativity, new solutions can be obtained from particular solutions by applying on them the operations of the group which leaves the equation invariant. Invariance properties assume therefore a special importance in non-linear theories.

(1) M. BORN: *Proc. Roy. Soc.*, A **143**, 410 (1934).

(2) W. HEISENBERG: *Physica*, **19**, 897 (1953).

(3) W. HEISENBERG: *Nachr. Göttingen Akad. Wiss.*, 111 (1953) and *Zeits. f. Naturf.*, **9a**, 292 (1954); W. HEISENBERG, F. KORTÉL und M. MITTER: *Zeits. f. Naturf.*, **10a**, 425 (1955).

Heisenberg's equation (1.1) does not possess any new invariance property over Dirac's equation, as the only requirement imposed on it is linearity with respect to the derivatives of  $\psi$  in addition to relativistic invariance. Hence, its arbitrary character. For instance, instead of (1.1) we could choose the equation

$$(1.2) \quad \gamma^\mu \partial_\mu \psi + l^{3n-1} (\bar{\psi} \psi)^n \psi = 0,$$

while keeping the equation dimensionally correct. The exponent of  $l$  is chosen by bearing in mind that  $\bar{\psi} \psi$  has the dimensions of an inverse cube length. In particular we obtain Heisenberg's form (1.1) by taking  $n = 1$ . HEISENBERG has decided on the choice (1.1) by reasons of formal simplicity. However, requirement of invariance under a new group of transformation seems to be a more important factor in restricting the possible equations since it leads to simplicity of solution and even to new physical properties.

In looking for the new invariance property we shall be guided by the example of Maxwell's equations which are Lorentz invariant. Equations describing matter in Newtonian mechanics were not Lorentz invariant, and their modification as to include the invariance property possessed by the electromagnetic equations led to relativistic mechanics and eventually to Dirac's wave equation. On the other hand, Maxwell's equations possess a further invariance property, namely, invariance under the conformal group which includes the Lorentz group as a subgroup. This was first shown by CUNNINGHAM<sup>(4)</sup> and BATEMAN<sup>(5)</sup> and it means physically that the equations keep the same form in different frames of reference moving relatively to each other with constant acceleration. The relativity theory of PAGE<sup>(6)</sup> based on the equivalence of such frames was shown to be invariant with respect to conformal transformations by ROBERTSON<sup>(7)</sup>. Later, HILL<sup>(8)</sup> gave a general proof of the connection between uniformly accelerated motions and the conformal group. Now, if we require that equations describing matter possess all the invariance properties of Maxwell's equations we are bound to modify Dirac's equation as to render it conform-invariant. Attempts were made in this direction by VEBLEN<sup>(9)</sup> and DIRAC<sup>(10)</sup> who developed a six-dimensional formalism, using homogeneous coordinates. However, HAANTJES<sup>(11)</sup> and later

(4) E. CUNNINGHAM: *Proc. London Math. Soc.*, **8**, 77 (1909).

(5) H. BATEMAN: *Proc. London Math. Soc.*, **8**, 223 (1910).

(6) L. PAGE: *Phys. Rev.*, **49**, 254 (1936).

(7) H. P. ROBERTSON: *Phys. Rev.*, **49**, 755 (1936).

(8) E. L. HILL: *Phys. Rev.*, **72**, 143 (1947).

(9) D. VEBLEN: *Proc. Nat. Acad. Sc.*, **21**, 484 (1935).

(10) P. A. M. DIRAC: *Ann. of Math.*, **37**, 429 (1936).

(11) J. HAANTJES: *Proc. Ned. Akad. Wet.*, **44**, 814 (1941).



INFELD and SCHILD <sup>(12)</sup> were able to show that, as it stands, Dirac's equation is conform-invariant except for its mass term which, therefore, has to be modified.

Fundamental length is not a conform-invariant concept. It follows that it should not appear in a conform-invariant theory. If the field equation we are seeking is of the type of Eq. (1.2), then, the fundamental length ought to have a null exponent, which gives us  $n = \frac{1}{3}$  instead of  $n = 1$ . As multiplication of one of the terms of the Eq. (1.2) by a conform-invariant coefficient will not destroy its conform-invariance, we may try an equation of the form

$$(1.3) \quad \gamma^\mu \partial_\mu \psi + \lambda (\bar{\psi} \psi)^{\frac{1}{3}} \psi = 0.$$

It now remains to show that Eq. (1.3) is indeed invariant under conformal transformations. For this purpose, after giving a convenient  $2 \times 2$  matrix representation of conformal transformations in section 2, we proceed to express Eq. (1.3) in the same matrix formalism in the following section. Section 4 is devoted to a direct proof of the conform-invariance in question and the relation of the new equation to Dirac's equation is discussed in section 5. The last section deals with the Lagrangian formulation of the theory.

In a sequel to this paper it will be shown how the conform-invariant wave equation can be brought within the frame of general relativity.

## 2. - $2 \times 2$ Matrix Representation of Conformal Transformations.

Conformal transformations in space-time have been studied by ROBERTSON <sup>(13)</sup>, SCHOUTEN and HAANTJES <sup>(14)</sup>, HAANTJES <sup>(15)</sup>, INFELD and SCHILD <sup>(16)</sup>, HILL <sup>(17)</sup> and INGRAHAM <sup>(18)</sup> among others. The general group depends on 15 parameters and is generated by

- 1) A constant uniform space-time dilatation (1 par.). Symbol:  $\mathcal{D}$ .
- 2) A translation defined by a constant 4-Vector (4 par.). Symbol:  $\mathcal{T}$ .
- 3) A constant Lorentz transformation (6 par.). Symbol:  $\mathcal{L}$ .
- 4) An inversion (Symbol:  $\mathcal{I}$ ) defined by

$$(2.1) \quad x'^0 = x^0 \tau^{-2}, \quad x'^n = -x^n \tau^{-2}, \quad (n = 1, 2, 3).$$

<sup>(12)</sup> L. INFELD and A. SCHILD: *Phys. Rev.*, **70**, 410 (1946).

<sup>(13)</sup> Cf. Ref. <sup>(7)</sup>.

<sup>(14)</sup> J. A. SCHOUTEN and J. HAANTJES: *Proc. Ned. Akad. Wet.*, **39**, 1063 (1936).

<sup>(15)</sup> J. HAANTJES: *Proc. Ned. Akad. Wet.*, **43**, 1288 (1940).

<sup>(16)</sup> L. INFELD and A. SCHILD: *Phys. Rev.*, **68**, 250 (1945).

<sup>(17)</sup> E. L. HILL: *Phys. Rev.*, **67**, 358 (1945); **68**, 232 (1945) and Ref. <sup>(8)</sup>.

<sup>(18)</sup> R. L. INGRAHAM: *Nuovo Cimento*, **12**, 825 (1954).



Here the interval  $\tau$  is defined by

$$(2.2) \quad \tau^2 = (x^0)^2 - (x^1)^2 - (x^2)^2 - (x^3)^2.$$

The index zero refers to the real time coordinate while the indices 1, 2, 3 refer to spatial coordinates. The total number of parameters is 15 since the inversion  $\mathcal{I}$  does not commute with the translation  $\mathcal{T}$ .

To each position vector  $x^\mu$  ( $\mu = 0, 1, 2, 3$ ) there corresponds a hermitian  $2 \times 2$  matrix

$$(2.3) \quad X = \begin{pmatrix} x^0 + x^3 & x^1 - ix^2 \\ x^1 + ix^2 & x^0 - x^3 \end{pmatrix}$$

in a one-to-one manner. This matrix can also be written as

$$X = x^\mu I_\mu,$$

where the  $I_\mu$  designate the four hermitian units which satisfy the relations

$$(2.4) \quad (I_\mu)^2 = 1, \quad I_1 I_2 = -I_2 I_1 = i I_3, \quad \text{etc.}$$

We assume that indices can be raised and lowered by means of the metric tensor  $\eta_{\mu\nu}$  of special relativity.  $I_0$  is the unit matrix and the hermitian units  $I_n$  which are related to the conventional unit quaternions  $e_n$  by

$$(2.5) \quad I_n = i e_n \quad (n = 1, 2, 3),$$

are represented by the three Pauli matrices. Hence,  $X$  can also be regarded as a special complex quaternion, the norm of which

$$(2.6) \quad \mathcal{N}(X) = |X|^2 = x_\mu x^\mu = \Delta(X),$$

is seen to be equal to the determinant of the matrix  $X$ . In general, any complex  $2 \times 2$  matrix  $\Phi$  can be written as

$$\Phi = \varphi^v I_v$$

and, therefore, corresponds to a complex quaternion. The quaternion conjugates of  $I_v$  are defined by

$$(2.7) \quad \bar{I}_n = -I_n, \quad \bar{I}_0 = I_0,$$

so that the quaternion conjugate of  $\Phi$ , namely

$$\bar{\Phi} = \varphi^v \bar{I}_v$$

corresponds to the adjoint matrix

$$(2.8) \quad \bar{\Phi} = \Phi^{-1} \Lambda(\Phi)$$

where  $\Phi^{-1}$  is the reciprocal matrix of  $\Phi$ . In the case of unimodular matrices we have

$$(2.9) \quad \Lambda(\Phi) = 1 \quad \text{and} \quad \bar{\Phi} = \Phi^{-1}.$$

The hermitian conjugate of  $\Phi$ , that is, the complex conjugate of the transposed matrix, is given by

$$(2.10) \quad \Phi^\dagger = (\varphi^\nu)^* I_\nu,$$

where the star indicates complex conjugation.

The four operations which generate the conformal group are now represented by the following  $2 \times 2$  matrix operations:

$$(2.11) \quad \mathcal{D}: \quad X' = fX = \mathcal{D}X,$$

where  $f$  is a constant real scalar.

$$(2.12) \quad \mathcal{C}: \quad X' = X + A = \mathcal{C}X,$$

where  $A$  is the hermitian matrix corresponding to a constant 4-vector  $A^\mu$ .

$$(2.13) \quad \mathcal{L}: \quad X' = Q^\dagger X Q = \mathcal{L}X,$$

where  $Q$  is a  $2 \times 2$  complex unimodular matrix. (This is just the 2-valued representation of the Lorentz group).

$$(2.14) \quad \mathcal{J}: \quad X' = X^{-1} = \mathcal{J}X.$$

It may be verified that the operations  $\mathcal{D}$ ,  $\mathcal{C}$  and  $\mathcal{L}$  are commutative (with however different values of the parameters) and satisfy the symbolic relations

$$(2.15) \quad \mathcal{D}\mathcal{D} = \mathcal{D}, \quad \mathcal{C}\mathcal{C} = \mathcal{C} \quad \text{and} \quad \mathcal{L}\mathcal{L} = \mathcal{L},$$

which express that each set of transformations enjoys the group property separately.

The inversion  $\mathcal{J}$  commutes with  $\mathcal{D}$  and  $\mathcal{L}$  but not with  $\mathcal{C}$ . It satisfies the equation

$$(2.16) \quad \mathcal{J}\mathcal{J} = I,$$

where  $I$  represents the identity transformation. On the other hand the transformation  $\mathcal{J}\mathcal{C}\mathcal{J}$  can always be expressed as an operation of the form  $\mathcal{L}\mathcal{C}\mathcal{D}\mathcal{J}\mathcal{C}$  where the parameters of each operation are determined in function of the parameters of the original translation, provided the latter is specified by a vector whose length does not vanish. Indicating the parameters of each operation explicitly between square brackets we have in fact.

$$(2.17) \quad \mathcal{J}\mathcal{C}[A]\mathcal{J} = \mathcal{L}[A/|A|]\mathcal{C}[A^{-1}]\mathcal{D}[-|A|^{-2}]\mathcal{J}\mathcal{C}[A^{-1}],$$

where  $A$  is the  $2 \times 2$  matrix of the form (2.3) belonging to the 4-vector  $A_\mu$ ,  $A^{-1}$  its reciprocal,  $\bar{A}$  defined by means of (2.8) and its length  $|A|$  by means of (2.6). Without specification of the parameters, (2.17) can be written symbolically as

$$\mathcal{J}\mathcal{C}\mathcal{J} = \mathcal{L}\mathcal{C}\mathcal{D}\mathcal{J}\mathcal{C},$$

thus, in a form where the inversion occurs once only. It follows that the most general transformation generated by the four operations  $\mathcal{D}$ ,  $\mathcal{C}$ ,  $\mathcal{L}$  and  $\mathcal{J}$  can always be written as

$$(2.18) \quad \mathcal{C} = \mathcal{D}\mathcal{L}\mathcal{C}\mathcal{J}\mathcal{C},$$

again, provided the translations are proper. The identity transformation is obtained as

$$(2.19) \quad I = \lim_{A \rightarrow 0} \mathcal{J}\mathcal{C}[A]\mathcal{J}$$

and can be included in the general form (2.18) by means of (2.17). The  $2 \times 2$  matrix form of the general conformal transformation (2.18) can now be obtained by using the matrix expressions (2.11) to (2.14) for each operation which occurs in (2.18). Thus we obtain

$$(2.20) \quad X' = \mathcal{C}X = \pm fQ^\dagger[(X - A)^{-1} + B]Q,$$

where  $A$  and  $B$  are hermitian,  $Q$  unimodular and  $f$  a positive constant. The identity transformation is obtained as the limit of the expression (2.17) for  $A \rightarrow 0$ .

The differentiation formula

$$(2.21) \quad d(X^{-1}) = -X^{-1}(dX)X^{-1}$$

gives

$$dX' = \mp fQ^\dagger(X - A)^{-1}dX(X - A)^{-1}Q$$

or

$$(2.22) \quad dX' = \mp I^{\dagger} dX I,$$

where

$$(2.23) \quad I = f^{\frac{1}{2}}(X - A)^{-1} Q.$$

Taking the norm of both sides of (2.22) and using (2.6) we obtain

$$(2.24) \quad d\tau' = k d\tau,$$

where

$$(2.25) \quad d\tau = |dX|, \quad d\tau' = |dX'|$$

and

$$k^2 = (I\bar{I})(I\bar{I})^*,$$

so that

$$(2.26) \quad k = f|X - A|^{-2} = f(|X|^2 + |A|^2 - 2A \cdot \bar{X})^{-1},$$

where the scalar  $A \cdot \bar{X}$  stands for

$$(2.27) \quad A \cdot \bar{X} = \frac{1}{2}(A\bar{X} + X\bar{A}),$$

again the bar denoting quaternion conjugation defined by (2.7) or (2.8). It may be verified that (2.27) is just the relativistic scalar product of the four-vectors  $A$  and  $X$ . We also have

$$(2.28) \quad A \cdot \bar{X} = \frac{1}{2} \text{Tr}(A\bar{X}).$$

The relation (2.24) shows that the transformation (2.20) is indeed conformal.

Now, let us introduce the matrix  $\bar{D}$  which corresponds to the gradient operator

$$\partial_{\mu} = \frac{\partial}{\partial x^{\mu}}.$$

With the help of the hermitian units defined by (2.4) and (2.7) we may write

$$\bar{D} = \bar{I}^{\mu} \hat{\gamma}_{\mu}$$

or

$$(2.29) \quad D = I^{\mu} \partial_{\mu} = \sum_{\mu} \bar{I}_{\mu} \partial_{\mu}.$$

The D'Alembertian operator is given by

$$(2.30) \quad \square = D\bar{D} = \partial^\mu \partial_\mu.$$

The following discussion is based on a theorem which may be stated: If we define the matrix  $\Phi$  corresponding to the conformal transformation (6.22) by

$$(2.31) \quad \Phi = \Gamma \bar{\Gamma} \Gamma = \Gamma \Lambda(\Gamma),$$

this matrix satisfies the partial differential equation

$$(2.32) \quad D\Phi = 0,$$

where  $D$  is defined by (2.29). From (2.30) it also follows that all the components of  $\Phi$  satisfy the homogeneous wave equation

$$\square \Phi = 0.$$

A direct proof of the above theorem can be given as follows. Using (2.23) we find

$$(2.33) \quad \Phi = |X - A|^{-2} (X - A)^{-1} f^3 Q.$$

Noting that

$$\Phi' = \Phi f^{-\frac{3}{2}} \bar{Q}$$

satisfies the same equation (2.32) as  $\Phi$ , we have to prove that

$$D\Phi' = 0$$

or

$$(2.34) \quad D\{|X - A|^{-4} (\bar{X} - \bar{A})\} = 0,$$

where we have used the definition (2.8). On the other hand

$$\partial_\nu |X - A|^{-4} = -4[(X - A) \cdot \bar{I}_\nu] |X - A|^{-6},$$

the dot product being defined by (2.27). Using (2.29) and (2.4) we find

$$D|X - A|^{-4} = -4(X - A) |X - A|^{-6}.$$

We also have

$$D(\bar{X} - \bar{A}) = D\bar{I}_\nu x^\nu = 1,$$



so that the left hand side of (2.34) is seen to vanish. This completes the proof of (2.32).

### 3. - $2 \times 2$ Matrix Formulation of Dirac's Equation.

Dirac's equation reads

$$(3.1) \quad (\gamma^\mu \partial_\mu + m)\psi = 0,$$

where  $\psi$  is a complex column matrix and the  $4 \times 4$  matrices  $\gamma^\mu$  satisfy the commutation relations

$$(3.2) \quad \gamma^\mu \gamma^\nu + \gamma^\nu \gamma^\mu = -2\eta^{\mu\nu},$$

where  $\eta^{\mu\nu}$  is the metric tensor of special relativity.

Let  $\Phi$  be a complex  $2 \times 2$  matrix. We define the operation  $\gamma^\mu$  on the matrix  $\Phi$  by the relation

$$(3.3) \quad \gamma^\nu \Phi = i\bar{I}^\nu (\bar{\Phi})^\dagger \mathbf{a}$$

where  $\bar{I}^\nu$  is defined by (2.7),  $\bar{\Phi}$  by (2.8), hermitian conjugacy by (2.10) and the matrix corresponding to a constant unit space vector  $\mathbf{a}^m$  by

$$(3.4) \quad \mathbf{a} = I_\nu \mathbf{a}^m \quad (m = 1, 2, 3).$$

We have

$$(3.5) \quad \mathcal{M}(\mathbf{a}) = -(\mathbf{a})^2 = -1 \quad \text{and} \quad \mathbf{a}^\dagger = \mathbf{a}.$$

From the definition (3.3) it follows that

$$\gamma^\mu (\gamma^\nu \Phi) = i\bar{I}^\mu [i\bar{I}^\nu (\bar{\Phi})^\dagger \mathbf{a}]^\dagger \mathbf{a} = -\bar{I}^\mu I^\nu \Phi.$$

Hence, we obtain

$$\gamma^\mu \gamma^\nu + \gamma^\nu \gamma^\mu = -(\bar{I}^\mu I^\nu + \bar{I}^\nu I^\mu) = -\text{Tr}(\bar{I}^\mu I^\nu),$$

or, using (2.27) and the orthogonality of the hermitian units we find (3.2). In particular we can choose

$$(3.6) \quad \mathbf{a} = I_3 = i\mathbf{e}_3,$$

where  $\mathbf{e}_3$  is the third quaternion unit defined by (2.5), and obtain the following realization of the operators  $\gamma^\nu$  <sup>(19)</sup>

$$(3.7) \quad \gamma^\nu \Phi = -\bar{I}^\nu (\bar{\Phi})^\dagger \mathbf{e}_3.$$

(19) F. GÜRSEY: *Phys. Rev.*, **77**, 844 (1950).

Now, taking as the wave function the  $2 \times 2$  complex matrix  $\Phi$  with 4 components instead of the column matrix  $\psi$  with 4 components, and remembering (3.7) we can write, instead of the  $4 \times 4$  matrix equation (3.1), the following  $2 \times 2$  matrix equation

$$-\bar{I}^\nu \partial_\nu (\bar{\Phi})^\dagger \mathbf{e}_3 + m\Phi = 0$$

or

$$I^\nu \partial_\nu \Phi + m(\bar{\Phi})^\dagger \mathbf{e}_3 = 0.$$

Using the  $2 \times 2$  matrix (2.29) corresponding to the gradient operator, we obtain finally

$$(3.8) \quad D\Phi + m(\bar{\Phi})^\dagger \mathbf{e}_3 = 0.$$

Written in quaternion notation this is equivalent to the quaternion form of Dirac's equation given previously by the author<sup>(20)</sup>.

This  $2 \times 2$  matrix equation is entirely equivalent to the standard equation (3.1). To each column matrix  $\psi$  there corresponds in a unique way a  $2 \times 2$  matrix with elements

$$(3.9) \quad \Psi = \begin{pmatrix} \psi_1 + \psi_3 & -\psi_2^* + \psi_4^* \\ \psi_2 + \psi_4 & \psi_1^* - \psi_3^* \end{pmatrix}.$$

Conversely, to each complex  $2 \times 2$  matrix  $\Psi$  there corresponds a 4-column  $\psi$  such that (3.9) is satisfied.

To the row-matrix  $\psi$  corresponds the transposed of the matrix (3.9).

Further, if  $\Omega$  is a hermitian operator and  $\omega$  is defined by

$$(3.10) \quad \omega = \psi^* \Omega \psi,$$

we have

$$(3.11) \quad \omega = \text{R}(\Psi^\dagger \cdot \Omega' \Psi) = \frac{1}{2} \text{R}(\text{Tr } \Psi^\dagger \Omega' \Psi),$$

where R denotes the real part of the complex scalar quantity in brackets, the dot product is that defined by (2.27) and  $\Omega'$  is the same operator  $\Omega$  which appears in (3.10), but in a  $2 \times 2$  matrix representation.  $\Psi$  is the matrix derived from  $\psi$  through (3.9).

The adjoint row matrix is defined by

$$\bar{\psi} = \psi^\dagger \gamma_4,$$

<sup>(20)</sup> Cf. Ref. <sup>(19)</sup> and F. GÜRSEY: *Ph. D. Thesis*, University of London (1950) (unpublished).

so that  $\bar{\psi}\psi$  is a relativistic invariant. The  $2 \times 2$  matrix form of  $\bar{\psi}$  is given by the transposed of the matrix which represents the column  $\bar{\psi}$ , namely

$$(3.12) \quad \bar{\Psi} = \begin{pmatrix} \psi_1^* - \psi_3^* & \psi_2^* - \psi_4^* \\ -\psi_2 - \psi_4 & \psi_1 + \psi_3 \end{pmatrix}$$

which is seen to be the adjoint of the matrix  $\Psi$ . Therefore, to the adjoint row matrix  $\bar{\psi}$  corresponds the adjoint of the matrix which represents the column matrix  $\psi$ . We have

$$(3.13) \quad \bar{\Psi}\Psi = \Psi\bar{\Psi} = \Delta(\Psi).$$

It can also be shown that if  $\psi$  and  $\varphi$  are column matrices represented by the  $2 \times 2$  matrices  $\Psi$  and  $\Phi$ , we have

$$(3.14) \quad R(\bar{\psi} \cdot \varphi) = \frac{1}{2} R(\text{Tr } \bar{\Psi}\Phi).$$

In particular, if  $\Omega$  is a hermitian operator,

$$(3.15) \quad \bar{\psi}\Omega\varphi = \frac{1}{2} R(\text{Tr } \bar{\Psi}\Omega'\Phi).$$

Thus we have <sup>(21)</sup>

$$(3.16) \quad \bar{\psi}\psi = \frac{1}{2} R(\text{Tr } \bar{\Psi}\Psi) = R(\bar{\Psi}\Psi)$$

and

$$(3.17) \quad \bar{\psi}\gamma_5\psi = \frac{1}{2} R(\text{Tr } \bar{\Psi}i\Psi) = \text{Im}(\bar{\Psi}\Psi),$$

where  $\text{Im}$  stands for «imaginary part».

Using (3.16) we are now in a position to write the non-linear eq. (1.3) in  $2 \times 2$  matrix form. Defining  $\Psi$  by (3.9) we obtain

$$(3.18) \quad D\Psi + \lambda(R\bar{\Psi}\Psi)^{\frac{1}{2}}(\bar{\Psi})^{\dagger}e_3 = 0$$

exactly in the same way as (3.8) was derived from (3.1).

#### 4. - Conformal Invariance of the New Wave Equation.

In order to show the conformal invariance of Eq. (3.18) we need the transformation formula for the matrix  $D$  (2.29) which represents the four-dimensional gradient operator. The components of  $D$ , namely  $\partial_\mu$  transform contra-

<sup>(21)</sup> For the details of this and similar statements contained in this section the reader is referred to Ref. <sup>(20)</sup> or to forthcoming papers in the *Rev. Fac. Sc. de l'Univ. d'Istanbul*, Série A.

gradiently to the component  $dx^\mu$  of the displacement vector  $dX$ . As the scalar product

$$dx^\mu \partial_\mu = \frac{1}{2} \text{Tr} (\bar{I}^\nu I_\nu) dx^\mu \partial_\nu = \frac{1}{2} \text{Tr} (d\bar{X} D) = d\bar{X} \cdot D$$

is to be invariant, it is seen that  $D$  transforms like the reciprocal of  $d\bar{X}$ . Since the transformation formula for  $(d\bar{X})^{-1}$  is

$$(d\bar{X}')^{-1} = (\bar{I}^\dagger)^{-1} (d\bar{X})^{-1} (\bar{I})^{-1}$$

if  $dX$  transforms according to (2.22), then, the transformation law for  $D$  must be

$$(4.1) \quad D' = (\bar{I}^\dagger)^{-1} I^\mu (\bar{I})^{-1} \partial_\mu .$$

Using the matrix  $\Phi$  defined by (2.31) we can also write (4.1) in the form

$$D' = (I\bar{I})^{-2} (\bar{I}^\dagger)^{-1} I^\mu \Phi \partial_\mu .$$

Now, the theorem expressed by (2.32) gives immediately,

$$(4.2) \quad D' = (I\bar{I})^{-2} (\bar{I}^\dagger)^{-1} D \Phi .$$

On the other hand we have

$$(4.3) \quad \Phi \bar{\Phi} = (I\bar{I})^3 ,$$

and, since according to (2.23)  $I\bar{I}$  is real, we can also write

$$(I\bar{I})^{-1} (\bar{I}^\dagger)^{-1} = (I^\dagger \bar{I}^\dagger)^{-1} (\bar{I}^\dagger)^{-1} = (\bar{\Phi}^\dagger)^{-1} ,$$

so that the final transformation law for  $D$  is

$$(4.4) \quad D' = (\Phi \bar{\Phi})^{-\frac{1}{2}} (\bar{\Phi}^\dagger)^{-1} D \Phi .$$

We have to show that if the wave equation holds true in the dashed coordinate system, that is, if we have

$$(4.5) \quad D' \Psi' + \lambda (\mathbf{R} \Psi' \bar{\Psi}')^{\frac{1}{2}} (\bar{\Psi}')^\dagger \mathbf{e}_3 = 0 ,$$

it can be restored to the same form in the non-dashed system by means of the conformal transformation (2.20). Indeed, insertion of (4.4) into (4.5) gives

$$(4.6) \quad (\Phi \bar{\Phi})^{-\frac{1}{2}} (\bar{\Phi}^\dagger)^{-1} D (\Phi \Psi') + \lambda (\mathbf{R} \Psi' \bar{\Psi}')^{\frac{1}{2}} (\bar{\Psi}')^\dagger \mathbf{e}_3 = 0 .$$

If we choose

$$(4.7) \quad \Psi' = \Phi^{-1}\Psi$$

as the transformation law for the wave function, we get

$$(4.8) \quad (\bar{\Psi}')^\dagger = (\bar{\Phi}^\dagger)^{-1}\bar{\Psi}^\dagger$$

and

$$(4.9) \quad R\Psi'\bar{\Psi}' = (\Phi\bar{\Phi})^{-1}R\Psi\bar{\Psi}.$$

When the remaining dashed functions in (4.6) are expressed in terms of the undashed functions by means of the above relations we obtain the original wave equation (3.18). The constant  $\lambda$  which has the same value in both systems is taken as a conform-invariant scalar.

It can also be shown that the normalization condition in the unquantized theory, i. e.

$$(4.10) \quad \int_{\Sigma} j^\mu d\sigma_\mu = 1,$$

or, the total charge in the quantized theory, i.e.

$$(4.11) \quad Q = e \int_{\Sigma} j^\mu d\sigma_\mu,$$

taken over any space-like surface  $\Sigma$  is conform-invariant. Here  $j^\mu$  is the probability density 4-vector and  $d\sigma_\mu$  the surface element directed along the normal to the surface. If  $J$  and  $d\Sigma$  denote the  $2 \times 2$  hermitian matrices corresponding to  $j^\mu$  and  $d\sigma^\mu$ , we have

$$(4.12) \quad j^\mu d\sigma_\mu = \frac{1}{2} \text{Tr} (\bar{J} d\Sigma) = \bar{J} \cdot d\Sigma,$$

where

$$(4.13) \quad J = \Psi\Psi^\dagger.$$

In a conformal transformation,  $d\Sigma$  transforms according to

$$(4.14) \quad d\Sigma' = \Phi^\dagger d\Sigma \Phi,$$

and the probability density 4-vector obeys the law

$$(4.15) \quad \bar{J}' = \Phi^{-1} \bar{J} (\Phi^\dagger)^{-1},$$



so that the scalar product

$$\bar{J}' \cdot d\Sigma' = \bar{J} \cdot d\Sigma$$

and, hence, the total charge remains invariant. This is a reasonable result since we do not expect the charge of a particle to change in an accelerated frame.

## 5. — Connection with Dirac's Equation.

Consider a plane wave solution of the Dirac equation

$$(5.1) \quad (\gamma^\mu \partial_\mu + m)\psi = 0$$

normalized in a volume  $a^3$  so that

$$(5.2) \quad \bar{\psi}\psi = a^{-3}.$$

Here  $a$  denotes a relativistically invariant length. Inserting this solution in the conform equation

$$(5.3) \quad \gamma^\mu \partial_\mu \psi + \lambda(\bar{\psi}\psi)^{\frac{1}{3}}\psi = 0,$$

we see that it satisfies

$$(\gamma^\mu \partial_\mu + \lambda a^{-1})\psi = 0.$$

That is, every normalized plane wave solution of Dirac's equation corresponding to the mass constant  $m$  satisfies the conform-invariant equation with the constant  $\lambda$ , provided that

$$(5.4) \quad \lambda a^{-1} = m.$$

In other words, if we hold  $\lambda$  constant and vary  $a$ , we obtain particular solutions of (5.3) which correspond to different mass values of Dirac's equation (5.1). This shows how we can get plane-wave solutions of (5.3) which are connected to Dirac plane waves with different rest-mass values.

In order to obtain new particular solutions of (5.3), all we have to do is to apply a conformal transformation to a particular plane wave solution. Thus, the column matrix  $\psi'$  which corresponds to the matrix

$$(5.5) \quad \Psi' = \Phi^{-1}(X)\Psi(X)$$

is the solution of the dashed equation if  $X$  is expressed as a function of  $X'$ .

To give an example, let the conformal transformation reduce to the inversion (2.14) together with a negative uniform dilatation (2.11). We have

$$(5.6) \quad X' = -l^2 X^{-1}$$

and

$$dX' = l^2 X^{-1}(dX)X^{-1}.$$

The surface element  $d\Sigma$  transforms according to

$$d\Sigma' = \Phi^\dagger(d\Sigma)\Phi,$$

where

$$\Phi(X) = l^3(X\bar{X}X)^{-1}.$$

From (5.6) we derive

$$X = -l^2(X')^{-1},$$

so that in terms of  $X'$

$$\Phi = l^{-3}X'\bar{X}'X'.$$

It follows that if  $\Psi(X)$  is a plane wave solution of Dirac's equation the function

$$\Psi' = \Phi^{-1}\Psi = -l^3(X'\bar{X}'X')^{-1}\Psi(-l^2X'^{-1})$$

is a particular solution of the conform-invariant equation (4.5). We can now drop the dashes and write the particular solution of (3.18) as

$$(5.7) \quad \Psi_1 = -l^3(X\bar{X}X)^{-1}\Psi(-l^2X^{-1}).$$

This illustrates how conform-invariance can be used to derive new particular solutions of the wave equation from known solutions.

## 6. - Lagrangian Considerations.

Having shown that the surmised equation (1.3) is indeed conform-invariant, we may ask whether there are other conform-invariant equations which are linear with respect to the derivatives of a spinor wave function. The most general procedure for finding such an equation would be to start from a conform invariant action integral defined by

$$(6.1) \quad I = \int \mathcal{L} d\omega,$$

where  $\mathcal{L}$  is the Lagrangian density and  $d\omega$  the 4-dimensional volume element. In a conformal transformation,  $dX$  and the element  $d\Sigma$  of a 3-dimensional surface transform respectively according to the laws

$$dX' = I^+(dX)I^-$$

and

$$d\Sigma' = \Phi^+(d\Sigma)\Phi$$

where  $\Phi$  is given by (2.31). Hence, the 4-dimensional volume element

$$d\omega = d\bar{X} \cdot d\Sigma = \frac{1}{2} \text{Tr} (d\bar{X} d\Sigma)$$

obeys the transformation law

$$(6.2) \quad d\omega' = k^4 d\omega,$$

where

$$(6.3) \quad k = I\bar{I} = (\Phi\bar{\Phi})^{\frac{1}{2}}.$$

Therefore, to ensure the conform-invariance of the action integral (6.1), the Lagrangian density must transform according to the law

$$(6.4) \quad \mathcal{L}' = k^{-4} \mathcal{L} = (\Phi\bar{\Phi})^{-\frac{4}{3}} \mathcal{L}.$$

Furthermore,  $\mathcal{L}$  must be relativistic invariant. Assume  $\mathcal{L}$  to be of the form

$$(6.5) \quad \mathcal{L} = \mathcal{L}_1 + \mathcal{L}_2,$$

where  $\mathcal{L}_1$  depends on the spinor wave function  $\Psi$  only, and  $\mathcal{L}_2$  depends on  $\Psi$ ,  $\partial\Psi$  and is linear with respect to the derivatives of  $\Psi$ . Since the transformation law for  $\Psi$  is

$$(6.6) \quad \Psi' = \Phi^{-1}\Psi,$$

it follows that the expression

$$(6.7) \quad \mathcal{L}_1 = \alpha(\bar{\Psi}\Psi)^{\frac{4}{3}}$$

transforms according to

$$\mathcal{L}'_1 = (\Phi\bar{\Phi})^{-\frac{4}{3}} \mathcal{L}_1.$$

Here  $\alpha$  is a conform-invariant constant. We also have

$$R\Psi'\bar{\Psi}' = (\Phi\bar{\Phi})^{-1}R\Psi\bar{\Psi}$$

and

$$\text{Im } \Psi' \bar{\Psi}' = (\Phi \bar{\Phi})^{-1} \text{Im } \Psi \bar{\Psi}.$$

On the other hand, in virtue of (3.16) and (3.17) we have

$$\omega_1 = \bar{\psi} \psi = \text{R} \Psi \bar{\Psi}$$

and

$$\omega_2 = \bar{\psi} \gamma_5 \psi = \text{Im } \Psi \bar{\Psi},$$

so that  $\omega_1$  is a scalar and  $\omega_2$  pseudoscalar. A new scalar can then be defined by taking the absolute value of  $\omega_2$ . If we assume that  $\mathcal{L}_1$  involves the scalar  $\omega_1$  only we find

$$\mathcal{L}_1 = \alpha \omega_1^{\frac{1}{2}} = \alpha (\psi \bar{\psi})^{\frac{1}{2}}.$$

To obtain the invariant  $\mathcal{L}_2$  which, under a conformal transformation, obeys the law

$$\mathcal{L}_2' = (\Phi \bar{\Phi})^{-1} \mathcal{L}_2$$

we form the matrix

$$D' \Psi' = (\Phi \bar{\Phi})^{-\frac{1}{2}} (\bar{\Phi}^\dagger)^{-1} D \Psi.$$

Here  $D$  is the gradient operator in matrix form.  $D$  and  $\Psi$  transform respectively according to (4.4) and (4.7). From (4.7) we also deduce that

$$\Psi'^\dagger = \Psi^\dagger (\Phi^\dagger)^{-1}.$$

Using the relation

$$(\Phi^\dagger)^{-1} (\bar{\Phi}^\dagger)^{-1} = (\Phi \bar{\Phi})^{-1},$$

we find

$$(6.8) \quad \Psi'^\dagger D' \Psi' = (\Phi \bar{\Phi})^{-\frac{1}{2}} \Psi^\dagger D \Psi.$$

Multiplying both sides by the matrix  $\mathbf{e}_3 = -iI_3$  and taking the real part of the trace of this matrix, we see that the real scalar

$$\mathcal{L}_2 = \frac{1}{2} \text{R Tr } (\Psi^\dagger D \Psi \mathbf{e}_3)$$

also has the required transformation property. As our Lagrangian (6.5) we can therefore choose.

$$\mathcal{L} = \frac{1}{2} \text{R Tr } (\Psi^\dagger D \Psi \mathbf{e}_3) + \alpha (\text{R} \Psi \bar{\Psi})^{\frac{1}{2}}.$$

In 4-spinor language, this reads

$$(6.9) \quad \mathcal{L} = \frac{1}{2}(\bar{\psi}\gamma^\mu\partial_\mu\psi - \partial_\mu\bar{\psi}\gamma^\mu\psi) + \alpha(\bar{\psi}\psi)^{\frac{4}{3}}.$$

By varying  $\psi$  and  $\bar{\psi}$  separately in this Lagrangian, we obtain the conform-invariant equation

$$\gamma^\mu\partial_\mu\psi + \frac{4}{3}\alpha(\bar{\psi}\psi)^{\frac{1}{3}}\psi = 0,$$

which is equivalent to (1.3) and the adjoint equation.

If the Lagrangian is also assumed to depend on the absolute value of the pseudoscalar  $\omega_2$ , we obtain Lagrangians more general than (6.9), which lead to modified equations of the Dirac-Heisenberg type. One such equation which derives from a Lagrangian depending only on  $\sqrt{\omega_1^2 + \omega_2^2}$  and which remains invariant against the transformation

$$(6.10) \quad \psi \rightarrow \exp[\gamma_5\theta]\psi$$

is encountered in general relativity and will be dealt with in the sequel to the present paper.

---

#### RIASSUNTO (\*)

Come possibile punto di partenza per una descrizione unitaria delle particelle, si propone una nuova equazione spinoriale d'onda, simile alla generalizzazione non lineare dell'equazione di Dirac data da HEISENBERG, ma dotata inoltre di invarianza rispetto alle trasformazioni conformi. Si sviluppa un formalismo basato sull'impiego di matrici  $2 \times 2$  onde ottenere un'espressione sintetica sia per le trasformazioni conformi che per le equazioni spinoriali del tipo di quelle di Dirac. Si dà poi per mezzo di detto formalismo una prova diretta dell'invarianza della nuova equazione rispetto alle trasformazioni conformi e si deriva una legge esplicita di trasformazione per la funzione d'onda. Si mostra inoltre che l'equazione non quantizzata esprime la propagazione di onde piane corrispondenti a particelle di differenti masse a riposo.

---

(\*) Traduzione a cura della Redazione.



## Solid Scintillators for Beta Ray Spectrometry.

A. BISI, E. GERMAGNOLI (\*) and L. ZAPPA

*Istituto di Fisica Sperimentale del Politecnico - Milano*

*(\*) Laboratori CISE - Milano*

(ricevuto il 15 Febbraio 1956)

**Summary.** — A beta ray spectrometer and a  $\beta$ - $\gamma$  coincidence spectrometer using anthracene crystals are described. The results of some measurements concerning simple and complex decays are given. In particular the decay of  $^{170}\text{Tm}$  has been reinvestigated.

### 1. — Introduction.

High  $Z$  inorganic crystals (e.g.  $\text{NaI}(\text{Tl})$ ), optically coupled to photomultipliers, have been extensively used in the last years as detectors of X- and  $\gamma$ -quanta. Their high efficiency and the proportionality, in a wide energy range, between the amplitude of light pulses and the energy of the absorbed radiations made it possible to build easily some kinds of satisfactory spectrometers for X- and  $\gamma$ -rays. With the help of coincidence techniques, such crystals have been found useful in investigating decay schemes of radioisotopes and analyzing  $\gamma$ -spectra due to nuclear reactions.

Their resolving power is of course rather low, but this disadvantage is often overcompensated by their peculiar high efficiency, which can be conclusive with regard to the practical possibility of carrying out a coincidence measurement. From this point of view the only serious inconvenience is that pulses emitted from inorganic crystals last one microsecond or about; an important limitation to their use in very fast coincidence arrangements will arise from this fact. There is no limitation of this kind with organic scintillators (anthracene, stilbene); their efficiency for  $\gamma$ -rays is not so high but on the other hand they give out very fast pulses.

What seems worthwhile to point out in this paper is however the usefulness of organic scintillators in revealing  $\beta$ -particles; many descriptions of expe-

rimental arrangements involving anthracene or stilbene crystals can be found in the literature, but it has not been adequately pointed out so far that they can be used in  $\beta$ -ray spectrometry as successfully as inorganic crystals are used for the analysis of  $\gamma$ -spectra. In particular the high fluorescent efficiency and the linearity of anthracene crystals for  $\beta$ -rays, make the  $\beta$  scintillation counter exceedingly useful in  $\beta$ - $\gamma$  coincidence arrangements as a complementary device for a magnetic spectrometer. It is in fact possible to determine quickly, with an often satisfactory resolution, the features of a  $\beta$ -spectrum, with the help of a multichannel pulse analyzer. Examples of such use of anthracene crystals will be given in the following sections.

## 2. — Experimental Arrangement.

For the  $\beta$ -ray spectrometer, a cylindrical anthracene crystal (2.5 cm in diameter and 2.5 cm high) and a Dumont 6292 photomultiplier were used. The flat surfaces of the crystal were smoothed with emery paper and later on the whole crystal was cleaned with benzene. Finally the crystal was introduced into a cylindrical Al container, at one end of which a thin optical glass window had been sealed. The optical coupling was obtained with Silicon DC 200 centistokes. As usual, MgO powder was put in between the walls of the container and the crystal to act as a light reflector. The surface of the anthracene crystal, which was opposite to the glass window, was covered with a thin Al sheet ( $\sim 0.2 \text{ mg cm}^{-2}$ ).

With the crystal assembled in this way a set of preliminary measurements was performed using thin  $\beta$  samples of  $^{32}\text{P}$ ,  $^{185}\text{W}$ ,  $^{60}\text{Co}$ , and  $^{137}\text{Cs}$ . The shapes of Kurie plots obtained with the first three samples and the electron line arising from  $K$  and  $L$  internal conversion of 662 keV  $\gamma$ -rays emitted from  $^{137}\text{Ba}$  were examined in different experimental conditions, in order to find out the most suitable geometrical arrangement.

A good agreement between the obtained values for the end points of Kurie plots and the energies associated to the  $\beta$  transitions was obtained in these measurements.

As regards the general trend of the Kurie plots, it was noticed a distinct deviation from a straight line at energies less than about one half of the maximum energy. As it is well known this deviation is due to backscattering effects, i.e. to the fact that a large fraction of  $\beta$ -rays entering the flat anthracene surface are scattered out of the crystal before being stopped. In order to minimize the backscattering effects, the technique of the hollow crystal spectrometer <sup>(1)</sup> was adopted.

<sup>(1)</sup> P. R. BELL in K. SIEGBAHN: *Beta and Gamma Ray Spectroscopy* (Amsterdam 1955), p. 136.

The experimental arrangement which was used for the undermentioned measurements is schematically given in Fig. 1. In this arrangement the dimensions of the source, of the hole within the crystal and the source-detector distance are determined in view of minimizing the scattering of the crystal and the air and of obtaining a high transmission.

Dimensions given in Fig. 1 are not too critical; the sample holder can, to some extent, be brought nearer to the surface of the crystal in order to get higher counting rates, without serious distortion in Kurie plots. That is the case, for instance, in coincidence measurements where the transmission must be kept as high as possible in order to reduce random coincidences when weak sources have to be used.

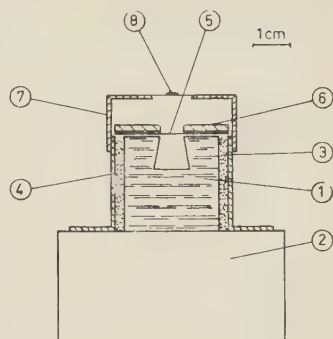


Fig. 1. - Experimental arrangement for the  $\beta$  spectrometer: 1. anthracene hollow crystal spectrometer; 2. phototube; 3. MgO reflector; 4. Al container; 5. thin Al foil; 6. brass collimator; 7. adjustable sample holder; 8.  $\beta$  source.

### 3. - Analysis of Simple $\beta$ Spectra.

Fig. 2 shows some  $\beta$ -spectra which were obtained with the above-described spectrometer connected to a conventional amplifying chain; pulses were analyzed by means of a twenty channel fast analyzer <sup>(2)</sup>. For these measurements care was taken to use only  $\beta$  emitters having simple and allowed spectra. Actually only  $^{185}\text{W}$  shows two groups of  $\beta$ -rays, which have almost the same maximum energy.

These results check the linear response of anthracene crystal and

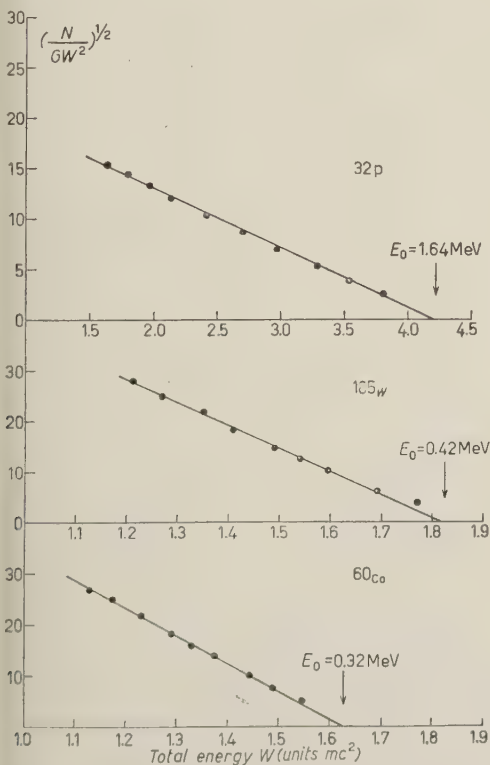


Fig. 2. - Kurie plots of simple  $\beta$  spectra.

<sup>(2)</sup> E. GATTI: *Nuovo Cimento*, **11**, 153 (1954).

provide a valuable indication as to the accuracy in the determination of energies involved in  $\beta$  transitions. Only the linear behaviour of the Kurie plot of

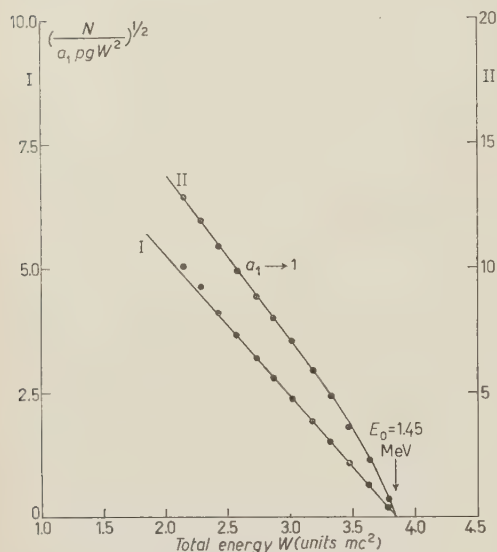


Fig. 3. — Conventional and corrected Fermi plot for the  $\beta$  spectrum of  $^{89}\text{Sr}$ . For a comparison with the results obtained with a magnetic spectrometer see A. BISI, S. TERRANI and L. ZAPPA: *Nuovo Cimento*, **2**, 1297 (1955).

$^{60}\text{Co}$  in the low energy range is scarcely significant because it results from a compensation of back scattering effects and of air scattering.

In Fig. 3 the results which have been obtained with a source of  $^{89}\text{Sr}$  are summarized. It is interesting to note that the  $\beta$ -spectrum of  $^{89}\text{Sr}$  has a first forbidden shape ( $\Delta I = 2$ ; yes); curve I shows the uncorrected Kurie plot and curve II has been deduced from I after correction for the shape factor. It is clear that the response of the  $\beta$ -ray spectrometer is sensitive to the type of spectrum and that a satisfactory accuracy in the measurement of  $\beta$  transition energy can be achieved also with forbidden spectra. In Table I the measured values of end points of  $\beta$ -spectra are collected and compared with the most accurate available determinations.

TABLE I.

$\beta$ emitter	End point (MeV) <sup>(3)</sup>	Present value	Percent difference
$^{32}\text{P}$	1.708	1.64	4
$^{185}\text{W}$	0.429	0.42	2
$^{60}\text{Co}$	0.310	0.32	3
$^{89}\text{Sr}$	1.464	1.45	1

#### 4. — Measurements with Plastics.

Some measurements were carried out with a plastic scintillator (Pamelen) <sup>(4)</sup> for the purpose of investigating whether it is suitable to use plastics in  $\beta$  spectrometry.

<sup>(3)</sup> Data taken from R. W. KING: *Rev. Mod. Phys.*, **26**, 327 (1954).

<sup>(4)</sup> Supplied by Isotope Development Limited (London).

The plastic scintillators have the advantage of being inexpensive and easily machinable.

The response linearity of the mentioned plastic was studied by plotting, versus energies the heights of pulses belonging to the Compton edges of the  $\gamma$  lines indicated in Table II. In the whole investigated energy interval, the pulse

TABLE II.

Source	$\gamma$ ray energy (MeV) <sup>(5)</sup>	Energy corresponding to Compton edge
<sup>51</sup> Cr	0.32	0.18
<sup>22</sup> Na	0.51	0.34
<sup>137</sup> Cs	0.66	0.48
<sup>56</sup> Mn	0.82	0.62
<sup>65</sup> Zn	1.12	0.91
<sup>22</sup> Na	1.28	1.07
<sup>208</sup> Tl (ThC'')	2.61	2.38

height was a strictly linear function of the maximum energy of Compton electrons, as it is shown in Fig. 4.

A cylindrical plastic, 3.7 cm in diameter and 2 cm high, was then shaped similar to the anthracene crystal (see Fig. 1).  $\beta$ -spectra and conversion electron

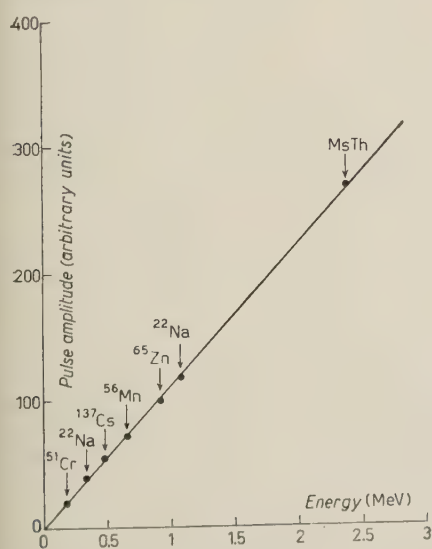


Fig. 4. — Linearity of the energy response of Pamelon.

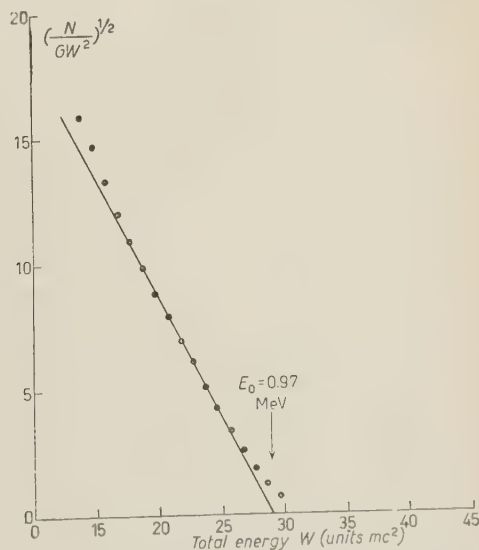


Fig. 5. — Kurie plot of the  $\beta^-$  spectrum of <sup>170</sup>Tm obtained with a Pamelon plastic.

<sup>(5)</sup> Data taken from J. M. HOLLANDER, I. PERLMAN and G. T. SEABORG: *Rev. Mod. Phys.*, **25**, 469 (1953).



lines were inspected. The results obtained suggest that the anthracene is preferable to plastic scintillators in view of its better resolution. Actually the relative half width of  $K$  conversion line from  $^{137}\text{Cs}$ , obtained with an anthracene crystal and a plastic scintillator were  $10 \div 11\%$  and  $15\%$  respectively.

A  $\beta$ -spectrum with a thin source of  $^{170}\text{Tm}$  is given in Fig. 5; the effect of the rather low resolving power can be seen from the deviation of the Kurie plot from a straight line near the end point.

## 5. - Use of $\beta$ Crystal Spectrometer in a Coincidence Arrangement.

In order to find out whether the hollow crystal spectrometer can be advantageously adopted in a coincidence arrangement,  $\beta$ - $\gamma$  coincidence experiments were carried out in well known and simple cases ( $^{137}\text{Ba}$  and  $^{170}\text{Tm}$ ).

For this purpose a NaI(Tl) scintillation counter was used as a detector of X- and  $\gamma$ -rays and placed behind the active sample. The distance between sample and crystal was taken as small as possible in order to give a large solid angle for the detection of the  $\gamma$ -rays. Only the pulses belonging to photopeaks at the output of the  $\gamma$  spectrometer were used to trigger the coincidence circuit <sup>(6)</sup>.

5.1. *K conversion electrons from isomeric level of  $^{137}\text{Ba}$ .* - A source of  $^{137}\text{Cs}$  was placed between the two spectrometers. By triggering the coincidence circuit with the pulses due to the  $K$  X-rays characteristic of Ba arising from  $K$  internal conversion of the 662 keV  $\gamma$ -rays, the peak due to the  $K$  conversion electrons could be easily revealed. With the  $\beta$  spectrometer alone, the peak shown in Fig. 6

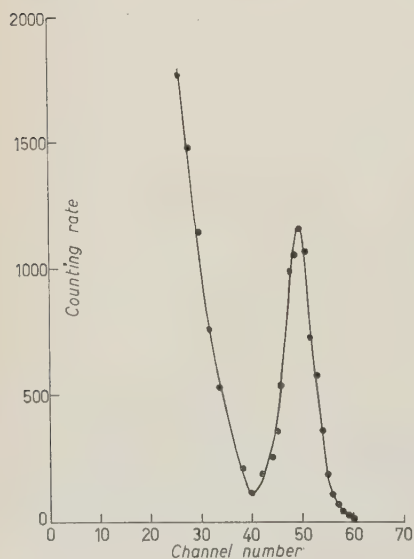


Fig. 6. - Spectrum of  $K$  conversion electrons of  $^{137}\text{Ba}$ : not in coincidence.

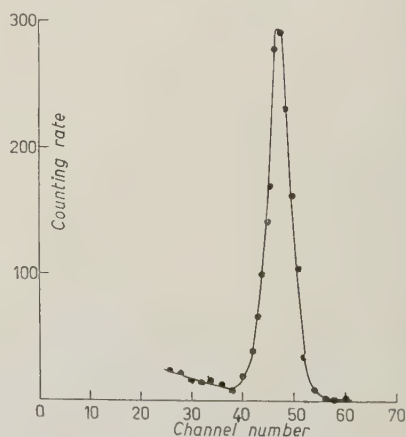


Fig. 7. - Spectrum of  $K$  conversion electrons of  $^{137}\text{Ba}$ : coincidence measurement.

<sup>(6)</sup> E. GERMAGNOLI, A. MALVICINI and L. ZAPPA: *Nuovo Cimento*, **10**, 1388 (1953).

was obtained. As it can be seen from Fig. 7, the pulse height distribution appears to be symmetric in a coincidence measurement, as both the continuous  $\beta$  spectrum from  $^{137}\text{Cs}$  and the  $L$  and  $M$  conversion electrons are obviously absent.

In this way the energy resolution of the  $\beta$  spectrometer was clearly put in evidence. The relative width of the peak at half maximum has the previously stated value.

**5.2. Decay of  $^{170}\text{Tm}$ .** — The decay of  $^{170}\text{Tm}$  is well known (7) and its decay scheme is given in Fig. 8. The  $\gamma$ - and X-ray spectrum was obtained by means of the NaI(Tl) crystal spectrometer and is shown in Fig. 9. If the areas under the two peaks are compared, the  $K$  internal conversion coefficient  $\alpha_K$  for the 84 keV  $\gamma$  transition can be deduced. We have, in fact:

$$(1) \quad I_K = \omega_K \varepsilon_K \alpha_K I$$

$$(2) \quad I_\gamma = \varepsilon_\gamma I,$$

where

$I_K$  and  $I_\gamma$  are the measured intensities of  $K$  X- and  $\gamma$ -rays;

$\varepsilon_K$  and  $\varepsilon_\gamma$  are the efficiencies of the detector for  $K$  X- and  $\gamma$ -radiations;

$I$  is the number of  $\gamma$ -rays emitted from the source;

$\omega_K$  is the fluorescence yield of the  $K$  shell in Yb.

From (1) and (2) we obtain:

$$\alpha_K = \frac{\varepsilon_\gamma}{\omega_K \varepsilon_K} \frac{I_K}{I_\gamma}$$

$\varepsilon_\gamma$  and  $\varepsilon_K$  are very closely the same and therefore the efficiencies could be taken into account by making a correction of a few percent to the experimental values  $I_K$  and  $I_\gamma$ .

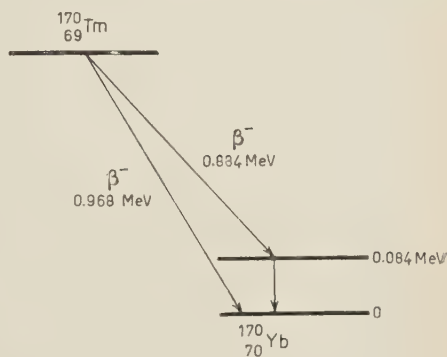


Fig. 8. — Decay scheme of  $^{170}\text{Tm}$ .

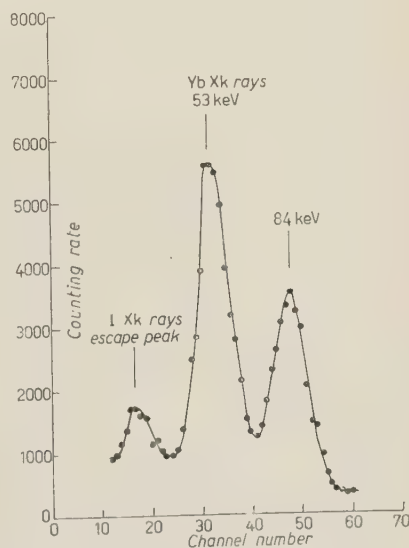


Fig. 9. — Spectrum of  $K$  X- and  $\gamma$ -rays emitted from  $^{170}\text{Tm}$ .

(7) R. W. KING: *Rev. Mod. Phys.*, **26**, 327 (1954).

By taking  $\omega_K = 0.93$  (\*) and after corrections for the escape peaks we found:

$$\alpha_K = 1.69 \pm 0.02.$$

With regard to the total  $\beta$ -spectrum, a Kurie plot is shown in Fig. 10. The end point occurs at  $950 \pm 5$  keV.

By triggering the coincidence circuit with the pulses belonging to the peak at 84 keV, a  $\beta$  spectrum was put into evidence, with its end point at  $867 \pm 5$  keV. This is also shown in Fig. 10. The difference between the end points of the two spectra is:

$$\Delta E = 83 \pm 7 \text{ keV}.$$

This value is in good agreement with the value obtained for the energy of the  $\gamma$ -ray. The same result was found by triggering the coincidence circuit with the pulses belonging to the peak of  $K$  X-rays of Yb.

In order to deduce quantitative informations from coincidence measurements, it is remarked that the  $K$  conversion coefficient can also be obtained in the following way: if  $I_{\beta K}$  and  $I_{\beta \gamma}$  are the

Fig. 10. - Kurie plots of  $\beta$  spectra of  $^{170}\text{Tm}$ : total spectrum and  $\beta$  spectrum in coincidence with  $K$  X- or  $\gamma$ -rays.

total numbers of  $\beta$ -particles which are coincident with the  $K$  X- and with the  $\gamma$ -rays, we have:

$$(3) \quad I_{\beta K} = \varepsilon_{\beta} \omega_K \varepsilon_K \alpha_K \Gamma$$

$$(4) \quad I_{\beta \gamma} = \varepsilon_{\beta} \varepsilon_{\gamma} \Gamma,$$

where  $\varepsilon_{\beta}$  is the efficiency of the anthracene crystal for  $^{170}\text{Tm}$   $\beta$ -rays. Consequently  $\alpha_K$  is also given by:

$$\alpha_K = \frac{\varepsilon_{\gamma}}{\omega_K \varepsilon_K} \frac{I_{\beta K}}{I_{\beta \gamma}}$$

$I_{\beta K}$  and  $I_{\beta \gamma}$  were obtained from the areas under ideal Fermi distributions and by taking into account once more the correction for escape peaks. Thus we

(\*) I. BERGSTRÖM, in K. SIEGBAHN: *Beta and Gamma Ray Spectroscopy* (Amsterdam, 1955), p. 630.

found:

$$\alpha_K = 1.61 \pm 0.10.$$

The agreement with the previously obtained value is quite satisfactory.

By a similar method the percentage of disintegrations in which a  $\gamma$ -ray is emitted and the relative intensities of the two  $\beta$  groups can be deduced. The total intensity  $I_\beta$  of  $\beta$  particles is in fact given by:

$$(5) \quad I_\beta = \frac{1 + \alpha}{B} \varepsilon_\beta \Gamma - \varepsilon_\beta N,$$

where  $N$  is the number of disintegrations within the source;

$\alpha$  is the total conversion coefficient ( $\alpha = \alpha_K + \alpha_L + \alpha_M$ );

$B$  is the branching ratio i.e. the ratio between the intensity of  $\beta$ -rays emitted in the transition towards the 84 keV level and the total intensity of  $\beta$ -rays.

If (5) and (3) or (5) and (4) are combined, we have alternatively:

$$B = \frac{1 + \alpha}{\omega_K \varepsilon_K \alpha_K} \frac{I_{\beta K}}{I_\beta},$$

$$B = \frac{1 + \alpha}{\varepsilon_\gamma} \frac{I_{\beta\gamma}}{I_\beta}.$$

The total conversion coefficient  $\alpha$  cannot obviously be deduced from the present measurements. We assumed  $\alpha = 8.7$ , which was obtained by averaging the values given by GRAHAM, WOLFSON and BELL<sup>(9)</sup> and by NOVEY<sup>(10)</sup>. We obtain in this way:

$$B = 0.258 \quad (\text{from (4) and (5)})$$

$$B = 0.223 \quad (\text{from (3) and (5)})$$

whose average is:

$$B = 0.24 \pm 0.02.$$

Finally, for the relative probability of emission of a  $\gamma$ -ray, we get from (5):

$$\frac{\Gamma}{N} = \frac{B}{1 + \alpha} = 0.025.$$

The results which were obtained for  $\alpha_K$ ,  $B$ , and  $\Gamma/N$  by means of  $\beta$ - $\gamma$  co-

<sup>(9)</sup> R. L. GRAHAM, J. L. WOLFSON and R. E. BELL: *Canad. Journ. Phys.*, **30**, 459 (1952).

incidence techniques agree satisfactorily with the known decay data of  $^{170}\text{Tm}$  <sup>(9,10)</sup>.

## 6 - Conclusions.

The above described results can be considered as an exemplification of the experimental possibilities of organic crystals in  $\beta$  spectrometry. The satisfactory linearity and the high efficiency of such devices make them very useful, particularly in preliminary researches, when more accurate measurements are planned with a high resolution apparatus, or when only weak sources are available, or when weak  $\beta$  groups have to be examined.

The possibility of getting rather accurate quantitative results out of coincidence measurements is also demonstrated by the agreement of the data concerning the decay of  $^{170}\text{Tm}$  with the previously published ones. Moreover the  $\beta$ - and  $\gamma$ -ray coincidence spectrometer, described in this work, is such an easily assembled and highly efficient apparatus that it can be favourably compared, at least in many cases, with a coincidence arrangement in which a  $\beta$ -ray magnetic spectrometer is used. The larger counting rates which are obtainable with a crystal spectrometer probably more than compensate the higher resolution of the magnetic spectrometer.

\* \* \*

The kind interest of Prof. G. BOLLA for the present work is gratefully acknowledged.

<sup>(10)</sup> T. B. NOVEY: reported in *Argonne National Laboratory Classified Report ANL*, 4427 (July 1950).

## RIASSUNTO

L'uso di cristalli di antracene come spettrometri  $\beta$  è descritto nel presente lavoro; la loro utilità in apparecchiature di coincidenze  $\beta$ - $\gamma$  viene discussa, e sono presentati i risultati di alcune misure in coincidenza. Il decadimento del  $^{170}\text{Tm}$  è stato riesaminato con lo spettrometro qui descritto.



## Sur les variations diurnes en temps solaire et en temps sidéral des grandes gerbes de l'air.

J. DAUDIN (\*), P. AUGER, A. CACHON et A. DAUDIN

*Laboratoire des Rayons Cosmiques de l'École Normale Supérieure - Paris*

(ricevuto il 15 Febbraio 1956)

**Resumé.** — Résultats de l'enregistrement permanent des grandes gerbes de l'air à l'Observatoire du Pic du Midi (2860 m), durant les années 1951, 1952, 1953 et 1954. Analyse en temps solaire et en temps sidéral.

Il est maintenant bien établi que le Rayonnement Cosmique est isotrope à moins de 1% près pour les basses et moyennes énergies (énergies primaires  $< 4 \cdot 10^{13}$  eV) (1). Ce résultat est expliqué par l'existence de champs magnétiques solaires et galactiques capturant, ou tout au moins déviant, les Rayons Cosmiques primaires, qui arrivent ainsi de toutes les directions. Cependant, ces champs magnétiques galactiques sont encore très mal connus, et en faisant différentes hypothèses concernant l'intensité et la répartition de ces champs d'une part, l'origine et le mode de propagation des Rayons Cosmiques dans la Galaxie d'autre part, on prévoit dans chaque cas l'existence d'une faible variation diurne du Rayonnement Cosmique en fonction du temps sidéral (2,3). La détermination expérimentale de cette anisotropie pourrait donc être d'un grand intérêt pour l'étude théorique du magnétisme galactique, de l'origine du Rayonnement Cosmique et peut-être aussi des émissions radioastronomiques.

(\*) Décédé le 24 Janvier 1954.

(1) P. BARRETT, G. COCCONI, Y. EISENBERG and K. GREISEN: *Phys. Rev.*, **95**, 1571 (1954).

(2) LEVERETT DAVIS: *Phys. Rev.*, **96**, 743 (1954).

(3) B. ROSSI: *Suppl. Nuovo Cimento*, **2**, 275 (1955).

Pour obtenir des hamiltoniens de cette sorte, le plus simple est probablement d'utiliser le procédé qui sera exposé dans la section suivante. Il est toutefois essentiel de remarquer dès maintenant que certaines conséquences expérimentalement vérifiables peuvent être obtenues sans construire explicitement ces hamiltoniens: il suffit d'utiliser la méthode employée par WATSON (7) pour l'application à la photoproduction du formalisme du spin isotopique. De telles déductions sont évidemment indépendantes de toute hypothèse sur le type des interactions (FERMI, YUKAWA...). La méthode est aisément applicable à chaque cas particulier. Nous reviendrons sur ce sujet dans la section 6.1 où des exemples seront donnés.

### 3. — Construction des hamiltoniens.

Soit  $x = \begin{pmatrix} x_a \\ x_b \end{pmatrix}$  un isospineur de 1<sup>ère</sup> espèce, indépendant des coordonnées d'espace, qui ne représente qu'un artifice de calcul et auquel nulle signification ou interprétation physique ne sont données (6). D'après les considérations de la référence (2), on doit formellement faire correspondre à  $x$  une valeur  $+1$  de  $U$  et à  $x_a$  et  $x_b$  des « états de charge »  $+1$  et  $0$  respectivement.

Pour construire l'hamiltonien des interactions faibles, on utilise les règles suivantes. Formellement,

- 1) l'interaction doit contenir linéairement l'isospineur  $x$ ;
- 2) elle doit conserver le  $U$  total;
- 3) elle doit être un isoscalaire vrai (conserver le  $I$  total);
- 4) l'isospineur  $x$  doit être tel que dans la représentation où  $\tau_3$  est diagonal,  $\tau_3 = \begin{pmatrix} 1 & 0 \\ 0 & -1 \end{pmatrix}$ , il ne possède que la composante neutre;
- 5) la conservation des baryons est bien entendu imposée.

Étant donné que  $x$  a une valeur de  $U$  égale à  $1$ , les conditions 1) et 2) fournissent la loi  $\Delta U = \pm 1$  pour les particules en jeu. De même des conditions 1) et 3) résulte la loi  $\Delta I = \pm \frac{1}{2}$  puisque le spin isotopique de  $x$  est égal à  $\frac{1}{2}$ .

La condition 4) conduit à la loi absolue de la conservation de la charge des particules. En effet les conditions  $\Delta I_{\text{total}} = \Delta U_{\text{total}} = 0$  fournissent  $\Delta Q_{\text{total}} = 0$  d'où, grâce à 4)  $\Delta Q_{\text{particules}} = 0$ .

Les règles données ci-dessus conduisent bien (après suppression du symbole  $x_b$  de l'écriture) à une composante d'un isospineur de 1<sup>ère</sup> espèce formé à

(7) K. M. WATSON: *Phys. Rev.*, **85**, 852 (1952).

l'aide des opérateurs  $\tau_k$  et dans des champs des particules mises en jeu. Noter que l'emploi du  $x$  est essentiellement un artifice commode pour construire de la manière la plus générale possible des composantes d'isospineurs qui satisfassent à la conservation de la charge, à la règle  $\Delta U = \pm 1$  et, bien entendu, à la règle  $\Delta I = \pm \frac{1}{2}$ .

Afin de montrer comment il convient de procéder dans la pratique considérons le cas d'une interaction  $\Lambda$ ,  $\mathcal{N}$ ,  $\pi$  ( $\mathcal{N}$ : nucléon) dans l'hypothèse où celle-ci est due à un couplage direct. Le seul produit qu'il soit possible de former avec les champs (\*)  $\Lambda$ ,  $\mathcal{N}$ ,  $\pi$ ,  $x$  et qui satisfasse aux conditions 1) à 5) est

$$(1) \quad g\mathcal{N}\tau x\Lambda\pi + \text{c.c.}$$

qui développé, s'écrit

$$(2) \quad g[\sqrt{2}\bar{p}x_0\Lambda\pi + \sqrt{2}\bar{n}x_+\Lambda\pi^* + (\bar{p}x_+ - \bar{n}x_0)\Lambda\pi^0] + \text{c.c.}$$

On ne conserve que les termes en  $x_0$ , soit

$$(3) \quad g[\sqrt{2}\bar{p}\Lambda\pi - \bar{n}\Lambda\pi^0] + \text{c.c.},$$

termes qui décrivent les désintégrations  $\Lambda \rightarrow p + \pi^-$  et  $\Lambda \rightarrow n + \pi^0$  respectivement. Le rapport des constantes de couplage pour ces deux processus est ainsi déterminé (noter que l'exemple du  $\Lambda$  est trop simple pour être intéressant: le rapport de branchement, 2, se déduit de façon générale de la règle  $\Delta I = \frac{1}{2}$  qui impose au système final d'être dans un état  $\frac{1}{2}$  pur).

De même s'il existe un couplage direct pour l'interaction  $\Sigma$ ,  $\mathcal{N}$ ,  $\pi$  celui-ci s'écrit généralement,

$$(4) \quad g\bar{\mathcal{N}}x\Sigma\cdot\pi + ig'\mathcal{N}\tau x[\Sigma\times\pi] + \text{c.c.} \rightarrow \\ \rightarrow g\bar{n}(\Sigma^+\pi^* + \Sigma^-\pi + \Sigma^0\pi^0) + g'[\bar{n}(\Sigma^-\pi - \Sigma^+\pi^*) + \sqrt{2}\bar{p}(\Sigma^0\pi - \Sigma^+\pi^0)] + \text{c.c.}$$

expression où apparaissent cette fois deux constantes de couplage,  $g$ ,  $g'$  a priori indépendantes.

On pourrait multiplier de tels exemples et écrire des couplages directs  $\Xi$ ,  $\Lambda$ ,  $\pi$ ;  $0$ ,  $\mathcal{N}$ ,  $\mathcal{N}$  etc., comme aussi des couplages directs,  $\Lambda$ ,  $\mathcal{N}$ ,  $\mathcal{N}$ ,  $\mathcal{N}$  etc. De façon générale il est clair que le présent formalisme réduit le nombre de constantes arbitraires (constantes de couplages relatives à chaque mode de désintégration).

(\*) Pour les opérateurs de champs  $\psi_\Lambda$ ,  $\psi_{\mathcal{N}}$  etc., la notation simplifiée  $\Lambda$ ,  $\mathcal{N}$  etc., est utilisée.

## 2. — Analyse statistique.

Cette étude porte d'abord sur les trois années 1951-52-53 groupées, la discussion expérimentale pour chacune de ces années ayant été faite antérieurement <sup>(6)</sup>. Nous étudierons ensuite les résultats de l'année 1954 seule, avant de les joindre aux précédents.

2.1. *Méthode.* — Pour étudier les variations diurnes des gerbes d'Auger en temps solaire, nous additionnons les valeurs horaires brutes fournies par chacun des 4 dispositifs d'enregistrement pour tous les jours de l'année; nous additionnons ensuite de la même façon les valeurs correspondantes de la pression atmosphérique, de la température, des fortuites, de la tension des compteurs, pour chaque enregistrement, afin d'effectuer globalement les corrections nécessaires. (Chaque jour plusieurs heures sont perdues pour les contrôles; aux heures manquantes est attribuée la valeur moyenne de l'intensité pour la journée, ce qui aura pour effet de diminuer l'amplitude de toute variation diurne observée).

Nous soumettons alors les totaux obtenus pour chacune des 24 heures de la journée moyenne à l'analyse de Fourier, afin de déterminer la phase et l'amplitude des 2 premiers harmoniques. Puis nous corrigeons successivement de l'onde de pression, de température, de fortuites, de tension des compteurs correspondante:

— les corrections de pression et de température sont faites en admettant qu'il existe un effet barométrique de  $-10\%$  par cm de Hg et un effet de température locale de  $-0.11\%$  par  $^{\circ}\text{C}$  pour D I et D II, de  $+0.15\%$  pour TI et TII. Ces valeurs ont été déterminées expérimentalement <sup>(5,7)</sup>;

— quant aux fortuites, sachant qu'elles représentent  $6\%$  et  $4\%$  des coïncidences sur D I et D II respectivement, on déduit de leur variation diurne la correction à effectuer;

— il y a eu correction de tension des compteurs pour l'année 1951 seule, la tension étant mieux stabilisée depuis, et enregistrée avec précision.

Parallèlement à l'analyse de Fourier, nous traçons les courbes de variations diurnes des grandes gerbes, et nous utilisons les courbes de pression, de température, etc., correspondantes, pour effectuer les corrections.

On opère de façon identique pour étudier les variations diurnes en temps sidéral, en groupant les données en fonction du temps sidéral.

<sup>(6)</sup> M.me A. DAUDIN: *Thèse* (Paris, 1954).

<sup>(7)</sup> J. et A. DAUDIN: *Journ. Atmos. Ter. Phys.*, **3**, 245 (1953).

2.2. *Résultats.*

2.2.1. Ondes diurnes et semi-diurnes solaires. — L'enregistrement D I donnant la plus grande précision statistique sera celui que nous étudierons le plus en détail.

Le Tableau II donne l'amplitude et l'heure du maximum des ondes de Fourier de 2 mois en 2 mois pour les années 1951 et 1952, les 2 dernières colonnes donnant l'amplitude et l'heure du minimum de pression pour les jours correspondants. On voit qu'il existe sur les ondes diurnes des gerbes d'Auger une variation saisonnière en opposition de phase avec celle de pression, avec maximum au solstice d'été, minimum en hiver.

TABLEAU II. — *Variation saisonnière, pour l'enregistrement D I.*

		Rayons Cosmiques		Pression	
		Heure du maximum	Amplitude en %	Heure du minimum	Amplitude
Janvier-Février	1951+52	5h 20 <sup>m</sup>	0.26	5h 50 <sup>m</sup>	0.12 mm
Mars-Avril	» »	5h 20 <sup>m</sup>	0.43	6h 00 <sup>m</sup>	0.23 mm
Mai-Juin	» »	3h 45 <sup>m</sup>	0.56	5h 15 <sup>m</sup>	0.38 mm
Juillet-Août	» »	4h 45 <sup>m</sup>	0.54	5h 12 <sup>m</sup>	0.36 mm
Septembre-Octobre	» »	4h 30 <sup>m</sup>	0.41	5h 50 <sup>m</sup>	0.16 mm
Novembre-Décembre	» »	7h 30 <sup>m</sup>	0.32	6h 00 <sup>m</sup>	0.15 mm
Années	1951+52	5h 00 <sup>m</sup>	0.41 ± 0.03	5h 40 <sup>m</sup>	0.20 mm

Étant donné le parallélisme entre les variations des gerbes et celles de la pression, on est tenté d'expliquer les premières par l'effet barométrique diurne. Ce parallélisme se retrouve entre la courbe (*Aa*) des grandes gerbes et celle (*B*) de la variation diurne de la pression, inversée, sur la fig. 2.

Mais les amplitudes de la variation des gerbes sont trop grandes pour être dues seulement à un effet barométrique de 10% par cm de Hg. Après correction barométrique, la courbe (*Ab*) de la fig. 2, ainsi que le tableau III, montre une variation en phase avec celle de la température (inversée) et celle des fortuites.

Si on fait les corrections de température et de fortuites, on obtient la courbe (*Ae*) qui ne met en évidence aucune variation résiduelle apparente: en effet, l'amplitude du 1<sup>er</sup> harmonique de Fourier pour cette courbe est 0.003% (tableau III).

On peut donc conclure que l'onde diurne en temps solaire des grandes gerbes D I est entièrement expliquée, après correction des fortuites, par les effets atmosphériques (pression, température) à 0.02% près, et que l'inten-



sité des particules de grande énergie des Rayons Cosmiques ne présente pas de variation diurne solaire d'origine extra-terrestre. Le soleil n'émettrait donc

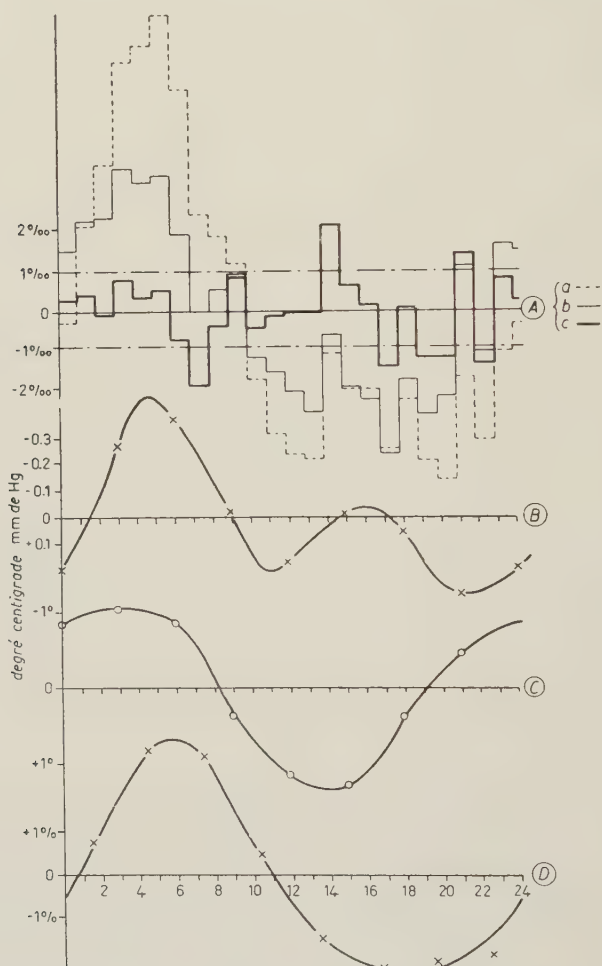


Fig. 2. — Enregistrement D I: variations en temps solaire, années 1951+52+53. Courbes A: variations des grandes gerbes: a) sans corrections; b) après correction barométrique. c) après correction barométrique, de température et de fortuites. — Courbe B: variation de la pression atmosphérique. — Courbe C: variation de la température. — Courbe D: variation des fortuites.

pas de Rayons Cosmiques d'énergie aussi élevée que  $3 \cdot 10^{14}$  eV, résultat en accord avec l'opinion suivant laquelle le soleil n'en émet pas d'énergie supérieure à  $5 \cdot 10^{11}$  eV. Cette opinion est basée sur le fait que, durant les accroissements brusques de l'intensité des Rayons Cosmiques, au moment d'éruptions

TABLEAU III. — Ondes diurnes de Fourier en temps solaire.

Années	Enre- gistre- ment	Grandes Gerbes		Minimum de Pression		Tempéra- ture		Fortuites		Nb. de jours
		Phase	Amplitude en %	Phase	Ampli- tude	Phase	Ampli- tude	Phase	Ampli- tude	
		h.m.		h.m.	mm.	h.m.	°C	h.m.		
+52+53	D I	05.00 ± 0.12	0.41 ± 0.02	6.10	0.21	12.10	0.9	4.00	2.7%	—
» »	D I <sub>p</sub>	03.06	0.26 ± 0.02	—	—	—	—	—	—	—
» »	D I <sub>p,T,f</sub>	13.10	0.093 ± 0.02	—	—	—	—	—	—	—
+52+53	T I	06.00 ± 1.30	0.16 ± 0.06	6.00	0.22	—	—	—	—	—
» »	T I <sub>p</sub>	20.40	0.13 ± 0.06	—	—	—	—	—	—	—
+52+53	T II	08.00	0.29 ± 0.13	6.00	0.22	—	—	—	—	—
+52+53+54	D I	04.50	0.75 ± 0.05	7.04	0.27	13.44	1.3	3.48	2.2%	267
	D I <sub>i</sub>	05.18	0.57 ± 0.05	—	—	—	—	—	—	—
	D I	05.06 ± 0.06	0.44 ± 0.01	6.32	0.22	—	—	—	—	—
+52+53+54	T I	02.54 ± 2.17	0.3 ± 0.18	7.20	0.24	—	—	—	—	149
	T I	03.50 ± 1.30	0.17 ± 0.06	6.16	0.23	—	—	—	—	—
	D II	06.00 ± 1.16	0.29 ± 0.09	7.04	0.23	—	—	—	—	—

D I<sub>p</sub> = enregistrement D I corrigé de la pression.

D I<sub>p,T,f</sub> = enregistrement D I corrigé de la pression, de la température et des fortuites.

D I<sub>p</sub> = enregistrement T I corrigé de la pression.

D I<sub>i</sub> = enregistrement D I corrigé de l'effet instrumental.

solaires, il n'y a pas eu d'augmentation à l'équateur, lequel ne peut être atteint que par les particules d'énergie supérieure à  $5 \cdot 10^9$  eV.

Nous avons essayé de confirmer ces résultats par l'étude des coïncidences de l'enregistrement D II. Mais l'onde diurne est déphasée: nous supposons qu'il y a eu un effet de température instrumental probablement dû à l'alimentation par piles.

Sur les gerbes de grande extension, l'erreur statistique est 3 à 6 fois plus grande que sur D I. Cependant il semble que l'amplitude trop faible (tableau III) et le maximum en avance par rapport à l'onde de correction barométrique, peut s'expliquer par l'effet de température positif trouvé par ailleurs<sup>(6)</sup> qui est en partie instrumental, en partie réel.

La fig. 3 montre la variation diurne de T I, avant correction barométrique: courbe (Aa), et après correction: courbe (Ab), déduite de la courbe (B).

La courbe (Ab) présente un maximum de variation d'amplitude 0.13%, plus faible que la courbe (Aa); mais bien qu'elle montre un certain parallélisme avec la courbe de température vers le milieu de la journée, son maximum

a lieu à 20<sup>h</sup> 40<sup>m</sup>, bien après celui de température, et la correction a pour effet d'augmenter l'amplitude de la courbe résiduelle. En fait le banc de compteurs

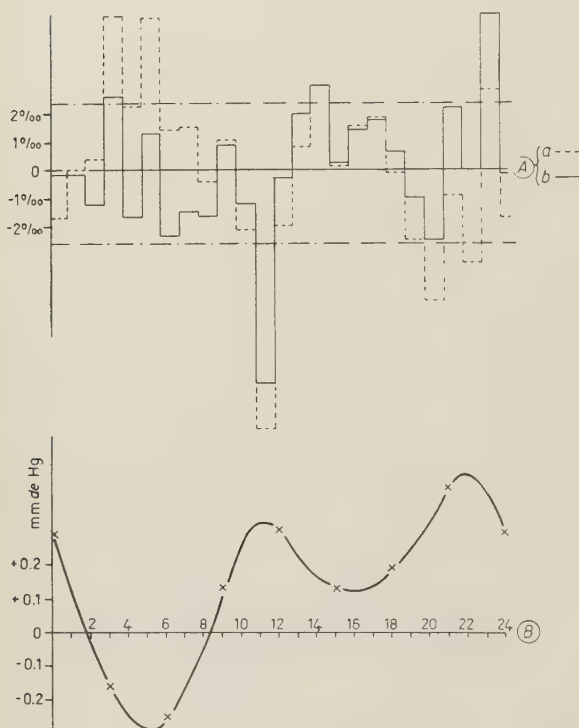


Fig. 3. — Enregistrement T I: variations en temps solaire, années 1951+52+53. Courbes A: variations des grandes gerbes: a) sans corrections; b) avec correction barométrique. — Courbe B: variation de la pression.

éloigné est situé dans une boîte chauffée, mais imparfaitement étanche jusqu'à la fin de 1953, et sa température était sensiblement différente de la température extérieure et plus basse les jours de grand vent que durant les journées foides, mais calmes. Et dans ces conditions une bonne correction de température est impossible; nous négligerons donc cette correction par la suite.

Le tableau IV montre que pour les 4 enregistrements l'onde semi-diurne des gerbes est en opposition de phase parfaite avec celle de pression. Les amplitudes correspondent très bien à la correction barométrique si on prend un coefficient de 10% par cm de Hg.

Cette onde n'est altérée par aucun effet de température, et ce résultat prouve

TABLEAU IV. — Ondes semi-diurnes solaires.

Années	Enregistre- ment	Rayons Cosmiques		Pression	
		Heure du maximum	Amplitude en %	Heure du minimum	Amplitude
1951+52+53	D I	4 <sup>h</sup> 44 <sup>m</sup>	(0.21 ± 0.02)	4 <sup>h</sup> 44 <sup>m</sup>	0.21 mm
1954	D I	5 <sup>h</sup> 14 <sup>m</sup>	0.21	4 <sup>h</sup> 28 <sup>m</sup>	0.17 mm
1951+52+53+54	D I	4 <sup>h</sup> 56 <sup>m</sup>	(0.21 ± 0.01)	4 <sup>h</sup> 40 <sup>m</sup>	0.20 mm
1951+52+53	T I	4 <sup>h</sup> 30 <sup>m</sup>	(0.28 ± 0.07)	4 <sup>h</sup> 40 <sup>m</sup>	0.21 mm
1951+52+53+54	T I	4 <sup>h</sup> 58 <sup>m</sup>	(0.23 ± 0.06)	4 <sup>h</sup> 38 <sup>m</sup>	0.22 mm
1951+52+53	D II	4 <sup>h</sup> 10 <sup>m</sup>	(0.21 ± 0.04)	—	—
1954	D II	4 <sup>h</sup> 48 <sup>m</sup>	0.25	4 <sup>h</sup> 12 <sup>m</sup>	0.18 mm
1951+52+53	T II	4 <sup>h</sup> 32 <sup>m</sup>	(0.27 ± 0.13)	—	—

que, en dehors des légers effets de température d'origine expérimentale que nous avons signalés, les appareils ont été fidèles et précis.

Enfin ce résultat prouve aussi que, après correction barométrique, il n'existe pas de variation semi-diurne sur les gerbes d'Auger. Or, en plus de la variation diurne solaire d'origine extra-terrestre, une variation semi-diurne a également été mise en évidence pour les Rayons Cosmiques de faible et moyenne énergie.

Ceci confirme notre conclusion précédente: le soleil n'émet pas de Rayons Cosmiques d'énergie égale ou supérieure à  $3 \cdot 10^{14}$  eV.

2°2.2. Ondes diurnes et semi-diurnes sidérales. — Le tableau V donne les coefficients de Fourier des ondes diurnes sidérales pour les 4 enregistrements, avant correction barométrique, toutes autres corrections d'ori-

TABLEAU V. — Ondes sidérales avant correction barométrique.

Années	Enregistrement	Nombre de jours	Rayons Cosmiques		Pression	
			Heure du maximum	Amplitude en %	Heure du minimum	Amplitude
1951	D I	192	21 <sup>h</sup> 35 <sup>m</sup>	0.10	3 <sup>h</sup> 25 <sup>m</sup>	0.13 mm
1952	»	295	0 20	0.13	23 20	0.08
1953	»	211	22 18	0.24	22 04	0.09
1951+52+53	»	698	22 20	0.15	0 45	0.08
1954	»	267	18 00	0.38	22 00	0.13
1951+52+53+54	»	965	20 30	0.17	23 20	0.10
1951	T I	265	21 <sup>h</sup> 40 <sup>m</sup>	0.43	01 <sup>h</sup> 00 <sup>m</sup>	0.08 mm
1952	»	315	23 55	0.23	22 00	0.075
1953	»	290	20 36	0.10	21 00	0.08
1951+52+53	»	870	21 50	0.23	22 00	0.07
1954	»	149	19 38	0.40	—	—
1951+52+53+54	»	1 019	21 50	0.24	22 30	0.08
1951	D II	280	22 <sup>h</sup> 30 <sup>m</sup>	0.15	—	—
1952	»	250	20 42	0.30	—	—
1953	»	306	19 00	0.12	—	—
1951+52+53	»	836	20 46	0.17	—	—
1951+52+53	T II	713	22 <sup>h</sup> 00 <sup>m</sup>	0.25	22 <sup>h</sup> 00 <sup>m</sup>	0.08 mm

gine expérimentale étant effectuées. Les 2 dernières colonnes donnent l'amplitude et l'heure du minimum des ondes barométriques correspondantes. On voit que l'accord entre les 4 enregistrements est bon pour les 3 années prises ensemble, et aussi pour chaque année en particulier.

Le tableau VI donne les coefficients de Fourier du 1<sup>er</sup> et du 2<sup>ème</sup> harmonique, après correction barométrique. Pour les 4 enregistrements, l'heure du maximum est environ 21<sup>h</sup>. L'amplitude semble augmenter faiblement avec l'énergie.

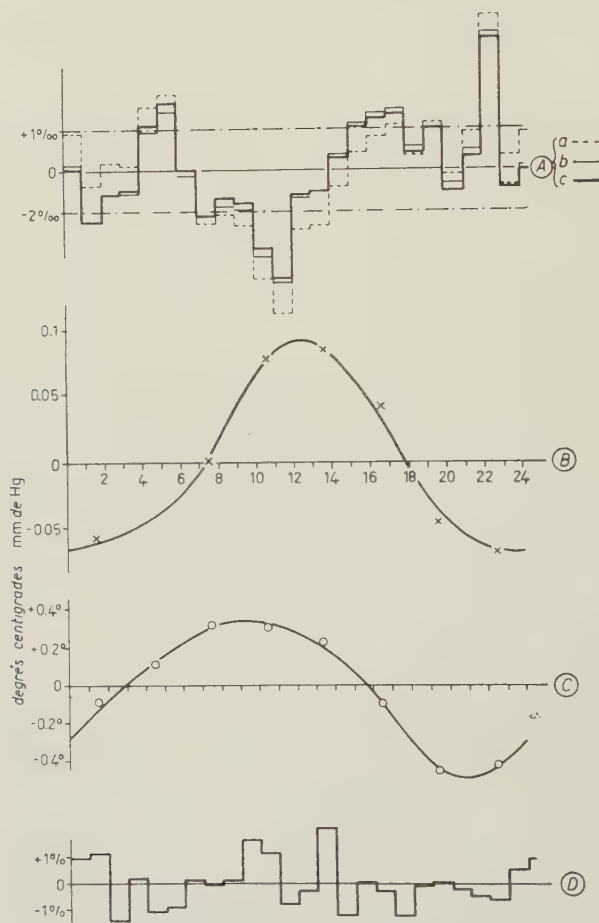


Fig. 4. — Enregistrement D I: variations en temps sidéral, années 1951+52+53. Courbes A: variations des grandes gerbes: a) sans corrections; b) après correction barométrique; c) après corrections barométrique, de température et de fortuites. — Courbe B: variation résiduelle en temps sidéral de la pression atmosphérique. — Courbe C: variation résiduelle en temps sidéral de la température. — Courbe D: variation résiduelle en temps sidéral des fortuites.

Les résultats obtenus fig. 2 montrant clairement le parallélisme des variations en temps solaire des grandes gerbes D I avec la pression, puis avec la température et les fortuites, et enfin l'absence de variations résiduelles après corrections, nous ont encouragé à faire le même travail pour les variations en temps sidéral (fig. 4). Les courbes (Aa), (Ab), (Ac), représentent comme



TABLEAU VI. — Ondes sidérales probables après correction barométrique.

Années	Enre-gistre-ment	Nb. de jours	1 <sup>er</sup> harmonique		2 <sup>ème</sup> harmonique	
			Heure du maximum	Amplitude en %	Heure du maximum	Amplitude en %
1951+52+53	D I	698	20 <sup>h</sup> 40 <sup>m</sup> ± 45 <sup>m</sup>	0.10 ± 0.02	5 <sup>h</sup> 30 <sup>m</sup>	0.07 ± 0.02
» » »	DI cor.	»	20 58	0.08	—	—
1954	D I	267	19 10	0.09	4 <sup>h</sup> 52 <sup>m</sup>	0.1
1951+52+53+54	»	965	20 22 ± 30	0.09 ± 0.015	5 20	0.09 ± 0.015
1951+52+53	T I	870	22 <sup>h</sup> 10 <sup>m</sup> ± 1 <sup>h</sup> 30 <sup>m</sup>	0.17 ± 0.07	7 <sup>h</sup> 00 <sup>m</sup>	0.12 ± 0.07
1954	»	149	18 00	0.22	—	—
1951+52+53+54	»	1019	21 22 ± 1 21	0.17 ± 0.06	7 18	0.09 ± 0.06
» » » »	T I cor.	»	21 58	0.16	—	—
1951+52+53	D II	836	19 <sup>h</sup> 50 <sup>m</sup> ± 1 <sup>h</sup> 30 <sup>m</sup>	0.12 ± 0.04	5 <sup>h</sup> 56 <sup>m</sup>	0.05 ± 0.04
1951+52+53	T II	713	22 <sup>h</sup> 20 <sup>m</sup> ± 3 <sup>h</sup> 00 <sup>m</sup>	0.18 ± 0.13	8 <sup>h</sup> 10 <sup>m</sup>	0.18 ± 0.13

précédemment les variations diurnes des gerbes, mais en temps sidéral, avant correction barométrique, après correction barométrique et après correction de température et de fortuites. La courbe (Ac) résiduelle montre une variation non nulle, et l'analyse de Fourier pour cette courbe indique un maximum à 20<sup>h</sup> 58<sup>m</sup> et une amplitude de 0.08 ± 0.02 %.

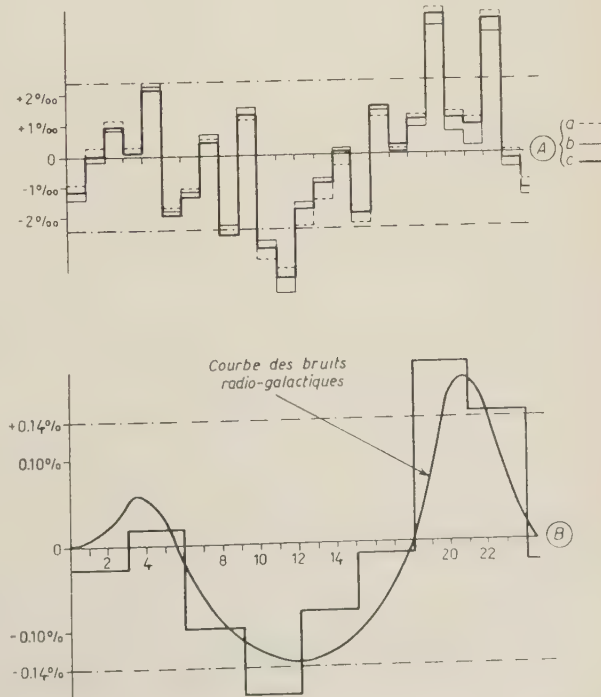


Fig. 5. — Enregistrement T I : variations en temp sidéral, années 1951+52+53. Courbes A : variations horaires des grandes gerbes : a) avant correction barométrique ; b) après correction barométrique ; c) après correction de température. - Courbe B : variation des grandes gerbes, groupées de 3 en 3 heures (la courbe superposée donne, en unités arbitraires, la variation correspondante des bruits radio-galactiques).

Les variations de température et de fortuites, qui sont à peu près en phase en temps solaire, sont en opposition de phase en temps sidéral (les amplitudes de température sont maxima l'été, celles des fortuites l'hiver); il en résulte une correction globale (température+fortuites) très faible.

La fig. 5 représente la variation diurne sidérale de l'enregistrement T I, avant correction barométrique: courbe (Aa) et après: courbe (Ab). Comme en temps solaire, et pour les mêmes raisons, nous n'effectuons pas les corrections de température. Celles-ci auraient tendance à augmenter l'amplitude de la variation, puisque l'effet de température est ici positif, et ont donc pour effet de diminuer l'intensité des gerbes à 21<sup>h</sup> sidérales (\*).

La courbe (B) de cette figure représente la même variation, mais est obtenue en groupant les intensités de 3 heures en 3 heures; nous avons superposé la courbe de variation des bruits radio-galactiques dans un demi-angle zénithal de 20° (unités arbitraires) obtenue par DENISSE et BLUM à Marcoussis.

### 2.3. Discussion. — Nos résultats indiquent:

— qu'il n'existe pas de variation diurne des grandes gerbes en fonction du temps solaire d'amplitude supérieure à 0.06 % pour D I, et à 0.21 % pour T I (limite supérieure obtenue en prenant 3 fois l'erreur probable);

— que s'il existe une variation diurne en temps sidéral, elle n'est pas supérieure à 0.14 % pour D I et à 0.35 % pour T I.

L'examen des courbes de variation nous incite à penser que les gerbes d'Auger présentent une faible variation diurne en temps sidéral, bien que l'amplitude soit trop faible par rapport à l'erreur pour que ce résultat puisse être considéré comme certain. Nous ne pensons pas que cette faible variation soit d'origine instrumentale car:

— nous avons fait une discussion expérimentale assez serrée pour éliminer toutes les causes d'erreur auxquelles on peut penser;

— bien que différentes critiques soient faites à chacun de nos 4 enregistrements, l'accord obtenu pour leur courbe de variation sidérale est bon;

— il existe un accord suffisant entre nos résultats et ceux de CITRON et KEHLER (\*) montrant que la variation ne peut être d'origine instrumentale.

Dans ces conditions, cette variation est-elle un résidu d'effets atmosphériques, ou est-elle d'origine astrophysique? Nous ne pensons pas qu'elle puisse être attribuée à un résidu d'effets atmosphériques, car nous avons montré

(\*) La courbe Ac est indiquée sur la figure pour montrer que, de toute façon, la différence entre Ab et Ac est très faible.

(§) A. CITRON et P. KEHLER: *Zeits. f. Naturforsch.*, 10a, 499 (1955).

que les effets observés en temps sidéral, sont toujours supérieurs aux effets solaires. L'examen de la fig. 5 (B) nous fait croire que la variation observée est d'origine astrophysique, les 2 maxima observés correspondant aux passages de la Voie lactée au zénith du Pic du Midi. C'est la région du Cygne qui est dans le bras galactique auquel appartient le système solaire, qui passe au zénith entre 19 et 22 heures, et la région de Persée, bras éloigné du système solaire, qui passe au zénith entre 4 et 6 heures.

### 3. — Résultats de 1954.

3.1. *Ondes diurnes et semi-diurnes solaires.* — Les résultats des ondes de Fourier sont indiqués dans les tableaux III et IV et la fig. 6 montre la variation diurne relative au dispositif D I: avant correction barométrique (Aa), et après correction (Ab).

Tandis que sur la fig. 2 la courbe (Aa) est en opposition de phase parfaite avec l'onde diurne de pression, ici elle apparaît surtout en opposition de phase avec la courbe de température ou en phase avec celle du mouvement propre des compteurs. En effet les compteurs utilisés en 1954 se sont montrés sensibles à la température.

Si on corrige la courbe (Aa) de l'effet de température et de fortuites com-

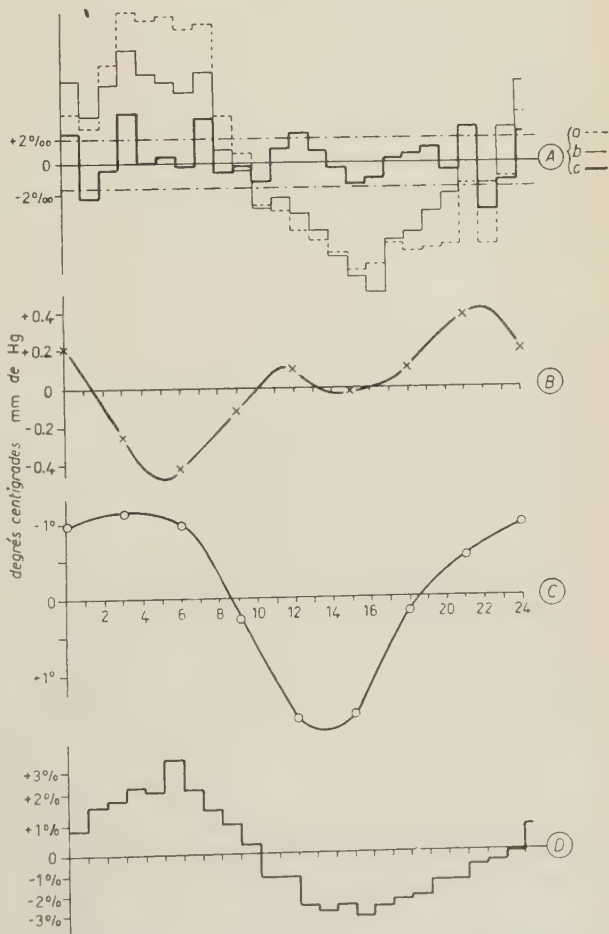


Fig. 6. — Enregistrement D I: variations en temps solaire pour l'année 1954. Courbes A: variations des grandes gerbes: a) avant correction barométrique; b) après correction barométrique; c) après toutes corrections. - Courbe B: variation de la pression. - Courbe C: variation de la température. - Courbe D: variation des fortuites.

me précédemment, et aussi de cet effet instrumental (correction forcément un peu arbitraire), on trouve la courbe ( $\Delta c$ ), ne montrant pas de variations diurnes solaires.

A cause de cet effet, les résultats relatifs à l'année 1954 comporteront quelque incertitude, cependant la fig. 6 montre que, après correction de cet effet instrumental, les résultats sont satisfaisants. Les résultats de l'analyse harmonique qui sont donnés dans les tableaux III et IV sont en bon accord avec ceux des années précédentes, et avec ceux des enregistrements D II.

Nous ne corrigeons pas les résultats de T I de l'effet de température négatif instrumental qui, pour cet enregistrement, est moins important. C'est pourquoi on constate par rapport aux années précédentes une avance de la phase et une augmentation de l'amplitude.

3.2. *Ondes sidérales.* — Les tableaux V et VI donnent les 2 premiers harmoniques des ondes sidérales pour l'année 1954, avant et après correction barométrique. Après correction de l'effet de température instrumental sur D I, l'accord avec les années précédentes est bon. T I n'étant pas corrigé de cet effet, il en résulte une légère avance de la phase et une augmentation de l'amplitude: l'onde sidérale de température étant maximum à  $2^h 44^m$  avec une amplitude de  $0.7^\circ\text{C}$ .

#### 4. — Conclusion.

Ainsi cette étude nous incite à interpréter la variation sidérale observée comme étant d'origine astrophysique. Cependant, les amplitudes des ondes pseudo-sidérales atmosphériques pouvant atteindre des grandeurs non négligeables, il est nécessaire d'étudier ces effets avec le plus grand soin. En outre, nous devons signaler que nous n'avons pas réussi à montrer que l'extrémité du vecteur solaire décrit une ellipse dans le sens inverse des aiguilles d'une montre durant l'année, comme ce devrait être le cas dans l'hypothèse d'une variation sidérale. Pour D I, l'amplitude trouvée est faible, et les corrections importantes (pression, température, fortuites); pour T I, l'amplitude est plus grande, mais la précision statistique est moins bonne. C'est pourquoi nous avons essayé d'étudier les variations diurnes sidérales pour chaque semestre: si l'origine de la variation observée est astrophysique, cette variation sera identique pour les deux semestres; si l'origine est atmosphérique, les variations diurnes pour chaque semestre seront à peu près en opposition de phase. Les résultats sont donnés dans le tableau VII pour les enregistrements D I et T I. On voit que les variations diurnes de la pression, de la température et des fortuites sont en effet pratiquement en opposition de phase pour les deux semestres.

TABLEAU VII. — *Décomposition en 2 semestres.*

	Grand Gerbes			Pression (min.)	
	Phase	Amplitude %		Phase	Ampli- tude
<i>Enregistrement T I: 1951+52+53+54:</i>					
1 <sup>er</sup> semestre: 549 jours, avant cor. bar.	21 <sup>h</sup> 18 <sup>m</sup> ± 1 <sup>h</sup> 08 <sup>m</sup>	0.30 ± 0.09		08 <sup>h</sup> 08 <sup>m</sup>	0.19 mm
2 <sup>ème</sup> » : 464 » » » »	23 50 ± 1 40	0.24 ± 0.10		16 24	0.10
1 <sup>er</sup> semestre: 549 jours, après cor. bar.	19 46 ± 2 50	0.11 ± 0.09			
2 <sup>ème</sup> » : 464 » » » »	22 06 ± 1 50	0.21 ± 0.10			
<i>Enregistrement D I: 1951+52+53 (*):</i>					
grandes gerbes (**)	(1 <sup>er</sup> semestre)	18 <sup>h</sup> 18 <sup>m</sup>		0.22 ± 0.04%	
	(2 <sup>ème</sup> » )	02 46		0.16 ± 0.04	
pression	(1 <sup>er</sup> semestre)	09 00		0.17 mm	
	(2 <sup>ème</sup> » )	16 48		0.12 mm	
température	(1 <sup>er</sup> semestre)	06 00		0.7 °C	
	(2 <sup>ème</sup> » )	16 00		0.7 °C	
fortuites	(1 <sup>er</sup> semestre)	16 00		1.4 %	
	(2 <sup>ème</sup> » )	07 10		1.2 %	
grandes gerbes après correction barométrique, de					
température et de fortuites: (1 <sup>er</sup> semestre)	19 <sup>h</sup> 18 <sup>m</sup> ± 2 <sup>h</sup> 10 <sup>m</sup>	0.07 ± 0.04			
	(2 <sup>ème</sup> » )	23 18 ± 1 16		0.12 ± 0.04	

(\*) Le premier semestre comporte 344 jours utilisables, le second 363.

(\*\*) Grandes gerbes corrigées de l'effet barométrique seul.

Pour T I, on voit que la correction barométrique a pour effet de diminuer la différence entre les heures de maximum trouvées pour les deux semestres. Tandis que la différence de phase est de 8<sup>h</sup> 10<sup>m</sup> pour la pression, elle est seulement de 2<sup>h</sup> 20<sup>m</sup> pour les grandes gerbes, c'est-à-dire à l'intérieur des erreurs.

Pour D I, la différence de phase entre les deux semestres ne cesse de diminuer après les diverses corrections: barométrique, de température et de fortuites. Elle est finalement de 4<sup>h</sup> 00<sup>m</sup>; elle reste un peu grande, l'erreur sur la différence de phase étant de 3<sup>h</sup> 26<sup>m</sup>, mais on peut supposer qu'on a imparfaitement corrigé des effets atmosphériques.

Done, si par suite d'une précision statistique encore insuffisante, cette dernière étude n'apporte pas une preuve définitive en faveur de l'origine astrophysique de la variation observée, elle fournit un bon argument supplémentaire à cette hypothèse.

En conclusion, les résultats de ce travail nous autorisent à penser:

- 1) que les gerbes de l'air ne présentent pas de variation d'origine solaire;
- 2) qu'elles présentent une variation diurne en temps sidéral d'amplitude 0.08 % à 0.16 %, pour des Rayons Cosmiques primaires ayant des énergies de l'ordre de  $3 \cdot 10^{11}$  eV à  $2 \cdot 10^{15}$  eV, avec maximum vers 21<sup>h</sup>. La probabilité



d'une origine astrophysique pour cette variation nous paraît beaucoup plus grande que celle d'une origine atmosphérique.

\* \* \*

Nous voudrions remercier ici Mr. CLAUDE MOSZKOWSKI, Ingénieur E.S.E., MMrs. GUY CARMOUZE et LOUIS PAILHÉ, qui ont assuré le fonctionnement des appareils à l'Observatoire du Pic du Midi, Madame L. PAILHÉ qui a participé aux calculs, ainsi que le Directeur et le personnel de l'Observatoire. Enfin, nous remercions également la Société Lumière qui nous a livré gracieusement le film nécessaire à tous ces enregistrements.

---

#### RIASSUNTO (\*)

Risultati della registrazione permanente dei grandi sciami dell'aria all'Osservatorio del Pic du Midi (2860 m) durante gli anni 1951, 1952, 1953 e 1954. Analisi in tempo solare e in tempo siderale.

---

(\*) *Traduzione a cura della Redazione.*

## Entropy in Quantum Mechanics.

U. FARINELLI and A. GAMBA

*Istituto di Fisica dell'Università - Torino*  
*Istituto Nazionale di Fisica Nucleare - Sezione di Torino*

(ricevuto il 19 Febbraio 1956)

**Summary.** — A critical discussion from a physical standpoint of the proofs given so far of the second principle of thermodynamics in quantum mechanics shows how information theory allows a much more satisfactory physical interpretation.

### 1. — Introduction.

The problem of explaining macroscopic irreversibility from reversible microscopic laws is an old one. The first attempt can be traced back to the famous Boltzmann  $H$ -theorem, and the difficulties of the classical proof are well known. New hopes arose with the advent of quantum mechanics: as a matter of fact, already in 1929 VON NEUMANN <sup>(1)</sup> claimed to have proved the  $H$ -theorem without the assumptions necessary in classical physics. This work was almost ignored by the great majority of physicists, even after PAULI and FIERZ <sup>(2)</sup> tried to smooth the difficulties of VON NEUMANN's paper <sup>(3)</sup>. Perhaps this was also due to the fact that an approach of this kind is rather unsuitable for practical purposes. Other types of approach, more similar to the classical Gibbs approach, cannot avoid assumptions and are, therefore, less satisfactory for a general discussion of basic principles.

The most rigorous proof of the second principle of thermodynamics is therefore still to be found in VON NEUMANN's work.

<sup>(1)</sup> J. VON NEUMANN: *Zeits. f. Phys.*, **57**, 30 (1929).

<sup>(2)</sup> W. PAULI and M. FIERZ: *Zeits. f. Phys.*, **106**, 572 (1937).

<sup>(3)</sup> « Da die Neumannsche Arbeit für den Physiker unübersichtlich ist... », PAULI and FIERZ: loc. cit., p. 573.

A rather detailed analysis of the present situation is contained in a recent review article by TER HAAR <sup>(4)</sup>. However, the questions are by no means settled: also in the von Neumann, Pauli and Fierz theory there are some questionable features, especially due to the appearance of exceptions to the second principle, in form of « non-thermodynamic » observers.

In the present paper we shall take the problem over from the beginning, starting from the more modern point of view that entropy is nothing but a measure of our ignorance of the state of a system. Our standpoint has many advantages for a physical interpretation of the results, as we shall see. In particular, in the case of von Neumann's proof, it solves the paradox of non-thermodynamical observers.

## 2. — Density Matrices and Measurements.

It is well known that the state of a quantum mechanical system can be represented by means of a density matrix  $\varrho(\psi)$  instead of a normalized state-vector  $\psi$ .

If the expansion of  $\psi$  as a function of an orthonormal system of basic vectors  $v_k$  is given by

$$(1) \quad \psi = \sum_k c_k v_k,$$

the density matrix  $\varrho(\psi)$  is an hermitian matrix whose elements  $\varrho_{mn}$  are

$$(2) \quad \varrho_{mn} = c_m c_n^*,$$

where  $c_n^*$  is the conjugate complex of  $c_n$ .

By using the density matrix some standard formulae of quantum mechanics appear in a very concise and elegant form. For example, the mean value  $\langle A \rangle$  of any observable  $A$ , in the state specified by the density matrix  $\varrho$ , is given by the trace of the product matrix  $\varrho A$ :

$$(3) \quad \langle A \rangle = \text{Tr}(\varrho A) = \text{Tr}(A \varrho).$$

However, the main advantage of the formalism of the density matrix is that « impure » states can be dealt with in the same way as « pure » states.

If  $\varrho(\psi_1)$ ,  $\varrho(\psi_2)$ ,... are the density matrices of the pure states  $\psi_1$ ,  $\psi_2$ ,... respectively, the density matrix of a mixture of these states with weights  $p_1$ ,  $p_2$ ,...

<sup>(4)</sup> D. TER HAAR: *Rev. Mod. Phys.*, **27**, 289 (1955). The reader is referred to this paper for a complete bibliography.

$(p_1 + p_2 + \dots = 1)$  is defined as follows:

$$(4) \quad \varrho = \sum_r p_r \varrho(\psi_r) .$$

We should like to emphasize a point, which has not received sufficient attention in current literature. When a quantum mechanical system is represented by the density matrix of a mixture, two interpretations are possible. Either the system is actually a mixture, i.e. all the different states of which the mixture is made up are present in the physical system according to their weights, or the system is in a pure state <sup>(5)</sup>. In the latter case, the density matrix represents *what we know of the system*, and not the real state. Think, for example, of a system of electrons represented by a density matrix corresponding to, say, 70% of the electrons polarized « spin up » and 30% « spin down ». The two interpretations are: 1) no frame of reference exists in which all electrons are polarized « spin up »; 2) perhaps such a frame exists but we cannot know it for sure: our knowledge on the system allows us to bet for no more than 70% in any frame. Taking into account the connection between information and entropy <sup>(6)</sup>, it is not difficult to foresee that we shall be mainly concerned with the second interpretation. However, both will be needed and, in any case, such a distinction is of paramount importance in order to avoid misunderstandings.

Let us now consider an observable  $A$ , with eigenvalues  $a_k$  and eigenfunctions  $e_k$ . We define a measurement of  $A$  as the experimental determination of a set of probabilities  $c_k c_k^*$  for each  $a_k$ . The information thus obtained can be expressed by means of a density matrix  $\varrho_A$ , in which the diagonal elements are the  $c_k c_k^*$  and the off-diagonal ones are all equal to zero. Off-diagonal elements depend on phase-relations. By measuring  $A$ , nothing can be said about phases; so we have to average over them, a process which corresponds to putting zero for all off-diagonal elements in  $\varrho_A$ .

When  $A$  is degenerate, a measurement of  $A$  cannot give each  $c_k c_k^*$  separately, but only the sum  $\sum c_k c_k^*$  of all terms corresponding to the same degenerate level. If  $s_v$  is the degree of degeneracy of the  $v$ -th level, the density matrix is a diagonal matrix in which the terms corresponding to the states which belong to this level are all equal to  $(\sum c_k c_k^*)/s_v$ . This is easily proved to be a consequence of eq. (4) when an average is made over all *a priori* possible states.

<sup>(5)</sup> Or, anyhow, in a state « less impure » than it is represented by our density matrix.

<sup>(6)</sup> L. BRILLOUIN: *Journ. Appl. Phys.*, **24**, 1152 (1953); **25**, 595 (1954); A. GAMBA: *Nuovo Cimento*, **1**, 358 (1955).

A similar situation arises when  $A$  is not actually degenerate, but, owing to the limited precision of our measuring instruments, we are unable to distinguish among the eigenvalues  $a_k$  of a set of levels. This is the general case of a macroscopic measurement of  $A$ . Here too we only measure a sum  $\sum c_k c_k^*$  for the set of levels we cannot separate. The density matrix expressing the information we get from this macroscopic measurement, is easily seen to be formally the same as in the case of true degeneracy. Therefore, by using the formalism of the density matrix, there is no need of a separate treatment of microscopic and macroscopic measurements. We may summarize this result, by saying that in any case *all the information obtained by measuring an observable  $A$  is contained in a density matrix  $\varrho_A$  diagonal in the  $A$ -representation.*

Suppose that another observable  $B$ , not commuting with  $A$ , is measured at the same time. This process is not in disagreement with the general principles of quantum mechanics, because of our definition of measurement. It amounts to preparing in the same way a great number of equal systems and performing on half of them the measurement of  $A$  and on the other half the measurement of  $B$ , in order to evaluate probabilities for the eigenvalues. All the information obtained by the measurement of  $A$  and  $B$  is then given by two density matrices  $\varrho_A, \varrho_B$  diagonal in the  $A$ - and  $B$ -representations respectively. Transforming  $\varrho_B$  in the  $A$ -representation, we obtain a density matrix  ${}_B\varrho$  which is no longer diagonal. Thus the results of the measurement of  $A$  and  $B$  can also be given by two density matrices  $\varrho_A, {}_B\varrho$ , both in the  $A$ -representation. What do we know of the physical system? It must be in such states that are compatible with, and therefore common to, both  $\varrho_A$  and  ${}_B\varrho$ . We are not going to discuss here the details of the calculation, but it should now be clear that the results of the two measurements can be expressed by a single density matrix, in general not diagonal in the  $A$ -representation. This matrix can, however, be diagonalized by means of a convenient unitary transformation.

This process can be repeated for any number  $n$  of non-commuting observables  $A, B, C, \dots$ , so that the results can eventually be expressed by a single diagonal matrix  $\varrho$ , instead of  $n$  diagonal matrices  $\varrho_A, \varrho_B, \varrho_C, \dots$ .

Consider now an observable  $K$  defining a representation in which  $\varrho$  is diagonal. The same  $\varrho$ -matrix could have been obtained by measuring  $K$  instead of the set  $A, B, C, \dots$ . This is not surprising. For example, the single measurement of an operator which has the state of the system as one of its non degenerate eigenstates, is already sufficient to determine completely the quantum mechanical system. Of course we cannot know beforehand which observable is better in order to get more information on the system, since its state is *a priori* unknown.

In conclusion: *all the information obtained by measuring a set of observables  $A, B, C, \dots$  is contained in a density matrix  $\varrho$  diagonal in some (a priori unknown)  $K$ -representation.*



### 3. - Time Dependence of the Density Matrix.

If  $\varrho(0)$  is the density matrix at time  $t = 0$ , the density matrix  $\varrho(t)$  at a later time  $t$  is given by

$$(5) \quad \varrho(t) = R(t) \cdot \varrho(0) R^{-1}(t),$$

where  $R(t)$  is a unitary matrix determined by the solution of the Schrödinger equation. This is standard quantum mechanics. However, we are going to show that the density matrix obtained by using formula (5) has no relevant physical meaning.

If  $\varrho(0)$  is a diagonal matrix,  $\varrho(t)$  in general is not. Assume we obtained the density matrix  $\varrho(0)$  by measuring the observable  $A$  at time  $t = 0$ ;  $\varrho(t)$  cannot be thought of as the density matrix obtained by measuring  $A$  at time  $t$ , since such a matrix would be diagonal.

In order to obtain physically the matrix (5) at time  $t$ , one ought to measure a new observable  $A(t)$  depending explicitly on time, such that in the  $A(t)$ -representation  $\varrho(t)$  be diagonal. This is hardly a practical procedure, since our laboratory equipment is mostly not such a function of time!

It is far more significant from a physical point of view to consider always the same observable  $A$  we measured at  $t = 0$ . The corresponding density matrix must then be diagonal in the  $A$ -representation.

Let us consider, therefore, the density matrix  $\varrho'(t)$  obtained by modifying the matrix (5) in the following way: all off-diagonal elements are put equal to zero. In other words, we introduce another time-dependent matrix  $\varrho'(t)$  whose elements are:

$$(5') \quad \varrho'_{mn}(t) = \varrho_{mn}(t) \cdot \delta_{mn},$$

where  $\delta_{mn}$  is the Kronecker symbol, and  $\varrho_{mn}(t)$  are the elements of matrix (5). Although in  $\varrho'(t)$  off-diagonal elements are no longer present, yet not all unmeasurable quantities have disappeared. In fact, when  $A$  is degenerate, be it true degeneracy or lack of precision of our instruments, we must average over all degenerate levels, with an averaging process of the type described in Sect. 2.

A density matrix, which contains only quantities that are physically meaningful with respect to a measurement of  $A$ , is the matrix  $\varrho''(t)$ , whose elements are

$$(5'') \quad \varrho''_{mn}(t) = \delta_{mn} \sum_{s_r} \varrho'_{kk}(t),$$

the sum being over all degenerate levels to which the  $m$ -th level belongs,  $s_r$  being the degree of degeneracy <sup>(7)</sup>.

$\varrho''(t)$  represents what we may expect to be the result of a measurement of  $A$  at time  $t$ , if  $\varrho(0)$  represented what we knew on the system at time  $t=0$ . This, of course, is the interpretation 2) of the meaning of a density matrix. Interpretation 1) would sound: if at  $t=0$  the state of the system was actually  $\varrho(0)$ ; then by measuring  $A$  at time  $t$  we would certainly find  $\varrho''(t)$ . On the contrary, according to the second interpretation, we cannot be sure of finding  $\varrho''(t)$  by measuring  $A$  at time  $t$ . In general some other result will be found, and we can infer that at  $t=0$  the state was not the « true » mixture  $\varrho(0)$ ; some supplementary information is obtained on the system by means of the measurement. This point will be further discussed in the next section.

The matrix  $\varrho'(t)$ , as we saw, is not completely free of unmeasurable quantities. We introduced it only because in the literature it was sometimes (wrongly) used to define entropy. This question too will be discussed in the next section.

#### 4. — The Entropy Concept.

We have seen that *what* we know of a quantum mechanical system is represented by a density matrix  $\varrho$ . In order to evaluate *how much* we know of the system, the quantity

$$(6) \quad I = -S = \text{Tr} (\varrho \ln \varrho)$$

has been introduced <sup>(8)</sup>. This quantity  $I$  is called the amount of information, or simply the « information » on the system, whereas its negative  $S$  is the entropy of the system in  $k$  units ( $k$  being the Boltzmann constant). The matrix  $\varrho$  we put in formula (6) always expresses what we know on the system, and not the state of the system itself (see interpretation 2) of Sect 2): in other words, it must depend on known quantities only.

Let us discuss the physical meaning of formula (6) when we put for  $\varrho$  the different matrices introduced in the previous section.

If  $\varrho(0)$  is the density matrix obtained by measuring  $A$  at time  $t=0$ ,  $S(0) = -\text{Tr} (\varrho(0) \ln \varrho(0))$  is the entropy at time  $t=0$ . With regard to the time dependence of entropy, when no measurement is made on the system

<sup>(7)</sup> Note that at  $t=0$ ,  $\varrho(0) = \varrho'(0) = \varrho''(0)$ .

<sup>(8)</sup> See J. VON NEUMANN: loc. cit.

after  $t = 0$ , we have three possible definitions,  $S$ ,  $S'$ ,  $S''$ , according to whether we use  $\varrho$ ,  $\varrho'$ ,  $\varrho''$  respectively in formula (6).

$S = -\text{Tr}(\varrho \ln \varrho)$  is constant in time, owing to the invariance of the trace for unitary transformations. This is the case of microscopic reversibility: it represents the entropy obtained by measuring the observable  $A(t)$  depending explicitly on time, defined in Sect. 3. As we have seen, this is not a very significant quantity from a physical point of view.

The definition  $S' = -\text{Tr}(\varrho' \ln \varrho')$  has been proposed by some authors<sup>(9)</sup>. This entropy is not a constant, since the time dependence of  $\varrho'$  is not given by a unitary transformation. It was possible for Klein to prove that

$$(7) \quad S'(t) \geq S'(0) \quad \text{for } t > 0.$$

Theorem (7) was thought by KLEIN, BORN and GREEN to be the quantum mechanical proof of the second law of thermodynamics.

However, the second law is more general, and it would imply that

$$(8) \quad S'(t_2) \geq S'(t_1) \quad \text{for } t_2 > t_1.$$

This statement cannot be derived from theorem (7), which makes essential use of the fact that at  $t = 0$ ,  $\varrho(0)$  is diagonal. This is no longer true at any later time  $t$ :  $\varrho(t)$  is not diagonal (although  $\varrho'(t)$  is always diagonal by definition!). Time  $t = 0$  is privileged, being the time of the first measurement. Putting  $\varrho'(t)$  for  $\varrho(t)$ , (in order to have  $\varrho(t)$  diagonal) would amount to introducing a disturbance on the system, which destroys the information obtained at  $t = 0$ . This disturbance cannot be a quantum mechanical effect, according to our definition of measurement, and has therefore no physical meaning. This point was already discussed by PAULI<sup>(10)</sup>.

Another objection to the definition of entropy as  $S'$  is that not all terms in  $\varrho'$  are physically measurable. The definition

$$(9) \quad S'' = -\text{Tr}(\varrho'' \ln \varrho''),$$

is far more satisfactory, since only measurable quantities appear.  $S''$  is, therefore, the best definition for macroscopic entropy<sup>(11)</sup>. It is for this quantity that the theorems of thermodynamics are to be proved.

Klein's theorem holds *a fortiori* for  $S''$ : but we are confronted with similar

<sup>(9)</sup> O. KLEIN: *Zeits. f. Phys.*, **72**, 767 (1931); M. BORN and H. S. GREEN: *Proc. Roy. Soc., A* **188**, 10 (1946).

<sup>(10)</sup> W. PAULI: *Suppl. Nuovo Cimento*, **6**, 223 (1949).

<sup>(11)</sup> Note that our definition of entropy is given with respect to a fixed observable or set of observables, as it is implied in the classical definition of entropy.

difficulties as before if we try to prove the generalization

$$(10) \quad S''(t_2) \geq S''(t_1) \quad \text{for } t_2 > t_1.$$

Actually statement (10) is certainly not true: in simple cases, the entropy can be shown to fluctuate. These fluctuations, however, are negligible for systems of physical interest, so that statement (10) can be assumed as correct for practical purposes. Therefore, although a rigorous proof of theorem (10) has no meaning, there is no objection to a « phenomenological » proof. This has in fact been given by PAULI <sup>(12)</sup> and more recently by VAN KAMPEN <sup>(13)</sup> with the help of some explicit disorder assumptions. This kind of approach (a « Gibbs approach ») is necessary for many practical calculations, as it considers the explicit time dependence of entropy, and is therefore useful for the treatment of non-equilibrium systems. However, for a general discussion a different approach (a « Boltzmann approach ») is more suited. This point is deferred to the next section: but first we should like to discuss another question.

The matrix  $\varrho''(t)$ , by means of which entropy is defined, is a forecast on the results of a measurement of the observable  $A$ . What happens, if we do measure  $A$  at time  $t$ ? If the result is  $\varrho''(t)$ , no information is added to what we already knew on the system.  $S''(t)$ , the entropy immediately before the measurement, remains unchanged. On the other hand, if the result we find is not given by  $\varrho''(t)$ , we get new information on the system. Immediately after the measurement,  $\varrho''(t)$  as defined by (5''), no longer expresses what we know on the system, since now we know something more.  $\varrho''(t)$  has to be replaced by another density matrix, in terms of which we define the entropy after the measurement. This sudden change (actually a reduction) of the value of entropy due to the measurement is not surprising, since entropy is not an intrinsic property of the system, but depends on how much we know of it. This reduction of entropy is equal to the amount of information conveyed by the measurement, in agreement with the general principles of information theory, and is paid for by an equal or greater increase in the entropy of the measuring apparatus <sup>(14)</sup>.

It is perhaps worth noticing that this variation of entropy during the measurement is a macroscopic effect present in any macroscopic measurement and has nothing to do with the quantum disturbances which appear in the Born and Green treatment. In our case, the disturbance due to the measurement

<sup>(12)</sup> W. PAULI: *Sommerfeld Festschrift* (Leipzig, 1928), p. 30.

<sup>(13)</sup> N. G. VAN KAMPEN: *Physica*, **20**, 693 (1954). This work is mainly concerned with the derivation of Onsager's relations.

<sup>(14)</sup> L. BRILLOUIN: loc. cit.



rement affects not the system itself, as in the quantum case, but what we know of the system. To emphasize the difference between the two «disturbances», note that in our case a measurement reduces the entropy, while in the Born and Green case it would tend to increase it.

## 5. — Physical Interpretation.

As we have seen, it has not yet been possible to derive a proof of the second principle of thermodynamics that considers the explicit time dependence of entropy without making some assumptions. On the other hand, a proof can be given by means of a « Boltzmann approach »: i.e., proving that the time average of entropy is equal to the equilibrium (or microcanonical) value. This proof has been carried out by VON NEUMANN and by PAULI and FIERZ, without making any explicit « disorder assumption » of the type required for Boltzmann's  $H$ -theorem. The procedure is formally correct, but the physical interpretation is not wholly satisfactory.

VON NEUMANN proved for a pure state that the probability for the time average of entropy to be significantly different from the microcanonical value is negligible. PAULI and FIERZ explicitly evaluated the probability that this should happen. Although the proof given by these authors is concerned with a pure state, it is *a fortiori* valid for a mixture, in particular for our matrix  $\varrho''$ .

According to our point of view, the result may be formulated as follows: it is highly improbable that a measurement at time  $t$  could reduce the entropy of the system by telling us something that we did not yet know before as a consequence of the first measurement of  $A$  at time  $t = 0$ .

However, there is another point which needs careful discussion, since it contains the most unsatisfactory features of the theory.

According to VON NEUMANN, PAULI and FIERZ, there are observables privileged with respect to the entropy: for them, the time average of entropy can be far from the microcanonical value. These observables, although very « improbable », certainly place the theory in a peculiar position, as remarked by FIERZ himself <sup>(15)</sup>. These observables are *a priori* known: therefore anybody could choose them in order to store information for the future. These observers—who are called by PAULI non-thermodynamic—drastically limit the validity of thermodynamical considerations also in practical cases.

This situation, in our opinion, must be handled in a way similar to that used to solve the classical paradox of the Maxwell demon <sup>(16)</sup>.

<sup>(15)</sup> M. FIERZ: *Helv. Phys. Acta*, **28**, 705 (1955).

<sup>(16)</sup> L. SZILARD: *Zeits. f. Physik*, **53**, 840 (1929); see also BRILLUOIN: loc. cit.



The point is that the definition of the microcanonical value of entropy has to be re-examined.

The microcanonical value  $S_\mu$  is defined by

$$(11) \quad S_\mu = -\text{Tr} (\varrho_H'' \ln \varrho_H''),$$

where  $\varrho_H''$  is the density matrix obtained by measuring the energy.  $\varrho_H''$  is constant in time, so that any information we got on the energy will never be lost.  $S_\mu$  is therefore an upper limit for entropy. In other words, no matter what variables we measure, the information on the system will never be less than what we knew on the energy distribution.

Clearly,  $S_\mu$  depends on the accuracy of our measurements, as it is implied in the concept of entropy. The precision of our instruments determines the energy shells and their degeneracy. With more precise instruments we could split an energy shell into subshells; process (5'') is altered, and a lower value is obtained for  $S_\mu$ , according to the fact that we have more information that keeps in time.

However, not only a direct measurement of energy can give such a splitting of the energy shells: we could get similar results by measuring other observables commuting with the Hamiltonian, or even, to some extent, observables which do not commute with the Hamiltonian. Think, for example, of a system of electrons in a magnetic field. Our energy measurement could be rather crude, and make it impossible for us to separate energetically the two different states of polarization. It is, anyhow, clear that measurements of polarization could give us information on the energy.

It is proved in the Appendix that it is always possible to split the information obtained by a measurement of  $A$  in two parts, so that the first one remains constant in time, the other one will be eventually lost. This corresponds to a splitting of the density matrix  $\varrho_A$  into the sum of two matrices:

$$(12) \quad \varrho_A = \bar{\varrho}_A + \overset{\circ}{\varrho}_A,$$

$\bar{\varrho}_A$  is diagonal in the energy representation; on the contrary,  $\overset{\circ}{\varrho}_A$  is such that in the energy representation all its diagonal elements are zero. The information conveyed by  $\bar{\varrho}_A$  is only information on energy, and is constant in time, whereas the information contained in  $\overset{\circ}{\varrho}_A$  yields nothing on the energy and gets eventually lost.

Therefore, in the definition (11) of the microcanonical entropy,  $\varrho_H''$  has to take into account *all* information on the energy distribution, not only that given by a direct measurement of  $H$ . The paradox of « non-thermodynamical » observers is now clear: the microcanonical entropy cannot be defined irrespect-

ively of the results of other measurements. A non-thermodynamical observer is no one else but an observer that knows something more about energy.

## APPENDIX

We want to split the density matrix  $\varrho_A$  obtained by measuring  $A$  at time  $t = 0$  into the sum of a matrix  $\bar{\varrho}_A$  commuting with the Hamiltonian and a matrix  $\overset{m}{\varrho}_A$  whose elements have a zero time average:

$$\varrho_A = \bar{\varrho}_A + \overset{m}{\varrho}_A.$$

Let us first transform  $\varrho_A$  into the reference system in which the Hamiltonian is diagonal:

$$U \cdot \varrho_A \cdot U^{-1} = \varrho_H,$$

where  $U$  is a unitary matrix, time independent if both  $A$  and  $H$  do not depend explicitly on time. In this reference system, the splitting

$$\varrho_H = \bar{\varrho}_H + \overset{m}{\varrho}_H,$$

is very easy:  $\bar{\varrho}_H$  must be diagonal, and we define its elements as follows:

$$(\bar{\varrho}_H)_{mn} = (\varrho_H)_{mn} \cdot \delta_{mn}.$$

As a consequence, we have:

$$(\overset{m}{\varrho}_H)_{mn} = (\varrho_H)_{mn} \cdot (1 - \delta_{mn}).$$

$\overset{m}{\varrho}_H$  is a matrix whose diagonal elements are all zero, and therefore gives no information on the results of a measurement of  $H$ .

$\bar{\varrho}_H$  is constant in time, so that the information it contains will never be lost. The time dependence of the elements of  $\overset{m}{\varrho}_H$  is given by

$$(\overset{m}{\varrho}_H(t))_{mn} = (\overset{m}{\varrho}_H(0))_{mn} \exp \left[ i \frac{E_m - E_n}{\hbar} t \right],$$

where  $E_m$  and  $E_n$  are the  $m$ -th and  $n$ -th eigenvalue of the Hamiltonian respectively, which we assume non degenerate, as required in von Neumann's proof. The time average of each element of  $\overset{m}{\varrho}_H$  is clearly zero: this matrix  $\overset{m}{\varrho}_H$  is the one giving the information which is lost as time goes on.

It is now sufficient to transform back into the original reference system to get the desired result:

$$Q_A = U^{-1} \cdot \bar{Q}_H \cdot U, \quad \overset{M}{Q}_H = U^{-1} \cdot \overset{M}{Q}_H \cdot U.$$


---

#### RIASSUNTO

Si fa una critica dal punto di vista fisico delle dimostrazioni finora date del secondo principio della termodinamica in meccanica quantistica, e si mostra come alla luce della teoria dell'informazione sia possibile darne un'interpretazione fisica assai più soddisfacente.

## Interactions faibles des hyperons et des mésons lourds.

B. D'ESPAGNAT et J. PRENTKI

*CERN - Genève*

(ricevuto il 20 Febbraio 1956)

**Summary.** — In order to account for the selection rule  $\Delta I = \pm \frac{1}{2}$ , which seems to govern the decays of hyperons and heavy mesons, the relevant interaction hamiltonian is taken as the component of a 1st kind spinor in isotopic space. Without any further hypothesis concerning the types of interaction and the number of independent hamiltonians this already provides some relations (see sect. 6) which could be tested by experiment and could also provide some information, especially on the spin and parity of the  $\Sigma$ . This is partly due to the fact that the scattering in the final state has some effect on the decay probabilities. A convenient mean for writing down explicitly such hamiltonians is also given. This leads to a discussion of the choice Fermi-type *versus* Yukawa-type. No convincing argument can be given at the present stage for any of the two types. On the assumption of a Yukawa-type, chosen because of its greater simplicity, the consequences of some natural choices of the coupling constants are investigated.

### 1. — Introduction.

Le problème des interactions faibles est sûrement très complexe. Les modes de désintégration des particules sont d'une grande variété et, en fait, toutes les particules élémentaires connues sont mises en jeu lors de ces processus. Il convient de remarquer que même pour les particules « anciennes », telles que les mésons  $\pi$  et  $\mu$  en liaison avec la radioactivité  $\beta$ , aucune théorie vraiment satisfaisante n'a pu être élaborée. L'apparition des particules « nouvelles » vient naturellement compliquer encore une situation qui devrait être envisagée dans son ensemble. Toutefois, si l'on porte son attention plus particulièrement sur le problème des hyperons et des mésons lourds, on voit se dégager certaines lois empiriques de nature à préciser quelque peu la forme des interactions.

Il est bien connu <sup>(1)</sup> que la considération des interactions fortes conduit à attribuer à chaque particule nucléaire (nucléons, mésons  $\pi$ , hypérons et mésons lourds) un spin isotopique  $I$  et un nombre quantique  $U$  liés à la charge par la relation

$$Q = I_3 + U/2$$

et que ces interactions sont régies par la conservation séparée des  $I$ ,  $I_3$  et  $U$  totaux. Les deux dernières lois de conservation entraînent la conservation de la charge qui, évidemment, est une loi absolue. Ceci constitue la base du modèle de GELL-MANN <sup>(1)</sup>. Dans le modèle phénoménologique on préfère parfois parler de conservation de l'étrangeté  $S = -U + N$  où  $N$ , le nombre de baryons (nombre de baryons moins nombre d'antibaryons) est bien entendu aussi une constante du mouvement.

Dans une formulation mathématique du modèle précédent <sup>(2)</sup>  $U$  s'interprète soit comme le nombre d'isofermions (nombre d'isofermions moins nombre d'antiisofermions) — nombre qui est donc, lui aussi, une constante du mouvement — soit encore, ainsi que l'a fait récemment remarquer RACAH <sup>(3)</sup> comme la conservation d'une « charge isofermionique » étroitement liée à la conservation de la parité intrinsèque des particules dans l'espace du spin isotopique.

PAIS et GELL-MANN ont constaté que toutes les désintégrations des hypérons et mésons lourds expérimentalement observées sont compatibles avec des sauts quantiques  $\Delta I = \pm \frac{1}{2}$  et  $\Delta S = \pm 1$ . Cette dernière condition est évidemment équivalente à  $\Delta U = \pm 1$  qui signifie que pour de tels processus le nombre d'isofermions change d'une unité. Cette dernière formulation nous semble plus adaptée à un traitement théorique car elle fournit une première indication pour la construction des hamiltoniens d'interaction.

La règle  $\Delta I = \pm \frac{1}{2}$  fut primitivement introduite par GELL-MANN et PAIS pour des raisons d'uniformité: elle s'impose dans les désintégrations du  $\Xi$  et du  $\Sigma$  alors que pour celles du  $\Lambda$  et des mésons lourds  $\Delta I = \pm \frac{3}{2}$  serait à priori tout aussi acceptable. Récemment cette règle a toutefois reçu d'intéressantes confirmations; elle a en effet permis à DALITZ <sup>(4)</sup> d'interpréter la différence des vies moyennes entre  $\theta^+$  et  $\theta^0$  à la condition (vraisemblablement satisfaite) que la particule soit scalaire. Elle permet de même, comme l'a fait remarquer WENTZEL <sup>(5)</sup>, de fixer entre des limites acceptables le rapport entre les deux modes de désintégration du  $\tau^+$ .

<sup>(1)</sup> M. GELL-MANN and A. PAIS: *Proceedings of Glasgow Conference on Nuclear and Meson Physics* (1954), p. 342.

<sup>(2)</sup> B. D'ESPAGNAT et J. PRENTKI: *Phys. Rev.*, **99**, 328 (1955); *Compt. Rend.*, **240**, 2486 (1955); *CERN Report* 55-11 (1955); *Nuclear Physics*, **1**, 33 (1956).

<sup>(3)</sup> G. RACAH: *Nuclear Physics*, sous presse.

<sup>(4)</sup> Remarque de R. H. DALITZ citée par R. E. MARSHAK: *Bull. Am. Phys. Soc.*, **30**, No. 8, 25 (1955).

<sup>(5)</sup> G. WENTZEL: *Phys. Rev.*, sous presse.



En raison des arguments rapportés ci-dessus, il est naturel d'admettre que les lois  $\Delta I = \pm \frac{1}{2}$ ,  $\Delta U = \pm 1$  gouvernent les interactions faibles des hyperons et des mésons lourds. Ces lois constituent la base de la théorie de ces interactions qui est présentée dans la section 2. Dans la section 3, le problème plus particulier de la construction explicite des hamiltoniens est étudié. Ceci conduit à la question de savoir si une théorie générale des interactions faibles est possible et au problème du choix des types d'interaction (concernant toutes les particules); tel est l'objet de la section 4. Dans la section 5 certaines répercussions des interactions fortes sur les processus de désintégration qui relèvent des interactions faibles sont étudiées à cause de leur importance dans l'interprétation des résultats expérimentaux. Enfin la section 6 est consacrée aux applications, d'une part de la théorie générale présentée dans la section 2, d'autre part des formalismes plus particuliers auxquels conduisent les méthodes de la section 3. Les applications de la théorie générale comportent en particulier une relation entre le rapport de branchement  $(\Sigma^+ \rightarrow n + \pi^+)/(\Sigma^+ \rightarrow p + \pi^0)$  d'une part et le rapport des vies moyennes de  $\Sigma^+$  et de  $\Sigma^-$  d'autre part. De telles relations, dont l'intérêt est d'être indépendantes du type de couplage choisi, semblent accessibles à l'expérience.

## 2. — Conséquences des règles $\Delta U = \pm 1$ , $\Delta I = \pm \frac{1}{2}$ .

La théorie des interactions fortes étant basée sur la notion d'espace du spin isotopique, il est naturel d'aborder celle des interactions faibles par des considérations portant sur le même espace. En ce qui concerne les interactions fortes on impose à l'hamiltonien d'être un isoscalaire vrai <sup>(2)</sup>. Il serait souhaitable d'obtenir pour les interactions faibles une règle analogue mais ici la non-conservation des quantités  $I$  et  $U$  rend la tâche moins aisée. Comme le nombre d'isofermions doit varier d'une unité, ainsi qu'il a été signalé plus haut, il est clair que chaque membre de l'hamiltonien doit contenir un nombre impair de champs isofermioniques. Ainsi la règle  $\Delta U = \mp 1$  a-t-elle pour conséquence nécessaire que  $\Delta I$  est demi-entier. Il convient maintenant d'introduire en outre la règle plus restrictive  $\Delta I = \pm \frac{1}{2}$ .

Cette règle est très analogue à celle qui régit les phénomènes nucléaires où un photon est émis ou absorbé, et qui s'exprime par  $\Delta I = \pm 1, 0$ . Or cette dernière loi se déduit mathématiquement du fait que l'hamiltonien d'interaction électromagnétique est la somme d'un isoscalaire et de la troisième composante d'un isopseudovecteur. Par analogie il est très naturel d'admettre dans le cas présent que l'hamiltonien des interactions faibles est une composante d'isospineur <sup>(6)</sup>, ce qui entraîne de la même manière la loi  $\Delta I = \pm \frac{1}{2}$ .

(6) B. D'ESPAGNAT et J. PRENTKI: *Compt. Rend.*, **242**, 740 (1956).

Pour obtenir des hamiltoniens de cette sorte, le plus simple est probablement d'utiliser le procédé qui sera exposé dans la section suivante. Il est toutefois essentiel de remarquer dès maintenant que certaines conséquences expérimentalement vérifiables peuvent être obtenues sans construire explicitement ces hamiltoniens: il suffit d'utiliser la méthode employée par WATSON <sup>(7)</sup> pour l'application à la photoproduction du formalisme du spin isotopique. De telles déductions sont évidemment indépendantes de toute hypothèse sur le type des interactions (FERMI, YUKAWA...). La méthode est aisément applicable à chaque cas particulier. Nous reviendrons sur ce sujet dans la section 6<sup>1</sup> où des exemples seront donnés.

### 3. — Construction des hamiltoniens.

Soit  $x = \begin{pmatrix} x_a \\ x_b \end{pmatrix}$  un isospineur de 1<sup>ère</sup> espèce, indépendant des coordonnées d'espace, qui ne représente qu'un artifice de calcul et auquel nulle signification ou interprétation physique ne sont données <sup>(8)</sup>. D'après les considérations de la référence <sup>(2)</sup>, on doit formellement faire correspondre à  $x$  une valeur  $+1$  de  $U$  et à  $x_a$  et  $x_b$  des « états de charge »  $+1$  et  $0$  respectivement.

Pour construire l'hamiltonien des interactions faibles, on utilise les règles suivantes. Formellement,

- 1) l'interaction doit contenir linéairement l'isospineur  $x$ ;
- 2) elle doit conserver le  $U$  total;
- 3) elle doit être un isoscalaire vrai (conserver le  $I$  total);
- 4) l'isospineur  $x$  doit être tel que dans la représentation où  $\tau_3$  est diagonal,  $\tau_3 = \begin{pmatrix} 1 & 0 \\ 0 & -1 \end{pmatrix}$ , il ne possède que la composante neutre;
- 5) la conservation des baryons est bien entendu imposée.

Étant donné que  $x$  a une valeur de  $U$  égale à  $1$ , les conditions 1) et 2) fournissent la loi  $\Delta U = \pm 1$  pour les particules en jeu. De même des conditions 1) et 3) résulte la loi  $\Delta I = \pm \frac{1}{2}$  puisque le spin isotopique de  $x$  est égal à  $\frac{1}{2}$ .

La condition 4) conduit à la loi absolue de la conservation de la charge des particules. En effet les conditions  $\Delta I_{\text{total}} = \Delta U_{\text{total}} = 0$  fournissent  $\Delta Q_{\text{total}} = 0$  d'où, grâce à 4)  $\Delta Q_{\text{particules}} = 0$ .

Les règles données ci-dessus conduisent bien (après suppression du symbole  $x_b$  de l'écriture) à une composante d'un isospineur de 1<sup>ère</sup> espèce formé à

<sup>(7)</sup> K. M. WATSON: *Phys. Rev.*, **85**, 852 (1952).

l'aide des opérateurs  $\tau_k$  et dans des champs des particules mises en jeu. Noter que l'emploi du  $x$  est essentiellement un artifice commode pour construire de la manière la plus générale possible des composantes d'isospineurs qui satisfassent à la conservation de la charge, à la règle  $\Delta U = \pm 1$  et, bien entendu, à la règle  $\Delta I = \pm \frac{1}{2}$ .

Afin de montrer comment il convient de procéder dans la pratique considérons le cas d'une interaction  $\Lambda$ ,  $\mathcal{N}$ ,  $\pi$  ( $\mathcal{N}$ : nucléon) dans l'hypothèse où celle-ci est due à un couplage direct. Le seul produit qu'il soit possible de former avec les champs (\*)  $\Lambda$ ,  $\mathcal{N}$ ,  $\pi$ ,  $x$  et qui satisfasse aux conditions 1) à 5) est

$$(1) \quad g\mathcal{N}\tau x\Lambda\pi + \text{c.c.}$$

qui développé, s'écrit

$$(2) \quad g[\sqrt{2}\bar{p}x_0\Lambda\pi + \sqrt{2}\bar{n}x_+\Lambda\pi^* + (\bar{p}x_+ - \bar{n}x_0)\Lambda\pi^0] + \text{c.c.}$$

On ne conserve que les termes en  $x_0$ , soit

$$(3) \quad g[\sqrt{2}\bar{p}\Lambda\pi - \bar{n}\Lambda\pi^0] + \text{c.c.},$$

termes qui décrivent les désintégrations  $\Lambda \rightarrow p + \pi^-$  et  $\Lambda \rightarrow n + \pi^0$  respectivement. Le rapport des constantes de couplage pour ces deux processus est ainsi déterminé (noter que l'exemple du  $\Lambda$  est trop simple pour être intéressant: le rapport de branchement, 2, se déduit de façon générale de la règle  $\Delta I = \frac{1}{2}$  qui impose au système final d'être dans un état  $\frac{1}{2}$  pur).

De même s'il existe un couplage direct pour l'interaction  $\Sigma$ ,  $\mathcal{N}$ ,  $\pi$  celui-ci s'écrit généralement,

$$(4) \quad g\bar{\mathcal{N}}x\Sigma\cdot\pi + ig'\mathcal{N}\tau x[\Sigma \times \pi] + \text{c.c.} \rightarrow \\ \rightarrow g\bar{n}(\Sigma^+\pi^* + \Sigma^-\pi + \Sigma^0\pi^0) + g'[\bar{n}(\Sigma^-\pi - \Sigma^+\pi^*) + \sqrt{2}\bar{p}(\Sigma^0\pi - \Sigma^+\pi^0)] + \text{c.c.}$$

expression où apparaissent cette fois deux constantes de couplage,  $g$ ,  $g'$  a priori indépendantes.

On pourrait multiplier de tels exemples et écrire des couplages directs  $\Xi$ ,  $\Lambda$ ,  $\pi$ ;  $\theta$ ,  $\mathcal{N}$ ,  $\mathcal{N}$  etc., comme aussi des couplages directs,  $\Lambda$   $\mathcal{N}$ ,  $\mathcal{N}$ ,  $\mathcal{N}$  etc. De façon générale il est clair que le présent formalisme réduit le nombre de constantes arbitraires (constantes de couplages relatives à chaque mode de désintégration).

(\*) Pour les opérateurs de champs  $\psi_\Lambda$ ,  $\psi_{\mathcal{N}}$  etc., la notation simplifiée  $\Lambda$ ,  $\mathcal{N}$  etc., est utilisée.

#### 4. — Discussion des différents types d'interaction.

Le formalisme décrit dans la section précédente, s'applique également bien aux divers types d'interactions faibles (Fermi, Yukawa, etc.), par suite il ne permet évidemment pas de faire un choix entre ces divers schémas possibles.

L'interaction universelle de Fermi rend remarquablement bien compte des phénomènes qui mettent uniquement en jeu les nucléons et les leptons. Une manière d'expliquer la désintégration du méson  $\pi$  est de la considérer comme un processus indirect faisant intervenir l'interaction précédente, à laquelle on doit alors donner la forme  $S \pm T + \sim 0.04A$ , forme qui n'est évidemment guère satisfaisante pour l'esprit. Il a été suggéré par DALLAPORTA <sup>(8)</sup> et GELL-MANN <sup>(9)</sup> d'étendre ce type d'interaction aux hyperons et aux mésons lourds et de supposer par conséquent que le couplage universel de Fermi régit toutes les interactions faibles. Ces auteurs ont montré que tous les différents modes de désintégration connus peuvent être décrits de cette manière, tout au moins qualitativement.

Il est difficile d'expliquer, si l'on s'en tient simplement à cette hypothèse, la différence des vies moyennes du  $\theta^+$  et du  $\theta^0$  par exemple. Remarquons toutefois qu'il est possible de conjuguer notre formalisme avec une telle théorie, mais uniquement bien entendu en ce qui concerne les interactions mettant en jeu un nombre impair d'isofermions.

Ceci permet de lever l'objection précédente mais risque d'en soulever de non moins graves. En effet, on ne voit actuellement aucune raison, si l'on fait usage dans la théorie des règles  $\Delta U = \pm 1$ ,  $\Delta I = \pm \frac{1}{2}$ , de traiter à pied d'égalité des processus qui, apparemment, n'obéissent pas à ces règles (radioactivité  $\beta$ , désintégration du méson  $\pi$ , ...) et des processus qui y obéissent. Il nous semble donc que la généralisation d'une interaction universelle de Fermi aux phénomènes en question, bien que possible et même sous certains aspects séduisante, constitue en définitive une hypothèse encore assez fragile qui est loin de donner entière satisfaction à certains égards.

Pour ces raisons on ne saurait à l'heure actuelle éliminer entièrement l'hypothèse selon laquelle existeraient aussi des interactions faibles du type de Yukawa. Il est en particulier fort concevable que les interactions qui mettent en jeu les règles  $\Delta U = \rightarrow 1$ ,  $\Delta I = \pm \frac{1}{2}$  soient de ce type. Peut être un avantage de cette manière de voir est-il de séparer de façon distincte les interactions qui conservent  $U$  de celles qui ne le conservent pas.

Bien entendu, cet avantage ne serait réel que dans le cas où la désintégra-

<sup>(8)</sup> N. DALLAPORTA: *Nuovo Cimento*, **1**, 962 (1955).

<sup>(9)</sup> M. GELL-MANN: *Report at the Pisa Conference on Elementary Particles* (1955), non publié.



tion  $\pi$ - $\mu$  pourrait s'expliquer à l'aide de la radioactivité  $\beta$ , qui du point de vue de la conservation de  $U$  est tout à fait analogue (\*). Ceci implique bien entendu la présence de 0.04 environ de couplage axial. Si l'analyse des spectres  $\beta$  en venait à exclure cette dernière possibilité il faudrait supposer un couplage direct de Yukawa entre  $\pi$ ,  $\mu$ ,  $\nu$ . Dans ces conditions, les hypothèses selon lesquelles les couplages  $\Delta U = \rightarrow 1$ ,  $\Delta I = \rightarrow \frac{1}{2}$  sont du type de Fermi ou du type de Yukawa, apparaîtraient a priori comme également légitimes.

Il nous semble donc que l'alternative suivante se pose: ou bien il existe environ 0.04 de couplage axial dans l'interaction  $\beta$  et l'on a uniquement deux genres d'interaction faibles ( $\Delta U = 0$ ,  $\Delta U = \pm 1$ ) qui peuvent être du même type (Fermi) ou de types différents (Fermi, Yukawa) ou bien la présence de couplage axial est définitivement exclue par l'expérience et alors trois genres d'interaction peuvent a priori exister: (Fermi,  $\Delta U = 0$ ), (Yukawa,  $\Delta U = 0$ ), (Fermi ou Yukawa,  $\Delta U = \pm 1$ ). D'une telle discussion on peut seulement conclure que la question de l'existence d'un faible pourcentage de couplage axial dans l'interaction  $\beta$  est d'un intérêt primordial.

## 5. — Effet des interactions fortes sur les désintégrations des hypérons et des mésons lourds.

Bien que les désintégrations soient essentiellement dues aux interactions faibles, il ne serait pas légitime de négliger complètement les influences que peuvent exercer sur ces processus, aux ordres supérieurs, les interactions fortes. Les corrections à apporter de ce fait peuvent être divisées en deux catégories, corrections de vertex et interactions dans l'état final.

On peut estimer raisonnablement que les corrections de vertex ne doivent pas apporter de modifications considérables: l'argument consiste à estimer l'« ordre » d'un graphe en utilisant la définition de l'« ordre » donnée par CHEW <sup>(10)</sup>: si  $f$  est la constante de couplage fort,  $g$  celle de couplage faible,  $n$  le nombre de vertex élémentaires d'interaction forte,  $m$  le nombre d'états intermédiaires pouvant « résonner » avec l'état initial, l'« ordre » défini par cet auteur est  $g \cdot f^{n-2m}$ . Il est alors facile de constater que toute correction de vertex est d'« ordre » supérieur ou égal à  $gf^2$ , c'est-à-dire d'« ordre » supérieur au graphe élémentaire dont on est parti: négliger de telles corrections constitue donc à tout le moins une approximation cohérente.

Il n'en va pas de même en ce qui concerne les interactions dans l'état final, les graphes correspondants pouvant très bien avoir l'« ordre »  $g$ : aussi convient-il d'étudier leur influence <sup>(6)</sup>.

(\*) Du moins dans l'hypothèse  $U_e - U_\mu - U_\nu = 0$ ; mais des hypothèses différentes ne semblent guère pouvoir améliorer la situation prise dans son ensemble.

<sup>(10)</sup> G. F. CHEW: *Phys. Rev.*, **94**, 1755 (1954).



Les états finaux sont composés soit de leptons pour lesquels cette interaction est négligeable, soit de deux ou plusieurs mésons  $\pi$  pour lesquels vraisemblablement l'interaction n'est pas encore appréciable aux énergies correspondant à la valeur  $Q$  des réactions, soit enfin d'un méson  $\pi$  et d'un baryon. C'est ce dernier cas qu'il convient d'examiner.

Soit d'abord un hyperon de spin isotopique  $(I, I_3)$  se désintégrant en un nucléon de spin isotopique  $(m = \frac{1}{2}, m_3)$  et un méson  $\pi$  de spin isotopique  $(t = 1, t_3)$  (\*). Soient, d'autre part,  $B_{I_3, m_3}^{I_3, m_3}$  ( $T_{I_3, m_3}^{I_3, m_3}$ ) les éléments de matrice des processus de désintégration lorsqu'on néglige (tient compte de) l'interaction dans l'état final. A partir d'un développement en approximations de Born successives on obtient l'équation (approximation de Tamm-Dancoff) reliant les  $T$  aux  $B$ , qui s'écrit

$$(6) \quad T_{I_3, m_3}^{I_3, m_3}(\mathbf{p}) = B_{I_3, m_3}^{I_3, m_3}(\mathbf{p}) + \sum_{m_3, \mathbf{q}} \frac{\mathcal{C}^{m_3, m_3'}(\mathbf{p}, \mathbf{q}) B_{I_3, m_3'}^{I_3, m_3'}(\mathbf{q})}{E_{\mathbf{p}} - E_{\mathbf{q}} + i\eta}$$

où  $\mathcal{C}^{m_3, m_3'}(\mathbf{p}, \mathbf{q})$  est l'élément de matrice de la diffusion élastique  $\pi$ -nucléon pris entre des états de moment relatif  $\mathbf{q}$  et  $\mathbf{p}$ .

On peut développer les quantités  $B_{I_3, m_3}^{I_3, m_3}$ ,  $T_{I_3, m_3}^{I_3, m_3}$  en valeurs propres du spin isotopique total  $i$  de l'état final. Anticipant légèrement sur ce qui formera le sujet de la section 6'1, on peut écrire de façon générale

$$(7) \quad B_{I_3, m_3}^{I_3, m_3} = \sum_i C_{1, \frac{1}{2}}(i, i_3, t_3, m_3) B_{I, i} C_{I_3, \frac{1}{2}}(i, i_3, I_3, -\frac{1}{2})$$

$$(8) \quad T_{I_3, m_3}^{I_3, m_3} = \sum_i C_{1, \frac{1}{2}}(i, i_3, t_3, m_3) T_{I, i} C_{I_3, \frac{1}{2}}(i, i_3, I_3, -\frac{1}{2}).$$

Portant (7) et (8) dans (6) on obtient après un calcul élémentaire

$$(9) \quad T_{I, i}(\mathbf{p}) = B_{I, i}(\mathbf{p}) + \sum_{\mathbf{q}} \frac{\mathcal{C}_i(\mathbf{p}, \mathbf{q}) B_{I, i}(\mathbf{q})}{E_{\mathbf{p}} - E_{\mathbf{q}} + i\eta}.$$

La matrice  $K$  correspondante est définie par

$$(10) \quad K_{I, i}(\mathbf{p}) = B_{I, i}(\mathbf{p}) + P \sum_{\mathbf{q}} \frac{\mathcal{K}_i(\mathbf{p}, \mathbf{q}) B_{I, i}(\mathbf{q})}{E_{\mathbf{p}} - E_{\mathbf{q}}},$$

la notation  $\mathcal{K}_i$  étant évidente.  $T$  et  $K$  sont alors liés par la relation

$$(11) \quad T_{I, i} = K_{I, i} - i\pi Q \mathcal{C}_i K_{I, i},$$

(\*) On a dans les cas étudié  $I_3 = m_3 + t_3 + \frac{1}{2} = i_3 + \frac{1}{2}$ .

où  $q$  est la densité des états finaux. La démonstration de (11) ne sera pas donnée ici car elle est très similaire à celle de l'équation de Heitler qui est bien connue <sup>(11)</sup>.

De (11) et de l'équation de Heitler relative à la diffusion élastique on déduit immédiatement que

$$(12) \quad T_{l,i} = K_{l,i} \frac{\mathcal{T}_i}{\mathcal{R}_i} = K_{l,i} \exp[i\delta_i] \cos \delta_i,$$

où  $\delta_i$  est le déphasage relatif à l'onde de spin isotopique  $i$ .  $\delta_i$  est une notation abrégée pour  $\delta_{l,J,i}$ , où  $J$ , le moment angulaire total, est égal au spin de l'hypéron initial et où  $l$  est déterminé par la parité de cet hypéron relative à celle du nucléon et par  $J$ .

On sait que la résolution numérique de l'équation de Tamm-Dancoff pour la diffusion élastique fournit  $\mathcal{R}_i(p, q)$  pour des valeurs arbitraires (non nécessairement égales), de  $p$  et de  $q$ . Ceci permet de calculer  $K_{l,i}$  à partir de l'équation (10). Si toutefois on désire seulement une première estimation il semble suffisant d'employer l'approximation

$$\frac{K_{l,i}}{\mathcal{R}_i} \approx \frac{B_{l,i}}{\mathcal{B}_i},$$

où  $\mathcal{B}_i$  est l'approximation de Born relative à la diffusion élastique dans l'onde  $i$ . L'équation (13) s'écrit alors

$$(14) \quad T_{l,i} = B_{l,i} z_i$$

avec

$$(15) \quad z_i = \frac{\mathcal{R}_i}{\mathcal{B}_i} \exp[i\delta_i] \cos \delta_i.$$

Étant donné que  $\mathcal{R}_i$  est pris maintenant pour  $q = p$  l'évaluation de  $\mathcal{R}_i/\mathcal{B}_i$  est simple. Un exemple sera donné dans la section suivante.

Connaissant les  $T_{l,i}$  on obtient les  $T_{l,i}^{I_3, m_3}$  nécessaires pour le calcul des diverses désintégration par la formule (8).

Le cas  $\Xi \rightarrow \Lambda + \pi$  se traite bien entendu de manière similaire mais nécessite une étude préalable de la diffusion  $\Lambda, \pi$ .

<sup>(11)</sup> M. GOLDBERGER: *Phys. Rev.*, **84**, 929 (1951).

## 6. — Désintégration des hyperons.

6.1. *Conséquences de la théorie générale.* — Comme il a été dit dans la section 2, il est possible de déduire certaines conséquences importantes du seul fait que l'hamiltonien est supposé être une composante d'isospineur, c'est-à-dire sans aucune hypothèse relative aux types des interactions faibles (Fermi ou Yukawa, par exemple).

Soit  $T_q^{\frac{1}{2}}$  une telle composante d'isospineur. Les éléments des matrices  $\langle i, i_3 | T_q^{\frac{1}{2}} | I, I_3 \rangle$  où  $(i, i_3)$  caractérise un état propre du spin isotopique total de l'état final peuvent s'écrire

$$(16) \quad \langle i, i_3 | T_q^{\frac{1}{2}} | I, I_3 \rangle = \langle i || T^{\frac{1}{2}} || I \rangle C_{I, \frac{1}{2}}(i, i_3, I_3, q).$$

Remarquons que si  $U_{in}$  et  $U_f$  sont les  $U$  initial et final, la conservation de la charge jointe à la relation  $Q = I_3 + U/2$  donne

$$(17) \quad q = i_3 - I_3 = \frac{U_{in} - U_f}{2} = -\frac{\Delta U}{2}.$$

Ainsi la loi  $\Delta U = \pm 1$  a-t-elle pour effet que la conservation de la charge est toujours satisfaite par l'une des deux valeurs possible du nombre quantique  $q$ , qui sont  $\pm \frac{1}{2}$ : par exemple pour la désintégration des hyperons  $q = -\frac{1}{2}$ .

Les formules (7) et (8) de la section 5, s'obtiennent immédiatement à l'aide de (16). La formule (8) entraîne, en ce qui concerne la désintégration des hyperons, les conséquences suivantes.

*Cas du  $\Lambda$ .* — D'après (8), ou d'après la règle  $\Delta I = \pm \frac{1}{2}$ , seul l'état final  $i = \frac{1}{2}$ ,  $i_3 = -\frac{1}{2}$  est possible. (8) donne le résultat connu

$$(18) \quad \frac{T_{(\Lambda \rightarrow p^-)}}{T_{(\Lambda \rightarrow n^0)}} = \frac{T_0^{0, \frac{1}{2}}}{T_0^{0, -\frac{1}{2}}} = -\sqrt{2},$$

le rapport de branchement des deux modes de désintégration du  $\Lambda$  est donc 2.

*Cas du  $\Xi$ .* — D'une manière analogue on peut calculer le rapport des vies moyennes du  $\Xi^0$  et du  $\Xi^-$ . Il vient

$$(19) \quad \tau^0/\tau^- = 2.$$

*Cas du  $\Sigma$ .* — Pour la désintégration du  $\Sigma^+$ , (8) donne

$$(20) \quad \frac{T(\Sigma^+ \rightarrow n^+)}{T(\Sigma^+ \rightarrow p^0)} = -\frac{2\sqrt{2} - \alpha}{2 + \sqrt{2}\alpha}$$

avec

$$(21) \quad \alpha = T_{1, \frac{3}{2}} / T_{1, \frac{1}{2}}.$$

Le rapport de branchement entre les deux modes de désintégration du  $\Sigma^+$ ,

$$(22) \quad \varrho = (\Sigma^+ \rightarrow n^+) / (\Sigma^+ \rightarrow p^0)$$

est donc

$$(22') \quad \varrho = \left| \frac{2\sqrt{2} - \alpha}{2 + \sqrt{2}\alpha} \right|^2.$$

D'autre part la probabilité totale de désintégration du  $\Sigma^+$  est proportionnelle à

$$(23) \quad |T(\Sigma^+ \rightarrow n^+)|^2 + |T(\Sigma^+ \rightarrow p^0)|^2 = |T_{1, \frac{1}{2}}|^2 + \frac{1}{4} |T_{1, \frac{3}{2}}|^2$$

et celle du  $\Sigma^-$  (avec le même coefficient de proportionnalité) à

$$(24) \quad \frac{3}{4} |T_{1, \frac{3}{2}}|^2$$

d'où, pour le rapport  $R$  des vies moyennes

$$(25) \quad R = \tau^- / \tau^+ = \frac{1}{3} + \frac{4}{3} |\alpha|^{-2}.$$

La quantité  $\alpha$  donnée par (22) est complexe. Il faut cependant noter que, grâce aux considérations de la section 5, l'argument de cette quantité complexe est connu si l'on connaît le spin et la parité du  $\Sigma$ , c'est-à-dire les moments angulaires total  $J$  et orbital  $l$  du système final: la formule (12) donne en effet

$$(26) \quad \alpha = \pm |\alpha| \exp [i(\delta_{l, J, \frac{3}{2}} - \delta_{l, J, \frac{1}{2}})],$$

où les  $\delta$  sont les déphasages de la diffusion élastique  $\pi$ -nucléon pour une énergie de  $Q = 115$  MeV dans le système c.m.

A l'aide de (26) il est possible d'éliminer  $\alpha$  entre (22') et (25). Ceci conduit à la relation

$$(27) \quad \cos^2 (\delta_{l, J, \frac{3}{2}} - \delta_{l, J, \frac{1}{2}}) = \frac{[9R - (3R + 1)(\varrho + 1)]^2}{8(\varrho + 1)^2(3R - 1)}$$

entre les rapports  $R$ ,  $\varrho$  et les déphasages. Une telle relation devrait être accessible à l'expérience. Il convient de remarquer que cette relation est très géné-

rale et découle uniquement du caractère isospinoriel de l'interaction. Si  $\Sigma$  est de la classe  $(\frac{1}{2}+)$  le premier membre de (27) est  $\cos^2(\delta_{31} - \delta_{11})$  selon les notations conventionnelles, donc très voisin de l'unité. Si  $\Sigma$  est de la classe  $(\frac{1}{2}-)$  ce même premier membre est  $\cos^2(\delta_3 - \delta_1)$ . Si  $\Sigma$  est de la classe  $(\frac{3}{2}+)$  il vaut  $\cos^2(\delta_{33} - \delta_{13})$ , quantité qui est voisine de zéro, enfin si  $\Sigma$  est de la classe  $(\frac{3}{2}-)$  ou de spin supérieur à  $\frac{3}{2}$  le premier membre de (27) fait intervenir uniquement les déphasages des ondes  $D$  et au dessus et est donc de nouveau très voisin de l'unité. On voit que de la mesure des rapports  $R$  et  $\varrho$  et de la relation (27) il est possible d'extraire certaines indications quant au spin et à la parité du  $\Sigma$ .

Le cas où  $\Sigma$  serait de la classe  $(\frac{3}{2}+)$  mérite une mention spéciale: en effet en raison du voisinage de la résonance il est alors hautement vraisemblable en raison de la formule (14), que  $|\alpha| \gg 1$  (cf. équ. (21)). (22') et (25) donnent alors <sup>(6)</sup> (\*):

$$(28) \quad \varrho \approx \frac{1}{2}; \quad R \approx \frac{1}{3}; \quad (\Sigma \in \frac{3}{2}+).$$

De façon générale (25) montre que  $1/R$  est nécessairement compris entre 0 et 3. Quant à  $\varrho$  on peut montrer par (22') que ses valeurs maxima et minimales sont données par les deux racines de l'équation

$$(29) \quad x^2 - x \left[ \frac{9}{2} \cot^2(\delta_{1,J,\frac{3}{2}} - \delta_{1,J,\frac{1}{2}}) + \frac{5}{2} \right] + 1 = 0.$$

6.2. *Usage d'interactions de Yukawa* - Les résultats de la section 6.1 sont comme il a été souligné, tout à fait généraux. Il faut s'attendre à ce que le formalisme développé dans la section 3 puisse apporter des précisions nouvelles en contrepartie des hypothèses qu'on est alors amené à introduire de surcroît. Si l'on admet par exemple que le type des interactions faibles est celui de Yukawa (cfr. section 4) il est possible à l'aide de la formule (4) d'évaluer les probabilités  $w$  des divers modes de désintégration des  $\Sigma$ . On a

$$(30) \quad w(\Sigma^+ \rightarrow n^+) = 2\pi\hbar^{-1} \left| \frac{2}{3}(-g + 2g')z_{\frac{1}{2}} - \frac{1}{3}(g + g')z_{\frac{3}{2}} \right|^2 \varrho_{\Sigma},$$

$$(31) \quad w(\Sigma^+ \rightarrow p^0) = 2\pi\hbar^{-1} \left| \frac{\sqrt{2}}{3}(-g + 2g')z_{\frac{1}{2}} + \frac{\sqrt{2}}{3}(g + g')z_{\frac{3}{2}} \right|^2 \varrho_{\Sigma}$$

$$(32) \quad 1/\tau_{\Sigma^-} = w(\Sigma^- \rightarrow n^-) = 2\pi\hbar^{-1}(g + g')^2(z_{\frac{3}{2}})^2 \varrho_{\Sigma},$$

(\*) En ce qui concerne la valeur de  $\varrho$  comparer avec HOLLADAY, réf. (12).

(12) W. G. HOLLADAY: *Bull. Am. Phys. Soc.*, II, 1, 51 (1956).



où  $\varrho_{\Sigma}$  est la densité des états finaux (\*). D'où en particulier

$$(33) \quad R = \tau^-/\tau^+ = (1 + 2\gamma^2)/3$$

avec

$$(34) \quad \gamma = z_{\frac{1}{2}}(z_{\frac{3}{2}})^{-1}(-g + 2g')(g + g')^{-1}.$$

Deux quelconques de ces quantités permettent d'obtenir les constantes  $g$  et  $g'$  relatives au  $\Sigma$ . On s'aperçoit aisément que le cas  $g = -g'$  et  $g = 2g'$  correspondent à des états finaux  $\frac{1}{2}$  pur et  $\frac{3}{2}$  pur respectivement. Ainsi le cas  $g = -g'$  doit être rejeté, à moins que la vie moyenne du  $\Sigma^-$  ne soit beaucoup plus longue que celle du  $\Sigma^+$ . Le cas  $g = g'$  impliquerait en approximation de Born ( $z_i = 1$ ) que  $\Sigma^-$  se désintègre uniquement en  $p + \pi^0$ . Toutefois l'interaction dans l'état final modifie ce résultat: si par exemple  $\Sigma$  a le spin  $\frac{1}{2}$  et la parité  $+$ , le rapport  $\varrho$  défini par (22) devient égal à  $2/25$ ; si  $\Sigma$  est une particule ( $\frac{3}{2}+$ ),  $\varrho$  devient égal à  $\frac{1}{2}$ , résultat déjà obtenu d'une manière plus générale (cf. section 6.1).

A partir de l'hamiltonien (3) on obtient d'une façon analogue les probabilités de désintégration du  $\Lambda$

$$(35) \quad w(\Lambda \rightarrow n^0) = \frac{1}{2}w(\Lambda \rightarrow p^+) = 2\pi\hbar^{-1}g_{\Lambda}^2(z_{\frac{1}{2}})^2\varrho_{\Lambda},$$

où cette fois  $z_{\frac{1}{2}}$  doit être évalué pour l'énergie 37 MeV.

Enfin pour  $\Xi$  on obtient de même

$$(36) \quad \frac{1}{2}w(\Xi^- \rightarrow \Lambda + \pi^-) = w(\Xi^0 \rightarrow \Lambda + \pi^0) = 2\pi\hbar^{-1}g_{\Xi}^2(z_1)^2\varrho_{\Xi}.$$

$z_1$  peut être calculé par une méthode de Tamm-Dancoff appliquée à la diffusion  $\pi$ - $\Lambda$ .

Les formules précédentes permettent en principe de déterminer les diverses constantes  $g$  à partir de l'expérience. Malheureusement les connaissances expérimentales dans ce domaine sont encore trop préliminaires. Il est clair que l'on peut toutefois faire à priori des hypothèses plus ou moins plausibles sur les valeurs relatives de ces constantes et en tirer des relations entre les diverses probabilités de désintégration. Ainsi, par exemple, il serait séduisant de supposer que toutes ces constantes sont égales. Cependant afin de vérifier une telle hypothèse il nous semble essentiel de tenir compte de l'influence des

(\*) Les  $z$  sont donnés par (15). Ainsi si  $\Sigma$  est de la classe ( $\frac{1}{2}+$ ) les formules (1') de CHEW (réf. (13)) fournissent aisément  $\mathcal{K}_{\frac{1}{2}}/\mathcal{B}_{\frac{1}{2}} \approx \frac{1}{3}$ ,  $\mathcal{K}_{\frac{3}{2}}/\mathcal{B}_{\frac{3}{2}} \approx \frac{2}{3}$ , ceci en raison du voisinage de la résonance  $I=J=\frac{3}{2}$ .

(13) G. F. CHEW: *Phys. Rev.*, **89**, 591 (1953).

interactions fortes, évaluée dans la section 5. Remarquons que l'hypothèse de constantes de Yukawa égales semble difficilement compatible avec celle d'un  $\Sigma$  de la classe  $(\frac{1}{2}+)$  étant donné la faible valeur du rapport de branchement dans ce cas (voir plus haut). Elle ne serait pas incompatible avec un  $\Sigma$  de la classe  $\frac{3}{2}+$ .

Du point de vue des considérations qui précèdent, l'hypothèse selon laquelle les interactions faibles seraient du type de Fermi est moins attrayante, non seulement à cause de la plus grande complexité des graphes mais surtout à cause du fait que le nombre de constantes arbitraires mises en jeu est alors plus grand.

## 7. — Conclusion.

Pour résumer, l'essentiel de ce travail se trouve dans l'hypothèse selon laquelle l'hamiltonien des interactions faibles est une composante d'un isospineur (règle  $\Delta I = \pm \frac{1}{2}$ ). De cette hypothèse des conclusions expérimentalement vérifiables peuvent être déduites, dont certaines sont tout à fait indépendantes de la forme exacte des termes d'interaction ainsi que des constantes de couplage: des exemples ont été donnés dans la section 6.1. Une autre propriété générale concerne, rappelons-le, les lois de désintégration du  $\theta^+$  et du  $\theta^0$ : la forme isospinorielle du terme d'interaction assurant la validité de la règle  $\Delta I = \pm \frac{1}{2}$  interdit de ce fait (\*)  $\theta^+ \rightarrow \pi^+ + \pi^0$ , ce qui signifie que la vie moyenne du  $\theta^+$  est beaucoup plus longue que celle du  $\theta^0$ .

D'autre part nous avons pu expliciter les hamiltoniens, ceci à l'aide de l'artifice de l'isospineur  $x$ , ce qui nous aurait permis, moyennant certaines hypothèses sur les constantes de couplage, d'obtenir des relations entre les probabilités des différents modes de désintégration des diverses particules et les vies moyennes. Le problème de l'influence des interactions fortes sur les processus de désintégration a été envisagé et il se trouve, tout au moins dans le cas des désintégrations des hypérons, que cet effet peut être important. On doit donc en tenir compte pour l'établissement ou la vérification de l'hypothèse attribuant aux rapports entre les constantes de couplage des valeurs numériques simples ou, ce qui serait plus séduisant encore, la valeur 1.

---

(\*) Pour  $\theta$  scalaire.

## Note sur épreuves.

Après envoi à l'Editeur du présent article, nous avons eu connaissance du travail de R. GATTO: *Nuovo Cimento*, 2, 318 (1956) qui propose la même hypothèse et parvient à des résultats similaires à plusieurs égards à ceux présentés ici.

Enfin il semble se dégager de la discussion de la section 4 qu'aucune raison profonde n'existe à l'heure actuelle pour croire à une interaction généralisée de Fermi représentant toutes les interactions faibles, y compris celles des hyperons et mésons lourds. Une interaction du type de Yukawa mettant en jeu ces particules aurait tout au moins le mérite de la simplicité.

#### RIASSUNTO (\*)

Per giustificare la regola di selezione  $\Delta I = \frac{1}{2}$  che sembra presiedere al decadimento degli iperoni e dei mesoni pesanti si prende la relativa hamiltoniana di interazione come la componente di uno spinore di prima specie nello spazio isotopico. Questo è sufficiente a fornire senza ulteriori ipotesi riguardo ai tipi di interazione e al numero di hamiltoniane indipendenti, alcune relazioni (v. Sez. 6) suscettibili di essere saggiate sperimentalmente e di fornire anche elementi, specialmente sullo spin e la parità dei  $\Sigma$ . Ciò è in parte dovuto al fatto che lo scattering nello stato finale influenza in una certa misura le probabilità di decadimento. Si dà anche un mezzo opportuno per scrivere le suddette hamiltoniane in forma esplicita. Ciò porta alla discussione sulla scelta tipo Fermi-tipo Yukawa. Allo stato attuale delle cose non si possono portare argomenti convincenti a favore di uno dei due tipi. Scegliendo, a causa della sua maggior semplicità, un tipo Yukawa, si esaminano le conseguenze di alcune scelte naturali delle costanti di accoppiamento.

---

(\*) Traduzione a cura della Redazione.

## On the Limit of Applicability of Quantum Electrodynamics.

S. KAMEFUCHI

*Institute of Theoretical Physics, Nagoya University, Japan*

H. UMEZAWA

*Department of Physics, University of Tokyo, Japan*

(ricevuto il 20 Febbraio 1956)

**Summary.** — The general features of the  $Z_3$ -factor or those of the *normal zone* of the renormalized charge in quantum electrodynamics are discussed in detail by use of the method of *renormalization cut-off* developed in our previous paper. It is found that the renormalization theory of quantum electrodynamics is consistent only when we introduce the cut-off momentum  $\Lambda$  which is smaller than  $\lambda = m \exp [3\pi \cdot 137/2]$ . The peculiar features are also discussed which appear in connection with the state of negative norm unless we introduce a suitable cut-off factor.

### 1. — Introduction.

As is well known the renormalized quantum electrodynamics needs to satisfy several requirements in order to be considered a consistent theory. At first, some formal conditions are to be satisfied for the  $Z$ -factors <sup>(1)</sup>, or what is the same thing, corresponding conditions must hold for the renormalized propagators  $S_c$  and  $D_c$ . Furthermore there is an important question to be examined of whether or not the *normal zone*  $N(e_r)$  for the renormalized charge  $e_r$  really includes the observed value  $e_{ob} = 1/\sqrt{137}$ . Recently, KÄLLÉN <sup>(2)</sup> has shown that at least one of the renormalization constants is to be divergent. But the most im-

<sup>(1)</sup> Throughout this paper we shall use the same notations as in our previous paper: H. UMEZAWA, S. KAMEFUCHI, Y. TOMOZAWA and M. KONUMA: *Nuovo Cimento*, **3**, 772 (1956), which will be referred to as I.

<sup>(2)</sup> G. KÄLLÉN: *Dan. Mat. Fys. Medd.*, **27**, No. 12 (1953).

portant criterion may be found in the condition for the  $Z_3$ -factor, since this is a gauge invariant quantity contrary to the factors  $Z_1$  or  $Z_2$  (cf. I, Sect. 5). From the arguments developed by LEHMANN<sup>(3)</sup>, it is an easy matter to show that, for the photon propagator,  $\int \kappa^2 \varrho(\kappa^2) d\kappa^2 = 0$ , that is,  $\varrho(\kappa^2) \propto \delta(\kappa^2)$ . This curious result seems to suggest that the normal zone for  $e_r$  is restricted only to the zero point. This may easily be anticipated if one remembers that in this case the transition matrix-elements, being functions of  $e_r$ , have vanishing values for the transition from one photon state to many particle states. It is the aim of the present paper to examine in detail the problem of the normal zone for  $e_r$  along the line of arguments developed in I and thus to make clear to what extent the present framework of quantum electrodynamics can give the correct answers for electromagnetic phenomena.

In the previous paper I, we described a way for calculating the renormalized propagators  $G_c$ . We shall now apply it to obtain the renormalized propagator  $D_c(k^2)$  of the photon. To do this, we should first calculate the factor  $Z_3(\Lambda^2, e_{ob})$  corresponding to various values of  $\Lambda$  by means of the *renormalization cut-off*. For we have already proved the relations (cf. (I.54))

$$(1) \quad D_c(k^2) = D_F(k^2) R_c(-k^2, e_{ob}),$$

$$(2) \quad R_c(-k^2, e_{ob}) = 1/Z_3(-k^2, e_{ob}).$$

As was discussed in I (Sect. 4), the real part of  $Z_3(\Lambda^2, e_{ob})$ , i.e.  $Z_3^R(\Lambda^2, e_{ob})$ , can be approximately calculated by means of the straight cut-off, instead of using the renormalization cut-off. The straight cut-off leads to  $Z_3^R(-k^2, e_{ob})$  with the error of  $O(m^2/k^2) \log(m^2/k^2)$ . On the other hand the imaginary part of  $Z_3(-k^2, e_{ob})$ , i.e.  $Z_3^I(-k^2, e_{ob})$  is known to be finite even if we go to the limit  $-k^2 \rightarrow \infty$ .

The calculation of  $Z_3(\Lambda^2, e_{ob})$  will be carried out in Sect. 2 under the assumption that the vacuum polarization comes mainly from the contribution of high energy-momenta ( $|k^2| \sim \Lambda^2$ ). This assumption may be justified if the vacuum polarization is given by a logarithmically divergent integral as it is in the perturbation expansion (\*).

Then, it will be found in Sect. 2 that the observed charge  $e_{ob} = 1/\sqrt{137}$

(3) H. LEHMANN: *Nuovo Cimento*, **11**, 342 (1954).

(\*) It may be instructive to remember LEHMAN's result<sup>(3)</sup> that the exact propagator of the electron has the same or a stronger singularity as that of the free electron, when there appear no contributions of states of negative probabilities to the propagator of the electron. This suggests that the vacuum polarization is given by a divergent integral. In such a case, our way for estimation of the vacuum polarization effect may give the highest order term of the divergence, which appears to be logarithmic.



is out of the normal zone  $N(e_r)$  of the renormalized charge, and the real part of  $R_c$  becomes negative for  $-k^2 > \lambda^2 \gg m^2$ . The value of  $\lambda^2$  will also be given there.

If we disregard the effects of particles with  $-k^2 > \lambda^2$  (and therefore simply replace  $G_c(k^2, e_{ob})$  for  $-k^2 > \lambda^2$  by zero), the normal zone  $N(e_A)$  turns out to include  $e_{ob} = 1/\sqrt{137}$ . Thus, we see that the renormalization theory may not lead to reasonable answers for high energy ( $-k^2 > \lambda^2$ ) phenomena, which depend essentially on  $G_c(k^2, e_{ob})$  with  $-k^2 > \lambda^2$ . To construct a consistent renormalization theory, therefore, it seems necessary to find out an other physical effect which radically changes the  $R_c(-k^2, e_{ob})$  for  $-k^2 > \lambda^2$ . Since we have never observed particles of masses larger than  $\lambda$  we cannot expect that to take account of any other effects due to mesons, nucleons and hyperons essentially improves the situation as far as they are subject to the renormalizable interactions (i.e., those of the first kind <sup>(4)</sup>). The detailed discussion of  $R_c(-k^2, e_{ob})$  in the renormalizable quantum electrodynamics will be given in Sect. 3.

## 2. - The Function $Z_3(-k^2, e_{ob})$ .

As shown in I, Sect. 5, the propagator  $D_{\mu\nu}(k)$  of a photon has the form:

$$(3) \quad D_{\mu\nu}(k) = \left\{ \delta_{\mu\nu} - \frac{k_\mu k_\nu}{k^2} \right\} D(k^2) + k_\mu k_\nu D_t(k^2).$$

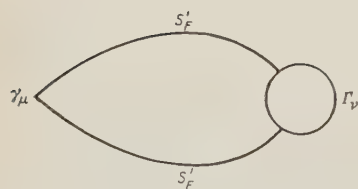


Fig. 1.

Here  $D(k^2)$  satisfies the equation:

$$(4) \quad \{k^2 + \Pi(k^2)\} D(k^2) = 1.$$

The function  $\Pi(k^2)$  is defined by the polarization operator  $\Pi_{\mu\nu}(k)$  in the following way:

$$(5) \quad \Pi_{\mu\nu}(k) = \left\{ \delta_{\mu\nu} - \frac{k_\mu k_\nu}{k^2} \right\} \Pi(k^2).$$

Fig. 1 shows the Feynman diagram corresponding to  $\Pi_{\mu\mu}$ : Thus,  $\Pi_{\mu\nu}$  is obtained in the form:

$$(6) \quad \Pi_{\mu\nu}(k) = e^2 \int d^4t \operatorname{Tr} [S'_F(k-t) \gamma_\mu S'_F(t) \Gamma_\nu(k-t, t)].$$

<sup>(4)</sup> S. SAKATA, H. UMEZAWA and S. KAMEFUCHI: *Phys. Rev.*, **84**, 154 (1951); *Prog. Theor. Phys.*, **7**, 377 (1952).

We now apply the renormalization cut-off (cf. I, Sect. 1) to all the calculations of integrals over internal momenta. Then, (I.18*a, b*) and (I.39) tell us that

$$(7a) \quad S'_F(t) = Z_2^R(\Lambda, e_A) S_{FC}(t, e_A),$$

$$(7b) \quad \Gamma_\mu(t_1, t_2) = (Z_1^R(\Lambda, e_A))^{-1} \Gamma_{\mu c}(t_1, t_2, e_A).$$

As shown in I, the renormalized quantities  $S_{FC}$  and  $\Gamma_{\mu c}$  are independently of  $\Lambda$  except through the renormalized charge  $e_A$ , which is defined by

$$(8) \quad \left\{ \begin{array}{l} e_A^2 = e^2 Z_3^R(\Lambda^2, e_A) (Z_2^R(\Lambda, e_A) / Z_1^R(\Lambda, e_A))^2 \\ \text{or} \\ \quad = e^2 Z_3^R(\Lambda^2, e_A) \end{array} \right.$$

on account of the relation (cf. (I.45)):

$$(9) \quad Z_1^R(\Lambda, e_A) = Z_2^R(\Lambda, e_A).$$

By substituting (7*a, b*) into (6), we obtain the  $\Pi_{\mu\nu}(k)$  calculated by the renormalization cut-off method:

$$(10) \quad \Pi_{\mu\nu}(k) = e_A^2 (Z_3^R(\Lambda^2, e_A))^{-1} Z_1^R(\Lambda, e_A) \cdot \int d^4t \operatorname{Tr} [S_{FC}(k-t, e_A) \gamma_\mu S_{FC}(t, e_A) \Gamma_{\nu c}(k-t, t, e_A)].$$

We now assume that the particles with large momentum (i.e.  $-i\gamma t \sim \Lambda$ ) mainly contribute to the integration (10). Then, we may disregard  $k$  as compared with  $t$  and may use the asymptotic expressions for  $S_{FC}$  and  $\Gamma_{\nu c}$  (I.52*b*) and (I.49) (\*);

$$(11) \quad S_{FC}(t, e_A) = S_F(t) / Z_2(-i\gamma t, e_A),$$

$$(12) \quad \Gamma_{\mu c}(t, t, e_A) = \gamma_\mu Z_1(-i\gamma t, e_A),$$

for  $-i\gamma t \sim \Lambda \gg m$ .

After replacing  $-i\gamma t$  in  $Z_1(-i\gamma t, e_A)$  and  $Z_2(-i\gamma t, e_A)$  with  $\Lambda$ , (10) turns out to be

$$(13) \quad \Pi_{\mu\nu}(k) = e_A^2 (Z_3^R(\Lambda^2, e_A))^{-1} \int d^4t \operatorname{Tr} [S_F(k-t, e_A) \gamma_\mu S_F(t) \gamma_\nu].$$

(\*) It should be noted that these asymptotic expressions also hold true in the space-like region of the argument.

Here we have neglected the imaginary term  $iZ'_3/Z^2_3$  which approaches zero in the limit  $\Lambda \rightarrow \infty$ . The integration in (13) is nothing but the lowest order term of the perturbation expansion for the vacuum polarization term.

We shall calculate the integration in (13) by using the straight cut-off instead of using the renormalization cut-off; the error induced in this way is made up of terms of  $O(m/\Lambda) \log(m/\Lambda)$  (cf. I, Sect. 6). Then, we obtain

$$(14) \quad \int d^4t \operatorname{Tr}[S_F(k-t)\gamma_\mu S_F(t)\gamma_\nu] \sim \\ \sim \left( \delta_{\mu\nu} - \frac{k_\mu k_\nu}{k^2} \right) k^2 \left\{ \frac{1}{3\pi} \log \frac{\Lambda^2}{m^2} + f(k^2) \right\} \quad \text{for } \Lambda^2 \gg m^2,$$

where  $f(k^2)$  is a function satisfying the relation

$$(15) \quad f(0) = 0.$$

From (13), (14) and (5) we obtain

$$(16) \quad \Pi(k^2) = \frac{1}{Z^R_3(\Lambda^2, e_A)} \left( \frac{e_A^2}{3\pi} \log \frac{\Lambda^2}{m^2} + e_A^2 f(k^2) \right) k^2 \quad \text{for } \Lambda^2 \gg m^2.$$

Using (I.83) we obtain

$$(17) \quad \frac{1}{Z^R_3(\Lambda^2, e_A)} = \frac{\partial}{\partial k^2} \{ k^2 + \Pi(k^2) \} \Big|_{k^2=0} = \\ = 1 + \frac{1}{Z^R_3(\Lambda^2, e_A)} \frac{e_A^2}{3\pi} \log \frac{\Lambda^2}{m^2} \quad \text{for } \Lambda^2 \gg m^2,$$

which finally leads to

$$(18) \quad Z^R_3(\Lambda^2, e_A) = 1 - \frac{e_A^2}{3\pi} \log \frac{\Lambda^2}{m^2} \quad \text{for } \Lambda^2 \gg m^2.$$

### 3. - Discussions.

The relation (17) leads to

$$(19) \quad e_A^2 = \frac{e^2}{1 + (e^2/3\pi) \log(\Lambda^2/m^2)} \quad \text{for } \Lambda^2 \ll m^2.$$

This shows that, when  $e^2$  runs from 0 to  $\infty$ ,  $e_A^2$  does from 0 to  $((1/3\pi) \log(\Lambda^2/m^2))^{-1}$ . This defines the normal zone  $N(e_A)$ . When taking  $\Lambda$  to

be infinite  $e_A$  and  $N(e_A)$  approach  $e_r$  and  $N(e_r)$ , respectively. Thus, we see that any real value (except zero) of the observed charge  $e_{ob}$  is out of  $N(e_r)$ .

The renormalized propagator of a photon can be obtained from (1) and (2), with  $R_c$  given by

$$(20) \quad R_c(-k^2, e_{ob}) = \frac{1}{1 - (e_{ob}^2/3\pi) \log(-k^2/m^2) + iZ^I(-k^2, e_{ob})} \quad \text{for } -k^2 \gg m^2.$$

Thus, we see that the real part of  $R_c$ ,  $\text{Re}[R_c]$ , changes its sign at

$$(21) \quad -k^2 = \lambda^2 \equiv m^2 \exp[3\pi/e_{ob}^2]$$

and

$$(22) \quad \text{Re}[R_c(-k^2, e_{ob})] < 0 \quad \text{for } -k^2 > \lambda^2.$$

Fig. 2 shows a qualitative feature of the real part of  $R_c$  for large  $|k^2|$ . It should be noted that the imaginary correction term, makes the real part of  $R_c$  continuous at  $k^2 = -\lambda^2$ , where  $\text{Re}[R_c]$  changes its sign (cf. Fig. 2 in I). Suppose  $\Lambda$  is left finite, and further, the cut-off procedure is applied to all the integrals appearing in the  $S$ -matrix. This means that  $D_c(k^2)$  for  $-k^2 > \Lambda^2$

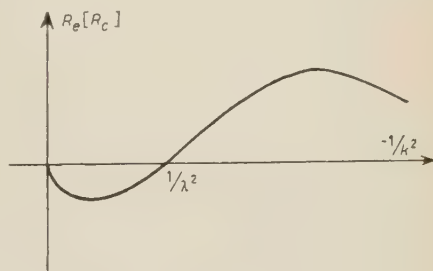


Fig. 2.

are all to be disregarded in the calculation. When  $\Lambda > \lambda$ , we find from (18) that  $Z_3^R(\Lambda, e_{ob})$  is still negative;  $e_{ob}$  is out of the normal zone  $N(e_A)$  for  $e_A$ .

When  $\Lambda < \lambda$ ,  $Z_3^R(\Lambda, e_{ob})$  turns out to be positive and  $N(e_A)$  now contains  $e_{ob}$ .

This can be more clearly seen from Fig. 3, which shows graphically the quantity:

$$(23) \quad \varepsilon^2(-k^2, e_{ob}) \equiv e_{ob}^3/Z_3^R(-k^2, e_{ob}).$$

Regarding  $e_{ob}$  as  $e_A$ , we see from (8) that

$$\varepsilon(\Lambda^2, e_{ob}) = e.$$

In other words,  $\varepsilon(-k^2, e_{ob})$  with  $-k^2 = \Lambda^2$  is equal to the unrenormalized charge

$e$ , which leads to  $e_A = e_{ob}$ . Fig. 3 shows that  $\varepsilon^2$  can be positive only when  $\Lambda < \lambda$ .

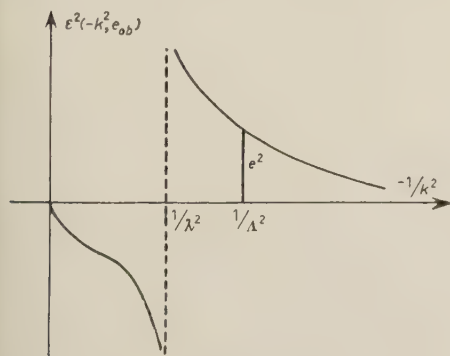


Fig. 3.

Thus, we see that, in order to make the renormalization theory consistent, we shall have to find some physical effects which change the sign of the real part of  $R_c(-k^2, e_{ob})$  (or of  $D_c(k^2)$  for  $-k^2 > \lambda^2$ ). It is quite interesting therefore to find high-energy phenomena, to which  $D_c(k^2)$  for  $-k^2 > \lambda^2$  gives essential contributions and, therefore to which the present renormalization theory cannot be applied. Since the observed value of charge is given by

$$e_{ob} = 1/\sqrt{137},$$

we obtain

$$(24) \quad \lambda^2 = m^2 \exp [3\pi \cdot 137].$$

So far we have considered only the system of electron (mass:  $m$ ) and photon. If we suppose that there exist in nature  $n$  charged spinor particles (mass:  $E_1m, E_2m, \dots, E_nm$ ) and  $l$  charged spinless particles ( $s_1m, s_2m, \dots, s_lm$ ), (18), (19), (20) and (21) shall be replaced, respectively, by

$$(25) \quad Z_3^R(\lambda^2, e_\lambda) = 1 - \frac{e_\lambda^2}{3\pi} K(\lambda^2),$$

$$(26) \quad e_{ob}^2 = \frac{e^2}{1 + (e^2/3\pi) K(\lambda^2)},$$

$$(27) \quad R_c(-k^2, e_{ob}) = \frac{1}{1 - (e_{ob}^2/3\pi) K(-k^2) + iZ_3^I(-k^2, e_{ob})} \quad \text{for } -k^2 \gg m^2,$$

$$(28) \quad \lambda^2 = m^2 \left[ \prod_{i=1}^n E_i \prod_{j=1}^l (s_j)^{\frac{1}{2}} \right]^{2/(n+(l/4))} \exp \left[ \frac{3\pi}{(n + (l/4))e_{ob}^2} \right].$$

Here  $K$  is defined by

$$(29) \quad K(-k^2) = \sum_{i=1}^n \log \left[ \frac{-k^2}{(E_i m)^2} \right] + \frac{1}{4} \sum_{j=1}^l \log \left[ \frac{-k^2}{(s_j m)^2} \right].$$

If  $\lambda$  is larger than the mass of any particle among them, the above results for  $R_c$  seem to be left unchanged, even if we take into account interactions of heavy particles as far as they are subject to renormalizable interactions (i.e., those of the first kind <sup>(4)</sup>). In other words, as far as we remain in the framework of renormalizable field theory, the inclusion of any other effects can never improve the situation. On the contrary, if  $\lambda$  were smaller than any one of the masses we would have no consistent electrodynamics for such a particle.



We are now in a position to discuss the reasons why the renormalization theory (with the use of perturbation approximation) has achieved brilliant successes in the realm of quantum electrodynamics. The first reason is found in the point that the magnitude of  $\lambda$  is quite large. This is an immediate consequence of the smallness of  $e_{ob}$  as seen from (21). The second reason lies in its property of gauge invariance. By virtue of this property, in the low energy limit on the one hand higher order radiative corrections contribute only to the renormalization of the lowest order term, and in the high energy region on the other the radiative corrections of vertices and propagators  $Z_1(-i\gamma t)$ ,  $Z_2(-i\gamma t)$  compensate each other to approach the lowest order term of the perturbation expansion but with the renormalized charge  $e$  (not  $e$ ).

If we assume  $\Lambda < \lambda$ , we find that

$$(30) \quad \frac{e_{ob}^2}{3\pi} \log \left( \frac{-k^2}{m^2} \right) < 1 \quad \text{for } -k^2 < \Lambda^2.$$

Thus, by taking  $e_{ob} = 1/137$ , we obtain

$$(31) \quad \frac{e_{ob}^2}{3\pi} e_{ob}^{2n} \log \left( \frac{-k^2}{m^2} \right) < \left( \frac{1}{137} \right)^n \quad \text{for } n \geq 1, -k^2 < \Lambda^2.$$

This shows the reason why our results for  $D_c(k^2)$  and  $e_{-1}^2$  agree with those obtained by LANDAU *et al.* <sup>(5)</sup>. Indeed, they assumed (30) in their discussion to derive asymptotic forms for  $S_F$ ,  $D_F$ ,  $\Gamma_\mu$ .

We shall now consider the Feynman diagram in Fig. 4. The matrix element corresponding to this diagram can be derived from that of the perturbation expansion by replacing  $e$  by the effective charge defined by

$$e_{eff}(-k^2) = e_{ob}(R_c(-k^2, e_{ob}))^{\frac{1}{2}}.$$

Thus, it appears possible that the scattering cross-section with high momentum transfer ( $|k^2| \gtrsim \lambda^2$ ) essentially depends on the effective charge, and therefore, on  $R_c(-k^2, e_{ob})$  with  $-k^2 \gtrsim \lambda^2$ . In this region of energy the Coulomb interaction takes the different sign from the usual one. We can expect that correct theory may change the sign of the real part of  $R_c$  with  $-k^2 > \lambda^2$  and so recover the

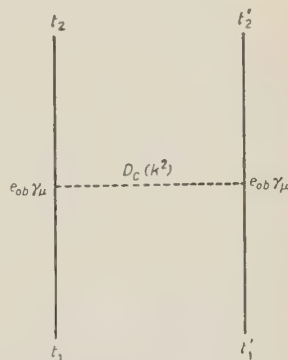


Fig. 4.

<sup>(5)</sup> L. D. LANDAU, A. A. ABRIKOSOV and I. M. HALATNIKOV: *Dokl. Akad. Nauk SSSR*, **95**, 497, 733, 1177 (1954); **96**, 261 (1954); L. D. LANDAU and I. POMERANČUK: *Dokl. Akad. Nauk SSSR*, **102**, 489 (1955). In this connection see also R. P. FEYNMAN: *Proc. Fifth Rochester Conference*, 95 (1955).

correct sign of the Coulomb interaction. In order to determine rigorously the effective charge by means of scattering experiments, we should calculate the function  $\Gamma_{\mu c}(t_1, t_2)$  because  $\gamma_\mu$  in Fig. 4 should be replaced by  $\Gamma_{\mu c}$ .

As stated above, in quantum electrodynamics the existence of other elementary particles cannot essentially change the difficult situation. The final solution of the difficulty may rather be sought in connection with the introduction of a new fundamental length or more specifically with the structure of space-time itself (the effect of the gravitational field) (\*). In  $(ps)$ -( $ps$ ) meson theory similar arguments seem to suggest that  $\lambda$  may take the order of magnitude of the nucleon mass. Thus, the failure of the theory may easily be found experimentally as far as we are only concerned with the meson-nucleon interaction. Hence, quite contrary to the situation in quantum electrodynamics, the existence of heavy mesons and hyperons, which have masses comparable to  $\lambda$ , may play a decisive role in the problem of the normal zone (+).

\* \* \*

The authors wish to express their appreciation of enlightening discussions by members of the symposium on field theory held on November 1955 at the Research Institute for Fundamental Physics. Thanks are also due to Professors H. YUKAWA, S. SAKATA, Z. Koba and Y. KATAYAMA for kind interest and encouragement and to Messrs. Y. TOMOZAWA and M. KONUMA for helpful conversation and assistance.

(\*) We can expect that the fundamental length may be introduced into quantum electrodynamics through the intermediary of interactions of the second kind (4) in which the electron participates, that is, the Fermi interaction ( $\mu$ -e-decay,  $\beta$ -decay) and the gravitational interaction. From order of magnitude considerations they are supposed to be effective in the energy region  $k \sim 5 \cdot 10^5 m$  and  $k \sim 2 \cdot 10^{22} m$ , respectively. As these values are small compared with the cut-off value (28) in the text  $\lambda = 10^{23} m$ , their contribution may play an essential role in the discussion of the limit of applicability.

(+) As to this point, authors are very much indebted to Dr. K. SAWADA for his inspiring discussions.

#### RIASSUNTO (\*)

Si discutono dettagliatamente, usando il metodo del *taglio di rinormalizzazione* esposto in un nostro precedente lavoro, le caratteristiche generiche del fattore  $Z_3$  o quelle della *zona normale* della carica rinormalizzata in elettrodinamica quantistica. Si trova che la teoria della rinormalizzazione dell'elettrodinamica quantistica è compatibile solo introducendo il momento di taglio  $\lambda$  che è minore di  $\lambda = m \exp [3\pi \cdot 137/2]$ . Si discutono anche gli aspetti particolari che sorgono in connessione allo stato di norma negativa a meno di introdurre un opportuno fattore di taglio.

(\*) Traduzione a cura della Redazione.

## The Evidence from Angular Correlations on the Spin of the $\Lambda^0$ .

G. MORPURGO

*Scuola di Perfezionamento in Fisica Nucleare dell'Università - Roma*

*Istituto Nazionale di Fisica Nucleare - Sezione di Roma*

(ricevuto il 22 Febbraio 1956)

**Summary.** — A method for establishing a lower limit to the spin of the  $\Lambda^0$  is described; the method is based on the observation that the possible simultaneous shapes of the two angular distributions in  $\cos \theta$  and  $\varphi$  ( $\varphi$  = angle between the plane of production and the plane of decay;  $\theta$  angle between the line of flight of the  $\Lambda^0$  and the line of flight of the decay products in the rest system of the same) are, for any assumed spin connected with each other and severely restricted. A detailed analysis is presented, for the cases of spins  $3/2$  and  $5/2$ . The insufficient statistics of the experimental data presently available (12 cases not of completely homogeneous nature) does not allow at the moment to express any definite conclusion. However if some trends now present in the data will be confirmed a spin of  $5/2$  or higher is necessary.

### 1. — Introduction.

It has been pointed out on several occasions <sup>(1)</sup> since the observation of the first few cases of  $\Lambda^0$  production that the angular distribution in the angle  $\varphi$  between the plane of production and the plane of decay might give informations about the spin of the  $\Lambda^0$ ; assuming that the  $\Lambda^0$  comes out partially polarized from the reaction in which it is produced it is possible in fact to show that the distribution in  $\varphi$  may tend to favour the smaller  $\varphi$  values and that, keeping constant the polarization, this tendency increases when the value of the spin increases; only in the case of spin  $\frac{1}{2}$  one obtains, independently from the polarization, an isotropic  $\varphi$  distribution. The experimental situation, as analyzed

<sup>(1)</sup> W. FOWLER, R. P. SHUTT, A. M. THORNDIKE and W. L. WHITEMORE: *Phys. Rev.*, **98**, 121 (1955).

in a recent paper by W. D. WALKER and W. D. SHEPHARD <sup>(2)</sup> seems to show that small  $\varphi$  values are favoured in the production of  $\Lambda^0$  and  $\Sigma^-$  from  $\pi^-$  in hydrogen, thus pointing to a spin higher than  $\frac{1}{2}$  (compare Fig. 1). The 12 cases

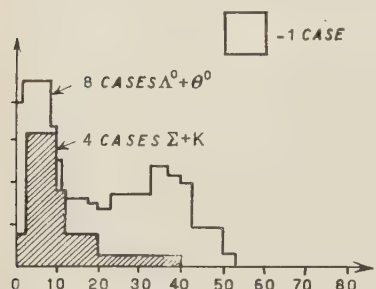


Fig. 1. — Number of cases in function of the dihedral angle between plane of decay and production (from ref. <sup>(2)</sup>).

to which Fig. 1, taken from their paper, refers, summarize the data obtained from FOWLER and coworkers (and a  $\pi^-$  nominal energy of 1.4 GeV) and the cases from WALKER and SHEPHARD (at 1 GeV). No case has a  $\varphi$  larger than  $45^\circ$ . It has to be noticed that, as discussed in reference <sup>(2)</sup>, there should be no bias for the observation of events with  $\varphi > 45^\circ$ ; for example the  $\Lambda^0$ 's produced in collisions against nuclei (and there are quite a lot of them) show an almost isotropic distribution in  $\varphi$  (Fig. 2) thus showing that nothing prevents the observation of large  $\varphi$  values; an isotropic distribution may be

expected in the production against nuclei due to the probable cancellation of polarization produced by the nucleus.

It may be remarked that in Fig. 1 the  $\Lambda^0$  and the charged  $\Sigma$  are both included; possibly they have different spins; moreover those cases of  $\Lambda^0$  production have also been included which have possibly to be interpreted as a  $\Sigma^0 + \Theta^0$  production, the  $\Sigma^0$  then decaying fast into a  $\Lambda^0$ . Finally it may be noticed that the polarization of the outgoing  $\Lambda^0$  depends on the angle which the  $\Lambda^0 \rightarrow \Theta$  line of flight forms with the  $\pi^-$  line of flight in the center of mass system; this angle is also different for the various cases. This mixing of various cases considerably reduces the values of the statistics. It has to be constantly kept in mind in the following.

WALKER and SHEPHARD have particularly emphasized that, besides the  $\varphi$  distribution, also another distribution is important in trying to find the spin of the  $\Lambda^0$ ; this is the distribution in  $\cos \theta$ , where  $\theta$  is the angle between

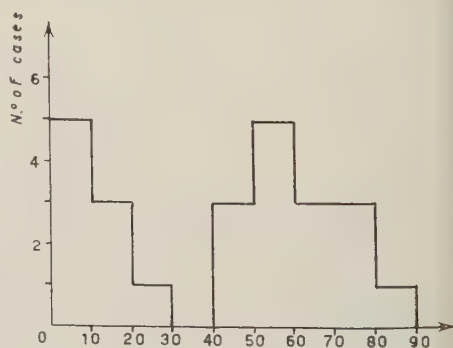


Fig. 2. — Number of cases in function of the dihedral angle between planes of production and decay for  $\Lambda^0$  from walls (from ref. <sup>(2)</sup>).

<sup>(2)</sup> W. D. WALKER and W. D. SHEPARD: preprint. I thank Dr. R. GATTO for having told me of this paper.



the line of flight of the  $\pi^-$  (and proton) produced in the decay, in the *rest system* of the decaying  $\Lambda^0$ , and the line of flight of the  $\Lambda^0$ . They point out that the mentioned distribution in  $\cos \theta$  should be always isotropical for a spin  $\frac{1}{2}$   $\Lambda^0$ , and should be peaked forward ( $\theta = 0^\circ$ ) and backward ( $\theta = 180^\circ$ ) for a spin  $> \frac{1}{2}$ , the more so the higher the value of the spin is, if the produced  $\Lambda^0$  is strongly polarized along the normal to the production plane. The distribution in  $\cos \theta$ , for the gas produced events is reported in Fig. 3, and shows peaks at  $\cos \theta \cong \pm 0.5$ , but only one event at  $\theta = 0^\circ$  or  $180^\circ$ ; though the total number of events is small this fact seems at first rather remarkable in view of the strong anisotropy in  $\varphi$ , which, would tend to suggest a value at least three half for the spin of the  $\theta$  and a strong polarization of the same.

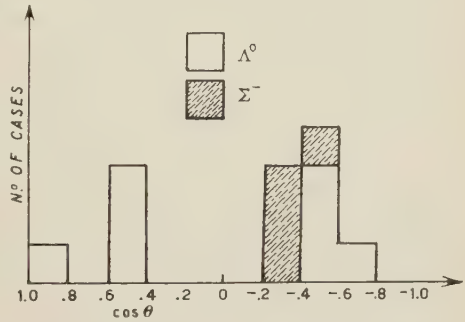


Fig. 3. —  $\cos \theta$  distribution for the twelve cases produced in  $H$  (from ref. (2)).

We may notice that according to WALKER and SHEPHARD there should be no bias in the  $\cos \theta$  distribution; for example in the  $\Lambda^0$ 's produced in the walls of the chamber the  $\cos \theta$  distribution is isotropic and the angles  $0^\circ$  and  $180^\circ$  are by no means missing. It may be further remarked that the  $\theta$  distribution (3) has, from first principles, so to say, to be symmetric with respect to  $90^\circ$ , so that the effective total number of cases per interval of  $\cos \theta$  in the  $\theta$  distribution is obtained adding together the cases belonging to the interval in consideration and the cases belonging to intervals symmetric with respect to  $\theta = 90^\circ$ ; in other words the really relevant diagram should be drawn with  $\theta$  varying in the interval  $180^\circ \dashv 90^\circ$  and all the cases of Fig. 3 with  $\theta = 90^\circ - \alpha$  ( $0^\circ < \alpha < 90^\circ$ ) should be reported at  $\theta = 90^\circ + \alpha$  in the new diagram (Fig. 4).

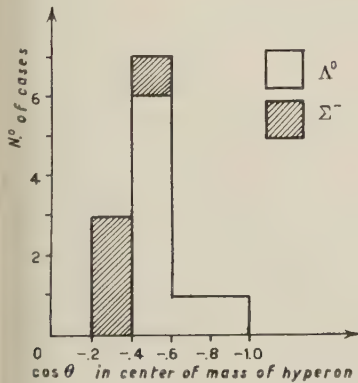


Fig. 4.

It will be one of the results of the present paper to show that, not necessarily a strongly peaked  $\varphi$  distribution as the one indicated by Fig. 1 does

(3) When speaking of the  $\theta$  distribution we always mean in this paper the distribution in  $\cos \theta$ .



correspond to a  $\theta$  distribution peaked at  $0^\circ$  and  $180^\circ$  <sup>(4)</sup>, so that in fact there is no contradiction between the fact that the  $\varphi$  distribution strongly favours small angles while the  $\theta$  distribution does not favour the angles  $0^\circ$  and  $180^\circ$ . More precisely, we shall show that the comparison of the  $\varphi$  and  $\theta$  distributions gives in general an information on the minimum values  $S$  of the spin which may be assigned to the  $\Lambda^0$ , *much stronger* than the information which one may get from the  $\varphi$  distribution alone or the  $\theta$  distribution alone. It has to be added that, though we are well aware of the insufficiency of the present data, the spirit which underlies the present work is to assume that the future data will show some of the strong anisotropy characteristics of the present ones. In the opposite case, the treatment presented here will have to be completed by a more detailed discussion of the process of production to be of some help; it has to be kept in mind that the spin of the  $\Lambda^0$  might be as high as one likes, but still the angular distributions be isotropical, in some cases.

Mention has to be made also of the interesting paper by S. B. TREIMAN and H. W. WYLD <sup>(5)</sup> which together with <sup>(2)</sup> has been the starting point of the present paper: these authors consider just the  $\varphi$  distribution and find the minimum spin value  $S$  of the  $\Lambda^0$  which is consistent with a given observed  $\varphi$  angular distribution; they show that the peaking of the  $\varphi$  distribution at  $0^\circ$  gives sensible information on the minimum value of the spin which has to be assigned to the  $\Lambda^0$ .

The results of the analysis presented here, will be summarized in Sect. 7. In Sect. 2 the notation and the general formalism to describe the decay of a spin  $S$ -particle are given; in Sect. 3 the  $\varphi$  and  $\theta$  angular distributions are discussed as functions of the polarization state of the decaying  $\Lambda^0$  under the assumption of spin  $\frac{3}{2}$ ; in Sect. 4 the same discussion is presented for a spin  $\frac{5}{2}$ ; in Sect. 5 a general discussion of the process of production of a  $\Lambda^0$  with a spinless  $\Theta^0$  by an unpolarized  $\pi^- \rightarrow p$  beam is presented; it is shown that the calculation of the angular distributions of the products of decay of the  $\Lambda^0$ , as well as of the polarization may be done as if the  $\Lambda^0$  at the moment of decay were in a pure state, thus justifying the treatment of the previous sections. Finally in Sect. 6 a proof is given that the polarization is normal to the plane of production and a short discussion on the polarization of a particle with  $S > \frac{1}{2}$  is presented.

<sup>(4)</sup> For instance it will be shown that, for spin  $3/2$ , to the most peaked  $\varphi$  distribution corresponds an isotropical  $\cos \theta$  distribution; though it is true that for the most polarized state the distribution in  $\theta$  has a maximum at  $0^\circ$  and  $180^\circ$ , while the distribution in  $\varphi$  is still considerably peaked at  $0^\circ$ . The point is that the state giving rise to the most peaked distribution is not the state of complete polarization (Sect. 3), though the polarizations are almost the same (respectively  $(\sqrt{3}+1)/2$  and  $3/2$ ); essentially similar statements may be made for spin  $5/2$ .

<sup>(5)</sup> S. B. TREIMAN and H. W. WYLD: *Phys. Rev.*, **100**, 879 (1955).

## 2. — The Description of the Decay Process.

First a few words on the notation! The system of coordinates to which we shall refer in the following is the rest system of the decaying  $\Lambda^0$ ; the  $z$  axis of the above system is oriented along the line of flight of the  $\Lambda^0$ , while the  $y$  axis is normal to the plane of production (the plane determined by the line of flight of the  $\Lambda^0$  and the line of flight of the  $\pi^-$  producing the  $\Lambda^0$ ) and the  $x$  axis is normal to the  $z$  and  $y$  axis. In such a system the line of flight of the  $\pi^-$  produced in the decay may be specified by the two angles  $\theta$  and  $\varphi$ , which are the usual polar coordinates connected to the cartesian ones in the usual way. It is then easy to realize that the angle  $\varphi$  so introduced is just the dihedral angle previously mentioned between the plane of production and the plane of decay, while the angle  $\theta$  is the same angle previously considered between the line of flight of the  $\Lambda^0$  and the line of flight of the products of decay. The situation is illustrated in the accompanying Fig. 5.

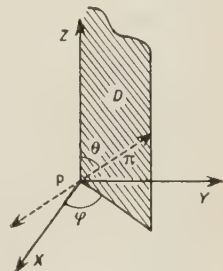


Fig. 5.

We now assume that the  $\Lambda^0$  in the decay of which we are interested is produced together with a spinless  $\Theta^0$  in a collision between a pion and a proton in an initially unpolarized beam.

We call  $\chi_s^M$  the spin functions of the  $\Lambda^0$ ,  $M$  being the projection of the  $\Lambda^0$  spin in the direction of the  $z$  axis (line of flight) and denote by  $\lambda_M$  ( $M = -S, -S+1, \dots, +S$ )  $2S+1$  complex numbers; the sum of the squares of the moduli of the  $\lambda_M$ 's is indicated by  $A$ ;  $A = \sum_M |\lambda_M|^2$ ; we call  ${}_x\chi_s$  the normalized function

$$(1)_\alpha \quad {}_\alpha\chi_s = A^{-\frac{1}{2}} \sum_M \lambda_M \chi_s^M$$

a general combination of spin functions  $\chi_s^M$ , with complex coefficients  $\lambda_M$  and introduce also the normalized function

$$(1)_\beta \quad {}_\beta\chi_s = A^{-\frac{1}{2}} \sum_M (-1)^{|M-\frac{1}{2}|} \lambda_M \chi_s^{-M},$$

where the  $\lambda_M$  are the same in function  ${}_\beta\chi_s$  as in function  ${}_x\chi_s$ . We shall prove in Sect. 5, by discussing the production process that if the  $\Lambda^0$  in which we are interested is produced in the process specified above, then, any quantity of interest, in particular the angular distributions of the decay products, the polarization tensor components of the  $\Lambda^0$  etc., has to be calculated by an averaging process of the following nature; first the calculation has to be performed as if the  $\Lambda^0$  were in the pure state  $(1)_\alpha$ , next as if it were in the pure state  $(1)_\beta$  adding then the results and dividing by 2.

It may however be easily proved, and it will become apparent from the following explicit expressions, that, since the two functions  ${}_{\alpha}\chi_s$  and  ${}_{\beta}\chi_s$  are obtained the one from the other simply through the substitution:

$$(1') \quad \lambda_M \rightarrow (-1)^{|M+\frac{1}{2}|} \lambda_{-M},$$

the quantities which we are going to evaluate in the following, namely the coefficients  $A_M^{(S)}$  and  $\mathcal{A}_M^{(S)}$  in (3) and (4), and the expectation value of the  $y$  component of the spin, are exactly the same if calculated with function  $(1)_{\alpha}$  or with the function  $(1)_{\beta}$ . It follows that as far as the above mentioned quantities are concerned we may proceed as if the  $\Lambda^0$  were in the pure state  ${}_{\alpha}\chi_s$  and forget about the averaging process. This we shall do in the following, keeping in mind however that a more general calculation has always to be performed according to the indicated procedure.

We now calculate the angular distributions from the  $\Lambda^0$  decay. For this observe first that each spin function  $\chi_s^M$ , gives rise to an outgoing  $\pi^- \rightarrow \pi^0$  wave the angular and spin part of which is indicated by  $\psi_s^M$ . With an obvious notation we have either:

$$(2)_1 \quad \psi_s^M = \left( \frac{S+M}{2S} \right)^{\frac{1}{2}} \alpha Y_{S-\frac{1}{2}}^{M-\frac{1}{2}} + \left( \frac{S-M}{2S} \right)^{\frac{1}{2}} \beta Y_{S-\frac{1}{2}}^{M+\frac{1}{2}},$$

or

$$(2)_2 \quad \psi_s^M = - \left( \frac{S+M-1}{2S+2} \right)^{\frac{1}{2}} \alpha Y_{S+\frac{1}{2}}^{M-\frac{1}{2}} + \left( \frac{S+M+1}{2S+2} \right)^{\frac{1}{2}} \beta Y_{S+\frac{1}{2}}^{M+\frac{1}{2}},$$

according to the parity of the decaying particle. However it is well known that, insofar angular distributions summed over the spins are considered, the two functions give the same results, and in the following use can be made of just one of them, for example  $(2)_1$ .

Starting then from equations  $(1)_{\alpha}$  and (2) the most general expressions for the angular distributions in  $\theta$  and in  $\varphi$  may be immediately written down. The expression for the  $\varphi$  distribution has already been given in ref. (5) and is (6):

$$(3) \quad I_s(\varphi) = \frac{2}{\pi} \left( 1 + \sum_{M=2, 4, \dots, 2S-1} A_M^{(S)} \cos M\varphi \right) \quad 0 \leq \varphi \leq 2\pi$$

(6) As pointed out in ref. (5) the most general distribution in  $\varphi$  is of the form:

$$(3') \quad I_s(\varphi) = \frac{1}{2\pi} \left( 1 + \sum_{M=2, 4, \dots} A_M^{(S)} \cos M\varphi + \sum_{M=2, 4, \dots} B_M^{(S)} \sin M\varphi \right) \quad (0 \leq \varphi < 2\pi)$$

However events produced in planes forming the angles  $\varphi$  or  $\varphi + \pi$  or  $2\pi - \varphi$  or  $\pi - \varphi$  are indistinguishable so that the effectively observed distribution is (3). Notice moreover that, quite apart from this consideration the coefficients of the terms in  $\sin M\varphi$  (3') vanish if the producing pion proton beam is unpolarized.

and the expression for  $I_s(\theta)$  may be easily shown to be of the form:

$$(4) \quad I_s(\theta) = \frac{1}{2} + \sum_{M=2, 4, \dots; 2S-1} \mathcal{A}_M^{(S)} P_M(\cos \theta),$$

where the  $P_M$  are the Legendre polynomials. Notice that  $I_s(\theta)$  and  $I_s(\varphi)$  (the suffix  $S$  is added to remember the spin with which we are dealing) are both normalized to one and all amounts now to determine the coefficients  $A_M^{(S)}$  and  $\mathcal{A}_M^{(S)}$  in the distributions (3) and (4) starting from (1)<sub>x</sub>, (2); the required expressions will give  $A_M^{(S)}$  and  $\mathcal{A}_M^{(S)}$  in terms of the  $\lambda_M$ .

By definition we have:

$$(5) \quad A_M^{(S)} = 2 \int_0^{2\pi} I_s(\varphi) \cos M\varphi d\varphi$$

and

$$(6) \quad \mathcal{A}_M^{(S)} = \frac{2M+1}{2} \int_0^\pi I_s(\theta) P_M(\cos \theta) d \cos \theta.$$

The intensities  $I_s(\varphi)$  and  $I_s(\theta)$  are simply expressed through the wave function (1) <sub>$\alpha$</sub>  as

$$(7) \quad I_s(\varphi) = A^{-1} \sum_{\text{spin}} \int_0^\pi \left| \sum_M \lambda_M \psi_S^M \right|^2 d \cos \theta$$

and

$$(8) \quad I_s(\theta) = A^{-1} \sum_{\text{spin}} \int_0^{2\pi} \left| \sum_M \lambda_M \psi_S^M \right|^2 d\varphi$$

so that, on inserting (7) and (8) respectively in (5) and in (6) the required expressions for  $A_M^{(S)}$  and  $\mathcal{A}_M^{(S)}$  are derived. We give the resulting expressions

$$(9) \quad A_M^{(S)} = 2A^{-1} \sum_{M'' M'} \lambda_{M''} \lambda_{M'}^* G_{M'', M'}^{(S, M)}$$

$$(10) \quad \mathcal{A}_M^{(S)} = \frac{2M+1}{2} \sum_{M'} |\lambda_{M'}|^2 I_{M'}^{(S, M)},$$

where the coefficients  $G_{M'', M'}^{(S, M)}$  and  $I_{M'}^{(S, M)}$  are easily calculated performing some integrals over the spherical harmonics; it is:

$$(11) \quad G_{M'', M'}^{(S, M)} = \frac{(S+M'')^{\frac{1}{2}} (S+M')^{\frac{1}{2}}}{2S} \int Y_{S-\frac{1}{2}}^{M''-\frac{1}{2}} Y_{S-\frac{1}{2}}^{(M'-\frac{1}{2})^*} \cos M\varphi d \cos \theta d\varphi + \\ + \frac{(S-M'')^{\frac{1}{2}} (S-M')^{\frac{1}{2}}}{2S} \int Y_{S-\frac{1}{2}}^{M''+\frac{1}{2}} Y_{S-\frac{1}{2}}^{(M'+\frac{1}{2})^*} \cos M\varphi d \cos \theta d\varphi$$

and

$$(12) \quad \Gamma_{M'}^{(S, M)} = \frac{(S + M')}{2S} \int |Y_{S-\frac{1}{2}}^{M'-\frac{1}{2}}|^2 P_M(\cos \theta) d \cos \theta d\varphi + \\ + \frac{(S - M')}{2S} \int |Y_{S-\frac{1}{2}}^{M'+\frac{1}{2}}|^2 P_M(\cos \theta) d \cos \theta d\varphi.$$

Through (11) and (12) both  $A_M^{(S)}$  and  $\mathcal{A}_M^{(S)}$  are expressed as quadratic forms in the  $\lambda_M$ ;  $\mathcal{A}_M^{(S)}$  is diagonal, while  $A_M^{(S)}$  is non diagonal. It may be mentioned that in their paper TREIMAN and WYLD have determined for some spin values the maximum eigenvalue of the quadratic form associated to  $A_M^{(S)}$  when the  $\lambda_M$  are varied. Our purpose is somewhat different; we want to discuss *together* the  $\theta$  and  $\varphi$  distributions and show that the requirement that one, say the  $\varphi$  distribution, has a certain behaviour implies a strong limitation and in some cases determines the possible behaviour of the other distribution, say the  $\theta$ . We shall show this in the next two sections for the cases of spin  $\frac{3}{2}$  and  $\frac{5}{2}$ .

### 3. — The Case of Spin $\frac{3}{2}$ .

In the case of spin  $\frac{3}{2}$  only  $A_2^{(\frac{3}{2})}$  and  $\mathcal{A}_2^{(\frac{3}{2})}$  are different from zero and the expressions (3) and (4) may be rewritten:

$$(13) \quad I_{\frac{3}{2}}(\varphi) = \frac{2}{\pi} (1 + A_2^{(\frac{3}{2})} \cos 2\varphi),$$

$$(14) \quad I_{\frac{3}{2}}(\theta) = \frac{1}{2} + \mathcal{A}_2^{(\frac{3}{2})} P_2(\cos \theta).$$

The expression (14) for  $I_{\frac{3}{2}}(\theta)$  does not seem to be at all compatible with the present experimental distribution; indeed due to the fact that only  $P_2(\cos \theta)$  appears in (14) the  $\cos \theta$  distributions which are contained in (14) are either peaked at  $90^\circ$ , or have maxima at  $0^\circ$  and  $180^\circ$  and a minimum at  $90^\circ$ , or finally are isotropical; no one of these three features appears in the experimental distribution and this fact alone may be an argument for a spin higher than  $\frac{3}{2}$ . However in view of the fact that the present statistics is very poor and that future data may change completely the shape of the  $\theta$  distribution we discuss extensively the case of spin  $\frac{3}{2}$ ; moreover this case is particularly illustrative of the sort of correlation between the  $\theta$  and  $\varphi$  distributions.

Using (9) and (10) and taking account of the fact that only a limited number



of  $G_{M', M'}^{(\frac{3}{2}, 2)}$  and  $I_{M'}^{(\frac{3}{2}, 2)}$  do not vanish <sup>(7)</sup> we get:

$$(15) \quad A_2^{(\frac{3}{2})} = -A^{-1} \sqrt{\frac{1}{3}} (\lambda_{\frac{3}{2}} \lambda_{-\frac{1}{2}}^* + \lambda_{\frac{1}{2}}^* \lambda_{-\frac{1}{2}} + \lambda_{-\frac{3}{2}} \lambda_{\frac{1}{2}}^* + \lambda_{-\frac{1}{2}}^* \lambda_{\frac{1}{2}}),$$

$$(16) \quad \mathcal{A}_2^{(\frac{3}{2})} = \frac{1}{2} A^{-1} (|\lambda_{\frac{1}{2}}|^2 + |\lambda_{-\frac{1}{2}}|^2 - |\lambda_{\frac{3}{2}}|^2 - |\lambda_{-\frac{3}{2}}|^2).$$

These expressions may be further simplified introducing <sup>(7)</sup> instead of the four complex  $\lambda_M$ , seven independent real parameters  $\gamma, \varepsilon, \delta, \psi_M$  ( $M = -\frac{3}{2}, -\frac{1}{2}, \frac{1}{2}, \frac{3}{2}$ ) satisfying the relation  $A = 1$  in terms of which the expressions (15) (16) take the form:

$$(17) \quad A_2^{(\frac{3}{2})} = -\sqrt{\frac{1}{3}} \sin 2\gamma [\cos \varepsilon \sin \delta \cos (\psi_{\frac{3}{2}} - \psi_{-\frac{3}{2}}) + \sin \varepsilon \cos \delta \cos (\psi_{-\frac{3}{2}} - \psi_{\frac{1}{2}})],$$

$$(18) \quad \mathcal{A}_2^{(\frac{3}{2})} = \frac{1}{2} \cos 2\gamma.$$

The parameters  $\gamma, \varepsilon, \delta$ , in these expressions, may assume any value in the interval  $0 \rightarrow \pi/2$ ; the  $\psi_M$ 's may vary from 0 to  $2\pi$ . For any choice of  $\gamma, \varepsilon, \delta, \psi_M$  in the above intervals we have from (17) and (18) possible values for  $A_2^{(\frac{3}{2})}$  and  $\mathcal{A}_2^{(\frac{3}{2})}$ ; and as a consequence, from (13) and (14) a definite shape of the  $\varphi$  and  $\theta$  angular distributions.

Moreover the polarization component  $\langle S_y \rangle_{\frac{3}{2}}$  of the decaying  $\Lambda^0$  that is the expectation value of the spin component  $S_y$  in the direction of the normal to the plane of production, may be also, of course, expressed through the  $\lambda_M$  or, equivalently, through the new parameters  $\gamma, \varepsilon, \delta, \psi_M$  <sup>(8)</sup>.

It is easy to show that:

$$(19) \quad \langle {}_\alpha \chi_{\frac{3}{2}} | S_y | {}_\alpha \chi_{\frac{3}{2}} \rangle = \langle S_y \rangle_{\frac{3}{2}} = \sqrt{3} [\sin (\psi_{\frac{1}{2}} - \psi_{\frac{3}{2}}) \cos \varepsilon \cos \delta - \\ - \sin (\psi_{-\frac{1}{2}} - \psi_{-\frac{3}{2}}) \sin \varepsilon \sin \delta] \cos \gamma \sin \gamma + 2 \cos^2 \gamma \cos \delta \sin \delta \sin (\psi_{-\frac{1}{2}} - \psi_{\frac{1}{2}}).$$

For any shape of the distributions in  $\theta$  and  $\varphi$  corresponding to a choice of the parameters, we may then calculate through (19) the value of the polarization.

To shorten the following discussion a distribution in  $\varphi$  peaked at  $0^\circ$  will

<sup>(7)</sup> Compare Appendix I.

<sup>(8)</sup> It may be added that, contrarily to the case of a spin 1/2 particle, there are also other expectation values which do not vanish and which together with  $\langle S_y \rangle$  characterize the polarization state of the  $\Lambda^0$ . However in the following, where it cannot produce confusion we shall call  $\langle S_y \rangle$  the « polarization » though a name like, e.g., « first order polarization » would be preferable; it must be kept in mind that the vanishing of  $\langle S_y \rangle$  does not mean that the  $\Lambda^0$  is unpolarized. Compare for questions of this kind Sect. 6, where it will be also shown that the expectation value of any component of  $\mathbf{S}$  in the plane of production is identically zero for an initially unpolarized pion proton beam; a theorem already well known particularly in the case of spin 1/2.

be simply called a « peaked » distribution; a convenient parameter for the  $\varphi$  distribution is the one already introduced by TREIMAN and WYLD, namely the fraction of the total number of events from  $\varphi = 0^\circ$  to a certain angle  $\varphi = \alpha$ ; in the following  $\alpha$  will be taken to be  $\pi/4$  and the corresponding integral of  $I(\varphi)$  from  $0^\circ$  to  $\pi/4$  will be denoted by  $P$ .

$$(20) \quad P^{(\frac{3}{2})} = \int_0^{\pi/4} I_{\frac{3}{2}}(\varphi) d\varphi = \frac{1}{2} + \frac{1}{\pi} A_2^{(\frac{3}{2})}.$$

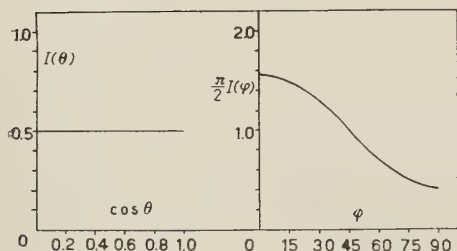


Fig. 6. — The distributions which correspond to the maximum peaking.

For the  $\theta$  distribution we shall consider in some cases the ratio  $R^{(\frac{3}{2})}$  between  $I_{\frac{3}{2}}(0^\circ)/I_{\frac{3}{2}}(90^\circ)$  (though experimentally this ratio is 0/0!).

We may first see that the most peaked  $\varphi$  distribution is obtained by choosing in (17)  $\sin 2\gamma = 1$ , and the values of  $\varepsilon$ ,  $\delta$ ,  $\psi_M$  in such a way that the expression in brackets has its minimum, namely  $-1$ . The corresponding (maximum) value of  $A_2^{(\frac{3}{2})}$  is

$\sqrt{\frac{1}{3}} = 0.577$  and is  $P^{(\frac{3}{2})} = 0.684$ ; from (18) the value of  $\mathcal{A}_2^{(\frac{3}{2})}$  turns out to be zero, the  $\cos \theta$  distribution being thus isotropical ( $R^{(\frac{3}{2})} = 1$ ), (Fig. 6). The values of the parameters are

$$(21) \quad \gamma = \frac{\pi}{4}, \quad \delta + \varepsilon = \frac{\pi}{2}, \quad \psi_{\frac{3}{2}} - \psi_{-\frac{1}{2}} = \pi, \quad \psi_{-\frac{3}{2}} - \psi_{\frac{1}{2}} = -\pi.$$

As one sees the parameters are not completely determined from the requirement of maximum peaking of the  $\varphi$  distribution; if we add however the requirement that the polarizatoion  $\langle S_y \rangle$  has its maximum value compatible with (21) then the further restrictions so introduced

$$\delta - \varepsilon = 0, \quad \psi_{\frac{1}{2}} - \psi_{\frac{3}{2}} = \frac{\pi}{2},$$

together with (21) determine completely the parameters as

$$\delta = \frac{\pi}{4}, \quad \varepsilon = \frac{\pi}{4}, \quad \gamma = \frac{\pi}{4}, \quad \psi_{\frac{3}{2}} = 0, \quad \psi_{-\frac{1}{2}} = \pi, \quad \psi_{\frac{1}{2}} = \frac{\pi}{2}, \quad \psi_{-\frac{3}{2}} = \frac{3}{2}\pi,$$

apart from an inessential overall phase factor.

The corresponding value of the polarization is

$$(22) \quad \langle S_y \rangle = \frac{\sqrt{3}}{2} + 1$$

and the wave function (compare Appendix I) may be written:

$$(23) \quad \chi'_{\frac{3}{2}} = \frac{1}{2}[(\chi_{\frac{3}{2}}^{\frac{3}{2}} - \chi_{\frac{3}{2}}^{-\frac{3}{2}}) - i(\chi_{\frac{3}{2}}^{-\frac{3}{2}} - \chi_{\frac{3}{2}}^{\frac{3}{2}})].$$

By a completely similar procedure it is possible to determine the distribution in  $\varphi$  and the polarization for the choice of the parameters which give rise to a distribution in  $\theta$  with a maximum value of  $\mathcal{A}_2^{(\frac{3}{2})}$  (or equivalently of the ratio  $R$ ): the maximum value of  $\mathcal{A}_2^{(\frac{3}{2})}$ , namely  $\frac{1}{2}$ , is obtained when  $\gamma = 0$ ; the corresponding  $R$  is equal to 4. The corresponding  $\varphi$  distribution is isotropical (Fig. 7); the maximum polarization is 1 and is obtained when  $\delta = \pi/4$  and  $\psi_{-\frac{1}{2}} - \psi_{\frac{1}{2}} = \pi/2$ ; the wave function is

$$\chi''_{\frac{3}{2}} = \frac{1}{\sqrt{2}}(\chi_{\frac{3}{2}}^{\frac{1}{2}} + i\chi_{\frac{3}{2}}^{-\frac{1}{2}}).$$

Similarly the choice of parameters which give a minimum value to  $\mathcal{A}_2^{(\frac{3}{2})}$  produces an isotropic  $\varphi$  distribution and corresponds to a vanishing  $\langle S_y \rangle$ ; the ratio  $R$  for this choice is  $R = 0$ , the intensity  $I_{\frac{3}{2}}(\theta)$  vanishing at  $0^\circ$  and  $180^\circ$  (Fig. 8).

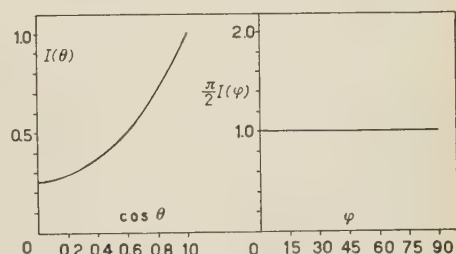


Fig. 7. — The distributions which correspond to the maximum  $(I(\theta = 180^\circ))/(I(\theta = 90^\circ))$ .

Finally we want to determine the shape of the  $\theta$  distribution and of the most peaked  $\varphi$  distribution, when the polarization has its maximum value  $\frac{3}{2}$  (Fig. 9).

This situation is obtained with the choice:

$$\gamma = \frac{\pi}{3}, \quad \delta = \frac{\pi}{4}, \quad \varepsilon = \frac{\pi}{4}, \quad \psi_{\frac{1}{2}} = 0, \\ \psi_{\frac{1}{2}} = \frac{\pi}{2}, \quad \psi_{-\frac{1}{2}} = \pi, \quad \psi_{-\frac{3}{2}} = \frac{3}{2}\pi,$$

Fig. 8. — The distributions which correspond to the requirement of a minimum in the  $\theta$  distribution at  $\theta = 180^\circ$ .

and corresponds to  $A_2^{(\frac{3}{2})} = 0.5$  and  $\mathcal{A}_2^{(\frac{3}{2})} = 0.25$ ; the values of  $R^{(\frac{3}{2})}$  and  $P^{(\frac{3}{2})}$  are respectively  $R = 2$ ,  $P = 0.659$ ; the corresponding wave function is

$$\chi''' = \frac{1}{2\sqrt{2}}[(\chi_{\frac{3}{2}}^{\frac{3}{2}} - \sqrt{3}\chi_{\frac{3}{2}}^{-\frac{1}{2}}) + i(\sqrt{3}\chi_{\frac{3}{2}}^{\frac{1}{2}} - \chi_{\frac{3}{2}}^{-\frac{3}{2}})].$$

The results of this discussion are summarized in Figs. 6, 7, 8, 9; any intermediate case may be calculated using the above formulae. It is remarkable

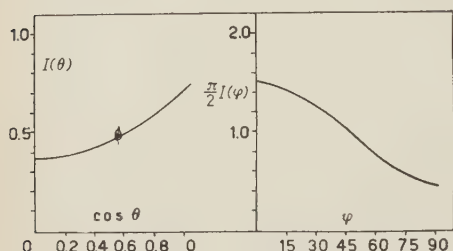


Fig. 9. — The distributions corresponding to the maximum  $\langle S_y \rangle_{\frac{5}{2}}$ .

that vary small variations in the first order polarization and in the peaking of the  $\varphi$  distribution may be accompanied by extremely large variations in the  $\theta$  distribution; comparing the first discussed case (wave function  $\chi'$ ) with the last one (wave function  $\chi''$ ) one realizes that the variation in  $P$  and in  $\langle S_y \rangle$  are only respectively from 0.684 to 0.659 and from 2.71/2 to 3/2; yet the shape of the  $\theta$  distribution is completely changed,  $R$  varying from 1 in case  $\chi'$  to 2 in case  $\chi''$  (Figs. 6 and 9).

#### 4. — Spin $5/2$ .

A similar discussion may be made when a spin  $\frac{5}{2}$  is assumed for the  $\Lambda^0$ . The expressions for  $I_{\frac{5}{2}}(\theta)$  and  $I_{\frac{5}{2}}(\varphi)$  have the general form:

$$(24) \quad I_{\frac{5}{2}}(\varphi) = \frac{2}{\pi} (1 + A_2^{(\frac{5}{2})} \cos 2\varphi + A_4^{(\frac{5}{2})} \cos 4\varphi)$$

and

$$(25) \quad I_{\frac{5}{2}}(\theta) = \frac{1}{2} + \mathcal{A}_2^{(\frac{5}{2})} P_2(\cos \theta) + \mathcal{A}_4^{(\frac{5}{2})} P_4(\cos \theta).$$

The new feature of this case is that now the  $\cos \theta$  distribution may have a non monotonous behaviour from  $\theta = 0^\circ$  to  $90^\circ$  due to the presence of  $P_4(\cos \theta)$ . The point is now to see, assuming a spin  $\frac{5}{2}$  which are the shapes of the distributions compatible with possible values of the coefficients in (24) (25) and in particular which are the shapes of the  $\theta$  distributions compatible with sufficiently peaked  $\varphi$  distributions. In a completely similar way as the one previously described <sup>(9)</sup>, it may be shown that the expressions for  $A_2^{(\frac{5}{2})}$ ,  $A_4^{(\frac{5}{2})}$ ,  $\mathcal{A}_2^{(\frac{5}{2})}$ ,  $\mathcal{A}_4^{(\frac{5}{2})}$  in terms of the  $\lambda_M$  ( $M = -\frac{5}{2}, \dots, +\frac{5}{2}$ ) are the following:

$$A_2^{(\frac{5}{2})} = -\frac{2}{\sqrt{8}} A^{-1} \left[ \frac{1}{\sqrt{5}} (\lambda_{\frac{5}{2}} \lambda_{\frac{1}{2}}^* + \lambda_{-\frac{1}{2}} \lambda_{-\frac{5}{2}}^* + \text{c. c.}) + (\lambda_{\frac{1}{2}} \lambda_{-\frac{3}{2}}^* + \lambda_{\frac{3}{2}} \lambda_{-\frac{1}{2}}^* + \text{c. c.}) \right]$$

(<sup>9</sup>) Compare Appendix II.

$$A_4^{(\frac{5}{2})} = \frac{1}{\sqrt{5}} A^{-1} [\lambda_{\frac{5}{2}} \lambda_{-\frac{5}{2}}^* + \lambda_{-\frac{3}{2}} \lambda_{\frac{3}{2}}^* + \text{c. c.}]$$

$$\mathcal{A}_2^{(\frac{5}{2})} = A^{-1} \left[ -\frac{5}{7} (|\lambda_{\frac{5}{2}}|^2 + |\lambda_{-\frac{5}{2}}|^2) + \frac{4}{7} (|\lambda_{\frac{1}{2}}|^2 + |\lambda_{-\frac{1}{2}}|^2) + \frac{1}{7} (|\lambda_{\frac{3}{2}}|^2 + |\lambda_{-\frac{3}{2}}|^2) \right]$$

$$\mathcal{A}_4^{(\frac{5}{2})} = A^{-1} \left[ \frac{3}{14} (|\lambda_{\frac{5}{2}}|^2 + |\lambda_{-\frac{5}{2}}|^2) + \frac{3}{7} (|\lambda_{\frac{1}{2}}|^2 + |\lambda_{-\frac{1}{2}}|^2) - \frac{9}{14} (|\lambda_{\frac{3}{2}}|^2 + |\lambda_{-\frac{3}{2}}|^2) \right].$$

By introducing <sup>(9)</sup> in place of the seven complex parameters  $\lambda_M$ , the 13 independent real parameters  $\Gamma, \gamma, \varepsilon, \gamma', \varepsilon', \psi_M$  ( $M = -\frac{5}{2}, \dots, \frac{5}{2}$ ) in such a way as to satisfy the condition  $A = 1$ , the above expressions take the form ( $\psi_{2M, 2M'}$  stays for  $\psi_M - \psi_{M'}$ )

$$(26) \quad A_2^{(\frac{5}{2})} = -\sqrt{2} \left[ \sin^2 \Gamma \cos \gamma \sin \gamma \left( \frac{\cos \varepsilon \cos \psi_{5,1}}{\sqrt{5}} + \sin \varepsilon \cos \psi_{1,-3} \right) + \cos^2 \Gamma \cos \gamma' \sin \gamma' \left( \frac{\cos \varepsilon' \cos \psi_{-5,-1}}{\sqrt{5}} + \sin \varepsilon' \cos \psi_{-1,3} \right) \right],$$

$$(27) \quad A_4^{(\frac{5}{2})} = \frac{2}{\sqrt{5}} [\sin^2 \Gamma \sin^2 \gamma \sin \varepsilon \cos \varepsilon \cos \psi_{5,-3} + \cos^2 \Gamma \sin^2 \gamma' \sin \varepsilon' \cos \varepsilon' \cos \psi_{3,-5}],$$

and

$$(28) \quad \mathcal{A}_2^{(\frac{5}{2})} = \left[ \sin^2 \Gamma \left( -\frac{5}{7} \sin^2 \gamma \cos^2 \varepsilon + \frac{4}{7} \cos^2 \gamma + \frac{1}{7} \sin^2 \gamma \sin^2 \varepsilon \right) + \cos^2 \Gamma \left( -\frac{5}{7} \sin^2 \gamma' \cos^2 \varepsilon' + \frac{4}{7} \cos^2 \gamma' + \frac{1}{7} \sin^2 \gamma' \sin^2 \varepsilon' \right) \right],$$

$$(29) \quad \mathcal{A}_4^{(\frac{5}{2})} = \left[ \sin^2 \Gamma \left( \frac{3}{14} \sin^2 \gamma \cos^2 \varepsilon + \frac{3}{7} \cos^2 \gamma - \frac{9}{14} \sin^2 \gamma \sin^2 \varepsilon \right) + \cos^2 \Gamma \left( \frac{3}{14} \sin^2 \gamma' \cos^2 \varepsilon' + \frac{3}{7} \cos^2 \gamma' - \frac{9}{14} \sin^2 \gamma' \sin^2 \varepsilon' \right) \right].$$

In these equations  $\Gamma, \gamma, \varepsilon, \gamma', \varepsilon'$  are free to vary in the interval  $0 \rightarrow \pi/2$  while the  $\psi_M$  may assume any value in the interval  $0 \rightarrow 2\pi$ .

Similarly the expression for the expectation value  $\langle S_y \rangle$  of the  $y$  component of the spin is, in terms of the  $\Gamma \dots \psi_M$  parameters,

$$(30) \quad \langle S_y \rangle_{\frac{5}{2}} = \sin \Gamma \cos \Gamma \left\{ \sqrt{5} \sin \gamma \sin \gamma' [\sin \varepsilon' \cos \varepsilon \sin \psi_{3,5} + \cos \varepsilon' \sin \varepsilon \sin \psi_{-3,-5}] + \sqrt{8} [\cos \gamma \sin \gamma' \sin \varepsilon' \sin \psi_{1,3} + \cos \gamma' \sin \gamma \sin \varepsilon \sin \psi_{-3,-1}] + 3 \cos \gamma \cos \gamma' \sin \psi_{-1,1} \right\}.$$



The following discussion will be based on the above expressions; its results are summarized in Fig. 10, 11, 12, 13.

The most peaked  $^{(10)}\varphi$  distribution (Fig. 10) is obtained when  $\gamma = \gamma' = \pi/4$ ,  $\psi_{5,1} = \psi_{-5,-1} = \psi_{1,-3} = \psi_{-1,3} = \pi$ ,  $\sin \varepsilon = \sin \varepsilon' = \sqrt{\frac{5}{6}}$  and corresponds to  $A_2^{(\frac{5}{2})} = \sqrt{\frac{3}{5}}$

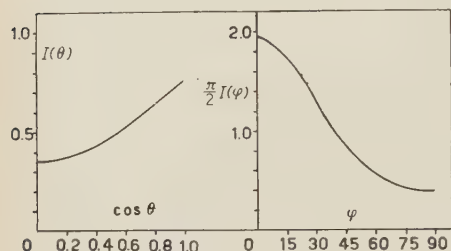


Fig. 10. — The distributions corresponding to the maximum  $\varphi$  peaking.

independently from  $\Gamma$ . The above parameters then determine  $A_4^{(\frac{5}{2})} = \frac{1}{6}$ ,  $\mathcal{A}_4^{(\frac{5}{2})} = -\frac{1}{28}$  and  $\mathcal{A}_2^{(\frac{5}{2})} = \frac{2}{7}$  always independently from  $\Gamma$ ; so the requirement that the distribution in  $\varphi$  is the most peaked one automatically determines the distribution in  $\theta$  and also the coefficient of  $\cos 4\varphi$  in the  $\varphi$  distribution itself. The corresponding value of  $\langle S_y \rangle^{\frac{5}{2}}$  still depends on the choice of  $\Gamma$  and  $\psi_{-1,1}$  and is a maximum when  $\Gamma = \pi/4$  and  $\psi_{-1,1} =$

$= \pi/2$ ; its value is then  $(7 + 2\sqrt{15})/6 \cong 14.7/6$ , a few percent smaller than the absolute maximum  $\frac{5}{2}$ .

In Fig. 11 we have reported, on the other hand, an illustration of the opposite situation: the distributions in  $\theta$  and  $\varphi$  which result from the requirement that the integral:  $\int_{30^\circ}^{90^\circ} I_{\frac{5}{2}}(\theta) d\cos \theta$

is a maximum; or, in other words from the requirement that the distribution in  $\theta$  correspond to the maximum percentage of events in the interval  $\theta = 0^\circ \vdash 30^\circ$  (as well as, of course  $\theta = 180^\circ \vdash 150^\circ$ ) a feature not at all indicated by the experimental data. This situation corresponds to  $\gamma = \gamma' = 0$  in (28), (29), that is to  $\mathcal{A}_2^{(\frac{5}{2})} = \frac{4}{7}$ ,  $\mathcal{A}_4^{(\frac{5}{2})} = \frac{3}{7}$ . It follows again that the  $\varphi$  distribution is determined:  $A_2^{(\frac{5}{2})} =$

$= A_4^{(\frac{5}{2})} = 0$ , an isotropical  $\varphi$  distribution; and the maximum value of the polarization in these conditions is obtained for  $\Gamma = \pi/4$ ,  $\psi_{-1,1} = \pi/2$ , and is  $\frac{3}{2}$ .

In Fig. 12 the distributions in  $\theta$  and in  $\varphi$  are reported which correspond to the requirement the  $\langle S_y \rangle$  has its maximum value  $\frac{5}{2}$ . This implies  $\Gamma = \pi/4$ ,

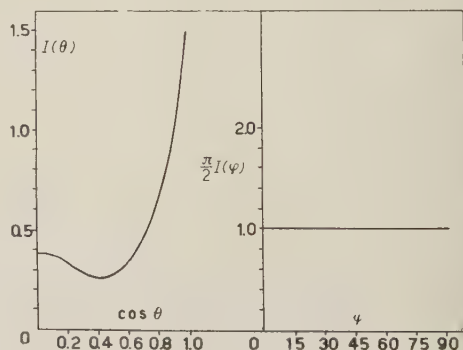


Fig. 11. — The distributions corresponding to the requirement of maximum intensity at  $\theta = 180^\circ$ .

<sup>(10)</sup> The definition of the most peaked  $\varphi$  distribution in this section is: the one which has the largest  $P^{(\frac{5}{2})}$ . Due to the presence of the  $\cos 4\varphi$  term in (24) this is not the one having the highest  $I(\varphi=0)$  value in (24).

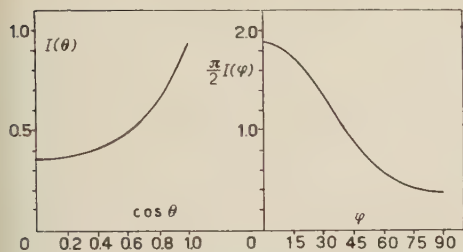


Fig. 12. — The distributions corresponding to the maximum  $\langle S_y \rangle_{\frac{5}{2}}$ .

gested by the *present* experimental data. A situation of this kind is provided by the choice  $\sin \gamma = \sin \gamma' = \sqrt{3}/2$ ,  $\sin \varepsilon = \sin \varepsilon' = \sqrt{5}/6$  which leads to  $\mathcal{A}_2^{(\frac{5}{2})} = \frac{1}{7}$ ,  $\mathcal{A}_4^{(\frac{5}{2})} = -\frac{15}{65}$ ; with the further condition  $\psi_{5,1} = \psi_{1,-3} = \psi_{-5,-1} = \psi_{-1,3} = \pi$  this leads to an  $A_2^{(\frac{5}{2})}$  value  $3/(2\sqrt{5})$  and to an  $A_4^{(\frac{5}{2})}$  value equal to  $\frac{1}{4}$ . The corresponding maximum polarization is obtained for  $\Gamma = \pi/4$ ,  $\psi_{-1,1} = \pi/2$ ; it is  $\langle S_y \rangle = 4.23/2$ . The resulting distributions are plotted in Fig. 13; it may be noticed that it is perhaps possible to obtain a slightly higher peak in the  $\cos \theta$  distribution than the one of Fig. 13, but then either the  $\varphi$  distribution is too flat or there is too much intensity at  $\theta = 0^\circ$  or at  $\theta = 90^\circ$ .

The conclusion is therefore the following: the distribution in  $\cos \theta$  may show a maximum in the angular region suggested by the experiments and still give rise to a sufficiently peaked  $\varphi$  distribution ( $P = 0.708$ ); however if the experimental data will confirm the pronounced maximum now existing at  $\cos \theta = 0.6$ , one will have to conclude that a spin  $\frac{5}{2}$  is insufficient to explain the data. It may also be remarked that in the case of spin  $\frac{5}{2}$  some intensity should be observed also at  $\varphi = 90^\circ$ , produced by the  $\cos 4\varphi$  term. However in this case  $A_4^{(\frac{5}{2})}$  is only 0.25.

## 5. — The Process of Production of a $\Lambda^0 \mapsto \Theta^0$ .

It is the purpose of this section to discuss shortly the process of production of a  $\Lambda^0$  and to justify the use of functions  $(1)_\alpha$  and  $(1)_\beta$  as well as the procedure illustrated at the beginning of Sect. 2 to calculate the decay of the  $\Lambda^0$ .

$\psi_{3,5} = \psi_{-5,-3} = \pi/2$ ,  $\psi_{1,3} = \psi_{-3,-1} = \pi/2$ ,  $\psi_{-1,1} = \pi/2$  and  $\sin \varepsilon' = \sin \varepsilon = \sqrt{5}/6$ ,  $\sin \gamma' = \sin \gamma = \sqrt{3}/8$ . The corresponding  $\theta$  and  $\varphi$  distributions have then the following coefficients:  $A_2^{(\frac{5}{2})} = \frac{3}{4}$ ,  $A_4^{(\frac{5}{2})} = \frac{1}{8}$ ,  $\mathcal{A}_2^{(\frac{5}{2})} = 5/14$ ,  $\mathcal{A}_4^{(\frac{5}{2})} = 9/112$ . Finally one may look if it is possible to find a  $\theta$  distribution which has a maximum at  $\cos \theta \cong 0.6$ , and if this is compatible with a sufficiently peaked  $\varphi$  distribution, a situation sug-

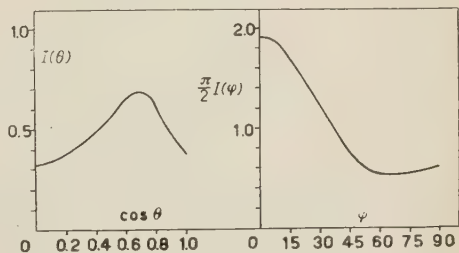


Fig. 13. — The distributions in  $\theta$  and  $\varphi$  corresponding to the requirement of a peaking in the  $\theta$  distribution at  $\cos \theta \cong 0.6$  and, at the same time, to a sufficient peaking in the  $\varphi$  distribution at  $\varphi = 0$ .

Moreover also some questions concerning the polarization of a particle of spin  $> \frac{1}{2}$  will be discussed.

Consider, in their center of mass the incoming  $\pi^-$  and the proton. Call  $z'$  their line of motion and  $\theta'$  the angle formed by the line of flight of the  $\Lambda^0$  with the axis  $z'$ ; the azimuthal angle of such line of flight may be, without loss of generality, taken to be zero (this defining the  $x'$  axis) due to the cylindrical symmetry around the  $z'$  axis; the «dashed» system of coordinates  $x', y', z'$ , is illustrated by Fig. 14. The third components of angular momenta

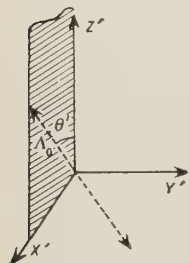


Fig. 14.

and spins are in the following referred to the  $z'$  axis, unless otherwise specified. The protons are initially unpolarized; this implies that we have to calculate the outgoing  $\Lambda^0 \rightarrow \Theta^0$  state, first when the proton spin is, say,  $\alpha$ , next when the proton spin is  $\beta$ ; any quantity of interest has to be calculated separately for the two pure states, the results added, and divided by 2.

If  $\bar{\chi}_s^M$  are the spin functions of the  $\Lambda^0$  with component  $M$  along the  $z'$  axis (this is not the line of flight of the  $\Lambda^0$  as in the previous sections) it is easy to realize that the most general angular and spin part of the outgoing  $\Lambda^0 \rightarrow \Theta^0$  amplitude produced when the spin of the proton is  $\alpha$  may be written:

$$(31) \quad \sum_M \sum_L H_L^M Y_L^{\frac{1}{2}-M}(\theta') \bar{\chi}_s^M.$$

Here the  $H_L^M$  are complex numbers, having in general a complicated expression through products or sums of products of Clebsch-Jordan coefficients and complex phase shifts; and the  $Y_L^{\frac{1}{2}-M}(\theta')$  are spherical harmonics which by our choice of the  $x'$  axis are independent from the azimuthal angle, hence real; the sum over  $L$  is extended to all the angular momenta which one may wish to consider in the outgoing wave; the spin of the  $\Theta^0$  is assumed to be zero: there is no spin function of the  $\Theta^0$  in (31).

To evaluate the cross-section for the process  $\pi^- + p \rightarrow \Lambda^0 + \Theta^0$  one should have to give explicit expressions for the  $H_L^M$  in terms of conveniently chosen phase shifts, or more generally collision parameters. This is not our purpose here. We simply notice that, on calling  $\bar{\lambda}_M(\theta')$  the expression:

$$(32) \quad \bar{\lambda}_M(\theta') = \sum_L H_L^M Y_L^{\frac{1}{2}-M}(\theta')$$

and calling  $A$  the expression  $\sum_M |\bar{\lambda}_M(\theta')|^2$ , the normalized amplitude  ${}_s\chi_s$  may be rewritten:

$$(33) \quad {}_\alpha\chi_s = A^{-\frac{1}{2}} \sum_M \bar{\lambda}(\theta') \bar{\chi}_s^M.$$

To express the spin functions  $\bar{\chi}_s^M$  in terms of the spin functions  $\chi_s^M$  used in the previous sections, where  $M$  is the spin component along the line of flight of the  $\Lambda^0$ , a rotation around the  $y'$  axis has to be performed, as characterized by an unitary matrix  $U_{M,M'}$ ; one has:

$$(34) \quad \bar{\chi}_s^M = \sum_{M'} U_{MM'} \chi_s^{M'}.$$

We then get from (33):

$$(35) \quad {}_\alpha \chi_s = A^{-\frac{1}{2}} \sum_M \lambda_M(\theta') \chi_s^M,$$

where we have put:

$$(36) \quad \lambda_M(\theta') = \sum_{M'} U_{MM'} \bar{\lambda}_{M'}(\theta').$$

We have thus obtained expression  $(1)_\alpha$  of Sect. 2.

A similar deduction is valid when the proton spin is  $\beta$ ; it may then be seen <sup>(11)</sup>, by simple symmetry arguments that in such case the wave function of the outgoing  $\Lambda^0 \mapsto \Theta^0$  wave, similar to (31) is simply

$$(37) \quad \sum_M \sum_L H_L^M Y_L^{M-\frac{1}{2}} \bar{\chi}_s^{-M},$$

where the  $H_L^M$  are the same coefficients as in (31); remembering (32) and:

$$(38) \quad Y_L^{M-\frac{1}{2}}(\theta') = (-1)^{|M-\frac{1}{2}|} Y_L^{\frac{1}{2}-M}(\theta'),$$

(37) may be rewritten:

$$(39) \quad {}_\beta \chi_s \equiv A^{-\frac{1}{2}} \sum_M (-1)^{|M-\frac{1}{2}|} \bar{\lambda}_M(\theta') \bar{\chi}_s^{-M},$$

which has to be compared with (33). By using again (34) and the property <sup>(12)</sup>:

$$(40) \quad U_{-M, -M'} = (-1)^{|M+M'|} U_{M, M'},$$

one gets for  ${}_\beta \chi_s$ , expressed in terms of the spin functions with respect to the line of flight of the  $\Lambda^0$

$$(41) \quad {}_\beta \chi_s = \sum_M (-1)^{|M-\frac{1}{2}|} \lambda_M(\theta') \chi_s^M,$$

<sup>(11)</sup> Compare Appendix III.

<sup>(12)</sup> Compare Appendix IV.

with the same definition (36) of the  $\lambda_M(\theta')$ . This is just expression  $(1)_\beta$  and the procedure used in the previous sections to describe the decay of the  $\Lambda^0$  is thus completely justified; at the same time this deduction makes it clear that the coefficients  $\lambda_M$  in  $(1)_\alpha$   $(1)_\beta$  are generally functions of the angle  $\theta'$  between the line of flight of the  $\Lambda^0 \mapsto \Theta^0$  and that of the producing  $\pi^- \mapsto p$  in their center of mass system. This expresses of course the fact that the polarization of the outgoing  $\Lambda^0$  depends on the angle of production; when the total number of observed events will be greater than actually is, it will be more meaningful to construct several diagrams similar to Fig. 1 and Fig. 4 each one referring to a given subregion of angles of emission of the  $\Lambda^0$  in the center of mass system, than to collect in one diagram all the events independently from the production angle. It may however be emphasized that the procedure of collecting all events, independently of the above production angle in one diagram like Fig. 1 or Fig. 4 may only smooth the possible anisotropies in  $\theta$  and in  $\varphi$  which would be present for each production angle separately; hence the conclusion that the value of the spin assigned to the  $\Lambda^0$  by the analysis of such diagrams is a lower limit, is not altered.

Moreover it should be desirable, in future, that all experiments be done at the same energy; the  $\lambda_M$  depend of course on the energy and one would like to get rid of complications of this sort; as far as one can tell 1.4 GeV is a good energy, particularly if the fact is confirmed that at that energy the produced  $\Lambda^0$  tends to go back in the center of mass system, thus reducing the production angle region.

## 6. — The Polarization of the $\Lambda^0$ .

We want now to examine some questions relative to the polarization of the outgoing  $\Lambda^0$ . In Sect. 3 and 4 the expectation value of the spin component normal to the plane of production was calculated for each case and its value was assumed to be a measure of the polarization.

This has to be justified, and the sense in which the above expectation value is a measure of the polarization made clear. For this we prove first the following theorem: consider any operator  $O$  which is a product of operators  $S_x$ ,  $S_y$ ,  $S_z$  of the  $\Lambda^0$  and let the coordinate system be so defined that  $S_x$  and  $S_z$  are components of the spin in the plane of production,  $S_y$  is normal to the plane of production. Consider then the expectation value of  $O$  in the state  $\chi_\alpha$ ,  $\langle \alpha | O | \alpha \rangle$  and the similar quantity  $\langle \beta | O | \beta \rangle$  for the state  $\beta \chi_\alpha$ . Then the average value of  $O$ , defined as

$$(42) \quad \text{av } O = \frac{1}{2} [\langle \alpha | O | \alpha \rangle + \langle \beta | O | \beta \rangle],$$



is certainly zero if the number of factors  $S_x$  plus the number of factors  $S_y$  in  $O$  is odd; if the above number is even, the average of  $O$  is equal to the expectation value of  $O$  in the pure state  ${}_{\Lambda}\chi_s$ :  $\text{av } O = \langle \alpha | O | \alpha \rangle$ , which may (or may not) be different from zero. Before proving the theorem we observe that the theorem is a generalization of a similar theorem well known for the case of spin  $\frac{1}{2}$ ; in the case of spin  $\frac{1}{2}$  the only independent spin operators are just  $\sigma_x$ ,  $\sigma_y$ ,  $\sigma_z$  and the theorem may be expressed as saying that the average value of the components of the spin in the plane of collision vanish, if the beam producing the collision is unpolarized.

For a spin higher than  $\frac{1}{2}$  there are many more independent operators constructed through  $S_x$ ,  $S_y$ ,  $S_z$  and the theorem says, not only that  $\text{av } S_x = \text{av } S_z = 0$  but also that, for example,  $\text{av } S_x S_y^2$ , or  $\text{av } S_z S_x^2$  or  $\text{av } S_x^3$  etc., vanish.

The proof of the theorem is as follows: observe first that the state  ${}_{\Lambda}\chi_s$  (35) or  $(1)_{\Lambda}$  is related simply to the state  ${}_{\beta}\chi_s$  (41) or  $(1)_{\beta}$  through  $(^{11})$ :

$$(43) \quad {}_{\beta}\chi_s = PR {}_{\Lambda}\chi_s,$$

where  $P$  is the parity operator producing a reflection of the  $z'$  axis and  $R$  is an operator which produces a rotation of  $180^\circ$  around the  $y'$  axis; notice that, in the notations of the previous sections, the  $y'$  axis coincides with the  $y$  axis, so that  $S_{y'} = S_y$ .

We remark now that the unitary operator  $PR$  commutes with  $S_y$  and anti-commutes with  $S_{x'}$  and  $S_{z'}$ , therefore also with  $S_x$  and  $S_z$ :

$$R^+P^+S_yPR = S_y; \quad R^+P^+S_xPR = S_x; \quad R^+P^+S_zPR = S_z.$$

On rewriting (42) as:

$$(44) \quad \text{av } O = \frac{1}{2}[\langle \alpha | O | \alpha \rangle + \langle \alpha | R^+P^+OPR | \alpha \rangle],$$

it is then obvious from the above commutation rules that, if the total number of  $S_x$  factors plus the total number of  $S_z$  factors contained in  $O$  is odd, the second term in (44) just cancels the first, while, if the above number is even, it adds to the first; this proves the theorem.

The calculation of  $\langle S_y \rangle$  performed in Sects. 3, 4 using just the functions  ${}_{\Lambda}\chi_s$  is thus justified; at the same time however it becomes clear that the quantity  $\langle S_y \rangle = \langle {}_{\Lambda}\chi_s | S_y | {}_{\Lambda}\chi_s \rangle$  which we have calculated in Sects. 3, 4, is only one among many other equally important « indicators » of the polarization: for example also the expectation values of such operators as  $S_x^2 S_y$  or  $S_x^2$ ,  $S_y^2$ ,  $S_z^2$ ,  $S_x S_y S_z$  or  $S_y^3$  and so on (or more convenient combinations of them), are measures of the polarization; we shall however not enter here in details on this point.

As a final remark for this section the following may be appropriate: it may happen that a more detailed discussion of the process of production of a  $\Lambda^0$  shows that the  $\lambda_M$  coefficients in (35) or (1)<sub>s</sub> have to satisfy some limitations; for example it may be easily proved that if for some reasons the sum over  $L$  in (37) reduces to just one term then  $\langle S_y \rangle$  is necessarily zero; this would imply a severe limitation on the coefficients  $\lambda_M$ ; a situation of this kind presents itself at energies near threshold, where the outgoing wave with  $L = 0$  is predominant over the others. In any case, if there are limitations on the  $\lambda_M$  depending from the mechanism of production, such limitations imply that the shapes of the possible angular distributions are further restricted with respect to the case, which was assumed in the discussion of Sects. 3 and 4, in which the  $\lambda_M$  were not subjected to limitations of any kind<sup>(13)</sup>. An examination of such possible limitations will become of interest when a better statistics will indicate more clearly than now the actual shape of the distributions.

## 7. - Final Remarks.

Some of the conclusions of the analysis presented in this paper are here shortly summarized. The limitation that the spin of the  $\Theta^0$  has been assumed to be zero has to be kept in mind. However a similar treatment may be done for a  $\Theta^0$  having a spin, by summing over the  $\Theta^0$  final spin orientations. Moreover we emphasize again the scarcity of the present experimental data: *we believe that presently they are not such as to exclude absolutely even the case of spin  $\frac{1}{2}$* . It must also be added that in the case the future data indicate isotropic or smooth distributions, a method like the one presented here is

---

<sup>(13)</sup> The manuscript of this paper was ready for publication when the issue of December 1, 1955 of the *Physical Review* arrived containing a letter by R. K. ADAIR on the same general subject. ADAIR makes not use of the limitations mentioned above and we report his observation in a somewhat different but essentially equivalent form: it is seen from (32) that if just the  $L=0$  wave is present in the outgoing  $\Lambda^0 \rightarrow \Theta^0$  beam, then, apart from a numerical factor (33) and (39) reduce respectively to  ${}_s\chi_s = \bar{\chi}_s^{\frac{1}{2}}$  and  ${}_s\chi_s = \bar{\chi}_s^{-\frac{1}{2}}$ . This wave functions, on decay, give rise to perfectly definite angular distributions, so that for any spin  $S$ , a completely definite angular distribution is obtained in the angle between the line of flight of the producing  $\pi^-$ , and the line of flight of the  $\pi^-$  produced on the decay. The same observation applies, (this is in fact the content of ADAIR's paper) if one considers, at any energy, the  $\Lambda^0$  produced along the line of flight of the producing  $\pi^-$ , and also if the  $\Theta^0$  has a value of the spin different from zero. The advantage of Adair's method is, of course, that a definite value for the spin may be obtained, and not just a lower limit; the disadvantage, of course, is that to restrict oneself to events near threshold only or to events produced into a narrow solid angle, makes it very difficult to collect a sufficient statistics. I thank Prof. M. KROLL for a discussion on the content of ADAIR's paper.

unable to lead to any definite conclusion; it has to be kept in mind that the following points may be then stated:

1) If the present data are taken as indications of anisotropies in either the  $\varphi$  or the  $\theta$  distributions, or in both, the spin of the  $\Lambda^0$  is at least  $\frac{3}{2}$ .

2) If the present data moreover are taken as indicating a maximum at some angle intermediate between  $0^\circ$  and  $90^\circ$  in the  $\cos \theta$  angular distribution then the spin of the  $\Lambda^0$  must be at least  $\frac{5}{2}$ .

3) If the future data shall confirm the extremely pronounced maximum in the  $\cos \theta$  distribution at  $\cos \theta \cong 0.5$  and at the same time the peaking in the  $\varphi$  distribution at  $0^\circ$ , the spin of the  $\Lambda^0$  should be larger than  $\frac{5}{2}$ .

4) In any case the information which one may get from the simultaneous consideration of the  $\varphi$  and  $\theta$  angular distribution, is extremely larger than the information which one may get from their separate consideration; it is therefore hoped that in every experimental paper the data necessary to the construction of diagrams Fig. 1 and Fig. 4 will be explicitly indicated.

\* \* \*

Several conversations with Prof. N. KROLL have been particularly stimulating. I would like to thank him; I thank also Prof. B. TOUSCHEK for an useful discussion on the material presented in Sect. 5.

#### APPENDIX I (to Section 3).

The only non vanishing  $G_{M^2, M}^{(\frac{3}{2}, 2)}$  are:

$$G_{\frac{3}{2}, -\frac{1}{2}}^{(\frac{3}{2}, 2)} = G_{-\frac{1}{2}, \frac{3}{2}}^{(\frac{3}{2}, 2)} = G_{\frac{1}{2}, -\frac{3}{2}}^{(\frac{3}{2}, 2)} = G_{-\frac{3}{2}, \frac{1}{2}}^{(\frac{3}{2}, 2)} = -\frac{1}{2\sqrt{3}}.$$

The values of the  $\Gamma_M^{(\frac{3}{2}, 2)}$  are as follows:

$$\Gamma_{\frac{1}{2}}^{(\frac{3}{2}, 2)} = \Gamma_{-\frac{1}{2}}^{(\frac{3}{2}, 2)} = \frac{1}{5}; \quad \Gamma_{\frac{3}{2}}^{(\frac{3}{2}, 2)} = \Gamma_{-\frac{3}{2}}^{(\frac{3}{2}, 2)} = \frac{1}{5}.$$

The relation between the  $\lambda_M$  and the parameters  $\gamma$ ,  $\varepsilon$ ,  $\delta$ ,  $\psi_M$  is:

$$\begin{aligned} \lambda_M = \varrho_M \exp[i\psi_M] \quad \text{and} \quad \varrho_{\frac{3}{2}} &= \sin \gamma \cos \varepsilon & \varrho_{-\frac{3}{2}} &= \sin \gamma \sin \varepsilon, \\ \varrho_{\frac{1}{2}} &= \cos \gamma \cos \delta & \varrho_{-\frac{1}{2}} &= \cos \gamma \sin \delta. \end{aligned}$$

The polarization may be calculated remarking that

$$\langle S_y \rangle = \frac{1}{2i} \langle (S_x + iS_y) - (S_x - iS_y) \rangle.$$

## APPENDIX II (to Section 4).

The non vanishing  $G_{M', M'}^{(\frac{5}{2}, 2)}$  are:

$$\begin{aligned} G_{\frac{5}{2}, \frac{1}{2}}^{(\frac{5}{2}, 2)} &= G_{\frac{1}{2}, \frac{5}{2}}^{(\frac{5}{2}, 2)} = G_{-\frac{1}{2}, -\frac{5}{2}}^{(\frac{5}{2}, 2)} = G_{-\frac{5}{2}, -\frac{1}{2}}^{(\frac{5}{2}, 2)} = -\frac{1}{\sqrt{40}}, \\ G_{\frac{1}{2}, -\frac{3}{2}}^{(\frac{5}{2}, 2)} &= \text{etc.} = . . . = -\frac{1}{\sqrt{8}}, \\ G_{\frac{3}{2}, -\frac{1}{2}}^{(\frac{5}{2}, 4)} &= \text{etc.} = . . . = \frac{1}{2\sqrt{5}}. \end{aligned}$$

The values of the  $\Gamma_M^{(\frac{5}{2}, 2)}$  are as follows:

$$\Gamma_{\frac{5}{2}}^{(\frac{5}{2}, 2)} = \Gamma_{-\frac{5}{2}}^{(\frac{5}{2}, 2)} = -\frac{2}{7}; \quad \Gamma_{\frac{3}{2}}^{(\frac{5}{2}, 2)} = \Gamma_{-\frac{3}{2}}^{(\frac{5}{2}, 2)} = \frac{2}{35}; \quad \Gamma_{\frac{1}{2}}^{(\frac{5}{2}, 2)} = \Gamma_{-\frac{1}{2}}^{(\frac{5}{2}, 2)} = \frac{8}{35},$$

The values of the  $\Gamma_M^{(\frac{5}{2}, 4)}$  are:

$$\Gamma_{\frac{5}{2}}^{(\frac{5}{2}, 4)} = \Gamma_{-\frac{5}{2}}^{(\frac{5}{2}, 4)} = \frac{1}{21}; \quad \Gamma_{\frac{3}{2}}^{(\frac{5}{2}, 4)} = \Gamma_{-\frac{3}{2}}^{(\frac{5}{2}, 4)} = -\frac{1}{7}; \quad \Gamma_{\frac{1}{2}}^{(\frac{5}{2}, 4)} = \Gamma_{-\frac{1}{2}}^{(\frac{5}{2}, 4)} = \frac{2}{21}.$$

The relation between the  $\lambda_M$  and the parameters  $\Gamma$ ,  $\gamma$ ,  $\varepsilon$ ,  $\gamma'$ ,  $\varepsilon'$ ,  $\psi_M$  is:

$$\begin{aligned} \lambda_M &= \varrho_M \exp[i\psi_M] \quad \text{and} \quad \varrho_{\frac{5}{2}} = \sin \Gamma \sin \gamma \cos \varepsilon; & \varrho_{-\frac{5}{2}} &= \cos \Gamma \sin \gamma' \cos \varepsilon', \\ \varrho_{-\frac{3}{2}} &= \sin \Gamma \sin \gamma \sin \varepsilon; & \varrho_{\frac{3}{2}} &= \cos \Gamma \sin \gamma' \sin \varepsilon', \\ \varrho_{\frac{1}{2}} &= \sin \Gamma \cos \gamma; & \varrho_{-\frac{1}{2}} &= \cos \Gamma \cos \gamma'. \end{aligned}$$

## APPENDIX III (to Section 5).

The proof of eq. (37) is as follows: the ingoing wave

$$\psi_{\beta}^{\text{in}} = \beta \sum_l A_l Y_l^0(\theta') \frac{\exp[-ikr]}{r},$$

which gives rise to the outgoing wave (37) is related to the ingoing wave

$$\psi_{\alpha}^{\text{in}} = \alpha \sum_l A_l Y_l^0(\theta') \frac{\exp[-ikr]}{r}$$

which gives rise to the outgoing wave (31) simply through

$$\psi_{\beta}^{\text{in}} = PR\psi_{\alpha}^{\text{in}},$$

where  $R$  is an operator effecting a rotation of  $180^\circ$  and  $P$  is the parity operator. Therefore since the operator  $PR$  commutes with the Hamiltonian, the outgoing wave, when the proton is initially in the state  $\beta$  is simply obtained from (31), by application of the operator  $PR$ . Now it is easy to see that apart from an inessential phase factor independent from  $M$  and  $L$

$$PR\tilde{\chi}_s^M = \tilde{\chi}_s^{-M},$$

$$PR Y_L^{M-\frac{1}{2}}(\theta') = P Y_L^{\frac{1}{2}-M}(\pi - \theta') = Y_L^{\frac{1}{2}-M}(\theta'),$$

thus proving (37).

#### APPENDIX IV (to Section 5).

The matrix  $U_{MM'}$  is defined by a set of equations of the form:

$$(aS_x + bS_z - M) \sum_{M'} U_{MM'} \chi_s^{M'} = 0,$$

where the  $x$  and  $z$  axes are the same as in Sect. 3;  $a$ ,  $b$  specify the rotation from the  $z'$  to the  $z$  axis around the  $y' = y$  axis. On writing explicitly the above equations as:

$$\begin{aligned} \frac{a}{2} [U_{M, M''-1} \sqrt{(S - M'' + 1)(S + M'')} + U_{M, M''+1} \sqrt{(S + M'' + 1)(S - M'')}] + \\ + b(M'' - M)U_{MM''} = 0, \end{aligned}$$

we see that they are invariant under the substitution (40).



## RIASSUNTO

Si descrive un metodo per stabilire un limite inferiore allo spin del  $\Lambda^0$ ; esso è basato sull'osservazione che, per ogni spin che si assume per il  $\Lambda^0$  le forme possibili che le distribuzioni in  $\cos \theta$  e in  $\varphi$  ( $\varphi$ =angolo tra il piano di produzione e quello di decadimento;  $\theta$  angolo tra la linea di volo del  $\Lambda^0$  e la linea di volo dei prodotti di decadimento nel sistema di riposo del  $\Lambda^0$ ) possono simultaneamente avere, sono legate tra di loro ed in numero limitato. Viene esposta una analisi dettagliata per i casi di spin  $3/2$  e  $5/2$ . La scarsità dei dati sperimentali attualmente disponibili (12 casi di natura non completamente omogenea) non permettono al momento di esprimere conclusioni sicure; tuttavia se alcune caratteristiche salienti dei dati attuali si manterranno in futuro, è necessario uno spin almeno pari a  $5/2$ .

## A Model for $\Lambda^0 - \theta^0$ Production (\*).

L. F. LANDOVITZ and J. LEITNER (\*\*)

*Nevis Cyclotron Laboratories, Columbia University, Department of Physics - New York*

(ricevuto il 6 Marzo 1956)

**Summary.** — A calculation of the perturbation theoretic angular distributions in the reaction  $\pi^- + p \rightarrow \Lambda^0 + \theta^0$  is reported. Some general implications of the model  $\pi^- + p \rightarrow \text{single particle} \rightarrow \Lambda^0 + \theta^0$  are described. The second order results for the productions distributions are of the form  $A + B \cos \theta$  for all choices of spin, coupling, etc. The exact center of mass distribution is identical in form to that above but is determined only to within an unknown parameter  $\xi$ . The nature of the distributions preclude the possibility of verification of the model on the basis of present data. The decay angular distributions of the spin  $\frac{1}{2}$   $\Lambda^0$  are isotropic for all values for the  $\theta^0$  spin. Possibilities for future comparison with experiment are discussed.

### 1. — Introduction.

Recent measurements at Brookhaven (<sup>1-3</sup>) of the center of mass angular distribution of  $\Lambda^0$  particles produced in the reaction  $\pi^- + p \rightarrow \Lambda^0 + \theta^0$ , indicate a surprisingly large anisotropy favoring the backward direction. Also, experiments (<sup>4</sup>) on production of  $\Lambda^0$ ,  $\theta^0$  in carbon and lead show that the emergent

---

(\*) This research was supported in part by the joint program of The Atomic Energy Commission and the Office of Naval Research.

(\*\*) Quincy Ward Boese Fellow.

(<sup>1</sup>) W. B. FOWLER, R. P. SHUTT, A. M. THORNDIKE and W. S. WHITEMORE: *Phys. Rev.*, **93**, 861 (1954).

(<sup>2</sup>) W. B. FOWLER, R. P. SHUTT, A. M. THORNDIKE and W. S. WHITEMORE: *Phys. Rev.*, **98**, 121 (1955).

(<sup>3</sup>) W. D. WALKER: *Phys. Rev.*, **98**, 1407 (1955).

(<sup>4</sup>) H. BLUMENFELD, E. T. BOOTH, L. M. LEDERMAN and W. CHINOWSKY: private communication.

$\Lambda^0$  has a small laboratory kinetic energy which is not inconsistent with a large center of mass production angle. This paper reports the results of an investigation undertaken to examine the possibility of comparison of observed distributions with those given by a perturbation theoretic calculation.

No general kinematical arguments are capable of predicting the center of mass distribution without assumptions concerning the relevant matrix elements. A unique description of the center of mass angular distribution (for various values of the  $\theta^0$  spin), is afforded only by assumptions as to the following:

- (1) A model for the reaction along with an appropriate interaction hamiltonian.
- (2) Relative parity of the  $\theta^0$ , nucleon fields.
- (3) Couplings consistent with the assumed  $\theta^0$  spin.
- (4) The  $\Lambda^0$  spin.

Little data, unambiguously pertinent as criteria for the spin of the  $\Lambda^0$ , are available. As pointed out by FOWLER *et al.*, this evidence is somewhat contradictory inasmuch as one appropriate angular correlation is present while another is not. Although much data <sup>(5,7)</sup> are available from production of  $\Lambda^0$ - $\theta^0$  pairs in heavy  $Z$  materials, the latter is of dubious worth since  $\Lambda^0$  scattering would almost certainly serve to destroy any polarization present at production. Moreover, some authors find a  $\gamma$  correlation <sup>(8)</sup> indicative of  $S_\Lambda > \frac{1}{2}$ , while others do not. It is felt therefore that the existing evidence is not conclusive enough to discard the benign possibility that the  $\Lambda^0$  is indeed a spin  $\frac{1}{2}$  Dirac particle. As regards assumption (3), since the  $\theta^0$  is known to have the decay scheme  $\theta^0 \rightarrow \pi^+ + \pi^-$ , its parity must be given by  $(-1)^{S_\theta}$  (where  $S_\theta$  is the  $\theta^0$  spin); all couplings inconsistent with the above criterion are neglected. Those couplings, inconsistent with the  $\theta^0$  parity which are present in Table I have been included, since this theory applies equally well to the associated production of  $\Lambda^0$ 's and  $\tau$ 's via the reactions:

$$\pi^+ + n \rightarrow p \rightarrow \Lambda^0 + \tau^+$$

$$\pi^- + p \rightarrow n \rightarrow \Lambda^0 + \tau^0$$

<sup>(5)</sup> D. GAYTHER and C. BUTLER: *Phil. Mag.*, **46**, 467 (1955).

<sup>(6)</sup> J. D. SORRELS: *Fifth Annual Rochester Conference*.

<sup>(7)</sup> J. BALLAM, A. L. HODSON, W. MARTIN, R. RAU, G. T. REYNOLDS and S. B. TRIEMAN: *Phys. Rev.*, **97**, 245 (1955).

<sup>(8)</sup>  $\gamma$  = angle between production and decay planes.

and since the parity of the  $\tau$  is probably negative. This follows from the known decay scheme for  $\tau$ :  $\tau^+ \rightarrow \pi^+ + \pi^+ + \pi^-$  and the fact that in at least one case the odd  $\pi^-$  is emitted in a  $S$ -state relative to the center of mass of the di- $\pi$  system ( $E_\pi \sim .5$  MeV), since then the  $\tau$  parity is given by  $P_\tau = (-1)^l$  where  $l$ , the relative angular momentum of a 2 boson system, must be even. In fact, the statistical analyses of DALITZ<sup>(9)</sup>, HARRIS *et al.*<sup>(10)</sup>, etc., show that 0, — are the most favorable values of the spin-parity; the 0, — cases are, thus, reported in Table I. Since the  $\Lambda^0$  decays into  $\pi^- + p$  its parity is given by  $(-1)^{j \pm \frac{1}{2}}$ ; hence all possibilities consistent with scalar Lagrangian are considered. Assumption (1) is discussed in detail below.

## 2. — General Consequences of the Model.

The strong Yukawa interaction suggests a single particle intermediate state as a model for the production of  $\Lambda^0$ ,  $\theta^0$ 's. The simplest phenomenological interaction consistent with the above, and which incorporates the strong conservation laws of charge and heavy particles, as well as the associated production hypothesis<sup>(11)</sup> is:  $\pi^- + p \rightarrow n \rightarrow \Lambda^0 + \theta^0$ <sup>(12)</sup> as shown in Fig. 1. For the neutron

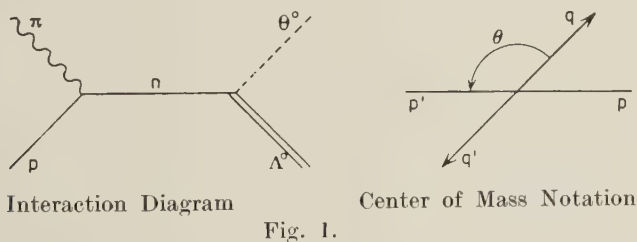


Fig. 1.

decay vertex the interaction hamiltonian is taken to be:  $H_{\Lambda^0\theta^0} = G \int \bar{\psi}_\Lambda O_j \psi_N \Phi_j \cdot d^3x + \text{c.c.}$ , where  $O_j$  is a coupling operator dependent upon the properties of the  $\theta^0$ . The forms assumed by  $H_{\Lambda^0\theta^0}$  for various values of  $S_\theta$  are given in

<sup>(9)</sup> R. DALITZ: *Proceedings of the Fifth Annual Rochester Conference*.

<sup>(10)</sup> G. HARRIS, J. OREAR and S. TAYLOR: in press.

<sup>(11)</sup> M. GELL-MANN and A. PAIS: *Proceedings of the Fifth Annual Rochester Conference on High Energy Nuclear Physics*, 1955.

<sup>(12)</sup> It has been brought to our attention that this production scheme has been investigated by MATTHEWS and SALAM. [P. T. MATTHEWS and A. SALAM: *Phil. Mag.*, **46**, 150 (1955)]. However they have limited their efforts to the derivation of some few second order results. Their results, wherever comparable to those given here, are in agreement with the latter.

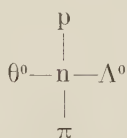
Table I. The total hamiltonian for the system is then,

$$H = H_{\pi} + H_n + N_{n\pi} + H_{\Lambda^0\theta^0},$$

where  $H_{\pi}$  and  $H_n$  are the free pion and nucleon hamiltonians respectively and  $H_{n\pi}$  is the usual charge independent pion-nucleon hamiltonian <sup>(13)</sup>:

$$H_{n\pi} = ig \int \bar{\psi} \boldsymbol{\tau} \cdot \boldsymbol{\Phi} \psi d^3x.$$

These hamiltonians have as a direct consequence the set of interactions:



hence only one type of interaction diagram is possible, namely that shown in Fig. 1. Thus, in spite of any self energy corrections etc., the intermediate state consists of a spin  $\frac{1}{2}$  neutron; the angular dependence of  $\sigma(\theta)$  is then determined by angular momentum considerations alone. This situation is quite similar to the compound nucleus theory for inelastic scattering of neutrons from nuclei where conservation of angular momentum determines the distribution of emergent particles. Since the intermediate state consists of a single particle, it has  $J = \frac{1}{2}$ ,  $J_z = \pm \frac{1}{2}$  only. Further, since the emergent particles are spin  $\frac{1}{2}$  and spin 0 or 1, the allowed orbital angular momenta are 0 and 1. Then the wave function of the intermediate states (for the  $S_0 = 0$  case) can be represented as:

$$\psi_{J_z = \frac{1}{2}} = \alpha |\frac{1}{2} \frac{1}{2}\rangle Y_0^0 + \beta [\sqrt{\frac{2}{3}} |\frac{1}{2}, -\frac{1}{2}\rangle Y_1^1 - \sqrt{\frac{1}{3}} |\frac{1}{2} \frac{1}{2}\rangle Y_1^0],$$

$$\psi_{J_z = -\frac{1}{2}} = \alpha |\frac{1}{2}, -\frac{1}{2}\rangle Y_0^0 + \beta [\sqrt{\frac{2}{3}} |\frac{1}{2}, -\frac{1}{2}\rangle Y_1^0 + \sqrt{\frac{1}{3}} |\frac{1}{2} \frac{1}{2}\rangle Y_1^{-1}].$$

Since the neutron has a definite parity one might expect the distribution to contain  $s$  waves or  $p$  waves only; however, the intermediate state contains neutrons or anti-neutrons and since  $\gamma_4$ , the relativistic inversion operator, gives

$$\gamma_4 u_0^{(-)} = -u_0^{(-)},$$

both signs for the parity of the intermediate state are permitted. The coef-

<sup>(13)</sup> G. WENTZEL: *Quantum Theory of Fields* (New York, 1949), p. 63.



ficients of the  $s$  and  $p$  waves are independent of  $J$  by symmetry, hence are identical.

Then

$$|\psi_{\frac{1}{2}}|^2 = |\psi_{-\frac{1}{2}}|^2 = \alpha^2 + \beta^2 + \gamma \cos \theta.$$

Averaging over intermediate states gives  $\sigma_{\text{scalar}}(\theta) \sim A + B \cos \theta$ . An identical result holds in the vector case.

Since only  $s$  and  $p$  waves are involved in the cross-sections quoted above, it follows from the general theory of partial waves since  $\sigma_{\text{max}} = \sum_l (2l+1)\pi\lambda^2$  that the maximum cross-section for production should be  $4\pi\lambda^2 \sim 8.3$  mb for  $E_\pi \sim 1.5$  GeV.

An angular momentum analysis identical to that above gives  $\sigma_{\frac{3}{2}}(\theta) = A + B \cos \theta$  also. Indications are that any spin for the  $\Lambda^0$  will give this distribution.

The  $\Lambda^0$  decay angular distribution can be written, on the basis of angular momentum conservation alone, as:

$$\sigma_0(\theta) = \sum_j \sum_{m_\Lambda} \sum_{m_p} |a_j| \left( C_{S_\Lambda S_\theta m_\Lambda m_\theta}^{S_\Lambda S_\theta J J_z} C_{S_p l m_p m_l}^{S_p l S_\Lambda m_\Lambda} \right) Y_l^{m_l} |^2.$$

Here, since  $J = \frac{1}{2}$ ,  $m_\Lambda + m_\theta = \pm \frac{1}{2}$ , the resultant distribution is identical to certain angular correlations found in the above model independent case, if one considers  $\Lambda^0$ 's and  $\theta^0$ 's produced in the forward or backward direction. Such correlations have been tabulated by ADAIR<sup>(14)</sup>; for spin  $\frac{1}{2}$   $\Lambda^0$ 's they are isotropic independent of the assumed  $S_\theta$ .

### 3. — Born Approximation.

From  $H$  it follows that the matrix element for production,  $M$ , is:

$$M \sim \bar{u}_{q,\sigma}^{(+)} O_i [-i\gamma(p_4 + p_4') + m] \gamma_5 u_{p,\sigma}^{(+)},$$

where  $u^{(\pm)}$  is a positive (negative) energy spinor and  $p_4, p_4', q_4, q_4'$  are the four-momenta of the proton, pion,  $\Lambda^0, \theta^0$  respectively. Hence,

$$\sigma_2(\theta) \sim \frac{1}{2} \sum_{\substack{\sigma, \sigma' \\ \text{pol.} \\ \text{of } \theta^0}} |M|^2 \sim A + B \cos \theta.$$

The results of this second order calculation are given in Table I. The following

(14) R. K. ADAIR: in press.

TABLE I.

K Particle Spin	Coupling	K Particle Parity	$H_{\Lambda,0}$	$\sigma_2(\theta) \sim A_i + B_i \cos \theta$	
				$A_i$	$B_i$
0	Scalar	+	$G \int \bar{\psi}_\Lambda \psi_N \Phi d^3x + \text{c. c.}$	$2E_q w_p r - \mu^2(E_p E_q + m M)$	$pq(2p^2 + 2E_p w_p + \mu^2)$
0	Pseudo scalar	—	$G \int \bar{\psi}_\Lambda \gamma_5 \psi_N \Phi d^3x + \text{c. c.}$	$2p^2 w_p E_q - \mu^2(E_p E_q - m M)$	$pq(2p^2 + \mu^2)$
0	Gradient	+	$\frac{G}{K} \int \bar{\psi}_\Lambda \gamma_\mu \psi_N \frac{\delta \Phi}{\delta x_\mu} d^3x + \text{c. c.}$	$\frac{2w_q s}{K^2} (-2w_p r + \mu^2 E_p) + 2w_p E_q r - \mu^2(E_p E_q + m M)$	$pq(\mu^2 + 2r) \left[ 1 + \frac{2s}{K^2} \right]$
0	Gradient	—	$\frac{G}{K} \int \bar{\psi}_\Lambda \gamma_5 \gamma_\mu \psi_N \frac{\delta \Phi}{\delta x_\mu} d^3x + \text{c. c.}$	$\frac{2w_p s}{K^2} (2w_q r - E_p \mu^2) - 2w_p E_q r + \mu^2(E_p E_q + m M)$	$-pq(\mu^2 + 2r) \left[ 1 + \frac{2s}{K^2} \right]$
1	Vector	+	$G \int \bar{\psi}_\Lambda \gamma_\mu \psi_N \Phi d^3x + \text{c. c.}$	$\frac{2w_q s}{K^2} (2w_p r - \mu^2 E_p) + 2w_p E_q r + \mu^2(3m M - E_p E_q)$	$pq(\mu^2 + 2r) \left[ 1 - \frac{2s}{K^2} \right]$

TABLE II. —  $\sigma(\theta) \sim \bar{A}_i + \bar{B}_i \cos \theta$ .

K Particle Spin	Coupling	K Particle Parity	$\bar{A}_i$	$\bar{B}_i$
0	Scalar	+	$A^2 A_s + 2AB\{mw_p E_q - M(p^2 + E_p w_p)\} + B^2(mM - E_p E_q)$	$A^2 B_s + 2mpqAB + pqB^2$
0	Pseudo Scalar	—	$A^2 A_{ps} - 2AB\{mw_p E_q - M(p^2 + E_p w_p)\} + B^2(mM + E_p E_q)$	$A^2 B_{ps} - 2mpqAB - pqB^2$
0	Gradient	+	$A^2 A_{q+} + AB[4mw_q w_p s - K^2 w_p E_q m + 2K^2 M(p^2 + E_p w_p)] + B^2(mM + E_p E_q)$	$A^2 B_{q+} - pqAB[4ms + K^2/2] - 2pqB^2(s + K^2/2)$
0	Gradient	—	$A^2 A_{q-} + AB[4mw_q w_p s + K^2 mw_p E_q + 2K^2 M(p^2 + E_p w_p)] - B^2[-2E_p w_q s + K^2(mM + E_p E_q)]$	$A^2 B_{q-} - pqAB[4ms - K^2/2] - 2pqB^2(s - K^2/2)$
1	Vector	+	$A^2 A_v + 2AB\left[3Ms + 3mw_p E_q - \frac{2mw_p w_q r}{K^2}\right] + B^2\left[-2E_p E_q + \frac{2s}{H^2} E_p w_q - 3mM\right]$	$A^2 B_v + 2mABpq\left[3 + \frac{2s}{K^2}\right] + B^2pq\left[3 + \frac{2s}{K^2}\right]$

notation is employed:

$m, \mu, M, K$  are the masses of the proton,  $\pi, \Lambda^0, \theta^0$  respectively, and  $E_p, w_p, \bar{E}_q, \bar{w}_q$  are the energies of the proton,  $\pi, \Lambda^0, \theta^0$  respectively;

$$r = p^2 + E_p w_p;$$

$$s = q^2 + E_q w_q.$$

#### 4. - Relation between Born Approximation and Exact Solution.

To obtain the relation between the second order results and the exact angular distribution the most general form of the matrix element for interaction:

$$(1) \quad M' \sim \bar{u}_{q,\sigma}^{(+)} O'_j S'_F \Gamma'_5 u_{p\sigma}^{(+)}$$

must be used. Since the hamiltonian is invariant, the transformation properties of  $O'_j, S'_F, \Gamma'_5$  must be the same as their counterparts  $O_j, S_F, \gamma_5$ :

Then,

$$(2) \quad S'_F \sim [-i\gamma(p_4 + p'_4) + m]f_1 + f_2,$$

$$(3) \quad \Gamma'_5 \sim \gamma_5 g_1 + [-i\gamma(p_4 + p'_4) + m]\gamma_5 g_2 + \gamma_5 [-i\gamma p_4 + m]g_3 + \\ + [-i\gamma(p_4 + p'_4) + m]\gamma_5 [-i\gamma p_4 + m]g_4,$$

$$(4) \quad \Gamma'_\mu \sim \gamma_\mu h_1 + [-i\gamma q_4 + M]\gamma_\mu h_2 + \gamma_\mu [-i\gamma(p_4 + p'_4) + m]h_3 + \\ + [-i\gamma q_4 + M]\gamma_\mu [-i\gamma(p_4 + p'_4) + m]h_4,$$

$$(5) \quad l' \sim l_1 + [-i\gamma q_4 + M]l_2 + [-i\gamma(p_4 + p'_4) + m]l_3 + \\ + [-i\gamma q_4 + M][-i\gamma(p_4 + p'_4) + m]l_4,$$

where  $f_j, g_j, h_j, l_j$  are unknown functions of  $p_4^2, p_4'^2, (p_4 - p_4')^2, q^2, q'^2$  (from covariance requirements); further, there can be no angular dependence in these functions for terms like  $q_4(p_4 + p'_4)$  can be replaced by  $q_4(q_4 + q'_4)$  because of energy conversation. As expected, substitution of (2), (3), (4), (5) into (1) yields  $\sigma(\theta) \sim \bar{A}_i + \bar{B}_i \cos \theta$  where  $\bar{A}_i, \bar{B}_i$  are appropriate composites of the functions  $f_j, g_j, h_j, l_j$  known parameters, and  $A_i, B_i$ , the Born approximation values of  $\bar{A}_i, \bar{B}_i$ . The resulting exact angular distributions <sup>(15)</sup> are tabulated for various  $\theta^0$  spins in Table II.

<sup>(15)</sup> Derivative couplings are included although they are non-renormalizable in power series, since if exact solutions obtainable by other methods *do* exist, the results quoted here will hold.

## 5. - Comparison with Experiment.

There are two distinct features of the calculation: the use of a particular model and application of perturbation theory to the problem. A comparison of decay angular distributions with experiment, since the former are independent of perturbation theory, is in principle a direct test of the validity of the model. However, the decay distributions are in all cases isotropic and since only two certain  $\Lambda^0$  decays from  $\Lambda^0$ ,  $\theta^0$  pairs produced in hydrogen have been reported such a comparison is not warranted at present.

A fit of the center of mass distributions to experiment on the other hand, provides a test of perturbation theory as well as the model. The quantity of interest here is the anisotropy in the distribution which can be described by means of the parameter

$$\varepsilon(\xi_i) \equiv \frac{\sigma(180^\circ)}{\sigma(0)} = \frac{\bar{A}(\xi_i) - \bar{B}(\xi_i)}{\bar{A}(\xi_i) + \bar{B}(\xi_i)},$$

where  $\xi_i = A_i/B_i$ : The condition  $\sigma(\theta) \geq 0$  requires that  $\xi_i$  lie outside the region given by the largest and smallest roots ( $\xi_{i_{\min}}^\pm$ ) of the equations  $\bar{A}_i \pm \bar{B}_i = 0$ . However  $\varepsilon(\xi_i)$  is completely unrestricted by the theory ( $0 \leq \varepsilon(\xi_i) \leq \infty$ ).

Consequently, almost any observed anisotropy can be fit to the exact theoretical anisotropy by proper choice of  $\xi_i$ . In the case  $|\xi_i| \gg 1$ , however,  $\varepsilon(\xi_i)$  becomes independent of the exact value of  $\xi_i$ , since then

$$\varepsilon(\xi_i) \sim \frac{A_i - B_i}{A_i + B_i} \equiv \varepsilon_2,$$

which is the unique Born approximation result; the latter can be calculated directly using Table I.

An exact application of the maximum likelihood procedure for fitting the observed data to the distribution is not possible in general since it requires a knowledge of the probability for detection of  $\Lambda^0$  decays.

Since a  $\Lambda^0$ ,  $\theta^0$  event is not seen unless the  $\Lambda^0$  (or  $\theta^0$ ) decay is detected, the observed distribution is effectively  $f(\theta) = \sigma(\theta)D(\theta)$  where  $D(\theta)$  is the probability for detection of  $\Lambda^0$  decays.  $D(\theta)$  is quite difficult to calculate exactly but can be approximated for various angular ranges of  $\theta$ ,  $\theta_i$ , and is of the form

$$D(\theta) = \exp\left[-\frac{\Delta x M}{P_{\Lambda}(\theta)\tau_0}\right] - \exp\left[-\frac{X_{A0}L_{A0}(\theta)}{P_{\Lambda}(\theta)\tau_0}\right],$$



where:  $\Delta x$  = the smallest recognizable distance between interactions in the chamber,

$P_{\Lambda}(\theta)$  = laboratory momentum of the  $\Lambda^0$ ;

$\tau_0$  = mean life for the  $\Lambda^0$ ;

$X_{\Delta\theta}$  = a function of chamber dimensions for the range  $\Delta\theta_i$ ;

$L_{\Delta\theta}(\theta)$  = a function of  $\theta$  defined for the range  $\Delta\theta_i$ .

Hence, the exact expression for the joint probability of observing the experimental distribution is

$$P = \pi\sigma(\theta_j)D_{\Delta\theta_j}(\theta_j),$$

where

$$\sum_i \int \Delta\theta_i \sigma(\theta) D_{\Delta\theta_i}(\theta) dw = 1,$$

normalizes the distribution. The best fit values of  $\bar{A}$ ,  $\bar{B}$ , namely  $\bar{A}^*$ ,  $\bar{B}^*$  are then given by

$$\frac{\delta P}{\delta \bar{A}} = \frac{\delta P}{\delta \bar{B}} = 0.$$

In practice, for the sake of ease of computation, one plots  $P$  for  $\bar{A} > \bar{B} > -\bar{A}$  and observes the maximum. A very crude calculation assuming  $D_{\Delta\theta_i}(\theta) = \text{const}$  yields a best fit value  $\bar{A}^*/\bar{B}^* \sim 1$  or  $\varepsilon^*(\xi_i^*) \sim 0$  which is expected for a large anisotropy. Correspondingly,  $\xi_i^* \sim \xi_{i \min}^{\pm}$  which since  $\xi_{i \min}^{\pm} \sim 1$  (for  $E_{\pi} \sim 1.5$  GeV) may indicate that the experimental anisotropy cannot be compared to the unique Born approximation result. It is important to note that in the above approximation the normalization does not restrict  $\bar{A}/\bar{B}$  while in a more exact calculation the normalization will in general require  $\bar{A}/\bar{B} = f(\bar{A}, \bar{B})$ . Since  $\varepsilon(\xi_i)$  depends on the ratio  $\bar{A}/\bar{B}$  only, it is indeed possible that in a more realistic approximation the best fit solution might be consistent with  $|\xi_i| \gg 1$  in which case  $\varepsilon(\xi_i^*)$  would be directly comparable to  $\varepsilon_{2i}$ . However, because of the small number of events, and the fact that they were observed in different chambers (hence with different  $D(\theta)$ 's) it is felt that a more detailed comparison should be deferred until more data are available.

\* \* \*

The authors are indebted to Professors A. PAIS, R. SERBER, and J. STEINBERGER for their many suggestions and constructive criticism. We should also like to express our thanks for helpful discussions with Doctors R. ADAIR and J. OREAR.

**Note Added in Proof.**

Recently, considerable data on  $\Lambda^0\theta^0$  production in hydrogen have been reported by STEINBERGER'S group at Columbia. Out of 23  $\Lambda^0$ 's seen, 18 have  $\theta_{\text{CM}} > 120^\circ$ . Such a large CM peaking indicates that many  $l$  values may be involved in production -- a feature which is not consistent with the model proposed here.

## RIASSUNTO (\*)

Si riferisce un calcolo delle distribuzioni angolari teoriche nella reazione  $\pi^+ + p \rightarrow \Lambda^0 + \theta^0$  quali risultano nella teoria delle perturbazioni. Si descrivono alcune conseguenze generali del modello  $\pi^+ + p \rightarrow$  particella singola  $\rightarrow \Lambda^0 + \theta^0$ . I risultati del secondo ordine per le distribuzioni dei prodotti sono della forma  $A + B \cos \theta$  per qualsiasi scelta di spin, accoppiamento ecc. La distribuzione nel sistema del centro di massa esatta è nella forma identica a quella suddescritta ma determinata solo a meno di un parametro  $\xi$  incognito. La natura delle distribuzioni preclude la possibilità di verificare il modello sulla base dei dati oggi disponibili. Le distribuzioni angolari nel decadimento dei  $\Lambda^0$  di spin  $\frac{1}{2}$  sono isotrope per qualsiasi valore dello spin del  $\theta^0$ . Si discutono le future possibilità di confronto con l'esperienza.

---

(\*) Traduzione a cura della Redazione.

## On the Pion-Nucleon Interaction.

P. BUDINI

*Istituto di Fisica dell'Università - Trieste*  
*Istituto Nazionale di Fisica Nucleare - Sezione di Padova*

(ricevuto il 15 Marzo 1956)

**Summary.** — A non local model for the pion-nucleon interaction is presented assuming that the pion interacts with the nucleon through an intermediate field. This internal field provides factors in the integral equations of the pion nucleon scattering which play the role of the usual mathematical form factors of the non local theories. With a proper choice of the mass of the internal quanta and of the coupling-constant and after renormalization of the integral equations on the Chew scheme the known behaviour of the  $P$  phases of pion nucleon scattering at low energy can be reproduced.

### 1. — Introduction.

The extended source model for the pseudovector symmetric pion-nucleon interaction seems to give a satisfactory account of part at least of the low energy pion-nucleon phenomenology <sup>(1)</sup>. Considering that the extended source theory is nothing other than the static limit of non local covariant theories <sup>(2)</sup>, its successes render interesting the discussion of the the physical content which may dwell in the non local theories, and on their capacity to represent the nucleon in its interaction with the pion at least as far as meson-nucleon physics is concerned. From a more theoretical standpoint, the opportunity to search for some form of non local theory for boson-fermion interactions is suggested by the difficulties that have been recently put in evidence for the local theories even if they are renormalizable <sup>(3)</sup>.

One of the classical typus of non local theories is the form factor theory, such as that discussed in ref. <sup>(2)</sup>. Such theory has the fundamental physical drawback that it postulates, in net contrast to experimental evidence, the

<sup>(1)</sup> G. F. CHEW: *Phys. Rev.*, **95**, 1669 (1954).

<sup>(2)</sup> P. BUDINI: *Nuovo Cimento*, **3**, 835 (1956).

<sup>(3)</sup> T. D. LEE: *Phys. Rev.*, **95**, 1329 (1954); V. HABER-SCHAIM and W. THIRRING: *Nuovo Cimento*, **2**, 100 (1955); G. KÄLLEN and W. PAULI: *Dan. Mat. Fys. Medd.*, **30**, n. 7 (1955).

vanishing of the interaction at high energy, and the theoretical drawback of the introduction a priori in the theory of the highly arbitrary form factor. Thus we are inclined to think that the form factor is to be considered as a device to cut-off as yet unknown pieces of the theory in a region where the extrapolation of the old theory would give wrong results. On the other hand it is reasonable to think that the newly discovered mesons will contribute to providing a sort of a form for the nucleon in its interaction with the pion at energies at which the new mesons can not yet be created (\*); and this form has to be such that at higher energy the interaction does not cease but rather is apt to describe the advent of new phenomena such as the creation of the new mesons.

In the following by non local pion-nucleon interaction we will intend that it is not expressible as the linear product of the nucleon current density and the pion field taken at the same point-event. Thus an indirect pion nucleon interaction is included in our definition of non local interaction. It has the advantage over the conventional form factor theories, that it does not postulate the vanishing of the interaction at high energy contrary to experimental evidence. We will take it into consideration in the present paper. In order to explore the possibility that the form of the source may be in some way connected with the existence of the strange mesons we shall take as intermediary a boson field. The problem that the formal elimination of the intermediate field may lead to a conventional form factor theory will not be considered in detail, in the present work.

The problem that has attracted much attention recently and on which the various theories of pion-nucleon interaction are usually tested is the pion-nucleon elastic scattering problem and in particular the resonance of the  $P = \frac{3}{2}$ ,  $T = \frac{3}{2}$  phase shift; so we have applied our model to the solution of this problem. We find in fact that the internal field renders the integral equation convergent and with a proper choice of the coupling constant and of the mass of the internal meson the essential feature of the low energy pion nucleon  $P$  waves can be reproduced.

## 2. — The Field Equations.

We will exemplify the line of thought exposed in the previous paragraph with the assumption that the pion interacts with the nucleon only through a meson  $X$ :

$$(1) \quad N \rightleftharpoons N + X \rightleftharpoons N + \pi.$$

(\*) It may well be that this effect may be produced also by nucleon pairs or by a non linearity of the pion field or better that these are partially equivalent, partially complementary rough representations of the reality.

As a first stage we intend to discuss the interaction pion-nucleon at low energy precisely such that the X-meson can not be created in a real state. Thus in order to keep the model as simple as possible we will not discuss the properties of X as a real particle nor try to compare it with some of the known mesons in view also of the possibility that the X-meson may be a rough way of representing a non linearity of the pion field. Then the only determining characteristic of X is its rest mass  $\mu_x$ , its parity spin and isotopic spin being the same as that of the pion. We thus take for the lagrangean density of the system:

$$(2) \quad L = L_{\text{Nucleons}}^0 + L_{\text{pions}}^0 + L_x^0 - \frac{F_x}{\mu_x} \bar{\psi}(x) \gamma_5 \gamma_\mu \nabla_\mu \tau_i \Phi_i(x) \psi(x) - F_\pi \frac{\mu_x^3}{\mu_\pi} \Phi_i(x) \varphi_i(x).$$

Where  $\Phi_i$  represents the X field,  $\mu_x$  its rest mass,  $F_x$  is the coupling constant X-nucleon and  $F_\pi$  is a numerical factor. From this follow the field equations:

$$(3) \quad \left\{ \begin{aligned} (\gamma_\mu \nabla_\mu + M) \psi &= - \frac{F_x}{\mu_x} \gamma_5 \gamma_\mu \nabla_\mu \tau_i \psi \Phi_i, \\ \bar{\psi} (\nabla_\mu \gamma_\mu - M) &= \frac{F_x}{\mu_x} \bar{\psi} \gamma_5 \gamma_\mu \tau_i \nabla_\mu \Phi_i, \\ (\square - \mu_x^2) \Phi_i &= \frac{F_x}{\mu_x} \nabla_\mu \bar{\psi} \gamma_5 \gamma_\mu \tau_i \psi - \frac{F_\pi \mu_x^3}{\mu_\pi} \varphi_i, \\ (\square - \mu_\pi^2) \varphi_i &= - \frac{F_\pi \mu_x^3}{\mu_\pi} \Phi_i. \end{aligned} \right.$$

The hamiltonian formalism of the theory can be formulated without difficulty and the system quantized. For the hamiltonian we obtain:

$$(4) \quad H = H_{\text{Nucleons}}^0 + H_{\text{pions}}^0 + H_x^0 + H_1 + H_2,$$

where

$$(5) \quad H_1 = \frac{-i F_x \tau_i}{(2\pi)^{\frac{3}{2}} \mu_x} \int \frac{d^3 k' d^3 k''}{\sqrt{2\omega_x''}} [\bar{\psi}(k' - k'') \gamma_5 \gamma_\mu k_\mu'' \psi(k') \Phi_i^+(k'') - \bar{\psi} \gamma_5 \gamma_\mu k_\mu'' \psi(k' - k'') \Phi_i^-(k'')]$$

$$(5') \quad H_2 = F_\pi \frac{\mu_x^3}{\mu_\pi} \int \frac{d^3 k'}{\sqrt{\omega_x' \omega_\pi}} [\varphi_i^+(k') \Phi_i^-(k') + \Phi_i^+(k') \varphi_i^-(k')]$$

with:

$$(6) \quad \left\{ \begin{aligned} [\varphi_i^-(k'), \varphi_j^+(k)] &= [\Phi_i^-(k'), \Phi_j^+(k)] = \delta_{ij} \delta^3(k - k') \\ \{ \psi(k), \bar{\psi}(k') \} &= \gamma^4 \delta^3(k - k') \end{aligned} \right.$$

and the other fields commute (anticommute).



$H_1$  represents the interaction X field-nucleon;  $H_2$  the interaction pion-X field.

### 3. — Pion-Nucleon Scattering.

As an example we have applied the model presented in the preceding Section to the problem of low energy pion-nucleon scattering. In order to compare the quantitative implications of this theory to experimental results, and especially to the published results of the cut-off theory, we have followed the methods given by CHEW <sup>(1)</sup> although today they may be already bettered <sup>(4)</sup> in some respects. We have adopted the Tamm-Dancoff method neglecting configurations containing three or more mesons. We have also neglected nucleon pairs. In fact it will be seen that, at low energy, in the integrals representing sums over the virtual states the contribution from energies larger than the rest mass of the nucleon is not important.

A state vector of the system of total momentum  $p$  can be expanded in terms of the number operators of the various free field quanta:

$$(7) \quad P_{p'} = \chi(p; 0; 0) \psi^+(p) |0\rangle + \int \chi_i(p-k_1; k_1; 0) \psi^+(p-k_1) q_i^+(k_1) d^3k_1 |0\rangle + \\ + \int \chi_i(p-k'_1; 0; k'_1) \psi^+(p-k'_1) \Phi_i^+(k'_1) d^3k'_1 |0\rangle + \\ + \frac{1}{\sqrt{2}} \int \chi_{ij}(p-k_1-k_2; k_1; k_2; 0) \psi^+(p-k_1-k_2) q_i^+(k_1) \Phi_j^+(k_2) d^3k_1 d^3k_2 |0\rangle + \dots,$$

where  $\chi(p-k_1-k'_1-k'_2-\dots; k_1\dots k_m; k'_1\dots k'_n)$  represents the amplitude of a state with a nucleon of momentum  $p-k_1-k_2-\dots$ ;  $m$   $\pi$ -mesons of momenta  $k_1\dots k_m$  and  $n$  X-mesons of momenta  $k'_1\dots k'_n$ . On dropping the fourth terms of  $\gamma_5\gamma_\mu k_\mu$  which is small at low energy and gives small contribution to  $P$  waves, which are the only ones considered in the present work, we then find for  $\chi_i(p-k; k; 0)$  the following integral equation:

$$(8) \quad (E-E_{p-k}-\omega)\chi_i(p-k; k; 0) = (2\pi)^{-3} \frac{F^2}{\mu_\pi^2} \int \frac{d^3k'}{2\sqrt{\omega_\pi\omega'_\pi}} \cdot \\ \cdot \left\{ r(k)r(k') \frac{(\sigma k)(\sigma k')}{E-E_p} \tau_i\tau_i + V(k, k') \frac{(\sigma k')(\sigma k)\tau_j\tau_j}{E-E_{p-k-k'}-\omega_\pi-\omega'_\pi} \right\} \chi_j(p-k'; k'; 0) + \\ + \frac{3}{2} (2\pi)^{-3} \frac{F^2}{\mu_\pi^2} \int \frac{V'(k, k')k'^2 d^3k'}{\omega'_\pi(E-E_{p-k-k'}-\omega_\pi-\omega'_\pi)} \chi_i(p-k; k; 0),$$

(4) G. F. CHEW and F. E. LOW: to be published.

where  $F^2 = F_x^2 F_\pi^2$ ;

$$(8') \quad \left\{ \begin{aligned} v(k) &= \frac{\mu_x^2}{\omega_x(E - E_{p-x} - \omega_x)}; \\ V(k, k') &= \frac{\mu_x^4}{\omega_x \omega_x'} \left\{ (E - E_{p-k-k'} - \omega_\pi - \omega_x')^{-1} (E - E_{p-k-k'} - \omega_\pi' - \omega_x)^{-1} + \right. \\ &+ \frac{E_{p-k-k'} - \omega_\pi' - \omega_\pi}{E_{p-k-k'} - \omega_x' - \omega_x} \left[ (E - E_{p-k-k'} - \omega_\pi - \omega_x')^{-1} (E - E_{p-k-k'} - \omega_\pi' - \omega_x)^{-1} + \right. \\ &+ (E - E_{p-k-k'} - \omega_\pi - \omega_x')^{-1} (E - E_{p-k'} - \omega_x')^{-1} + (E - E_{p-k-k'} - \omega_\pi' - \omega_x)^{-1} + \\ &\left. \left. + (E - E_{p-k} - \omega_x)^{-1} + (E - E_{p-k} - \omega_x)^{-1} (E - E_{p-k'} - \omega_x')^{-1} \right] \right\}; \\ V'(k, k') &= \frac{\mu_x^4}{\omega_\pi'^2 (E - E_{p-k-k'} - \omega_\pi - \omega_x')^2}. \end{aligned} \right.$$

Of the self-energy terms only the one proportional to  $F^2 F_\pi^2$  has been kept (the last term on the right hand side of (8)) as it is the only one to give, after renormalization, observable effects on the pion-nucleon scattering problem. It can be seen that (8) has a form which is a generalization of the last equation of ref. (2). That is the internal meson provides factors which are similar to those obtained in the form-factor theory, but are not particular cases of these.

Equation (8) can be easily separated for eigenstates of isotopic spin and angular momentum; we obtain in the center of the mass system the following equation for  $\chi_{ij}(k) = \chi_{ij}(-k; k; 0)$  (as usual the first index refers to isotopic spin and the second to angular momentum):

$$(9) \quad \left\{ \begin{aligned} (E - E_k - \omega_\pi) \chi_{13}(k) &= -\frac{F^2 |k|}{\mu_\pi^2 6\pi^2} \int \frac{V(k, k')}{\sqrt{\omega_\pi \omega_\pi'}} \frac{\chi_{13}(k')}{E - E_{k+k'} - \omega_\pi - \omega_\pi'} k'^3 dk' \\ \chi_{31} &= \chi_{13} \\ (E - E_k - \omega_\pi) \chi_{11}(k) &= \frac{F^2 |k|}{\mu_\pi^2 4\pi^2} \int \frac{1}{\sqrt{\omega_\pi \omega_\pi'}} \left[ \frac{3v(k)v(k')}{E - M} + \right. \\ &\quad \left. + \frac{1}{3} \frac{V(k, k')}{E - M - \omega_\pi - \omega_\pi'} \right] \chi_{11}(k') k'^3 dk' \\ (E - E_k - \omega_\pi) \chi_{33}(k) &= \frac{F^2 |k|}{\mu_\pi^2 3\pi^2} \int \frac{V(k, k')}{\sqrt{\omega_\pi \omega_\pi'}} \frac{\chi_{33}(k')}{E - E_{k+k'} - \omega_\pi - \omega_\pi'} k'^3 dk'. \end{aligned} \right.$$

These equations present singularities at  $E = E_k + \omega_\pi$ ;  $E = E_{k+k'} + \omega_\pi + \omega_\pi'$ ;

$E = E_k + \omega_x$ ;  $E = E_{k+k'} + \omega_\pi + \omega'_x$ ; ... the first two correspond to incoming waves and the creation of a further pion in a real state respectively, and in our problem the principal value at these poles is to be taken. Further poles contained in the factors  $v$  and  $V$  correspond to the possibility of the creation of X-meson in real states but they do not need to be taken into consideration at low energy as far as  $E < M + \mu_x$ .

The form factors  $v$  and  $V$  are approximately 1 for low  $k$  and  $k'$ ; and tend to 1 when  $\mu_x/\mu_\pi$  tend to infinity. Increasing  $k$  or  $k'$  they converge rapidly to zero as  $k$  or  $k'$  get larger than  $\mu_x$ . In the interval from  $k = k' = 0$  to  $k \sim k' \sim \mu_x$  they can, especially  $V(k, k')$ , even encrease with  $k$  or  $k'$ . In general it is clear that the form which the nucleon presents to the pion depends on the energy and the spins of the system.

#### 4. — Renormalization.

Equations (9) can be easily renormalized with the procedure suggested by CHEW (\*). Then to second order of the coupling constant equations for  $\chi_{31}$ ,  $\chi_{13}$  and  $\chi_{33}$  need not be formally modified. Only the equation for  $\chi_{11}$  will be altered for the self-energy for the nucleon in the field of the pion, in those states which have a bare nucleon line in a virtual state. These states are represented by the term with the factor  $(E - M)^{-1}$ . Now this term contrary to the local theory, gives convergent results even without renormalization, and this is so because the self-energy of the nucleon in the field of the pion is finite. Renormalization brings about a factor  $1 + \Delta_r(E - M)$  with

$$(10) \quad \Delta_r(x) = \frac{3}{4\pi^2} \frac{F^2}{\mu_\pi^2} \int_{\mu_\pi}^{\infty} \frac{x k'^3 V'^2(k_0, k')}{(\omega'_\pi - x)(E_{k_0} - E_{k_0+k'} - \omega'_\pi)^2} d\omega',$$

in the denominator of the first term of the kernel of the equation for  $\chi_{11}$  which does not alter essentially the behaviour of  $\chi_{11}$  at low energies.

To fourth order, renormalization implies essentially the correction of all nucleon lines for the self-energy of the nucleon in the field of the pion, the

(\*) For the renormalization of problems of this type it is perhaps preferable to use a model approach of the type of those of LEE (3) or THIRRING-HABER-SCHAIM (3), or, better to start directly on the Low (4) line. But as already stated we prefer in this work, in order to compare numerical results, to remain close to the Chew procedure.

equations for  $\chi_{13}(k)$  and  $\chi_{33}(k)$  modified in this way then become:

$$(11) \quad (E - E_k - \omega_\pi)[1 + \Delta(E - E_k - \omega_\pi)]\chi_{13}(k) = -\frac{F'^2}{\mu_\pi^2} \frac{|k|}{6\pi^2} \int \frac{V(k, k')}{\sqrt{\omega_\pi \omega'_\pi}} \cdot \frac{\chi_{13}(k')}{(E - E_{k+k'} - \omega_\pi - \omega'_\pi)[1 + \Delta(E - E_{k+k'} - \omega_\pi - \omega'_\pi)]} k'^3 dk',$$

$$(11') \quad (E - E_k - \omega_\pi)[1 + \Delta(E - E_k - \omega_\pi)]\chi_{33}(k) = -\frac{F'^2}{\mu_\pi^2} \frac{|k|}{3\pi^2} \int \frac{V(k, k')}{\sqrt{\omega_\pi \omega'_\pi}} \frac{\chi_{33}(k')}{(E - E_{k+k'} - \omega_\pi - \omega'_\pi)[1 + \Delta(E - E_{k+k'} - \omega_\pi - \omega'_\pi)]} k'^3 dk',$$

where  $F'^2$  is now the renormalized coupling constant.

## 5. - Results and Conclusion.

Our integral equations can be put in the form:

$$(12) \quad \chi(\omega) = \delta(\omega_0 - \omega) + \int K(\omega_0, \omega, \omega') \chi(\omega') d\omega',$$

then the first term of the Fredholm series gives:

$$(13) \quad \chi(\omega) = \delta(\omega_0 - \omega) + \frac{K(\omega_0, \omega, \omega_0)}{1 - \int K(\omega_0, \omega', \omega') d\omega'},$$

this reinserted in (12) gives:

$$(14) \quad \chi(\omega) = \delta(\omega_0 - \omega) + \frac{\int K(\omega_0, \omega, \omega') K(\omega_0, \omega', \omega_0) d\omega'}{1 - \int K(\omega_0, \omega', \omega') d\omega'}.$$

This solution coincides with the one proposed by GAMMEL<sup>(5)</sup> and adopted by CHEW. We have applied the method to the calculation of the  $\delta_{33}$  phase shift and we obtain

$$(15) \quad \tan \alpha_{33} = \frac{F'^2 k_0^3 V(k_0 k_0)}{3\pi\omega_0 [1 + A_r(-\omega_0)]} \left[ 1 + \frac{A_r(\omega_0)}{1 - A_r(\omega_0)} \right],$$

<sup>(5)</sup> J. L. GAMMEL: *Phys. Rev.*, **95**, 209 (1954).

with

$$(16) \quad \left\{ \begin{aligned} \Delta_c(\omega_0) &= \frac{F'^2}{3\pi^2\mu_\pi^2} \int_{\mu_\pi}^{\infty} \frac{V(k'k_0)V(k_0k')}{V(k_0k_0)} \cdot \frac{\omega_0[1 + \Delta_r(-\omega_0)]}{\omega'^2(\omega' - \omega_0)[1 + \Delta_r(-\omega')]^2[1 + \Delta_r(\omega_0 - \omega')]} k'^3 d\omega' \\ \Delta_F(\omega_0) &= \frac{F'^2}{3\pi^2\mu_\pi^2} \int_{\mu_\pi}^{\infty} \frac{V(k'k')k'^3 d\omega'}{(2\omega' - \omega_0)(\omega' - \omega_0)[1 + \Delta_r(\omega_0 - 2\omega')][1 + \Delta_r(\omega_0 - \omega')]} \end{aligned} \right.$$

We have taken account of the recoil of the nucleon only in the form factors where energies of the order of  $M$  and higher play a role but not in the kernel of the equation in accordance with CHEW.

The  $\chi_{33}$  phase shift presents the possibility of resonance because of the sign of the kernel in equation (11') which in turn is determined only by the spins state of the system. Thus at low energy the  $\chi_{33}$  phase shift is higher and the other lower than the Born approximation.

With  $\mu_\pi = 5\mu_\pi$  and  $F'^2/4\pi\mu_\pi^2 = 0.0559$  we obtain resonance at 198 MeV (lab.) of the incoming pion, beyond this energy the phase increases but slower than the experimental one; at intermediate energies the theoretical values of  $\delta_{33}$  are somewhat higher than the experimental ones ( $\sim 20\%$  higher than the Chew values). The  $\delta_{13}$ ,  $\delta_{31}$  and  $\delta_{11}$  phases are small and present the known behaviour at low energy.

Concluding we think that a physical non local theory of the pion-nucleon interaction of the type of the example presented in this work can give with a proper choice of the parameters results in accordance with experimental evidence about the nucleon interaction, at least as well as the extended source theory does.

\* \* \*

We wish to thank Dr. L. FONDA and Dr. I. REINA for help in the solution of the integral equations and numerical calculations.

#### RIASSUNTO

Si studia un modello basato sull'ipotesi che il pione interagisca col nucleone tramite un campo intermedio. Si applica il modello alla trattazione adiabatica del problema della diffusione pione-nucleone. Il campo intermedio introduce nei nuclei delle equazioni di diffusione fattori di convergenza del tipo di quelli che si ottengono nelle teorie non locali. I risultati quantitativi per le fasi  $P$  sono dello stesso tipo di quelli che si ottengono con la teoria della sorgente estesa.



**The Increase in the Total Cosmic Ray Intensity  
and in the Positive Excess  
due to the Solar Flare of 23rd February 1956.**

I. FILOSOFO (\*), I. MODENA (+), E. POHL (×) and J. POHL-RÜLING

*Istituto di Fisica dell'Università - Padova  
Istituto Nazionale di Fisica Nucleare - Sezione di Padova*

(ricevuto il 16 Marzo 1956)

**Summary.** — Increases in the total flux and in the positive excess of the Cosmic Radiation have been detected which were clearly associated with the large solar flare of the 23th Feb. 1956. The differential and integral spectra for the additional  $\mu$ -mesons produced in the atmosphere have been derived. The nature of the positive excess of these mesons leads to the conclusion that the particles coming from the flare were mainly protons. Their energy is estimated to lie between 4 and 10 GeV. In this band the primary flux increased to about 25 times normal during the flare.

For over a year three independent groups of apparatus have been measuring variations of the total cosmic ray intensity and of the positive excess. This experiment has been conducted at Padua (longitude 11°53' E, latitude 45°24'5 N) at an effective altitude of 25 m above sea-level.

The first of these groups of apparatus (set A) consists of two identical Geiger telescopes and serves for the measurement of the total intensity. Each telescope is made up of three trays of six counters (5×90 cm working length) having an acceptance angle in the NS direction of 92° and in the EW direction of 42°. 10 cm of lead situated between the second and third trays

(\*) Now at the Betatron Lab. University of Illinois, Urbana Ill.

(+) Now A.U.C. G.A.r.i., at the Scuola di Guerra Aerea, Firenze, Italy.

(×) Now at the Abteilung für Radiologie und Isotopenforschung, Physiologisches Institut der Universität Innsbruck, Innsbruck, Austria.

functions as an absorber. The combined mean hourly counting rate of the two telescopes is about 29000.

The second apparatus (set *B*) measures the positive excess of  $\mu$ -mesons in the vertical direction and is substantially the same as that already described in a previous publication <sup>(1)</sup>. An electromagnet separates the positive and negative  $\mu$ -mesons which are then counted by means of 16 triple coincidence channels each having an angular aperture of  $70^\circ$  in the NS direction and  $8^\circ 45'$  in the EW direction. It has a mean hourly counting rate of 430 in an energy band of width 0.6 GeV with a mean value at 1.0 GeV.

A further improvement in this apparatus since our previous publication has been the incorporation of suitable circuits for the counting of the total

TABLE I.

Set	Energy in GeV	<i>a</i> mean two hourly counting rate	23-2-1956 0259 to 0459 h U.T.		
			<i>b</i> total two hourly counting rate	<i>b</i> - <i>a</i> increase	( <i>b</i> - <i>a</i> ) · 100/ <i>a</i> increase in %
<i>A</i>	> 0.16	58 313	91 328	33 015	$56.6 \pm 0.5$
<i>B</i> (total intensity)	> 0.70	15 648	21 328	5 680	$36.3 \pm 0.9$
<i>B</i> ( $\mu^+ + \mu^-$ )	min 0.7 max 1.3	867	1 669	802	$93 \pm 5$
<i>C</i> ( $\mu^+ + \mu^-$ ) $15^\circ$ S	min 0.9 max 1.5	128	211	83	$65 \pm 14$
<i>B</i> <sub><math>\mu^+</math></sub>	min 0.7 max 1.3	471	986	515	$109 \pm 5$
<i>B</i> <sub><math>\mu^-</math></sub>	min 0.7 max 1.3	395	683	288	$73 \pm 7$
<i>C</i> <sub><math>\mu^+</math></sub> $15^\circ$ S	min 0.9 max 1.5	70	127	57	$82 \pm 11$
<i>C</i> <sub><math>\mu^-</math></sub> $15^\circ$ S	min 0.9 max 1.5	58	84	26	$45 \pm 13$

<sup>(1)</sup> I. FILOSOFO, E. POHL and J. POHL-RÜLING: *Nuovo Cimento*, **12**, 809 (1954).

intensity. This is measured over a vertical solid angle of  $70^\circ$  in the NS direction and  $22^\circ$  in the EW direction. The particles pass through the 50 cm of iron forming the nuclei of the magnet and are naturally subject to the magnetic field of 13000 gauss. The total intensity as measured in this way shows a cut-off at about 0.7 GeV and corresponds to a mean hourly counting rate of 7830.

The third apparatus (set C) also measures the positive excess, but it differs from set B in that it is smaller and freely orientable at various angles to

the vertical and to the NS line. Its 8 triple coincidence channels have an angular aperture of  $34^\circ \times 8^\circ 45'$ . With the apparatus inclined at  $15^\circ$  from the vertical towards South, the hourly counting rate is about 65.

Records for each apparatus are taken every two hours and in particular at 0059, 0259 h U.T., etc.

On the 23rd of February 1956, between 0259 and 0459 h U.T. all three sets showed a remarkable sudden increase in their counting rates, but in the following two hours all were nearly back to normal, only set A being slightly above its average  $[(5.1 \pm 0.7) \text{ \%}]$ .

The increase in the various intensities during the critical hours is shown in Table I and in Fig. 1. This increase was confined to a period of time much shorter than the interval of the two hours in which it was registered. A minimum value for the true maximum of the increase may thus be obtained from the apparent increase (shown in Table I and Fig. 1) by multiplying by 4.35. This takes into account both the fact that the increase actually

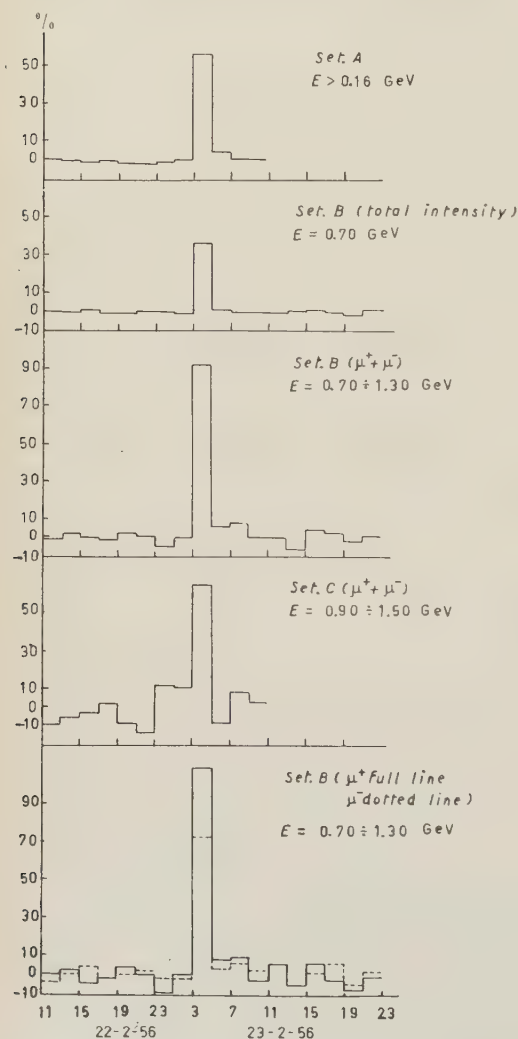


Fig. 1. - Percentage variation from the mean values for various intensities as recorded by our apparatus.

started at 0345 h U.T. instead of 0259 h U.T., and the profile of the increase (\*).

In addition to these quantities, which have been directly obtained from the counting rates, one may calculate the increase in the energy band from 0.16 to 0.70 GeV by making use of the known integral energy spectrum <sup>(2,3)</sup> of  $\mu$ -mesons at sea-level and the difference between the normalized counting rates for the total intensity as obtained from sets *A* and *B*, which have different cuts-off. In the same way one may obtain the increase for energies above 1.3 GeV from the difference between the total intensity and the combined positive and negative  $\mu$ -meson counting rates which are both supplied by set *B*.

Combining the calculated results with those obtained directly from the apparatus one may derive both the integral and differential energy spectra for the increase (i.e. of those  $\mu$ -mesons produced by the extra particles coming from the flare). These spectra are represented in Table II and Fig. 2. From the integral spectrum it is evident that in whatever manner it is extrapolated, the maximum energy of the extra  $\mu$ -mesons is about 2 GeV and therefore the corresponding primaries must also have been particles having low energy.

From the separate counting rates for positive and negative  $\mu$ -mesons we

TABLE II.

Integral spectrum of the increase		Differential spectrum of the increase	
cut-off energy in GeV	percentage increase	energy band in GeV	percentage increase in this band
0.16	$56.6 \pm 0.5$	min 0.16 max 0.7	$128.5 \pm 6$
0.70	$36.3 \pm 0.9$	min 0.7 max 1.3	$93 \pm 5$
1.3	$16.5 \pm 3$	min 0.9 max 1.5	$65 \pm 14$
—	—	min 1.3 max $\sim 2.0$	$16.5 \pm 3$

(\*) We are indebted to Dr. H. ELLIOT for sending us the profile of the increase as measured at the University of Manchester. This profile indicates a maximum between 03.45 h U.T. and 04.00 h U.T. and we have assumed that it lasted for the whole of this interval. Thus we can only give a minimum value for the true peak.

(2) B. ROSSI: *Rev. Mod. Phys.*, **20**, 537 (1948).

(3) G. PUPPI: *Progress in Cosmic Ray Physics* (1955).

have obtained the percentage positive excess by means of  $\varepsilon = 2(\mu^+ - \mu^-) \cdot 100/(\mu^+ + \mu^-)$ . This is given in Table III.

From the data of set *B* one notes that the positive and negative  $\mu$ -mesons did not increase in the same proportion: the additional particles show a positive excess of about three times normal (\*). This apparent preference for the pro-

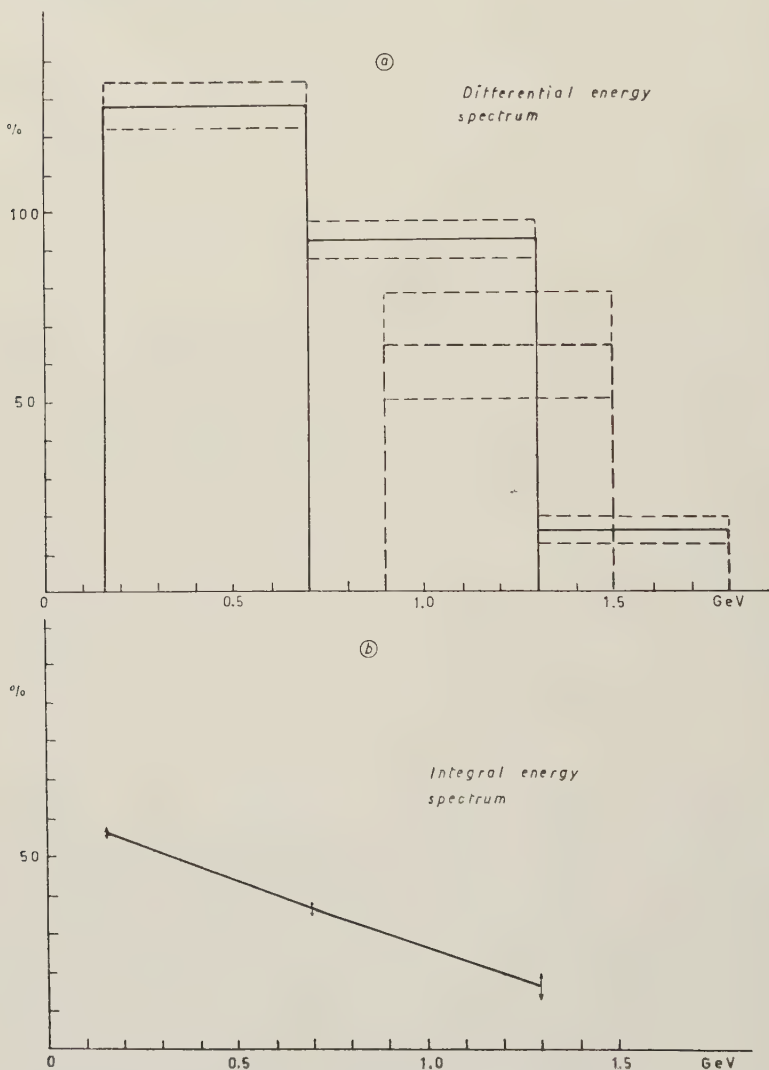


Fig. 2. — Differential and integral energy spectra of the extra  $\mu$ -mesons recorded at sea-level during the flare.

(\*) Since the counting rate of set *C* is comparatively low and is consequently subject to relatively large errors we have not used its results in our calculations. However it has provided a good confirmation of the general features of the increase.



TABLE III.

	Energy band in GeV	normal excess $\varepsilon$	total excess $\varepsilon$ in critical hours	excess $\varepsilon$ of increase
Set B	min 0.7 max 1.3	$18.3 \pm 0.2$	$36.4 \pm 7$	$57 \pm 10$
Set C 15 °S	min 0.9 max 1.5	$19.6 \pm 1.5$	$41 \pm 14$	$75 \pm 20$

duction of positive  $\mu$ -mesons leads to the conclusion that the corresponding primaries were also positive, and in particular it can be shown that the majority were low-energy protons only capable of about one pion producing collision in the atmosphere. This may be demonstrated from the following considerations.

The positive excess resulting from interactions of low multiplicity may be estimated from the over all positive excess in the atmosphere (<sup>1,3</sup>), and from experiments with artificially accelerated particles (<sup>4,5</sup>). In both cases it is about 50%, which is in agreement with our results. This fact confirms that the primaries responsible for the increase are mainly protons having relatively low energies. For such particles the process of multiplication in cascade through the atmosphere is very much reduced, at least as far as their contribution to the sea-level  $\mu$ -meson intensity is concerned.

One may exclude that neutral particles or alphas represent an appreciable fraction of the extra primaries.

Bearing in mind that the protons make only one meson producing collision we are able to obtain the ratio of the mean energy of the pions so produced to that of the protons which create them (<sup>4,5</sup>); it may then be inferred when one takes into account the various possible levels of the atmosphere at which this collision may occur, the greater part of the additional  $\mu$ -mesons at sea-level are due to primary protons lying in the energy band between 4 and 10 GeV.

To estimate the increase in the primaries one may consider the difference in the cosmic ray primary flux between those two geomagnetic latitudes which have cuts-off representing the lower and upper limits of the energy band between 4 and 10 GeV; these turn out to be lat. 45° and lat. 23° respectively (<sup>6</sup>). The difference in intensity at sea-level between lat. 45° and lat. 23°, which is about 10% of the total (<sup>3</sup>), thus represents the contribution to the sea-level

(<sup>4</sup>) Private communication from V. T. COCCONI.

(<sup>5</sup>) A. H. ROSENFELD: *Phys. Rev.*, **96**, 130 (1954).

(<sup>6</sup>) G. PUPPI and N. DALLAPORTA: *Progress in Cosmic Ray Physics* (1952), p. 320.

(<sup>7</sup>) J. R. WINCKLER, T. STIX, K. DWIGHT and R. SABIN: *Phys. Rev.*, **79**, 656 (1950).

intensity by this band of primary energies. Therefore on comparing the relative increases at sea-level we can estimate the relative intensity of the primaries in the 4 to 10 GeV interval during the flare, with respect to normal conditions. At sea-level the increase as registered by our apparatus is 57%, and so we have concluded that the true extra flux of primaries in the 4 to 10 GeV band is about 25 times normal.

We are not in a position to say anything about primaries of lower energy.

\* \* \*

We are indebted to Prof. G. PUPPI who has been supervising our work. Thanks are also due to Drs. C. MARONI and U. FASOLI for help in running the apparatus and to G. SALMASO for the execution of numerical computations.

---

#### RIASSUNTO

È stato misurato l'aumento dell'intensità e dell'eccesso positivo dei raggi cosmici in relazione al brillamento solare del 23-2-1956. Si sono ricavati gli spettri differenziale ed integrale di quei mesoni  $\mu$  prodotti in seguito al brillamento. Dal valore dell'eccesso positivo di questi mesoni si può concludere che la primaria dovuta all'attività solare è principalmente costituita da protoni, la cui energia risulta compresa fra 4 e 10 GeV. In questa banda di energia, il flusso della primaria durante il brillamento è aumentato di circa 25 volte il valore normale.

## NOTE TECNICHE

### Le coefficient de température et la stabilité thermique des compteurs de Geiger-Müller autocoqueurs contenant une vapeur organique.

D. BLANC et R. VISTE

*Laboratoire de Physique Atomique et Moléculaire du Collège de France - Paris*

(ricevuto il 25 Dicembre 1955)

**Résumé.** — Dans le but d'expliquer les résultats assez contradictoires obtenus antérieurement, nous avons effectué un ensemble d'expériences sur l'effet thermique des compteurs de Geiger-Müller entre 20 °C et 250 °C, en utilisant divers remplissages autocoqueurs et des détecteurs à cathode interne ou à parois de verre et graphitage externe. Le coefficient de température, proportionnel à la pression partielle du constituant polyatomique, est dû à sa désorption régulière depuis les parois. La caractéristique de palier s'améliore lorsque la température augmente, et l'effet néfaste d'ions négatifs possibles, produits par la vapeur de mercure existant en très faibles proportions dans le remplissage, est nul, contrairement à certaines hypothèses antérieures. La détérioration progressive de la caractéristique au dessus d'une certaine température est due à un phénomène étranger à la décharge, réversible (dégagement de vapeur d'eau depuis les parois, augmentation du mouvement propre) ou irréversible (décomposition de la vapeur polyatomique ou réaction chimique sur les parois): Les compteurs à parois de verre non étuvés manifestent une stabilité remarquable: jusqu'à 250 °C ne se produit aucune augmentation sensible du fond, et, jusqu'à une température  $t_0$  voisine de 100 °C, leur coefficient thermique est très inférieur à celui des compteurs à cathode interne du type classique. Au dessus de  $t_0$ , la variation est plus rapide.

#### 1. — Introduction.

Les recherches antérieures sur le comportement thermique des compteurs autocoqueurs ont conduit à des conclusions souvent contradictoires. Un certain nombre de publications ont été faites sur cette question, et le Tableau I résume leurs résultats essentiels.

TABLEAU I.

Auteurs et Références	Zône de tempé- ratures (°C)	Nature de la cathode	Remplissage cm <sup>3</sup> Hg	Coefficient de tempé- rature (volt/degé)	Sens de variation de la pente avec la température	Sens de variation de la longueur du palier avec la température	Traitement thermique prélimi- naire	Nature des parois externes
S. A. KORFF W. D. B. SPATZ W. HILBERRY ( <sup>1</sup> )	-22, + 55	Métal non précisé	Alcool Argon	Nul au dessus de 0 °C	Pas indiqué	0 → ↗ - 22	Pas indiqué	Pas indiqué
G. JOYET M. SIMON ( <sup>2</sup> )	+ 5, + 45	Aluminium	Alcool Argon	+ 14	↗	↗	Pas d'étuvage	Aluminium
O. PARKASH ( <sup>3</sup> )	+ 20, + 180	Cu oxydé	Alcool 1.5 Argon 8.5	Sensibl. + 0.17	↗	↗	Pas indiqué	Pas indiqué
O. PARKASH P. L. KAPUR ( <sup>4</sup> )	+ 8, + 60	Cathode externe	Alcool Argon	Semble négligé > 9 °C	↗	↗	Pas d'étuvage	Verre « Novo »
W. R. LOOSEMORE D. TAYLOR ( <sup>5</sup> )	+ 15, + 100	Carbone (interne)	Alcool Argon	+ 9 entre + 15° et + 50°	↗	↗	Pas indiqué	Pas indiqué
W. R. LOOSEMORE D. TAYLOR ( <sup>6</sup> )	+ 15, + 100	Cuivre	Alcool Argon	+ 1.50 entre 15, °C et 80 °C	75 ↗ ↗ 100 15	↗	Pas indiqué	Pas indiqué
G. FUJIOKA I. KITAHARA ( <sup>7</sup> )	+ 15, + 170	Cuivre	Alcool 1 Argon 9	Nul	+ 18 °C ↗ ↗	↗	Chauffage à 400 °C	Verre dur type Pyrex

C. CASTAGNOLI G. CREA A. GIGLI ( <sup>8</sup> )	15, +100	Métal non précisé	Alcool 0.8 Argon 9	0 > 15°C +28 < 15°C	Non précisé	+6 ↗ -15 ↘ +100	Pas indiqué	Métal
R. SEIDL ( <sup>9</sup> )	0, + 40	Dural	Méthylal 1.5 Argon 8.5	Nul	↗	Non précisé	Pompage sans étuvage (araldite)	Verre Jena Normalglas 16/III
C. P. JOSHI ( <sup>10</sup> )	+25, + 80	Cuivre	Éther de pétrole 2 Argon 7	+2.1	↗	↗	Pompage sans étuvage	Verre
J. H. MADER ( <sup>11</sup> )	+20, +110	Cuivre recouvert de C	Alcool 1.5 Argon 8.5	Variation parabolique du seuil	↗ ↘ T <sub>0</sub> (70 °C)	T <sub>0</sub> (70 °C) ↗ ↘	Pas indiqué	Laiton Isolant: céramique
R. MEUNIER M. BONPAS J. P. LEGRAND ( <sup>12</sup> )	0, + 200	Al, Mo, Ta, Ni, Bi, Cu, Fe, Ag	Méta, para- xylène saturé Argon (10 à 30)	+17 à +30 < 60 °C +0.1 > 60°C	↗ ↘ T <sub>0</sub> (70 °C)	↗ ↘ T <sub>0</sub> (70 °C)	Pas indiqué	Verre dur type Moly ou verre Novo

(<sup>1</sup>) S. A. KOREF, W. D. B. SPATZ et N. HILBERRY: *Rev. Sci. Instr.*, **13**, 127 (1942).

(<sup>2</sup>) G. JOYET et M. SIMON: *Helv. Phys. Acta*, **21**, 180 (1947).

(<sup>3</sup>) O. PARKASH: *Phys. Rev.*, **76**, 568 (1949).

(<sup>4</sup>) O. PARKASH et P. L. KAPUR: *Proc. Phys. Soc.*, A **63**, 457 (1950).

(<sup>5</sup>) W. R. LOOSEMORE et D. TAYLOR: *Proc. Phys. Soc.*, B **63**, 728 (1950).

(<sup>6</sup>) G. FUJIOKA, I. KITA et O. MINAKAWA: *Journ. Phys. Soc. Japan*, **6**, 103 (1951).

(<sup>7</sup>) O. STANISZ: *Acta Phys. Pol.*, **11**, 140 (1951).

(<sup>8</sup>) C. CASTAGNOLI, G. CREA et A. GIGLI: *Rev. Sem. Ist. Fis. Univ. Roma*, **2**, n. 78 (1952).

(<sup>9</sup>) R. SEIDL: *Czechoslov. Journ. Phys.*, **1**, 160 (1952).

(<sup>10</sup>) C. P. JOSHI: *Indian Journ. Phys.*, **27**, 393 (1953).

(<sup>11</sup>) J. H. MADER: *Zeits. f. Phys.*, **137**, 216 (1954).

(<sup>12</sup>) R. MEUNIER, M. BONPAS et J. P. LEGRAND: *Journ. Phys. et Rad.*, **16**, 145 (1955).



Ces travaux ont porté, presque dans tous les cas, sur les détecteurs classiques à cathode interne. Seuls PARKASH et KAPUR <sup>(12)</sup>, ont étudié les compteurs à coque de verre et graphitage externe au dessus de la température ambiante (jusqu'à 60 °C) pour un remplissage argon-alcool classique: le coefficient de température, très faible, n'a pas été précisé. A. et J. DAUDIN <sup>(13)</sup> notent, sans donner de précisions, le bon fonctionnement de compteurs en verre « novo » contenant un remplissage (argon+méthylal) à -18 °C, pour la détection du rayonnement cosmique. Les propriétés thermiques des compteurs à coque de verre — très mal connues, comme on le voit — sont soumises aux considérations suivantes:

1) Au dessous de la température ambiante, s'ajoutent à la condensation possible de la vapeur polyatomique, les effets électriques de la résistance, alors très élevée, de la paroi de verre. Le seuil de Geiger augmente trop rapidement avec le taux de comptage, et l'emploi d'un verre très conducteur est nécessaire <sup>(14)</sup>.

2) Au dessus de la température ambiante, par contre, la résistivité du verre devient beaucoup plus faible et le seuil de Geiger est pratiquement indépendant du taux de comptage. D'autre part, la simplicité mécanique et la robustesse de ces compteurs les adaptent particulièrement à être utilisés à température élevée. C'est pourquoi notre étude a été faite dans ce domaine.

L'intérêt pratique d'une telle recherche est important, les réalisations de compteurs pour températures élevées étant peu nombreuses et conduisant en général à des solutions compliquées <sup>(15)</sup>. Nous avons déjà eu l'occasion de signaler les qualités des compteurs à parois de verre à haute température <sup>(16)</sup>, et ce fait a été confirmé dans une publication récente <sup>(17)</sup> portant sur les compteurs proportionnels.

## 2. — Dispositif expérimental.

Les compteurs à coque de verre, d'un diamètre interne  $b$  de 1 à 3 cm, sont constitués par un cylindre de verre « novo » (T K 100=143 °C) épais de 0.5 à 1 mm, suivant l'axe duquel est tendu un fil de tungstène d'un diamètre  $a=0.1$  mm, relié à chacune de ses extrémités à un fil de copperclad permettant une soudure directe au verre. Le ressort placé habituellement à l'extrémité du fil de tungstène est supprimé, la tension voulue étant obtenue par étirage du verre; jusqu'à 250 °C, la tension ainsi réalisée est suffisante.

Nous avons utilisé une méthode précédemment décrite <sup>(18)</sup> pour définir avec précision la longueur efficace  $L$  de la cathode. Les sections graphitées sont séparées par

<sup>(13)</sup> A. DAUDIN et J. DAUDIN: *Journ. Phys. et Rad.*, **12**, 564 (1951); **14**, 169 (1953).

<sup>(14)</sup> D. BLANC: *Journ. Phys. et Rad.*, **16**, 681 (1955).

<sup>(15)</sup> ANONYME: *Instruments*, **24**, 1067 (1951).

<sup>(16)</sup> D. BLANC et R. VISTE: *Compt. Rend. Acad. Sci.*, **240**, 2405 (1955).

<sup>(17)</sup> A. MOLJK, R. W. P. DREVER et S. C. CURRAN: *Rev. Sci. Instr.*, **26**, 1034 (1955).

<sup>(18)</sup> D. BLANC: *Nuovo Cimento*, **1**, 1280 (1955).

des couches très résistantes de vernis à l'amiante qui éliminent toute conductibilité de surface.

Les compteurs sont pompés durant trois heures avant remplissage, sous la pression de  $0.1 \mu\text{m}$  de mercure, *sans étuvage* qui brise les couches polymoléculaires d'eau existant sur la surface du verre, modifie profondément le seuil photoélectrique et introduit des effets incontrôlables sur la caractéristique de comptage à la température ambiante <sup>(19,20)</sup>. Les remplissages sont constitués d'éthanol ou de méthylal, additionnés (ou non) d'argon ou d'hydrogène spectroscopiquement purs.

Les compteurs à cathode interne sont d'un modèle industriel éprouvé <sup>(21)</sup>. Ils comportent des cathodes de graphite ou de plomb, et des remplissages (alcool+argon) ou (formiate d'éthyle+argon).

Les compteurs sont placés dans une étuve donnant toutes les températures entre  $20^\circ\text{C}$  et  $250^\circ\text{C}$  à  $0.5^\circ\text{C}$  près. L'armature métallique de l'étuve sert de blindage; le fil de jonction au préamplificateur est un câble coaxial isolé par de la laine de verre.

Le circuit de comptage est constitué d'un préamplificateur, d'un circuit normalisateur, d'une échelle de 1000 (temps de résolution égal à  $5 \mu\text{s}$ ) et d'un numéroteur mécanique. Le seuil est de  $0.8 \text{ V}$ .

### 3. — Coefficient de température.

**3.1. Compteur à coque de verre.** — Nous avons expérimenté des remplissages (éthanol+argon), (éthanol+hydrogène), (méthylal+argon) et méthylal pur <sup>(22)</sup>. La variation thermique du seuil du palier  $V_P$ , quel que soit le remplissage, a l'allure donnée dans la Fig. 1.

La variation est linéaire jusqu'à une température  $t_0$  au dessous de laquelle le coefficient de température  $c_0$  (volts par degré) est donc constant. Au dessus de  $t_0$ , la courbe est une parabole. Prenant  $t=20^\circ\text{C}$  comme température de référence:

$$\begin{aligned} t \leq t_0 & \quad V_P^t - V_P^{20} = c_0(t - 20), \\ t > t_0 & \quad \begin{cases} V_P^t - V_P^{t_0} = c_0(t - t_0) + c_1(t - t_0)^2 & \text{ou} \\ V_P^t - V_P^{20} = c_0(t - 20) + c_1(t - t_0)^2. \end{cases} \end{aligned}$$

Le Tableau II et le Fig. 2 donnent la variation de  $c_0$  avec la pression  $P_v$  de la vapeur organique. La courbe est une droite passant par l'origine.  $P_v$  étant exprimée en centimètres de mercure:

$$\text{Méthylal:} \quad c_0 = 0.16 P_v \text{ (volts par degré),}$$

$$\text{Éthanol:} \quad c_0 = 0.50 P_v \text{ (volts par degré).}$$

<sup>(19)</sup> R. MAZE: *Journ. Phys. et Rad.*, **7**, 164 (1946).

<sup>(20)</sup> M. GRENON: *Compt. Rend. Acad. Sci.*, **236**, 1772 (1953).

<sup>(21)</sup> N. B. BALAAM: *Electron. Engineering*, **12**, 558 (1952).

<sup>(22)</sup> D. BLANC: *Nuovo Cimento*, **11**, 231 (1954).

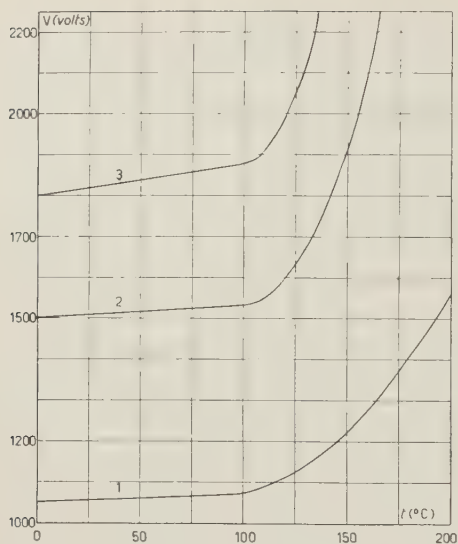


Fig. 1. - Variation thermique du seuil  $V_p$ ; (1) Méthylal 1 cm<sub>Hg</sub> + Argon 10.6 cm<sub>Hg</sub>; (2) Méthylal pur 2.3 cm<sub>Hg</sub>; (3) Méthylal pur 5.4 cm<sub>Hg</sub>.

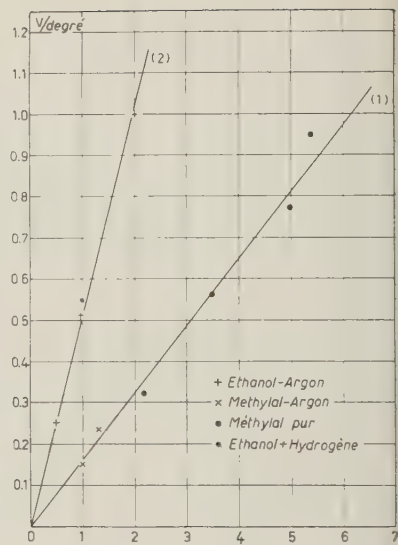


Fig. 2. -  $c_0 = f(P_v)$  pour mélanges autocoupeurs classiques et vapeur pure (compteurs à graphitage externe).

TABLEAU II.

Méthylal cm <sub>Hg</sub>	Argon cm <sub>Hg</sub>	$c_0$ (volts/degré)	$t_0$ °C	Nombre de compteurs étudiés
1.0	10.6	0.15	$90 \pm 8$	4
1.3	8.3	0.23	$95 \pm 8$	3
2.3	0	0.32	$102 \pm 6$	4
3.5	0	0.56	$105 \pm 5$	2
5.0	0	0.77	$100 \pm 5$	3
5.4	0	0.85	$107 \pm 5$	4
Alcool cm <sub>Hg</sub>	Argon cm <sub>Hg</sub>			
0.5	4.5	0.25	$105 \pm 8$	2
1.0	9.0	0.51	$105 \pm 8$	5
2.0	7.7	1.00	$95 \pm 0$	2
Alcool cm <sub>Hg</sub>	Hydrogène cm <sub>Hg</sub>			
1.0	9.7	0.55	$105 \pm 8$	2

Les valeurs de  $t_0$  portées dans le Tableau II ont été déterminées graphiquement par raccordement de la droite et de la parabole (Fig. 1). La Fig. 3 donne la courbe  $t_0 = f(P_v)$ . Aux erreurs expérimentales près,  $t_0$  est indépendante de  $P_v$ . Ces résultats conduisent aux conclusions suivantes:

1)  $c_0$  ne dépend pas de la géométrie du compteur; il est également indépendant de la nature et de la pression du gaz permanent additif. La courbe  $c_0 = f(P_r)$  passe par l'origine et le constituant polyatomique explique seul ce coefficient. La variation linéaire de seuil avec la température montre qu'il se produit un dégagement régulier de vapeur organique depuis les parois. Les études antérieures concernant les compteurs non autocoupeurs à remplissages de gaz permanent (hydrogène, air, argon pur, etc.) confirment que, en l'absence d'une vapeur organique, les seuils n'augmentent pas avec la température (<sup>23,24</sup>).

2) Au dessus de  $t_0$  intervient un effet supplémentaire;  $c_1$  dépend de  $P_r$  et de la géométrie du compteur. A titre d'exemple, pour  $a = 0.1$  mm et  $b = 2$  cm:

$P_v = 1.3$ cm de mercure	$c_1$ (volts/degré) = 0.09
» = 2.5 » » »	» » » = 0.15
» = 5.4 » » »	» » » = 0.25

Cet effet est attribuable à un dégagement progressif de vapeur d'eau depuis la paroi de verre. Le rôle de la vapeur d'eau s'introduisant ainsi dans le remplissage serait:

a) D'augmenter rapidement  $V_p$  en fonction de  $t$ . Ce fait est corroboré par les expériences de M. GRENON, qui étuvait des compteurs de ce type pour éliminer l'eau absorbée, puis les remplissait d'un mélange argon-alcool classique, additionné de vapeur d'eau sous la pression de 5 mm de mercure; à la température ambiante, le seuil initial était de 2000 V, le palier revenant ensuite très lentement à la normale, par retour progressif de l'eau sur les parois. La tension de la vapeur d'eau produite ici serait de plusieurs millimètres de mercure au dessus de 200 °C.

b) De détériorer progressivement le palier des remplissages argon-vapeur organique au dessus de  $t_0$ , comme nous l'indiquerons plus loin. Le rôle néfaste de la vapeur d'eau, source d'ions négatifs, est bien connu (<sup>25</sup>).

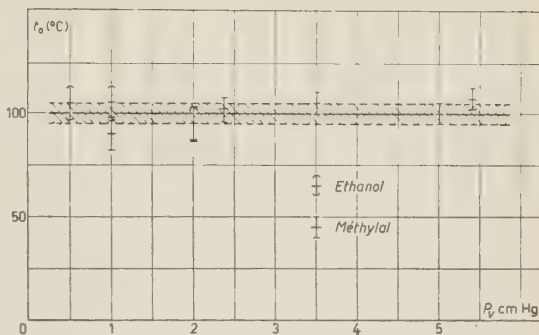


Fig. 3. -  $t_0 = f(P_v)$ .

(<sup>23</sup>) G. MEDICUS: *Zeits. f. Phys.*, **103**, 76 (1936).

(<sup>24</sup>) R. D. EVANS et R. A. MUGELE: *Rev. Sci. Instr.*, **7**, 441 (1936).

(<sup>25</sup>) M. GRENON et R. VIALARD: *Journ. Chim. Phys.*, **49**, 623 (1952).

### 3.2. Compteurs à cathode interne.

a) Argon 9 cm<sub>Hg</sub> + éthanol 1 cm<sub>Hg</sub>, avec cathode de carbone ( $a=0.127$  mm,  $b=1.6$  cm,  $L=6$  cm). Les résultats sont résumés dans la Fig. 4. Jusqu'à 80 °C environ, la variation du seuil de Geiger est linéaire,  $c_0$  étant égal à 2 V par degré. Au dessus de cette température, la variation du seuil est beaucoup moins rapide, la plus grande partie de l'éthanol adsorbé sur les parois étant passée à l'état de vapeur. Ce phénomène se manifeste jusqu'à 210 °C environ. Un effet thermoionique sensible a lieu au dessus de 160 °C, et nous y reven-

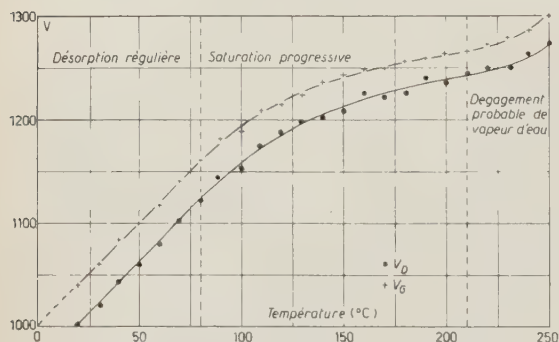


Fig. 4. — Variation du seuil de démarrage et du seuil de Geiger en fonction de la température pour un compteur à cathode interne de carbone. Éthanol 1 cm<sub>Hg</sub> + Argon 9 cm<sub>Hg</sub>.

refroidissement à la température ambiante, le seuil reste plus élevé qu'initialement et ne revient que très lentement à sa valeur primitive.

b) Argon 9 cm<sub>Hg</sub> + formiate d'éthyle 1 cm<sub>Hg</sub>, avec cathode constituée par un dépôt de plomb sur un cylindre de cuivre ( $a=0.127$  mm ( $b=3$  cm,  $L=20$  cm).

JENKINS et TAYLOR <sup>(26)</sup> préconisent l'utilisation de formiate d'éthyle pour son coefficient de température inférieur à celui de l'éthanol. La Fig. 5 donne l'évolution du seuil de Geiger. Au des-

seins plus loin. Après chauffage à une température inférieure à 210 °C et refroidissement à la température ambiante, le compteur reprend rapidement sa caractéristique initiale: il n'y a donc aucune décomposition du constituant polyatomique. Ces résultats s'accordent avec les expériences de LOOSEMORE et TAYLOR <sup>(5)</sup>.

A partir de 210 °C, le seuil varie de façon sensiblement parabolique en fonction de la température. Ce phénomène est à rapprocher de celui observé au dessus de  $t_0$  dans les compteurs à coque de verre. Après

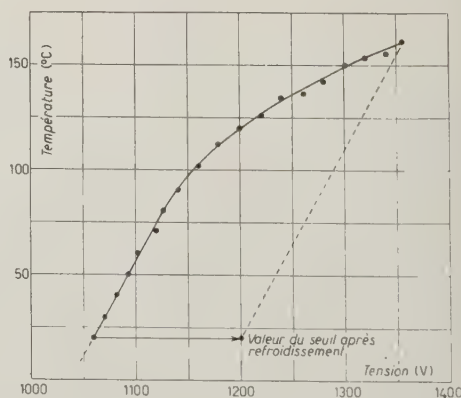


Fig. 5. — Variation du seuil de Geiger en fonction de la température pour un compteur à cathode interne de (Pb-Cu). Formiate d'éthyle 1 cm<sub>Hg</sub> + Argon 9 cm<sub>Hg</sub>.

<sup>(26)</sup> R. O. JENKINS et R. W. TAYLOR: *Journ. Sci. Instr.*, **27**, 254 (1950).



sous de 85 °C environ, le seuil varie linéairement avec la température et  $e_0$  est de 1.1 V par degré.

Au dessus de 85 °C, la variation est plus rapide et ressemble à celle observée sur les compteurs à coque de verre au dessus de  $t_0$ , mais le seuil ne reprend plus, après refroidissement, sa valeur initiale, et la translation qu'il subit est égale à sa variation entre 85 °C et la température maximum à laquelle a été porté le compteur. De plus, le palier est fortement altéré. Une décomposition chimique irréversible du formiate d'éthyle semble avoir lieu.

c) Des mesures comparatives montrent que, pour des compteurs à halogène (brome), le coefficient de température est de l'ordre de 0.10 à 0.16 V par degré. A une température supérieure à 150 °C, le brome attaque la cathode, ce qui détruit de façon définitive les qualités d'autocoupage du compteur.

#### 4. — Évolution de la caractéristique de palier.

Pour les remplissages autocoupeurs classiques, quel que soit le type de compteur étudié, la longueur du palier augmente et sa pente diminue lorsque la température s'élève. La caractéristique atteint une qualité maximum pour une certaine température et se détériore lentement au dessus. La température optimum coïncide sensiblement :

— avec la température  $t_0$  pour les compteurs à parois de verre;

— avec la température pour laquelle se manifeste un effet thermoionique sensible, pour les compteurs à cathode interne et lorsqu'il n'y a pas de décomposition du constituant polyatomique;

— dans le cas du formiate d'éthyle, avec la température pour laquelle la détérioration de la vapeur commence à se manifester.

La Fig. 6 donne l'exemple d'un compteur à coque de verre ( $a = 0.1$  mm,  $b = 0.95$  cm,  $L = 6.2$  cm). La température du maximum est de 100 °C, valeur identique à celle de  $t_0$  donnée par la Fig. 3.

La Fig. 7 concerne un compteur à cathode interne de carbone ( $a = 0.127$  mm,  $b = 1.6$  cm,  $L = 6$  cm) pour lequel la variation du seuil de Geiger a été décrite plus haut (Fig. 4): au dessous de 160 °C, la longueur de palier augmente avec la température, en même temps que la pente diminue, comme dans le cas des compteurs à coque de verre. Ces résultats s'accordent avec les expériences de FUJIOKA *et al.* <sup>(6)</sup>. Au dessus de 160 °C, l'effet thermoionique se manifeste de façon sensible et les qualités du compteur s'altèrent lentement. Au dessus de 210 °C, enfin, s'ajoute à l'émission

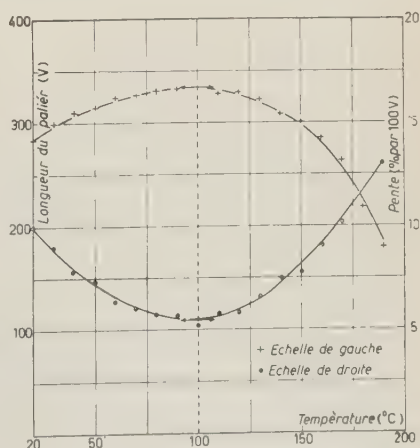


Fig. 6. — Pente et longueur du palier en fonction de la température pour un compteur à coque de verre ( $a = 0.1$  mm,  $b = 0.95$  cm,  $L = 6.2$  cm). Éthanol 0.5 cm<sub>Hg</sub> + Argon 4.5 cm<sub>Hg</sub>.

depuis le cylindre l'effet supplémentaire signalé plus haut : la longueur du palier tend rapidement vers zéro.

Pour les compteurs à graphitage externe contenant du méthylal pur, cet effet est

inversé : la pente augmente d'abord, passe par un maximum puis diminue, alors que la longueur du palier diminue, passe par un minimum puis augmente. Les températures du maximum et du minimum coïncident et sont égales à  $t_0$  aux erreurs expérimentales près.

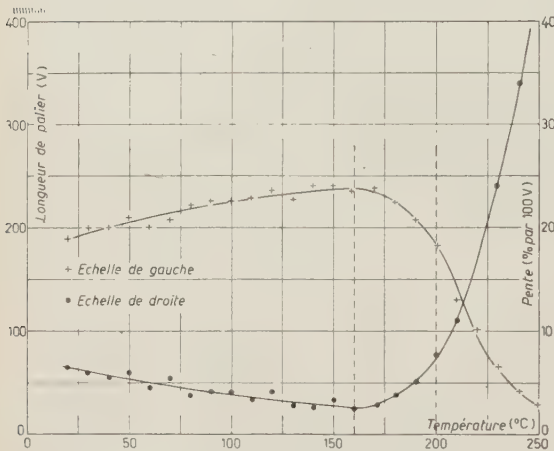


Fig. 7. — Pente et longueur du palier en fonction de la température. Compteur à cathode interne de carbone. Éthanol; 1 cm<sub>Hg</sub> + Argon: 9 cm<sub>Hg</sub>.

## 5. — Effet thermoïonique.

L'émission spontanée d'électrons [ou d'ions (12)] depuis le cylindre se traduit par une augmentation du mouvement propre.

1) Pour les compteurs à coque de verre, quelle que soient la géométrie, la nature du verre et le remplissage, le fond reste constant jusqu'à 250 °C. L'émission spontanée est donc négligeable, ce qui confirme la stabilité remarquable de la surface cathodique des compteurs de ce type.

2) Pour les divers compteurs à cathode interne étudiés, l'augmentation du fond commence à être sensible pour une température comprise entre 100 °C et 200 °C. On trouvera sur la Fig. 8 l'augmentation thermique du fond pour un compteur (alcool+argon) à cathode de carbone décrit plus haut. Le fond est  $N_0=50$  impulsions pour 30 secondes à la température ambiante. La variation du taux de comptage  $N$  avec la température est donnée par la courbe (1). La courbe (2) donne la différence

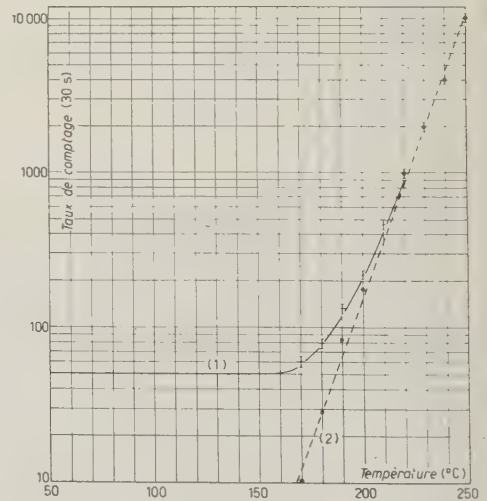


Fig. 8. — Variation du mouvement propre en fonction de la température pour une cathode interne de carbone ( $a = 0.127$  mm,  $b = 1.6$  cm,  $L = 6$  cm). Éthanol 1 cm<sub>Hg</sub> + Argon 9 cm<sub>Hg</sub>.

$n = N - N_0$ , égale à l'émission spontanée. Les résultats confirment les expériences de SEIDL<sup>(9)</sup>, GROTOWSKI *et al.*<sup>(27)</sup>, R. MEUNIER *et al.*<sup>(12)</sup>.

## 6. — Confirmation de la stabilité des compteurs à coque de verre.

Un compteur n'est réellement utilisable dans une gamme étendue de températures que dans la mesure où une variation thermique rapide n'altère pas ses propriétés.

M. KIMURA<sup>(28,29)</sup> a constaté sur des compteurs à cathode métallique (fer, laiton, nickel, aluminium) qu'une variation rapide de la température (2° par minute) entraîne une augmentation considérable du fond, multiplié par plus de 50 dans certains cas; le comptage ne revient à la normale qu'après plus de deux heures lorsque la température est maintenue constante. Il étudia des remplissages argon-éthanol, argon-éther et argon-éthylène: l'effet existe dans tous les cas et provient d'une émission spontanée depuis la cathode.

Pour contrôler la stabilité des compteurs à coque de verre, nous avons effectué deux séries d'expériences:

1) Le compteur est placé dans l'étuve, dont on augmente la température d'une façon sensiblement linéaire en fonction du temps (2°5 par minute environ). Le fond est contrôlé de façon continue à l'aide d'un enregistreur graphique à bande. La température ayant atteint une valeur de 150 à 180 °C, on laisse l'étuve revenir à la température ambiante. Tous les compteurs étudiés ont été soumis à cet essai: dans aucun cas le phénomène décrit par KIMURA n'a été observé, et le fond reste parfaitement constant.

2) Le compteur est introduit rapidement dans l'étuve, où est maintenue une température constante (de 100 à 150 °C). La variation thermique est brutale mais le taux de comptage ne subit cependant aucune perturbation.

## 7. — Conclusion.

Cette étude montre que la robustesse et la faible valeur du coefficient thermique des compteurs à graphitage externe les rendent particulièrement intéressants lorsque des augmentations de température sont à envisager. Un étuvage préliminaire modéré devrait permettre de les utiliser, sans l'effet parasite observé, à des températures très supérieures à  $t_0$ . En particulier, des compteurs non étuvés remplis de vapeur pure, pour lesquels l'effet est inversé, restent excellents au dessus de 150 °C, dans la mesure où la vapeur ne subit pas de décomposition thermique.

D'autre part, pour les remplissages autocoupeurs classiques, les résultats

(27) K. GROTOWSKI, A. Z. HRYNKIEWICZ et H. NIEWODNICZANSKI: *Acad. Polon. Sci.*, **1**, 109 (1953).

(28) M. KIMURA: *Phys. Rev.*, **80**, 761 (1950).

(29) M. KIMURA: *Journ. Phys. Soc. Japan*, **6**, 141 (1951).

généraux suivants ont été obtenus:

1) Le coefficient de température, proportionnel à la pression partielle du constituant polyatomique, est dû à une désorption régulière de celui-ci depuis les parois.

2) L'amélioration thermique du palier montre que l'effet néfaste d'ions négatifs venant de la vapeur de mercure présente en très faibles proportions dans le remplissage initial est nul, contrairement à certaines hypothèses antérieures (<sup>3,10</sup>).

3) La détérioration du compteur au dessus d'une certaine température critique est due — dans tous les cas — à un phénomène étranger à la décharge. Ce phénomène peut être réversible (dégagement de vapeur d'eau depuis les parois, émission depuis la cathode) ou irréversible (réaction chimique à l'intérieur du remplissage dans le cas d'une vapeur organique, ou sur les parois dans le cas d'un halogène).

---

#### RIASSUNTO (\*)

Allo scopo di spiegare i risultati alquanto contraddittori ottenuti in precedenza, abbiamo eseguito una serie d'esperienze sull'effetto termico dei contatori di Geiger-Müller tra 20 °C e 250 °C, utilizzando diversi riempimenti autoestintori e rivelatori a catodo interno o a pareti di vetro grafitate esternamente. Il coefficiente di temperatura, proporzionale alla pressione parziale del costituente poliatomico è dovuto alla regolare riemissione dalla parete. La caratteristica di soglia migliora con l'aumentare della temperatura e l'effetto nocivo dei possibili ioni negativi prodotti dal vapore di mercurio esistente in piccolissima proporzione nel riempimento è nullo, contrariamente a certe ipotesi precedenti. Il deterioramento progressivo della caratteristica al disotto di una data temperatura è dovuto a un fenomeno estraneo alla scarica, reversibile (sviluppo del vapore acqueo dalle pareti, aumento del moto proprio) o irreversibile (decomposizione del vapore poliatomico o reazione chimica sulle pareti). I contatori a pareti di vetro non trattati in stufa manifestano una notevole stabilità: fino a 250 °C non si produce alcun aumento sensibile del fondo e fino a una temperatura  $t_0$  prossima a 100 °C il loro coefficiente termico è molto inferiore a quello dei contatori a catodo interno di tipo classico. Al disopra di  $t_0$  la variazione è più rapida.

---

(\*) Traduzione a cura della Redazione.



# LETTERE ALLA REDAZIONE

(La responsabilità scientifica degli scritti inseriti in questa rubrica è completamente lasciata dalla Direzione del periodico ai singoli autori)

## A Note on the Decay of $^{185}\text{W}$ .

S. K. BHATTACHERJEE and SHREE RAMAN

Tata Institute of Fundamental Research - Bombay

(ricevuto il 6 Febbraio 1956)

There has been much controversy on the mode of decay of 75 day  $^{185}\text{W}$  in recent years. It was found to have a simple decay with one  $\beta$ -group of maximum energy ( $^{1,3}$ ) of about 430 keV. Conversion lines corresponding to a  $\gamma$ -ray of 134 keV were reported by CORK ( $^4$ ) *et al.* and quite recently supported by MIJOTOVIC ( $^5$ ). A strong electromagnetic radiation of energy 60 keV was observed in scintillation spectrometer and was ascribed to  $K$  X-rays from the capture decay of  $^{181}\text{W}$  ( $^6$ ). BISI ( $^7$ ) *et al.* studied the radiations of  $^{183}\text{W}$  with magnetic spectrometer, scintillation and proportional counter spectrometers. They found the  $\beta$ -decay simple; no higher energy electromagnetic radiation was reported by them besides the one at 57 keV,

which was shown to be a  $\gamma$ -ray and not the  $K$  X-rays of Re. The proposed decay scheme necessitates the presence of an inner  $\beta$ -group of about 370 keV maximum energy.

This note reports on work on the existence of an inner group of  $\beta$ -rays in  $^{185}\text{W}$  decay done with a coincidence scintillation spectrometer.

The whole  $\gamma$ -spectrum was accepted in a NaI(Tl) spectrometer while the  $\beta$ -spectrum was taken with an anthracene (4 mm thick) scintillation spectrometer. Only one  $\gamma$ -ray corresponding to an energy of about 58 keV was found. The anthracene crystal spectrometer records the total  $\beta$ -distribution from which a linear Fermi plot can be drawn; the  $\gamma$ -channel accepting the full photopeak of 57 keV  $\gamma$ -ray, the coincidence  $\beta$ -spectrum was taken; it clearly showed the inner group in  $^{185}\text{W}$  in coincidence with the 57 keV  $\gamma$ -ray (resolving time  $2.5 \cdot 10^{-7}$  s). The end-point energy determination from the Fermi plot of the coincidence spectrum cannot be done accurately because of the very low energy difference between the two end points ( $\sim 57$  keV) and of the poor resolution of the spectrometer (28% for 624 keV conversion line of  $^{137}\text{Cs}$ ).

( $^1$ ) D. SAXON: *Phys. Rev.*, **74**, 1264 (1948).

( $^2$ ) F. B. SHULL *et al.*: *Phys. Rev.*, **74**, 917 (1948).

( $^3$ ) C. L. PEACOCK *et al.*: *Phys. Rev.*, **74**, 297 (1948).

( $^4$ ) J. M. CORK, H. B. KELLER and A. E. STODDARD: *Phys. Rev.*, **76**, 575 (1949).

( $^5$ ) A. M. MIJOTOVIC: *Bull. Inst. Nu. Sci. (Boris Kidrich)*, **4**, 75 (1954).

( $^6$ ) W. E. KREGER *et al.*: *Bull. Am. Phys. Soc.*, **30**, no. 5, **4** (1955).

( $^7$ ) A. BISI, S. TERRANI and L. ZAPPA: *Nuovo Cimento*, **1**, 291 (1955).



From the gross  $\beta$ - $\gamma$  coincidences of  $^{185}\text{W}$  we can roughly estimate the  $\beta$ -branching ratio;  $^{170}\text{Tm}$  being used as a comparator source because it has known  $\beta$ -branching ratio, its mode of decay is identical to that of  $^{185}\text{W}$  and the energies involved in both cases are comparable. Performing the ( $\beta$ - $\gamma$ ) coincidence experiments at identical  $\beta$  as well as  $\gamma$ -geometry, the inner  $\beta$ -group intensity of  $^{185}\text{W}$  is found to be about 15%.

In order to find the total conversion coefficient  $\alpha_T$  for the 57 keV transition, we followed the method due to SUNYAR<sup>(8)</sup> using  $^{170}\text{Tm}$  as the standard source for comparison.

For identical geometry of  $\gamma$ -detection

$$(N_{\beta\gamma}/N_{\beta})_{\text{Tm}} = f_{\beta}\omega_{\gamma} \left[ \frac{1 + \omega_k\alpha_k}{1 + \alpha_T} \right]_{\text{Tm}},$$

$$(N_{\beta\gamma}/N_{\beta})_{\text{W}} = f'_{\beta}\omega_{\gamma} \left[ \frac{1 + \omega_{LL}\alpha_L}{1 + \alpha_T} \right]_{\text{W}},$$

<sup>(8)</sup> A. W. SUNYAR: *Phys. Rev.*, **93**, 1344 (1954).

where  $\omega_{\gamma}$  is the  $\gamma$ -detection solid angle, the efficiency of detection for 84 keV  $\gamma$ -ray of Tm and 57 keV  $\gamma$ -ray of  $^{185}\text{W}$  is taken to be unity;  $f_{\beta}$  is the  $\beta$ -branching ratio of  $^{170}\text{Tm}$  and is 0.24<sup>(9)</sup> and  $\omega_k^{\text{Tm}} = 0.93$ . The value of  $\omega_{LL}$ , the  $L$ -fluorescence yield of Re has been calculated by BISI *et al.*<sup>(7)</sup> and is 0.11; putting the measured value for  $\alpha_L \cong 3$  by BISI *et al.*<sup>(7)</sup> we get from the above 2 expressions

$$\alpha_T \cong 3.3.$$

Thus one concludes that the conversion of the 57 keV transition accompanying the  $\beta$ -decay of  $^{185}\text{W}$  takes place wholly from the  $L$ -shell, and from the theoretical value of  $\alpha_L$  from ROSE<sup>(10)</sup> *et al.* one can easily classify this as an  $M1$  transition in accordance with the assignment of BISI and others and hence the decay scheme proposed by them is fully confirmed.

<sup>(9)</sup> R. L. GRAHAM, J. L. WOLFSON and R. E. BELL: *Can. Journ. Phys.*, **30**, 459 (1952)

<sup>(10)</sup> M. E. ROSE *et al.*: See Appendix IV *Beta and Gamma-ray Spectroscopy*, edited by K. SIEGBAHN, p. 908.

## On the Meaning of Fermi Coupling.

B. JOUVET

*CERN (\*), Theoretical Study Division  
at the Institute for Theoretical Physics, University of Copenhagen*

(ricevuto il 16 Febbraio 1956)

Various authors have attempted to account for elementary particles, starting from a theory of Fermi-type coupling between some Fermion fields. However, no quantum attempt has been clearly successful so far. We shall here investigate the simplest example, that of a scalar self-coupling of a spinor  $\psi$ , and show that this theory is identical with a Yukawa-type theory of a scalar meson whose experimental mass  $\mu$  and coupling constant  $G$  are given functions of the Fermion constants<sup>(†)</sup>. This identity will be used to express the unrenormalized quantities of the Fermi-theory in terms of the renormalized ones. We assume that both theories have a solution and that the Yukawa-theory still has a meaning when the renormalization constants tend to the critical values given below.

Let  $L_F = L_1(m_0, \psi_0) + (g_0/2)(\bar{\psi}_0\psi_0)(\bar{\psi}_0\psi_0)$  be the Fermi-Lagrangian, as a function of the unrenormalized quantities, where  $L_1$  is the free particle of the Dirac Lagrangian;  $S_F$  will be the corresponding  $S$ -matrix. The Yukawa-Lagrangian  $L_Y = L_1(m_0, \psi_0) + L_2(\mu_0, A_0) + G_0 A_0 \bar{\psi}_0 \psi_0$ , again in unrenormalized form ( $L_2$  being the free meson part), will lead to an  $S$ -matrix  $S_Y$ , of which these matrix elements in which no real mesons appear are denoted by  $(\langle S_Y \rangle_0 \text{ meson})$ . Comparing the matrix elements of  $(\langle S_Y \rangle_0 \text{ meson})$  proportional to  $G^{2N}$  with those of  $S_F$  proportional to  $g^N$ , one sees that one would obtain

$$(1) \quad S_F = (\langle S_Y \rangle_0 \text{ meson})$$

provided that

$$(2) \quad g_0 = \frac{G_0^2}{p^2 + \mu_0^2}.$$

(\*) European Organization for Nuclear Research.

(†) This demonstration has been carried out in more general and physical cases (but using regularization to treat the infinities) and various consequences explored by the author in a former work<sup>(1)</sup>. The model given here is easily generalized for different types of Fermi-coupling, and couplings between different spinor fields.

(1) B. JOUVET: *Journ. de Math.*, **33**, 201 (1954) or *Thèse de Doctorat*, Paris (1954); *Suppl. Nuovo Cimento*, **2**, 941 (1955); *Proceed. Pisa Conf.* (1955).

Both  $G_0^2$  and  $\mu_0^2$  must be infinite if this equality is to hold; thus the (contact) Fermi-interaction is equivalent to that resulting from the exchange of mesons of infinite mass  $\mu_0$ , with coupling constant  $G_0$ , also infinite. The point of interest is, however, that both these parameters are the unobservable unrenormalized ones. Because of the occurrence of  $g_0$  in the divergent quantities, care must be taken to show that (2) actually leads to (1). By using a limiting process with a cut-off on the Fermion momentum,  $\mu^2 < \Lambda$ , one can give this proof providing that  $G_0^2(\Lambda)$  and  $\mu_0^2(\Lambda)$  satisfy

$$(3) \quad \left( \frac{\partial}{\partial \Lambda} \left( \frac{1}{G_0^2(\Lambda)} \right) \ll \frac{a}{\Lambda} \right)_{\Lambda \rightarrow \infty}; \quad a = \text{const}; \quad \mu_0^2(\Lambda) = \frac{G_0^2(\Lambda)}{g_0}.$$

Let us now deal with the renormalized quantities. If we assume that the usual renormalization constants of the Yukawa-theory are determined as functions of the observable parameters ( $m, \mu, G$ ), only the meson quantities may be renormalized at first

$$(4) \quad A_0 = Z_3^{\frac{1}{2}} A, \quad \mu_0^2 = \mu^2 + (\delta\mu^2/Z_3), \quad G_0 = G_1 Z_3^{-\frac{1}{2}} = \frac{Z_1}{Z_2} Z_3^{-\frac{1}{2}} G.$$

Expressing  $\langle S_Y \rangle_{0 \text{ meson}}$  in terms of these quantities, the equality (1) holds when

$$(5) \quad Z_3 = 0, \quad \delta\mu^2 = G_1^2/g_0$$

and condition (3) leads to

$$(6) \quad \frac{\partial Z_3(\Lambda)}{\partial \Lambda} \ll a G_1^2/\Lambda.$$

The unitarity of  $S_F^-$  and  $S_Y$  can be shown to imply that

$$(7) \quad S_Y |\text{meson}\rangle = 0,$$

which is the case if  $\mu > 2m$  so that the meson has a finite life-time;  $\Lambda_F'$  then has a complex pole, and  $\delta\mu^2$  is defined as the real part of the usual quantity  $(^+)$ . One may then renormalize the  $\psi$  field in the usual way. Finally, one may renormalize the constant  $g_F$ , which is the value of the total Fermi-interaction between free particles when the exchanged momentum tends to zero, with

$$(8) \quad g_0 = g_F \cdot Z_F^2 Z_2^{-2}; \quad g_F = G^2(\mu^2 + iG^2 K_{\text{ren}}^Y(p^2 = 0))^{-1}.$$

$K_{\text{ren}}^Y(p^2)$  is the meson renormalized polarization operator. From this treatment one obtains two relations that we expect would determine the observable parameters

$$(9) \quad Z_3(m, \mu, G) = 0; \quad \delta\mu^2(m, \mu, G) Z_F^2(m, \mu, G) g_F = G^2 Z_1^2(m, \mu, G).$$

---

(<sup>+</sup>) A similar case has been studied in detail in connection with the Lee model by V. GLASER (*Colloquium*, October 31st, 1955, Copenhagen).

Analogous equations should enable one to calculate, in principle, physical constants of elementary particles, such as electric charge, through the appropriate modifications of the old schematic model.

\* \* \*

The author wishes to thank many members of the Theoretical Group in the Institute for Theoretical Physics in Copenhagen for their stimulating criticism.

On  $\Lambda^0$ -Binding Energies in Hyperfragments.

T. TATI and H. TATI

*Physics Department, Kanazawa University - Kanazawa, Japan*

(ricevuto il 20 Febbraio 1956)

A considerable number of data of  $\Lambda^0$ -binding energies  $B_\Lambda$ 's in hyperfragments has been reported, although they are not accurate and some of them are uncertain. Theoretical considerations on  $B_\Lambda$  have also been given by many authors <sup>(1)</sup>, but we want to emphasize in this note the difference of the qualitative character between  $B_\Lambda$ 's and nucleon-separation energies (Binding energies of the last nucleons). The neutron or proton separation energy from the nucleus with nucleon numbers  $N$  and  $Z$  varies in a complicated way with  $N$  and  $Z$  ranging from a negative value to about 20 MeV, and the main part of this variation is explained by the variation of the difference between the symmetry energies of the nucleus  $(N, Z)$  and of the nucleus  $(N-1, Z)$  or  $(N, Z-1)$  <sup>(2)</sup>. The symmetry energy is caused by the effect of the Pauli-principle but since the Pauli-principle is not effective to the  $\Lambda^0$ -particle bound in a nucleus we can

expect that  $B_\Lambda(A)$  of the fragment of mass number  $A$  varies relatively smoothly with  $A$ . In Fig. 1, measured  $B_\Lambda$ 's are plotted against  $A$ . It seems remarkable that the probable values of  $B_\Lambda(A)$ 's of the fragments which have the same  $A$  and the different  $Z$  are nearly equal and  $B_\Lambda(A)$  increases gradually with  $A$ . For comparisons, in Fig. 2 the separation energies of neutrons  $S_n(N, Z)$ 's from the nuclei  $(N, Z)$  are plotted against  $A$  and the contributions of the symmetry energies to  $S_n(N, Z)$ 's are also plotted. The contribution of the symmetry energy to  $S_n(N, Z)$  was estimated <sup>(3,2)</sup> by

$$V^s(N, Z) - V^s(N-1, Z),$$

where

$$V^s(N, Z) = (1.75T^2 + A + A_0)L_1A^{-1},$$

$$T = (N - Z)/2, \quad L_1 = 44 \text{ MeV},$$

and

$$A = \begin{cases} 0 & \text{for odd } A \text{ nuclei} \\ 0.81 & \text{for odd-odd nuclei} \\ -0.81 & \text{for even-even nuclei,} \end{cases}$$

$$A_0 = \begin{cases} 0.25 & \text{for odd-odd } N=Z \text{ nuclei} \\ -0.63 & \text{for even-even } N=Z \text{ nuclei} \\ 0 & \text{for } N \neq Z \text{ nuclei.} \end{cases}$$

<sup>(1)</sup> R. GATTO: *Nuovo Cimento*, **1**, 372 (1955); F. DUIMIO: *Nuovo Cimento*, **1**, 688 (1955); E. DIANA and F. DUIMIO: *Nuovo Cimento*, **2**, 373 (1955); R. H. DALITZ: *Phys. Rev.*, **99**, 1475 (1955); J. T. JONES and J. K. KNIPP: *Nuovo Cimento*, **2**, 857 (1955); R. GATTO: *Nuovo Cimento*, **2**, 373 (1955).

<sup>(2)</sup> T. TATI: *Progr. Theor. Phys.*, **14**, 107 (1955).

<sup>(3)</sup> J. N. BLATT and V. F. WEISSKOPF: *Theoretical Nuclear Physics* (1952).



The symmetry energy  $V^s(N, Z)$  was derived assuming that the nucleus  $(N, Z)$  has the potential energy which is proportional to the number of symmetric pairs in the nucleus.

We will estimate  $B_\Lambda(A)$  by the simplest model which assumes that (1) nucleons are distributed uniformly in a fragment and (2) the range of the  $\Lambda^0$ -nucleon force is considerably smaller than

the range of the nucleon-nucleon force (1), and (3) the change of the residual nucleus in the fragment when the  $\Lambda^0$ -particle is removed is small. Then  $B_\Lambda(A)$  is the difference of the potential energy  $V(A)$  and the kinetic energy  $T(A)$  of the  $\Lambda^0$ -particle bound in the fragment,

$$(1) \quad B_\Lambda(A) = \frac{1}{2}V(A) - T(A).$$

When the  $\Lambda^0$ -particle is distributed uni-

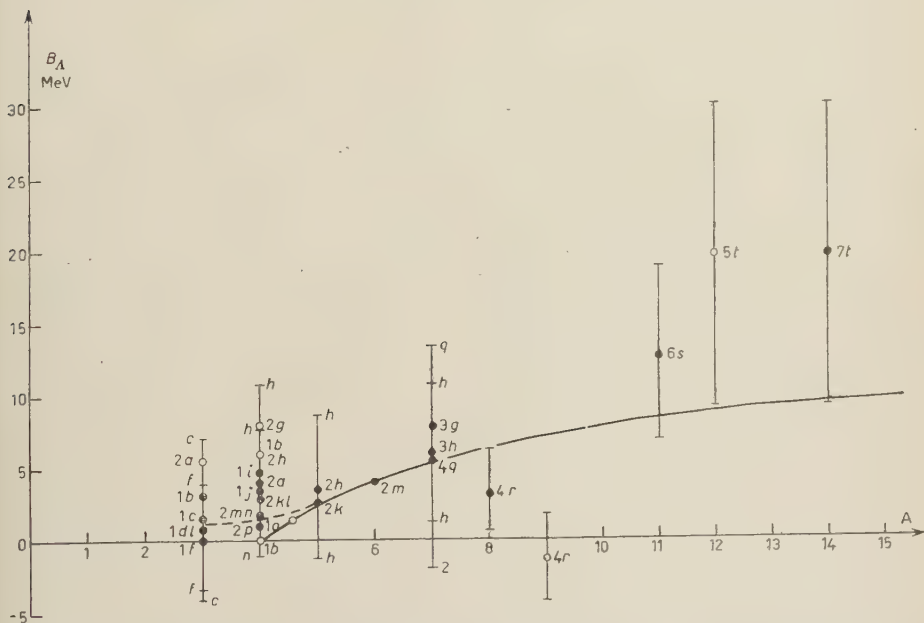


Fig. 1. —  $\Lambda^0$ -binding energies in hyperfragments. Numbers near points representing  $B_\Lambda$ 's are the atomic numbers of fragments. Letters labelling the points indicate the events from which the  $B_\Lambda$ 's are derived. — a) W. F. FRY, J. SCHNEPS and M. S. SWAMI: *Phys. Rev.*, **97**, 1189 (1955); b) H. YAGODA: *Phys. Rev.*, **98**, 153 (1955); J. T. JONES jr. and J. K. KNIPP: *Nuovo Cimento*, **2**, 855 (1955); c) C. CASTAGNOLI, G. CORTINI and C. FRANZINETTI: *Nuovo Cimento*, **2**, 550 (1955); d) A. BONETTI, R. LEVI SETTI, M. PANETTI, L. SCARSI and G. TOMASINI: *Nuovo Cimento*, **11**, 330 (1954); e) M. BALDO, G. BELLIBONI, M. CECCARELLI, M. GRILLI, B. SECHI, B. VITALE and G. T. ZORN: *Nuovo Cimento*, **1**, 1180 (1955); f) A. DEBENEDETTI, C. M. GARELLI, L. TALLONE and M. VIGONE: *Nuovo Cimento*, **12**, 466 (1954); g) J. CRUSSARD and D. MORELLET: *Compt. Rend.*, **236**, 64 (1953); h) C. CASTAGNOLI, G. CORTINI and C. FRANZINETTI: *Nuovo Cimento*, **2**, 550 (1955); i) J. HORNOSTEL and E. O. SALANT: *Phys. Rev.*, **98**, 218 (1955); j) M. SCHEIN, D. M. HASKIN and D. LEENOV: *Phys. Rev.*, **100**, 1455 (1955); k) R. D. HILL, E. O. SALANT, M. WIGDOFF, L. S. OSBORNE, A. PEVSNER, D. M. RITSON, J. CRUSSARD and W. D. WALKER: *Phys. Rev.*, **79**, 797 (A) (1954); R. H. DALITZ: *Phys. Rev.*, **99**, 1475 (1955); l) J. E. NAUGLE, E. P. NEY, P. S. FRIEDER and W. B. CHESTON: *Phys. Rev.*, **96**, 1383 (1954); m) A. BALDO, G. BELLIBONI, M. CECCARELLI, M. GRILLI, B. SECHI, B. VITALE and G. T. ZORN: *Nuovo Cimento*, **1**, 1180 (1955); n) N. SEEMAN, M. M. SHAPIRO and B. STILLER: *Phys. Rev.*, **100**, 1480 (1955); o) M. W. FRIEDLANDER, D. KEEFE and M. G. K. MENON: *Nuovo Cimento*, **2**, 663 (1955); p) W. F. FRY, J. SCHNEPS and M. S. SWAMI: cited in R. H. DALITZ's paper (reference (1)); q) W. F. FRY, J. SCHNEPS and M. S. SWAMI: *Phys. Rev.*, **97**, 1189 (1955); r) W. F. FRY and S. R. WHITHE: *Nuovo Cimento*, **11**, 551 (1954); W. F. FRY, J. SCHNEPS and M. S. SWAMI: *Phys. Rev.*, **97**, 1189 (1955); t) P. S. FRIEDER, G. W. ANDERSON and J. E. NAUGLE: *Phys. Rev.*, **94**, 677 (1954).

formly in the fragment, we can estimate  $V(A)$  as follows under our assumptions

$$(2) \quad V(A) = (b^3v/R_A^3)(A-1) - (9/16) \cdot$$

$$\cdot (b^4v/R_A^4)(A-1) = V^0 - V'(A-1)^{-\frac{1}{2}},$$

$\theta$ -mesons and  $\Lambda^0$ -n and n-n potentials have the form of a Yukawa well,  $b^3v$  is 1/9 times the corresponding quantity for the nucleon-nucleon force <sup>(1)</sup> and  $V^0$  will be much smaller than the average potential depth for a nucleon in the nucleus.

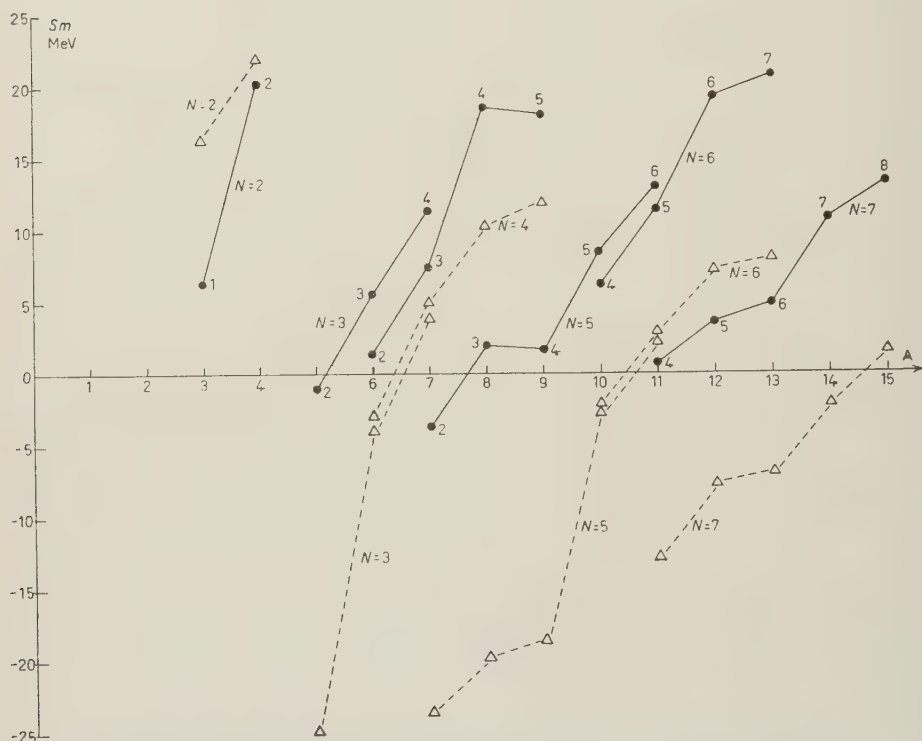


Fig. 2. — Neutron-separation energies  $S_n(N, Z)$ 's from the nuclei  $(N, Z)$  are plotted against  $A$  (Binding energies of the last neutrons). Numbers near points representing  $S_n$ 's are the atomic numbers of nuclei.  $S_n(N, Z)$ 's of given  $N$  are connected.  $\Delta$  represents the contribution of the symmetry energy to  $S_n(N, Z)$ .

where  $b$  and  $v$  are the effective range and depth of the  $\Lambda^0$ -nucleon force.  $R_A$  is the radius of the fragment and if  $R_A = r_0(A-1)^{\frac{1}{3}}$ ,  $V^0$  and  $V'$  are independent of  $A$ . The second term represents the surface effect in this model which has a sharp boundary. When  $b$  is much smaller than  $r_0$ ; the surface energy term is neglected, and under the assumption (2),  $V'/V^0$  is smaller than the corresponding quantity for a nucleon. If the  $\Lambda^0$ -nucleon force is carried mainly by

But there seems to be some possibilities that  $V^0$  has larger values. ( $\alpha$ ) The ratio of the corresponding quantities  $b^3v$  for the  $\Lambda^0$ -n and n-n potentials depends on their detailed nature and is larger than 1/9 if the potentials are more singular than the Yukawa well. ( $\beta$ ) If the probability of finding a  $\Lambda^0$ -particle and a nucleon within the distance  $b$  in the fragment is larger than  $(b^3/R_A^3)$  (position correlations), we have larger values of  $V^0$  than the value estimated in (2).

The estimation of the kinetic energy  $T(A)$  of  $\Lambda^0$ -particle is also difficult. We estimate  $T(A)$  here by the energy of the 1s level of the square well potential of depth  $V^0$  and range  $R_A$ . (This is allowable when the mean free path of the  $\Lambda^0$ -particle is not much smaller than the radius of the fragment.) In Fig. 1, a curve is shown which is calculated by Eqs. (1) and (2) assuming  $V^0 = 20$  MeV and  $R_A = 1.45 \cdot 10^{-13} (A-1)^{1/3}$  cm and  $V' = 0$ . The dotted curve represents a probable correction taking into account relatively diffuse boundaries<sup>(4)</sup> of  ${}^2\text{H}$ ,  ${}^3\text{H}$  or  ${}^3\text{He}$  (hence radii of  ${}^3\text{H}^*$ ,  ${}^4\text{H}^*$  or  ${}^4\text{He}^*$ ).

In the present stage where even for a nucleon in the nucleus the correct values of the potential and kinetic energies are not known, we can not obtain the correct values for  $V(A)$  and  $T(A)$ . In addition statistical considerations are

inadequate for the lightest nuclei. But we may expect that in the nucleus  $(N, Z)$  the potential energy of the  $\Lambda^0$ -particle is a much more smooth function of  $(N, Z)$  than the potential energy of a nucleon since the symmetry effect on the latter is very large in light nuclei while  $V(A)$  has no symmetry effect when the spin-dependence of the  $\Lambda^0$ -n force is neglected. If we can expect that the  $B_\Lambda(A)$  lies near a smooth  $V_\Lambda(A) - A$  curve contrary to the case of nucleon separation energies, we can choose a more probable scheme when the two or more decay schemes of a hyperfragment are possible in the interpretation of an event. In Fig. 1, when two or more decay schemes are possible, the values of  $B_\Lambda$ 's which are less probable in the above mentioned sense are represented by open circles. More exact values of  $B_\Lambda(A)$ 's and of  $B_\Lambda(A)$ 's of various mass numbers will give important information about nuclear structures.

(4) A. E. S. GREEN and K. LEE: *Phys. Rev.*, **99**, 772 (1955).

# A $\tau$ -Decay with a Secondary of Extremely Low Energy.

N. BRENE

*Institute for Theoretical Physics, University of Copenhagen, Denmark*

(ricevuto il 23 Febbraio 1956)

The relative probability that one of the mesons produced in the decay of a  $\tau$ -meson at rest takes only a very small proportion of the total energy available may be shown to depend strongly on the spin and parity of the  $\tau$ -meson <sup>(1-3)</sup>. Events of this type are expected to be most common if the  $\tau$ -meson has spin 0 and negative parity. It should be stressed, however, that information from individual events of this type can only be used in the context of the general  $\tau$ -meson statistics.

An event of this sort was found in the K<sub>1</sub>-stack (120 Ilford G5 stripped emulsion 25 × 40 cm<sup>2</sup>), exposed to a beam of positive secondary particles of unique momentum from the Berkeley Bevatron, in the course of an experiment to analyze the relative composition of the heavy meson beam.

The particles are picked up about 3 or 5 cm before they reach the area where K-mesons normally stop and if they have the correct grain density (visually estimated) they are followed to their stopping point and their decay, if any, is examined.

In this way we have so far recorded 426 K-mesons and 33  $\tau$ -mesons.

From one of the  $\tau$ -events emerges a positive secondary of very short range. The details of the measurements made on the decay particles are set out in Table I.

TABLE I.

Particle	Range
1	$12.0 \pm 1.0 \mu\text{m}$
2	$24.1 \pm 1.0 \text{ mm}$
Angle ( $p_2, p_3$ ) = $176^\circ 48' \pm 0^\circ 18'$	

As the range of one of the particles, which escaped from the available portion of the emulsion, is not known, and as direction measurements on the very short secondary are ambiguous, it is not possible to make a complete analysis of the momentum balance. However, on the assumption that the event does represent the decay of a  $\tau$ -meson at rest according to the usual mode, it is possible to calculate the momentum of the escaping particle and the direction of motion of the slow  $\pi$ -meson. The additional data so obtained are set out in Table II.

From the triangle of momentum there are two possible solutions from one of which the  $Q$ -value ( $73.0 \pm 3.5 \text{ MeV}$ ) is in good agreement with the accepted one

<sup>(1)</sup> R. H. DALITZ: *Phil. Mag.*, **44**, 1068 (1953).

<sup>(2)</sup> R. H. DALITZ: *Phys. Rev.*, **94**, 1046 (1954).

<sup>(3)</sup> E. FABRI: *Nuovo Cimento*, **11**, 479 (1954).

TABLE II.

Particle	Charge	$pc$ (MeV)	$E$ (MeV)	$Q$ -value (MeV)
1	+	$11.4 \pm 0.3$	$0.467 \pm 0.025$	—
2	—	$112 \pm 2$	$39.5 \pm 1.2$	—
3	(+)	102 (121)	33.0 (45.3)	$73.0 \pm 3.5$ $(85.3 \pm 3.5)$

$(75.0 \pm 1.5 \text{ MeV})$  <sup>(4)</sup>. This solution also

agrees best with the apparent direction of particle 1.

<sup>(4)</sup> E. AMALDI: *Pisa Conference Report* (1955).

A more complete description of all our  $\tau$ -data will shortly be published.



# Remarks on the Absorption of Negative K-mesons by Protons.

R. GATTO

*Istituto di Fisica e Scuola di Perfezionamento dell'Università - Roma*  
*Istituto Nazionale di Fisica Nucleare - Sezione di Roma*

(ricevuto il 24 Febbraio 1956)

In this paper we give a brief discussion on the absorption of slow negative K-mesons by hydrogen nuclei. The time taken by a low energy ( $\sim 10$  MeV) negative heavy meson to be slowed down and captured in liquid hydrogen is estimated to be  $\sim 10^{-10}$  s <sup>(1)</sup>, therefore appreciably smaller than the measured lifetime  $\sim 10^{-8}$  s. Some of the possible reactions which are expected to occur in the framework of Gell-Mann's theory have been already observed in nuclear emulsions. We report here some considerations about the different possible absorption modes of a bound K-meson by a proton. The angular correlations for the decay products of the hyperon (or of the possible K-meson) produced by the absorption deserve particular attention since they may give information on the spins. We give here the general form of these correlations. We also discuss in some detail the important physical point of the possible absorption from orbits with higher angular momentum.

The reactions

$$(1') \quad K^- + p \rightarrow \Sigma^+ + \pi^-$$

$$(1'') \quad K^- + p \rightarrow \Sigma^0 + \pi^0$$

$$(1''') \quad \rightarrow \Sigma^- + \pi^+$$

$$(2) \quad \rightarrow \Lambda^0 + \pi^0$$

are fast reactions. Assuming that  $(\bar{K}N, \Sigma)$ ,  $(\bar{K}N, \Lambda)$ ,  $(\Sigma, \Sigma\pi)$ ,  $(\Lambda, \Sigma\pi)$  are strong interactions, one can imagine (1) and (2) as occurring for instance through the virtual sequence: initial state goes over into a  $\Sigma^0$  or  $\Lambda^0$  which goes over into the final state. In (1'') the virtual hyperon cannot be a  $\Sigma^0$ , because the coupling constant of  $(\Sigma^0, \Sigma^0\pi^0)$  must be zero to satisfy charge independence, and in (2) the virtual hyperon cannot be a  $\Lambda^0$  because the coupling constant of  $(\Lambda^0, \Lambda^0\pi^0)$  must also be zero for charge independence. In (1'') the final state has  $I = 0$  and this leads to the inequality

$$\sigma(K^-p|\Sigma^0\pi^0) <$$

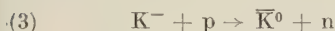
$$< \frac{1}{2}[\sigma(K^-p|\Sigma^+\pi^-) + \sigma(K^-p|\Sigma^-\pi^+)].$$

The ratio between the statistical weight of the final state of (1'), or of (1''), or of (1'''), and that of the final state of (2) is  $\sim 0.59$ . Multiplying by a factor  $\sim 5$  to account for the various isotopic

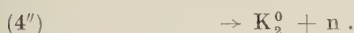
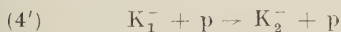
<sup>(1)</sup> A. WIGHTMAN: *Phys. Rev.*, **77**, 521 (1950).

spin states the ratio is raised to  $\sim 3$ .

One can imagine a charge exchange reaction

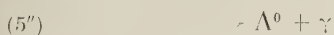


and, if two different kinds of heavy mesons exist,  $K_1$  and  $K_2$ , supposing  $K_1$  to be the heavier of the two one can also imagine the reactions



The rates of (3) and (4) would depend very sensibly on the mass differences. For reactions (3) and (4'') to occur the mass difference between the initial and the final K must be  $> 1.3$  MeV. For reaction (4') the mass difference only needs to be  $> \sim 10^4$  eV. The ratio of the statistical weight of one of the reactions (3) and (4) to the statistical weight of (2) is  $0.14\sqrt{Q}$ , where  $Q$  (in MeV) is the excess energy available. Therefore these reactions are expected to be less probable than (1) and (2). Reactions (4) would be of interest also in connection with the recent suggestion of two different K-mesons with very different lifetimes<sup>(2)</sup>.

The possible reactions



are expected to be still more improbable. If we compare, for instance, (5') with (1'), we find that the statistical weight of (5') is  $\sim 0.50$  that of (1'), but the squared matrix element for (5') is expected to be much smaller than for (1') [a rough estimate leads to

$$4\pi w_\pi / 137g^2 m_K$$

for the ratio between the squared ma-

trix element of (5') and that of (1'), with  $g$  = coupling constant of  $(K^-p, \Sigma^0)$ , and  $w_\pi$  energy of the pion in (1'), assuming  $g^2 \sim 3$ , the ratio is  $\sim 1.4 \cdot 10^{-2}$ ].

The observation of the subsequent decay of the hyperons emitted in (1) and (2) may furnish information on the spins. Consider the angle  $\theta$  between the line of flight of the hyperon and the direction of emission (in the center of mass system of the hyperon) of its decay pion. Let us call  $J$  the value of the spin of the bound  $(K^-, p)$  system when the absorption of the  $K^-$  occurs,  $s$  the spin of the emitted hyperon,  $l_1$  the relative orbital angular momentum between the emitted  $\Sigma^+$  and  $\pi^0$  ( $l_1$  can take different values), and  $l_2$  the unique value permitted for the relative orbital angular momentum between the final nucleon and pion when the hyperon disintegrates. The distribution for the angles  $\theta$ ,  $f(\cos \theta)$ , has the same formal expression as that obtained in the case of the cascade decay of the  $\Xi^-$ <sup>(3)</sup>.

$$(6) \quad f(\cos \theta) = \sum c_{l_1} c_{l_1'} F_\nu(l_1 l_1' J s) b_\nu(l_1 l_1') \cdot \\ \cdot F_\nu(l_2 l_2 \frac{1}{2} s) b_\nu(l_2 l_2) P_\nu(\cos \theta),$$

where  $F_\nu$  are defined according to FERENTZ and ROSENZWEIG<sup>(4)</sup>, and  $b_\nu$  are particle parameters

$$(6') \quad b_\nu(l_1 l_1') = 2 \frac{[l_1(l_1 + 1)l_1'(l_1' + 1)]^{\frac{1}{2}}}{\nu(\nu + 1) - l_1(l_1 + 1) - l_1'(l_1' + 1)}.$$

The  $c_{l_1}$  are unknown real coefficients proportional to the reduced matrix elements. If the K-mesons of (1) and (2) have spin zero and if absorption occurs from  $s$  states, then  $J = \frac{1}{2}$ , and only one value of  $l_1$  is permitted. The angular correlation in this case only depends on the hyperon spin. This case has

<sup>(3)</sup> R. GATTO: *Proc. of Pisa Conference*, 1955.

<sup>(2)</sup> T. D. LEE and J. ORAER: *Phys. Rev.*, **100**, 932 (1955).

<sup>(4)</sup> M. FERENTZ and N. ROSENZWEIG: *ANL*-5234.

been discussed independently by TREIMAN<sup>(5)</sup>. If the absorption occurs from an higher orbit, then, for a fixed  $J$ , more values of  $l_1$  are allowed. In such cases the correlation depends on some unknown parameters which should be determined by the experiment. Anyhow it must be remarked that the state of polarization of the emitted hyperons is described by some density matrix the coefficients of which are fixed numbers which depend on the physical mechanism of the reaction, but, differently from other cases, as for instance the case of associated production etc., they have not to depend on energy, on the angle of emission, and so on. From a well known general theorem the maximum power of  $\cos \theta$  (only even powers are permitted) contained in the angular correlation is less than  $2s - 1$ . Therefore, for instance, if  $s = \frac{3}{2}$ , the correlation has the form  $1 + a \cos^2 \theta$  (if the absorption occurs from  $s$  states one finds, from (6):  $a = 3$ ).

In the case of  $\pi^-$  capture in hydrogen the absorption is known to occur predominantly from  $s$  states. It was shown by BRUECKNER, SERBER and WATSON<sup>(6)</sup> that for deuterium the  $\gamma$ -transition probability from the  $2p$  to the  $1s$  state  $w_\gamma(2p \rightarrow 1s)$ , is of the order of 20 times larger than the absorption probability from the  $2p$  state. The absorption of  $\pi^-$  in hydrogen occurs through the reactions  $\pi^- + p \rightarrow n + \pi^0$  (for which the energy release is very small) and  $\pi^- + p \rightarrow n + \gamma$  with about equal probabilities. The ratio between the statistical weight of (1'), multiplied by a factor of 6 to account approximately for (1''), (1'''), and (2) in the various isotopic spin states, and the statistical weight of  $\pi^- + p \rightarrow n + \pi^0$ , multiplied by a factor of 2 to account approximately for the other possible reaction  $\pi^- + p \rightarrow$

$n + \gamma$ , is  $\sim 47$ . Moreover for a  $p$ -state the probability of finding the meson in a given small region around the proton increases as  $\mu^5$ , where  $\mu$  is the reduced mass of the meson-proton system—on the other hand the radius of the interaction region may be rather smaller in the case of K-mesons. The  $2p \rightarrow 1s$   $\gamma$ -transition probability is only proportional to the reduced mass, and can be calculated to be for K-mesons  $\sim 4.7 \cdot 10^{11} \text{ s}^{-1}$ . One can alternatively try to estimate the  $2p$  absorption probability by comparing with the cross-sections for K-meson absorption in flight. Such cross-sections are known to be geometric as to their order of magnitude<sup>(7)</sup>. Assuming that the ratio between the  $2p$  absorption rate and the absorption rate from the continuum is approximately given by the ratio between the square of the gradient of the bound wavefunction and that of the free wavefunction<sup>(6)</sup>, we obtain an estimate  $\sim \alpha \cdot 2 \cdot 10^{11} \text{ s}^{-1}$  for the  $2p$  absorption rate, taking the cross-section for absorption from the continuum equal to  $\alpha(1/m_\pi)^2$ , where  $\alpha$  is presumably of the order of unity. Therefore the direct  $2p$  absorption could compete with the  $2p \rightarrow 1s$  transition probability and even be preferred. The measurement of the angular correlation itself or direct measurement of the optical  $\gamma$ -ray spectrum may resolve this point.

\* \* \*

I would like to thank Prof. E. AMALDI for stimulating discussions on the subject. I would also like to thank Dr. S. B. TREIMAN for the useful correspondence.

<sup>(6)</sup> K. A. BRUECKNER, R. SERBER and K. WATSON: *Phys. Rev.*, **81**, 575 (1951).

<sup>(7)</sup> J. HORNOSTEL and E. O. SALANT: *Phys. Rev.* (in the press).

<sup>(5)</sup> S. B. TREIMAN: *Phys. Rev.* (in the press).

# Note on the Technique of Experiments on Air Shower Time Variations.

K. SITTE

*Department of Physics, Technion, Israel Institute of Technology - Haifa, Israel*

(ricevuto il 25 Febbraio 1956)

It has long been known that the variation with sidereal time of the frequency of air showers may well provide the most decisive clue in the decision between the rival theories of the origin of cosmic radiation. In spite of their importance, however, experiments hitherto performed have remained singularly inconclusive, and their results range all the way between large amplitudes of daily or semi-diurnal variations (FARLEY and STOREY <sup>(1)</sup>, CRANSHAW and GALBRAITH <sup>(2)</sup>) to barely observable effects (HODSON <sup>(3)</sup>, DAUDIN and DAUDIN <sup>(4)</sup>) and complete absence of significant variations (CITRON <sup>(5)</sup>). Clearly, one has to look for technical reasons for this discrepancy. In the following, two fallacies in the customary thinking about experiments on the time variation of air showers will be discussed.

It must be kept in mind, first of all, that the expected effect—if it exists—will

be appreciable only for the highest primary energies, while there is certainly no anisotropy at the common air shower energies of, say,  $10^{14}$  eV. It follows from this that an ordinary double or triple coincidence arrangement is not an effective apparatus to study this question: in any such arrangement, a very large fraction of the recorded events will always be due to showers of comparatively low density; that is, to primaries in the time-independent energy range. To see this, one has only to remember that the relative contributions to the counting rate, of showers of density  $\Delta$  in an arrangement of counter area  $S$ , is proportional to  $(1 - \exp[-\Delta S])^n$  for  $n$ -fold coincidences: and for  $\Delta \rightarrow 0$ , this expression takes the approximate form  $\Delta^{n-1}$ . Contrary to often-heard arguments, this weakness is not remedied by spreading the two or three counters over a wider area. By thus accepting showers incident, on the average, at a larger distance, this procedure does raise the average energy of the showers recorded with counters of a given size; but it does *not* change the fraction of showers below average energy that the equipment registers.

Clearly, the simplest way to exclude those—relatively—low-density showers, is to use a larger number of counters in coincidence. As an illustration, the relative contributions as a function of shower

<sup>(1)</sup> F. J. M. FARLEY and J. R. STOREY: *Proc. Phys. Soc.*, A **67**, 996 (1954).

<sup>(2)</sup> T. E. CRANSHAW and W. GALBRAITH: *Phil. Mag.*, **45**, 1109 (1954); T. E. CRANSHAW: *International Conference on Cosmic Radiation*, Guanajuato (1955).

<sup>(3)</sup> A. L. HODSON: *Proc. Phys. Soc.*, A **64**, 106 (1951).

<sup>(4)</sup> A. DAUDIN and J. DAUDIN: *Compt. Rend.*, **234**, 1551 (1952); A. CACHON: *International Conference on Cosmic Radiation*, Guanajuato (1955).

<sup>(5)</sup> A. CITRON: *Zeits. f. Naturf.*, **7**, 712 (1952).



density for a 3-, 6- and 9-fold coincidence are represented, with arbitrary ordinates, in Fig. 1. The calculations were, of course, not done for equal counter area  $S$

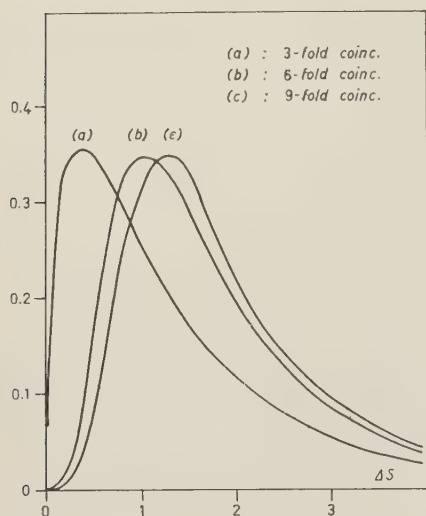


Fig. 1. — Relative contribution to 3-fold, 6-fold and 9-fold coincidences, as a function of the shower density ( $\Delta S$ ). The abscissae are calibrated to give for all three arrangements the same average density of the recorded showers: the values shown refer to the triple coincidences)

in the three cases; instead, the areas were chosen so as to give the same *average* density recorded in all three arrangements. This is more in accordance with the principles of proper design of the equipment. The advantage of a larger  $n$  is evident, and it should be remembered that this simple coincidence method is by no means always the best solution. In fact, frequently a coincidence-anti-coincidence arrangement—providing sharper energy resolution—will do much better.

As a practical example, records from a series of air shower experiments <sup>(6)</sup>

carried out between 1950 and 1953 at Echo Lake and Mt. Evans, Colorado, were re-examined. None of these experiments was designed for a study of time variations, but since time records were kept, an analysis was possible. A certain difficulty arose from the fact that only for part of the runs exact pressure records were available, and since all the observations were made in the summer, pressure corrections are necessary. Where more precise data were missing, reduction was made according to the *average* daily pressure variation. In all the experiments, extension hodoscope trays permitted a rough determination of the shower density, and a classification of the events as to their primary energy. Wherever possible, the three energy groups of the Kasnitz-Sitte experiment were used as a standard; «A-showers» of approximately  $10^{14}$  eV average energy, «B-showers» with  $10^{15}$  eV, and «C-showers» with  $10^{16}$  eV, each with a half width of acceptance corresponding to a factor 10 in primary energies. Altogether, about 13000 showers could thus be analyzed; about 5650 belonged to group A, 5050 to group B and 2250 to group C. The result of the analysis is the following: for showers of  $10^{14}$  eV: no detectable time variation;

for showers of  $10^{15}$  eV: diurnal variation with an amplitude of  $< 2\%$  and a maximum at about 19 h LST, semi-diurnal variation with an amplitude of  $3.1\%$  and maxima at 5 h and 17 h LST;

for showers of  $10^{16}$  eV: diurnal variation with an amplitude of  $< 3\%$  and a maximum at about 20 h LST, semi-diurnal variation with an amplitude of  $4.1\%$  and maxima at 6 h and 18 h LST.

However, owing to the poor statistics

<sup>(6)</sup> K. SITTE: *Phys. Rev.*, **78**, 721 (1950); **87**, 351 (1952); H. L. KASNITZ and K. SITTE;

*Phys. Rev.*, **94**, 977 (1954); K. SITTE, D. L. STIERWALT and I. L. KOFSKY: *Phys. Rev.*, **94**, 988 (1954); and hitherto unpublished results.



it is also found that for *B*-showers the probability for the observed semi-diurnal variation to be due to a chance distribution is about 55%, while for *C*-showers it is about 30%. For the diurnal variation, the corresponding figures are in both cases  $\sim 67\%$ . Even so, and although the experiments were not planned for this study, the results are of some interest, and are in contrast to the results of an analysis of the undivided total of 13 000 showers which gives no significant daily or semidiurnal variation.

The second fallacy to be pointed out, lies in the assumption that for experiments of this kind, it is always of great value to go to as high altitude as possible. This is not necessarily true. As far as the total rates are concerned, one does, of course, gain by moving to high mountains—at least, as long as he does not pass through the cascade maximum of the most energetic showers, and that is scarcely a serious limitation. But one

also loses in resolution; that is again, the arrangement will accept an increasingly larger fraction of low-energy events which « dilute » the observed effect and thus outweigh the gain in statistical accuracy. A glimpse at the numbers —vs.—altitude curves of air showers will prove this point: the ratio of the densities of, say, a  $10^{15}$  eV and a  $10^{16}$  eV shower is more favourable for discrimination at, say, 3 000 m than at 5 000 m. But for this effect, no answer can be given in general terms. Frequently, and depending on the energy range in which one wishes to work, it may well be worth while to set up the experiment at very high altitude. But it should be made a more general practice then it appears to have been up to now, to determine carefully the optimum operating conditions for a given experiment on the time variation of air showers—including the optimum altitude. The benefit will prove well worth the time spent.

## Dependence of Alpha Disintegration Energy on Proton and Neutron Numbers.

Y. PAL VARSHNI

*Department of Physics, Allahabad University - Allahabad. India*

(ricevuto il 28 Febbraio 1956)

The variation of  $\alpha$  disintegration energy  $E_\alpha$  (or  $\alpha$ -particle energy  $E_\alpha$ ) with mass number  $A$ , atomic number  $Z$  and neutron number  $N$  ( $= A - Z$ ) has been extensively studied [PERLMAN, GHIORSO and SEABORG <sup>(1)</sup> and the references given therein, FEATHER <sup>(2)</sup>, CHAUDHURY <sup>(3)</sup>, SENGUPTA <sup>(4)</sup>, etc.].

It is possible to calculate the  $\alpha$  disintegration energy from the semi-empirical mass formula. Such calculations have been carried out by PRYCE <sup>(5)</sup>, DAS <sup>(6)</sup> and DUBE and SINGH <sup>(7)</sup>. Usually the calculated values differ much from the observed values. PRYCE <sup>(5)</sup> has shown that the differences between the observed and calculated values vary smoothly with the mass number  $A$ . Recently ROGER <sup>(8)</sup>

has proposed a formula connecting the  $\alpha$  disintegration energy with  $N$  and  $Z$ .

The present note suggests a simple empirical relation for  $E_\alpha$  in terms of  $N$  and  $Z$  for nuclei having  $N > 132$ . The formula is

$$E_\alpha = .4Z - 1.795(N - 132)^{\frac{1}{2}} - 26.208.$$

The observed and calculated values have been tabulated in Table I. Observed values have been taken from SENGUPTA <sup>(4)</sup>. All values are in MeV.

TABLE I.

$Z$	$N$	$E_\alpha$ obs. MeV	$E_\alpha$ calc. MeV	Percentage error
85	133	6.84	6.00	— 12.3
86	133	6.68	6.40	— 4.2
	134	6.39	5.65	— 11.5
87	133	6.81	6.80	— .1
	134	6.42	6.05	— 5.8
88	133	6.83	7.20	+ 5.4
	134	6.62	6.45	— 2.6
	135	5.82	5.88	+ 1.0
	136	5.78	5.40	— 6.6
	138	4.88	4.60	— 5.7

<sup>(1)</sup> I. PERLMAN, A. GHIORSO and G. T. SEABORG: *Phys. Rev.*, **77**, 26 (1950).

<sup>(2)</sup> N. FEATHER: *Nuclear Stability Rules* (Cambridge, 1952).

<sup>(3)</sup> M. L. CHAUDHURY: *Phys. Rev.*, **88**, 137 (1952); *Zeits. f. Phys.*, **133**, 561 (1952).

<sup>(4)</sup> S. SENGUPTA: *Phys. Rev.*, **87**, 1136 (1952); *Zeits. f. Phys.*, **134**, 413 (1953).

<sup>(5)</sup> M. H. L. PRYCE: *Proc. Phys. Soc.*, **63**, 692 (1950).

<sup>(6)</sup> R. K. DAS: *Ind. Journ. Phys.*, **24**, 525 (1950).

<sup>(7)</sup> G. P. DUBE and L. S. SINGH: *Curr. Sci.*, **23**, 84 (1954); *Ind. Journ. Phys.*, **28**, 177 (1954).

<sup>(8)</sup> F. ROGER: *Compt. Rend. Acad. Sci.*, **240**, 858 (1955).

TABLE I (continued)

Z	N	$E_a$ obs. MeV	$E_a$ calc. MeV	Percentage error
89	133	7.08	7.60	+ 7.3
	134	6.76	6.85	+ 1.3
	135	6.28	6.28	— 0
	136	5.90	5.80	— 1.7
	138	5.04	5.00	— .8
	139	4.58	4.64	+ 1.3
90	134	7.33	7.25	— 1.1
	135	6.68	6.68	0
	136	6.41	6.20	— 3.3
	137	5.97	5.78	— 3.2
	138	5.52	5.40	— 2.2
	139	5.14	5.04	— 1.9
	140	4.76	4.72	— .8
	142	4.09	4.12	+ .7
91	135	6.93	7.08	+ 2.2
	136	6.57	6.60	+ .4
	137	6.20	6.18	— .3
	138	5.79	5.80	+ .2
	139	5.50	5.44	— 1.1
	140	5.09	5.12	+ .6
92	136	6.83	7.00	+ 2.5
	137	6.53	6.58	+ .8
	138	5.96	6.20	+ 4.0
	139	5.6	5.84	+ 4.3
	140	5.4	5.52	+ 2.2
	142	4.84	4.92	+ 1.6
	144	4.58	4.38	— 4.4
	146	4.30	3.88	— 9.8

TABLE I (continued)

Z	N	$E_a$ obs. MeV	$E_a$ calc. MeV	Percentage error
93	138	6.31	6.60	+ 4.6
	140	5.65	5.92	+ 4.8
	142	5.15	5.32	+ 3.3
	144	4.85	4.78	— 1.4
94	138	6.72	7.00	+ 4.2
	140	6.3	6.32	+ .3
	142	5.85	5.72	— 2.2
	144	5.6	5.18	— 7.5
	146	5.2	4.68	— 10.0
95	144	5.87	5.58	— 4.9
	146	5.58	5.08	— 8.9
96	142	6.6	6.52	— 1.2
	144	6.37	5.98	— 6.1
	146	6.18	5.48	— 11.1

The average percentage error is  $\pm 3.6$ , which is quite satisfactory considering that the variation of  $E_a$  with  $N$  and  $Z$  is often not very regular.

\* \* \*

The author is thankful to Professor K. BANERJEE for his kind interest in the work.

## The Flux of the Helium Component of the Primary Cosmic Radiation at Geomagnetic Latitude $41^{\circ}$ N.

A. DE MARCO and A. MILONE

*Istituto di Fisica dell'Università - Genova*

*Istituto Nazionale di Fisica Nucleare - Sezione Aggregata di Genova*

M. REINHARZ

*Centro Studi di Geologia Nucleare dell'Università - Pisa*

(ricevuto il 14 Marzo 1956)

The intensity of the primary helium component of the cosmic radiation has been determined several times and at various latitudes (<sup>1-15</sup>). All but three

determinations have been made using counter or chamber techniques. Determinations using the photographic plate were made by BRADT and PETERS, PETERS, and WADDINGTON.

BRADT and PETERS (<sup>3</sup>) determined the  $\alpha$  flux at  $30^{\circ}$  and  $51^{\circ}$  N geomagnetic latitude by selecting all particles in a certain grain density interval and by subtracting from these the background due to the secondary particles; recently (<sup>11</sup>) PETERS has published a second determination at  $30^{\circ}$  N using combined measurements of ionization and range. WADDINGTON (<sup>12</sup>) who determined the  $\alpha$  flux at  $55^{\circ}$  N, used the ionization-scattering method.

In view of this scarcity of data from nuclear emulsions, and having at our disposal a group of well processed plates from the Sardinian expedition of 1953 (\*), it seemed not unprofitable to try to determine the  $\alpha$  flux at the latitude  $41^{\circ}$  N of the flight.

(<sup>1</sup>) F. FREIER, E. J. LOFGREN, E. P. NEY and F. OPPENHEIMER: *Phys. Rev.*, **74**, 1818 (1948).

(<sup>2</sup>) M. A. POMERANTZ and F. L. HEREFORD: *Phys. Rev.*, **76**, 997 (1949).

(<sup>3</sup>) H. L. BRADT and B. PETERS: *Phys. Rev.*, **77**, 54 (1950).

(<sup>4</sup>) F. S. SINGER: *Phys. Rev.*, **80**, 47 (1955).

(<sup>5</sup>) E. P. NEY and D. M. THON: *Phys. Rev.*, **81**, 1069 (1951).

(<sup>6</sup>) G. J. PERLOW, L. R. DAVIS, C. W. KISSINGER and J. D. SHIPMANN: *Phys. Rev.*, **88**, 321 (1952).

(<sup>7</sup>) L. R. DAVIS, H. M. CAULT and C. Y. JONSON: *Phys. Rev.*, **91**, 431 (1953).

(<sup>8</sup>) J. LINSLEY: *Phys. Rev.*, **93**, 899 (1954).

(<sup>9</sup>) M. A. POMERANTZ: *Phys. Rev.*, **95**, 1691 (1954).

(<sup>10</sup>) C. W. MCCLURE: *Phys. Rev.*, **96**, 1391 (1954).

(<sup>11</sup>) B. PETERS: *Proc. Ind. Acad. Sci.*, **40**, 6, 230 (1954).

(<sup>12</sup>) C. J. WADDINGTON: *Phil. Mag.*, **45**, 1312 (1954).

(<sup>13</sup>) N. HORWITZ: *Phys. Rev.*, **98**, 165 (1955).

(<sup>14</sup>) J. R. WINCLER and L. PETERSON: *Phys. Rev.*, **99**, 608 (1955).

(<sup>15</sup>) W. R. WEBBER and F. B. McDONALD: *Phys. Rev.*, **100**, 1460 (1955).

(\*) Glass-backed emulsions G5 600  $\mu$ m, flight no. 15, effective altitude 28  $\mu$ m, duration of flight 6<sup>h</sup>40<sup>m</sup>; see J. DAVIES and C. FRANZINETTI: *Suppl. Nuovo Cimento*, **12**, 480 (1954).

At the geomagnetic latitude of  $41^\circ$  N, the geomagnetic cut-off is 1.5 GeV/nucleon (\*). At and above this energy, the  $\alpha$  particles have an ionization very near the plateau for a particle of charge 2. For particles of charge 1, the plateau grain density in our plates was found to be  $24 \pm 0.5$  grains/100  $\mu$ m. The plateau for charge 2 was determined on 4 tracks of certified  $\alpha$  particles. The values obtained was  $85 \pm 1$  grains/100  $\mu$ m.

From a scanned area of 9.25 cm<sup>2</sup> a first selection was made of all tracks longer than 4 mm and with a grain density higher than 70 grains/100  $\mu$ m. This limit was chosen so as to be more than two standard deviations below the grain density of an  $\alpha$  particle at plateau. Of the 170 tracks chosen in this way, 4 were recognized as heavy nuclei and were rejected.

With our routine microscopes we were able to eliminate by rough scattering measurements the greater part of the mesons and protons among the remaining 166 tracks, their mean angle of scattering being greater than  $10^{-1}$  degrees/100  $\mu$ m. The scattering of the 74 tracks finally selected was measured with greater precision with the sagitta method using a Koristka MS2 microscope kindly put at our disposal by the Rome group.

The results of our sagitta measurements have been plotted in Fig. 1. As can be seen there is a distinct group of tracks having a small angle of scattering; these we assumed to consist of  $\alpha$  primaries. The bulk of these tracks have a mean angle of scattering about

twice the maximum expected at this latitude.

Although noise had been eliminated between cells of different length and the regular distortion by the method of third differences, it would seem that a source of spurious scattering remained. This may be of the type found by BISWAS *et al.* <sup>(16)</sup>, FAY <sup>(17)</sup> and LOHRMANN and TEUCHER <sup>(18)</sup>. The fact that the shorter tracks show in general a higher scattering tends to confirm this.

Taking this into account, we included in the group assumed to be primary, all tracks having a scattering angle smaller than  $5 \cdot 10^{-2}$  degrees/100  $\mu$ m.

These tracks had all a grain density around 85 grains/100  $\mu$ m.

Using the values for  $\lambda_{\text{air}} = 44$  g/cm<sup>2</sup>;  $\lambda_{\text{emulsion}} = 60$  g/cm<sup>2</sup>,  $\lambda_{\text{glass}} = 53$  g/cm<sup>2</sup> as given by WADDINGTON <sup>(12)</sup>, and taking only tracks having an incident angle smaller than  $60^\circ$ , we obtain:

$$I_x = 39 \pm 8.6 \text{ He/m}^2 \text{ s ster.}$$

A comparison with other determinations, made at the same geomagnetic latitude (G. I. PERLOW *et al.* <sup>(6)</sup>:  $I_\alpha = 110 \pm 20$  He/m<sup>2</sup> s ster; N. HORWITZ <sup>(13)</sup>:  $I_\alpha = 99 \pm 16$  He/m<sup>2</sup> s ster; WILLIAM *et al.* <sup>(15)</sup>:  $I_\alpha = 82 \pm 9$  He/m<sup>2</sup> s ster) shows that our value is decisively lower. Even including all the tracks with a scattering angle between 5 and  $10 \cdot 10^{-2}$  degrees/100  $\mu$ m, thus certainly including also tritons and deuterons, the intensity remains still low ( $I_\alpha = 52 \pm 9$  He/m<sup>2</sup> s ster). Such a low intensity cannot be explained by scanning loss, since the scanning was very slow, under immersion objective, and in a rescanning of a portion of the surface all the tracks and no more were found again. In addition, the fact that the number of tracks of length  $l$  is propor-

(\*) The geomagnetic latitude has been determined with the relation

$$\sin \lambda = \cos 78.5^\circ \cos (\Omega - 69^\circ) \cos A + \sin 78.5^\circ \sin A$$

using the centered dipole, where  $A$  and  $\Omega$  are the mean geographic latitude North ( $39^\circ 20'$ ) and the mean geographic longitude West ( $-7^\circ 26'$ ) respectively. The cut-off energy for our latitude has been taken from the curves of VALLARTA (M. S. VALLARTA: *Phys. Rev.*, **74**, 1837 (1948)) for vertical incidence.

<sup>(16)</sup> S. BISWAS, B. PETERS and RAMA: *Proc. Ind. Acad. Sci.*, **41**, 154 (1955).

<sup>(17)</sup> H. FAY: *Zeits. f. Naturf.*, **10**, 572 (1955).

<sup>(18)</sup> E. LOHRMANN and M. TEUCHER: *Nuovo Cimento*, **3**, 59 (1956).





Fig. 1. — Scattering distribution of all tracks on which sagitta scattering measurements were made (values larger than  $20 \cdot 10^{-3} \mu\text{m}$  have been emitted). The hatched part represents all tracks having lengths between 4 and 5 cm.

tional to  $1/l^2$  (Fig. 2) shows that there was no selective loss depending on the dip of the tracks.

We have also calculated the intensity for two intervals of the incident angle,  $0^\circ \div 20^\circ$  and  $20^\circ \div 60^\circ$ , for which we

found  $36 \pm 14$  and  $40 \pm 10$   $\text{He}/\text{m}^2 \text{ster}$  respectively.

FAY<sup>(17)</sup> who determined the primary flux for  $Z > 2$  with plates flown at the same expedition, also obtained a value much smaller than that obtained by others. The same effect obtained independently in two laboratories with plates from the same expedition but exposed in different flights, seems to exclude a possible explanation as eventual errors of flights registration.

A fuller account of the present work, including also a determination of the primary protonic flux, will be given later.

\*\*\*

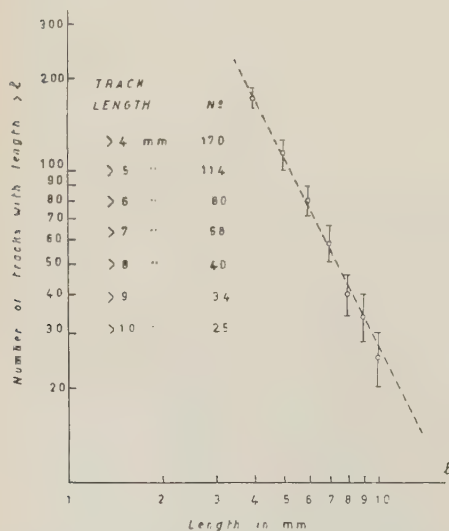


Fig. 2. — The experimental points indicate the number of tracks with length  $> l$  in function of  $l$ . The drawn line represents  $N_{>l} \propto 1/l^2$ .

We would like to thank the Rome group for their kind permission to use their Koristka MS2 Microscope for our measurements. We would also like to thank Prof. E. PANCINI for his interest in this work and Prof. G. OCCHIALINI for helpful discussions and criticism. We are indebted to Miss M. PUPPO for the very efficient and reliable scanning of our plates.

**Increase of Cosmic Ray Intensity  
Associated with the Solar Flare of February 23, 1956.**

F. BACHELET and A. M. CONFORTO

*Istituto di Fisica dell'Università - Roma  
Comitato Nazionale per l'Anno Geofisico Internazionale*

(ricevuto il 16 Marzo 1956)

An extraordinary increase in Cosmic Ray Intensity has been recorded on February 23, 1956, in Rome (s.l.;  $42.5^\circ$  N geom.) with an unshielded threefold counter telescope set.

The apparatus <sup>(1)</sup> consists of 12 counter telescopes altogether, 4 independent in each direction (Zenith,  $30^\circ$  North, and  $30^\circ$  South), with effective areas of  $15 \times 50 \text{ cm}^2$  each, and a distance of 29 cm between the extreme trays (openings of  $55^\circ$  in the North-South plane and  $120^\circ$  in the East-West plane, for the vertical telescopes, and  $45^\circ$  and  $112^\circ$  respectively for the inclined telescopes). The counts of each telescope are automatically registered at intervals of 15 minutes. The normal counting rate is approximately 47 000 counts per hour for the set of 4 vertical telescopes and 27 000 counts per hour for each of the two sets of inclined telescopes (North  $\sim$  South). The apparatus has been permanently running since October 1953, in the course of an investigation of the time variations of Cosmic Ray intensity.

The recorded increase of Cosmic Rays was presumably associated with an intense solar flare of importance 3, occurred in a very active sunspot region, and observed optically in Tokyo (Japan) and Kodaikanal (India): the observation in Tokyo started at 0334 U.T. and the flare lasted about 40 minutes. Also radio fadeouts and radiowave bursts have been observed. Moreover a worldwide geomagnetic storm occurred about 48 hours later (sudden commencement at 0306 U.T. February 25, 1956), the decrease in H amounting to  $\sim 250 \gamma$  in Gibilmanna (Sicily). Cosmic Ray increases have been registered almost simultaneously to the solar flare also in many other stations in Europe, America and Asia by neutron- as well as ionizing particle-recorders. This shows that the event is of a worldwide character and similar—although apparently much more intense—to four cosmic ray events observed in association with large solar flares during the past eleven year sunspot cycle <sup>(2)</sup>.

In Rome the increase of counting rates

<sup>(1)</sup> For more details see: F. BACHELET and A. M. CONFORTO: *Nuovo Cimento*, **12**, 923 (1954).

<sup>(2)</sup> H. ELLIOT: *Progress in Cosmic Ray Physics*, **1** (Amsterdam, 1952), Chap. VIII.

for all the 12 telescopes started between 0330 and 0345 U.T. (0430 and 0445 local time), maximum intensity being reached between 0345 and 0400 U.T. Then the intensity recovered towards its normal value over the next two hours. The 15 mi-

notes rates agree very well within the statistical errors in each telescope set, while definitely significant is the difference between the percentage increase of the vertical telescopes and the inclined ones.

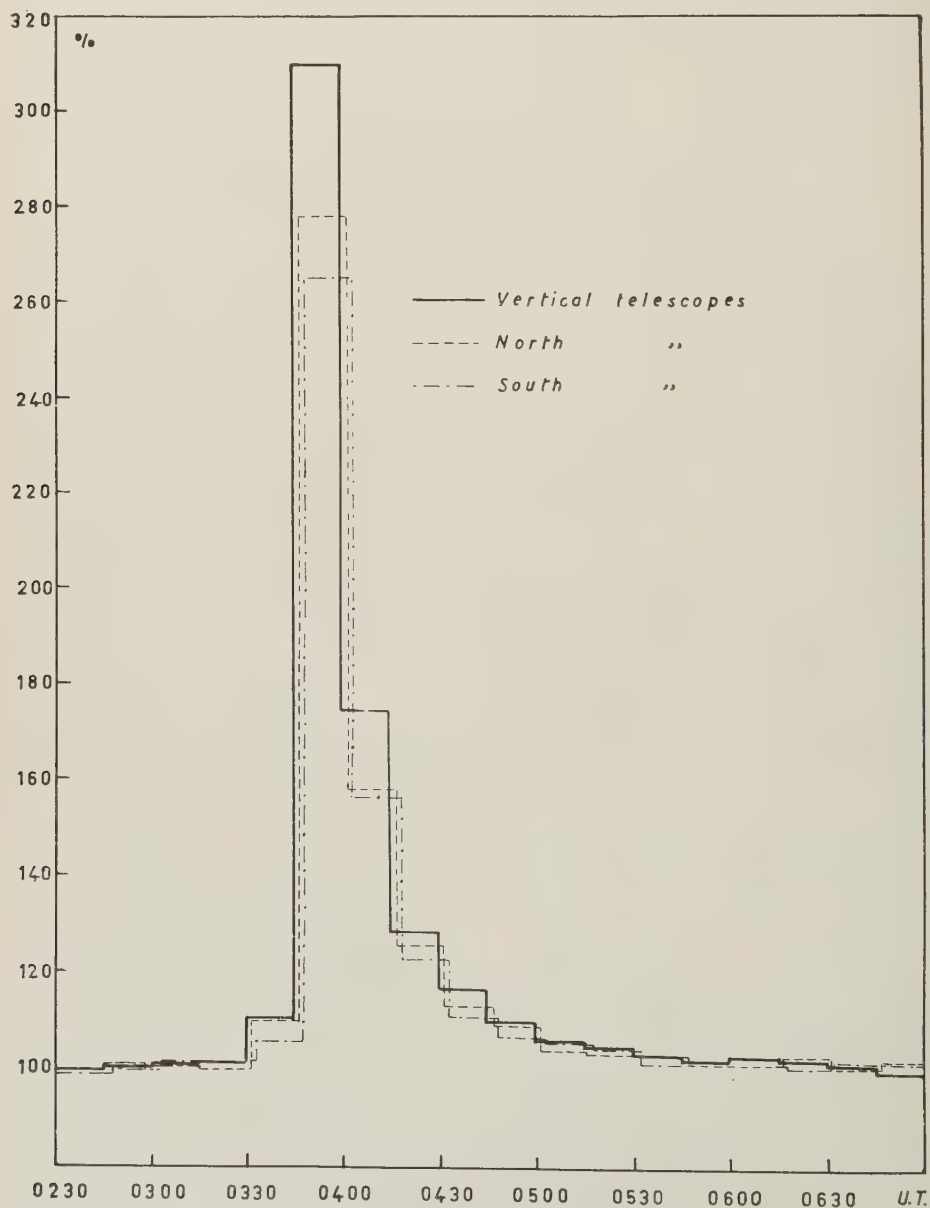


Fig. 1. — Cosmic ray intensity recorded in Rome during the solar flare of February 23, 1956.  
Statistical error: vertical telescopes 0.9 % inclined telescopes 1.2 %.

In Fig. 1 the percentage values of intensity in the three directions with respect to the two hours preceding the event are shown between 0230 and 0700 U.T. of February 23, 1956. The data are not corrected for the atmospheric effects since the barometric effect can be estimated as negligible during these few hours ( $\Delta B = 0.9 \text{ mm}_{\text{Hg}}$ ) and no upper atmosphere data at that time are available. The regression atmospheric coefficients of the apparatus have been determined <sup>(3)</sup> to be.  $\Gamma_B = -2.47\%/\text{cm}_{\text{Hg}}$ ;  $\Gamma_H = -3.25\%/\text{km}$ ,  $\Gamma_T = +0.09\%/^{\circ}\text{C}$  ( $B$  = barometric pressure,  $H$  = height of 100 mb level,  $T$  = temperature of 100 mb level).

From a comparison of the magnitude of the increase recorded by the vertical and the inclined telescopes, an absorption coefficient much larger than that obtained from the normal rates would be deduced. This would be well in agreement with the fact already pointed out <sup>(4,5)</sup>, that the primary particles responsible for the increase associated

with solar flares belong to a low energy range.

The data of our apparatus during the days following the flare, corrected for barometric pressure, give only an indication of a small intensity decrease associated with the magnetic storm of February 25, 1956. Also an indication of a small decrease is shown in the days preceding the flare, to be related to the magnetic storm ( $\sim 90 \gamma$  in  $H$  in Gilmanna) of February 19, 1956 and to the intense solar activity of that period.

As soon as more and more precise data are available, both of the cosmic ray events and of astronomical and geomagnetic observations, a more comprehensive discussion will be possible.

\* \* \*

We are deeply indebted to Dr. F. MOLINA of the Istituto Nazionale di Geofisica for geomagnetic data, and to Dr. K. O. KIEPENHEUER of the Fraunhofer Institut of Freiburg i.B. and Dr. W. O. ROBERTS of the High Altitude Observatory of the University of Colorado for astronomical information.

<sup>(3)</sup> Paper to be published.

<sup>(4)</sup> S. E. FORBUSH, T. B. STINCHCOMB and M. SCHEIN: *Phys. Rev.*, **79**, 501 (1950).

<sup>(5)</sup> J. FIROR: *Phys. Rev.*, **94**, 1017 (1954).

## The Conversion Length of High Energy Photons.

K. PINKAU

*H. H. Wills Physical Laboratory - University of Bristol*

(ricevuto il 22 Marzo 1956)

Recently, KOSHIBA and KAPLON <sup>(1)</sup> have raised some doubts about the validity of cross-sections derived from Quantum Electrodynamics in energy regions above  $10^3$  MeV. These authors report a cross-section for trident production higher than predicted by BHABHA <sup>(2)</sup> in the theoretical framework of the Bethe-Heitler theory. If conventional Quantum Electrodynamics is seriously in error in this energy region, one might similarly expect a shortening of the conversion length for  $\gamma$ -rays above  $10^3 \div 10^4$  MeV. To give agreement with the higher trident cross-section, the conversion length would have to be reduced by a factor of about 1.5 as was mentioned by KOSHIBA and KAPLON.

In order to investigate this possibility, the conversion length has been determined from measurements in a number of stacks of Ilford G 5 stripped emulsions.

If  $x_i$  is the distance along the photon path between the edge of the emulsions and the point of creation of a high energy electron pair which gives rise to an

electromagnetic cascade, then a method of maximum likelihood <sup>(3)</sup> may be applied to the measured  $x_i$  values to obtain the mean free path for conversion.

The conversion length,  $\lambda$ , expected theoretically is defined by the equation

$$\lambda \sim \frac{9}{7} X_0,$$

where  $X_0$  is the radiation length, given by the formula

$$\frac{1}{X_0} = 4\alpha \frac{N}{A} Z^2 r_0^2 \log 183 Z^{-\frac{1}{3}},$$

in the notation of ROSSI and GREISEN <sup>(4)</sup>.

For average values  $A = 28$  and  $Z = 12.5$  in Ilford G 5 emulsion of about 60% relative humidity one obtains a value of  $\lambda = 3.75$  cm. Variations up to about 5% from this value may occur with variation of the composition and humidity of the emulsion.

24 high energy electromagnetic cascades, each initiated by a single photon, have been found in 5 stacks of stripped

<sup>(1)</sup> M. KOSHIBA and M. F. KAPLON: *Phys. Rev.*, **100**, 327 (1955).

<sup>(2)</sup> H. BHABHA: *Proc. Roy. Soc., A* **152**, 559 (1935).

<sup>(3)</sup> M. S. BARTLETT: *Phil. Mag.*, **44**, 249 (1953).

<sup>(4)</sup> B. ROSSI and K. GREISEN: *Rev. Mod. Phys.*, **13**, 240 (1941).



emulsions [for details see BRISBOUT *et al.* (5)]. It was assumed that a given shower was created by a single photon, when the second pair appeared late enough to be explained by a process of radiation from the first pair, followed by conversion, and had no significant lateral displacement. In the most likely case of multiple photon origin, namely the decay of a  $\pi^0$ , the mean opening angle of the two  $\gamma$ -rays will be about 200 times larger than that of the first electron pair (assuming equipartition of energy).

Although the probability that the cascades are initiated by single photons is very great, it should be remarked here that higher photon multiplicities would give rise to smaller values of  $x_i$ . Thus the obtained conversion length is a lower limit if such alternative initiating processes have actually occurred.

The numbers of electrons present at a convenient distance between 1 and 2 radiation lengths from the origin (point of creation of the first pair) and parallel to the shower core have been counted. In comparison with previous results (6) this number has been taken as a rough estimate of the numbers of electrons above 100 MeV present at the particular distance from the origin, where the errors of losses of tracks (through high angular divergence or large lateral displacement from the core) and the false inclusion of particles with energy below 100 MeV may partly cancel each other. The minimum number of tracks at 1.3 radiation lengths was 7, so all photons included will probably have an energy above  $10^4$  MeV.

The data available have been divided into two groups, 12 cascades with a primary photon energy between  $10^4$  and  $2 \cdot 10^5$  MeV (called later the group of «low energy»), and 12 showers with

a photon energy exceeding  $2 \cdot 10^5$  MeV (called the «high energy» group).

For the calculation of  $\lambda$ , formula (2) of ref. (3) has been used in the form

$$(1) \quad \lambda = \frac{1}{n} \sum_{i=1}^n \left( x_i + \frac{y_i}{\exp[y_i/\lambda] - 1} \right);$$

$x_i < y_i$ .

Here we use the following notations:

—  $x_i$  is the conversion distance of the photon, measured as distance between emulsion edge and point of conversion along the photon path (given by the direction of the induced shower), and diminished by 10%, since the photon travels for about 1/10-th of its way in the air gap between the emulsion sheets.

—  $y_i$  is the distance of possible detection. Only cascades with more than about  $10 \div 20$  particles and not too diffuse will have a high probability of being detected during scanning. As a safety limit it was assumed that no photon converting within 5 cm from the scanning line in the stack would give rise to a sufficient number of secondaries to be detected. Thus  $y_i$  is taken as distance between emulsion edge and scanning line minus 5 cm along the photon path.

Formula (1) can be used only if all photons have been created outside the stack. It might be thought that there is a certain possibility for some of the photons to be locally produced, i.e. in high energy nuclear interactions occurring within the stack. These photons could convert at large distances from the emulsion edge, leading to an overestimation of the true conversion length.

However, all the observed photons which converted at more than 2.5 cm from the emulsion edge (2.5 cm would represent a conversion length of 3.75 cm reduced by a factor of 1.5 [KOSHIBA and KAPLON (1)]) had energies which were probably of the order of  $10^5$  MeV or more, and no associated shower tracks have been observed. On the other hand,

(5) F. A. BRISBOUT, C. DAHANAYAKE, A. ENGLER, Y. FUJIMOTO and D. H. PERKINS: to be published in *Phil. Mag.* (1956).

(6) K. PINKAU: to be published in *Nuovo Cimento* (1956).

it would appear very unlikely that nuclear interactions of this high energy should give rise to  $\gamma$ -rays either indirectly (from  $\pi^0$ ) or directly (perhaps from some as yet undetected other process) and yet be of such a low multiplicity that no shower tracks would be observed in the neighbourhood of the photon. It should be noted here that events such as these would not be generally detected even if a search for them were made along the path of the photon.

The decay of incoming unstable particles, which is relatively unimportant in the stack, will either produce recognizable events near the initiating  $\gamma$ -ray, or produce discrete cascades.

Furthermore, the expected distribution of the conversion distance  $x_i$  from the edge of the stack for locally produced  $\gamma$ -rays is nearly flat at distances larger than 1 radiation length inside the stack, because the mean free path for nuclear interaction is much larger than the conversion length. The stacks used provided a detection length  $y_i$  of the order of  $20 \div 30$  cm. Thus, if a considerable contamination of locally produced photons existed, many cascade origins would also be at distances up to  $20 \div 30$  cm. In fact, no origin has been found further than 12 cm away from the emulsion edge.

It is believed therefore that locally produced photons exist in such small numbers amongst the sample considered that they can have no appreciable effect on the results.

The values of maximum likelihood for  $\lambda$  are presented in the table and may be compared with the theoretical conversion length of  $\lambda = 3.75$  cm. The error given is one standard deviation.

low energy	high energy	all energies
$4.4^{+1.6}_{-1.0}$ cm	$4.2^{+1.8}_{-1.0}$ cm	$4.3^{+1.1}_{-0.8}$ cm

The results from the table seem to indicate fairly good agreement with the theoretical value. A shortening of the conversion length by a factor of 1.5 as mentioned by KOSHIBA and KAPLON seems unlikely from the given results.

\* \* \*

The author is indebted to Professor C. F. POWELL for the facilities of this laboratory, and to Professor E. BAGGE, the Rotary-Club Hamburg and the Studienstiftung des deutschen Volkes for a scholarship.

He wants to thank Dr. D. H. PERKINS for suggesting this experiment.

## Probable Evidence for $Y_0$ -Events.

C. CASTAGNOLI, C. FRANZINETTI and A. MANFREDINI

*Istituto di Fisica dell'Università - Roma*

*Istituto Nazionale di Fisica Nucleare - Sezione di Roma*

(ricevuto il 23 Marzo 1956)

In a research on  $Y$ -particles reported in a previous paper <sup>(1)</sup>, same indication was obtained of the existence of  $Y_0$ -particles (i.e.  $Y$ -particles ending in the emulsion without decaying nor producing a visible disintegration).

A systematic search for  $Y_0$ -events was then started in this laboratory. As a result, two events have been observed which are most probably due to interactions of negative hyperons with matter leading to the emission of no ionizing particle.

In one of the parent stars a  $K$ -meson is also produced.

The emulsions in which these two events have been found, were exposed at an altitude of  $\sim 27$  km during the Sardinian Expedition 1953.

### 1. - Experimental method.

Masses of a large number of particles in nuclear disintegrations have been measured. The tracks have been selected according to the following criteria:

1) they appeared to be due to particles of protonic mass or heavier;

2) their end was definitely associated with a « blob » or a slow electron;

3) their angle of dip, with respect to the plan of the emulsion, was smaller than  $12^\circ$  and they had a range longer than 1 cm.

Mass measurements were carried on measuring the average gap length  $\bar{x}$  as a function of the residual range. As it was shown by CASTAGNOLI *et al.* <sup>(2)</sup> the average gap length  $\bar{x}$  is the most convenient parameter to use on particles of reduced residual range  $r = R/M$  lying in the interval between 0 and 18.7 mm/ $m_p$  of emulsion ( $m_p$  being the protonic mass).

A number of measurements of  $\bar{x}$  (we shall denote them by the suffix  $i$ ) have been made at different positions  $R_i$ . The corresponding value of  $r_i$  was then deduced from a calibration graph and a value of  $M$  deduced from the relation  $M_i = R_i/r_i$ . The distribution of the  $M_i$  plotted on a logarithmic scale should result nearly symmetric with respect to

<sup>(1)</sup> C. CASTAGNOLI, G. CORTINI and A. MANFREDINI: *Nuovo Cimento*, **2**, 565 (1955).

<sup>(2)</sup> C. CASTAGNOLI, G. CORTINI and A. MANFREDINI: *Nuovo Cimento*, **2**, 301 (1955).

its average value which can be easily calculated.

Alternatively, from the same set of data, one could estimate the mass from the ratio  $(\bar{x}_p)_i/\bar{x}_i$  where  $\bar{x}_i$  is the average gap length as measured on a track at a position  $R_i$  from the end of its range and  $(\bar{x}_p)_i$  is the expected value of the same parameter for protons of the same residual range. The mass is then obtained from the relation

$$M = M_p[(\bar{x}_p)_i/\bar{x}_i]^{1.88}.$$

The results shown in Fig. 1 and indicated

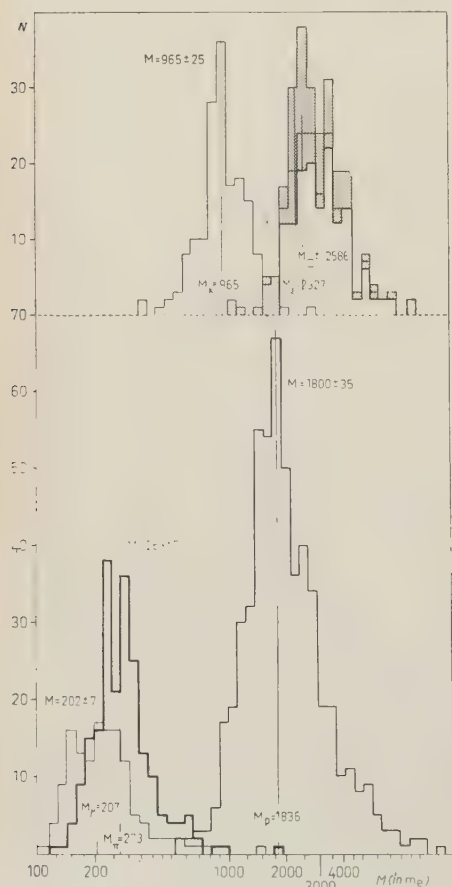


Fig. 1. - Results of mass measurements performed on the two tracks considered here (shaded area), together with a number of measurements on  $\mu$ 's,  $\pi$ 's, K's, protons and Y's, the identity of which could be established independently.

below as  $m_{\text{gap}}$  have been obtained using this method.

Scattering and range measurements have been performed using the constant sagitta method.

## 2. - Details on the observed $Y_0$ -particles.

*Event A.* - From a star of type  $36+16p$  two tracks are emitted which have been interpreted as an Y-particle and a K-meson respectively.

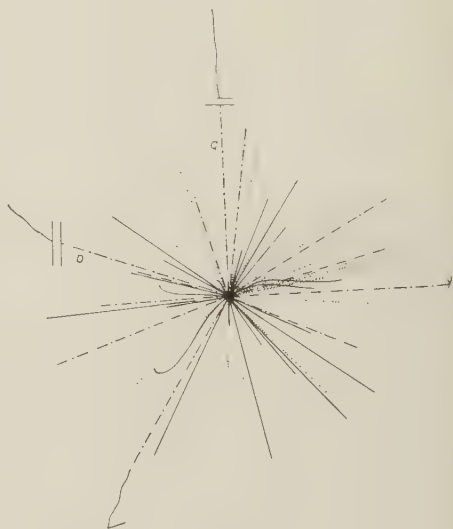


Fig. 2.

The first one (track *b* in Fig. 2) is  $7400 \mu$  long and its end is associated with a short blob. Scattering-range and gap-range methods yielded for the mass the following values

$$m_{\text{scatt}} = (2380 \pm 450) m_e,$$

$$m_{\text{gap}} = (2513 \pm 150) m_e.$$

The particle responsible for it has then be assumed to be a hyperon.

Searching for masses different from  $p$  or nucleons amongst the secondaries emitted in the same event, a K-mesons has been identified, (track *a*) which covers a range of 20 mm and then decays into a minimum ionizing particle ( $p\beta = 200 \pm 10 \text{ MeV/c}$ ;  $g/g_0 = 0.95 \pm 0.05$ ).

The mass of the decaying particle as obtained from gap length measurements, is  $1\,035 \pm 270 m_e$ .

The  $p\beta$  value of the secondary particle is very close to the value expected for  $K_{\mu 2}$  decay.

*Event B.* - From a jet-type star (4+8p) (see Fig. 3) a track has been

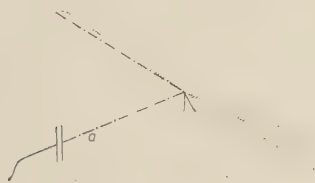


Fig. 3.

observed which is  $24\,300\ \mu\text{m}$  long. From its end, were the particle responsible for it stops, an electron of a few MeV escapes. Scattering, gap and grain density measurements give for the mass of the track the following values

$$\begin{aligned} m_{\text{scatt}} &= (1\,960 \pm 300) m_e, \\ m_{\text{gap}} &= (2\,840 \pm 110) m_e, \\ m_{\text{gr}} &= (2\,300 \pm 110) m_e. \end{aligned}$$

We feel that we can confidently assume that this is a hyperon.

### 3. - Conclusion.

The respective average values, obtained from the above quoted independent results each taken with a weight proportional to the inverse of their statistical error, are:

$$\begin{aligned} \text{A)} \quad & (2\,500 \pm 160) m_e, \\ \text{B)} \quad & (2\,740 \pm 100) m_e, \end{aligned}$$

to be compared with the values of

$$\begin{aligned} m_{\Sigma^-} &= 2\,327 \pm 1 m_e, \\ m_{\Xi^-} &= 2\,586 \pm 6 m_e. \end{aligned}$$

The values obtained make almost certain their interpretation in terms of hyperons. Their interaction with matter can then take place according to the following schemes <sup>(3)</sup>

$$(1) \quad \Sigma^- + p \rightarrow \Lambda^0 + n,$$

$$(2) \quad \rightarrow \Sigma^0 + n,$$

and

$$(3) \quad \Xi^- + p \rightarrow \Lambda^0 + \Lambda^0,$$

$$(4) \quad \rightarrow \Xi^0 + n \rightarrow \text{and possibly } \Lambda^0 + \Lambda^0.$$

The average values of their masses quoted above seem to favour an interpretation in terms of  $\Xi^-$ . Of the two schemes (3) and (4) the latter one seems more probable: in fact the ratio between the two statistical weights of the final states

$$P = \frac{\varrho(\Xi^0, n)}{\varrho(\Lambda^0, \Lambda^0)} = 0.18\sqrt{\Delta - 1.3}$$

where  $\Delta$  is the difference between the masses of the  $\Xi^-$  and  $\Xi^0$ . If the probability of each of the two schemes is taken to be proportional to  $\varrho$ , the quantity  $P$  gives the branching ratio between (3) and (4). Since  $\Delta$  presumably is of the order of a few MeV the scheme (3) should be considerably more frequent than the other.

A zero prong star then is possible if both the neutral disintegration products escape from the nucleus.

\* \* \*

Thanks are due to Prof. E. AMALDI for his interest shown during the work and to Dr. R. GATTO for helpful suggestions.

<sup>(3)</sup> R. GATTO: *Nuovo Cimento*, **1**, 372 (1955); M. W. FRIEDLANDER, Y. FUJIMOTO, D. KEEFE and M. G. K. MENON: *Nuovo Cimento*, **2**, 90 (1955).



# Gamma-Gamma Angular Correlation in $^{160}\text{Dy}$ .

G. BERTOLINI, M. BETTONI and E. LAZZARINI

*Istituto di Fisica Sperimentale del Politecnico - Milano*

(ricevuto il 29 Marzo 1956)

The  $\gamma$ -decay of  $^{160}\text{Dy}$  following the  $\beta$ -decay of  $^{160}\text{Tb}$  has been investigated by a number of authors (see the bibliography on the preceding paper <sup>(1)</sup>). In the latest papers the authors are in agreement on indicating the predominant  $\gamma$ -decay of  $^{160}\text{Dy}$  as shown in Fig. 1. The half life of the first excited level and the internal conversion coefficient of the  $\gamma$ -transition from this level to the ground state indicate that the spin of this level is 2 and the parity plus. In the preceding work we found an  $E2$  character of the 880 and 970 keV  $\gamma$ -transition through their internal conversion coefficients, but considering the uncertainty in the experimental method used, it seemed reasonable to confirm it with the angular correlation data.

NaI(Tl) scintillation counters were used as radiation detectors. The NaI(Tl) crystals in optical joint with RCA type 5819 photomultipliers were cut in the form of right circular cylinders (1" diameter, 1" thickness). The counters were laterally shielded against scattered radiation by a minimum thickness of 1.5 cm of lead.

The geometry of the lead shielding was such that only for angles between  $170^\circ$  and  $180^\circ$  one crystal can look

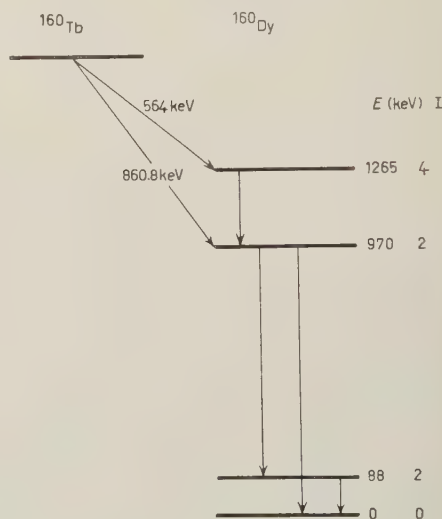


Fig. 1. - Simplified decay scheme of  $^{160}\text{Tb}$ .

directly at the other. However in these conditions the detector-detector solid angle for scattered radiation is so far reduced that the perturbation of the angular correlation is negligible.

Furthermore the crystals were fron-

<sup>(1)</sup> G. BERTOLINI, M. BETTONI and E. LAZZARINI: *Nuovo Cimento*, **3**, 754 (1956).

tally shielded with 3 mm thick polythene against electrons.

Fig. 2 is the block diagram of the coincidence spectrometer. It consists of two fast channels which have a resolving

seriminator  $D_2$  is adjusted at the maximum sensibility and the single channel selects the peak at 300 keV energy.

A dry source of  $\text{TbCl}_3$  was prepared in an aluminium cylindrical holder of

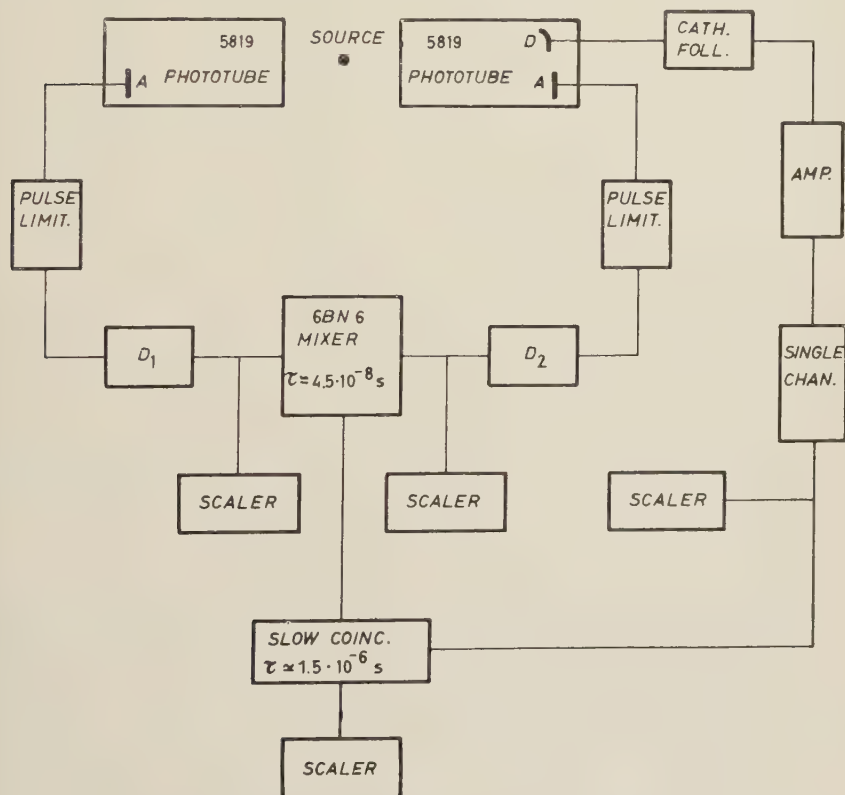


Fig. 2. — Block diagram of the coincidence spectrometer.

time of 45 nps in parallel with a slower energy selection channel.

The coincidence circuit consists of two fast discriminators according to MOODY *et al.* <sup>(2)</sup> and a 6 BN 6 mixer tube according to FISHER and MARSHALL <sup>(3)</sup>.

The discriminator  $D_1$  discriminates all the pulses which are corresponding to energies inferior to  $\approx 750$  keV, the di-

0.3 mm thickness and of 2 mm inner diameter.

Coincidences were taken for angles between the counter axes of  $90^\circ$ ,  $110^\circ$ ,  $130^\circ$ ,  $150^\circ$ ,  $168^\circ$ ,  $180^\circ$ ,  $192^\circ$ ,  $210^\circ$ ,  $230^\circ$ ,  $250^\circ$ ,  $270^\circ$ .

The experimental data were treated according to FRANCKEL <sup>(4)</sup> in the same way as in praevious paper <sup>(5)</sup>.

<sup>(2)</sup> N. E. MOODY, G. J. R. MACLUSKY and M. O. DEIGHTON: *Electronic Eng.*, **24**, 214 (1952).

<sup>(3)</sup> J. FISHER and J. MARSHALL: *Rev. Sci. Instr.*, **23**, 117 (1952).

<sup>(4)</sup> S. FRANCKEL: *Phys. Rev.*, **83**, 673 (1951).

<sup>(5)</sup> G. BERTOLINI, M. BETTONI and E. LAZZARINI: *Nuovo Cimento*, **3**, 800 (1956).

The angular efficiency of the two detectors 1 and 2 for  $\gamma$ -rays respectively of  $E_\gamma = 750$  keV and  $E_\gamma = 300$  keV have been determined experimentally, according to LAWSON and FRAUENFELDER<sup>(6)</sup>, with a well collimated beam ( $< 0.6^\circ$ ) of

The measured correlation is really a composite of two separate correlations, 300-880 keV and 300-970 keV.

The knowledge of the decay probability from the 960 keV level to the first excited state and to the ground

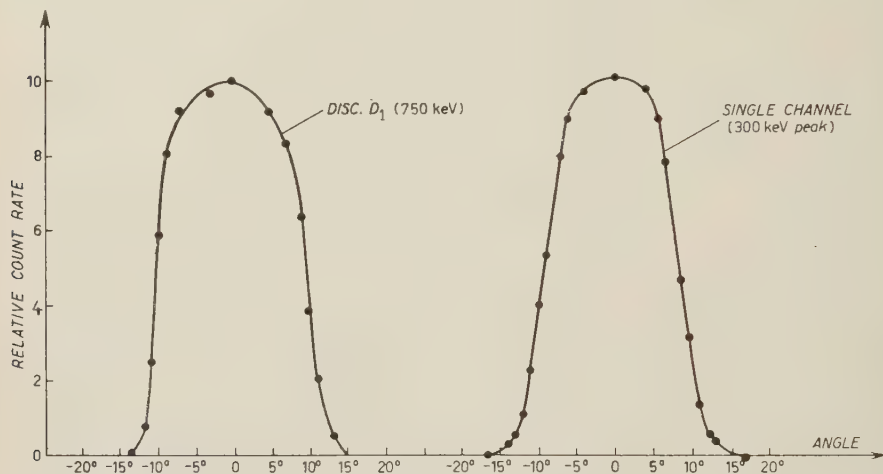


Fig. 3. — Experimental angular efficiency curves.

$\gamma$ -rays coming from a strong source of  $^{160}\text{Tb}$ . Fig. 3 shows the experimentally determined angular efficiencies.

The solid angle correction factors, determined by numerical integration of the measured angular resolution curves are:

$$\frac{Q_0}{Q_2} = 1.032, \quad \frac{Q_0}{Q_4} = 1.175.$$

Therefore the last square fit to the experimental points corrected for finite geometry is given by:

$$W(\theta) = (1 \pm 0.023) + (0.105 \pm 0.035) \cdot P_2(\cos \theta) - (0.0014 \pm 0.036) P_4(\cos \theta).$$

Fig. 4 shows the result of the measurements.

state makes possible the construction of the single correlations. This value un-

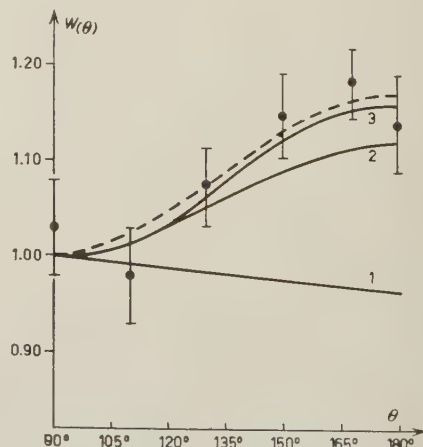


Fig. 4. — Angular correlation of the (300 — 880 + 970) keV  $\gamma$ -rays. The dashed curve in the least squares fit to the experimental points and has been corrected for finite geometry. Curves 1, 2 and 3 are the theoretical curves for the basic 4 (2) 2 (2) 2, 4 (2) 2 (1) 2 and 4 (2) 2 (2) 0 correlations respectively.

<sup>(6)</sup> J. L. LAWSON and H. FRAUENFELDER: *Phys. Rev.*, **91**, 649 (1953).

fortunately is not obtainable from the relative intensities of the 880 and 970 keV  $\gamma$ -rays (27.5 to 100) because two different transitions contribute to the 970 keV line.

From the theory of Bohr and Mottelson (7) a probability of 0.4 and 0.7 is

---

(7) K. SIEGBAHN:  *$\beta$  and  $\gamma$ -ray Spectroscopy* (Amsterdam, 1955), p. 468.

obtained ( $P_{970}/P_{880} = 0.4$  or  $0.7$ ) on the hypothesis that the 970 keV  $\gamma$ -ray has  $E2$  character and the 880 keV  $\gamma$ -ray  $M1$  or  $E2$  character respectively.

If one assumes for the 300-880 keV correlation a greater weight or even the same weight of the 300-970 keV correlation, one sees that the experimental result is best fitted to 4 (2) 2 (2) 0 and 4 (2) 2 (1) 2 assignments.

Radioactivité  $\alpha$  spécifique des plaques Ilford pour recherches nucléaires.

## II. Activité de surface.

S. DEUTSCH (\*)

*Laboratoire de Physique Nucléaire, Université Libre de Bruxelles*

(ricevuto il 6 Aprile 1956)

Dans une note antérieure <sup>(1)</sup>, les résultats des mesures de radioactivité  $\alpha$  spécifique des émulsions nucléaires Ilford C-2 ont été communiqués. Cette activité fixe une limite inférieure aux concentrations mesurables de radioéléments introduits dans l'émulsion. Dans le cas d'un échantillon extérieur à l'émulsion, soit qu'on veuille observer des  $\alpha$  provenant d'une radioactivité naturelle ou artificielle ou encore d'une réaction nucléaire, la limite inférieure de l'activité détectable est fixée par la contamination de la surface de l'émulsion. Cette contamination est de plus un facteur gênant la localisation de l'activité des échantillons faiblement radioactifs.

Nous avons déjà mis en évidence que plus de 90 % des particules traversant la surface des plaques examinées provenaient de l'extérieur et non des radioéléments contaminant l'émulsion.

A l'occasion d'une étude sur des météorites métalliques <sup>(2)</sup> qui sont parmi

les matériaux naturels les moins radioactifs connus, on a été amené à étudier de plus près l'activité  $\alpha$  de surface des émulsions.

On a essayé de déterminer l'origine de cette activité  $\alpha$  afin de pouvoir éliminer la contamination responsable.

L'observation, faite au microscope binoculaire Leitz Ortholux avec un grossissement de 1000 fois, a porté sur 4 plaques (5  $\times$  10 cm) Ilford C.2 « purifiées » de 200  $\mu$ m d'épaisseur. Elles ont été débarrassées de leur boîte et conservées 116 jours (comptés depuis la date de la coulée) émulsion contre émulsion, dans une atmosphère sèche à 4°. Elles ont été développées avec un révélateur à l'amidol suivant la méthode à deux températures <sup>(3)</sup>. L'absence de fading a été contrôlée par l'aspect des traces et par la radioactivité spécifique du verre.

Sur une surface de 19.25 cm<sup>2</sup>, on a compté 786  $\alpha$ , ayant une extrémité au moins en contact avec la surface de l'émulsion et ne faisant pas partie d'étoile. On n'a tenu compte que des traces inférieures à 50  $\mu$ m, ce parcours correspon-

(\*) Attachée à l'Institut Interuniversitaire des Sciences Nucléaires.

(1) S. DEUTSCH et E. C. DODD: *Nuovo Cimento*, **10**, 858 (1953).

(2) S. DEUTSCH, F. G. HOUTERMANS et E. E. PICCIOTTO: à paraître dans *Geochim. et Cosmochim. Acta*.

(3) C. C. DILWORTH, G. OCCHIALINI et L. VERMAESEN: *Bull. Centre Phys. Nucl. U.L.B.*, n. 13a (1950).



dant à celui de l' $\alpha$  le plus long émis dans la famille de l'Uranium et du Thorium. La majorité des traces provenant du rayonnement cosmique dont le nombre total est d'ailleurs négligeable (<sup>4,5</sup>) a ainsi été éliminée.

L'activité  $\alpha$  de surface trouvée est de  $0.24 \pm 0.03 \alpha$  par  $\text{cm}^2$  et par jour. Cette valeur concorde avec la moyenne des déterminations faites précédemment sur des émulsions Ilford C-2 purifiées. Celle-ci était de  $0.25 \alpha$  par  $\text{cm}^2$  et par jour. Ces résultats confirment qu'une telle activité ne peut provenir que d'émetteurs situés à l'extérieur de l'émulsion vu la faible radioactivité spécifique de l'émulsion elle-même (<sup>1</sup>).

Pour identifier les émetteurs responsables des  $\alpha$  de surface, on a mesuré les projections horizontales et verticales de 493  $\alpha$  à l'aide d'un micromètre oculaire (1 division =  $1.1 \mu\text{m}$ ) dont l'étalonnage a été vérifié d'après un micromètre objectif Zeiss. Les graduations (1 division =  $1 \mu\text{m}$ ) de la vis micrométrique de profondeur du microscope ont été vérifiées à l'aide d'un comparateur. Le calcul de la longueur des  $\alpha$  a été fait en prenant un facteur de contraction de l'émulsion de 2.5. Celui-ci a été évalué en mesurant l'épaisseur des plaques après développement et en admettant une épaisseur de  $200 \mu\text{m}$  indiquée par le fabricant pour l'émulsion non développée. La Fig. 1 donne l'histogramme des parcours de 493  $\alpha$  de surface, groupés par intervalle de  $5 \mu\text{m}$ . On n'a tenu compte que des  $\alpha$  ayant un parcours résiduel dans l'émulsion supérieur à  $5 \mu\text{m}$ .

La distribution des parcours montre deux maximum: l'un à  $39 \mu\text{m}$ , l'autre à  $29 \mu\text{m}$ .

Une telle distribution ne peut être due à une émission en couche épaisse des  $\alpha$  provenant des radioéléments contenus

dans l'émulsion. Elle semble causée par une émission en couche mince; le pic à  $39 \mu\text{m}$  est attribuable à l' $\alpha$  du RaC' et celui de  $29 \mu\text{m}$  à l' $\alpha$  du RaA mais il

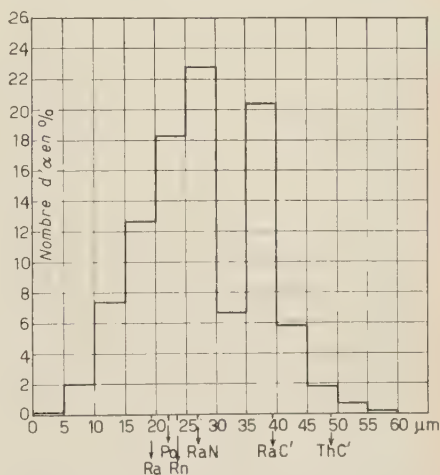


Fig. 1. — Histogramme des parcours des  $\alpha$  de surface dans les plaques Ilford C 2 sur 493 traces.

couvre aussi les parcours des  $\alpha$  du Radium, du Radon et du Polonium. Ainsi 85 % des  $\alpha$  sont attribuables aux Radon, Radium A et RaC'. Ce Radon circulerait dans la mince couche d'air séparant les deux plaques. En admettant pour cette couche une épaisseur moyenne de  $0.1 \text{ mm}$  et en supposant que le Radon est en équilibre avec l'air ambiant, l'activité de surface trouvée de  $0.24 \alpha$  par  $\text{cm}^2$  et par jour serait due à une concentration en Radon de  $5 \cdot 10^{-12}$  curie par litre, ce qui est une valeur plausible.

Le Radon provenant du Radium contenu dans l'émulsion (environ  $10^{-15}$  curie par  $\text{cm}^3$  d'émulsion sèche) et diffusant hors des plaques ne pourrait causer cette contamination de surface. Les 15% des  $\alpha$  restant sont attribuables à l'activité propre de l'émulsion et des poussières portant des radioéléments à vie longue. Ces poussières de surface ne peuvent pas supporter le dépôt actif du Radon sinon 5 % des  $\alpha$  du RaA et du RaC' devraient former des étoiles à 2 branches, alors

(<sup>4</sup>) D. H. PERKINS: *Nature*, **160**, 707 (1947); M. MORAND et P. CÜRR: *Cosmic Radiation* (Londres, 1949).

(<sup>5</sup>) S. LATTIMORE *Phil. Mag.*, **41**, 819 (1950).

que nous n'avons trouvé que des traces simples. Le Thoron et ses descendants à vie courte ne semblent pas intervenir.

En conclusion, on voit que l'activité superficielle des émulsions photographiques correspond à celle d'un échantillon épais contenant par gramme  $5 \cdot 10^{-8}$  g de Thorium ou  $1.5 \cdot 10^{-8}$  g d'Uranium (en supposant le Thorium et l'Uranium en équilibre avec leurs descendants). Ces teneurs sont calculées d'après les formules classiques d'Evans <sup>(6)</sup> et de Curie <sup>(7)</sup>, en prenant pour l'échantillon, la composition d'une roche granitique. Dans le cas de réactions (n,  $\alpha$ ) par exemple, induites dans une cible par un flux de neutrons thermiques de  $4 \cdot 11^{11}$  n/cm<sup>2</sup> (ce qui semble être la limite de la dose supportable par l'émulsion nucléaire pour une bonne discrimination des  $\alpha$ ) <sup>(8,9)</sup>, le background de surface des plaques limiterait la mise en évidence de telles réactions à celles ayant une section efficace supérieure à  $10^{-30}$  cm<sup>2</sup>.

= On a montré que 90 % de cette activité superficielle dans notre cas proviennent de l'extérieur de l'échantillon, plus particulièrement du Radon de l'air

et de ses descendants à vie courte, le spectre des longueurs des  $\alpha$  de surface s'étendant de 0 à 50  $\mu$ m dans l'émulsion photographique. Il faut souligner l'importance que prend la notion de plaque témoin, dans la mesure de très faibles activités  $\alpha$  comme le montre clairement la discussion des résultats sur la mesure de l'activité  $\alpha$  de météorites métalliques <sup>(2)</sup>, et celle relative à la section efficace de la réaction Fe(n,  $\alpha$ )Cr <sup>(9,10)</sup>. Les conditions de coulée, de conservation et de manipulation des plaques appliquées contre l'échantillon et de leurs témoins sont très critiques. Il semble que l'activité de surface pourrait être abaissée d'un ordre de grandeur en séchant et conservant les plaques dans une atmosphère privée de Radon. L'activité de surface serait alors de  $2 \cdot 10^{-2}$   $\alpha$ /cm<sup>2</sup>/jour: elle correspondrait à celle d'un échantillon épais contenant  $5 \cdot 10^{-9}$  g de Thorium ou  $1.5 \cdot 10^{-9}$  g d'Uranium par gramme. Ces valeurs fixent la limite inférieure de l'activité détectable d'un échantillon par autoradiographie alpha avec les émulsion actuelles.

\* \* \*

<sup>(6)</sup> R. D. EVANS: *Phys. Rev.*, **45**, 29 (1934).

<sup>(7)</sup> I. CURIE: *Journ. Phys. et Rad.*, **7**, 11 (1946).

<sup>(8)</sup> H. FARAGGI et R. BERNAS: *Compt. Rend.*, **234**, 1684 (1952).

<sup>(9)</sup> H. FARAGGI: *Journ. Phys. et Rad.*, **14**, 160 (1953).

Je remercie vivement le Docteur E. E. PICCIOTTO qui a dirigé ce travail.

<sup>(10)</sup> S. LONGCHAMP: *Journ. Phys. et Rad.*, **13**, 333 (1952).

On the Mass of the  $K^-$ -Meson.

F. HÄNNI, CH. LANG, M. TEUCHER and H. WINZELER

*Physikalisches Institut der Universität - Bern (Schweiz)*

E. LOHRMANN

*Hochspannungslaboratorium Hechingen - Deutschland*

(ricevuto il 20 Aprile 1956)

In a stack of 108 stripped emulsions Ilford G5  $20 \times 30$  cm<sup>2</sup>, 600  $\mu$ m thick each, which was flown in Texas at an altitude of 29 km for 8 hours, a three prong event (A) was found (Fig. 1). The particle producing track no. 2 of this event

comes to rest in the emulsion after 328  $\mu$ m and produces another star (B). According to scattering measurements using the constant sagitta cell scheme of FAY *et al.* <sup>(1)</sup> the mass of this particle is  $740^{+540}_{-260} m_e$ . Track no. 6 of star B produces another star (C) after 54  $\mu$ m. Since it is completely black no ionization measurements are possible. The details of all the stars are given in Table I. Star B seems to be due to the nuclear capture of a  $K^-$ -meson, star C could be produced by the nuclear capture of a meson or a hyperon. The possibility of a non mesonic decay of an excited fragment of  $Z \leq 3$  cannot be excluded. But all these possibilities are consistent with the assumption that track no. 2 is due to a  $K^-$ -meson. Track no. 3 is a proton coming to rest after  $8400 \pm 126 \mu$ m corresponding to a kinetic energy of  $47.6 \pm 0.4$  MeV. This is calculated from the tables of FAY *et al.* <sup>(1)</sup> corrected according to range-energy calibrations with  $\pi$ - $\mu$ -decays in our plates (range of the  $\mu$   $597 \pm 3 \mu$ m). Track no. 1 leads

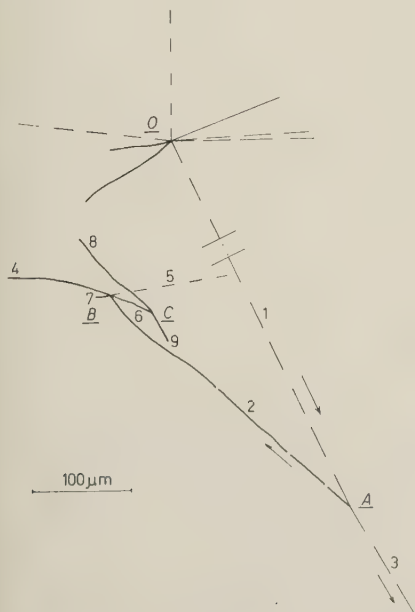


Fig. 1.

<sup>(1)</sup> H. FAY, K. GOTTSTEIN and K. HAIN: *Suppl. Nuovo Cimento*, **11**, 234 (1954).

TABLE I.

Track no.	Identity	Range ( $\mu\text{m}$ )	Energy (MeV)
1	$\text{K}^-$	13500	—
2	$\text{K}^-$	328	$5.7 \pm 0.1$
3	p	8400	$47.6 \pm 0.4$
4	p (?)	137	—
5	$\pi$ (*)	—	$100^{+70}_{-30}$ (+) $133 \pm 22$ (-)
6	$\Sigma^-$ (?)	54	—
7	p (?)	14.4	—
8	p (?)	187	—
9	p (?)	> 2000	—

(\*) An electron cannot be excluded.  
(+) Scattering measurement.  
(-) Mean gap length measurement.

after 13500  $\mu\text{m}$  to a star *O* of the type 7+0p. Its ionization *g* measured by the mean gap length method is 3.4  $g_{\text{plateau}}$  near *A*, 2.4  $g_{\text{plateau}}$  near *O*. Therefore it is clear that track no. 1 runs from *O* to *A*. From the variation of mean gap length vs. range one calculates a mass of  $1320 \pm 320 m_e$  for this particle and a kinetic energy of  $51 \pm 5$  MeV near event *A* assuming a mass of 965  $m_e$ . For energetic reasons *A* cannot be a «star». Since tracks no. 1, 2 and 3 are coplanar within the errors of measurement the assumption seems justified that event *A* is due to an elastic nuclear scattering of a  $\text{K}^-$ -meson by a free proton. It should give a rather precise mass

estimate for the  $\text{K}^-$ -meson. The angle between tracks no. 1 and 2 is  $35^\circ \pm 2^\circ$ , between tracks 1 and 3  $172^\circ \pm 1^\circ$ . Using energy and momentum balance the calculation for the mass of the  $\text{K}^-$ -meson gives.

$$m_{\text{K}^-} = 979 \pm 11 m_e.$$

The error is mainly due to the range-straggling of the  $\text{K}^-$  on its way from *A* to *B* and to the uncertainties of the angular measurements. Our value is in good agreement with measurements in Berkeley (<sup>2</sup>), which give  $963 \pm 12 m_e$ .

\*\*\*

We wish to thank Prof. F. G. HOUTERMANS for giving us the possibility of this work, Prof. CH. PEYROU for stimulating discussions and Dr. P. WALOSCHEK for valuable criticism. The event was found by Mrs. S. SCHILT.

The Texas flights were organized by the Office of Naval Research, our special thanks are due to Dr. A. ROBERTS.

Our participation in these flights was sponsored by the «Schweizer Nationalfonds». One of us (E.L.) wants to thank Prof. F. G. HOUTERMANS for the hospitality in his institute, Prof. E. SCHOPPER for granting leave of absence and the «Deutsche Forschungsgemeinschaft» for a maintenance grant.

(<sup>2</sup>) F. H. WEBB, W. W. CHUPP, G. GOLDHABER and S. GOLDHABER: *UCRL-Report* 3226, December 1955.

## A New Detector of Ionizing Radiation. The Gas Bubble Chamber.

P. E. ARGAN and A. GIGLI

*Istituto di Fisica dell'Università - Genova*

*Istituto Nazionale di Fisica Nucleare - Sezione Aggregata di Genova*

(ricevuto il 23 Aprile 1956)

A few years ago, D. A. GLASER <sup>(1)</sup> devised and put into operation a new type of recording instrument which was capable of visualizing the path of ionizing particles. The device, known as the bubble chamber, is based on the formation of vapor bubbles around ion clusters in a superheated liquid. Other types of metastabilities however can be imagined to occur in the liquid phase, for example the supersaturation of a gas-liquid solution; it may be possible that in such a metastable condition bubbles can be formed around ion clusters at the expenses of the dissolved gas.

With the same type of arguments used by GLASER <sup>(2)</sup> to explain the behaviour of a superheated liquid in the presence of ion charges, one concludes that the most favorable condition for the formation of the bubbles in a supersaturated solution is to be expected when the surface tension and the dielectric constant of the gas-liquid system are sufficiently small, namely for high gas concentration, i.e. high pressure.

Having this in mind, we have suc-

ceeded in putting into operation a bubble chamber, using a supersaturated solution of a gas in the liquid at room temperature.

The «a priori» choice of a suitable solution is somewhat tedious, since in the literature only few data are available on the surface tension and dielectric constant of solutions of gases in liquids. As liquid we have chosen the ethyl ether, because of the low values of surface tension (17 CGS units) and dielectric constant at room temperature; on the other hand, the carbon dioxide appeared to be very convenient as the dissolved gas, since it is strongly soluble in ethyl ether at moderate pressures, with a remarkable decrease of surface tension <sup>(3)</sup> and dielectric constant of the system. No other gas-liquid systems were tried, but it is possible that other solutions are as suitable as the CO<sub>2</sub>-ether system.

We have used a stainless steel chamber, cylindrical in shape (volume 200 cm<sup>3</sup>), and closed at the ends by two thick glass windows for illuminating and photographing its interior. The pressure of

<sup>(1)</sup> D. A. GLASER: *Phys. Rev.*, **91**, 762 (1953); **87**, 665 (1952).

<sup>(2)</sup> D. A. GLASER: *Suppl. Nuovo Cimento*, **11**, 361 (1954).

<sup>(3)</sup> *Int. Crit. Tab.* IV, 474-475 (1928); *Tab. Ann. Const. Donn. Num.*, VI, 77 (1923-1924).



the  $\text{CO}_2$ -ether system ranged from 40 to 50 atm at which pressures the bubble formation appeared to be possible by a rough estimate on the basis of the few surface tension data available in the literature. The chamber is connected to an expansion vessel situated at the bottom. The expansion is provided by means of a polythene diaphragm moved under the action of compressed air. A simple mechanical device makes possible a rapid release of the compressed air with the result that the pressure inside the chamber is reduced to 1 atm in a time interval of 6 to 7 ms.

Fig. 1 shows a photograph of the chamber (pre-expansion pressure of 47 atm) taken 14.6 ms after the beginning of the rapid expansion. The effect of a 10mC radium source placed at the side of the chamber is shown in Figs. 2 and 3. In Fig. 2 the radium source was held 45 cm from the center of the chamber in the plane of the photograph, whereas in Fig. 3 the source was at 25 cm and the photograph was taken 9.6 ms after the expansion. Electron tracks from the  $\gamma$ -rays of radium are clearly visible in both pictures; however, in the last photograph much less «old tracks» are present, due to the shorter time interval between the expansion and the flashing.

These preliminary results show that a supersaturated solution of a gas in a liquid can be conveniently used for detecting and visualizing the path of ionizing particles. The construction and operation of a bubble chamber based on this new principle is not a hard problem. In particular the operation of the chamber is not critical and no difficulties are encountered as far as the bubble formation on the walls and on the gaskets is concerned. No special polishing of the inside walls was used and the gaskets were cut from commercially available

polythene sheet. No effect of room temperature variations was observed during the experiments.

It is to be noted that in a supersaturated solution the bubble growth is much slower than in a supersaturated liquid, since the rate of growth is determined by the diffusion coefficient of the gas in the liquid, at least in the final stage of the bubble formation. In such a circumstance, use can be made of ordinary flashlamps; the flash duration in our photographs is about 100  $\mu\text{s}$ .

Moreover, the sensitive time of this chamber is likely to be larger than that of a «dirty» chamber of the Glaser type. Experiments are in progress to throw more light on this important feature of the chamber. As to the recycling time, we are not able to estimate it at the present time, since our device for expanding the  $\text{CO}_2$ -ether system is as yet too rough for such an evaluation.

Further work is in progress and more detailed information will be given at a later time.

\*\*\*

We wish to thank Prof. E. PANCINI whose advice and helpful interest was a determining factor for the success of this work. The aid of Mr. O. ROSATI for the design and construction of the mechanical parts is gratefully acknowledged.

### *Note Added in Proof.*

When this letter was already completed we received the last number of *Soviet Physics, JETP* (November 1955, 571) in which G. A. ASKAR'IAN discusses briefly the possibility of a new particle detector on the same principles considered by us. No information is given about any realisation of his proposal.



Fig. 1.



Fig. 2.



Fig. 3.





H. HERMES: *Einführung in die Verbandstheorie*, Springer Verlag (1955) p. VIII-164.

La teoria dei reticoli è da collocarsi in prima linea nel fronte in progressione della matematica astratta verso l'astrazione sempre più spinta, senza badare in alcun modo a esigenze o meno di intuizione. Due sono le vie principali verso l'astrazione: Costruzioni logiche assiomatiche sempre più ricche di enti astratti mutuamente collegati da assiomi sempre più complessi e l'altra consistente nell'assumere il minor numero possibile di assiomi e svolgere la teoria con grandi ricchezze di dettagli tutti basati su quel minimo di postulati iniziali. La teoria dei reticoli (« Verbandstheorie » in tedesco, « Lattice theory » in inglese) è più che altro da collocarsi in questo secondo ramo. Entrambi questi rami sono potenti e dominano sempre più vasi campi della matematica, almeno nel suo ordinamento classico, ed entrambi hanno un potere di sintesi notevolissimo. Le due correnti non sono naturalmente del tutto distinte e in molte applicazioni si collegano e si fondono.

La teoria dei reticoli si presenta formalmente come l'astrattizzazione delle operazioni di riunione e di intersezione (somma e prodotto secondo un altro fra-sario altrettanto in voga) per le parti di un dato insieme astratto, tuttavia questa posizione è in sostanza soltanto apparen-

temente antecedente il concetto di insieme; questa teoria è da ritenersi piuttosto in realtà una semplice costruzione logica, tra le più semplici, e come tale da far rientrare nel primo ramo di cui abbiamo parlato sopra.

La ragion d'essere della teoria dei reticoli non è però strettamente legata alle operazioni sulle parti di un insieme, ma piuttosto alla teoria dei gruppi, e precisamente alla considerazione dell'insieme di tutti i sottogruppi di un gruppo dato. Per questo insieme di sottogruppi esistono due particolari operazioni: l'intersezione di due sottogruppi distinti, che è il più grande sottogruppo contenuto in entrambi, e la quale, cioè la congiunzione, consistente nell'associare ai due sottogruppi il più piccolo sottogruppo che li contiene entrambi. Queste due operazioni sono legate da proprietà formali notevoli che si lasciano facilmente dominare astrattizzando le due suddette operazioni e giungendo pertanto alla teoria dei reticoli. L'insieme dei sottogruppi di un gruppo dato è per l'appunto un esempio di reticolo, e la considerazione di questa qualità per il suddetto insieme è fatta specialmente in vista del problema della classificazione dei gruppi astratti. Oltre questa applicazione la teoria dei reticoli ne trova molte altre nei campi più svariati della matematica, e ciò grazie all'alto livello di astrazione in cui si pone e alla semplicità dei suoi postulati.

Essa ebbe soprattutto sistemazione e affermazione come ramo autonomo della matematica attraverso il trattato *Lattice Theory*, scritto nel 1940 dal BIRKHOFF, il famoso matematico che dimostrò fra l'altro il celebre « Ultimo teorema di geometria » di Poincaré. Il presente trattato, del tutto recente, si presenta come una ideale continuazione dell'opera del BIRKHOFF. Esso è una esposizione completa dei principi della teoria e delle varie particolarizzazioni del concetto di reticolo, partendo dal concetto generale di reticolo senza specificazioni e dalle sue proprietà (cap. I), attraverso lo studio dei reticoli, sempre di carattere generale ma soddisfacenti a varie proprietà di tipo elementare (cap. II), lo studio dettagliato di particolari reticoli detti modulari e delle loro proprietà (cap. III), lo studio e le applicazioni dei reticoli di Boole nel campo dell'algebra e della topologia, e dei reticoli distributivi (cap. IV) e concludendo con varie applicazioni e concetti ad essi collegati, quali il lemma di Zorn e l'algebra di Boole (cap. V) e in appendice l'« algebra universale ».

In conclusione il trattato è da porsi anche se di modesta mole, tra le pietre miliari della matematica moderna astratta, sia per l'argomento che per la sobrietà e la finezza di esposizione e per la notorietà della collezione in cui esso appare: la famosissima serie di trattati: *Die Grundlehren der Mathematischen Wissenschaften* (della casa editrice Springer Verlag), ben nota a ogni matematico.

M. VACCARO

W. THIRRING — *Einführung in die Quantenelektrodynamik*, pagg. VI + 122. F. Deuticke, Wien 1955.

Questo volumetto di W. THIRRING è scritto per coloro che hanno già ragionevoli basi di teoria dei campi, quali possono essere date dalla preventiva lettura, ad esempio, del WENTZEL e dell'HEITLER,

e che vogliano mettersi rapidamente al corrente dei metodi moderni. Dopo una breve introduzione relativa all'elettrodinamica classica, si passa subito a sviluppare le idee fondamentali della teoria quantistica dei campi, considerando prima i campi non in interazione, poi i campi in interazione; vengono, in questa ultima parte, trattati anche esempi particolari come la interazione di due elettroni o la polarizzazione del vuoto ecc. Le ultime otto pagine sono dedicate alla teoria della rinormalizzazione.

Ciò che questo volume ha di nuovo è di avere impostato tutta la teoria sulla base del metodo di Schwinger, il più vicino al principio di corrispondenza.

Piuttosto che un libro di testo esso potrebbe essere considerato un'elegante traccia, del resto completa in se stessa, di un corso di elettrodinamica e di teoria dei campi in genere; sotto tale luce esso è certamente un libro utile e bello; fatto più per il docente che per lo studente.

G. MORPURGO

L. COLLATZ — *Numerische Behandlung von Differentialgleichungen* (Zweite Auflage). Springer-Verlag, Berlin-Göttingen-Heidelberg, pag. xv + 528, 1955. DM. 56, Leg. tela DM. 59.60.

A soli quattro anni dalla prima edizione, l'Autore ha dato alla stampa questa seconda edizione del libro di cui qui si tratta. Al pari del precedente volume anche qui le questioni riguardanti i metodi per la risoluzione numerica delle equazioni differenziali, risultano accuratamente esposti.

La presente edizione differisce però in molti punti dalla precedente, sia per quanto riguarda l'ordinamento generale della materia, sia per le numerose ed opportune aggiunte.

Riesce particolarmente felice l'aggiunta di un nuovo capitolo (il primo)



nel quale, oltre a varie generalità sui metodi di calcolo numerico, sono condensate nozioni sulle formule di quadratura (quelle classiche) e sui problemi al contorno lineari e non lineari.

Il presente volume risulta dotato in quasi tutti i paragrafi di notevoli esempi applicativi, ciò che ne aumenta i pregi e contribuisce a renderlo più facile ed accessibile anche ai meno esperti in questioni di calcolo numerico.

Nel complesso il volume si presenta sensibilmente migliorato rispetto alla sua prima edizione.

Accurata come al solito la bibliografia, ed ottima la veste tipografica.

FRANCESCO ROSATI

*The Physics of the Ionosphere* - The Physical Society, London - Un volume di 406 pagine (18 cm × 26 cm) con 187 figure e 3 tavole fuori testo. Prezzo 40 s.

Il volume contiene le memorie presentate alla Conferenza sulla fisica della ionosfera tenuta sotto gli auspici della Physical Society al Cavendish Laboratory di Cambridge dal 6 al 9 Settembre 1954.

Le 50 memorie (in lingua francese o tedesca alcune, in inglese tutte le altre) sono ordinate in 4 parti dedicate rispettivamente agli strati E e D, alle irregolarità e movimenti della ionosfera, allo strato  $F_2$  ed alla matematica della propagazione delle onde attraverso la ionosfera.

Ognuna delle 4 parti è preceduta da una memoria introduttiva, che fa il punto sullo stato attuale della ricerca in quel settore della fisica della ionosfera, con un addendum che tiene conto dei contributi portati nel corso della Conferenza stessa. Le memorie introduttive sono di A. H. WAYNICK, J. A. RATCLIFFE, D. F. MARTYN, K. O. BUDDEN.

Com'è noto le caratteristiche della parte ionizzata dell'alta atmosfera sono

state indagate negli ultimi 3 decenni con l'impiego quasi esclusivo delle tecniche radio ed una massa veramente notevole di dati è stata raccolta. Tuttavia il numero e la complessità dei problemi insoluti rimane quasi sconcertante (WAYNICK). Le recenti misure dirette in loco di molti parametri fisici con l'aiuto dei razzi e la misura di numerose grandezze in laboratorio, permettono oggi, insieme con i dati radio, una conoscenza più sicura della fisica della ionosfera (legge di distribuzione della densità elettronica, della frequenza di collisione, del coefficiente di ricombinazione, legge di formazione degli strati e influenze delle diverse porzioni dello spettro della radiazione solare, dinamica degli strati), senza che, peraltro, si possa parlare di risposte definitive. Allo studioso italiano interessato ai più recenti sviluppi della ricerca ionosferica ed ai problemi che essa solleva il volume qui recensito si raccomanda per l'autorità degli autori delle memorie e per la mole dei risultati raccolti.

Non è possibile naturalmente, dare qui notizia del contenuto di tutte le memorie. Ricorderemo solo quelle che costituirono gli « high lights » della Conferenza.

Le memorie n. 21, 33 e 34 illustrano, nei suoi diversi aspetti, la nuova teoria della dinamo di D. F. MARTYN, che riprende con essa la teoria delle variazioni geomagnetiche di Balfour e Schuster, tenendo presente però l'effetto Hall. Ne risulta una nuova distribuzione del potenziale elettrostatico nella regione della dinamo, per cui quasi tutte le anomalie dello strato  $F_2$  si spiegano, anche *quantitativamente*, come distorsioni dello strato dovute a correnti elettriche generate dal campo di polarizzazione della regione della dinamo.

La memoria n. 12 è il riassunto preparato da J. A. RATCLIFFE di una conversazione tenuta alla conferenza da D. K. BAILEY del National Bureau of Standards americano. D. K. BAILEY

appartiene a quel gruppo di studiosi che nel 1952 annunziarono la scoperta di un nuovo tipo di propagazione VHF basato su un meccanismo di scattering dovuto alle irregolarità *sempre presenti* nella ionosfera. A Cambridge sono state rese note, per la prima volta, alcune delle conclusioni a cui gli studiosi americani sono giunti dopo anni di intense ricerche: l'altezza dove ha luogo lo scattering è stata localizzata tra i 75 e i 90 km, sono state determinate le variazioni diurne e stagionali dell'intensità del segnale, la periodicità del fading, la funzione di autocorrelazione con la distanza.

La memoria n. 8, infine, dovuta al noto studioso indiano S. N. MITRA dà una conferma qualitativa e quantitative del fenomeno della self-girointerazione (autogirodemodulazione).

F. IMMIRZI

R. T. COX — *Statistical mechanics of irreversible change*. The John Hopkins Press, Baltimore, pagina 130.

Questo libretto è una esposizione dei fatti già noti di Termodinamica dei processi irreversibili, con continuo riferimento alla statistica di Gibbs. Non viene mostrata anche la trattazione cinetica di questi processi che è la parte più viva e ancora in formazione; perciò i metodi recenti sviluppati da Kirkwood sono rimasti esclusi.

Il libro risente della trattazione piuttosto formale e astratta tipica della Termodinamica.

La teoria del moto browniano e quella dei processi di trasporto, sono espone in modo abbastanza particolareggiato.

G. CARERI

---

PROPRIETÀ LETTERARIA RISERVATA

---